



Terms and Conditions of Use of Digitised Theses from Trinity College Library Dublin

Copyright statement

All material supplied by Trinity College Library is protected by copyright (under the Copyright and Related Rights Act, 2000 as amended) and other relevant Intellectual Property Rights. By accessing and using a Digitised Thesis from Trinity College Library you acknowledge that all Intellectual Property Rights in any Works supplied are the sole and exclusive property of the copyright and/or other IPR holder. Specific copyright holders may not be explicitly identified. Use of materials from other sources within a thesis should not be construed as a claim over them.

A non-exclusive, non-transferable licence is hereby granted to those using or reproducing, in whole or in part, the material for valid purposes, providing the copyright owners are acknowledged using the normal conventions. Where specific permission to use material is required, this is identified and such permission must be sought from the copyright holder or agency cited.

Liability statement

By using a Digitised Thesis, I accept that Trinity College Dublin bears no legal responsibility for the accuracy, legality or comprehensiveness of materials contained within the thesis, and that Trinity College Dublin accepts no liability for indirect, consequential, or incidental, damages or losses arising from use of the thesis for whatever reason. Information located in a thesis may be subject to specific use constraints, details of which may not be explicitly described. It is the responsibility of potential and actual users to be aware of such constraints and to abide by them. By making use of material from a digitised thesis, you accept these copyright and disclaimer provisions. Where it is brought to the attention of Trinity College Library that there may be a breach of copyright or other restraint, it is the policy to withdraw or take down access to a thesis while the issue is being resolved.

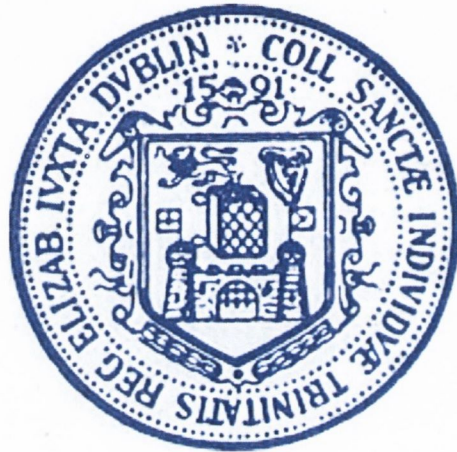
Access Agreement

By using a Digitised Thesis from Trinity College Library you are bound by the following Terms & Conditions. Please read them carefully.

I have read and I understand the following statement: All material supplied via a Digitised Thesis from Trinity College Library is protected by copyright and other intellectual property rights, and duplication or sale of all or part of any of a thesis is not permitted, except that material may be duplicated by you for your research use or for educational purposes in electronic or print form providing the copyright owners are acknowledged using the normal conventions. You must obtain permission for any other use. Electronic or print copies may not be offered, whether for sale or otherwise to anyone. This copy has been supplied on the understanding that it is copyright material and that no quotation from the thesis may be published without proper acknowledgement.

The role of TLRs and T cells in modulating glial activation; Implications for Alzheimer's disease

Tara Browne



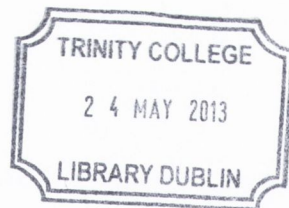
A thesis submitted to
University of Dublin, Trinity College
for the degree of
Doctor of Philosophy

Supervisor: Prof. Marina Lynch
Trinity College Institute of Neuroscience

2013

“You have to begin to lose your memory, if only in bits and pieces, to realise that memory is what makes our lives. Life without memory is no life at all, just as an intelligence without the possibility of expression is not really an intelligence. Our memory is our coherence, our reason, our feeling, even our action. Without it, we are nothing.”

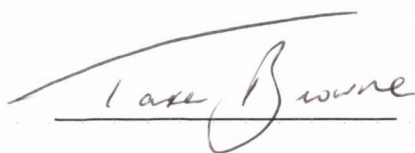
Luis Bunuel 1900-1993



Thesis 10002

I. Declaration

This thesis is submitted by the undersigned for the degree of Doctor of Philosophy at the University of Dublin. I declare that this thesis is entirely my own work with the following exceptions; certain results were produced in collaboration with Dr. Anthony Lyons, Dr. Keith McQuillan and Roisin McManus. This work has not been submitted in whole or part to this or any other university for any other degree. The author gives permission to the library to lend or copy this work upon request.

A handwritten signature in cursive script, reading "Tara Browne", written over a horizontal line.

Tara Browne

II. Abstract

Microglia are the key immune mediators of the CNS but, while astrocytes are primarily involved in maintaining homeostasis, they also exhibit immune functions. Both microglial and astrocytic activation is associated with autoimmune and neurodegenerative diseases such as multiple sclerosis (MS), Parkinson's disease and Alzheimer's disease (AD). Activation by a stimulus, such as a toll like receptor (TLR) agonist, or amyloid-beta ($A\beta$) results in the rapid production and secretion of pro-inflammatory cytokines and chemokines by these cells. However, under normal conditions, microglia are maintained in a quiescent state by interaction with other cells. Specifically, activation of the microglial receptor CD200R by its ligand, which is expressed on many cells including neurons, is important in this role, and disruption of the CD200-CD200R interaction results in increased microglial activation, neuroinflammation and autoimmune inflammation.

In this study, glial activation was assessed *in vitro* and *in vivo* in wildtype and CD200 knockout (CD200^{-/-}) mice following treatment with a TLR2 agonist, Pam₃Csk₄. It was found that Pam₃Csk₄ induced a significant increase in the expression of markers of glial activation and the production of pro-inflammatory cytokines and chemokines *in vitro* and *in vivo*. Furthermore, the loss of CD200 significantly enhanced cytokine and chemokine production in response to Pam₃Csk₄ *in vitro* and *in vivo*. In addition, it was found that TLR2 expression was increased on microglia cultured from CD200^{-/-}, compared with wildtype, mice suggesting a possible mechanism for the exaggerated response seen in CD200^{-/-} mice.

There is evidence that $A\beta$ induces some of its actions by interacting with TLR2 and the data from this study revealed that $A\beta$ mimicked many of the effects of Pam₃Csk₄. Significantly, incubation of cells in the presence of an anti-TLR2 antibody significantly attenuated $A\beta$ -induced cytokine and chemokine production by glia. These data provide evidence that activation of TLR2, either by the commonly-used agonist, Pam₃Csk₄, or by $A\beta$ triggered released of inflammatory mediators from glia and, importantly, provided support for the hypothesis that $A\beta$ -induced changes are TLR2-mediated.

Infiltration of T cells into the central nervous system (CNS) is believed to be involved in the pathogenesis of MS and a number of studies have reported that T cells infiltrate the brains of patients with AD. This is significant because T cells have been shown to interact with microglia and modulate their function. In this study, Th1, Th2 and Th17 cell lines were assessed for their ability to modulate glial activation *in vitro*. It was found that Th1 cells and Th17 cells increased glial activation as measured by CD40 and CD86 expression and IL-6 and TNF α production. Th2 cells had no effect on glial activation.

Having established that Th1 cells and Th17 cells impacted on glial activation *in vitro*, this was assessed *in vivo*. A transgenic mouse model of AD, which over-expresses amyloid precursor protein (APP) and presenilin-1 (PS1) (APP/PS1 mice) was used to examine the effect of Th1 and Th17 cells in modulating microglial activation and amyloid deposition. The data shows that T cells were present in greater numbers in the brains of APP/PS1 mice compared with wildtype mice and these cells secreted interferon (IFN)- γ and interleukin (IL)-17. Adoptive transfer of $A\beta$ -specific Th1 or Th17 cells into APP/PS1 mice increased microglial activation, as measured by CD11b immunoreactivity, while Th1 cells increased the number of $A\beta$ -containing plaques in hippocampus and cortex of APP/PS1.

In order to further examine the impact of Th1 cells on microglial activation and $A\beta$ plaque burden, mice were injected with an anti-IFN- γ antibody prior to, and on several days after, injection of $A\beta$ -specific Th1 cells. The data show that treatment of mice with anti-IFN- γ antibody attenuated the Th1 cell-induced increase in microglial activation and $A\beta$ deposition.

The results reveal that microglial activation is modulated by several factors including activation of CD200R and TLR2, as well as interaction with T cells. The evidence suggests that glial activation induced by Th1 cells in APP/PS1 mice is a result of release of IFN- γ . It remains to be established whether targeting T cell infiltration or IFN- γ release or activation of IFN- γ receptors may be beneficial in limiting disease progression in APP/PS1 mice and ultimately be of benefit in the treatment of AD.

III. Acknowledgements

Well where to begin, it's been an amazing chapter of my life that couldn't have happened without the support of an endless amount of people and to them I am truly grateful.

Firstly and most importantly, I'd like to sincerely thank my supervisor Professor Marina Lynch for her continual support, advice and incredible patience on matters both inside the lab and outside. Thank you so much for everything you have done for me over the last three years!! I'd also like to thank my funding body HRB who have kindly funded this project.

To everyone in the MAL lab, both members past and present including: Anto, Downer, Derek, Noreen, Aedin, Niamh, Julie-Ann, Anne-Marie, Thelma, Claire, Ronan, Belinda, Rodrigo, Raasay, Roisin, Jimmy, Steph, Lorraine and Donal, thanks for all your helping hands and advice throughout my project!! Thank you guys!! To my fellow PhD writers; Donal, Steph, Lorraine and Raasay well done guys, we made it!!

I'd also like to thank Professor Kingston Mills for his help and guidance with my project and thanks to everyone in Kingston's lab who helped me with my experiments!! An enormous thank you to Barry "FACS god" Moran, who offered endless help with my FACS analysis-thank you so much!!

I would like to thank the greater TCIN and physiology family especially the other supervisors, whose doors are always open to offer advice! To Quentin, Lesley, Ann, Alice, Kieran, Lisa, Barbara and Ciaran thank you for all your help!!

To the girlies in Dublin, Julie-Ann, Steph and Lorraine, I can't really put into words how amazing you guys have been!! You've been the best of friends and always put a smile on my face no matter what and been there for me especially when the road got a bit bumpy!! We've had some great laughs and nights out and I look forward to many more!! To my friends at home especially Dawn, Amy and Caitrin, I'm very lucky to have such great friends, always at the end of the phone and there for me when I need you the most, thank you for everything!

To Maria and Jim, who have had to live with not just one, but two, PhD students writing up!! I 'am enormously grateful for your never ending generosity, time and support. I can't thank you enough!!

To "Uncle" Bill and Shelley thank you for everything you have done for me, you've been amazing!! Especially getting up at early hours, in the pouring rain, to bring me and my horse eventing!! I'm truly grateful and I can't tell you how much I appreciate you! To the rest of the West Cork crew, you've provided never ending entertainment and fun over the last few years and I owe a lot of people drinks-thanks guys!!

Last but by no means least, this wouldn't have been possible without my amazing family!! Mum and Dad thank you for everything, your encouragement, guidance, support, help and belief in me!! You got me to where I' am!! From the bottom of my heart a huge thanks for everything!! To my brothers, Rory and Frazer, and my sister Kerry, you've all had individual inputs over the last few years but above all you have always been there for me, thank you!! To my auntie Mags, I'm massively grateful for your endless support, in more ways than one, and help over the past few years, thank you so much!!

IV. Table of Contents

I.	Declaration of authorship	i
II.	Abstract	ii
III.	Acknowledgements	iii
IV.	Contents Page	v
V.	List of Figures	x
VI.	List of Tables	xv
VII.	Abbreviations	xvi
Chapter 1.	Introduction	1
1.1.	The immune system	2
1.1.1.	The innate immune system	2
1.1.1.1.	<i>TLRs</i>	3
1.1.1.2.	<i>TLR structural characteristics and signalling pathways</i>	3
1.1.1.3.	<i>TLR ligands</i>	7
1.1.2.	The adaptive immune system	7
1.1.2.1.	<i>CD4⁺ T cell subpopulation induction and cytokine secretion</i>	9
1.1.2.2.	<i>CD4⁺ T cells and disease</i>	11
1.2.	The CNS	11
1.2.1.	CNS immunity and inflammation	12
1.2.2.	The BBB	12
1.2.3.	Astrocytes	15
1.2.4.	Microglia	15
1.2.5.	Markers of glial activation	17
1.2.5.1.	<i>CD11b</i>	17
1.2.5.2.	<i>MHC class II and co-stimulatory molecules CD80 and CD86</i>	17
1.2.5.3.	<i>CD40</i>	19
1.2.5.4.	<i>TLRs</i>	19

1.2.6. Cytokines	21
1.2.6.1. <i>TNFα</i>	21
1.2.6.2. <i>IL-6</i>	22
1.2.6.3. <i>IL-1β</i>	23
1.2.7. Chemokines	24
1.2.7.1. <i>IP-10</i>	24
1.2.7.2. <i>MCP-1</i>	25
1.2.7.3. <i>RANTES and MIP-1α</i>	26
1.2.8. Modulators of microglial activation: Maintaining microglial quiescence	26
1.2.8.1. <i>Fractalkine</i>	27
1.2.9. CD200	27
1.2.9.1. <i>CD200 and CD200R</i>	27
1.2.9.2. <i>CD200 signalling</i>	28
1.2.9.3. <i>CD200-CD200R interaction modulates inflammation</i>	31
1.2.9.4. <i>The role of CD200 in neurodegeneration</i>	32
1.3. AD	33
1.3.1. A β ; processing, production and overproduction	34
1.3.2. Role of the innate and adaptive immune system in AD	35
1.3.2.1. <i>Role of Microglia in AD</i>	35
1.3.2.2. <i>A role for TLRs in AD</i>	37
1.3.2.3. <i>A role for T cells in AD</i>	38
1.3.3. Transgenic mouse models of AD	39
1.4. Study aims	41
Chapter 2. Methods	42
2.1. Preparation, treatment and harvesting of primary glia	43
2.1.1. Preparation of primary mixed glia	43
2.1.2. Preparation of primary astrocytes and microglia	43
2.1.3. Treatment of mixed glia	44
2.1.4. Harvesting of mixed glia	44
2.2. Cell counts	45

2.3. Amyloid-beta (Aβ)	45
2.3.1. Preparation of A β ₁₋₄₂ and A β ₁₋₄₀	45
2.3.2. Testing of A β aggregation by thioflavin T assay	45
2.4. Animals	47
2.5. Treatment of animals for Pam₃Csk₄ study	47
2.6. Genotyping of APP/PS1 mice	47
2.6.1. Isolation of genomic DNA	47
2.6.2. Polymerase chain reaction (PCR) for APP ^{swe} and PS1 ^{dE9} genes	48
2.7. T cell study protocols	50
2.7.1. Generation of T cell lines from APP/PS1 and littermate control mice	50
2.7.1.1. <i>Preparation of spleen cell culture</i>	50
2.7.1.2. <i>Generation of non-specific Th1, Th2 and Th17 cell lines</i>	51
2.7.1.3. <i>Generation of Aβ-specific Th1, Th2 and Th17 cell lines</i>	51
2.7.2. Co-culture and treatment of specific T cell lines and glia	51
2.7.2.1. <i>Non-specific T cell co-culture with glia</i>	51
2.7.2.2. <i>Aβ-specific T cells co-culture with glia and incubation with Aβ₁₋₄₂</i>	52
2.7.3. Generation of Th1 and Th17 cell line from C57BL/6 mice and co-culture with mixed glia	54
2.7.3.1. <i>Generation of Th1 and Th17 cell lines</i>	54
2.7.3.2. <i>Co-culture and treatment of Th1 and Th17 cell lines with mixed glia</i>	54
2.7.4. Generation of T cells for adoptive transfer APP/PS1 <i>in vivo</i> study	55
2.7.4.1. <i>Generation of Aβ-specific T cell lines</i>	55
2.7.4.2. <i>Intravenous injection of Th1 cells for anti-IFN-γ study</i>	55
2.8. Mononuclear cell isolation from CNS tissue	56
2.9. Flow cytometry	58
2.9.1. Flow cytometry of T cells and glia	58
2.9.2. Flow cytometry of mononuclear cells	58

2.10. Protein quantification	60
2.11. Quantitative Polymerase Chain Reaction (QPCR)	60
2.11.1. RNA extraction	60
2.11.2. cDNA synthesis	61
2.11.3. QPCR	61
2.12. Analysis of cytokine and chemokine expression by ELISA	64
2.13. Determination of Aβ concentrations in tissue samples using multi-spot ELISA	66
2.13.1. Extraction of soluble and insoluble A β from brain tissue	66
2.13.2. Detection of soluble and insoluble A β concentrations in cortical tissue by multi-spot ELISA	66
2.14. Immunohistochemical analysis	67
2.14.1. Subbing of slides	67
2.14.2. Preparation of tissue sections for immunohistochemistry	67
2.14.3. Immunohistochemical staining for CD11b	68
2.14.5. Quantification of CD11b immunohistochemical analysis using Image J	69
2.14.6. Immunohistochemical staining for A β plaques using Congo red	69
2.14.7. Double-immunofluorescence staining for A β and CD11b	70
2.15. Statistical analysis	70
Chapter 3.	71
3.1. Introduction	72
3.2. Methods	75
3.3. Results	76
3.4. Discussion	100

Chapter 4.	112
4.1. Introduction	113
4.2. Methods	114
4.3. Results	115
4.4. Discussion	134
Chapter 5.	142
5.1. Introduction	143
5.2. Methods	148
5.3. Results	149
5.4. Discussion	167
Chapter 6.	177
6.1. Introduction	178
6.2. Methods	183
6.3. Results	185
6.4. Discussion	205
Chapter 7. General Discussion	211
Chapter 8. Bibliography	222
Appendix I List of Publications	246
Appendix II List of Materials	247
Appendix III List of Solutions	251
Appendix IV List of Company Addresses	253

V. List of Figures

- Figure 1.1.** TLR signalling via MyD88-dependent and MyD88-independent signalling cascades.
- Figure 1.2.** Naïve CD4⁺ T cell clonal expansion following antigen presentation and co-stimulation.
- Figure 1.3.** Migration of leukocytes requires the upregulation of adhesion molecules and signalling by chemokines and chemokine receptors.
- Figure 1.4.** The structure of CD200 and CD200R and the signalling pathway initiated following CD200-CD200R interaction.
- Figure 2.1.** Measurement of A β aggregation by thioflavin T assay
- Figure 2.2.** Timeline of generation of T cell lines from APP/PS1 and littermate control mice and co-culture with microglia or astrocytes.
- Figure 2.3.** Diagram of Percoll separation used to isolate mononuclear cells from the CNS.
- Figure 3.1.** Pam₃Csk₄ increased CD11b and CD40 mRNA expression
- Figure 3.2.** Pam₃Csk₄ decreased CD68 mRNA expression.
- Figure 3.3.** Pam₃Csk₄ increased production of TNF α .
- Figure 3.4.** Pam₃Csk₄ increased production of IL-6.
- Figure 3.5.** Pam₃Csk₄ increased production of MCP-1.
- Figure 3.6.** Pam₃Csk₄ increased production of IP-10.
- Figure 3.7.** Pam₃Csk₄ increased TLR mRNA expression.
- Figure 3.8.** Increased number of TLR2 expressing CD11b⁺ cells in CD200^{-/-}, compared with wildtype, mice.
- Figure 3.9.** TLR2 mRNA expression was increased by A β _{1-40/1-42}.
- Figure 3.10.** The A β -induced increase in CD86 and CD40 mRNA expression was attenuated by anti-TLR2.
- Figure 3.11.** CD11b and CD68 mRNA expression was unaffected by A β _{1-40/1-42} or anti-TLR2.
- Figure 3.12.** The A β -induced increase in TNF α mRNA expression was attenuated by anti-TLR2.

- Figure 3.13.** The A β -induced increase in IL-6 production was attenuated by anti-TLR2.
- Figure 3.14.** The A β -induced increase in IP-10 mRNA expression was attenuated by anti-TLR2.
- Figure 3.15.** The A β -induced increase in MCP-1 production was attenuated by anti-TLR2.
- Figure 3.16.** The A β -induced increase in MIP-1 α production was attenuated by anti-TLR2.
- Figure 3.17.** The A β -induced increase in RANTES production was attenuated by anti-TLR2.
- Figure 3.18.** A $\beta_{1-40/1-42}$ increased CD200R but not CD200L mRNA expression.
- Figure 3.19.** A $\beta_{1-40/1-42}$ exerted different effects on fractalkine receptor and fractalkine ligand mRNA expression.
- Figure 4.1.** Pam₃Csk₄ increased TNF α mRNA expression in hippocampal and cortical tissue prepared from wildtype and CD200^{-/-} mice.
- Figure 4.2.** Pam₃Csk₄ increased IL-1 β mRNA expression in hippocampal and cortical tissue prepared from wildtype and CD200^{-/-} mice.
- Figure 4.3.** Pam₃Csk₄ increased IL-6 mRNA expression in hippocampal and cortical tissue prepared from wildtype and CD200^{-/-} mice.
- Figure 4.4.** Pam₃Csk₄ increased IP-10 mRNA expression in hippocampal and cortical tissue prepared from wildtype and CD200^{-/-} mice.
- Figure 4.5.** Pam₃Csk₄ increased MIP-1 α mRNA expression in hippocampal and cortical tissue prepared from wildtype and CD200^{-/-} mice.
- Figure 4.6.** Pam₃Csk₄ increased MCP-1 mRNA expression in hippocampal and cortical tissue prepared from wildtype and CD200^{-/-} mice.
- Figure 4.7.** Pam₃Csk₄ increased RANTES mRNA expression in hippocampal and cortical tissue prepared from wildtype and CD200^{-/-} mice.
- Figure 4.8.** Pam₃Csk₄ treatment had no effect on the number of TLR2 expressing CD11b⁺ cells in wildtype and CD200^{-/-} mice.
- Figure 4.9.** Pam₃Csk₄ increased TLR2 mRNA expression in hippocampal and cortical tissue prepared from wildtype and CD200^{-/-} mice.

- Figure 4.10.** Pam₃Csk₄ increased TLR1 mRNA expression in hippocampal and cortical tissue prepared from wildtype and CD200^{-/-} mice.
- Figure 4.11.** Pam₃Csk₄ treatment had no effect on the number of MHC class II and CD40 expressing CD11b⁺ cells in wildtype and CD200^{-/-} mice.
- Figure 4.12.** CD40 mRNA expression was decreased in hippocampal and cortical tissue prepared from CD200^{-/-} mice.
- Figure 4.13.** CD86 mRNA expression was decreased in hippocampal and cortical tissue prepared from CD200^{-/-} mice.
- Figure 4.14.** CD68 mRNA expression was decreased in hippocampal and cortical tissue prepared from CD200^{-/-} mice.
- Figure 5.1.** Generation of non-specific Th1, Th2 and Th17 T cell lines.
- Figure 5.2.** Increased CD40 expression on microglia and astrocytes co-cultured with Th1 cells.
- Figure 5.3.** Increased cytokine production by microglia and astrocytes following co-culture with Th1 cells.
- Figure 5.4.** CD40 and CD86 expression is unaltered on microglia and astrocytes following co-culture with Th2 cells.
- Figure 5.5.** Cytokine production by microglia and astrocytes is unaltered following co-culture with Th2 cells.
- Figure 5.6.** Increased CD40 expression on astrocytes following co-culture with Th17 cells.
- Figure 5.7.** IL-6 production is increased by astrocytes following co-culture with Th17 cells
- Figure 5.8.** Generation of A β -specific Th1, Th2 and Th17 T cell lines.
- Figure 5.9.** CD40 and CD86 expression is unaltered on microglia and astrocytes following co-culture with A β -specific Th1 cells.
- Figure 5.10.** TNF α production was increased by microglia and astrocytes following co-culture with A β -specific Th1 cells.
- Figure 5.11.** CD40 and CD86 expression is unaltered on microglia and astrocytes following co-culture with A β -specific Th2 cells.
- Figure 5.12.** Cytokine production by microglia and astrocytes is unaltered following co-culture with A β -specific Th2 cells.

- Figure 5.13.** CD40 and CD86 expression is unaltered on microglia and astrocytes following co-culture with A β -specific Th17 cells.
- Figure 5.14.** Cytokine production by microglia and astrocytes is unaltered following co-culture with A β -specific Th17 cells.
- Figure 6.1.** CD3⁺CD4⁺ cells infiltrate the brains of wildtype and APP/PS1 mice.
- Figure 6.2.** CD3⁺CD8⁺ cells infiltrate the brains of wildtype and APP/PS1 mice.
- Figure 6.3.** Generation of Th1 and Th17 cell lines.
- Figure 6.4.** Expression of CD40 and CD86 on microglia was assessed following co-culture with Th1 cells and incubation with IFN- γ and A β ₁₋₄₂.
- Figure 6.5.** Expression of MHC class II on microglia was assessed following co-culture with Th1 cells and incubation with IFN- γ and A β ₁₋₄₂.
- Figure 6.6.** Expression of CD40 and CD86 on microglia was assessed following co-culture with Th17 cells and incubation with IL-17 and A β ₁₋₄₂.
- Figure 6.7.** Expression of MHC class II on microglia was assessed following co-culture with Th17 cells and incubation with IL-17 and A β ₁₋₄₂.
- Figure 6.8.** CD11b expression is increased in cortical sections prepared from APP/PS1, compared to wildtype, mice.
- Figure 6.9.** CD11b expression is increased in hippocampal sections prepared from APP/PS1, compared with wildtype, mice.
- Figure 6.10.** Anti-IFN- γ antibody attenuates the A β -specific Th1-induced increase in A β ₁₋₃₈, A β ₁₋₄₀ and A β ₁₋₄₂ concentrations in APP/PS1 mice.
- Figure 6.11.** A β -specific Th1 cells increase the number of A β -plaques in APP/PS1 mice and this effect is attenuated by anti-IFN- γ treatment.
- Figure 6.12.** CD11b expression was assessed in cortical sections prepared from wildtype and APP/PS1 mice.

- Figure 6.13.** CD11b expression was assessed in hippocampal sections prepared from wildtype and APP/PS1 mice.
- Figure 6.14.** Pan A β and CD11b expression was co-localised in cortical sections prepared APP/PS1 mice.
- Figure 6.15.** Pan A β and CD11b expression was co-localised in hippocampal sections prepared APP/PS1 mice.

VI. List of Tables

- Table 2.1.** Primers used for DNA amplification.
- Table 2.2.** Co-culture of Th1 and Th17 cells with mixed glia and treatments.
- Table 2.3.** Antibodies used in flow cytometry.
- Table 2.4.** QPCR primers gene expression assay numbers.
- Table 2.5.** Origin and specificities of antibodies for ELISA.
- Table 3.1.** Results summary of inflammatory markers assessed in mixed glia prepared from wildtype and CD200^{-/-} mice.
- Table 3.2.** Results summary of mRNA expression of inflammatory markers assessed in mixed glia treated with A β _{1-40/1-42} and anti-TLR2.
- Table 3.3.** Results summary of supernatant concentrations of cytokines and chemokines assessed in mixed glia treated with A β _{1-40/1-42} and anti-TLR2.
- Table 4.1.** Results summary of mRNA expression of inflammatory markers assessed in hippocampal and cortical tissue prepared from wildtype and CD200^{-/-} mice.
- Table 4.2.** Results summary of cell surface receptor expression on microglia prepared from wildtype and CD200^{-/-} mice.
- Table 5.1.** Results summary of the expression of co-stimulatory molecules and production of cytokines following co-culture of non-specific T cells with microglia and astrocytes.
- Table 5.2.** Results summary of the expression of co-stimulatory molecules and production of cytokines following co-culture of A β -specific T cells with microglia and astrocytes.

VII. Abbreviations

AD	Alzheimer's disease
APP	Amyloid precursor protein
A β	Amyloid-beta peptide
ANOVA	Analysis of variance
APC	Antigen presenting cell
ApoE	Apolipoprotein E
BCR	B cell receptor
BBB	Blood brain barrier
BSA	Bovine serum albumin
CNS	Central nervous system
CSF	Cerebrospinal fluid
CD11b	Cluster of differentiation 11b
CD200	Cluster of differentiation 200
CD28	Cluster of differentiation 28
CD3 ⁺	Cluster of differentiation 3
CD4 ⁺	Cluster of differentiation 4
CD8 ⁺	Cluster of differentiation 8
CD40	Cluster of differentiation 40
CD68	Cluster of differentiation 68
CD80	Cluster of differentiation 80
CD86	Cluster of differentiation 86
CIA	Collagen induces arthritis
CR3	Complement receptor 3
cDNA	Complementary deoxyribonucleic acid
CFA	Complete freund's adjuvant
dH ₂ O	Deionised water
DC	Dendritic Cell
DNA	Deoxyribonucleic acid
dNTP	Deoxyribonucleotide triphosphate
DAB	Diaminobenzidine

DMSO	Dimethylsulphoxide
DMEM	Dulbecco's modified eagle medium
ELISA	Enzyme linked immunosorbent assay
EAE	Experimental autoimmune encephalomyelitis
FAD	Familial Alzheimer's disease
FACS	Fluorescent-activated cell sorting
FBS	Foetal bovine serum
Fc	Fusion protein
GFAP	Glial fibrillary acidic protein
g	Gram
GFP	Green fluorescent protein
HBSS	Hank's balanced salt solution
HRP	Horse radish peroxidase
H ₂ O ₂	Hydrogen peroxide
IL-1RAcP	IL-1R accessory protein
IRAK	IL-1R associated kinases
Ig	Immunoglobulin
IP-10	Interferon gamma-induced protein 10
IFN- γ	Interferon-gamma
IL-1 β	Interleukin-1 beta
IL-1R	Interleukin-1 receptor
IL-12	Interleukin-12
IL-4	Interleukin-4
IL-6	Interleukin-6
ICAM-1	Intracellular adhesion molecule-1
i.p.	Intraperitoneally
i.v.	Intravenously
JAK	Janus kinase
-/-	Knock out
LRR	Leucine rich repeats
L	Ligand
LPS	Lipopolysaccharide
MIP-1	Macrophage inflammatory protein-1

MHC class II	Major histocompatibility complex class II
mRNA	Messenger ribonucleic acid
μ	Micro
ml	Milliliter
mm	Millimetre
MAPK	Mitogen-activated protein kinases
mM	Molar
OX6	Monoclonal antibody clone for MHC class II
MCP-1	Monocyte chemotactic protein-1
MS	Multiple sclerosis
MBP	Myelin basic protein
MyD88	Myeloid differentiation factor 88
nm	Nanometre
NK	Natural killer
NO	Nitric oxide
NGS	Normal goat serum
NHS	Normal horse serum
NF-κB	Nuclear factor-κB
OCT	Optimal cooling temperature
Pam ₃ Csk ₄	Pam ₃ CysSerLys ₄
PAMPs	Pathogen associated molecular patterns
PRRs	Pathogen recognition receptors
PMA	Phorbol myristate acetate
PBS	Phosphate buffered saline
PBS-T	Phosphate buffered saline containing tween
PCR	Polymerase chain reaction
PS	Presenilin
RANTES	Regulated and normal T cell expressed and secreted
RNase	Ribonuclease
RNA	Ribonucleic acid
RT	Room temperature
RPMI	Roswell Park Memorial Institute
SEM	Standard error of mean

Strep-HRP	Streptavidin-horseradish peroxidase linked
H ₂ SO ₄	Sulphuric acid
TCR	T cell receptor
Th	T helper cell
Treg	T regulatory Cell
TMB	Tetramethylbenzidine
ThT	Thioflavin T
TNFR	TNF receptor
TRAF	TNF receptor associated factor
TLR	Toll like receptor
TE	<i>Toxoplasma</i> encephalitis
Tg	Transgenic
TNF- α	Tumour necrosis factor-alpha
BACE	β -APP Cleaving Enzyme

Chapter 1

Introduction

Chapter 1

1.1. The immune system

The immune system, an organism's defence mechanisms against invading or self pathogens, is fundamental to survival. It consists of a network of proteins, cells, tissue and organs that respond to a given insult in a manner which preserves homeostasis and prevents tissue damage. The immune system has evolved to distinguish between host cells and pathogens and comprises a non-specific innate immune system and a specific adaptive immune system. The innate immune system is the first line of defence and consists of physical barriers and cells that react if the physical barriers are breached. Although the innate immune system responds rapidly following pathogen detection it is unable to generate immunological memory as it is non-specific. Immunological memory is generated by the adaptive immune system which requires antigen presentation for its activation. While defined as separate systems, they are functionally intertwined and the action of one system has a direct effect on the other (Becher *et al.*, 2000).

1.1.1. The innate immune system

The functions of the innate system include directly killing a pathogen with its own cells or initiating an appropriate adaptive immune response that will clear the pathogen (Medzhitov and Janeway, 1997). The cells involved are derived from the myeloid lineage such as granulocytes (neutrophils, basophils, eosinophils and mast cells) and monocytes (dendritic cells and monocytes). These cells act as antigen presenting cells (APCs) and phagocytes, and secrete cytokines to communicate with other cells of the immune system (Becher *et al.*, 2000). Once a pathogen has breached the physical barriers, pathogen recognition receptors (PRR) found on the cells of the innate immune system are required to identify pathogens by their specific pathogen-associated molecular patterns (PAMPs) (Medzhitov & Janeway, 1997). Recognition of PAMPs by immune cells results in the activation of signalling pathways leading to antigen presentation, co-stimulatory molecule upregulation and the release of cytokines and chemokines.

The most-studied PRRs are the Toll-like receptors (TLRs) (Laflamme *et al.*, 2001; Takeda & Akira, 2004).

1.1.1.1. TLRs

TLRs were first identified in *Drosophila* as receptors involved in dorso-ventral patterning in embryos and, since then, evidence for a role in immunity was provided by Hoffmann and colleagues in 1996 who found that Toll-mutant flies were highly susceptible to fungal infection (Takeda & Akira, 2004). TLRs play a pivotal role in identifying invading pathogens and producing the appropriate immune response (Pandey & Agrawal, 2006). TLRs are expressed on a wide array of immune cell types including B cells, T cells, macrophages, monocytes, neutrophils, basophils, dendritic cells and natural killer cells (Hopkins and Sriskandan, 2005). Furthermore, TLRs are expressed by cells of the central nervous system (CNS) including microglia (Applequist *et al.*, 2002) and astrocytes (Bowman *et al.*, 2003). TLRs are expressed both on the cell surface (TLRs 1, 2, 4, 5 and 6) and intracellularly (TLRs 3, 7, 8 and 9) (Pandey & Agrawal, 2006). Although the activation of TLRs is crucial to mount an appropriate immune response, their activation or dysregulation is also implicated in the pathogenesis of autoimmune, chronic inflammatory and infectious diseases including cancer, asthma, psoriasis, inflammatory bowel disease, Alzheimer's disease (AD) and multiple sclerosis (MS) (Chen *et al.*, 2007; O'Neill *et al.*, 2009). The activation of TLRs and their implication in the pathogenesis of diseases, be it beneficial or detrimental, has led to widespread research investigating the precise role of individual TLRs in diverse diseases as they may be targets for therapeutic intervention (Chen *et al.*, 2007).

1.1.1.2. TLR structural characteristics and signalling pathways

TLRs are a family of type 1 integral membrane glycoproteins which consist of an extracellular domain made up of leucine-rich repeats (LRR) in the pathogen-binding ectodomains (ECD), and a cytoplasmic domain referred to as Toll/IL-1R (TIR) domain as it shows striking similarity to the cytoplasmic domain of the interleukin (IL)-1 receptor family (Takeda & Akira, 2004; Pandey &

Agrawal, 2006). To date, thirteen mammalian TLRs (TLR1-13) have been identified, each with their own set of PAMPs and signalling pathways. TLR signalling has been widely reviewed and it is known that TLRs may signal via the myeloid differentiation factor 88 (MyD88)-dependent pathway (all TLRs) or via the MyD88-independent pathway (selective for TLR3 and TLR4) (Takeda & Akira, 2004; Pandey & Agrawal, 2006; Chen *et al.*, 2007). The TIR domain of the TLRs acts as a scaffold for protein-protein interactions allowing for the activation of signalling cascades including mitogen-activated protein kinases (MAPKs), phosphoinositide 3-kinase (P13K) and nuclear factor- κ B (NF- κ B) (Chen *et al.*, 2007). These signalling pathways employ different adaptor proteins that are recruited in different combinations to different TLRs allowing for individual responses to diverse pathogens (O'Neill *et al.*, 2009).

The MyD88-dependent pathway employs several molecules to initiate downstream signalling including members of the IL-1R associated kinase (IRAK) family and tumour necrosis factor (TNF) receptor associated factor (TRAF-6) (Pandey & Agrawal, 2006). Furthermore, the linker molecules transforming growth factor β -activated kinases (TAK-1) and TAK-binding protein (TAB)-1 and -2 are recruited, which activate downstream I κ B kinase kinases (IKK) (Pandey & Agrawal, 2006). IKK is composed of IKK α , IKK β and NEMO which induce the phosphorylation of the I κ B family proteins and nuclear translocation of NF- κ B enabling the upregulation of genes involved in pro-inflammatory cytokine and chemokine production (Pandey & Agrawal, 2006; Chen *et al.*, 2007). TAK-1 can also activate the MAPK pathway such as c-Jun N-terminal kinases (JNK) thereby inducing activating protein-1 (AP-1), resulting in similar upregulation of genes encoding inflammatory cytokines (Takeda & Akira, 2004; Chen *et al.*, 2007).

The MyD88-independent pathway uses the TIR-domain containing adaptor-inducing interferon- β (TRIF)-related adaptor molecule (TRAM) which binds to TRIF which, in turn, mediates signalling in several ways including a TRAF-6-dependent or -independent manner. The TRAF-6-independent pathway is mediated through the kinase receptor-interacting protein (RIP)-1. TRIF also binds with TRAF family member-associated NF- κ B activator (TANK)-binding kinase 1 (TBK-1) and inducible I κ B kinase (IKK- ϵ), which in turn, phosphorylates interferon regulatory factor (IRF)-3 and IRF-7. Phosphorylation of IRF-3 and IRF-7 allows for their nuclear translocation resulting in the

upregulation of type 1 interferon (IFN) genes (Pandey & Agrawal, 2006). Figure 1.1 illustrates the essential components of TLR activation inducing the MyD88-dependent and MyD88-independent signalling cascades.

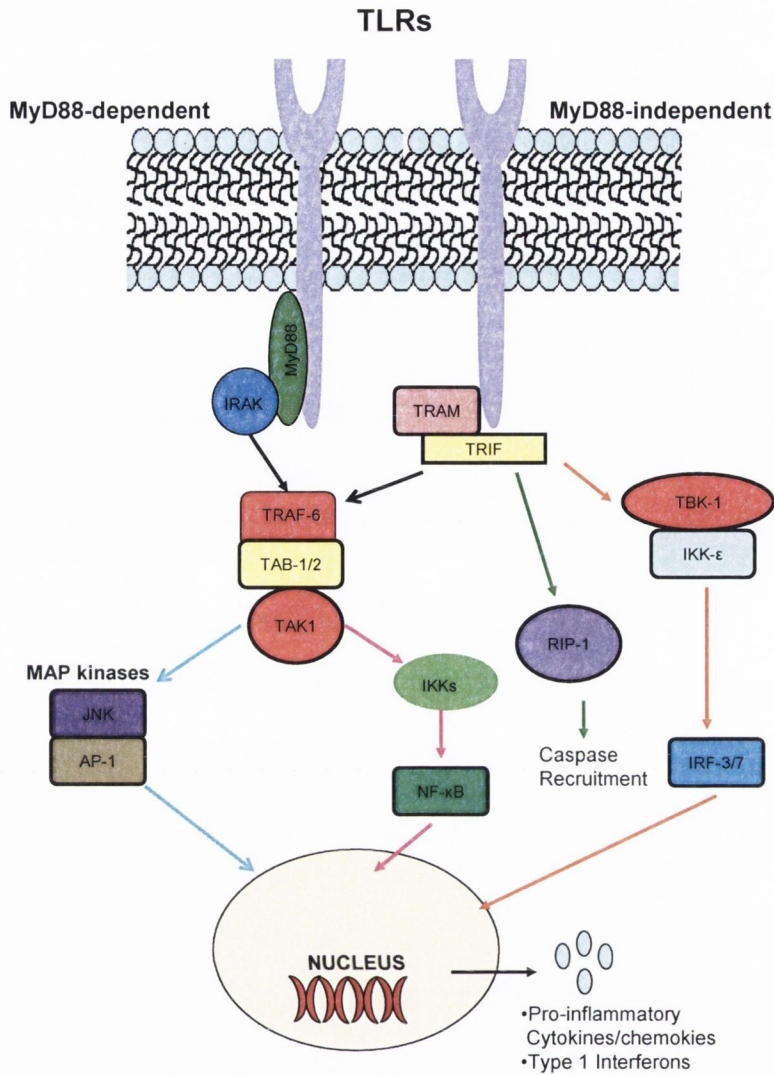


Figure 1.1. TLR signalling via MyD88-dependent and MyD88-independent signalling cascades.

TLRs mediate cytokine and chemokine production through MyD88-dependent and MyD88-independent pathway. These pathway results in downstream recruitment of signalling molecules with eventual translocation of NF-κB, AP-1 and IRF-3/7 to the nucleus and the upregulation of genes encoding cytokines and chemokines.

Adapted from Pandey & Agrawal (2006)

1.1.1.3. TLR ligands

TLRs respond to numerous ligands (Pandey & Agrawal, 2006). It has been suggested that TLR2 and TLR4 primarily recognise bacteria through differential cell wall components (Chen *et al.*, 2007), while TLR3, TLR7, TLR8 and TLR9 are endosomal and sense nucleic acid-based ligands, through their LRR domains (O'Neill, 2008). TLR3, TLR5 and TLR9 are involved in the recognition of double-stranded ribonucleic acid (RNA), bacterial flagellin and bacterial CpG-containing oligodeoxynucleotide (CpG) deoxyribonucleic acid (DNA), respectively (Takeda *et al.*, 2002). TLR4 recognises a component of the cell wall of gram-negative bacteria, lipopolysaccharide (LPS), and is critical for an LPS-induced immune response as shown in studies in which TLR4 was absent (Takeuchi *et al.*, 1999). TLR2 recognises the widest array of PAMPs including surface proteins on gram-negative and gram-positive bacteria, lipoteichoic acids, peptidoglycans (PGN), mycoplasma, mycobacteria and zymosan (Kielian, 2006). However, TLR2 has been shown to work as a heterodimer, with TLR1 and TLR6, to discriminate between lipopeptides (Ozinsky *et al.*, 2000). MALP-2, a synthetic mycoplasmal lipopeptide, which contains a diacylated cysteine residue is recognised by TLR2/TLR6 heterodimer while, Pam₃CysSerLys₄ (Pam₃Csk₄) which contains a triacylated cysteine residue is recognised by TLR2/TLR1 heterodimer (Takeda *et al.*, 2002). Triacylated lipopeptides interact with the TLR2/TLR1 heterodimer through the insertion of two ester-bound lipid chains into a pocket in TLR2 and the insertion of an amide-bound lipid chain into the hydrophobic channel in TLR1 (O'Neill, 2008).

1.1.2. The adaptive immune system

The adaptive immune system is more complex than the innate immune system in that it involves antigen-specific responses and the development of immunological memory for specific pathogens. Activation of the adaptive immune system depends on cells of the lymphoid lineage namely B and T progenitor cells. B cells develop in the foetal liver and later mature in the bone marrow and are mainly involved in humoral responses whereas T cells mature in the thymus and are responsible for cell-mediated immune responses.

B cells require signalling from the B cell receptor (BCR) and an additional signal from T helper (Th) cells to trigger their activation (Geisberger *et al.*, 2006). Once activated, they differentiate into either plasma cells or memory B cells. Plasma cells are terminally-differentiated B cells that secrete five different antibodies, including immunoglobulin (Ig) M, IgD, IgG, IgA, and IgE, which provide immediate and long-term protection against pathogens (Hoyer *et al.*, 2005). Once these antibodies are secreted they bind to their specific antigen, in a process called opsonisation, marking pathogens for phagocytosis.

T cells are involved in cell-mediated immune responses and are subdivided into cluster of differentiation (CD)8⁺ T cells or CD4⁺ T cells. Naïve CD8⁺ T cells can be divided into cytotoxic effector CD8⁺ cells or memory CD8⁺ T cells. CD8⁺ T cells recognise endogenous antigens, mainly viral particles, through major histocompatibility complex (MHC) class I allowing for the secretion of perforin and granulysin which lyse infected cells. Similarly CD4⁺ T cells can be divided into effector or memory cells. Activation of naïve CD4⁺ cells into appropriate effector cells requires two signals. The first signal is delivered through interaction of MHC class II on cells of the innate immune system with their specific T cell receptors (TCRs) (Sharpe & Freeman, 2002). This process is accompanied by a secondary signal from co-stimulatory molecules CD80 and CD86 on innate immune cells, to CD28 on T cells. Once both signals are present, naïve CD4⁺ T cells will rapidly divide into a subpopulation of T cells with effector functions (Sharpe & Freeman, 2002). In the absence of the second signal from co-stimulatory molecules, on APCs, T cells fail to respond and are rendered anergic or, if the secondary signal is a negative signal, T cell tolerance appears to be induced (Sharpe & Freeman, 2002). The phenotype of the activated CD4⁺ T cells generated depends not only on the antigen presented but on the cytokine environment present at the time of clonal expansion (Mosmann *et al.*, 1986). These CD4⁺ T cells subpopulations include Th1, Th2, Th17 and regulatory T (Treg) cells.

1.1.2.1. CD4⁺ T cell subpopulation induction and cytokine secretion

The distinct CD4⁺ T cell subtypes, termed Th1 and Th2 cells, were first discovered by Mosmann and colleagues (1986) and since then several other subtypes have been discovered, including Treg and Th17 cells (Mills, 2008).

Th1 cells are derived from naïve CD4⁺ T in the presence of interleukin (IL)-12, transforming growth factor- β (TGF- β) and interferon- γ (IFN- γ). IL-12 is thought to be the main factor in directing Th1 cell development and is produced by macrophages in response to microbial products (O'Garra, 1998). Th1 cells secrete an array of cytokines which correlate well with their function including IFN- γ , IL-2 and lymphotoxin (LT). Th1 cell cytokines are involved in macrophage activation as well as cytotoxic and inflammatory functions leading to the eradication of pathogens (Mosmann & Sad, 1996), however their dysregulation is also involved in immunopathologies and autoimmune diseases (O'Garra, 1998). Th2 cells divide in the presence of IL-4 which is secreted by mast cells and basophils (Constant & Bottomly, 1997). Th2 cells secrete cytokines including IL-4, IL-6, IL-10 and IL-5 which, in turn, can activate eosinophils and mast cells and induce B cells to produce IgE. Th2 cells are thought to control parasitic infections and their dysregulation has been implicated in atopy and allergic inflammation (O'Garra, 1998; Harrington *et al.*, 2005). Th17 cells divide in the presence of IL-1 and IL-23 and secrete IL-17, IL-17A, IL-21, IL-22, TNF α and IL-6. Th17 cells play an important role, through their secreted cytokines, in anti-microbial immunity at epithelial and mucosal barriers. Th17 cells are also involved in inflammation and autoimmunity (Mills, 2008).

Th1, Th2 and Th17 cells are able to regulate the induction of each other through the secretion of their cytokines in that Th1 cell-secreted IFN- γ inhibits Th2 cell development and humoral responses while, Th2 cell-secreted IL-4 and IL-10 inhibits Th1 development and macrophage activation (O'Garra, 1998). Similarly Th17 cells are regulated by Th1 cells (Mills, 2008). Figure 1.2 illustrates CD4⁺ clonal expansion.

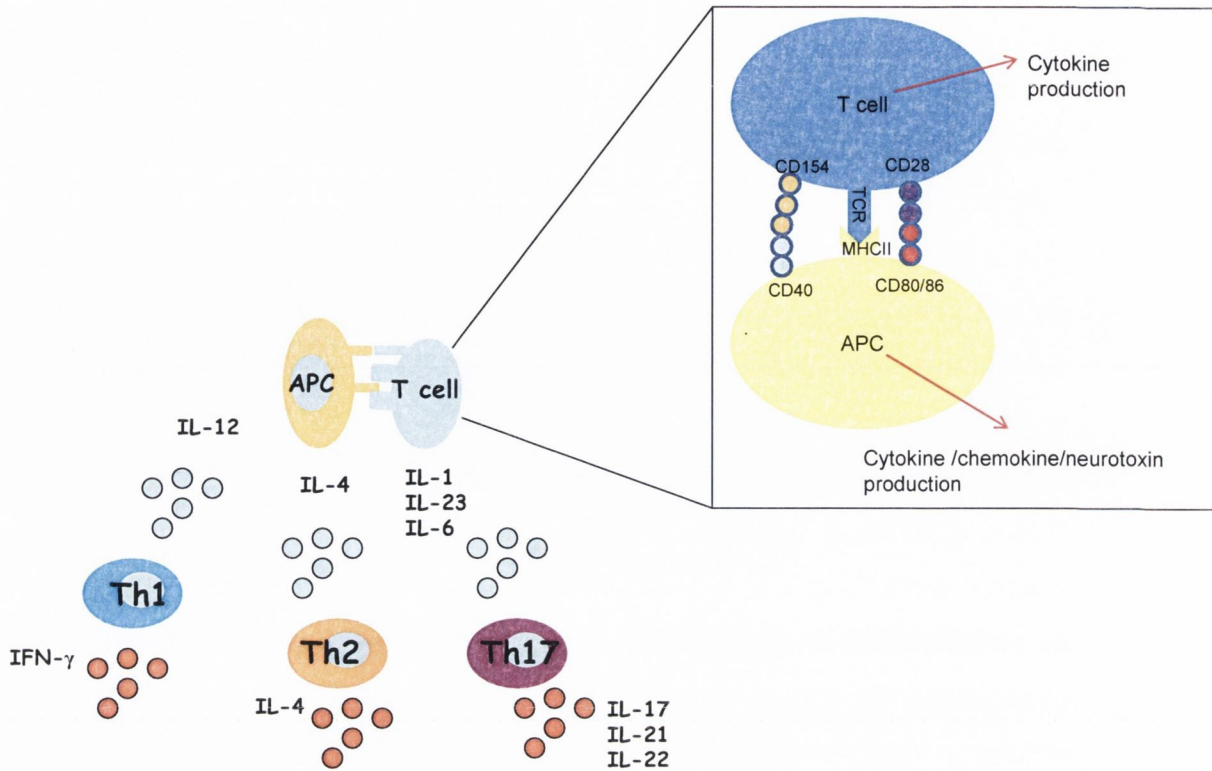


Figure 1.2. Naïve CD4⁺ T cell clonal expansion following antigen presentation and co-stimulation.

Following antigen presentation and the interaction of MHC class II with the TCR and co-stimulation from the CD28 and CD80/CD86 interaction naïve CD4⁺ T cell will differentiate into different T cell subsets depending on the cytokine environment present at the time of naïve T cell activation. CD4⁺ T cells activated in the presence of IL-12 will divide into Th1 effector cells, whereas IL-4 will shift the immune response towards Th2 effector cells. While, IL-1, IL-23 and IL-6 allow for Th17 effector cell development.

Adapted from Mills (2008) and Benveniste *et al.*, (2001)

1.1.2.2. $CD4^+$ T cells and disease

Despite the role of T cells in host defence their dysregulation or unchecked activation has been associated with a range of immune pathologies such as MS and type II collagen-induced arthritis (Harrington *et al.*, 2005). Knowledge of the role of specific T cell subgroups in MS has come from studies in the animal model experimental autoimmune encephalomyelitis (EAE) (Finsen & Owens, 2011). Originally studies in the EAE model suggested that Th1 cells mediated disease progression however more recently this view has been redefined (Becher *et al.*, 2006). This is based on the evidence from Billiau and colleagues (1987) demonstrating that blocking IFN- γ enhanced EAE and that mice deficient in IFN- γ or its receptor developed EAE (Chu *et al.*, 2000). It is now thought that both Th1 and Th17 cells can induce EAE but the pathology induced by Th1 cells differs to that of Th17 cells. For example Th1 cells have been found to facilitate macrophage recruitment into the CNS while, Th17 cells facilitate neutrophil recruitment (Kroenke *et al.*, 2008). Furthermore it has been shown that Th17 and $CD4^+$ cells secreting both IFN- γ and IL-17 infiltrate the CNS of mice undergoing EAE and exacerbate clinical symptoms accompanied by the activation of microglia and the secretion of pro-inflammatory cytokines (Murphy *et al.*, 2010). A role for Th2 cells in EAE is more controversial. Lafaille and colleagues (1997) suggest that Th2 cells can induce EAE in immuno-compromised RAG-1 knockout mice, whereas others suggest an anti-inflammatory role for Th2 cells and that Th2 cells can reverse Th1 cell-induced inflammatory changes (Gimsa *et al.*, 2001).

1.2. The CNS

The brain has evolved to be one of the most sophisticated and complex organs that nature has derived. Neurons roughly make up about 10% of the total cell number whereas glia make up about 90% of the total cell number and provide nutrients, support and defense for neurons but also interact with neurons in a complex and intricate fashion, such that deficits in glial function profoundly impact on neuronal function (Streit, 2005). Malfunction or disruption of this mutually-beneficial interaction is implicated in every major neurodegenerative disease (Moore & Thanos, 1996).

1.2.1. CNS immunity and inflammation

The CNS has developed both physiologically and anatomically to protect itself from damaging immune mediated inflammation (Aloisi, 2001). The proposal that the brain was “immunologically privileged” isolated from the periphery by the blood brain barrier (BBB) was supported with evidence from several investigators demonstrating that tissue transplanted into the brain survived for a longer period than tissue transplanted into the peripheral system (Medawar, 1948). The presence of the BBB, lack of lymphatic drainage and the lack of MHC antigens added to the proposed “immunoprivileged” notion however, this concept has now been revised. It is now accepted that the CNS can only employ a limited array of immune-defence components and that peripheral immune cells can cross the BBB and aid the resident immune cells in specific immune responses (Ransohoff *et al.*, 2003). These resident immune cells include astrocytes (Dong & Benveniste, 2001) and microglia. Microglia are considered the chief resident immunocompetent cells within the brain (Aloisi, 2001) and, as such assist in the recruitment of peripheral immune cells; however both microglia and astrocytes can upregulate the expression of adhesion molecules, as well as cytokines and chemokines which orchestrate the invasion of peripheral immune cells into the CNS through chemotaxis (Aloisi, 2001). Thus, regardless of the presence of the BBB, the CNS can facilitate its own immune surveillance (Hickey, 2001).

1.2.2. The BBB

The BBB consists of brain microvascular endothelial cells, a basement membrane, pericytes and glial cell elements, specifically astrocytic endfeet (Prat *et al.*, 2001). The specialized endothelial cells are linked together by tight junctions which are comprised of adhesion molecules including cadherins, occludin and claudins (Wilson *et al.*, 2010). These endothelial cells need constant input from the other neuroglia cells to maintain their BBB related properties (Prat *et al.*, 2001). The BBB is designed to selectively minimize the trafficking of cells and macromolecules into the CNS, however peripheral cells possess the ability to cross the BBB in search of specific antigens (Hickey, 2001). It is thought that leukocytes can migrate into the CNS through several routes including the choroid

plexus, subarachnoid space and the parenchymal perivascular space (Wilson *et al.*, 2010). Migration into the CNS is dependent on interacting pairs of selectins and their ligands, integrins and adhesion molecules, and chemokines and chemokine receptors (Ransohoff *et al.*, 2003). Figure 1.3 illustrates this process of migration.

Several studies suggest that CNS inflammation can disrupt the BBB integrity. Interestingly studies have found that both the expression of adhesion molecules and chemokines are increased in normal ageing and in response to cytokines which are released during CNS inflammation (Xu *et al.*, 2010). Furthermore, activation of endothelial cells and astrocytes during CNS injury can reduce tight junction integrity and increase BBB permeability aiding in the recruitment of peripheral cells (Wilson *et al.*, 2010). For instance, animal models of stroke exhibit decreased occludin expression following cerebral ischemia (Hua *et al.*, 2008). Previous studies from this laboratory have observed decreased expression of the tight junction molecules, occludin and claudin, and increased BBB permeability, measured by gadolinium extravasation, in APP/PS1 mice and CD200 knockout (CD200^{-/-}) mice, two mouse models which exhibit exacerbated inflammation (Kelly *et al.*, unpublished data). Importantly dysfunction of the BBB integrity has been described in several pathologies including AD, MS and vascular dementia (Campbell *et al.*, 2010), as well as in normal ageing (Farrall & Wardlaw, 2009).

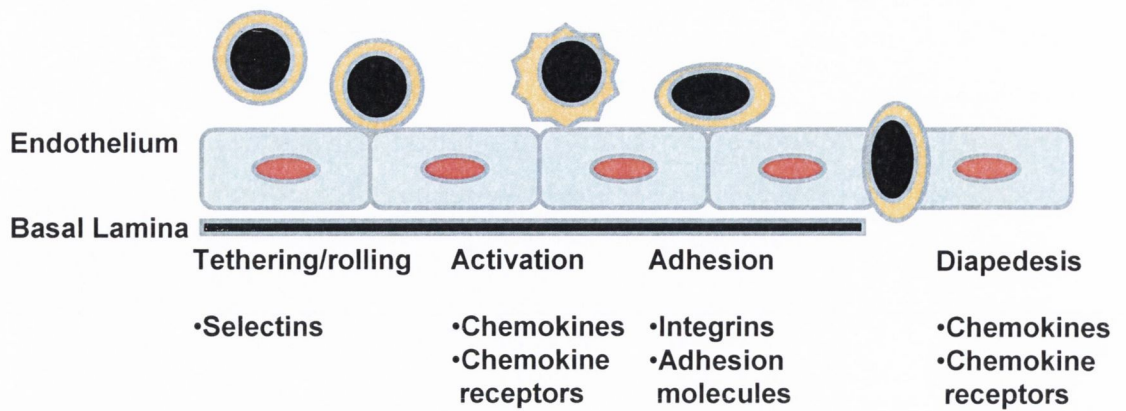


Figure 1.3. Migration of leukocytes requires the upregulation of adhesion molecules and signalling by chemokines and chemokine receptors.

Leukocyte extravasation into areas of inflammation has been separated into several steps. The first step is referred to as tethering and requires contact between the leukocyte and the endothelial cell followed by rolling. Both of these steps require interaction of selectins with their ligands. The next step, activation, requires the interaction of chemokines and their receptors which activate integrins. Integrin interaction with cell adhesion molecules results in the flattening of the leukocyte. The final stage is diapedesis which requires cytoskeletal reorganization that requires signalling from chemokines through their receptors.

Adapted from Ransohoff *et al.*, (2003)

1.2.3. Astrocytes

Astrocytes belong to the family of macroglia and are the most abundant glial cells within the CNS. Astrocytes are essential in development, maintaining homeostasis, survival of neurons and efficient running of the CNS (Bowman *et al.*, 2003). However, there is now considerable evidence suggesting a role for astrocytes in immune functions and inflammation (Dong & Benveniste, 2001). These cells express several TLRs which are important in recognizing bacterial products and mounting an effective immune response (Bowman *et al.*, 2003; Carpentier *et al.*, 2005). Furthermore, studies have found that astrocytes can produce chemokines (Babcock *et al.*, 2003; Dimitrijevic *et al.*, 2006) as well as cytokines which are integral to modulate immune responses. Astrocytes respond to both innate immune signals (e.g. TLR agonists) and adaptive immune signals (e.g. IFN- γ); studies from Carpentier and colleagues (2005) observed increased cytokine and chemokines secretion, as well as increased adhesion molecule, antigen presentation machinery and co-stimulatory molecule expression following stimulation with polyinosinic-polycytidylic acid (Poly I:C), LPS, IFN- α . and TNF α . Additionally, both the secretion of TNF α and IL-6 by astrocytes can lead to increased BBB permeability allowing for T cell entry (Carpentier *et al.*, 2005), and astrocytes have been shown to secrete IL-12 which is an important cytokine in T cell proliferation (Gurley *et al.*, 2008). In turn, T cells by releasing their cytokines can increase astrocyte activation (Giuliani *et al.*, 2003).

Evidence suggests that exacerbated astrocytic activation may have a role in neurodegenerative disease; reactive astrocytes are observed in the AD brain and are found in close association with amyloid (A β) deposits (Xia *et al.*, 2000), while it has been suggested that astrocytes respond more profoundly in the aged brain to inflammatory insults due to an age-related increase in basal astrocytic activation (Deng *et al.*, 2006).

1.2.4. Microglia

Microglial cells are the principal resident immune cells of the brain that were first described by Franz Nissl in the 1880s. As microglia are the resident brain macrophages they exhibit many of the features of other tissue macrophages

including phagocytosis, antigen presentation, production of chemokines and cytokines, complement components and reactive oxygen species (Benveniste *et al.*, 2001). They respond rapidly to endogenous insults (e.g. signals from stressed or dying cells as well as immune signals like cytokines and T cells) and exogenous insults such as those of pathogens (Aloisi, 2001). Under normal conditions they demonstrate a downregulated immunophenotype tailored to the specific microenvironment of the CNS. Interaction with neurons through ligand-receptor interactions is believed to aid in the maintenance of a downregulated phenotype. These ligand-receptor pairs include; CD200-CD200R, fractalkine-fractalkine receptor and signal regulatory protein- α (SIRP α)-CD47 (Hanisch & Kettenmann, 2007). However, microglia respond rapidly to a range of signalling molecules suggesting that their apparent quiescence represents a state of vigilance to disruptions in their extracellular surroundings (Kreutzberg, 1996). Traditionally, it was thought that microglia possessed only two states of activation a non-phagocytic phenotype and a phagocytic phenotype however, it is now acknowledged that this is not the case and multiple activation states exist (Lynch, 2009). Indeed microglia are very plastic and their activation state depends on the inflicted insult/pathology (Kreutzberg, 1996) and, more importantly, different phenotypes means functional diversity (Hanisch & Kettenmann, 2007). The transformation of microglia into an activated phenotype is characterized by increased expression of cell surface markers including those involved in antigen presentation and phagocytosis, and increased secretion of several inflammatory mediators namely cytokines and chemokines (Gehrmann *et al.*, 1995; Lynch, 2009).

Microglial activation is associated with an array of disease pathologies including neurodegenerative diseases such as MS, AD and Parkinson's disease (PD). Furthermore, studies suggest that microglial activation increases with ageing and this can be associated with an exacerbated response to an inflammatory insult (Deng *et al.*, 2006). Despite extensive research, the role of microglia in neurodegenerative diseases still remains unclear and their activation has been associated with both neuroprotective and neurotoxic effects (Hanisch & Kettenmann, 2007).

1.2.5. Markers of glial activation

Under resting conditions, glia express low basal levels of markers including CD11b (microglia only), CD40, CD86, CD80, MHC class II and TLRs however, CNS pathologies and systemic infections upregulates expression of these markers (Frank *et al.*, 2007). Further it has been established that microglia display different expression of these markers depending in the state of activation (Lynch, 2009).

1.2.5.1. CD11b

The integrin, CD11b, forms a heterodimer with CD18 to make up the complement receptor-3 (CR3), also known as MAC-1 (Lynch, 2009). The extent of CD11b expression is reported to correlate with the degree of microglial activation (Roy *et al.*, 2008). The CR3 receptor uses a lectin binding site to bind to an array of microbial molecules and behaves as a powerful mediator of the immune response particularly as it activates protein kinase cascades that are crucial for leukocyte activation (Aloisi, 2001). Recent studies have reported that CD11b is upregulated on microglia in response to an array of pro-inflammatory cytokines including TNF α , IFN α , IL-1 β and IL-6 and by fibronectin and vitronectin, which are extracellular matrix substrates that are released during BBB breakdown (Milner & Campbell, 2003). Consistently, LPS increases CD11b expression on microglial cell lines and also *in vivo* in the striatum of mice injected with LPS (Roy *et al.*, 2008). In addition, microglia have been observed expressing CD11b in close proximity to A β -plaques in a mouse model of AD (Bornemann *et al.*, 2001).

1.2.5.2. MHC class II and co-stimulatory molecules CD80 and CD86

MHC class II expression is a hallmark of APCs and is expressed at low levels on resting microglia however, its upregulation is an early consequence of microglial activation that may even precede morphological changes (McGeer *et al.*, 1993). Although MHC class II expression is generally found on professional APCs, such as microglia, it is also expressed on astrocytes although to a much

lesser extent (Lynch, 2009). MHC class II interaction with the TCR, expressed on CD4⁺ T cells, in the presence of co-stimulatory molecules initiates the activation of signalling cascades as well as the upregulation of CD40 and CD40L on their respective cells (Dong & Benveniste, 2001). Several factors increase the expression of MHC class II; IFN- γ , the Th1 cell secreted cytokine, is perhaps the most potent inducer of MHC class II expression on microglia (Xu & Ling, 1995), and astrocytes (Dong & Benveniste, 2001). Studies from Milner and Campbell (2003) demonstrated that microglia expressed MHC class II following IFN- γ stimulation. Others have observed basal expression of MHC class II on *ex vivo* human microglia and its upregulation following IFN- γ and LPS stimulation (Becher & Antel, 1996). MHC class II expression is enhanced in mixed glia treated with both IFN- γ and A β (McQuillan *et al.*, 2010). In addition, MHC class II expression is upregulated on microglia during ageing (Henry *et al.*, 2009) and following inescapable shock (Frank *et al.*, 2007).

The expression of MHC class II has been linked with neurodegenerative diseases. Lopes and colleagues (2008) reported MHC class II-positive microglia in close proximity to senile plaques in post-mortem tissue from AD patients. Although aberrant expression of MHC class II is implicated in the pathogenesis of autoimmune diseases its expression is also essential for normal immune function, as seen in Bare Lymphocyte Syndrome, where these individuals have severe immunodeficiency due to the lack of MHC class II (Benveniste *et al.*, 2001).

CD80 (B7-1) and CD86 (B7-2) are transmembrane glycoproteins which are expressed on APCs, including microglia and astrocytes, and signal via CD28 and cytotoxic T lymphocytes antigen 4 (CTLA-4) expressed on T cells (Lynch, 2009). CD80 and CD86 engagement along with MHC class II and TCR engagement is essential for T cell proliferation. Several stimuli have been observed to upregulate CD80 and CD86 expression. CD80 expression is upregulated in human microglial cultures following IFN- γ and LPS stimulation (Becher & Antel, 1996) and in microglial cell lines following PGN stimulation (Kielian *et al.*, 2002). CD86 and CD80 expression are enhanced in murine mixed glia following A β treatment (McQuillan *et al.*, 2010).

1.2.5.3. CD40

CD40 is a member of the TNF-receptor family found on APCs and interacts with its ligand (CD40L), also known as CD154, on activated T cells (Aloisi, 2001; Benveniste *et al.*, 2001) and astrocytes (Townsend *et al.*, 2005). Interaction between CD40-CD40L results in the upregulation of co-stimulatory molecules (CD80 and CD86) and increased secretion of cytokines and chemokines (Aloisi, 2001; Benveniste *et al.*, 2001). CD40 is expressed at low levels on microglia and its expression is greatly enhanced in response to several stimuli including IFN- γ (Benveniste *et al.*, 2001), LPS (Lyons *et al.*, 2009a), and A β (Tan *et al.*, 1999).

The expression of CD40 has been linked with neurodegenerative diseases including MS and AD. It has been found that engagement of CD40 on microglia results in the production of IL-12, a cytokine involved with Th1 cell development (Aloisi *et al.*, 2000b; Becher *et al.*, 2000a). Increased CD40 expression has been observed in MS lesions and it has been reported that blocking the CD40-CD40L interaction significantly reduces disease severity in EAE, a mouse model of MS (Gerritse *et al.*, 1996). Similarly decreased microgliosis and astrocytosis has been observed in an APP mouse model of AD with deficiencies in CD40L (Tan *et al.*, 2002). Townsend and colleagues (2005) demonstrated that CD40 shifted microglia away from a phagocytic phenotype to an APC phenotype when stimulated by A β . These studies found that, following CD40 ligation and the presence of Th1 cytokines, the expression of MHC class II was upregulated on microglia and these microglia were found to be co-localized with A β accumulations (Townsend *et al.*, 2005).

1.2.5.4. TLRs

TLRs are expressed on both microglia (Applequist *et al.*, 2002) and astrocytes (Bowman *et al.*, 2003). Jack and colleagues (2005) observed the expression of TLR1-9 in human glial cells, and microglia had higher TLR expression levels than that of astrocytes. Additionally, studies have shown the expression of TLR co-receptor CD14 in microglial cell lines (Chen *et al.*, 2006) and in human microglial cultures (Becher & Antel, 1996). Comparable to other

cell surface markers TLR expression is upregulated upon glial activation. TLR2 gene transcription is upregulated in several brain regions, including the circumventricular organs, following stimulation with gram-negative and gram-positive cell wall components (Laflamme *et al.*, 2001). Zhou and colleagues (2008) observed enhanced TLR2 expression accompanied by enhanced MHC class II and co-stimulatory molecule expression, in both astrocytes and microglia, following lymphocytic choriomeningitis virus infection (LCMV). There is an extensive literature describing the impact of TLR activation on modulating the production of cytokines and chemokines by glial cells. Stimulation of human glial cultures with TLR agonists, LPS, Pam₃Csk₄ and a synthetic dsRNA (PIC), results in the secretion of pro-inflammatory cytokines IL-6 and TNF α as well as T cell polarizing cytokines IL-12 and IL-10 (Jack *et al.*, 2005). Stimulation of murine microglial cultures with LPS and Pam₃Csk₄ results in the secretion of IL-6 and TNF α (Shah *et al.*, 2009), as well as the release of nitric oxide (NO) (Ebert *et al.*, 2005). Other studies have observed the secretion of chemokines in microglial cultures following TLR stimulation with fibronectin and increased phagocytic activity following co-stimulation of microglia with fibronectin and other TLR agonists (Ribes *et al.*, 2010). Murine astrocyte cultures stimulated with TLR agonists secrete cytokines including IL-1 β , TNF α , IL-6 and chemokines including macrophage inflammatory protein (MIP)-1 β , MIP-2 and monocyte chemotactic protein (MCP)-1 (Esen *et al.*, 2004).

Recent evidence suggests that chronic TLR expression, like other glial cell markers, may have a role in neurodegenerative diseases. TLR expression is increased in MS lesions and microglia isolated from MS patients express several TLRs (Bsibsi *et al.*, 2002). Furthermore studies in EAE have found that TLR1, TLR2, TLR4, TLR6-9 expression is increased in the spinal cord of these animals accompanied by an increase in MyD88 (Prinz *et al.*, 2006). Expression of TLR2 and TLR4 is increased in the brains of AD patients (Walter *et al.*, 2007), and TLR2 and TLR7 expression (Letiembre *et al.*, 2009), as well as CD14 overexpression (Fassbender *et al.*, 2004) is observed in a mouse model of AD. Additionally studies from Letiembre and colleagues (2007) show an age-related increase in the expression of TLR1-7 and CD14 in mice.

1.2.6. Cytokines

Cytokines are a family of pleiotropic proteins that are involved in cell-to-cell communication and cellular activation. They have been described as immunoregulatory and neuromodulators and are subdivided into anti- and pro-inflammatory categories (Szelenyi, 2001). Cytokines are key regulators of innate and adaptive immune responses (Aloisi, 2001), yet chronic cytokine elevation leads to neuroinflammation and is a pathological feature of many neurodegenerative diseases. Cytokines and their receptors are expressed at low levels throughout the brain (Szelenyi, 2001) but are promptly upregulated in response to various environmental stimuli as a consequence of astrocytic (Dong & Benveniste, 2001; Carpentier *et al.*, 2005) and microglial (Aloisi, 2001) activation, and infiltration of monocytes and activated lymphocytes (Ghirnikar *et al.*, 1998).

1.2.6.1. TNF α

TNF α is a multipotent cytokine which is involved in the pathogenesis of inflammatory and autoimmune diseases (Probert *et al.*, 2000). It is described as one of the master pro-inflammatory cytokines and is secreted by microglia and peripheral macrophages during CNS inflammation. TNF α binds to two receptors the TNFR1 and TNFR2 (Aloisi, 2001). The role of TNF α in CNS inflammation is compounded by its ability to induce cell adhesion molecules allowing for the recruitment of peripheral immune cells; Milner and Campbell (2003) observed that TNF α increased the expression of the integrins $\alpha_4\beta_1$ and CD11b on microglia. TNF α is secreted *in vitro* in response to an array of stimuli including LPS (Szczepanik *et al.*, 2001) and Pam₃Csk₄ (Jack *et al.*, 2005; Shah *et al.*, 2009). TNF α has been shown to collaborate with IFN- γ , a Th1 cell cytokine, in the induction of inducible NO synthase (iNOS) and NF- κ B activation in astrocytes (Falsig *et al.*, 2004; Hsiao *et al.*, 2007) and microglia (Mir *et al.*, 2008). Furthermore its secretion has been observed following A β treatment in mixed glial cultures (McQuillan *et al.*, 2010) and in human macrophages and murine microglial cell lines (Szczepanik *et al.*, 2001). Butovsky and colleagues (2005)

observed upregulated TNF α in rodent organotypic hippocampal slice cultures in response to both LPS and A β .

There is a vast amount of literature implicating a role for TNF α in disease pathology. TNF α is secreted by microglia and astrocytes in the AD brain (Lue *et al.*, 2001a). TNF α expression is elevated in the cerebrospinal fluid (CSF) of MS patients (Sharief & Hentges, 1991), and is present in MS lesions as well as in EAE (Probert *et al.*, 2000). While, some studies have suggested that TNF α may have a protective role in disease; Liu and colleagues (1998) observed that TNF $^{-/-}$ mice developed a more severe disease progression following myelin oligodendrocyte glycoprotein (MOG)-induced EAE.

1.2.6.2. IL-6

IL-6 is a pluripotent cytokine, with diverse biological function, that in recent years has received attention for its involvement in regulating inflammation and immunological responses. IL-6 has been found to be both beneficial and destructive, within the CNS, as it protects neurons from ischemic damage yet promotes astrocyte proliferation (Dong & Benveniste, 2001). IL-6 is expressed at low levels within the CNS however in inflammation, infection and disease, IL-6 levels become rapidly elevated (Van Wagoner & Benveniste, 1999). IL-6 binds to its plasma membrane receptor IL-6R resulting in the activation of signalling cascades JAK and MAPK (Heinrich *et al.*, 2003). IL-6 is produced by glial cells and neurons and its synthesis can be increased by other cytokines, namely IL-1 β and TNF α (Gadient & Otten, 1997) and IL-17 (Ma *et al.*, 2010). A β increases the expression of IL-6 in murine mixed glia cultures (McQuillan *et al.*, 2010) and in murine microglia cell lines (Szczepanik *et al.*, 2001). Additionally A β , linked with advanced glycation endproducts (AGE), in combination with IFN- γ and LPS profoundly induces the secretion of IL-6 from murine microglia and to a far greater extent than any of the stimuli alone (Gasic-Milenkovic *et al.*, 2003).

Like most cytokines, IL-6 dysregulation and overexpression has been implicated in several pathophysiological events (Gadient & Otten, 1997). IL-6 expression is elevated in the CSF of both patients with AD and PD (Blum-Degen *et al.*, 1995). IL-6 has also been shown to have a role in EAE; IL-6-deficient mice are resistant to EAE (Eugster *et al.*, 1998). Because of the dual effects of IL-6 it is

unclear if IL-6 is causative in these neurodegenerative diseases or is merely a reflection of the ongoing chronic inflammation as a result of progressive neuronal damage (Gadient & Otten, 1997).

1.2.6.3. *IL-1 β*

IL-1 β was first described in the 1980s by several laboratories working on inflammation. It has been described as a key mediator of immune responses and has been found to affect most cell types within the body resulting in inflammation (O'Neill, 2008). IL-1 β belongs to the family of IL-1 which includes IL-1 α . It binds to its receptor IL-1 type I receptor (IL-1R1) expressed on an array of cells, resulting in the release of other pro-inflammatory cytokines including IL-6 and TNF α (Mills & Dunne, 2009). IL-1 β is formed as pro-IL-1 β and then cleaved by caspase-1 to produce the activated form of IL-1 β (Mills & Dunne, 2009). IL-1 β is produced by neuronal and glial cells and is released after their stimulation due to injury, insult or stress (Murray & Lynch, 1998). IL-1 β can trigger neuronal cell death and, interestingly, the presence of glial cells is required for IL-1 β -induced neuronal cell death (Thornton *et al.*, 2006). Specifically Thornton and colleagues (2006) observed that astrocytes were the primary mediators of IL-1 β -induced neuronal death through the release of free radicals and this effect was blocked by IL-1RA the endogenous antagonist for the IL-1R1. IL-1 β concentrations are increased in both aged and stressed animals as well as animals treated with IL-1 β itself (Murray & Lynch, 1998). In addition, an age-related increase in IL-1 β expression and concentration is associated with an age-related increase in caspase-1 activity (Lynch *et al.*, 2007). Furthermore, IL-1 β expression is increased in the response to LPS and is significantly exacerbated in aged animals in response to LPS (Henry *et al.*, 2009).

There is evidence implicating IL-1 β in neurodegenerative diseases; microglia expressing IL-1 are found in association with plaques in brain tissue and this expression correlates with neuronal death (Mrak, 2012). IL-1 β is increased in the hippocampus of wildtype mice (Zaheer *et al.*, 2008), and in murine microglial cultures, following A β stimulation (Szczepanik *et al.*, 2001). Studies in IL-1R1-deficient mice suggest a role for IL-1 in mediating neurodegenerative autoimmune diseases; it has been shown that IL-1 β in combination with IL-23 promotes Th17

cell expansion, a T cell subtype involved in MS, and the secretion of IL-17 (Sutton *et al.*, 2006).

1.2.7. Chemokines

The infiltration of leukocytes from the periphery into the CNS is crucial for host defense responses as well as the initiation and maintenance of CNS autoimmunity (Aloisi, 2001). Chemokines are 8-14 kDa plurifunctional secreted proteins that are instrumental in this process of leukocyte trafficking (Cartier *et al.*, 2005). Currently there are more than 40 known human chemokines and 19 known G-protein coupled chemokine receptors. Chemokines are divided into 4 subfamilies (CXC, CC, C and CX3C) based on the sequence of their conserved cysteine residue but are also classified into inflammatory or homeostatic according to their function (Aloisi, 2001; Cartier *et al.*, 2005). Inflammatory chemokines are produced in response to cytokines and recruit monocytes, granulocytes and T cells to sites of inflammation. Homeostatic chemokines are expressed in discrete environments and recruit cells of the adaptive immune system (Cartier *et al.*, 2005). During CNS inflammation, several cell types are known to produce chemokines including endothelial cells, astrocytes and microglia (Aloisi, 2001). Chemokines play an important role in the development of CNS pathologies; chemokines and chemokine receptor expression upregulated in neurodegenerative diseases allowing for increased leukocyte infiltration and enhanced inflammation (Cartier *et al.*, 2005). Our knowledge of chemokine production by microglia and astrocytes has been greatly facilitated by studies in MS and EAE (Owens *et al.*, 2005). These studies have established that different chemokines may have diverse roles in disease mechanisms (Tran *et al.*, 2000a). However it must be noted that chemokines also have neuroprotective effects, such as fractalkine which inhibits microglial activation (Biber *et al.*, 2007).

1.2.7.1. IP-10

IP-10, also known as CXCL10, is secreted during inflammation by cells such as monocytes, lymphocytes, neutrophils and endothelial cells (Xia *et al.*, 2000). IP-10 binds to its G coupled receptor, CXCR3, expressed on activated T

cells. Several stimuli increase its expression; IP-10 mRNA expression is upregulated in response to IFN- γ (Xia *et al.*, 2000). Furthermore, A β treatment significantly increases the expression of IP-10 hippocampal concentrations in rodents (Clarke *et al.*, 2007). IP-10 plays a significant role in the recruitment of T cells to sites of inflammation and IP-10 expression correlates with T cell infiltration into diseased tissue (Dufour *et al.*, 2002). It has been shown that IP-10^{-/-} mice, infected with hepatitis virus, have decreased cell infiltration into the CNS associated with decreased IFN- γ expression and levels of demyelination (Dufour *et al.*, 2002).

Studies have suggested a significant role for IP-10 in neurodegenerative diseases (Cartier *et al.*, 2005). Xia and colleagues (2000) observed an increase in IP-10-positive astrocytes in post-mortem tissue from AD patients and a frequent association of these IP-10-positive astrocytes with A β deposits. In MS, IP-10 is significantly elevated in the CSF of MS patients (Sorensen *et al.*, 1999), as well as in the CNS of animal undergoing MOG-induced EAE (Tran *et al.*, 2000a).

1.2.7.2. MCP-1

MCP-1, also known as CCL2, recruits monocytes, memory T cells and dendritic cells to the site of injury. It binds to its receptor, CCR2, which is expressed on active monocytes, endothelial cells and leukocytes. MCP-1 was one of the first chemokines to be identified and associated with inflammation (Mahad *et al.*, 2006). Studies have implicated MCP-1 not only in leukocyte recruitment but also in BBB disruption; MCP-1 binding to its receptor expressed on endothelial cells, alters endothelial tight junction structure, resulting in increased BBB permeability following ischemic inflammation (Dimitrijevic *et al.*, 2006). Microglia and astrocytes are prominent sources of MCP-1; glial cells produce MCP-1 following axonal injury and this is associated with the infiltration of leukocytes into the CNS (Babcock *et al.*, 2003). Several different stimuli have been shown to increase MCP-1 expression. MCP-1 expression is increased in progenitor-derived astrocytes and neurons in response to the pro-inflammatory cytokines IFN- γ and TNF α (Lawrence *et al.*, 2006). In addition MCP-1 has been shown to be increased in rodent hippocampal tissue following intracerebroventricular injection of A β (Clarke *et al.*, 2007). Furthermore, it has

been shown that A β can upregulate the expression of MCP-1 receptor on endothelial cells and trigger T cell infiltration (Li *et al.*, 2009).

Evidence suggests that MCP-1 has a role in neurodegenerative diseases. Acute and active MS lesions display MCP-1 and MCP-2 immunoreactivity in post-mortem tissue from MS patients (McManus *et al.*, 1998), and MCP-1 is observed in the CNS of MOG-induced EAE (Tran *et al.*, 2000a). MCP-1 has been reported in mature senile plaques (Ishizuka *et al.*, 1997), and in CSF samples from AD patients (Galimberti *et al.*, 2003).

1.2.7.3. RANTES and MIP-1 α

RANTES, also known as CCL5, is involved in the recruitment of granulocytes, monocytes and effector T cells to sites of inflammation (Cartier *et al.*, 2005). Its receptor, CCR5, also acts as a receptor for MIP-1 α , and is expressed by activated/memory T cells and upregulated in inflammatory conditions; T cells expression of CCR5 is increased in rheumatoid synovial fluid (Qin *et al.*, 1998). Both astrocytes and microglia produce RANTES following LCMV infection (Zhou *et al.*, 2008). The expression of RANTES is increased following entorhinodentate axotomy (Babcock *et al.*, 2003), as well as traumatic brain injury (Ghirnikar *et al.*, 1998).

Like MCP-1 and IP-10, both RANTES and MIP-1 α are associated with neurodegenerative diseases. RANTES is increased in the CSF of MS patients (Tran *et al.*, 2000a), and its receptor has been detected on lymphocytic cells, macrophages and microglia in actively demyelinating MS lesions (Sorensen *et al.*, 1999). CCR5 expression is increased on reactive microglia in AD and this is associated with an increase in MIP-1 α expression on reactive astrocytes which are found in association with A β deposits (Cartier *et al.*, 2005). Furthermore microglia isolated from AD brain tissue treated with A β increase the production of MIP-1 α (Lue *et al.*, 2001a).

1.2.8. Modulators of microglial activation: Maintaining microglial quiescence

Many different factors, including secreted factors and cell surface receptors, play a role in modulating the inflammatory and activated states of

microglia. There is extensive literature reviewing the role that neurons play in delivering “on” and “off” signals to microglia. For example CD200, fractalkine, CD47 and high mobility group box 1 (HMGB1) expressed on healthy neurons antagonise the pro-inflammatory activity of microglia, while damaged or dying neurons are thought to produce chemokines that activate microglia (Biber *et al.*, 2007).

1.2.8.1. *Fractalkine*

Fractalkine, also known as CX3CL1, is a chemokine which is expressed on neurons and its receptor, CX3CR, which is expressed mainly on microglia (Lynch, 2009). Fractalkine can exist as a membrane-bound and soluble form. The membrane bound form displays adhesion properties while, the soluble form is involved in chemotaxis (Gemma *et al.*, 2010). It has been shown that both the soluble and the membrane form of fractalkine can attenuate LPS-induced microglial activation (Lyons *et al.*, 2009a). These authors also demonstrated an age-related decrease in fractalkine expression correlated with an upregulation in CD40 and MHC class II expression and the production of IL-1 β . Gemma and colleagues (2010) proposed that decreased fractalkine with ageing results in increased microglial activation and cognitive dysfunction. These authors found that administering soluble fractalkine to 22 month-old rats resulted in decreased MHC class II expression and increased neurogenesis in these animals. Interestingly a decrease in plasma levels of fractalkine has been observed in patients with AD (Kim *et al.*, 2008), and APP transgenic mice display decreased expression of neuronal fractalkine (Duan *et al.*, 2008).

1.2.9. CD200

1.2.9.1. *CD200 and CD200R*

CD200, previously known as OX2, is a 41-47 kDa type-1 cell surface glycoprotein with two immunoglobulin domains and looks like the TCR β sheet chain or an Ig light chain with a membrane integration segment (Clark *et al.*, 1985). CD200 is unable to signal due to its short cytoplasmic tail and the absence

of any known signalling motifs (Mukhopadhyay *et al.*, 2010). The structure of CD200 is closely related to the T cell co-stimulatory molecules CD80 and CD86 (Jenmalm *et al.*, 2006). CD200 is widely expressed within the CNS including on neurons, endothelial cells, activated T cells (Broderick *et al.*, 2002; Jenmalm *et al.*, 2006) and astrocytes (Costello *et al.*, 2011). CD200 interacts with CD200R expressed on cells of the myeloid lineage such as microglia and macrophages (Meuth *et al.*, 2008). The structure of CD200R is similar to that of CD200 but it contains a larger cytoplasmic tail for signalling (Wright *et al.*, 2000). Currently five CD200Rs have been reported in mice (CD200R1-5) (Gorzynski *et al.*, 2004). The CD200-CD200R interaction is believed to protect the CNS from excessive inflammation by exerting an inhibitory signal suppressing IFN- γ -induced proliferation, activation and secretion of NO, IL-6 and IL-13 by cells (Feuer, 2007; Meuth *et al.*, 2008). Furthermore, it has been demonstrated that disruption of this interaction between CD200-CD200R results in increased microglial activation and neuroinflammation (Masocha, 2009).

1.2.9.2. CD200 signalling

CD200R signalling differs from that of most immune inhibitory receptors, in that it lacks the cytoplasmic acid sequence termed immunoreceptor tyrosine-based inhibitory motif (ITIM), and contains an NPxY sequence in its cytoplasmic domain instead (Zhang *et al.*, 2004). The CD200 signalling pathway has not yet been fully elucidated, although it is proposed that the NPxY motifs interact with adaptor molecules through their phosphotyrosine-binding (PTB) domains. The NPxY motif contains three tyrosine residues as potential phosphorylation sites following CD200-CD200R engagement (Snelgrove *et al.*, 2008). Once phosphorylated adaptor molecules downstream of tyrosine kinase (Dok) 1 and Dok 2, are recruited and in turn are phosphorylated and associate with Ras GTPase-activating protein (RasGAP) and src homology 2 domain containing phosphatases (SHIP) (Snelgrove *et al.*, 2008). Dok2 primarily recruits RasGAP and non-catalytic region of tyrosine kinase adaptor protein 1 (Nck) while, Dok1 preferentially recruits Crk-like protein (CrkL) (Mihirshahi & Brown, 2010). The downstream signalling events result in the inhibition of the Ras/MAPK pathway including extracellular signal-regulated kinase (ERK), p38 MAPK and JNK

(Zhang *et al.*, 2004). Ultimately this inhibition of signalling cascades results in the decrease in the production of inflammatory cytokines. Figure 1.4 illustrates the structure of CD200 and its receptor and the signalling cascade initiated following CD200-CD200R interaction.

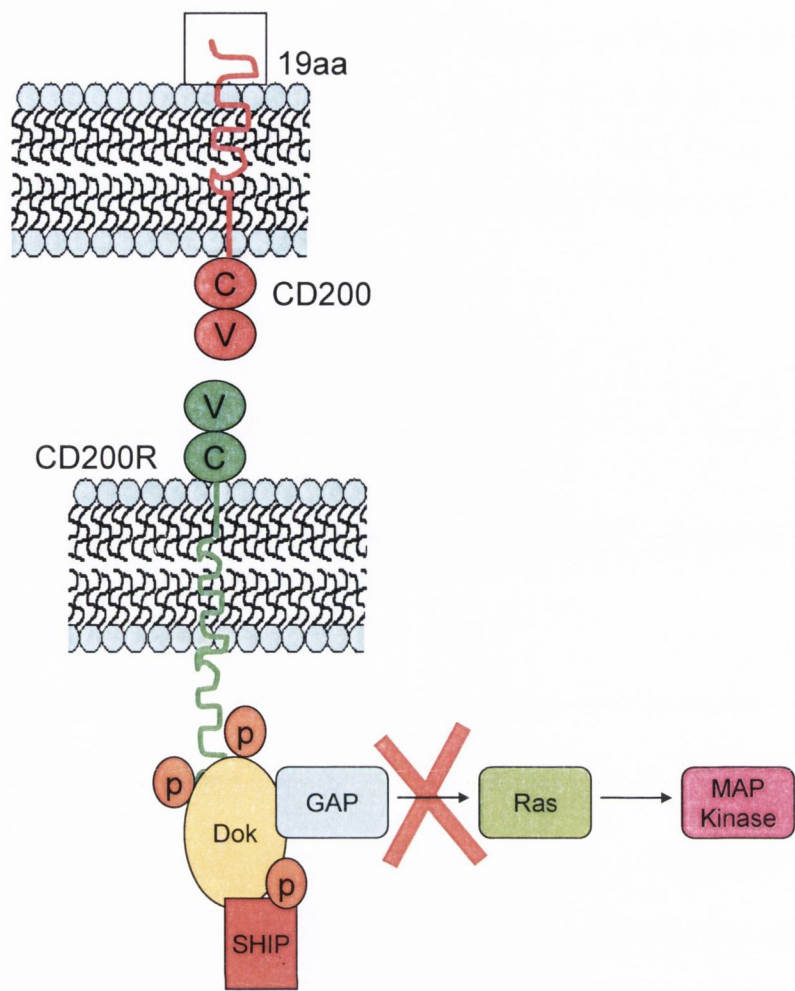


Figure 1.4. The structure of CD200 and CD200R and the signalling pathway initiated following CD200-CD200R interaction.

CD200 has a short cytoplasmic tail while the CD200R has a longer cytoplasmic tail which contains 3 tyrosine residues which when phosphorylated recruit Dok 1 and Dok 2, in turn these activate SHIP and RasGAP resulting in the inhibition of MAP kinases and inhibition of cytokine production.

Adapted from Miller *et al.*, (2011)

1.2.9.3. CD200-CD200R interaction modulates inflammation

The hypothesis that CD200 binding CD200R induces immune suppression was originally proposed by Hoek and colleagues (2000). Most of the studies which have evaluated the role of CD200 have come from the deletion of the CD200 gene in mice. These CD200^{-/-} mice have a normal lifespan and are grossly normal in appearance but are more susceptible to autoimmune diseases (Hoek *et al.*, 2000). Some of the earliest studies demonstrated that microglia obtained from CD200^{-/-} mice have increased activity compared to microglia obtained from healthy wildtype animals. Hoek and colleagues (2000) used several different models, including facial nerve transection model, EAE and collagen-induced arthritis (CIA), to examine the effect of CD200 on disease progression; the data showed that CD200^{-/-} mice had enhanced microglial responses and activation levels compared with wildtype animals. It was hypothesized that the increase in myeloid activation in CD200^{-/-} animals was due to the lack of inhibitory signalling through CD200R (Hoek *et al.*, 2000).

It has been established that *in vivo* disruption of the CD200-CD200R interaction aggravated the clinical course and outcome of EAE in rats (Meuth *et al.*, 2008). These authors reported that neutralizing the CD200-CD200R interaction significantly amplify IFN- γ -induced IL-6 response by macrophages. Furthermore it was observed that disruption of the CD200-CD200R interaction was accompanied by a significant increase in infiltrating immune cells into the spinal cord of MOG-induced EAE animals (Meuth *et al.*, 2008). While studies in Wld^S mice, which exhibit unique protection against neurodegenerative conditions like EAE, have been shown to overexpress CD200 possibly due to impaired protein ubiquitination and degradation (Chitnis *et al.*, 2007). Chitnis and colleagues (2007) observed that increased CD200 expression was able to protect neurons and axon, both *in vitro* and *in vivo*, from microglia-induced damage.

The importance of the CD200-CD200R interaction in maintaining microglial quiescence has also been confirmed by the use of CD200R antibodies and by CD200 fusion protein (CD200Fc). It was established that a rat anti-mouse CD200R monoclonal antibody (DX109), which activated CD200 signalling, suppressed experimental autoimmune uveoretinitis (EAU) progression while, CD200^{-/-} mice displayed early onset EAU (Copland *et al.*, 2007). These results

were in consensus with an earlier report from Broderick and colleagues (2002) who reported that CD200^{-/-} mice had accelerated onset of EAU associated with increased microglial activation, and increased number of infiltrating cells resulting in photoreceptor death. Similarly in CIA it was found that CD200Fc not only suppressed CIA but also caused decreased levels of TNF α and IFN- γ both of which drive myeloid cell activation and CIA disease progression (Gorczyński *et al.*, 2002a). More recent evidence, using an influenza model, highlighted the use of CD200Fc and an agonist antibody to CD200R as a method of resolving inflammation in cases of extensive inflammation and myeloid activation (Snelgrove *et al.*, 2008). These authors reported that a nonlethal dose of the influenza virus delivered to CD200^{-/-} mice resulted in death. Delivery of CD200Fc or OX110, an agonist monoclonal antibody to CD200R, to mice following influenza infection did not compromise viral clearance but decreased the expression of IFN- γ and TNF α in the airways and lung tissue of these animals (Snelgrove *et al.*, 2008).

From the evidence published to date it is clear that the CD200-CD200R interaction indeed plays a key role in immunoregulation. The presence of CD200 in immune-privileged sites and sites accessible to antigen challenge indicates that the CD200-CD200R interaction is involved in anti-inflammatory responses at these specific sites (Minas & Liversidge, 2006).

1.2.9.4. The role of CD200 in neurodegeneration

Several lines of evidence now suggest that the loss of CD200 may contribute to some of the microglial-induced inflammatory changes seen in neurodegenerative diseases like MS and AD. Most neurodegenerative diseases are characterized by an uncontrolled neuroinflammatory environment which has been attributed largely to microglial activation. The majority of these neurodegenerative disorders, but not all, are age-related diseases and evidence suggests that CD200 expression is decreased with age; CD200 expression is decreased in the hippocampus of aged rats accompanied by increased expression of MHC class II and IFN- γ (Frank *et al.*, 2006).

A role for CD200 has also been described in AD. Studies have found decreased expression of CD200 and CD200R in post-mortem brain tissue from

AD patients (Walker *et al.*, 2009). Specifically, these authors describe a deficit in neuronal CD200 expression in brain areas affected by AD pathology. Though it is possible that this is due to a decrease in viable neurons as a result of neurodegeneration (Masocha, 2009). Furthermore, microglial activation in the hippocampus of aged and A β -treated rats correlates with a decrease in neuronal CD200 expression (Lyons *et al.*, 2007). These studies reported that CD200-CD200R interaction decreased expression of MHC class II and the accompanied production of pro-inflammatory cytokines by A β -treated glia (Lyons *et al.*, 2007). These authors suggested that the expression of CD200 may be modulated by the anti-inflammatory cytokine IL-4; it was found that IL-4 markedly increases CD200 expression *in vitro* and that IL-4^{-/-} mice have exacerbated microglial activation associated with a decrease in CD200 expression (Lyons *et al.*, 2007).

Studies in post-mortem brain tissue from MS patients have demonstrated that both the expression of CD200 and its receptor could be found in peri-plaque regions of human MS (Meuth *et al.*, 2008). More importantly, it has been found that the expression of both CD200 and CD47, another macrophage modulatory protein, are downregulated in human MS lesions (Koning *et al.*, 2007). Together, these findings have suggested that enhancing the CD200-CD200R interaction may have therapeutic potential in neurodegenerative diseases such as AD and MS.

1.3. AD

AD is a devastating age-dependent neurodegenerative disease that is the most frequent cause of dementia in the ageing population. The majority of AD cases are sporadic with risk factors including head injury, stroke and even diet although about 5% of all AD cases are familial (FAD). FAD cases have a rare autosomal dominant mutation in genes that effect the expression levels of amyloid precursor protein (APP), presenilin (PS) 1 and 2 genes (Wyss-Coray, 2006). AD is characterised by progressive cognitive decline and memory loss associated with dramatic neuronal death and loss of synapses particularly in brain regions critical for learning and memory including the hippocampus, cerebral cortex and basal forebrain (Nagele *et al.*, 2004). The neuropathological hallmarks include neurofibrillary tau tangles, neuritic plaques, reactive gliosis and inflammation (Nagele *et al.*, 2004). Neurofibrillary tau tangles are inclusions within neurons

which consist of hyperphosphorylated tau, a protein associated with microtubules, which assembles into paired helical filaments. Neuritic plaques are composed of a dense core of A β fibrils, dystrophic neurons, microglia and astrocytes (Benveniste *et al.*, 2001; Nagele *et al.*, 2004).

The identification of these features of AD lead to the development of several hypotheses suggesting the mechanisms by which neurodegeneration occurs in AD including the “A β hypothesis”. The “A β hypothesis” suggests that an imbalance between the production and clearance of A β in the brain gives rise to the accumulation and the formation of A β plaques, exacerbated glial activation, prolonged inflammation and neuronal loss which ultimately causes cognitive decline (Karran *et al.*, 2011). The basis of this hypothesis has greatly influenced the research of current AD therapies especially investigating mechanisms which may aid the removal of A β or inhibit its overproduction (Karran *et al.*, 2011).

1.3.1. A β ; processing, production and overproduction

The fact that A β accumulates in the brain before disease onset, and that Down syndrome patients that have tri-chromosome 21, suffer from AD suggests a role for A β as a mediator of AD (Farfara *et al.*, 2008). A β peptides are natural occurring products of metabolism made up of 36-43 amino acids (Querfurth & LaFerla, 2010). A β is a 4kD peptide which maps to chromosome 21 and is highly expressed on neuronal cells (Farfara *et al.*, 2008). It is generated from the type I integral membrane protein, APP. APP is cleaved by α - and β -secretase (also known as BACE1) to generate two C-terminal fragments α APP and β APP which become inserted into the membrane (Sastre *et al.*, 2008). These fragments are cleaved by the γ -secretase complex (consisting of; PS1, nicastrin, anterior pharynx defective 1 (APH-1) and presenilin enhancer 2 (PEN-2)) resulting in the release of two peptides, P3 and A β (Walsh & Selkoe, 2007; Sastre *et al.*, 2008). When β APP is cleaved by γ -secretase at different points, three types of A β namely A β ₁₋₃₈, A β ₁₋₄₀ and A β ₁₋₄₂ are formed (Walsh & Selkoe, 2007). It is the overproduction of all three A β peptides, or a bias towards production of A β ₁₋₄₂, that is implicated in AD (Walsh & Selkoe, 2007).

A β self-aggregates into several coexisting physical forms including oligomers which can form into intermediate assemblies and fibrils, ultimately

forming insoluble fibrils when arranged as β -pleated sheets (Querfurth & LaFerla, 2010). It has been suggested that the assembly state of the A β peptide is central in determining the microglial response induced; A β ₁₋₄₂ oligomers and fibrils are actively taken up by microglia and induce neuronal toxicity while A β ₁₋₄₀ oligomers are not taken up by microglia nor do they induce neuronal toxicity yet they induce cytokine expression by microglia (Parvathy *et al.*, 2009).

Overproduction of A β is attributed to altered activation of the enzymes that process APP and several factors have been shown to be involved in altering these enzymes. BACE1 activity increases with age in both mouse models of AD and non-transgenic mouse models (Fukumoto *et al.*, 2004); knocking out BACE1 in APP transgenic mice reduces A β production (Ohno *et al.*, 2004). Additionally, factors associated with increased microglial activation alter BACE1; TNF α upregulates BACE1 expression in cultured astrocytes and this effect can be blocked by anti-TNF α antibodies (Yamamoto *et al.*, 2007), while oxidative stress alters PS1 and BACE1 activity (Tamagno *et al.*, 2008).

1.3.2. Role of the innate and adaptive immune system in AD

Neuroinflammatory changes are observed in both familial and sporadic cases of AD (McGeer & McGeer, 2003). Persuasive evidence that the inflammatory process plays an important role in AD comes from studies in which patient populations, treated with non-steroidal anti-inflammatory drugs (NSAIDs), have decreased incidence of AD (Bamberger & Landreth, 2001). Furthermore, administration of NSAIDs to transgenic animal models of AD significantly decreases the amount of reactive microglia in association with A β -plaques (Bamberger & Landreth, 2001).

1.3.2.1. Role of Microglia in AD

Although microglia provide the first line of defense in acute situations the function of microglia in the case of chronic situations like AD, is not clear (Streit, 2005). Microglial activation appears to occur in a very early stage of disease even prior to cognitive decline (McGeer & McGeer, 2003). It has been suggested that increased microglial activation, may be accounted for by an age-related decrease

in the neuronal-glial interactions, which maintain microglia in a quiescent state (Biber *et al.*, 2007). One such interaction that may contribute to this is the CD200-CD200R interaction which is altered with age (Lyons *et al.*, 2007) and in AD (Walker *et al.*, 2009).

While activated microglia are found in close proximity to A β -plaques in mouse models of AD (Bornemann *et al.*, 2001) and in the brains of AD patients (McGeer *et al.*, 1993), one of the central paradoxes surrounding the role of microglia in AD is their failure to phagocytose A β deposits (Bamberger & Landreth, 2001). It has been proposed by Streit (2004) that, in the AD brain, microglia are “dysfunctional” rather than activated and this results in decreased plaque removal and increased production of inflammatory mediators. Thus it has been suggested that activating microglia into a phagocytic phenotype may have beneficial effects in plaque clearance; administration of anti-A β antibodies results in decreased plaque load in Tg2576 mice (Wilcock *et al.*, 2004). Similarly following systemic LPS injection, increased microglial phagocytic activation and an associated clearance of diffuse A β , but not that of fibrillar A β , has been observed in Tg2576 mice (Herber *et al.*, 2007). In contrast, decreased microglial and astrocytic activity is associated with decreased plaque number, A β concentration and phosphorylated tau protein in APP transgenic iNOS^{-/-} mice (Nathan *et al.*, 2005).

There is extensive literature describing the effects of A β peptides in modulating glial activation both *in vivo* and *in vitro*; A β induces the production of cytokines, chemokines and the upregulation of APC molecules *in vitro* (Szczepanik *et al.*, 2001; Jana *et al.*, 2008; McQuillan *et al.*, 2010) and *in vivo* (Clarke *et al.*, 2007). The A β -induced effect on glial activation is even greater in the presence of augmenting factors such as LPS and IFN- γ (Gasic-Milenkovic *et al.*, 2003). Despite these studies, the mechanisms by which A β -induces microglial activation are poorly understood. It has been suggested that A β mediates its interaction with microglia through a receptor complex consisting of $\alpha_6\beta_1$ integrin, CD47, CD36 and the scavenger receptor A (Bamberger *et al.*, 2003). However, another mechanism which is receiving recent consideration is the interaction of TLRs with A β . There is a growing body of evidence suggesting that these innate immune receptors, which have significant effects on tailoring glial activation

(Jack *et al.*, 2005), may play a critical role in the pathogenesis of AD (Liu *et al.*, 2012).

1.3.2.2. A role for TLRs in AD

Expression of TLRs and the TLR co-receptor CD14 (Fassbender *et al.*, 2004) is increased in the brains of AD patients (Walter *et al.*, 2007) and in animal models of AD (Letiembre *et al.*, 2009). Furthermore, increased expression of CD14 in areas of the brain which are pathophysiologically relevant to AD has been observed (Liu *et al.*, 2005). The increased expression of TLRs in AD places them as prospective players in neurodegenerative mechanisms and disease progression (Okun *et al.*, 2009). However the role of TLRs in AD is unclear with reports arguing both beneficial and destructive effects through their ability to tailor microglial responses. Several recent reports have observed that TLR2, TLR4 (Udan *et al.*, 2008), and CD14 deficiency significantly reduces A β -induced microglial activation (Reed-Geaghan *et al.*, 2009). Consistently A β_{1-42} mediates pro-inflammatory cytokine production by microglia and increased expression of integrin markers through its interaction with TLR2 and this effect is blocked in TLR2^{-/-} mice (Jana *et al.*, 2008). Liu and colleagues (2012) established that microglia can interact with A β through TLR2/TLR1 heterodimer to induce pro-inflammatory cytokine production and that TLR2 deficiency shifts microglia away from an inflammatory state to a phagocytic phenotype. In addition it has been observed that A β -induced microglial activation via TLR2, TLR4 and CD14 initiates activation of MAP kinases and the induction of phagocytosis, reactive oxygen species (ROS) and NF- κ B (Reed-Geaghan *et al.*, 2009). CD14 deficiency or neutralization of CD14 with antibody significantly decreases A β -induced microglial production of cytokines and nitric oxide (Fassbender *et al.*, 2004). In addition, TLR2-deficient APP/PS1 mice exhibit decreased plaque burden at 6 months of age although they have comparable plaque burden to wildtype animals by 9 months of age (Richard *et al.*, 2008).

In vitro studies suggest that activation of TLR2, TLR4 and TLR9 with respective ligands PGN, LPS and CpG-ODN, increases the removal of A β from cultures (Tahara *et al.*, 2006). These authors also observed increased plaque burden in TLR4 mutant APP/PS1 mice at 14-16 months of age. The current

literature suggests that a better understanding of the interaction of innate immune TLRs with A β in AD may be useful in establishing effective therapeutic strategies.

1.3.2.3. A role for T cells in AD

While peripheral T cells were not traditionally associated with the progression of AD, this view has changed following several observations. T cells are present in the AD brain in a greater number than healthy individuals (Rogers *et al.*, 1988; Togo *et al.*, 2002; Monsonogo *et al.*, 2003), particularly in areas of the brain that are devastated during AD such as the hippocampus and limbic structures (Togo *et al.*, 2002). Furthermore, these studies have established that these T cells are activated and in the process of becoming effector T cells (Togo *et al.*, 2002). However, the role of T cells in disease pathology is still unclear with contradictory reports in the literature suggesting both beneficial and detrimental effects by T cell subtypes (Th1, Th2 and Th17). The possibility that T cell activation is influenced by their interaction with glia, and vice versa, needs to be explored.

A maladaptive role for T cells is mainly attributed to Th1 cells and their signature cytokine, IFN- γ , as well as Th17 cells. Th1 cells interact with microglia and upregulate the expression of antigen presentation machinery, co-stimulatory molecules and adhesion molecules resulting in Th1 cell activation (Aloisi *et al.*, 2000a). Similarly, studies from McQuillan and colleagues (2010) observed that both A β -specific Th1 and Th17 cells increased the expression of MHC class II and co-stimulatory molecules and an associated increase in the release of pro-inflammatory cytokine production. Supernatants from Th1 cells upregulate a similar pattern of antigen presentation molecules on microglia and the secretion of cytokines and chemokines and these effects can be blocked by anti-IFN- γ treatment (Seguin *et al.*, 2003). In addition treatment of microglial cultures with CD40L and IFN- γ increased chemokine secretion (D'Aversa *et al.*, 2002), as well as inhibiting microglial uptake of A β ₁₋₄₂ (Townsend *et al.*, 2005); interestingly the effect of IFN- γ and IL-17 on glial activation is greater in the presence of A β (McQuillan *et al.*, 2010) Furthermore, IFN- γ deficient APP mice have significantly reduced A β deposition in the cortex and hippocampus compared with

controls and this correlated with decreased astrogliosis and microgliosis (Yamamoto *et al.*, 2007).

T cells may have a beneficial effect through enhanced A β clearance and decreased production of glial inflammatory mediators. *In vitro* studies have suggested that Th2 cells and Th2 cell-secreted cytokines fail to induce antigen presentation machinery on microglia (Aloisi *et al.*, 2000a; Seguin *et al.*, 2003) but can enhance microglial uptake of A β ₁₋₄₂ (Townsend *et al.*, 2005). IL-4 has been shown to selectively inhibit the secretion of IL-1 β and IL-6 from microglia stimulated with A β or LPS (Szczepanik *et al.*, 2001). In addition Th2 cells can attenuate Th1 and Th17-induced glial activation (McQuillan *et al.*, 2010). Moreover, APP/PS1 mice which received A β -stimulated T cells exhibit decreased numbers of plaque-associated microglia and decreased cognitive decline, although interestingly this effect was associated with Th2 cells, and not Th1 cells, suggesting that different T cell subsets mediate different functions in AD (Ethell *et al.*, 2006). Cao and colleagues (2009) observed decreased pro-inflammatory cytokine production and plaque-associated microglia in APP/PS1 mice treated with A β -specific Th2 cells.

1.3.3. Transgenic mouse models of AD

Transgenic mouse models that have behavioral and pathological aspects of AD have enabled the generation and testing of therapies for AD (Gelinas *et al.*, 2004). The identification of genes that encode APP, PS1 and PS2 has revolutionized the use of animal models of AD and lead to the generation of several transgenic mouse models. However, these models only exhibit some of the pathological features including A β deposition and progressive memory loss, but they lack neurofibrillary tau tangles and neuronal loss (Ashe, 2001). Although it is possible to generate mouse models with both amyloid plaques and neurofibrillary tangles these animals are not suitable for investigating learning and memory as they become paralyzed (Ashe, 2001). The transgenic models currently used are based on mutations in APP, PS1 and PS2 resulting in a greater production and aggregation of A β peptides. These genes include the “Swedish” mutation which occurs at the β -secretase site and increases the production of A β ₁₋₄₀ and A β ₁₋₄₂ through preferential cleavage of APP by β -secretase rather than α -secretase

(Higgins & Jacobsen, 2003). Mutations in PS1 and PS2, which play a critical role in γ -secretase activity, also results in the overproduction of $A\beta_{1-42}$ (Higgins & Jacobsen, 2003).

The first transgenic model generated displaying neuritic $A\beta$ -plaques was the PDAPP mouse which overexpressed APP containing the V717F mutation. These animals have accelerated production of $A\beta_{1-40}$ and $A\beta_{1-42}$ resulting in plaque deposition, astrogliosis and microgliosis (Games *et al.*, 1995). Several other mouse models with mutations in APP exist including the Tg2576 model which was first examined by Hsiao and colleagues (1996), and is one of the most widely-studied mouse model of AD. The Tg2576 expresses the APP695 isoform with the Swedish mutation under the control of the prion protein promoter (Higgins & Jacobsen, 2003). These mice display increased $A\beta$ production coupled with cognitive impairment in spatial learning tasks (Hsiao *et al.*, 1996). The APP23 developed at Novartis expresses the APP751 isoform with the Swedish mutation under the control of a Thy1 promoter (Higgins & Jacobsen, 2003). Sturchler-Pierrat and colleagues (1997), reported that these APP23 mice display similar features to both the PDAPP and Tg2576 mouse model, including neuritic plaque deposition, astrogliosis and microgliosis particularly in areas devastated in AD including the hippocampus and neocortex.

Following on from these single transgenic models was the development of double transgenic models. Duff and colleagues (1996) reported that mice overexpressing a mutant PS1 gene had accelerated production of $A\beta_{1-42}$. It was found that crossing Tg2576 mice with mice that overexpressed mutant PS1 (PSAPP) had accelerated plaque development and substantial gliosis by 6 months of age, far earlier than the single transgenic mice (Holcomb *et al.*, 1998). A more recent double transgenic mouse model the APP^{swe}/PS1^{dE9}, and the model of choice in this study, is perhaps the model of preference for AD. The APP^{swe}/PS1^{dE9} model is generated by co-injection of plasmid constructs encoding the APP695 isoform and the Swedish mutation with exon-9 deleted into pronuclei. These genes are driven by an independent prion protein promoter (Jankowsky *et al.*, 2001). These mice display enhanced $A\beta_{1-42}$ production and exacerbated plaque burden in the cortex and hippocampus by 6 months of age (Garcia-Alloza *et al.*, 2006). Garcia-Alloza and colleagues (2006) observed increased ratio of insoluble $A\beta_{1-42}/A\beta_{1-40}$ as well as diffuse $A\beta$ deposition around

compact A β -plaques contributing to the increased size of plaques in mice by 8 months of age. Behavioral testing of these mice indicates significant deficits in spatial memory as assessed by the water maze (Cao *et al.*, 2007).

1.4. Study aims

The aims of this study were:

- To investigate the modulation of glial activation by CD200-CD200R interaction following TLR stimulation *in vitro* and *in vivo*.
- To investigate if A β -induced glial activation could be modulated by TLR2.
- To investigate the interaction between T cells and glia *in vitro* and establish if specific T cell subtypes could modulate glial activation.
- To investigate the role of T cells in modulating microglial activation in a mouse model of AD.

Chapter 2
Methods

Chapter 2

2.1. Preparation, treatment and harvesting of primary glia

2.1.1. Preparation of primary mixed glia

Primary glial cells were prepared from 1-day-old wildtype (C57BL/6) and CD200^{-/-} mice (Bioresource Unit, Trinity College, Dublin 2, Ireland). Neonates were sacrificed by decapitation and the brains were removed into a sterile petri-dish (Fisher Scientific, UK). The tissue was bi-directionally chopped using a sterile scalpel (Swann-Morton, UK) and transferred to 15 ml falcon tubes (Fisher Scientific, UK) containing warm Dulbecco's Modified Eagle Medium (DMEM; 2 ml; Gibco, UK) containing penicillin (100 µg/ml; Gibco, UK) and fetal bovine serum (FBS; 10 % w/v; Gibco, UK). The tissue was incubated for 5 minutes in 5 % CO₂ at 37 °C in a Nuaire Flow CO₂ incubator (Jencons, UK). Using sterile Pasteur pipettes the tissue was filtered through 50 µl sterile nylon mesh filters (BD Bioscience, USA) into 50 ml falcon tubes (Fisher Scientific, UK). The tubes were centrifuged at 1200 x g for 5 minutes at 20 °C, the supernatant was discarded, and the remaining pellet reconstituted in warm DMEM (6 ml). The resuspended glia were plated in 6-well plates (Fisher Scientific, UK) and incubated for 12-14 days in 5 % CO₂ at 37 °C. DMEM was replaced with fresh media every 2-3 days until the glia were ready for treatment.

2.1.2. Preparation of primary astrocytes and microglia

Primary glial cultures were prepared from 1-day-old wildtype mice as per section 2.1.1 with the exception that the mixed glia were maintained in T25 flasks (Fisher Scientific, UK). After 12 days glia were separated by shaking at 110 rpm for 2 hours at room temperature (RT). Supernatants were removed to 50 ml falcon tubes and centrifuged at 1200 x g for 5 minutes at 20 °C. The supernatant was discarded and the remaining pellet was reconstituted in warm DMEM (1 ml) and viable microglial cells were counted using trypan blue (Sigma-Aldrich, UK). Microglia were plated in 24-well plates (1 x 10⁵ cells/well; Fisher Scientific, UK) and incubated for 24 hours in 5 % CO₂ at 37 °C before co-culture with specific T

cells. Astrocytes were harvested by trypsinization (0.25% trypsin, 0.02% ethylenediaminetetraacetic acid EDTA; Invitrogen, UK) for 5 minutes. DMEM was then added to the flasks and supernatants were removed to 50 ml falcon tubes and centrifuged at 1200 x g for 5 minutes at 20 °C. Viable astrocytes were counted and plated in 6-well plates (3×10^5 cells/well) and incubated for 24 hours in 5 % CO₂ at 37 °C prior to co-culture with specific T cells.

2.1.3. Treatment of mixed glia

After 14 days in culture cells prepared from wildtype and CD200^{-/-} mice were treated. DMEM was removed from each well and replaced with fresh pre-warmed DMEM (1 ml) before treatment. Each plate was divided into control or treatment groups; controls received DMEM only. Cells were treated with Pam₃Csk₄ (100 ng/ml; Invivogen, France) for 24 hours prior to harvest.

Cells prepared from wildtype mice for the anti-TLR2 study were prepared for treatment as above. Cells were pre-treated with anti-TLR2 (2.5 µg/ml; Hycult Biotech, Netherlands) for 2 hours prior to treatment with Aβ_{1-40/1-42} cocktail (10 µM; Invitrogen, US) for 24 hours. After 24 hours the cells were harvested.

2.1.4. Harvesting of mixed glia

Plates were removed from the incubator one at a time and placed on ice for the duration of the harvest. Supernatants were removed through aspiration and stored in 1.5 ml tubes (Sarstedt, Germany) at -80 °C for cytokine analysis. Each well was washed with ice-cold phosphate-buffered saline (PBS; Sigma-Aldrich, UK) and harvested for gene or protein analysis. RA1 buffer (Macherey-Nagel, Germany) containing β-mercaptoethanol (1:100; Sigma-Aldrich, UK) was added to each well (353.5 µl/well), cells were scraped and the buffer removed and stored in sterile RNase free tubes at -80 °C until required for gene analysis. For protein analysis, cells were harvested for fluorescent activated cell sorter (FACS) analysis. Cells were trypsinised (150 µl/well) for 5 minutes, FACS buffer (800 µl/well; PBS/FBS 2 %) was added, and cells were immediately transferred to FACS tubes (BD Biosciences, UK) for cell marker expression analysis.

2.2. Cell counts

Cell counts were performed by diluting cells (1:10) in Ethidium Bromide Acridine Orange (EBAO) or trypan blue. The cell suspension (10 μ l) was loaded into a disposable haemocytometer (Hycor Biomedical, UK). Viable cells which stained green (EBAO method) or did not stain (trypan blue method) were counted under a fluorescent microscope (EBAO method) or light microscope (trypan blue method).

2.3. Amyloid-beta ($A\beta$)

2.3.1. Preparation of $A\beta_{1-42}$ and $A\beta_{1-40}$

$A\beta_{1-42/40}$ (Invitrogen, US) was dissolved in high-performance liquid chromatography-grade water and sterile PBS to generate a 1 mg/ml stock solution. $A\beta_{1-42}$ was allowed to aggregate for 48 hours at 37 °C and $A\beta_{1-40}$ was allowed to aggregate for 48 hours at RT. $A\beta$ was used immediately or stored at -20 °C until required.

2.3.2. Testing of $A\beta$ aggregation by thioflavin T assay

The presence of fibrillar $A\beta$ was assessed using a thioflavin T assay (ThT, Sigma-Aldrich, UK). ThT stock (2 mM) was diluted (1:20) to give a working concentration (100 μ M). Aliquots of PBS, freshly-reconstituted $A\beta$ and aggregated $A\beta$ were thawed on ice and samples (5 μ l) were added in triplicate to a black ELISA plate (Labsystems, Finland). Glycine (185 μ l; 50 mM; Sigma-Aldrich, UK) and ThT solution (10 μ l) was added to each well and the plates were read immediately at 435-485 nm using a 96-well plate reader (Biotek, Mason Technology, Ireland). Aggregation of $A\beta$ was measured by an increase in fluorescence intensity.

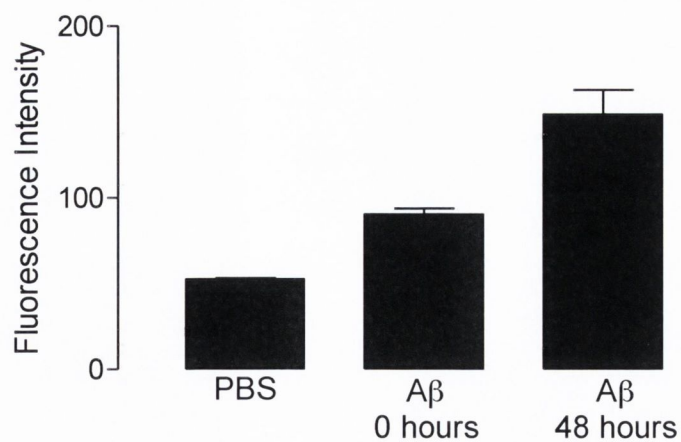


Figure 2.1. Measurement of A β aggregation by thioflavin T assay.

A β was aggregated as described in section 2.3.1 and aggregation was measured as described in section 2.3.2, and the aggregation was expressed as units of fluorescence intensity.

2.4. Animals

Specific pathogen free C57BL/6 mice were obtained from Harlan UK Ltd., Bicester, UK and CD200^{-/-} mice were gifted from Jonathan D Sedgwick. APP/PS1 mice were obtained from the Jackson Laboratory, Maine, US, and subsequently bred in a specific pathogen free units. All animals were housed and maintained under the required guidelines of the Irish Department of Health including veterinary supervision, light and temperature control (12 hour light-dark cycle and 22–23 °C); food and water were available *ad libitum*. All experiments on animals were performed under a license granted by the Minister for Health and Children (Ireland) under the Cruelty to Animals Act 1876.

2.5. Treatment of animals for Pam₃Csk₄ study

Male and female wildtype and CD200^{-/-} mice (2-3 months old) were randomly assigned to control or treatment groups (n=8). Mice were injected intraperitoneally (i.p) with either saline or Pam₃Csk₄ (100 µg/100 µl). Animals were sacrificed 5 hours post treatment and tissue was harvested for analysis.

2.6. Genotyping of APP/PS1 mice

2.6.1. Isolation of genomic DNA

Tail snips were taken from APP/PS1 and littermate control mice and stored at -20 °C until required. All solutions and reagents used to isolate genomic DNA were from a DNeasy[®] blood and tissue kit (Qiagen, US). The buffers AW1, AW2 and AL were prepared by the addition of ethanol (96-100 %) and brought to RT prior to use. Tail snips (0.5 cm) were placed in 1.5 ml microcentrifuge tubes and brought to RT. Buffer ATL (180 µl) and Proteinase K (20 µl) were added and the tubes were incubated overnight at 56 °C. Tubes were vortexed for approximately 15 seconds and buffer AL (200 µl) was added. Tubes were vortexed and ethanol (200 µl, 96-100 %) was added to the tubes. The mixture was transferred to DNeasy Mini spin columns in 2 ml collection tubes. Tubes were centrifuged at 8,000 rpm for 1 minute at RT. The flow-through was discarded and the column

placed in a new 2 ml collection tube. Buffer AW1 (500 μ l) was added and tubes were centrifuged at 8,000 rpm for 1 minute at RT. The column was placed in a new 2 ml collection tube and buffer AW2 (500 μ l) was added and tubes were centrifuged at 14,000 rpm for 3 minutes at RT to dry the membrane. The column was placed in a fresh 1.5 ml microcentrifuge tube and buffer AE (200 μ l) was added and incubated for 1 minute at RT. Tubes were centrifuged at 8,000 rpm for 1 minute at RT to elute the DNA and stored at 4 °C overnight to ensure that the DNA was completely solubilised. DNA concentrations were quantified using a NanoDrop Spectrophotometer (ND-1000 v3.5, NanoDrop Technologies Inc., US).

2.6.2. Polymerase chain reaction (PCR) for APPswe and PS1dE9 genes

The presence of APPswe and PS1dE9 mutations were assessed using PCR. Mastermix was prepared by addition of DNase-free water, GoTaq[®] qPCR mastermix (Promega, US) and sense and antisense primers (100 μ M, MWG Biotech, Germany) to a sterile tube. The mastermix for the PS1dE9 gene also contained sense and anti-sense primers for the PrP genes as an internal control. DNA and mastermix were added to fresh tubes, which were then placed in a thermocycler (MJ Research Peltier Thermal Cycler-200, Biosciences, Ireland). The amplification process consisted of an initial denaturing step at 94 °C for 30 seconds, an annealing step at 67 °C for 1 minute, and an extension step at 72 °C for 1 minute. After 35 cycles of amplification, a final extension step at 72 °C for 10 minutes was applied to ensure complete extension of PCR products. Equal volumes (10 μ l) of each sample and a 100 base pair ladder (Promega, US) were mixed with loading buffer (2 μ l; Promega, US), and loaded onto a 1 % (w/v) agarose gel containing gel red (1;10,000, Biotium, US). Samples were separated by application of 90 volts for 120 minutes. PCR products were visualised under an ultraviolet light and photographed using an ultraviolet transilluminator (Labworks, Ultra Violet, Bioimaging Systems, US). Table 2.1 summarises the primers used for DNA amplification.

Table 2.1. Primers used for DNA amplification.

Target	Primer sequence	Size (bp)
APPswe forward: APPswe reverse:	5'-AGGACTGACCACTCGACCAG-3' 5'-CGGGGGTCTAGTTCTGCAT-3'	377bp product
PSEN forward: PSEN reverse:	5'-GCCATGAGGGCACTAATCAT-3' 5'-GCCATGAGGGCACTAATCAT-3'	608bp product
Prion forward: Prion reverse:	5'-CTAGGCCACAGAATTGAAAGATCT-3' 5'-GTAGGTGGAAATTCTAGCATCATCC- 3'	324bp product

2.7. T cell study protocols

2.7.1. Generation of T cell lines from APP/PS1 and littermate control mice

2.7.1.1. Preparation of spleen cell culture

APP/PS1 and littermate control mice (12-months-old) were sacrificed by cervical dislocation and spleens were harvested to 50 ml falcon tubes containing x-vivo media (2 ml; Lonza, Belgium) containing penicillin (100 µg/ml), L-glutamine (100 mM; Gibco, UK) and β-mercaptoethanol (2 µl). Spleens were homogenized and passed through 40 µm sterile nylon mesh filters to obtain a single cell suspension. Cells were centrifuged at 1,200 rpm for 5 minutes and resuspended in x-vivo media (2 ml). The cell suspension was divided into two 50 ml falcon tubes allowing for the generation of non-specific T cells and Aβ-specific T cells from each spleen. For the generation of specific T cells, x-vivo media (9 ml) was added and cells were counted as per section 2.2. Cells were centrifuged at 1,200 rpm for 5 minutes and supernatants removed. CD4⁺ T cells were isolated using a magnetic activated cell sorter (MACS) column (Miltenyi Biotec, UK) and a CD4⁺ T cell isolation kit (Miltenyi Biotec, UK). Cells were resuspended in MACS buffer (40 µl/per 10⁷ cells; PBS containing 0.5 % bovine serum albumin (BSA) and 2 mM EDTA; Sigma-Aldrich, UK) and incubated in antibody cocktail (10 µl/per 10⁷ cells; Miltenyi Biotec, UK) for 10 minutes at 4 °C. Cells were flooded with MACS buffer (30 µl/per 10⁷ cells) and incubated with anti-biotin microbeads (20 µl/per 10⁷ cells; Miltenyi Biotec, UK) for 15 minutes at 4 °C. Cells were flooded in MACS buffer (20 x volume of antibody added), centrifuged at 1,200 rpm for 5 minutes and resuspended in MACS buffer (500 µl). The MACS column was flooded with MACS buffer (3 ml) and cells were transferred to the MACS column for magnetic sorting. T cells were centrifuged at 1,200 rpm for 5 minutes and resuspended in x-vivo media (2 ml). Cells were counted and plated in 24-well plates (200 µl/well, 2 x 10⁶ cells/ml).

For the generation of T cells that would later be stimulated into Aβ-specific T cell lines, red blood cells were lysed by the addition of ammonium chloride solution (1 ml; 0.87 %) for 2-3 minutes at RT. Cells were flooded with x-vivo media (30 ml) and centrifuged at 1,200 rpm for 5 minutes. Supernatants were

removed and the cell pellet was resuspended in x-vivo media (10 ml). Cells were counted and plated in 24-well plates (250 μ l/well, 4×10^6 cells/ml).

2.7.1.2. Generation of non-specific Th1, Th2 and Th17 cell lines

T cell lines were cultured for 5 days at 37 °C in a humidified 5 % CO₂ environment. All T cell lines were developed in the presence of anti cluster of differentiation 3/28 (α CD3/CD28; 4 μ g/ml, BD Biosciences, US) at the beginning of the culture. Th1 cell lines were developed in the presence of IL-12 (500 ng/ml, R&D Systems), Th2 cell lines in the presence of IL-4 (10 ng/ml, R&D Systems) and anti-IFN- γ (5 μ g/ml, BD Biosciences US) and Th17 cell lines in the presence of IL-1 β (25 ng/ml, R&D Systems), IL-23 (50 ng/ml), anti-IFN- γ (5 μ g/ml) and TGF β (5 ng/ml, R&D Systems). On the 3rd day of the culture media was changed on the T cell lines and cytokines were added in fresh x-vivo media without α CD3/CD28. T cell lines were harvested on the 5th day for co-culture with glia.

2.7.1.3. Generation of A β -specific Th1, Th2 and Th17 cell lines

A β -specific T cell lines were cultured as per section 2.7.1.2 with the exception that A β ₁₋₄₂ (15 μ g/ml) was included in the culture media instead of α CD3/CD28 at the beginning of the culture. On the 3rd day of the culture, media was changed on the T cell lines and cytokines were added without A β ₁₋₄₂. T cell lines were harvested on the 5th day for co-culture with glia.

2.7.2. Co-culture and treatment of specific T cell lines and glia

2.7.2.1. Non-specific T cell co-culture with glia

Supernatants were removed from T cell lines and stored at -20 °C for later cytokine analysis. T cells were transferred from the 24-well plates to 50 ml falcon tubes by pipetting up and down. Tubes were centrifuged at 1,200 rpm for 5 minutes and resuspended in DMEM (500 μ l). Cells were counted and resuspended in DMEM allowing for 1.5×10^5 cells/ml. T cells were cultured at a 1:2 ratio with microglia (300 μ l/well) and astrocytes (1000 μ l/well) for 24 hours at 37 °C in a

humidified 5 % CO₂ environment. Supernatants were removed for cytokine analysis by enzyme linked immunosorbent assay (ELISA) and cells were harvested for flow cytometry.

2.7.2.2. A β -specific T cells co-culture with glia and incubation with A β ₁₋₄₂

Supernatants were removed from A β -specific T cell lines and stored at -20 °C for later cytokine analysis. T cells were removed from the 24-well plates, as per section 2.7.2.1, and resuspended in x-vivo media (2 ml), counted, and CD4⁺ T cells were isolated using a MACS sort column and a CD4⁺ T cell isolation kit as per section 2.7.1.1. Following MACS sort A β -specific T cell lines were re-counted and resuspended in DMEM allowing for 1.5 x 10⁵ cells/ml. A β -specific T cell lines were cultured at a 1:2 ratio with microglia (300 μ l/well) and astrocytes (1000 μ l/well) in the presence of A β ₁₋₄₂ (15 μ g/ml) for 24 hours at 37 °C in a humidified 5 % CO₂ environment. Supernatants were removed for cytokine analysis by ELISA and cells were harvested for flow cytometry. Figure 2.2 summarises the generation of T cell lines from APP/PS1 and littermate control mice and co-culture with microglia and astrocytes.

2.7.3. Generation of Th1 and Th17 cell line from C57BL/6 mice and co-culture with mixed glia

2.7.3.1. Generation of Th1 and Th17 cell lines

C57BL/6 mice (2 month-old) were sacrificed by cervical dislocation and spleens were harvested for generation of T cell lines as per section 2.7.1.1. T cell lines were cultured for 5 days at 37 °C in a humidified 5 % CO₂ environment and generated in the presence of polarising cytokines as per section 2.7.1.2.

2.7.3.2. Co-culture and treatment of Th1 and Th17 cell lines with mixed glia

Supernatants were removed from T cell lines and cells were transferred to 50 ml falcon tubes and centrifuged at 1,200 rpm for 5 minutes. T cell lines were resuspended in DMEM (500 µl), counted and resuspended in the appropriate volume of DMEM allowing for 0.5 x 10⁵ cells/ml. T cells were cultured at a ratio of 1:2 with mixed glia (1x 10⁵ cells/ml). Mixed glia were also treated in the presence or absence of IFN-γ (20 ng/ml; R&D Systems, US) or IL-17 (20 ng/ml; R&D Systems, US). After 1 hour, co-cultures were stimulated with Aβ₁₋₄₂ (10 µM) for 24 hours at 37 °C in a humidified 5 % CO₂ environment. Supernatants were removed for cytokine analysis by ELISA and cells were harvested for flow cytometry. Table 2.2 summarises the co-culture of Th1/Th17 cells with mixed glia and their treatment with either IFN-γ/IL-17 and Aβ₁₋₄₂.

Table 2.2. Co-culture of Th1 and Th17 cells with mixed glia and treatments.

	Mixed glia co-culture with Th1 cells	Mixed glia co-culture with Th17 cells
Treatments	Control (± Aβ)	Control (± Aβ)
	Th1cells (± Aβ)	Th17 cells (±Aβ)
	IFN-γ (± Aβ)	IL-17 (± Aβ)

2.7.4. Generation of T cells for adoptive transfer APP/PS1 *in vivo* study

2.7.4.1. Generation of A β -specific T cell lines

C57BL/6 mice received a footpad immunisation of A β (75 μ g/mouse) and CpG-containing oligodeoxynucleotide (CpG, 25 μ g/mouse; Sigma-Aldrich, UK) into each paw (25 μ l/paw). After 21 days the mice were boosted with A β and CpG. Mice were sacrificed 7 days after the booster injection and the spleens were harvested. The spleens were restimulated *ex vivo* with A β (25 μ g/ml) and an array of cytokines and antibodies depending on the type of T cell line being developed. At the beginning of the culture Th1 cells were incubated with IL-12 (10 ng/ml), Th2 cell lines with dexamethasone (1×10^{-8} M, Sigma-Aldrich, UK), IL-4 (10 ng/ml), and anti-IFN- γ (5 μ g/ml). Th17 cell lines were incubated with IL-1 β (10 ng/ml), IL-23 (10 ng/ml), and anti-IFN- γ . After 4 days of incubation, Th1 and Th2 cell cultures received IL-2 (5 ng/ml R&D Systems), while Th17 cell cultures received Roswell Park memorial institute medium (RPMI; Gibco, US). After a further 7 days of incubation, surviving T cells (1×10^5 cells/ml) were restimulated with irradiated APCs (2×10^6 cells/ml), generated from spleens irradiated at a dose of 30 Gy in an irradiation chamber of a Nordian Gammcell 3000 irradiator, and A β (25 μ g/ml) for 4 days followed by 7 days of incubation with IL-2.

Following generation of A β -specific T cell lines, A β -specific Th1, Th2, and Th17 cells (15×10^6 cells/mouse), cells were washed and injected intravenously (i.v.) (15×10^6 cells/mouse in 300 μ l serum-free medium) into 6-7 month-old APP/PS1 mice. Control animals received 300 μ l serum-free medium alone. After 2 weeks APP/PS1 mice were anaesthetised with sodium pentobarbital (40 μ l; Euthatal, Merial Animal Health, UK) and perfused intracardially with ice-cold PBS (20 ml). The brains were rapidly removed, bisected and snap-frozen for later analysis by multi-spot ELISA and immunohistochemistry

2.7.4.2. Intravenous injection of Th1 cells for anti-IFN- γ study

APP/PS1 and littermate control mice received an i.p. injection of either anti-IFN- γ (600 μ g/mouse) or a control antibody (β -galactosidase: 600 μ g/mouse, R&D Systems, US). Twenty four hours later, Th1 cells (15×10^6 cells/mouse) in

serum-free RPMI were injected (300 μ l) into the lateral tail vein of the mice. Serum-free RPMI was injected into the tail vein of mice from other groups as a control. Anti-IFN- γ or β -galactosidase antibody injections were repeated on days 3, 7, 10, 14, 17, 21, 24, 28 and 31 after T cell transfer, in order to ensure that no IFN- γ was present in these animals. Mice were killed 34 days after T cell transfer by cervical dislocation and tissue was taken for analysis. The procedure described above was carried out by Dr Keith Mc Quillan. The tissue was gifted to me for analysis described hereafter.

2.8. Mononuclear cell isolation from CNS tissue

Animals were anaesthetised with sodium pentobarbital (40 μ l) and perfused intracardially with sterile ice-cold PBS (20 ml). The brain was removed and placed into a 50 ml falcon tube containing Hank's buffered saline solution (2 ml) containing 3 % FBS (HBSS/FBS; Sigma-Aldrich, UK). Tissue was dissociated through a sterile 70 μ m nylon mesh filter, washed with HBSS/FBS and centrifuged at 170 x g for 10 minutes at RT. The supernatant was removed and the remaining pellet resuspended in HBSS/FBS (2 ml) containing collagenase D (1 mg/ml, Roche, Ireland) and DNase I (10 μ g/ml, Sigma-Aldrich, UK), and incubated for 1 hour at 37 °C. Cells were washed in HBSS/FBS and centrifuged at 1,200 rpm for 5 minutes. Supernatants were removed and cells were resuspended in 1.088 g/ml Percoll (9 ml; Sigma-Aldrich, UK). This was underlayered with 1.122 g/ml Percoll (5 ml), and overlaid with 1.072 g/ml Percoll (9 ml) followed by 1.030 g/ml Percoll (9 ml), and finally PBS (9 ml). Percoll gradients were centrifuged at 1,250 x g for 45 minutes at 18 °C. Mononuclear cells were removed from between the 1.088:1.072 and 1.072:1.030 g/ml interfaces and placed in 50 ml falcon tubes. Cells were washed twice in HBSS/FBS and counted to obtain absolute numbers before being transferred to FACS tubes for assessment by flow cytometry. Figure 2.3 illustrates the Percoll separation method and isolation of mononuclear cells.

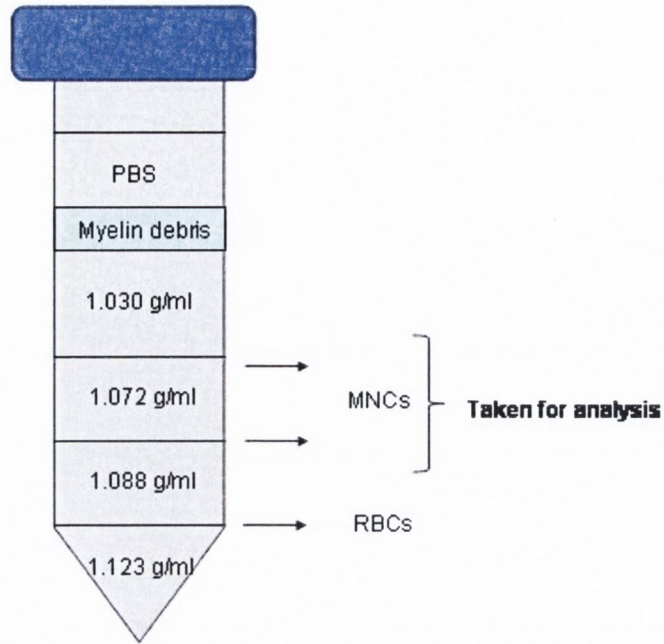


Figure 2.3. Diagram of Percoll separation used to isolate mononuclear cells from the CNS.

Diagram illustrating Percoll separation of cells, Red blood cell and dead cells are found at the 1.123:1.088 g/ml interface. Myelin debris is found at the 1.030 g/ml:PBS interface. Mononuclear cells are found at the 1.088:1.072 and 1.072:1.030 g/ml interfaces.

2.9. Flow cytometry

2.9.1. Flow cytometry of T cells and glia

Expression of cell surface markers was assessed on T cells and glial cells from *in vitro* and *in vivo* studies by flow cytometry using a DAKO CyAN_{ADP} flow cytometer, calibrated using Flow-Check Fluorospheres (Beckman Coulter, Ireland). T cells were removed from glia by pipetting up and down several times and transferred to respective FACS tubes. Mixed glia, microglia and astrocytes were harvested by addition of Trypsin-EDTA (150-300 μ l/well) to the wells, and incubated for 5 minutes. Cells were transferred to respective FACS tubes and centrifuged at 1,200 rpm for 5 minutes and resuspended in FACS buffer (100 μ l). Cells were blocked by incubating with anti-CD16/CD32 Fc γ RIII block (1:100; BD Biosciences, US) for 15 minutes at RT. Cells were incubated with the appropriate FACS antibodies or isotype control antibodies (see Table 2.3 for details) for 30 minutes at RT in the dark. Cells were then washed with FACS buffer to remove excess antibody, centrifuged at 1,200 rpm for 5 minutes between washes, resuspended in FACS buffer (400 μ l) and analysed using Summit software and FlowJo software.

2.9.2. Flow cytometry of mononuclear cells

Mononuclear cells prepared from CNS tissue were prepared for intracellular staining using a cell permeabilisation kit (Dako, Denmark). Cells were centrifuged at 1,200 rpm for 5 minutes before stimulation with *x-vivo* media (200 μ l) containing phorbol myristate acetate (PMA; 10 ng/ml; Sigma-Aldrich, US), Ionomycin (1 μ g/ml; Sigma-Aldrich, US) and brefeldin A (BFA; 5 μ g/ml; Sigma-Aldrich, US) for 4/5 hours. Following stimulation, cells were centrifuged at 1,200 rpm for 5 minutes and resuspended. Low-affinity IgG receptors (Fc γ RIII) were blocked by incubating cells in FACS buffer (50 μ l/sample) containing anti-CD16/CD32 Fc γ RIII (1:100) for 10 minutes at RT. Cells were then incubated in 50 μ l/sample FACS buffer containing the appropriate FACS antibodies (see Table 2.3 for details) for 15 minutes at RT, and fixed in IntraStain Reagent A (50 μ l/sample; Dako, Denmark) for 15 minutes at RT. Cells were washed twice with FACS buffer, centrifuged at 1,200 rpm for 5 minutes, and permeabilised with

IntraStain Reagent B (50 µl/sample; Dako, Denmark) plus intracellular antibodies (see Table 2.3 for details) for 15 minutes at RT in the dark. Cells were washed twice in FACS buffer and centrifuged at 1,200 rpm for 5 minutes. Immunofluorescence analysis was performed using Summit software (Dako, Denmark) and the results analysed using FlowJo software (Tree Star, US).

Table 2.3. Antibodies used in flow cytometry.

Surface Marker	Fluorescent Label	Dilution Factor	Supplier
CD11b	APC/PeCy7	1/100	BD Biosciences
CD3	V500/APC/A780	1/100-200	eBioscience
CD4	FITC/V450/PeCy7	1/100-200	BD Biosciences
CD8	A780	1/50	BD Biosciences
CD40	FITC/PE	1/100	BD Biosciences
MHCII	PE/PeCy5	1/100	BD Biosciences
CD86	PerCPcy5.5/FITC	1/100	BD Biosciences / Biolegend
IFN- γ	PerCPcy5.5/FITC	1/100	BD Biosciences
IL-17	V450/PE	1/100	BD Biosciences
TLR2	FITC	1/100	BD Biosciences
CD45	PeCy7	1/100	BD Biosciences
Live Dead marker	APCcy7	1/500	Biolegend

2.10. Protein quantification

Protein quantification was assessed using the bicinchoninic acid (BCA) assay. Protein standards were prepared from a stock solution of 2000 µg/ml BSA. A range of standards (0 to 2000 µg/ml) was generated by diluting the stock solution in sample buffer. Standards and samples (25 µl) were added to a 96-well plate in triplicate (Sarstedt, Ireland). BCA reagent was added and the samples were incubated at 37 °C for 30 minutes and absorbance assessed at 562 nm using a 96-well plate reader (Biotek, Mason Technology, Ireland). A regression line was plotted (GraphPad Prism, USA) to enable determination of the protein concentration.

2.11. Quantitative Polymerase Chain Reaction (QPCR)

2.11.1. RNA extraction

Messenger RNA (mRNA) was extracted from snap-frozen brain tissue from the *in vivo* studies and from cells from the *in vitro* studies. Tissue from the *in vivo* studies was homogenised in cell lysis mastermix (350 µl; Nucleospin RNA II, Macherey-Nagel, Germany) using a Polytron homogenizer (Kinematica, Switzerland). Cells from *in vitro* studies were harvested in lysis buffer as per section 2.1.4. The lysate from both *in vitro* and *in vivo* studies was filtered through a Nucleospin filter (Macherey-Nagel, Germany), and centrifuged at 11,000 x g for 1 minute. Lysates were mixed with ethanol (350 µl; 70 %) and loaded onto Nucleospin RNA II columns (Macherey-Nagel, Germany). Samples were centrifuged at 8,000 x g for 30 seconds allowing the RNA to bind to the columns. The silica membrane was desalted with membrane desalting buffer (350 µl; Macherey-Nagel, Germany) and centrifuged at 11,000 x g for 1 minute to dry the membrane. DNase reaction mixture (95 µl) was added directly onto the centre of the silica membrane column and incubated for 15 minutes at RT. The silica membrane was washed and dried 3 times. In the first wash, RA2 buffer (200 µl; Macherey-Nagel, Germany) was added to the Nucleospin RNA II column and centrifuged at 8,000 x g for 30 seconds. For the second wash, RA3 buffer (600 µl; Macherey-Nagel, Germany) was added to the Nucleospin RNA II column and

centrifuged at 8,000 x g for 30 seconds. In the final wash, RA3 buffer (250 µl) was added to the Nucleospin RNA II column and centrifuged at 11,000 x g for 2 minutes to dry the membrane completely. The RNA was eluted in nuclease-free water (60 µl; Macherey-Nagel, Germany) and centrifuged at 11,000 x g for 1 minute. The RNA concentration was quantified using a NanoDrop Spectrophotometer.

2.11.2. cDNA synthesis

Extracted mRNA was reverse-transcribed into complementary DNA (cDNA) using the high capacity cDNA reverse transcription kit (Applied Biosystems, Germany). RNA was equalised with nuclease-free water, the sample was vortex-mixed and stored on ice. A 2X mastermix was prepared containing the appropriate volumes of 10X RT buffer, 25X dNTPs, 10X random primers, multiscribe reverse transcriptase (50 U/µl) and nuclease-free water and kept on ice. Mastermix (25-30 µl) was added to equalised RNA samples (25-30 µl) to make a total volume of 50-60 µl. Samples were incubated for 10 minutes at 25 °C followed by 120 minutes at 37 °C on a thermocycler (PTC-200, Peltier Thermal Cycler, MJ Research, Biosciences Ireland). cDNA was stored at -20 °C until analysis.

2.11.3. QPCR

QPCR primers and probes were delivered as “TaqMan® Gene Expression Assays” (see Table 2.4 for details; Applied Biosystems, Germany). Quantitative Real-time PCR was performed on Applied Biosystems ABI Prism 7300 Sequence Detection System v1.3.1 in 96 well format where there was 25 µl reaction volume per well (3 µl cDNA and 22 µl PCR mastermix). The cDNA was mixed with Taqman universal PCR mastermix (Applied Biosystems, Germany) and the respective gene target assay. Mouse β-actin RNA primers (Applied Biosystems, Germany) were added as the reference guide. Each sample was measured in duplicate in a single RT-PCR run. Forty cycles were allowed run under the following conditions: 2 minutes at 50 °C, 10 minutes at 95 °C, and for denaturing 15 seconds at 95 °C and 1 minute at 60 °C for transcription. Analysis of the gene

expression values was carried out using the efficiency-corrected comparative CT method determining target gene expression relative to the β -actin endogenous control expression and relative to a control samples.

Table 2.4. QPCR primers gene expression assay numbers.

Gene name	Gene Description	Taqman Gene expression Assay number
TNF α	Tumour Necrosis Factor alpha	Mm00443258_m1
CD68	Cluster of Differentiation 68	Mm03047340_m1
CD200R	Cluster of Differentiation 200 receptor	Mm00491164_m1
CCL2	Chemokine Ligand 2	Mm00441242_m1
CXCL10	C-X-C motif Chemokine 10	Mm00445235_m1
IFN- γ	Interferon-gamma	Mm00801778_m1
CD11b	Cluster of Differentiation 11b	Mm01271265_m1
ICAM-1	Inter-Cellular-Adhesion-Molecule-1	Mm00516027_g1
IL-4	Interleukin-4	Mm00445259_m1
IL-6	Interleukin-6	Mm00446190_m1
IL-1 β	Interleukin-1 beta	Mm00434228_m1
CD200L	Cluster of Differentiation 200 ligand	Mm00487740_m1
TLR2	Toll-like receptor 2	Mm00442336_m1
TLR1	Toll-like receptor 1	Mm00446095_m1
TLR4	Toll-like receptor 4	Mm00445273_m1
CCL3	Chemokine ligand 3	Mm00441259_g1
CD40	Cluster of Differentiation 40	Mm00441891_m1
CD86	Cluster of Differentiation 86	Mm01344638_m1

2.12. Analysis of cytokine and chemokine expression by ELISA

The concentrations of the cytokines TNF α , IL-1 β , IL-6, IL-17, IFN- γ and chemokines MCP-1, RANTES, MIP-1 α and IP-10 were measured using commercially available ELISA kits (See Table 2.5 for details; R&D Systems, UK). Plates (Nunc-Immuno plate, Thermo Fisher Scientific, UK) were coated with 100 μ l/well of rat anti-mouse TNF α (0.8 μ g/ml), IL-1 β (4 μ g/ml), IL-6 (2 μ g/ml), IL-17 (2 μ g/ml), IFN- γ (4 μ g/ml), MCP-1 (0.2 μ g/ml), RANTES (2 μ g/ml), MIP-1 α (0.4 μ g/ml) and IP-10 (2 μ g/ml) capture antibody in PBS, and incubated at 4 $^{\circ}$ C overnight. Plates were washed several times with PBS containing 0.05 % Tween-20 (PBS-T), blocked for a minimum of 1 hour at RT with diluent (200 μ l/well; 0.1 M PBS, pH 7.3, with 1 % BSA), and washed several times with PBS-T. Plates were incubated with 100 μ l/well of recombinant mouse TNF α (0-2000 pg/ml), IL-1 β (0-1000 pg/ml), IL-6 (0-5000 pg/ml), IL-17 (0-1000 pg/ml), IFN- γ (0-2000 pg/ml), MCP-1 (0-250 pg/ml), RANTES (0-2000 pg/ml), MIP-1 α (0-500 pg/ml) and IP-10 (0-4000 pg/ml) in 1 % BSA/PBS or sample for 2 hours at RT. Plates were washed three times with PBS-T and incubated with 100 μ l/well of secondary antibody, biotinylated goat anti-mouse, TNF α (200 ng/ml), IL-1 β (100 ng/ml), IL-6 (200 ng/ml), IL-17 (400 ng/ml), IFN- γ (100 ng/ml), MCP-1 (50 ng/ml), RANTES (400 ng/ml), MIP-1 α (100 ng/ml) and IP-10 (50 ng/ml) in 1 % BSA for 2 hours at RT. Plates were washed three times in PBS-T, incubated with horse radish peroxidase (HRP)-conjugated streptavidin (100 μ l/well; 1:200 in 1 % BSA; R&D Systems, UK) for 20 minutes in the dark at RT, washed three times in PBS-T and substrate solution (100 μ l/well; R&D Systems, UK) was then added to the plates. The reaction was stopped with 1 M H $_2$ SO $_4$ (50 μ l/well). Absorbance was read at 420 nm within 30 minutes of stopping the reaction. A standard curve was generated by plotting the standards and their absorbance values and the concentrations were corrected allowing for protein concentrations. Protein concentrations from tissue were expressed as pg/mg and for supernatants as pg/ml (GraphPad Prism v 4.0; GraphPad Software, US).

Table 2.5. Origin and specificities of antibodies for ELISA.

Antibody specificity	Catalogue number	Supplier
Mouse IL-6	DY406	R&D Systems
Mouse IL-1 β	DY401	R&D Systems
Mouse TNF α	DY410	R&D Systems
Mouse MCP-1	DY479	R&D Systems
Mouse IP-10	DY466	R&D Systems
Mouse RANTES	DY478	R&D Systems
Mouse MIP-1 α	DY450	R&D Systems
Mouse IFN- γ	DY485	R&D Systems
Mouse IL-17	DY421	R&D Systems

2.13. Determination of A β concentrations in tissue samples using multi-spot ELISA

2.13.1. Extraction of soluble and insoluble A β from brain tissue

Snap-frozen cortical tissue from wildtype and APP/PS1 mice were homogenised in 5 volumes (w/v) of homogenising buffer (SDS/NaCl in dH₂O with proteases). The samples were centrifuged at 15,000 rpm for 40 minutes at 4 °C. The supernatant samples were removed to extract SDS-soluble A β and the pellets were kept for extraction of insoluble A β .

Supernatants were equalised (3 mg/ml) with homogenising buffer using a BCA protein assay as per section 2.10. Equalised supernatant samples were neutralised by the addition of 10 % (w/v) 0.5 M Tris-HCl (pH 6.8). Samples were stored at -20 °C for later detection of soluble A β .

Pellets were incubated in guanidine buffer (50 μ l; 5 M guanidine-HCl/50 mM Tris-HCl, pH 8, Sigma-Aldrich, UK) for 4 hours on ice, and centrifuged at 15,000 rpm for 30 minutes at 4 °C. Supernatant samples were equalised (0.3 mg/ml) with guanidine buffer and stored at -20 °C for later detection of insoluble A β .

2.13.2. Detection of soluble and insoluble A β concentrations in cortical tissue by multi-spot ELISA

Concentrations of soluble and insoluble A β were determined using “MSD® 96-well multi-spot 4G8 A β triple ultra-sensitive assay” kits (Meso Scale Discovery, USA). All solutions and reagents used were supplied by Meso Scale Discovery. Multi-spot A β 3-plex plates were blocked with 1 % Blocker A (150 μ l/well; 50 ml 1 X Tris wash buffer: 0.5 g Blocker A) for 1 hour at RT with vigorous shaking (300-1000 rpm). Plates were washed 3 times in 1 X Tris wash buffer (TWB) and detection antibody solution (25 μ l/well; 60 μ l 50 X SULFO-TAG 4G8 detection antibody, 30 μ l 100 X Blocker G in 2910 μ l 1 % Blocker A solution) was added. SDS-solubilised samples were diluted in Blocker A (200 μ g/ml) plus protease inhibitors (1: 100) and guanidine-treated samples were diluted in Blocker A (0.3 μ g/ml) solution. Standards were prepared by serial

dilutions of recombinant human A β ₁₋₃₈ (0-3,000 pg/ml), A β ₁₋₄₀ (0-10,000 pg/ml) and A β ₁₋₄₂ (0-3,000 pg/ml) in 1% Blocker A. Samples and standards (25 μ l/well) were added in duplicate to the appropriate wells of the 96-well plates which were incubated for 2 hours at RT with vigorous shaking (300-1000 rpm). Plates were washed in wash buffer and 2 X MSD read buffer (150 μ l/well; 10 ml dH₂O: 10 ml 4 X MSD read buffer) was added. Plates were read immediately using a Sector Imager plate reader (Meso Scale Discovery, US) and A β concentrations in test samples were evaluated with reference to the standard curve prepared using A β ₁₋₃₈ (0-3,000 pg/ml), A β ₁₋₄₀ (0-10,000 pg/ml) and A β ₁₋₄₂ (0-3,000 pg/ml).

2.14. Immunohistochemical analysis

2.14.1. Subbing of slides

Glass slides were coated in a subbing solution prior to sectioning of tissue to ensure adhesion of the tissue to the slide. Gelatine (2.5g; Fluka, Switzerland) and chromium potassium sulphate (0.25g; Sigma-Aldrich, UK) was dissolved in 500 ml dH₂O and heated to 60 °C. Subbing solution was filtered through Whatman filter paper (Whatman International, UK) and clean glass slides (Fluka, Switzerland) were submerged into the solution for 1 minute. Slides were removed and allowed to dry overnight.

2.14.2. Preparation of tissue sections for immunohistochemistry

Sections were prepared from tissue obtained from wildtype mice and APP/PS1 mice treated with Th1, Th17, Th1 and anti-IFN- γ or anti-IFN- γ . The left hemisphere of each brain was placed onto cork discs and coated with optimum cooling temperature compound (OCT; Sakura Tissue-Tek, Netherlands), snap frozen in pre-chilled isopropanol and stored at -80 °C. Before sectioning the tissue was allowed to equilibrate to -20 °C for 30 minutes. Sagittal sections (10 μ m thick) were cut using a cryostat (Leica, Meyer, UK), mounted on gelatine-coated glass slides, allowed to dry for 20 minutes and stored at -20 °C for later immunohistochemical analysis.

2.14.3. Immunohistochemical staining for CD11b

Frozen brain section from wildtype and APP/PS1 mice were thawed and brought to RT for approximately 30 minutes. Individual brain sections were surrounded in a hydrophobic well using a cytomation pen (Dako, Denmark). Sections were fixed in an acetone and ethanol mixture (1:1, Sigma-Aldrich, US) for 5-10 minutes and endogenous peroxidase activity was blocked with 0.3 % H₂O₂ (Sigma-Aldrich, US) in PBS for 5 minutes. Sections were washed with PBS (2 x 10 minute washes), and 10 % normal rabbit serum was added to block non-specific binding (NRS; Vector Laboratories, UK). Sections were incubated with rat anti-CD11b (1:100; clone 5C6, AbD Serotec, UK) in 5 % NRS in PBS overnight at RT. Negative controls were incubated in 5 % NRS in PBS. Sections were washed in PBS (2 x 10 minute washes) and incubated in secondary antibody, biotinylated rabbit anti-rat IgG (1:200; Vector, US) in 5 % NRS in PBS for 2 hours at RT. Sections were washed again and incubated with Vectostain Elite ABC reagent (2 drops of A/B in 5 ml PBS, Vector Laboratories, US) for 1 hour at RT. Sections were re-washed to remove excess ABC with PBS and developed using the substrate 3, 3 diaminobenzidine (DAB) enhanced liquid substrate system tetrahydrochloride (1 drop of solution B in 1 ml of solution A, Sigma-Aldrich, US) for approximately 10 minutes until the colour developed. Sections were immediately counterstained with 1 % methyl green (w/v, Sigma-Aldrich, UK) for 10 minutes and dehydrated by dipping for 5 seconds in 70 %, 80 %, 95 % and 2 minutes in 100 % ethanol followed by 2 x 4 minute incubations in xylene (VWR International Ltd., UK). Sections were mounted with xylene-based mountant dibutyl phthalate (DPX; VWR International Ltd., UK) and allowed to dry overnight in the fume hood. The sections were stored at RT until analysis. Sections were examined and analysed using a light microscope. The areas assessed for evidence of microglial activation were the dentate gyrus of the hippocampus and the cortex. The slides were visualized with an Olympus 1 x 51 light microscope (Tokyo, Japan) and micrographs were taken using an Olympus UCMAD3 (Japan) at 40 x magnification.

2.14.5. Quantification of CD11b immunohistochemical analysis using Image J

CD11b positive immunoreactivity was analysed using Image J software. Micrographs of cortical and hippocampal sections were converted to Tiff-tag images and opened in the Image J software. Images were then converted to 8 bit and the threshold adjusted. CD11b positive cells were then identified using the analyze particles tool. All images were analysed at the same threshold, cell circularity and pixel size.

2.14.6. Immunohistochemical staining for A β plaques using Congo red

Congo red solution was made by adding Congo red powder (0.1 g; Sigma-Aldrich, US) to saturated sodium chloride (NaCl; 500 ml; 50 grams in 80 % ethanol, Sigma-Aldrich, UK) and the solution was stirred overnight before use. Frozen brain sections from wildtype and APP/PS1 mice were stained for A β plaques using congo red. Sections were thawed and brought to RT for 30 minutes. Individual brain sections were surrounded in a hydrophobic well using a cytostation pen. The brain sections were fixed using ice-cold ethanol and washed 3 x 5 minutes in PBS. During the washes, sodium hydroxide (NaOH 1M; 2 ml, Sigma-Aldrich, UK) was added to saturated NaCl (200 ml) to produce an alkaline solution. Sections were incubated for 20 minutes at RT in the alkaline solution. During the incubation, Congo red solution (200 ml) was filtered through a 50 ml syringe using a cellulose acetate membrane filter (0.2 μ M Supor membrane Acrodisc syringe filters, Pall Corporation, US). The filtered Congo red solution (200 ml) was added to 1 M NaOH (2 ml) to generate an alkaline solution. The sections were incubated in the Congo red solution for 30 minutes at RT. Sections were rinsed in dH₂O to remove excess Congo red stain and sections were counterstained in 1 % methyl green solution for 10 minutes. Sections were dehydrated by dipping 5/6 times in 80 %, 95 %, 100 % and 100 % ethanol and 3 x 5 minute incubations in xylene. Slides were mounted in DPX and allowed to dry in the fume hood overnight. The slides were visualized with an Olympus 1 x 51 light microscope (Tokyo, Japan) and micrographs were taken using an Olympus UCMAD3 (Japan) at 40 x magnification. Positively-stained A β plaques were counted in representative sections from each animal under the same light and

magnification settings and results were expressed as the average number of plaques per sections.

2.14.7. Double-immunofluorescence staining for A β and CD11b

Frozen brain section from wildtype and APP/PS1 mice were thawed and brought to RT for approximately 30 minutes. Individual brain sections were surrounded with a cytomation pen and fixed in ice-cold methanol for 10 minutes followed by 3 x 1 minute washes in PHEM (HEPES sodium salt 25 mM; EGTA 10 mM; PIPES 60 mM; MgCl₂ 2 mM; pH6.9; Sigma-Aldrich, UK). Sections were permeabilized in 0.1 % Triton (Sigma-Aldrich, UK) in PHEM for 10 minutes followed by 3 x 1 minute washes in PHEM. Non-specific binding was blocked by incubating sections in 10 % normal goat serum (NGS) for 2 hours at RT. Sections were incubated overnight with primary antibodies: Pan A β (1:1000, Calbiochem, US) and rat anti-CD11b (1:100, clone 5C6, AbD, Serotec, UK) in 5 % NGS in PHEM. Sections were washed 3 x 1 minute washes in PHEM and incubated in secondary antibody ALEXA 488 (1:4000, Invitrogen, US) and ALEXA 546 (1:1000, Invitrogen, US) in 5 % NGS for 90 minutes at RT. Sections were washed every 10 minutes for 90 minutes, mounted with dapi-containing mounting medium (Vector Labs, US) and analysed using a confocal microscope (Axioplan 2, Zeiss, Germany).

2.15. Statistical analysis

Statistical analysis was performed using GraphPad Prism. Data were analysed using student's *t* test, two-way ANOVA or one-way ANOVA followed by Newman-Keuls post-hoc test. Data are expressed as means with standard errors (SEM) and deemed statistically significant when $p < 0.05$.

Chapter 3

Chapter 3

3.1. Introduction

The immune system is crucial for the maintenance of tissue homeostasis, clearing pathogens and responding to injury. It has been well documented that microglia are the major resident CNS immune cell, constantly surveying their microenvironment and participating in innate and adaptive responses resulting in the release of pro-inflammatory cytokines and chemokines, phagocytosis and the regulation of T cell responses (Aloisi, 2001). Astrocytes have also been implicated in immune functions and the development of CNS inflammation (Dong & Benveniste, 2001). There is extensive literature describing the phenotypical transformation of 'resting' microglia into 'activated' microglia. These phenotypical changes include the upregulation of various cells surface markers including CD11b (Roy *et al.*, 2008), CD40 and MHC class II (Benveniste *et al.*, 2001). Furthermore, Cytokines become promptly unregulated as a consequence of microglial (Aloisi, 2001) and astrocytic activation (Dong & Benveniste, 2001; Carpentier *et al.*, 2005), which in turn is associated with the expression of inflammatory chemokines.

It is imperative that activated microglia ultimately return to an inactivated state, when the insult is cleared to prevent unwanted tissue damage. In the normal brain, interaction of microglia with other glia and neurons can act to suppress 'activation' and dampen the pro-inflammatory response (Colton, 2009). The interaction of receptor-ligand pairs such as CD200, expressed on neurons and astrocytes, and CD200R, expressed on microglia, acts to inhibit the production of pro-inflammatory mediators by microglia (Lyons *et al.*, 2007; Meuth *et al.*, 2008; Masocha, 2009; Walker *et al.*, 2009). The importance of the CD200-CD200R interaction has been demonstrated in several different models including the facial nerve transection model, EAE and CIA (Hoek *et al.*, 2000). The use of CD200 fusion protein (Gorzynski *et al.*, 2002b) and CD200 antibodies (Copland *et al.*, 2007) have confirmed the anti-inflammatory potential of CD200-CD200R interaction. Interestingly, both CD200 and CD200R levels are decreased in brain tissue of AD patients (Walker *et al.*, 2009).

Microglia possess a number of receptors involved in immune function, most notably the TLRs, which allow them to rapidly detect pathogens and prevent unwanted tissue damage (Palm & Medzhitov, 2009). Similarly, astrocytes have also been found to express TLRs (Bowman *et al.*, 2003). To date, thirteen mammalian TLRs (TLR1-13) have been identified, each with their own set of PAMPs and signalling pathways. The pattern of TLRs expressed by glial cells and the signalling pathways employed play a significant role in determining the inflammatory response occurring within the CNS (Jack *et al.*, 2005). This study focuses on TLR2, which recognises the largest array of PAMPs including lipoteichoic acids, PGN, surface proteins on both gram-negative and gram-positive bacteria, mycobacteria and zymosan (Kielian, 2006). Previous studies have found that TLR2 works as a heterodimer with TLR1 and TLR6 to discriminate between lipopeptides (Ozinsky *et al.*, 2000). Studies using TLR1 and TLR6 knockout animals have demonstrated that TLR2 uses TLR1 to recognise triacyl lipopeptides such as Pam₃CysSerLys₄ (Pam₃Csk₄) a TLR2 agonist (Takeda *et al.*, 2002). Further investigations of the TLR2/TLR1 relationship, using Pam₃Csk₄, established that Pam₃Csk₄ was needed to bridge the two TLRs together thus aiding in the formation of the heterodimer facilitating downstream signalling activation (O'Neill *et al.*, 2009).

Although the activation of TLRs is crucial to mount an appropriate immune response, their activation comes at a cost and this is implicated in the pathogenesis of autoimmune, chronic inflammatory and infectious diseases (Chen *et al.*, 2007; O'Neill *et al.*, 2009) and in the pathogenesis of neurodegenerative diseases (Cameron & Landreth, 2010). There is a growing body of evidence suggesting that TLRs namely TLR2 and TLR4 and the TLR co-receptor, CD14, participate in microglial responses to A β . It is now understood that TLRs can regulate microglial phenotypes and responses in the AD brain (Landreth & Reed-Geaghan, 2009). Recognition of A β through TLRs and other cell surface receptors results in the production and secretion of pro-inflammatory cytokines (Cameron & Landreth, 2010). Several studies have found increased expression of TLR2 and TLR4 in mouse models of AD and the AD brain (Fassbender *et al.*, 2004; Walter *et al.*, 2007; Letiembre *et al.*, 2009), furthermore plaque-associated microglia have increased expression of TLRs (Frank *et al.*, 2009). Previous studies emphasise the role of TLR2 in A β -induced microglial activation. It has been

found that blocking TLR2 through neutralising antibodies or siRNA knockdown prevents A β -induced secretion of cytokines IL-6 and TNF α (Jana *et al.*, 2008; Udan *et al.*, 2008).

The aims of this study were to:

- Investigate *in vitro* the role of CD200 on microglial activation following stimulation with a TLR2 agonist Pam₃Csk₄.
- Investigate *in vitro* the effect of A β on microglial activation and to establish whether A β -induced changes are dependent on activation of TLR2.

3.2. Methods

Mixed glia were prepared from neonatal C57BL/6 wildtype and CD200^{-/-} mice and cultured for 14 days before incubation with Pam₃Csk₄ (100 ng/ml) for 24 hours (see section 2.1. for details). Similarly, mixed glia were prepared from neonatal C57BL/6 mice and cultured for 14 days before incubation with A β _{1-40/1-42} (10 μ M, 24 hours) or pre-incubation with anti-TLR2 (2.5 μ g/ml), for 2 hours, and A β _{1-40/1-42} for 24 hours (see section 2.1.3 for details). Supernatant samples were taken to determine cytokine and chemokine concentrations by ELISA and cells were taken to determine mRNA expression of surface proteins by QPCR (see sections 2.11 and 2.12 for details). Data are expressed as means \pm SEM. ANOVA and student's *t*-test were performed to determine whether significant differences existed between treatment groups and Bonferroni post-hoc test was applied where appropriate.

3.3. Results

3.3.1. Pam₃Csk₄ increased CD11b and CD40 and decreased CD68 mRNA expression in mixed glia prepared from wildtype and CD200^{-/-} mice.

TLRs are expressed on cells of the immune system and play a critical role in pathogen recognition and tailoring of the adaptive immune response (Medzhitov & Janeway, 1997). Microglia and astrocytes are capable of recognising a wide array of pathogens through TLRs. Ligation of TLRs allows for the progressive transformation of glia into a more “activated” phenotype which is measured here by assessing expression of markers of activation. Pam₃Csk₄, a synthetic TLR2 agonist, induced a significant increase in mRNA expression of CD11b and CD40 in mixed glia prepared from wildtype and CD200^{-/-} mice (***p*<0.001, ANOVA; Figures 3.1A and B). There was no genotype effect observed as the effect of Pam₃Csk₄ was similar in mixed glia prepared from wildtype and CD200^{-/-} mice. Basal mRNA expression of CD40 was significantly increased in glia prepared from CD200^{-/-}, compared with wildtype, mice (⁺*p*<0.05, student’s *t* test; Figure 3.1b).

Pam₃Csk₄ induced a significant decrease in the mRNA expression of CD68 in mixed glia prepared from wildtype and CD200^{-/-} mice (***p*<0.001, ANOVA; Figure 3.2). While no significant genotype effect was observed, there was a trend towards an increase in basal mRNA expression of CD68 in glia prepared from CD200^{-/-}, compared with wildtype, mice.

3.3.2. Pam₃Csk₄ increased TNF α and IL-6 in mixed glia prepared from wildtype and CD200^{-/-} mice.

TLR activation, through interaction with different pathogen-associated molecules, results in activation of signalling cascades resulting in the production of pro-inflammatory cytokines tailored to the activating stimulus (Jack *et al.*, 2005). Previously Pam₃Csk₄ has been found to increase pro-inflammatory cytokine production by microglia including TNF α and IL-6 (Ebert *et al.*, 2005; Jack *et al.*, 2005; Shah *et al.*, 2009). The present data show that Pam₃Csk₄ significantly increased mRNA expression of TNF α and supernatant

concentrations of TNF α in mixed glia prepared from wildtype and CD200^{-/-} mice (**p<0.001, ANOVA; Figure 3.3A and B) and significantly enhanced TNF α supernatant concentration obtained from mixed glia prepared from CD200^{-/-}, compared with wildtype, mice (***p<0.001, ANOVA; Figure 3.3B).

Pam₃Csk₄ also induced a significant increase in mRNA expression of IL-6 and supernatant concentrations of IL-6 in mixed glia prepared from wildtype and CD200^{-/-} mice (**p<0.001, ANOVA; Figure 3.4A and 3.4B). Both were further increased in mixed glia prepared from CD200^{-/-}, compared with wildtype, mice (***p<0.01, ***p<0.001, ANOVA; Figure 3.4A and B).

3.3.3. Pam₃Csk₄ significantly increased MCP-1 and IP-10 in mixed glia prepared from wildtype and CD200^{-/-} mice.

Expression and supernatant concentrations of the chemokines MCP-1 and IP-10, were assessed in mixed glia following Pam₃Csk₄ incubation. Pam₃Csk₄ significantly increased mRNA expression of MCP-1 and IP-10 (**p<0.001, ANOVA; Figure 3.5A and 3.6A) and supernatant concentrations of MCP-1 and IP-10 in mixed glia prepared from wildtype and CD200^{-/-} mice (**p<0.001, ANOVA; Figure 3.5B and 3.6B). The data show that the effect of Pam₃Csk₄ on the mRNA expression of MCP-1 and supernatant concentration was significantly greater in mixed glia prepared from CD200^{-/-}, compared with wildtype, mice (***p<0.01, ***p<0.001, ANOVA; Figure 3.5A and B). The effect of Pam₃Csk₄ on supernatant concentrations of IP-10 was significantly greater in cells prepared from CD200^{-/-}, compared with wildtype, mice (+p<0.05, ANOVA; Figure 3.6B).

3.3.4. Pam₃Csk₄ increased TLR mRNA expression in mixed glia prepared from wildtype and CD200^{-/-} mice.

A previous study demonstrated that TLR2 works in conjunction with TLR1 to recognise triacylated lipoproteins (Takeuchi *et al.*, 1999). In this study, it was found that Pam₃Csk₄ significantly increased both mRNA expression of TLR2 and TLR1 in mixed glia prepared from wildtype and CD200^{-/-} mice (**p<0.001, ANOVA; Figure 3.7A and B). No genotype effect on mRNA expression of TLR2 was observed following Pam₃Csk₄ incubation. Basal mRNA expression of TLR2

was greater in mixed glia prepared from CD200^{-/-}, compared with wildtype, mice but the difference was not statistically significant (Figure 3.7A). To further assess whether expression of TLR2 on microglia was altered, FACS analysis was performed on mixed glia. The data, (kindly donated by Dr Anthony Lyons), revealed that expression of TLR2 on CD11b⁺ cells was significantly increased in cells prepared from CD200^{-/-}, compared with wildtype, mice (**p<0.01, student's *t*-test; Figure 3.8). Table 3.1 summarises the mRNA expression results and supernatant concentration results.

3.3.5. A β -induced mRNA expression of markers of microglial activation were attenuated by anti-TLR2.

Microglia and astrocytes are capable of responding to A β through TLRs resulting in an inflammatory immune response (Landreth & Reed-Geaghan, 2009). Previously it has been found that A β ₁₋₄₂ increases the expression of TLR2 in microglial cultures (Jana *et al.*, 2008). Here the effect of A β _{1-40/1-42} on mRNA expression of TLRs in mixed glia, prepared from neonatal C57BL/6 mice, was investigated. It was found that incubation of mixed glia in the presence of A β _{1-40/1-42} significantly increased mRNA expression of TLR2 in mixed glia (*p<0.05, student's *t* test; Figure 3.9A). However mRNA expression of neither TLR1 (Figure 3.9B) nor TLR4 (Figure 3.9C) were affected by A β _{1-40/1-42}.

Studies by Jana and colleagues (2008) found that increased TLR2 expression was accompanied by increased production of pro-inflammatory markers and that knockdown of TLR2 suppressed the induction of these pro-inflammatory molecules and expression of integrin markers on microglia. In this study, several markers of microglial activation were investigated. Incubation of mixed glia in the presence of A β _{1-40/1-42} significantly increased mRNA expression of CD86 and CD40 (*p<0.05, **p<0.01, ANOVA; Figure 3.10A and B) and pre-incubation of mixed glia with anti-TLR2 significantly attenuated the A β -induced increase in mRNA expression of CD86 and CD40 (⁺p<0.05, ⁺⁺p<0.01, ANOVA; Figure 3.10A and B). Incubation of mixed glia in the presence of A β _{1-40/1-42} significantly decreased mRNA expression of CD11b but had no effect on CD68 (**p<0.01, ANOVA; Figure 3.11A and B). No significant effect of anti-TLR2 was observed in either CD11b or CD68 (Figure 3.11A and B).

3.3.6. A β -induced production of pro-inflammatory cytokines and chemokines was attenuated by anti-TLR2.

Data from several studies have demonstrated that TLR2 deficiency or knockdown decreases the production of A β -induced pro-inflammatory cytokines and chemokines by microglia (Udan *et al.*, 2008; Liu *et al.*, 2012). Here the production of cytokines and chemokine by mixed glia was assessed and the role of TLR2 in their production was investigated. Incubation of mixed glia in the presence of A β _{1-40/142} significantly increased mRNA expression of TNF α and IL-6 (***p*<0.001, **p*<0.05, ANOVA; Figure 3.12 and 3.13A). Incubation of mixed glia with anti-TLR2 significantly decreased mRNA expression of TNF α and IL-6 in mixed glia (****p*<0.001, +*p*<0.05, ANOVA; Figure 3.12 and 3.13A). A β _{1-40/1-42} incubation significantly increased supernatant concentrations of IL-6 in mixed glia (***p*<0.01, ANOVA; Figure 3.13B) and this A β -induced increase was attenuated by pre-incubation with anti-TLR2 (+*p*<0.01, ANOVA; Figure 3.14B). Supernatant concentrations of TNF α were not detectable.

Incubation of mixed glia in the presence of A β _{1-40/1-42} significantly increased mRNA expression of IP-10, MCP-1, MIP-1 α and RANTES (***p*<0.01, ****p*<0.001; ANOVA; Figures 3.15A-3.17A). The A β -induced increases in mRNA expression of IP-10, MCP-1, MIP-1 α and RANTES were significantly attenuated by pre-incubation with anti-TLR2 (+*p*<0.05, ++*p*<0.01, +++*p*<0.001, ANOVA; Figures 3.14A-3.17A). A β _{1-40/1-42} incubation significantly increased supernatant concentrations of MCP-1 and RANTES in mixed glia (***p*<0.001, ***p*<0.01, ANOVA; Figure 3.15B and 3.17B). Incubation with anti-TLR2 significantly decreased supernatant concentrations of MCP-1 and RANTES (+*p*<0.05, ANOVA; Figure 3.15B and 3.17B). Supernatant concentrations of IP-10 and MIP-1 α were not significantly changed by A β _{1-40/1-42} incubation or anti-TLR2 pre-incubation (Figure 3.14A and 3.16A).

3.3.7. A β - and anti-TLR2-treatment induced different mRNA expression of immunosuppressant receptors and ligands on glia.

Several receptors expressed on neurons and astrocytes play an important role in suppressing microglial activation. Interaction of fractalkine and CD200

with their respective ligands plays an important role in dampening the pro-inflammatory response (Cameron & Landreth, 2010). In this study, both CD200 receptor and fractalkine receptor-ligand interactions were investigated. It was found that incubation of mixed glia in the presence of $A\beta_{1-40/1-42}$ increases mRNA expression of CD200R ($^{\#}p < 0.05$, student's *t*-test; Figure 3.18a) but not that of CD200L (Figure 3.18B). Incubation of mixed glia with anti-TLR2 had no significant effect on mRNA expression of CD200R (Figure 3.18A). CD200L mRNA expression was significantly increased in mixed glia incubated with anti-TLR2 ($^{**}p < 0.01$, ANOVA; Figure 3.18B) and this effect was attenuated in cells which were incubated in the presence of $A\beta_{1-40/1-42}$ and anti-TLR2 ($^{++}p < 0.01$, ANOVA; Figure 3.18B).

Incubation of mixed glia in the presence of $A\beta_{1-40/1-42}$ significantly decreased mRNA expression of fractalkine receptor ($^{***}p < 0.001$, ANOVA; Figure 3.19A), whereas anti-TLR2-incubation significantly increased mRNA expression of fractalkine receptor in mixed glia ($^{+}p < 0.05$, ANOVA; Figure 3.19A). Incubation of mixed glia in the presence of $A\beta_{1-40/1-42}$ significantly increased mRNA expression of fractalkine ($^{***}p < 0.001$, ANOVA; Figure 3.20B), whereas anti-TLR2-incubation significantly decreased mRNA expression of fractalkine in mixed glia ($^{+++}p < 0.001$, ANOVA; Figure 3.19B).

Table 3.2 summarises the mRNA expression results and Table 3.3 summarises the supernatant concentration results.

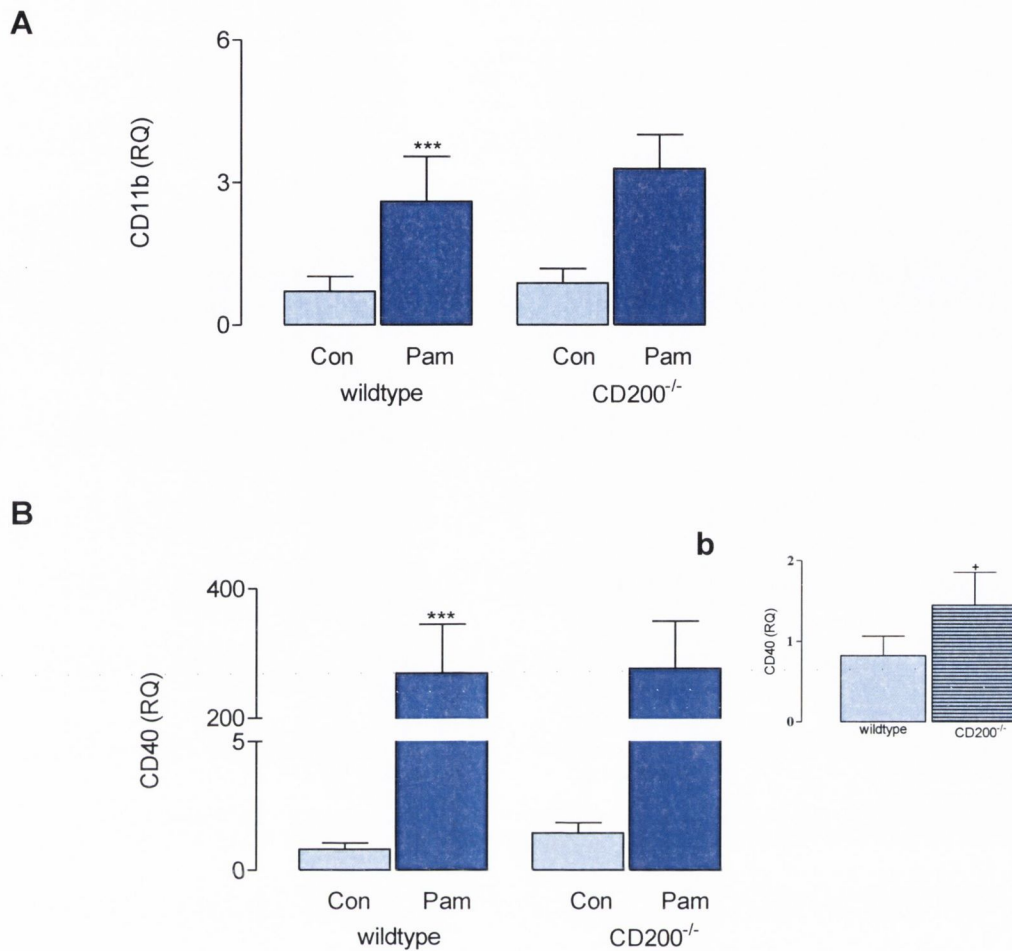


Figure 3.1. Pam₃Csk₄ increased CD11b and CD40 mRNA expression.

Pam₃Csk₄ (100 ng/ml; 24 hours) significantly increased CD11b (A) and CD40 (B) mRNA expression in mixed glia prepared from wildtype and CD200^{-/-} mice (***p*<0.001, ANOVA). Basal CD40 mRNA expression was significantly increased in CD200^{-/-}, compared with wildtype, mice (b) (⁺*p*<0.05, student's *t*-test). Values are expressed as means ± SEM (n=3-5).

(A) 2-way ANOVA: Pam₃Csk₄ effect **F (1,13) = 15.25; p<0.0001**, Genotype effect **F (1,13) = 2.059; p= 0.175**, Interaction effect **F (1,13) = 0.7202; p=0.414**

(B) 2-way ANOVA: Pam₃Csk₄ effect **F (1,10) = 114.7; p<0.0001**, Genotype effect **F (1,10) = 0.02292; p= 0.8827**, Interaction effect **F (1,10) = 0.01606; p=0.9017**

(b) ⁺*p*=0.0384; 0.8208 ± 0.1215; n=4 versus 1.447 ± 0.2037; n=4

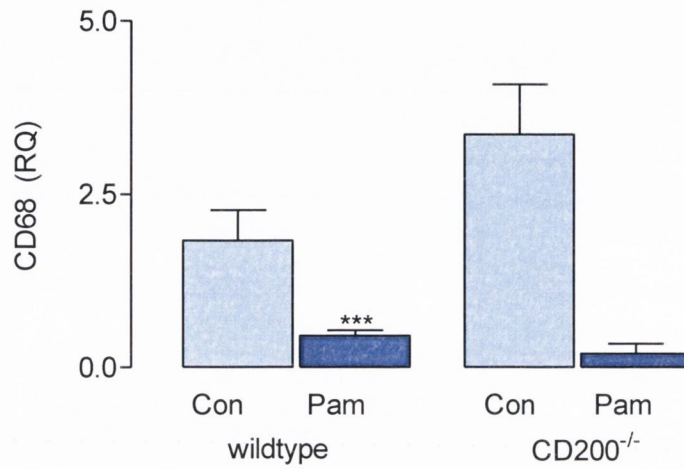


Figure 3.2. Pam₃Csk₄ decreased CD68 mRNA expression.

Pam₃Csk₄ (100 ng/ml; 24 hours) significantly decreased CD68 mRNA expression in mixed glia prepared from wildtype and CD200^{-/-} mice (**p<0.001, ANOVA). Values are expressed as means ± SEM (n=4).

2-way ANOVA: Pam₃Csk₄ effect F (1,11) = 23.91; p=0.0005, Genotype effect F (1,11) = 1.874; p=0.1983, Interaction effect F (1,11) = 3.708; p=0.0804

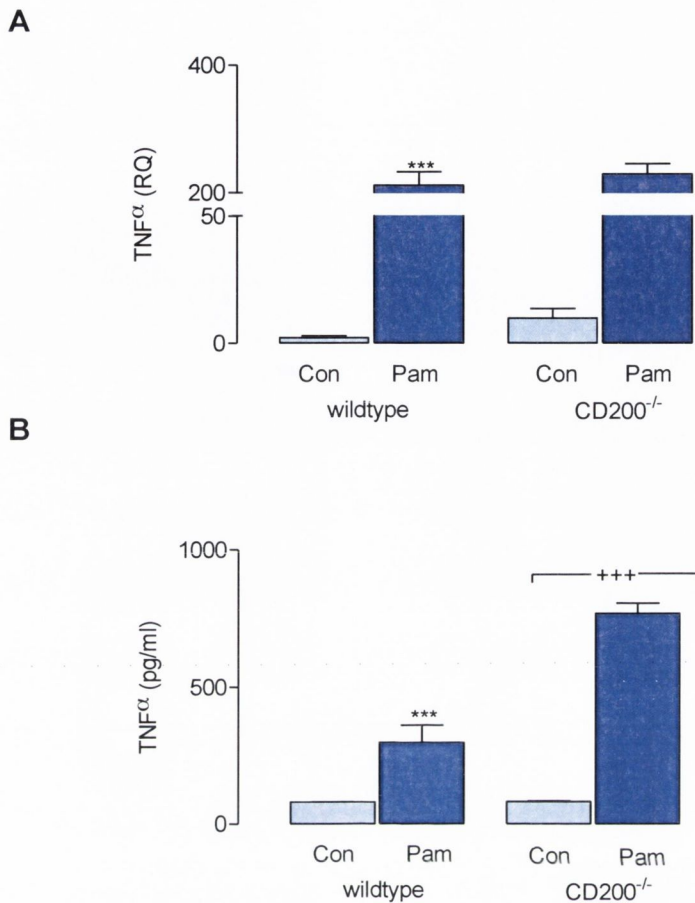


Figure 3.3. Pam₃Csk₄ increased production of TNF α .

Pam₃Csk₄ (100 ng/ml; 24 hours) caused a significant increase in TNF α mRNA expression (A) and supernatant concentration (B) in mixed glia prepared from wildtype and CD200^{-/-} mice (***p*<0.001, ANOVA). There was a significant increase in supernatant concentration (B) of TNF α in mixed glia prepared from CD200^{-/-}, compared with wildtype, mice (++++*p*<0.001, ANOVA), and a significant interaction between Pam₃Csk₄ and genotype was observed (B) (++)*p*<0.01, ANOVA). Values are expressed as means \pm SEM (n=3-4).

(A) 2-way ANOVA: Pam₃Csk₄ effect F (1,9) = 297.2; *p*<0.0001, Genotype effect F (1,9) = 1.072; *p*= 0.3275, Interaction effect F (1,9) = 0.1757; *p*=0.6850

(B) 2-way ANOVA: Pam₃Csk₄ effect F (1,10) = 123.2; *p*<0.0001, Genotype effect F (1,10) = 33.70; *p*= 0.0002, Interaction effect F (1,10) = 33.29; *p*=0.0002

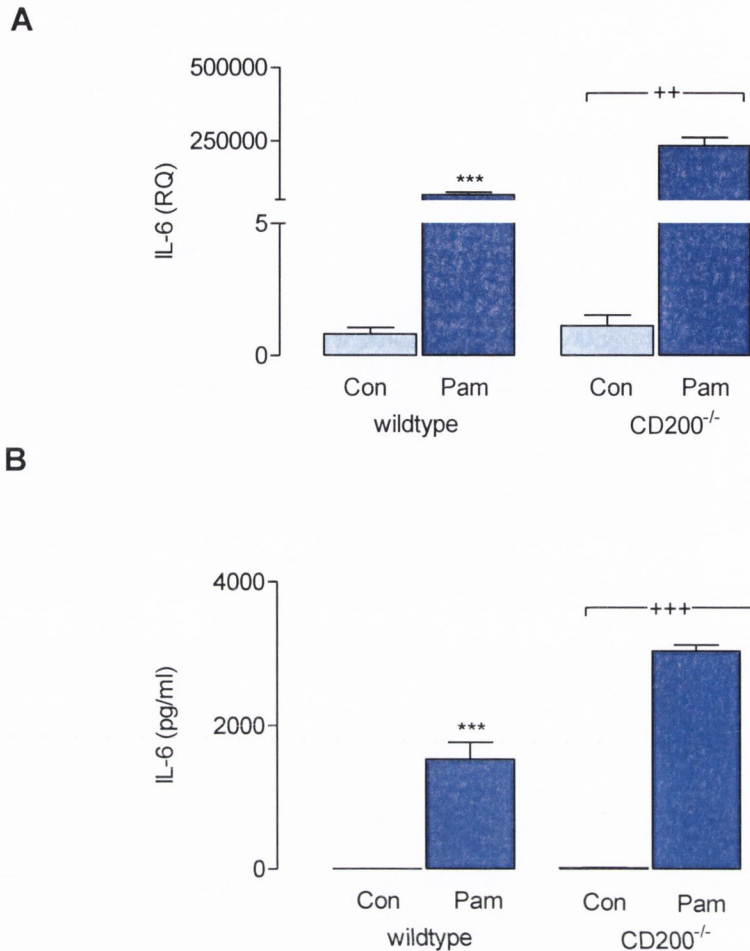


Figure 3.4. Pam₃Csk₄ increased production of IL-6.

Pam₃Csk₄ (100 ng/ml; 24 hours) caused a significant increase in IL-6 mRNA expression (A) and supernatant concentration (B) in mixed glia prepared from wildtype and CD200^{-/-} mice (** p<0.001, ANOVA). There was a significant increase in IL-6 mRNA expression (A) and supernatant concentration (B) in mixed glia prepared from CD200^{-/-}, compared with wildtype, mice (** p<0.01, *** p<0.001, ANOVA). A significant interaction between Pam₃Csk₄ and genotype was observed (A and B) (** p<0.01, *** p<0.001, ANOVA). Values are expressed as means ± SEM (n=3-4).

(A) 2-way ANOVA: Pam₃Csk₄ effect F (1,7) = 85.78; p<0.001, Genotype effect F (1,7) = 26.47; p=0.0013, Interaction effect F (1,7) = 26.47; p=0.0013

(B) 2-way ANOVA: Pam₃Csk₄ effect F (1,10) = 236.4; p<0.0001, Genotype effect F (1,10) = 26.20; p=0.0005, Interaction effect F (1,10) = 55.12; p=0.0005

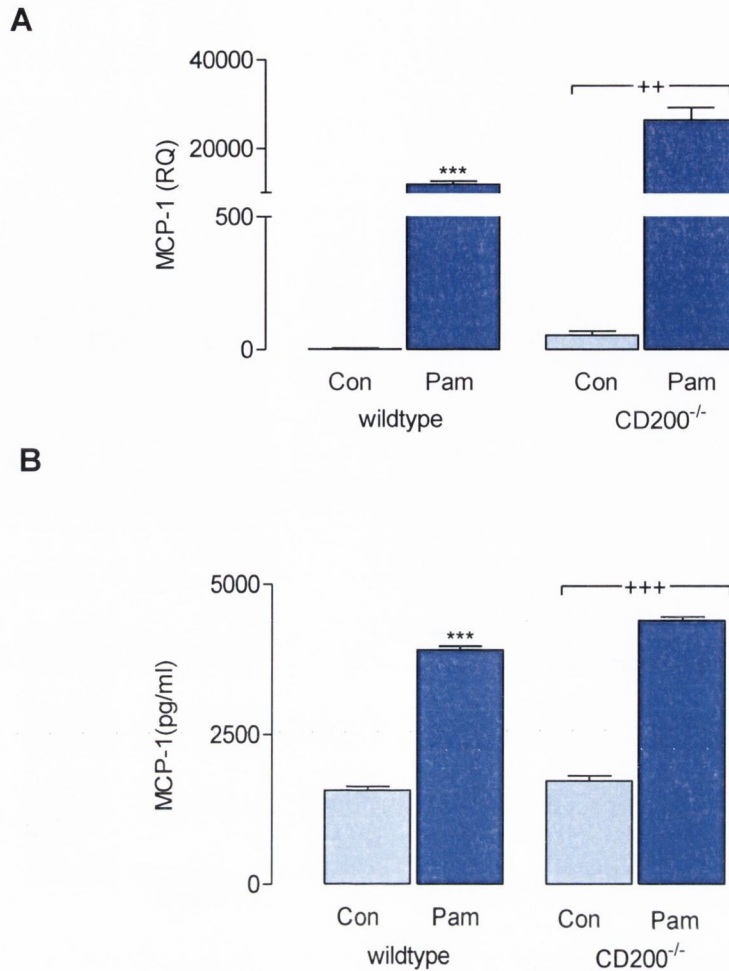


Figure 3.5. Pam₃Csk₄ increased production of MCP-1.

Pam₃Csk₄ (100 ng/ml; 24 hours) caused a significant increase in MCP-1 mRNA expression (A) and supernatant concentration (B) in mixed glia prepared from wildtype and CD200^{-/-} mice (***p*<0.001, ANOVA). There was a significant increase in MCP-1 mRNA expression (A) and supernatant concentration (B) in mixed glia prepared from CD200^{-/-}, compared with wildtype, mice (***p*<0.01, ****p*<0.001, ANOVA). A significant interaction between Pam₃Csk₄ and genotype was observed (A and B) (**p*<0.05, ***p*<0.01, ANOVA). Values are expressed as means ± SEM (n=3-6).

(A) 2-way ANOVA: Pam₃Csk₄ effect *F* (1,9) = 109.7; *p*<0.0001, Genotype effect *F* (1,9) = 15.92; *p*= 0.0032, Interaction effect *F* (1,9) = 15.70; *p*=0.0033

(B) 2-way ANOVA: Pam₃Csk₄ effect *F* (1,17) = 1281; *p*<0.0001, Genotype effect *F* (1,17) = 21.33; *p*= 0.0002, Interaction effect *F* (1,17) = 5.752; *p*=0.0282

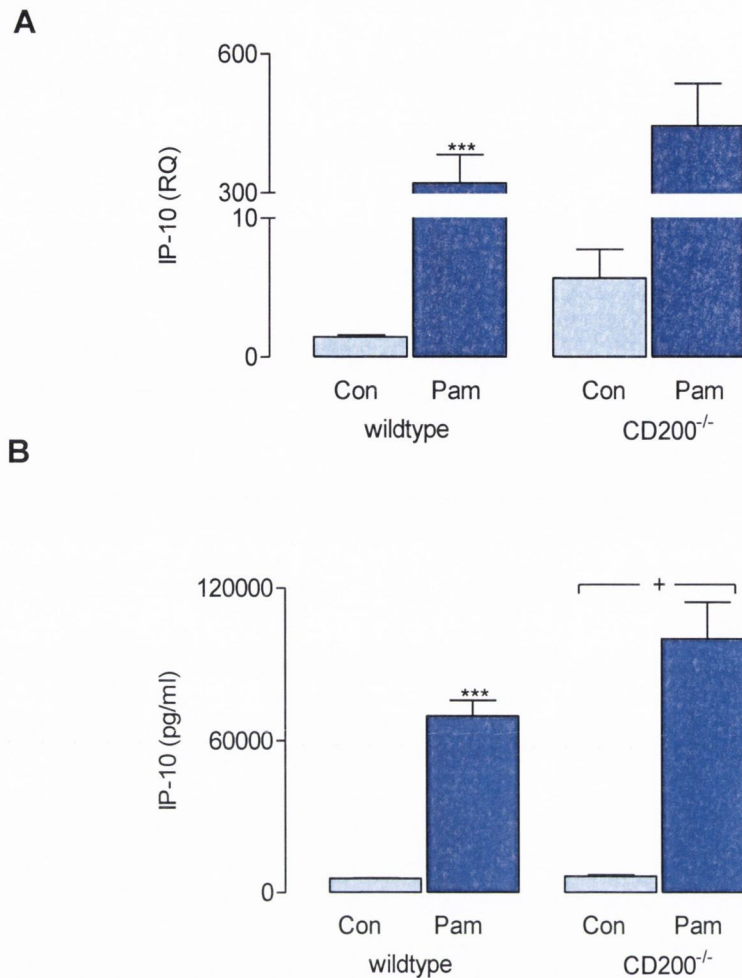


Figure 3.6. Pam₃Csk₄ increased production of IP-10.

Pam₃Csk₄ (100 ng/ml; 24 hours) caused a significant increase in IP-10 mRNA expression (A) and supernatant concentration (B) in mixed glia prepared from wildtype and CD200^{-/-} mice (***p*<0.001, ANOVA). There was a significant increase in IP-10 supernatant concentration (B) in mixed glia prepared from CD200^{-/-}, compared with wildtype, mice ([†]*p*<0.05, ANOVA). A significant interaction between Pam₃Csk₄ and genotype was observed (B) ([†]*p*<0.05, ANOVA). Values are expressed as means ± SEM (n=4-5).

(A) 2-way ANOVA: Pam₃Csk₄ effect *F* (1,12) = 47.56; *p*<0.0001, Genotype effect *F* (1,12) = 1.355; *p* = 0.2671, Interaction effect *F* (1,12) = 1.181; *p*=0.2985

(B) 2-way ANOVA: Pam₃Csk₄ effect *F* (1,15) = 134.8; *p*<0.0001, Genotype effect *F* (1,15) = 5.280; *p* = 0.0364, Interaction effect *F* (1,15) = 4.703; *p*=0.0466

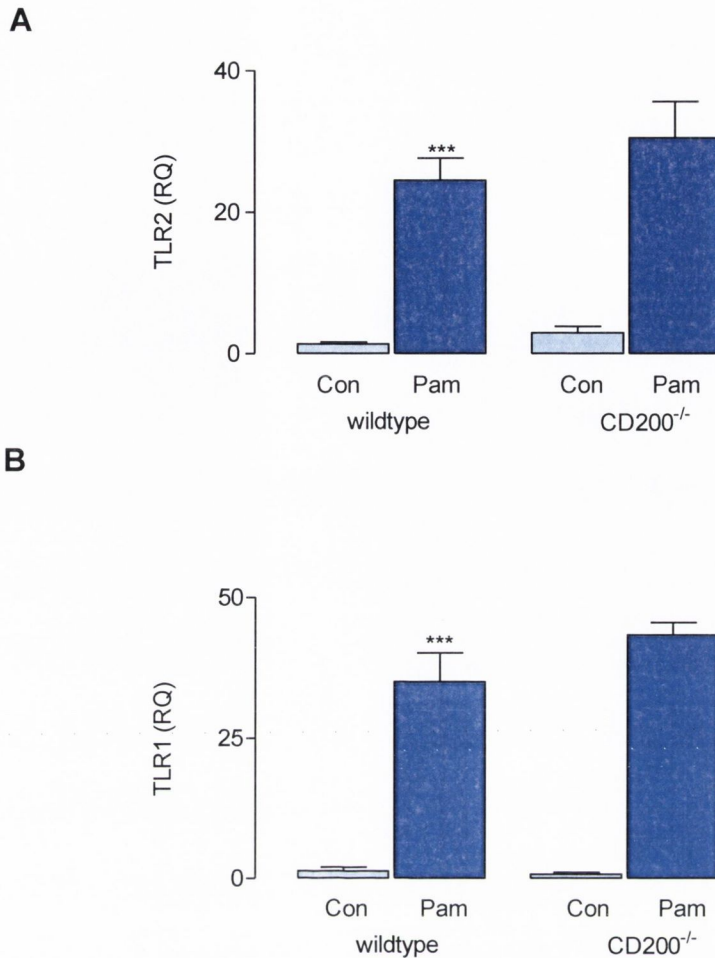


Figure 3.7. Pam₃Csk₄ increased TLR mRNA expression.

Pam₃Csk₄ (100 ng/ml; 24 hours) significantly increased TLR2 (A) and TLR1 (B) mRNA expression in mixed glia prepared from wildtype and CD200^{-/-} mice (***) p<0.001, ANOVA). Values are expressed as ± SEM (n=4-5).

(A) 2-way ANOVA: Pam₃Csk₄ effect F (1,12) = 68.61; p<0.0001, Genotype effect F (1,12) = 1.530; p= 0.2397, Interaction effect F (1,12) = 0.5228; p=0.4835

(B) 2-way ANOVA: Pam₃Csk₄ effect F (1,13) = 208.6; p<0.0001, Genotype effect F (1,13) = 2.118; p= 0.1693, Interaction effect F (1,13) = 2.854; p=0.115

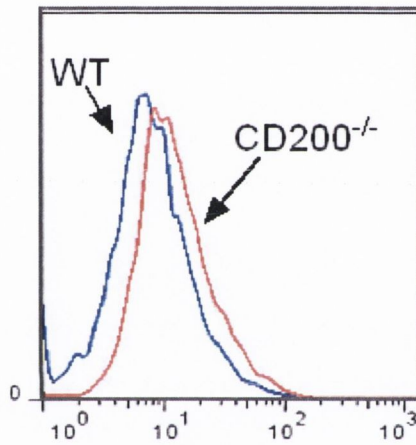
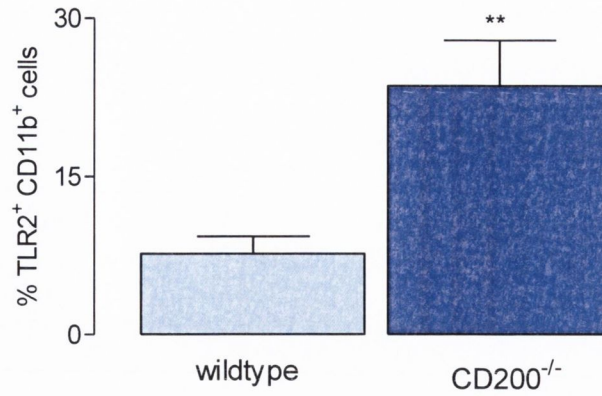


Figure 3.8. Increased number of TLR2 expressing CD11b⁺ cells in CD200^{-/-}, compared with wildtype, mice.

There was a significant increase in TLR2 expression on CD11b⁺ cells in mixed glia prepared from CD200^{-/-}, compared with wildtype, mice (***p*<0.01, student's *t*-test). Values are expressed as ± SEM (n=3-5).

***p*=0.006; 7.676 ± 1.634; n=5 versus 23.58 ± 4.318; n=4

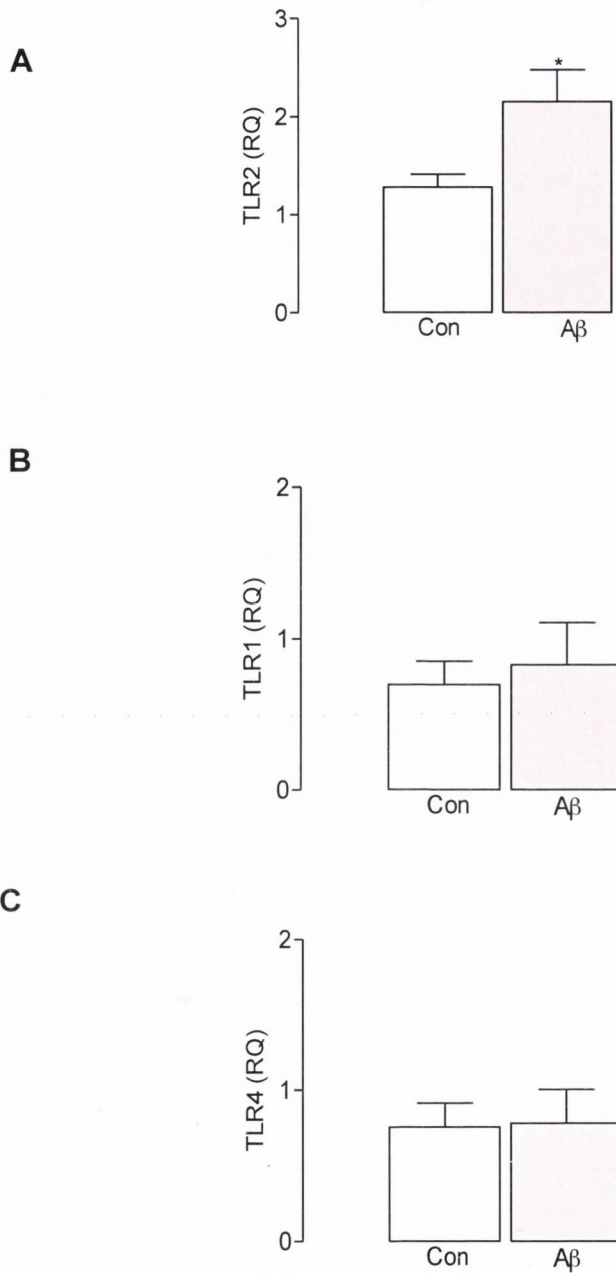


Figure 3.9. TLR2 mRNA expression was increased by Aβ_{1-40/1-42}.

Aβ_{1-40/1-42} (10 μM; 24 hours) significantly increased TLR2 mRNA expression (A) in mixed glia prepared from neonatal C57BL/6 mice (*p<0.05, student's *t*-test). TLR1 (B) and TLR4 (C) mRNA expression was not affected by Aβ_{1-40/1-42}. Values are expressed as means ± SEM (n=6).

(A) *p=0.0320; 1.281 ± 0.1333; n=6 versus 2.154 ± 0.3242; n=6

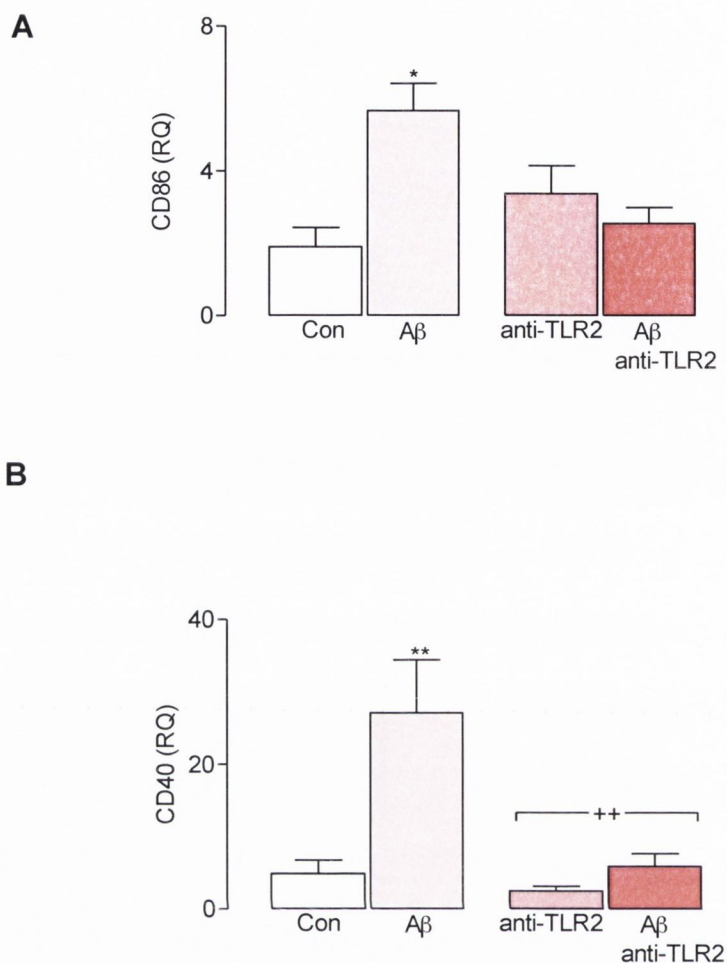


Figure 3.10. The A β -induced increase in CD86 and CD40 mRNA expression was attenuated by anti-TLR2.

Incubation of mixed glia in the presence of A $\beta_{1-40/1-42}$ (10 μ M; 24 hours) significantly increased CD86 and CD40 mRNA expression (A and B) (* p <0.05, ** p <0.01, ANOVA). Incubation of mixed glia with anti-TLR2 (2.5 μ g/ml; 2 hours) significantly decreased CD40 mRNA expression (B) (++) p <0.01, ANOVA). A significant interaction between A $\beta_{1-40/1-42}$ and anti-TLR2 pre-incubation was observed (A and B) (+ p <0.05, ++ p <0.01, ANOVA). Values are expressed as means \pm SEM (n=5-6).

(A) 2-way ANOVA: A β effect F (1,16) = 5.191; p =0.0368, anti-TLR2 effect F (1,16) = 1.641; p =0.2184, Interaction effect F (1,16) = 12.77; p =0.0025

(B) 2-way ANOVA: A β effect F (1,20) = 10.95; p =0.0035, anti-TLR2 effect F (1,20) = 9.241; p =0.0065, Interaction effect F (1,20) = 5.892; p =0.0248

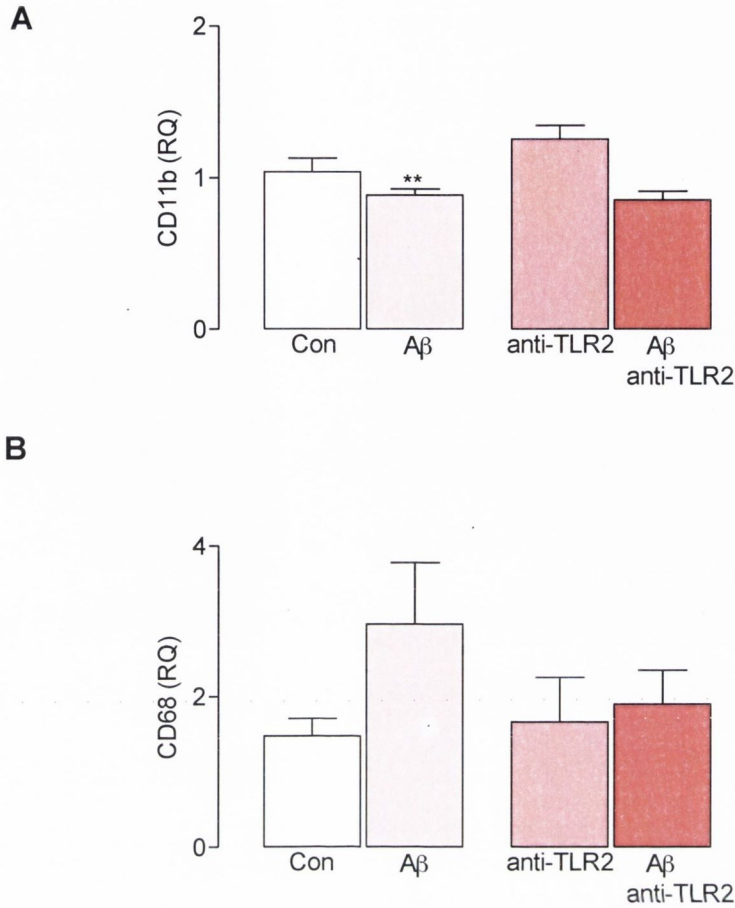


Figure 3.11. CD11b and CD68 mRNA expression was unaffected by A β _{1-40/1-42} or anti-TLR2.

Incubation of mixed glia in the presence of A β _{1-40/1-42} (10 μ M; 24 hours) significantly decreased CD11b mRNA expression (A) (** p <0.01, ANOVA) whereas CD68 mRNA expression was unaffected (B). Anti-TLR2 incubation (2.5 μ g/ml; 2 hours) had no significant effect on the mRNA expression of either CD11b or CD68 (A and B). Values are expressed as means \pm SEM (n=5-6).

(A) 2-way ANOVA: A β effect $F(1,120) = 14.19$; $p=0.0012$, anti-TLR2 effect $F(1,20) = 1.574$; $p=0.2240$, Interaction effect $F(1,19) = 2.878$; $p=0.1053$

(B) 2-way ANOVA: A β effect $F(1,17) = 2.108$; $p=0.1648$, anti-TLR2 effect $F(1,17) = 0.5450$; $p=0.4704$, Interaction effect $F(1,17) = 1.104$; $p=0.3081$

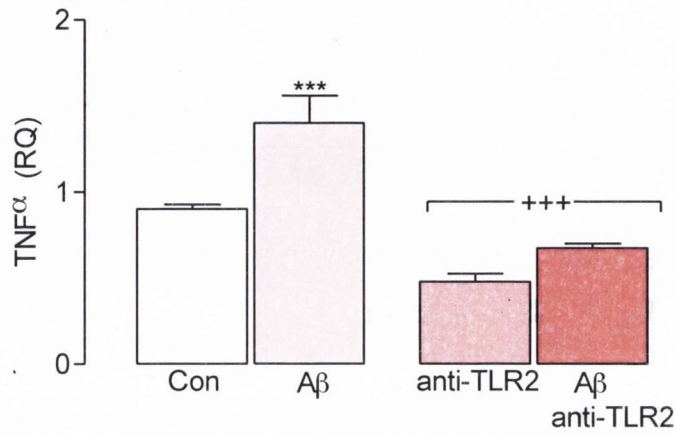


Figure 3.12. The Aβ-induced increase in TNFα mRNA expression was attenuated by anti-TLR2.

Incubation of mixed glia in the presence of Aβ_{1-40/1-42} (10 μM; 24 hours) significantly increased TNFα mRNA expression (**p<0.001, ANOVA). Incubation of mixed glia with anti-TLR2 (2.5 μg/ml; 2 hours) significantly decreased TNFα mRNA expression (***p<0.001, ANOVA). Values are expressed as means ± SEM (n=6).

2-way ANOVA: Aβ effect F (1,20) = 16.63; p=0.0006, anti-TLR2 effect F (1,20) = 45.58; p<0.0001, Interaction effect F (1,20) = 3.155; p=0.0909

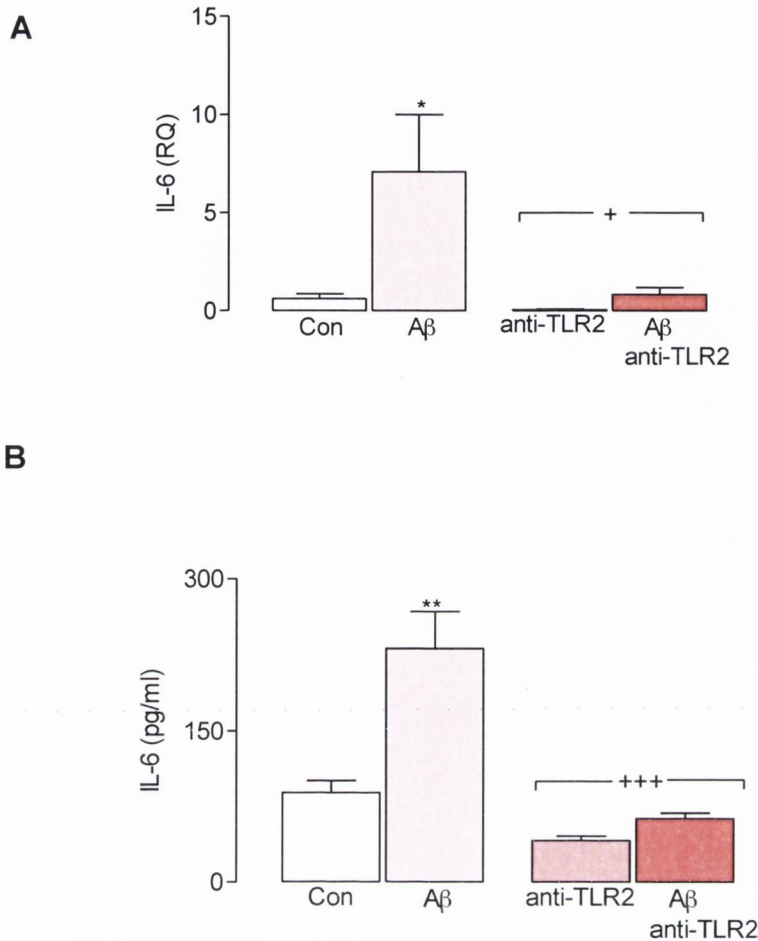


Figure 3.13. The A β -induced increase in IL-6 production was attenuated by anti-TLR2.

Incubation of mixed glia in the presence of A $\beta_{1-40/1-42}$ (10 μ M; 24 hours) significantly increased IL-6 mRNA expression (A) and supernatant concentration (B) (* p <0.05, ** p <0.01, ANOVA). Incubation of mixed glia with anti-TLR2 (2.5 μ g/ml; 2 hours) significantly decreased IL-6 mRNA expression (A) and supernatant concentration (B) (⁺ p <0.05, ⁺⁺⁺ p <0.001, ANOVA). A significant interaction between A $\beta_{1-40/1-42}$ and anti-TLR2 pre-incubation on IL-6 supernatant concentrations was observed (B) (⁺⁺ p <0.01, ANOVA). Values are expressed as means \pm SEM (n=4-6).

(A) 2-way ANOVA: A β effect $F(1,19) = 5.462$; $p=0.0305$, anti-TLR2 effect $F(1,19) = 4.846$; $p=0.0403$, Interaction effect $F(1,19) = 3.400$; $p=0.0809$

(B) 2-way ANOVA: A β effect $F(1,12) = 17.62$; $p=0.0012$, anti-TLR2 effect $F(1,12) = 30.38$; $p=0.0001$, Interaction effect $F(1,12) = 9.540$; $p=0.0094$

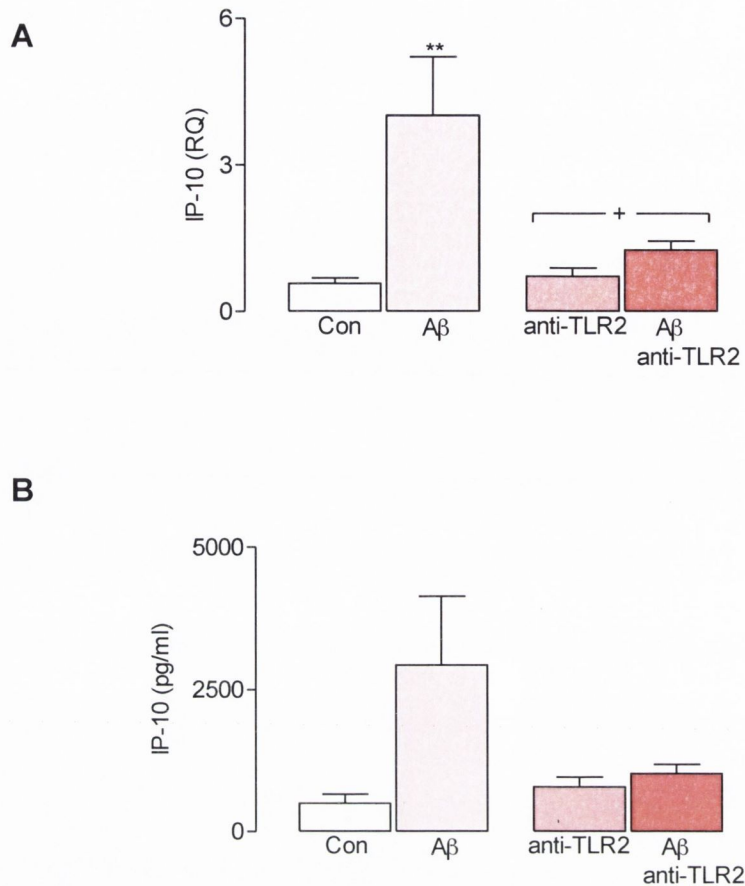


Figure 3.14. The A β -induced increase in IP-10 mRNA expression was attenuated by anti-TLR2.

Incubation of mixed glia in the presence of A $\beta_{1-40/1-42}$ (10 μ M; 24 hours) significantly increased IP-10 mRNA expression (A) (** p<0.01, ANOVA). Incubation of mixed glia with anti-TLR2 (2.5 μ g/ml; 2 hours) significantly decreased IP-10 mRNA expression (A) ($^{+}$ p<0.05, ANOVA), and a significant interaction between A $\beta_{1-40/1-42}$ and anti-TLR2 pre-incubation was observed (A) ($^{+}$ p<0.05, ANOVA). IP-10 supernatant concentrations (B) were unaltered following incubation of mixed glia in the presence of A $\beta_{1-40/1-42}$ with or without anti-TLR2 pre-incubation. Values are expressed as means \pm SEM (n=3-6).

(A) 2-way ANOVA: A β effect F (1,19) = 7.384; p=0.0014, anti-TLR2 effect F (1,19) = 5.975; p=0.0244, Interaction effect F (1,19) = 13.90; p=0.0137

(B) 2-way ANOVA: A β effect F (1,9) = 2.855; p=0.1254, anti-TLR2 effect F (1,9) = 1.055; p=0.3311, Interaction effect F (1,9) = 1.941; p=0.1970

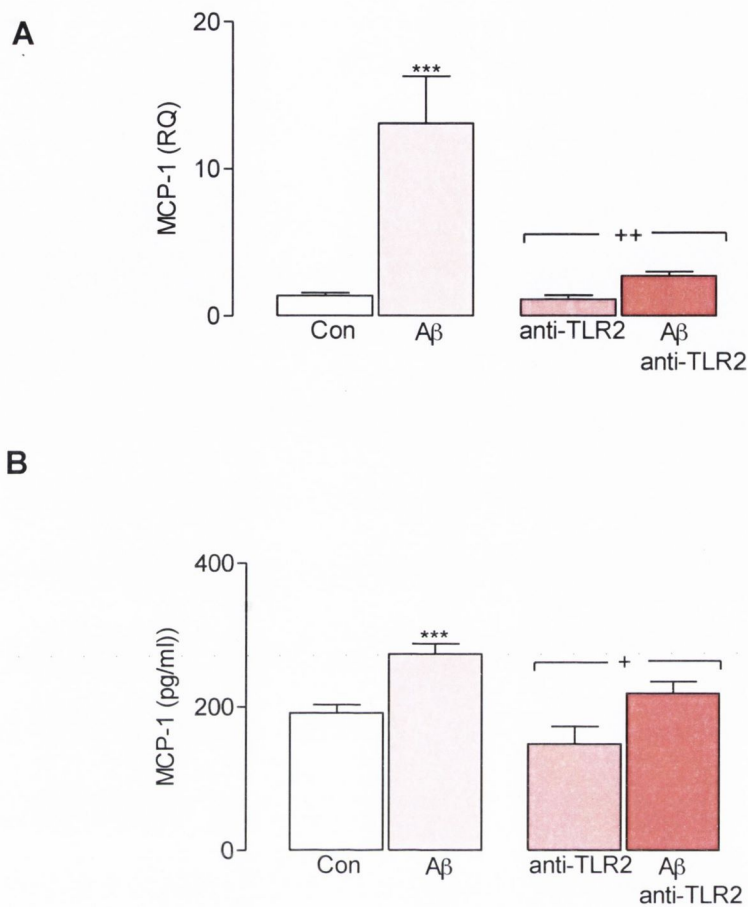


Figure 3.15. The A β -induced increase in MCP-1 production was attenuated by anti-TLR2.

Incubation of mixed glia in the presence of A $\beta_{1-40/1-42}$ (10 μ M; 24 hours) significantly increased MCP-1 mRNA expression (A) and supernatant concentration (B) (** p <0.001, ANOVA). Incubation of mixed glia with anti-TLR2 (2.5 μ g/ml; 2 hours) significantly decreased MCP-1 mRNA expression (A) and supernatant concentration (B) (** p <0.01, + p <0.05, ANOVA). A significant interaction between A $\beta_{1-40/1-42}$ and anti-TLR2 pre-incubation on MCP-1 mRNA expression was observed (A) (** p <0.01, ANOVA). Values are expressed as means \pm SEM (n=4-6).

(A) 2-way ANOVA: A β effect $F(1,19) = 22.59$; $p=0.0001$, anti-TLR2 effect $F(1,19) = 14.28$; $p=0.0013$, Interaction effect $F(1,19) = 13.02$; $p=0.0019$

(B) 2-way ANOVA: A β effect $F(1,12) = 19.16$; $p=0.0009$, anti-TLR2 effect $F(1,12) = 7.712$; $p=0.0167$, Interaction effect $F(1,12) = 0.1034$; $p=0.7533$

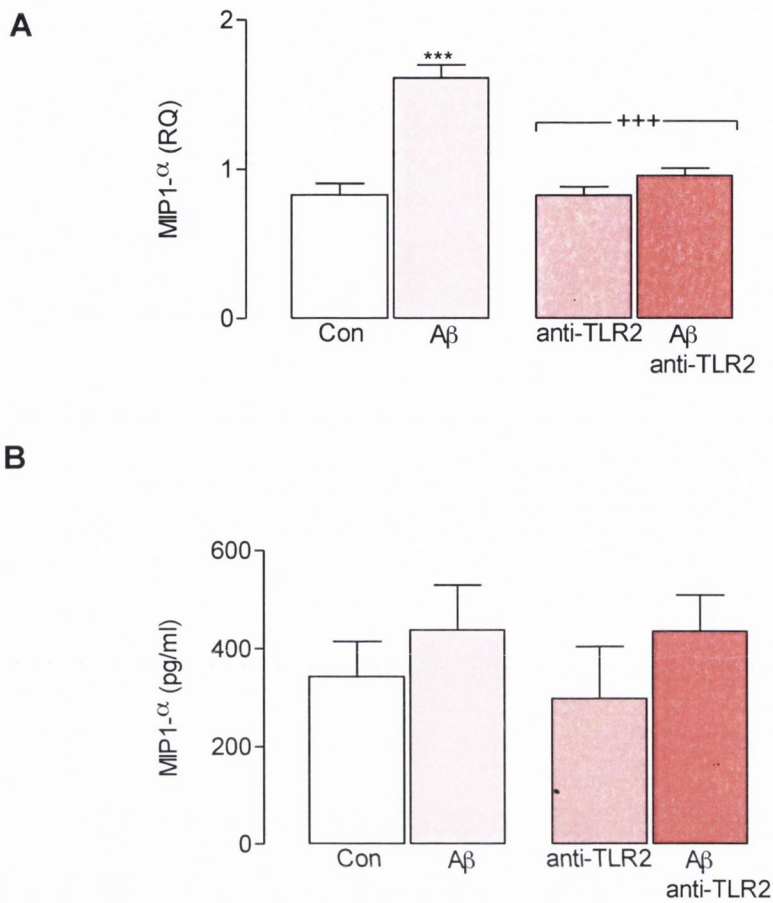


Figure 3.16. The A β -induced increase in MIP-1 α production was attenuated by anti-TLR2.

Incubation of mixed glia in the presence of A $\beta_{1-40/1-42}$ (10 μ M; 24 hours) significantly increased MIP-1 α mRNA expression (A) (** p <0.001, ANOVA). Incubation of mixed glia with anti-TLR2 (2.5 μ g/ml; 2 hours) significantly decreased MIP-1 α mRNA expression (A) (*** p <0.001, ANOVA) and a significant interaction between A $\beta_{1-40/1-42}$ and anti-TLR2 pre-incubation was observed (A) (*** p <0.001, ANOVA). MIP-1 α supernatant concentrations (B) were unaffected by incubation of mixed glia in A $\beta_{1-40/1-42}$ with or without anti-TLR2. Values are expressed as means \pm SEM (n=6-8).

(A) 2-way ANOVA: A β effect $F(1,20) = 43.48$; $p < 0.0001$, anti-TLR2 effect $F(1,20) = 22.59$; $p = 0.0001$, Interaction effect $F(1,20) = 222.14$; $p = 0.0001$

(B) 2-way ANOVA: A β effect $F(1,12) = 19.16$; $p = 0.0009$, anti-TLR2 effect $F(1,12) = 7.712$; $p = 0.0167$, Interaction effect $F(1,12) = 0.1034$; $p = 0.7533$

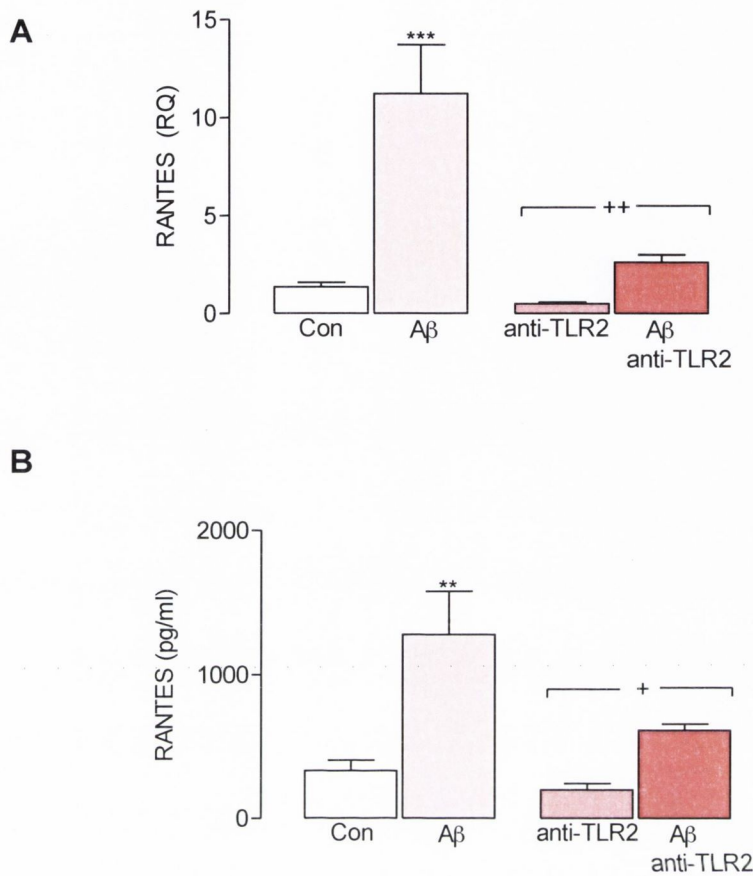


Figure 3.17. The A β -induced increase in RANTES production was attenuated by anti-TLR2.

Incubation of mixed glia in the presence of A $\beta_{1-40/1-42}$ (10 μ M; 24 hours) significantly increased RANTES mRNA expression (A) and supernatant concentration (B) (** p <0.001, * p <0.01, ANOVA). Incubation of mixed glia with anti-TLR2 (2.5 μ g/ml; 2 hours) significantly decreased RANTES mRNA expression (A) and supernatant concentration (B) (⁺⁺ p <0.01, ⁺ p <0.05, ANOVA). A significant interaction between A $\beta_{1-40/1-42}$ and anti-TLR2 pre-incubation on RANTES mRNA expression was observed (A) (⁺⁺ p <0.01, ANOVA). Values are expressed as means \pm SEM (n=4-6).

(A) 2-way ANOVA: A β effect $F(1,19) = 20.05$; $p=0.0003$, anti-TLR2 effect $F(1,19) = 12.50$; $p=0.0022$, Interaction effect $F(1,19) = 8.397$; $p=0.0092$

(B) 2-way ANOVA: A β effect $F(1,11) = 16.24$; $p=0.0020$, anti-TLR2 effect $F(1,11) = 5.598$; $p=0.0374$, Interaction effect $F(1,11) = 2.481$; $p=0.1436$

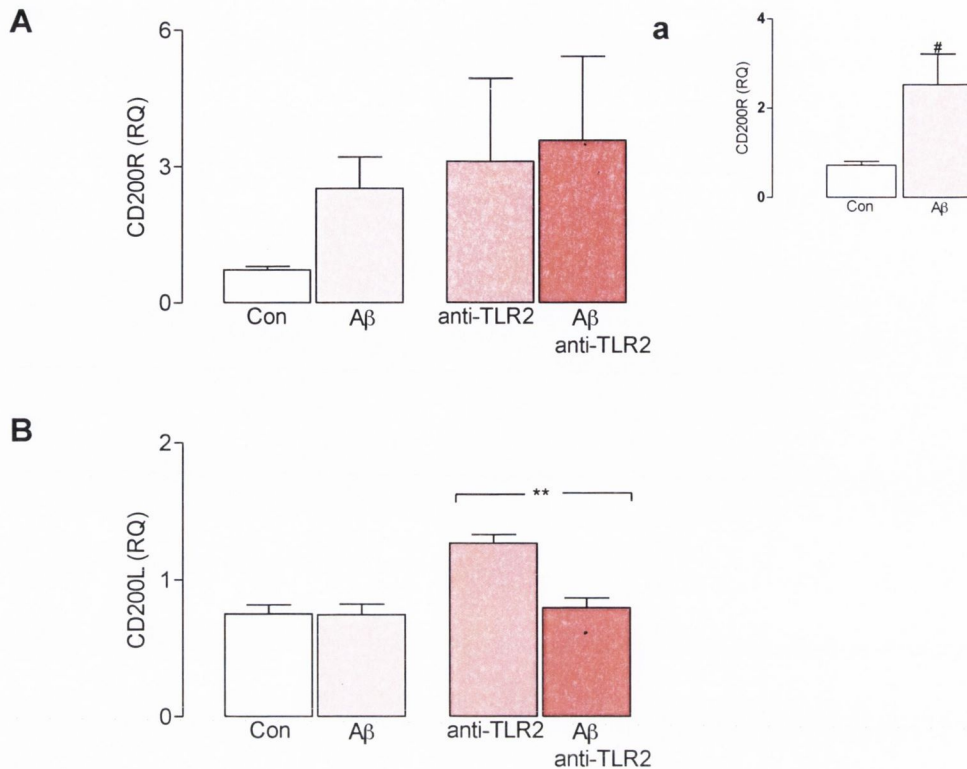


Figure 3.18. A β _{1-40/1-42} increased CD200R but not CD200L mRNA expression.

Incubation of mixed glia in the presence of A β _{1-40/1-42} (10 μ M; 24 hours) increased CD200R mRNA expression (A) ([#] $p < 0.05$, Student's *t*-test). Incubation of mixed glia with anti-TLR2 (2.5 μ g/ml; 2 hours) had no effect on CD200R mRNA expression (A). Incubation of mixed glia in the presence of A β _{1-40/1-42} (10 μ M; 24 hours) had no effect on CD200L mRNA expression (B). CD200L mRNA expression was significantly increased in mixed glia incubated with anti-TLR2 (B) (^{**} $p < 0.01$, ANOVA). A significant interaction between A β _{1-40/1-42} and anti-TLR2 pre-incubation was observed. A β _{1-40/1-42} incubation attenuated the significant anti-TLR2-induced increase in CD200L mRNA expression (B) (⁺⁺ $p < 0.01$, ANOVA) Values are expressed as means \pm SEM (n=6).

(A) 2-way ANOVA: A β effect $F(1,18) = 0.6840$; $p = 0.4190$, anti-TLR2 effect $F(1,18) = 1.594$; $p = 0.2229$, Interaction effect $F(1,18) = 0.2423$; $p = 0.6285$

(B) 2-way ANOVA: A β effect $F(1,18) = 15.29$; $p = 0.0010$, anti-TLR2 effect $F(1,18) = 10.78$; $p = 0.0041$, Interaction effect $F(1,18) = 10.37$; $p = 0.0047$

(a) [#] $p = 0.0425$; 0.7224 ± 0.08632 ; n=5 versus 2.525 ± 0.6870 ; n=6

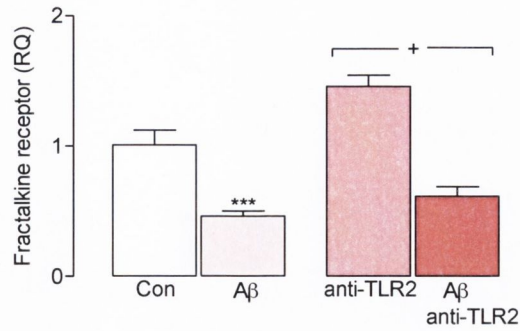
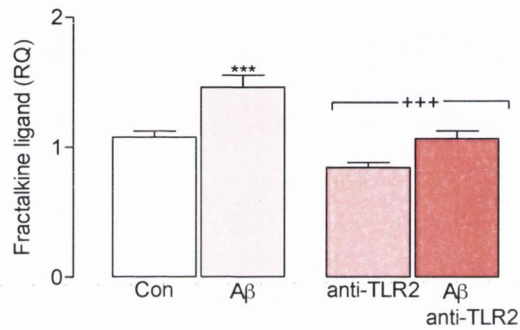
A**B**

Figure 3.19. A β _{1-40/1-42} exerted different effects on fractalkine receptor and fractalkine ligand mRNA expression.

Incubation of mixed glia in the presence of A β _{1-40/1-42} (10 μ M; 24 hours) significantly decreased mRNA expression of fractalkine receptor (A) (***p*<0.001, ANOVA). Incubation of mixed glia with anti-TLR2 (2.5 μ g/ml for 2 hours) significantly increased fractalkine receptor mRNA expression in mixed glia compared with controls (A) (⁺*p*<0.05, ANOVA). Incubation of mixed glia in the presence of A β _{1-40/1-42} (10 μ M; 24 hours) significantly increased mRNA expression of fractalkine ligand (B) (***p*<0.001, ANOVA). Incubation of mixed glia with anti-TLR2 (2.5 μ g/ml; 2 hours) significantly decreased fractalkine ligand mRNA expression (B) (⁺⁺⁺*p*<0.001, ANOVA). Values are expressed as means \pm SEM (n=6).

(A) 2-way ANOVA: A β effect *F* (1,19) = 38.39; *p*<0.0001, anti-TLR2 effect *F* (1,19) = 6.886; *p* = 0.0167, Interaction effect *F* (1,19) = 1.616; *p*=0.2191

(B) 2-way ANOVA: A β effect *F* (1,20) = 24.24; *p*<0.0001, anti-TLR2 effect *F* (1,20) = 26.12; *p*<0.0001, Interaction effect *F* (1,20) = 1.689; *p*=0.2085

3.4. Discussion

The aims of this study were to investigate changes induced by the TLR2 agonist Pam₃Csk₄ in mixed glia prepared from CD200^{-/-}, compared with wildtype, mice and to examine the role of the CD200-CD200R interaction in modulating microglial activation. To establish whether activation of TLR2 modulates Aβ-induced changes in these cells.

During neuroinflammation microglia become progressively more activated. This activation is associated with a morphological change and the upregulation of several cell surface markers including CD11b and CD40. These cell surface markers enable interaction with other cells like T cells to initiate an immune response but can also be used to measure the extent of microglial activation. Roy and colleagues (2008) reported that increased expression of CD11b correlates with the degree of microglial activation. Microglial stimulation by *S. aureus* and PGN, both of which activate TLR2, elevates expression of MHC class II, CD40, CD80 and CD86 (Kielian *et al.*, 2002). Furthermore, stimulation of microglial cultures with Pam₃Csk₄ leads to microglial morphological changes resulting in the more activated amoeboid form (Ebert *et al.*, 2005). In this study, Pam₃Csk₄ increased CD11b and CD40 mRNA expression in mixed glia prepared from wildtype and CD200^{-/-} mice yet no exaggerated increase was observed in glia prepared from CD200^{-/-} mice. Further, CD40 but not CD11b mRNA expression was increased in cells prepared from CD200^{-/-}, compared with wildtype, mice. These results are consistent with previous findings from this laboratory suggesting that CD200R engagement maintains microglia in a quiescent phenotype (Lyons *et al.*, 2007). CD68, a marker of phagocytic activity, has been found to be increased in CD200^{-/-} mice infected with EAE (Hoek *et al.*, 2000). CD68 mRNA expression was found to be decreased in mixed glia prepared from wildtype and CD200^{-/-} mice following Pam₃Csk₄ incubation. CD68 is a lysosomal protein and it appears to be cycled to the membrane when the cell is undergoing phagocytic activity. The expression of CD68 measured here was at the gene level and perhaps any changes in expression may have been observed at the protein level. Furthermore, the cells may be activated as measured by other markers (CD40 and CD11b) but simply not involved in phagocytosis.

TLR activation through differential pathogen-associated molecules leads to the activation of signalling cascades which result in the production of a tailored pro-inflammatory cytokine response (Jack *et al.*, 2005). Both microglia (Appelquist *et al.*, 2002) and astrocytes (Bowman *et al.*, 2003) are reported to express an array of TLRs including TLR2. Studies using human microglial and astrocyte cultures (Jack *et al.*, 2005) and murine microglial cultures (Shah *et al.*, 2009) found that TNF α and IL-6 concentrations were increased following Pam₃Csk₄ incubation. Du and co-authors (2011) demonstrated that Pam₃Csk₄ treatment significantly increased IL-6 production in brain homogenate samples from murine pups and this effect was significantly greater than that induced by LPS (Du *et al.*, 2011). Additionally, PGN, another TLR2 agonist, induces astrocytes to produce TNF α and IL-6 (Esen *et al.*, 2004). Here Pam₃Csk₄ increased the mRNA expression and release of TNF α and IL-6 from mixed glia prepared from wildtype and CD200^{-/-} mice and the effects were enhanced in glia prepared from CD200^{-/-}, compared with wildtype, mice. These results are consistent with previous studies from this laboratory and others which demonstrate an increase of IL-6 and TNF α in glial cultures in the absence of CD200 (Lyons *et al.*, 2007; Lyons *et al.*, 2009b). Studies using macrophages prepared from CD200^{-/-} animals have demonstrated increased IL-6 and TNF α levels in response to LPS (Snelgrove *et al.*, 2008). Furthermore, neutralizing the receptor-ligand interaction significantly amplifies IFN- γ induced IL-6 secretion in macrophages (Meuth *et al.*, 2008) whereas the use of DX109, a CD200R agonist, can inhibit IL-6 production from IFN- γ -stimulated bone-marrow derived macrophages (Copland *et al.*, 2007). In contrast it has been shown that macrophages from the colon of CD200R1^{-/-} mice do not have exacerbated TNF α production in response to TLR ligands compared with wildtype macrophages (Bain & Mowat, 2012). The discrepancy between studies in macrophages suggests that perhaps the CD200-CD200R interaction may not be a universal inhibitor of macrophage function and may have differential control mechanisms based on the microenvironment of the tissue.

Chemokines and their receptors are upregulated in neurodegenerative diseases and this probably contributes to increased infiltration of leukocytes into the brain and exacerbated inflammation (Mennicken *et al.*, 1999; Cartier *et al.*, 2005). Both microglia and astrocytes upregulate chemokine production following

TLR activation and cytokine stimulation (Okun *et al.*, 2009). There are several publications emphasizing the potency of Pam₃Csk₄ stimulation on chemokine secretion from various cell types. It has been demonstrated that human monocytes have increased secretion of MCP-1 following Pam₃Csk₄ stimulation (Dasu *et al.*, 2009). These authors found a significant increase in NF- κ B p65 dependent DNA binding activity in response to Pam₃Csk₄ which accounts for the large increase in cytokines and chemokines following TLR2 stimulation. A study by Gurley and colleagues (2008) investigating TLRs modulation by peroxisome proliferator-activated receptor (PPAR)- γ agonists revealed a similar increase in CXCL2 concentrations, a chemokine of the same family as IP-10, in murine astrocytes and microglia stimulated with Pam₃Csk₄ alone. This group also found an increase in MCP-1 concentrations in astrocytes and microglia treated with Pam₃Csk₄ compared with controls (Gurley *et al.*, 2008). Currently there are few publications on the impact of CD200 on chemokine production by microglia and astrocytes however, here it was found that Pam₃Csk₄ induced a significant increase in both MCP-1 and IP-10 mRNA expression, with enhanced MCP-1 mRNA expression and MCP-1 and IP-10 release in mixed glia prepared from CD200^{-/-}, compared with wildtype, mice. Previously it has been shown that a CD200R agonist can inhibit IFN- γ induced production of IP-10 and other chemokines in human monocytic cells (Jenmalm *et al.*, 2006). Inhibition of chemokines such as IP-10 would reduce recruitment of peripheral inflammatory cells such as neutrophils and Th1 cells to sites of inflammation (Proudfoot, 2002). This suggests that the loss of the CD200-CD200R inhibitory signal allows for increased chemokine production which may, in turn, facilitate increased inflammatory cell infiltration to sites of tissue damage.

Pam₃Csk₄ is a synthetic tripalmitoylated lipopeptide that is specifically recognized by a heterodimer of TLR2 and TLR1 (Takeda *et al.*, 2002; Du *et al.*, 2011). Previous studies have established that microglia constitutively express TLR2 (Laflamme *et al.*, 2001; Kielian *et al.*, 2002; Olson & Miller, 2004). TLR2 expression has been observed on human (Jack *et al.*, 2005) and murine (Kielian *et al.*, 2002) microglia cells. Several studies have demonstrated enhanced TLR2 and TLR1 expression following administration of TLR agonists including LPS (Laflamme *et al.*, 2001), *S. aureus* and PGN (Laflamme *et al.*, 2001; Kielian *et al.*, 2002). TLR2 and TLR1 mRNA expression was investigated in the present

study and the data shows that expression of both TLRs was increased in mixed glia prepared from wildtype and CD200^{-/-} mice in response to Pam₃Csk₄. There was no difference in TLR1 or TLR2 expression in mixed glia prepared from CD200^{-/-}, compared with wildtype, mice. However assessment of mRNA expression may not be a reflection of cell surface expression of the receptor therefore TLR2 surface expression on microglia prepared from wildtype and CD200^{-/-} mice was investigated. Flow cytometric analysis revealed that there was significantly greater surface expression of TLR2 on CD11b⁺ cells prepared from CD200^{-/-}, compared with wildtype, mice.

These data suggest that the greater response in glia prepared from CD200^{-/-}, compared with wildtype, mice to Pam₃Csk₄ may be due, at least in part, to the increased expression of TLR2. Taken together, the *in vitro* data suggests that enhanced activation seen in glia prepared from CD200^{-/-} mice may be due to both the absence of the CD200-CD200R interaction and also due to increased expression of TLR2 on CD200^{-/-} microglia. It is possible that increased expression of TLR2 on CD200^{-/-} microglia may allow for their over-activation and the increased inflammatory profile. CD200 is now implicated in the pathology of both neurodegenerative and autoimmune diseases. Thus the role of CD200 and its interaction with TLRs needs to be further investigated in an *in vivo* model as both these receptors may be targeted for therapeutic manipulation. The role of CD200-CD200R in an *in vivo* model is investigated in the next chapter.

A specific aim of this study was to investigate the role of TLR2 in mediating glial activation in responses to A β and development of a pro-inflammatory environment. While it is important for microglia to become “activated” resulting in an inflammatory environment for an effective response for elimination of pathogens, it is maladaptive when microglial activation is initiated by disease processes that originate within CNS and to date there is clear evidence implicating microglia in the pathogenesis of neurodegenerative diseases (Cameron & Landreth, 2010). It has been demonstrated that the extent of inflammation and the phenotype adopted by glial cells may rely on what receptors are activated and which inflammatory molecules are present at the time of stimulation. Increasing evidence now suggests that TLRs may play a significant role in the neuroinflammation seen in the pathogenesis of AD. Studies from mouse models of AD have found that TLR2 and TLR7 expression are upregulated (Letiembre *et*

al., 2009). TLR2 and TLR4 expression are increased in the post-mortem brain of AD patients (Walter *et al.*, 2007). Evidence from other studies have implicated TLRs and their co-receptor, CD14, in neurodegeneration (Liu *et al.*, 2005; Jana *et al.*, 2008; Udan *et al.*, 2008). Together, these studies suggest that the increase in TLRs may make them potential players in neurodegenerative mechanisms however, it is still unclear if TLRs activation is beneficial or detrimental. Several studies have established that microglia constitutively express TLR2 (Kielian, 2006) and that it becomes robustly upregulated on microglia during infection and disease (Glezer *et al.*, 2007). Here it was found that incubation of mixed glia in the presence of A β significantly increased TLR2 expression but not that of TLR4 or TLR1. The increase in TLR2 expression is consistent with a study from Jana and co-workers (2008) who similarly found increased TLR2 expression in both microglial cultures and BV-2 cell lines in response to A β . It is interesting that there was no change seen in TLR1 expression as a recent study by Liu and colleagues (2012) found that TLR2 interacting with TLR1, rather than TLR6, enhanced A β -triggered inflammation.

Previous investigators have found that cultured microglia deficient in CD14, TLR2 and TLR4 exhibit significantly reduced A β -induced microglial activation (Walter *et al.*, 2007; Jana *et al.*, 2008; Udan *et al.*, 2008; Reed-Geaghan *et al.*, 2009). Furthermore it has been demonstrated that A β -induced TLR2 expression, in microglial cultures, is associated with increases in markers of microglial activation (Jana *et al.*, 2008). Here it was found that A β increased the expression of CD40 and CD86 and this was attenuated by pre-treatment with anti-TLR2. CD68, a marker of phagocytosis, and CD11b, an integrin marker, were also investigated and it was found that CD68 expression was unchanged while CD11b was significantly decreased following A β -treatment. These results were a little surprising as both CD68 and CD11b have previously been found to be increased in microglial cultures in response to A β ₁₋₄₂ (Jana *et al.*, 2008). However, previously it has been described that ligation of CD40 significantly decreases phagocytosis of A β by microglia (Townsend *et al.*, 2005). It is possible that increases in CD40 and CD86 rather than CD68 suggest the cells have adopted an APC phenotype rather than a phagocytic phenotype. At present it still remains unclear under what circumstances and by what mechanism TLR activation may promote A β phagocytosis. Studies suggest that both TLR2 and TLR4 are involved

in the phagocytosis of A β . Chen and colleagues (2006) describe the internalisation of A β through TLR2 and TLR9 activation via the activation of the murine G-protein-coupled formyl peptide receptor 1 (mFPRL1). Similarly TLR4-induced A β phagocytosis requires mFPRL1 and can be blocked by the G-protein inhibitor pertussis toxin (Tahara *et al.*, 2006). Furthermore, investigators have found that murine microglial cultures (Chen *et al.*, 2006) and BV-2 cell lines increase A β uptake when stimulated with TLR2, TLR4 and TLR9 agonists (Tahara *et al.*, 2006). Conversely a recent study reports that microglia from TLR2-deficient mice phagocytose significantly more A β than cells from wildtype mice, (Liu *et al.*, 2012), suggesting that TLR2 activation by A β leads to a pro-inflammatory response rather than phagocytic response. Importantly caution has been suggested when interpreting some results as the discrepancies seen between studies may be due to the contamination of the A β preparation with bacterial components (Kielian, 2006). It is worth noting that previous reports suggest that both TLR2 and TLR4 are needed for A β -stimulated phagocytosis, (Reed-Geaghan *et al.*, 2009), and in the cultures used here no significant increase in TLR4 expression was observed which may account for the lack of change in CD68 expression.

There is a wealth of literature describing the production of cytokines and chemokines by glial cells following TLR ligation by an array of ligands (Jack *et al.*, 2005; Kielian, 2006). The recent appreciation that A β also acts as a ligand for TLRs may account, in part, for microglial responses to A β and the production of pro-inflammatory cytokines. The production and secretion of two pro-inflammatory cytokines was investigated and it was found that the A β -induced increases in TNF α expression and IL-6 expression and production were attenuated by anti-TLR2 treatment. Consistent with the present findings, previous studies have found that blocking TLR2 through antibodies (Udan *et al.*, 2008) and anti-sense knockdown (Jana *et al.*, 2008) prevents A β -induced IL-6 and TNF α production.

Under normal circumstances, chemokine expression within the CNS is low however several chemokines including MCP-1, IP-10, MIP-1 α and RANTES become unregulated during diverse pathological states including neurodegenerative diseases (Cartier *et al.*, 2005). The implications of chemokines in CNS pathologies such as MS and HIV has already been widely investigated. Both IP-10 and RANTES have been detected in CSF samples taken from MS

patients (Sorensen *et al.*, 1999) and increased MCP-1 (McManus *et al.*, 1998), RANTES (Sorensen *et al.*, 1999) and MIP-1 α (Simpson *et al.*, 1998) expression has been demonstrated in MS lesions. Furthermore, it has been found that antibodies against MIP-1 α reduced inflammation and inhibited development of symptoms in an adoptively-transfer model EAE while antibodies against MCP-1 inhibited relapses (Karpus & Kennedy, 1997). Similarly MCP-1 and MIP-1 α have been detected in the CNS of HIV patients (Conant *et al.*, 1998; McManus *et al.*, 2000). Although chemokines and their receptors were only thought to play a role in neurological disorders such as MS, there is now growing evidence to support the role of chemokines in AD (Cartier *et al.*, 2005). Previously it has been found that there is a marked IP-10 upregulation in reactive astrocytes in post-mortem brain tissue from AD patients and a frequent association between IP-10 positive astrocytes and amyloid deposits has been observed (Xia *et al.*, 2000). Furthermore, the presence of MCP-1 has been reported in mature senile plaques of brain tissue from AD patients (Ishizuka *et al.*, 1997). More recently IP-10 and MCP-1 levels have been found to be increased in CSF samples from AD patients (Galimberti *et al.*, 2003).

One aim was to investigate if TLR2 activation played a role in A β -induced production of chemokines. It was found that the A β -induced increase in the mRNA expression of the chemokines MCP-1, IP-10, MIP-1 α and RANTES was attenuated by anti-TLR2. At the protein level, A β -induced an increase in MCP-1 and RANTES supernatant concentrations and this was also ameliorated by anti-TLR2 although concentrations of IP-10 and MIP1- α were unchanged. These data are consistent with previous *in vitro* studies in astrocytes, oligodendrocytes and human monocytes which demonstrated an A β -induced increase in MCP-1, RANTES and MIP-1 α (Cartier *et al.*, 2005). However the finding that the A β -induced increases in chemokine expression was attenuated by anti-TLR2 treatment has not been demonstrated before. It is worth noting that A β increased CD40; CD40 has been associated with promoting increased chemokine secretion by microglia which in turn facilitates leukocyte infiltration and an amplified inflammatory process in HIV post-mortem brain tissue (D'Aversa *et al.*, 2002). One possibility is that the increase in CD40 and chemokine production would allow for peripheral cell infiltration in an *in vivo* setting resulting in exacerbated inflammation.

Numerous inhibitory receptors have been described on microglia and are therefore likely to be involved in immune responses (Mukhopadhyay *et al.*, 2010). Receptor-ligand interaction such as the CD200-CD200 receptor and the fractalkine-fractalkine receptor interactions are both implicated in “dampening” down the inflammatory response and aiding the return to homeostasis (Cameron & Landreth, 2010). Previous studies from this laboratory have found that CD200R is decreased in the brain with age (Lyons *et al.*, 2007) and also in APP/PS1 mice (unpublished observation). Walker and colleagues (2009) reported a decrease in both CD200 receptor and ligand in the AD brain (Walker *et al.*, 2009). The data presented here found that A β increased CD200R expression which was unchanged with anti-TLR2. A recent study using macrophages has suggested that TLRs induce the expression of CD200 receptor and CD200 ligand which in turn act as a feedback loop to control expression of TLRs (Mukhopadhyay *et al.*, 2010). Interestingly treatment of mixed glia with anti-TLR2 increased the expression of CD200L and this increase in CD200L was decreased in glia treated with anti-TLR2 and A β together.

Fractalkine is a transmembrane chemokine that exists in both soluble and membrane-bound forms and acts as a neuroimmune regulatory protein. Fractalkine acts *in vitro* as an anti-inflammatory molecule by downregulating the production of pro-inflammatory cytokines (Gemma *et al.*, 2010). Previous studies from this laboratory have reported that both soluble and membrane-bound fractalkine attenuates LPS-induced microglial activation. Furthermore age-related increases in microglial activation are accompanied by a decrease in fractalkine expression, and age-related microglial activation is attenuated in rats treated with fractalkine (Lyons *et al.*, 2009a). Here the effect of A β and anti-TLR2 on fractalkine and fractalkine receptor expression in mixed glia was investigated. Fractalkine receptor was found to be significantly decreased in response to A β -treatment and significantly increased by anti-TLR2. The opposite was seen for fractalkine ligand as it was increased in response to A β -stimulation and significantly decreased by anti-TLR2 treatment.

Together these data show that a significant part of the inflammatory response induced by A β in glia was due to TLR2 activation and blocking TLR2 dampens the development of a pro-inflammatory environment. At present it remains unclear if the activation of TLRs by A β contributes to, or inhibits AD

progression. It has been suggested that mild TLR activation may be beneficial in promoting A β uptake and clearance whereas excessive TLR activation may lead to accumulation of cytotoxic molecules like cytokines and reactive oxygen species (Okun *et al.*, 2009). The present data favour the latter proposal as anti-TLR2 attenuated the A β -induced cytokine and chemokine production in cultured cells. Furthermore, glia appeared to have adopted an APC phenotype rather than a phagocytic phenotype. Together the present findings and those of other research groups implicate TLR2 as a major player in neuroinflammation and suggest that targeting these receptors may have potential therapeutic benefits for the treatment of neuroinflammation in neurodegenerative diseases.

Table 3.1. Results summary of inflammatory markers assessed in mixed glia prepared from wildtype and CD200^{-/-} mice.

mRNA expression			
	Pam ₃ Csk ₄ effect	Genotype effect	Interaction effect
CD11b	↑↑↑		
CD40	↑↑↑	↑	
CD68	↓↓↓		
TNFα	↑↑↑		
IL-6	↑↑↑	↑	↑↑
MCP-1	↑↑↑	↑↑	↑
IP-10	↑↑↑		
TLR2	↑↑↑		
TLR1	↑↑↑		
Supernatant concentrations			
	Pam ₃ Csk ₄ effect	Genotype Effect	Interaction effect
TNFα	↑↑↑	↑↑↑	↑↑
IL-6	↑↑↑	↑↑↑	↑↑↑
MCP-1	↑↑↑	↑↑↑	↑↑
IP-10	↑↑↑	↑	↑

Table 3.2. Results summary of mRNA expression of inflammatory markers assessed in mixed glia treated with A β _{1-40/1-42} and anti-TLR2.

	A β _{1-40/42} effect	Anti-TLR2 effect	Interaction effect
CD86	↑		↓
CD40	↑↑	↓↓	↓↓
CD11b	↓↓		
CD68			
TNF α	↑↑↑	↓↓↓	
IL-6	↑	↓	
IP-10	↑↑	↓	↓
MCP1	↑↑↑	↓↓	↓↓
MIP-1 α	↑↑↑	↓↓↓	↓↓↓
RANTES	↑↑↑	↓↓	↓↓
CD200R	↑		
CD200L		↑↑	↓↓
Fractalkine receptor		↑	
Fractalkine ligand	↑↑↑	↓↓↓	
TLR2	↑↑	Not assessed	Not assessed
TLR4		Not assessed	Not assessed
TLR1		Not assessed	Not assessed

Table 3.3. Results summary of supernatant concentrations of cytokines and chemokines assessed in mixed glia treated with A β _{1-40/1-42} and anti-TLR2.

	A β _{1-40/42} effect	Anti-TLR2 effect	Interaction effect
IL-6	↑↑	↓↓↓	↓↓
IP-10			
MCP1	↑↑↑	↓	
MIP-1 α			
RANTES	↑↑	↓	

Chapter 4

Chapter 4

4.1. Introduction

Evidence from the previous chapter *in vitro*, which examined the effect of CD200-deficiency on Pam₃Csk₄-induced changes in glia and recent reports, have highlighted the importance of CD200-CD200R engagement in limiting the magnitude of inflammation and promoting inflammatory resolution. Markers of microglial activation, cytokine and chemokine expression and production have been shown to be increased in mixed glia prepared from CD200^{-/-}, compared with wildtype, mice. Indeed recent evidence from this laboratory has identified an exaggerated inflammatory response in mixed glia prepared from CD200^{-/-}, compared with wildtype, mice following both LPS and Pam₃Csk₄ stimulation (Costello *et al.*, 2011). Consistent with studies *in vitro* several studies in CD200^{-/-} mice (Hoek *et al.*, 2000; Snelgrove *et al.*, 2008) have demonstrated the importance of the CD200R as an inhibitory receptor in inflammation. The data has been consolidated by analysis of the effect of CD200R antibodies (Meuth *et al.*, 2008).

The aims of this study were to:

- Investigate *in vivo* the role of CD200 on inflammation and microglial activation following stimulation with a TLR2 agonist Pam₃Csk₄.
- Assess whether changes in TLR2 expression may be accountable for increased inflammation *in vivo* as seen *in vitro*.

4.2. Methods

Male and female C57BL/6 wildtype and CD200^{-/-} mice (2-3 months old) were randomly assigned to control or treatment groups (n=8). Mice were injected i.p. with either saline or Pam₃Csk₄ (100 µg/100 µl) and 5 hours later animals were anaesthetised with urethane (1.5 g/kg) and perfused intracardially with sterile ice-cold PBS (see section 2.5 for details). Brains were removed and hippocampal and cortical tissue was taken to determine mRNA expression of surface proteins by QPCR (see section 2.11 for details). The remainder of the brain tissue was harvested for microglial isolation by the 5 layer Percoll method (see section 2.8 for details) and markers of microglial activation were assessed by FACS (see section 2.9 for details). Data are expressed as means ± SEM. ANOVA was performed to determine whether significant differences existed between treatment groups and Bonferroni post-hoc test was applied where appropriate.

4.3. Results

4.3.1. Pam₃Csk₄ increased cytokine mRNA expression in hippocampal and cortical tissue prepared from wildtype and CD200^{-/-} mice.

The immunosuppressive role of the CD200-CD200R interaction was investigated *in vitro* in the previous chapter, here the same parameters were investigated *in vivo*. The results from the previous chapter demonstrated that mixed glia generated from CD200^{-/-} mice have an exaggerated inflammatory phenotype in response to Pam₃Csk₄ compared with mixed glia from wildtype mice. Thus it was hypothesised that i.p. injection of Pam₃Csk₄ would initiate an exaggerated cytokine response in CD200^{-/-}, compared with wildtype, mice. Pam₃Csk₄ treatment significantly increased mRNA expression of TNF α (** $p < 0.001$, ANOVA; Figure 4.1) and IL-1 β (** $p < 0.001$, ANOVA; Figure 4.2) in both hippocampal (Figure 4.1A and 4.2A) and cortical (Figure 4.1B and 4.2B) tissue prepared from wildtype and CD200^{-/-} mice. TNF α ($^{++}p < 0.01$, ANOVA; Figure 4.1A) and IL-1 β ($^{+}p < 0.05$, ANOVA; Figure 4.2A) mRNA expression was significantly increased in hippocampal tissue prepared from CD200^{-/-}, compared with wildtype, mice. Further analysis of the data revealed a significant interaction between Pam₃Csk₄ treatment and genotype ($^{++}p < 0.01$, $^{+}p < 0.05$, ANOVA; Figure 4.1A and 4.2A). In contrast, in the cortex there was no significant change in mRNA expression of TNF α (Figure 4.1B) or IL-1 β (Figure 4.2B) in tissue prepared from CD200^{-/-}, compared with wildtype, mice and no interaction was observed.

Pam₃Csk₄ induced a significant increase in the mRNA expression of IL-6 in both hippocampal (** $p < 0.001$, ANOVA; Figure 4.3A) and cortical ($^{*}p < 0.05$, ANOVA; Figure 4.3B) tissue prepared from wildtype and CD200^{-/-} mice. IL-6 mRNA expression was not significantly changed in hippocampal (Figure 4.3A) tissue prepared from CD200^{-/-}, compared with wildtype, mice. IL-6 mRNA expression was significantly decreased in cortical tissue prepared from CD200^{-/-}, compared with wildtype, mice ($^{+}p < 0.05$, ANOVA; Figure 4.3B). There was no significant interaction observed between Pam₃Csk₄ treatment and genotype in either hippocampal (Figure 4.3A) or cortical (Figure 4.3B) tissue.

4.3.2. Pam₃Csk₄ increased chemokine mRNA expression in hippocampal and cortical tissue prepared from wildtype and CD200^{-/-} mice.

Expression of chemokines, IP-10, MIP-1 α , MCP-1 and RANTES was assessed in hippocampal and cortical tissue harvested from wildtype and CD200^{-/-} mice following Pam₃Csk₄ treatment. Pam₃Csk₄ treatment significantly increased mRNA expression of IP-10 (***p*<0.001, ANOVA; Figure 4.4) and MIP-1 α (***p*<0.001, ANOVA; Figure 4.5) in both hippocampal (Figure 4.4A and 4.5A) and cortical (Figure 4.4B and 4.5B) tissue prepared from wildtype and CD200^{-/-} mice. IP-10 mRNA expression was increased in hippocampal (⁺*p*<0.05, ANOVA; Figure 4.4A) and cortical (⁺*p*<0.05, ANOVA; Figure 4.5B) tissue prepared from CD200^{-/-}, compared with wildtype, mice. MIP-1 α mRNA expression was increased in hippocampal (⁺*p*<0.05, ANOVA; Figure 4.5A), but not cortical (Figure 4.5B), tissue prepared from CD200^{-/-}, compared with wildtype, mice. Further analysis of the data revealed a significant interaction between Pam₃Csk₄ treatment and genotype on mRNA expression of IP-10 (⁺*p*<0.05, ANOVA; Figure 4.4A) and MIP-1 α (⁺*p*<0.05, ANOVA; Figure 4.5A) in hippocampal tissue. In cortical tissue there was no significant interaction observed between Pam₃Csk₄ treatment and genotype on mRNA expression of either IP-10 (Figure 4.4) or MIP-1 α (Figure 4.5).

Pam₃Csk₄ treatment significantly increased mRNA expression of MCP-1 (Figure 4.6) and RANTES (Figure 4.7) in both hippocampal (***p*<0.001, ANOVA; Figure 4.6A and 4.7A) and cortical (***p*<0.001, ***p*<0.01, ANOVA Figure 4.6B and 4.7B) tissue prepared from wildtype and CD200^{-/-} mice. Neither mRNA expression of MCP-1 (Figure 4.6) nor RANTES (Figure 4.7) was further increased in hippocampal (Figure 4.6A and 4.7A) or cortical (Figure 4.6B and 4.7B) tissue prepared from CD200^{-/-}, compared with wildtype, mice. No significant interaction was observed between Pam₃Csk₄ treatment and genotype on mRNA expression of either MCP-1 (Figure 4.6) or RANTES (Figure 4.7) in hippocampal (Figure 4.6A and 4.7A) and cortical (Figure 4.6B and 4.7B) tissue.

4.3.3. Pam₃Csk₄ increased TLR mRNA expression in hippocampal and cortical tissue prepared from wildtype and CD200^{-/-} mice.

Evidence from the literature suggests that TLR2 works in conjunction with TLR1 to recognise triacylated lipoproteins, such as Pam₃Csk₄, to exert a pro-inflammatory response. In the previous chapter it was found that that expression of TLR2 on CD11b⁺ cells was significantly increased in cells prepared from CD200^{-/-}, compared with wildtype, mice. Furthermore Pam₃Csk₄ treatment was found to increase both mRNA expression of TLR2 and TLR1 in mixed glia prepared from both wildtype and CD200^{-/-} mice. Here expression of TLR2 was assessed in whole brain tissue by FACS analysis and QPCR in hippocampal and cortical tissue harvested from wildtype and CD200^{-/-} mice following Pam₃Csk₄ treatment. FACS analysis revealed that Pam₃Csk₄ treatment had no significant effect on TLR2 expression on CD11b⁺ cells prepared from wildtype and CD200^{-/-} mice (Figure 4.8B). There was an apparent, but not significant, increase in TLR2 expression on CD11b⁺ cells prepared from CD200^{-/-} mice (Figure 4.8B). Further analysis of TLR2 expression by QPCR revealed that Pam₃Csk₄ treatment significantly increased mRNA expression of TLR2 in both hippocampal (**p<0.001, ANOVA; Figure 4.9A) and cortical (**p<0.001, ANOVA; Figure 4.9B) tissue prepared from wildtype and CD200^{-/-} mice. TLR2 mRNA expression was not further increased in hippocampal (Figure 4.9A) or cortical (Figure 4.9B) tissue prepared from CD200^{-/-}, compared with wildtype, mice and no significant interaction was observed between Pam₃Csk₄ treatment and genotype in either hippocampal (Figure 4.9A) or cortical (Figure 4.9B) tissue.

Pam₃Csk₄ treatment significantly increased mRNA expression of TLR1 in both hippocampal (**p<0.001, ANOVA; Figure 4.10A) and cortical (**p<0.001, ANOVA; Figure 4.10B) tissue prepared from wildtype and CD200^{-/-} mice. TLR1 mRNA expression was unaltered in hippocampal tissue (Figure 4.10A) but significantly decreased in cortical (+p<0.05, ANOVA; Figure 4.10B) tissue prepared from CD200^{-/-}, compared with wildtype, mice. No significant interaction was observed between Pam₃Csk₄ treatment and genotype in either hippocampal (Figure 4.10A) or cortical (Figure 4.10B) tissue.

4.3.4. Markers of microglial activation were differentially altered in hippocampal and cortical tissue prepared from wildtype and CD200^{-/-} mice.

There is a wealth of literature demonstrating that CD200 contributes to maintaining microglia in a quiescent state (Barclay *et al.*, 2002; Lyons *et al.*, 2007) and it has been established that CD200^{-/-} mice have increased microglial activation in models of disease (Hoek *et al.*, 2000). Expression of markers of microglial activation were assessed in whole brain tissue by FACS analysis and QPCR in hippocampal and cortical tissue harvested from wildtype and CD200^{-/-} mice following Pam₃Csk₄ treatment. FACS analysis revealed that Pam₃Csk₄ treatment had no significant effect on MHC class II (Figure 4.11B) and CD40 (Figure 4.11C) expression on CD11b⁺ cells prepared from wildtype and CD200^{-/-} mice (Figure 4.8B). There was a significant increase in MHC class II expression on CD11b⁺ cells prepared from CD200^{-/-} mice compared with wildtype mice (***) ($p < 0.0001$, ANOVA; Figure 4.11B). There was no significant change reported in CD40 expression on CD11b⁺ cells prepared from CD200^{-/-} mice compared with wildtype mice (Figure 4.11C). No significant interaction was observed between Pam₃Csk₄ treatment and genotype on the percentage expression of either MHC class II (Figure 4.11B) or CD40 (Figure 4.11C) on CD11b⁺ cells. CD40 expression was also assessed in hippocampal and cortical tissue by QPCR. Pam₃Csk₄ treatment had no significant effect on mRNA expression of CD40 in either hippocampal (Figure 4.12A) or cortical (Figure 4.12B) tissue prepared from wildtype and CD200^{-/-} mice. In contrast to the findings *in vitro* in the previous chapter, mRNA expression of CD40 was significantly decreased in both hippocampal (** $p < 0.01$, ANOVA; Figure 4.12A) and cortical (** $p < 0.01$, ANOVA; Figure 4.12B) tissue prepared from CD200^{-/-}, compared with wildtype, mice. No significant interaction was observed between Pam₃Csk₄ treatment and genotype in either hippocampal (Figure 4.12A) or cortical (Figure 4.12B) tissue.

Pam₃Csk₄ treatment significantly increased mRNA expression of CD86 in hippocampal (***) ($p < 0.001$, ANOVA; Figure 4.13A), but not cortical (Figure 4.13B), tissue prepared from wildtype and CD200^{-/-} mice. Pam₃Csk₄ treatment had no effect on mRNA expression of CD68 in hippocampal and cortical tissue prepared from wildtype and CD200^{-/-} mice (Figure 4.14A and B). However both mRNA expression of CD86 (Figure 4.13) and CD68 (Figure 4.14) was

significantly decreased in hippocampal ($^{++}p<0.01$, $^*p<0.05$, ANOVA; Figure 4.13A and 4.14A) and cortical ($^{***}p<0.001$, ANOVA; Figure 4.13B and 4.14B) tissue prepared from CD200^{-/-}, compared with wildtype, mice. No significant interaction was observed between Pam₃Csk₄ treatment and genotype on either mRNA expression of CD86 (Figure 4.13) or CD68 (Figure 4.14) in hippocampal (Figure 4.13A and 4.14A) or cortical (Figure 4.13B and 4.14B) tissue.

Table 4.1 summarises the mRNA expression results and Table 4.2 summarises the FACS results.

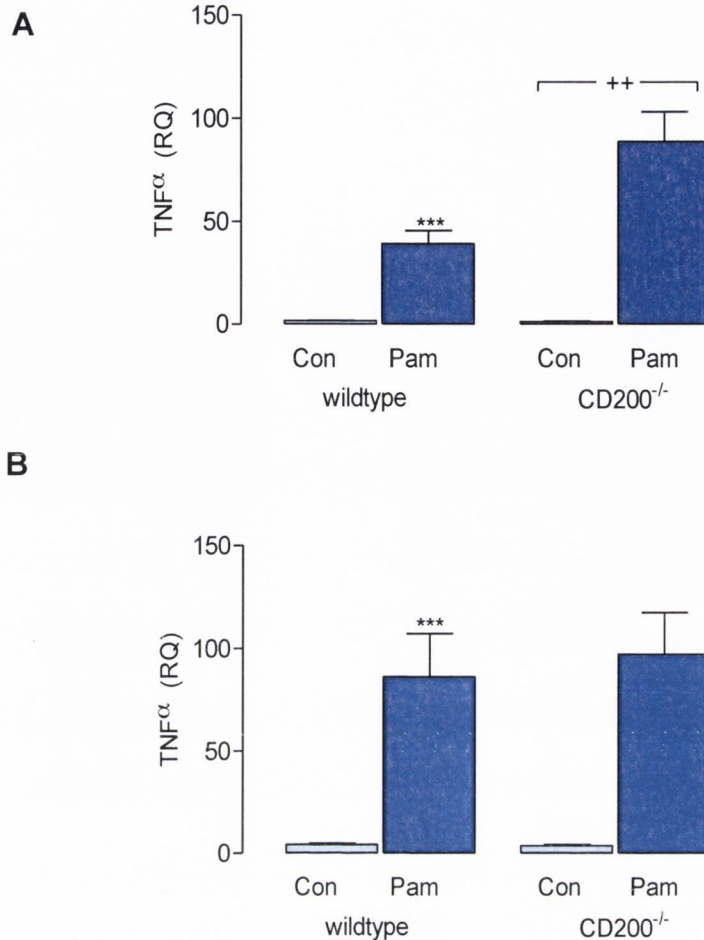


Figure 4.1. Pam₃Csk₄ increased TNF α mRNA expression in hippocampal and cortical tissue prepared from wildtype and CD200^{-/-} mice.

Wildtype and CD200^{-/-} mice received an i.p. injection of sterile saline (100 μ l) or Pam₃Csk₄ (100 μ g/ml). After 5 hours mice were perfused intracardially and sacrificed. Cortex and hippocampus was harvested for QPCR analysis. Pam₃Csk₄ treatment significantly increased TNF α mRNA expression in both hippocampal (A) and cortical (B) tissue prepared from wildtype and CD200^{-/-} mice (** p <0.001, ANOVA). TNF α mRNA expression (A) was significantly increased in hippocampal tissue prepared from CD200^{-/-}, compared with wildtype, mice (** p <0.01, ANOVA), and a significant interaction between Pam₃Csk₄ treatment and genotype was observed (A) (** p <0.01, ANOVA). Values are expressed as means \pm SEM (n=7-8).

(A) 2-way ANOVA: Pam₃Csk₄ effect F (1,25) = 52.48; p <0.0001, Genotype effect F (1,25) = 8.117; p = 0.0087, Interaction effect F (1,25) = 8.381; p =0.0078

(B) 2-way ANOVA: Pam₃Csk₄ effect F (1,24) = 36.34; p <0.0001, Genotype effect F (1,24) = 0.1261; p =0.7256, Interaction effect F (1,24) = 0.1563; p =0.6961

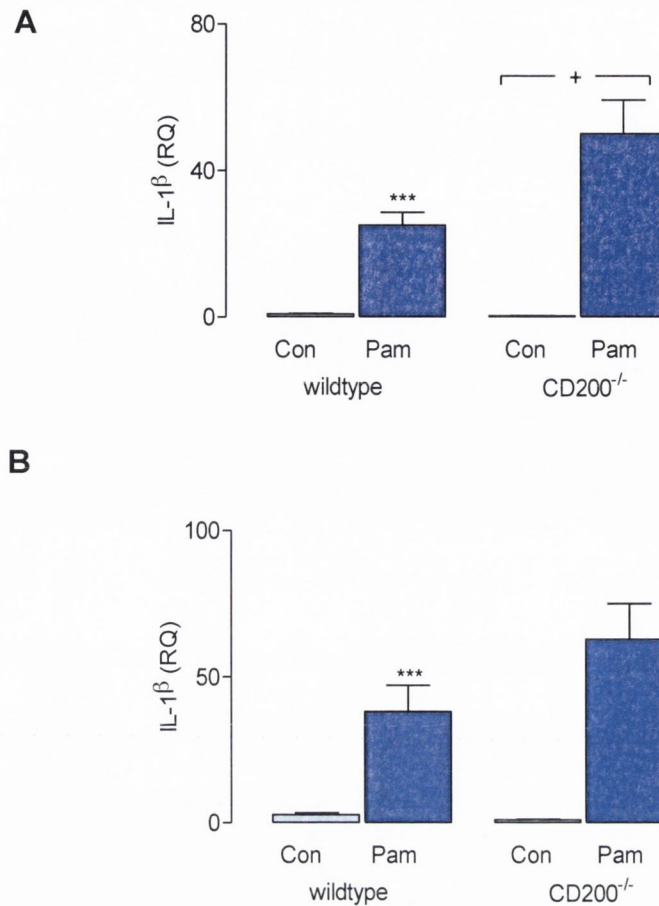


Figure 4.2. Pam₃Csk₄ increased IL-1 β mRNA expression in hippocampal and cortical tissue prepared from wildtype and CD200^{-/-} mice.

Hippocampal and cortical tissue was prepared from wildtype and CD200^{-/-} mice for QPCR analysis as described in Figure 4.1. Pam₃Csk₄ treatment significantly increased IL-1 β mRNA expression in both hippocampal (A) and cortical (B) tissue prepared from wildtype and CD200^{-/-} mice (***p*<0.001, ANOVA). IL-1 β mRNA expression was significantly increased in hippocampal (A) tissue prepared from CD200^{-/-}, compared with wildtype, mice (⁺*p*<0.05, ANOVA), and a significant interaction between Pam₃Csk₄ treatment and genotype was observed (A) (⁺*p*<0.05, ANOVA). Values are expressed as means \pm SEM (n=6-8).

(A) 2-way ANOVA: Pam₃Csk₄ effect F (1,25) = 47.30; *p*<0.0001, Genotype effect F (1,25) = 5.162; *p*= 0.0319, Interaction effect F (1,25) = 5.630; *p*=0.0257

(B) 2-way ANOVA: Pam₃Csk₄ effect F (1,25) = 39.93; *p*<0.0001, Genotype effect F (1,25) = 2.234; *p*=0.1475, Interaction effect F (1,25) = 2.985; *p*=0.0964

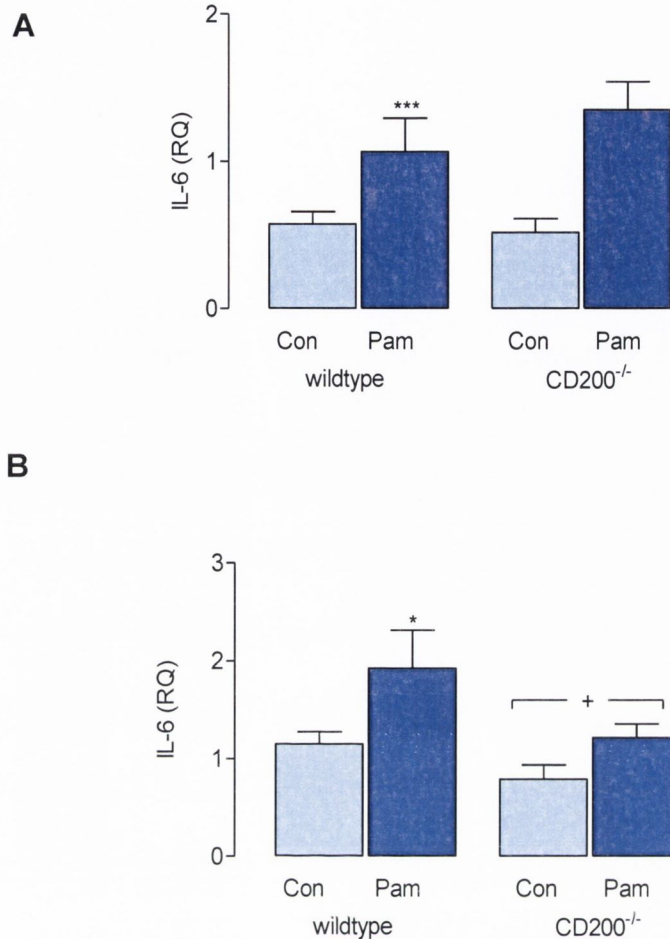


Figure 4.3. Pam₃Csk₄ increased IL-6 mRNA expression in hippocampal and cortical tissue prepared from wildtype and CD200^{-/-} mice.

Hippocampal and cortical tissue was prepared from wildtype and CD200^{-/-} mice for QPCR analysis as described in Figure 4.1. Pam₃Csk₄ treatment significantly increased IL-6 mRNA expression in both hippocampal (A) and cortical (B) tissue prepared from wildtype and CD200^{-/-} mice (***p*<0.001, **p*<0.05, ANOVA). IL-6 mRNA expression was significantly decreased in cortical (B) tissue prepared from CD200^{-/-}, compared with wildtype, mice (⁺*p*<0.05, ANOVA). Values are expressed as means ± SEM (n=6-8).

(A) 2-way ANOVA: Pam₃Csk₄ effect *F* (1,25) = 16.25; *p*=0.0005, Genotype effect *F* (1,25) = 0.4842; *p*= 0.4929, Interaction effect *F* (1,25) = 1.087; *p*=0.3072

(B) 2-way ANOVA: Pam₃Csk₄ effect *F* (1,23) = 6.452; *p*=0.0183, Genotype effect *F* (1,23) = 5.135; *p*=0.00332, Interaction effect *F* (1,23) = 0.5557; *p*=0.4635

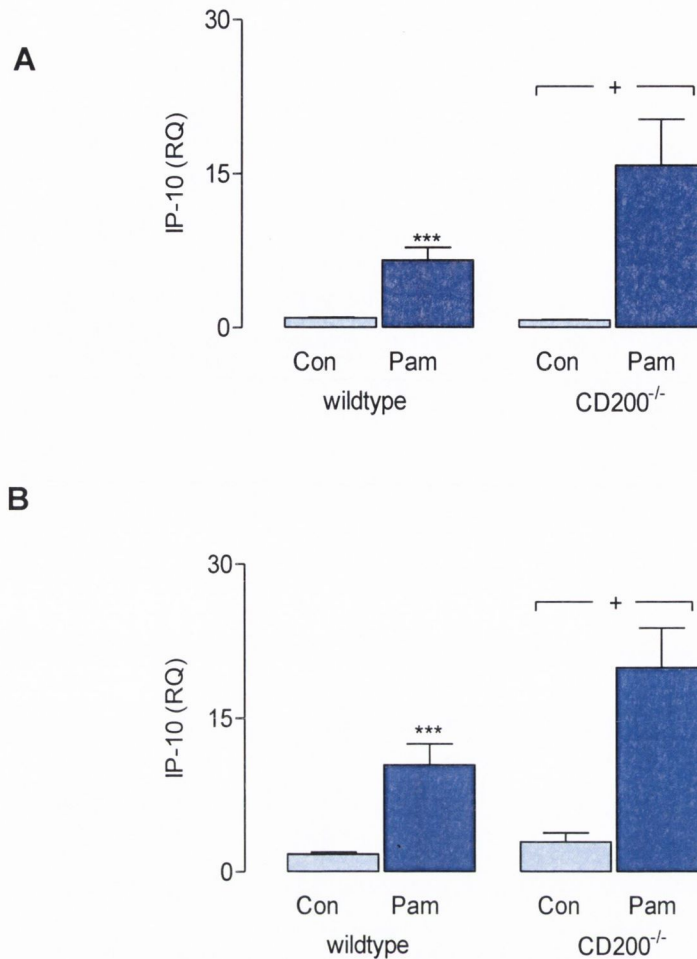


Figure 4.4. Pam₃Csk₄ increased IP-10 mRNA expression in hippocampal and cortical tissue prepared from wildtype and CD200^{-/-} mice.

Hippocampal and cortical tissue was prepared from wildtype and CD200^{-/-} mice for QPCR analysis as described in Figure 4.1. Pam₃Csk₄ treatment significantly increased IP-10 mRNA expression in both hippocampal (A) and cortical (B) tissue prepared from wildtype and CD200^{-/-} mice (***p*<0.001, ANOVA). IP-10 mRNA expression was significantly increased in hippocampal (A) and cortical (B) tissue prepared from CD200^{-/-}, compared with wildtype, mice (⁺*p*<0.05, ANOVA). A significant interaction between Pam₃Csk₄ treatment and genotype in hippocampal tissue was observed (A) (⁺*p*<0.05, ANOVA). Values are expressed as means ± SEM (n=6-8).

(A) 2-way ANOVA: Pam₃Csk₄ effect *F* (1,25) = 31.38; *p*<0.0001, Genotype effect *F* (1,25) = 4.052; *p*= 0.0550, Interaction effect *F* (1,25) = 4.459; *p*=0.0449

(B) 2-way ANOVA: Pam₃Csk₄ effect *F* (1,24) = 33.15; *p*<0.0001, Genotype effect *F* (1,24) = 5.733; *p*=0.0248, Interaction effect *F* (1,24) = 3.414; *p*=0.0770

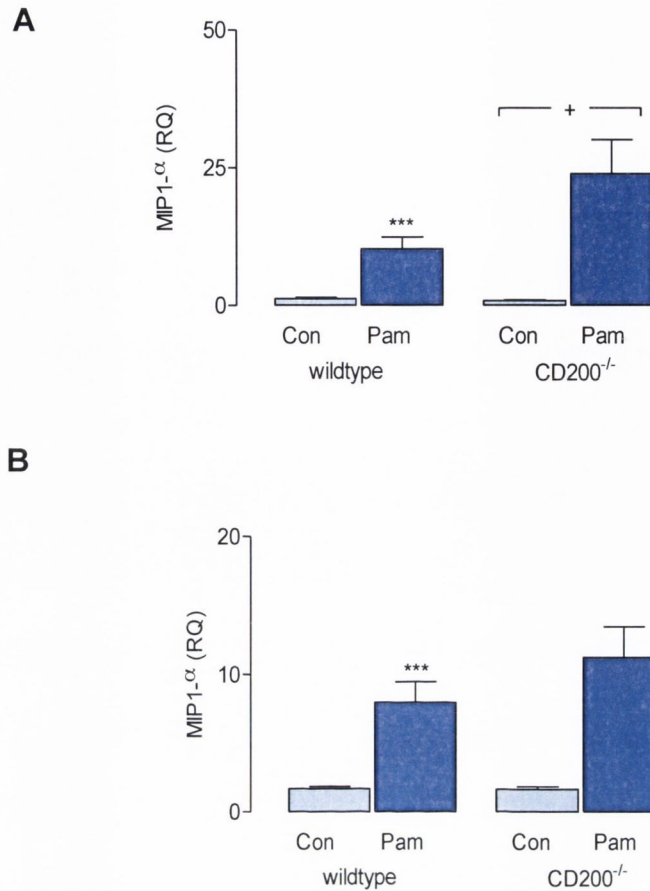


Figure 4.5. Pam₃Csk₄ increased MIP-1 α mRNA expression in hippocampal and cortical tissue prepared from wildtype and CD200^{-/-} mice.

Hippocampal and cortical tissue was prepared from wildtype and CD200^{-/-} mice for QPCR analysis as described in Figure 4.1. Pam₃Csk₄ treatment significantly increased MIP-1 α mRNA expression in both hippocampal (A) and cortical (B) tissue prepared from wildtype and CD200^{-/-} mice (***p*<0.001, ANOVA). MIP-1 α mRNA expression was significantly increased in hippocampal (A) tissue prepared from CD200^{-/-}, compared with wildtype, mice (⁺*p*<0.05, ANOVA), and a significant interaction between Pam₃Csk₄ treatment and genotype was observed (A) (⁺*p*<0.05, ANOVA). Values are expressed as means \pm SEM (n=7-8).

(A) 2-way ANOVA: Pam₃Csk₄ effect *F* (1,25) = 24.44; *p*<0.0001, Genotype effect *F* (1,25) = 4.206; *p*= 0.0509, Interaction effect *F* (1,25) = 4.672; *p*=0.0404

(B) 2-way ANOVA: Pam₃Csk₄ effect *F* (1,25) = 36.96; *p*<0.0001, Genotype effect *F* (1,25) = 1.516; *p*=0.2297, Interaction effect *F* (1,25) = 1.624; *p*=0.2143

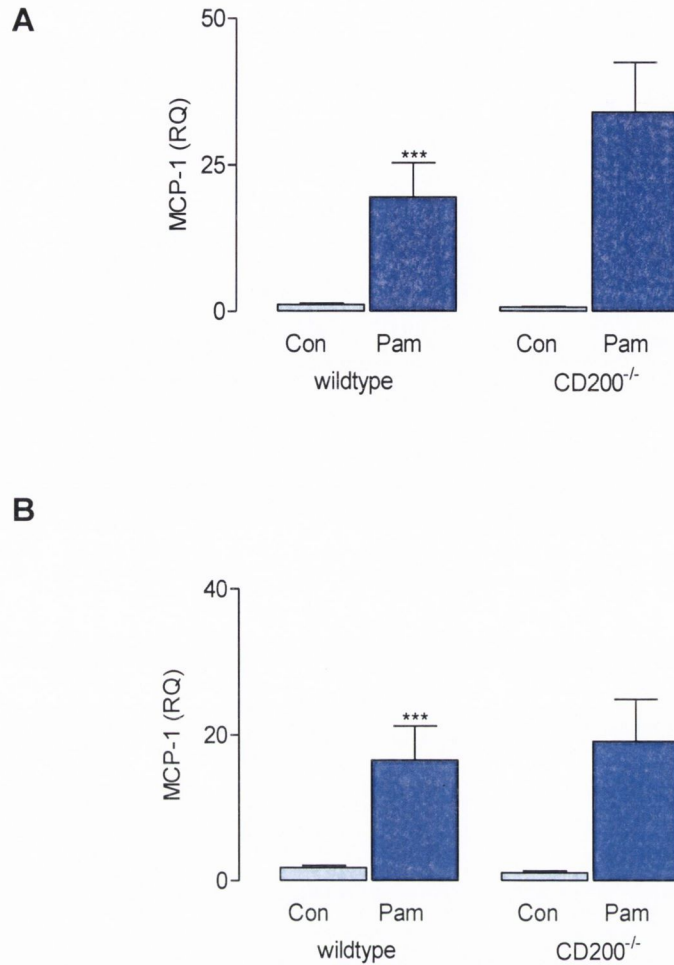


Figure 4.6. Pam₃Csk₄ increased MCP-1 mRNA expression in hippocampal and cortical tissue prepared from wildtype and CD200^{-/-} mice.

Hippocampal and cortical tissue was prepared from wildtype and CD200^{-/-} mice for QPCR analysis as described in Figure 4.1. Pam₃Csk₄ treatment significantly increased MCP-1 mRNA expression in hippocampal (A) and cortical (B) tissue prepared from wildtype and CD200^{-/-} mice (***p*<0.001, ANOVA). Values are expressed as means ± SEM (n=6-8).

(A) 2-way ANOVA: Pam₃Csk₄ effect *F* (1,24) = 21.82; *p*<0.0001, Genotype effect *F* (1,24) = 1.607; *p* = 0.2171, Interaction effect *F* (1,24) = 1.826; *p*=0.1892

(B) 2-way ANOVA: Pam₃Csk₄ effect *F* (1,24) = 19.45; *p*=0.0002, Genotype effect *F* (1,24) = 0.06390; *p*=0.8026, Interaction effect *F* (1,24) = 0.1939; *p*=0.6636

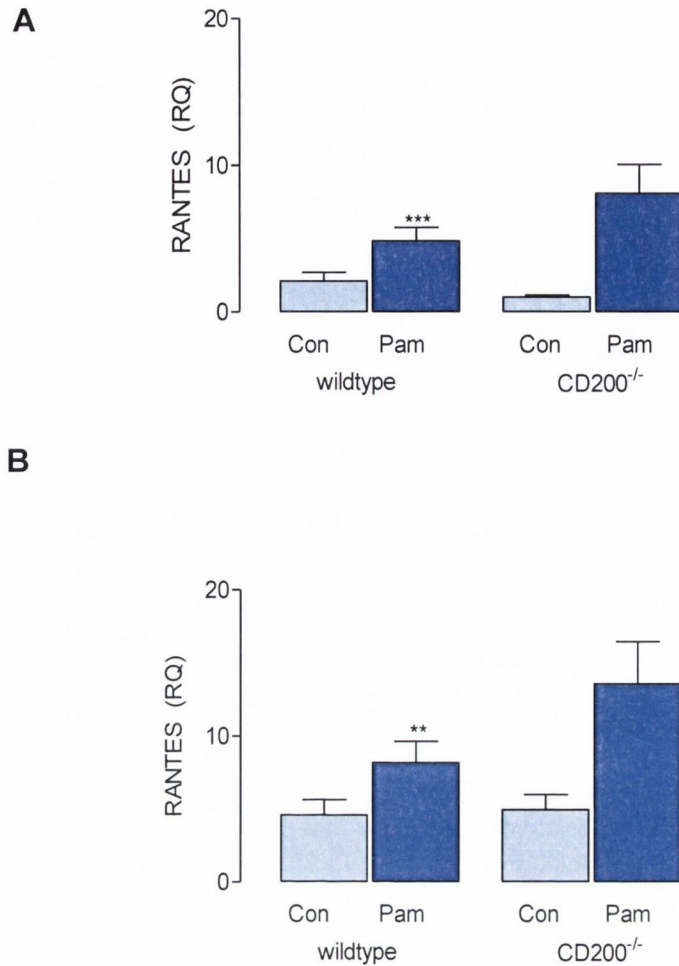


Figure 4.7. Pam₃Csk₄ increased RANTES mRNA expression in hippocampal and cortical tissue prepared from wildtype and CD200^{-/-} mice.

Hippocampal and cortical tissue was prepared from wildtype and CD200^{-/-} mice for QPCR analysis as described in Figure 4.1. Pam₃Csk₄ treatment significantly increased RANTES mRNA expression in hippocampal (A) and cortical (B) tissue prepared from wildtype and CD200^{-/-} mice (*** p<0.001, ** p<0.01, ANOVA). Values are expressed as means ± SEM (n=7-8).

(A) 2-way ANOVA: Pam₃Csk₄ effect F (1,24) = 18.95; p=0.0002, Genotype effect F (1,24) = 0.9015; p= 0.3519, Interaction effect F (1,24) = 3.729; p=0.0654

(B) 2-way ANOVA: Pam₃Csk₄ effect F (1,24) = 10.88; p=0.0030, Genotype effect F (1,24) = 2.728; p=0.1116, Interaction effect F (1,24) = 2.169; p=0.1538

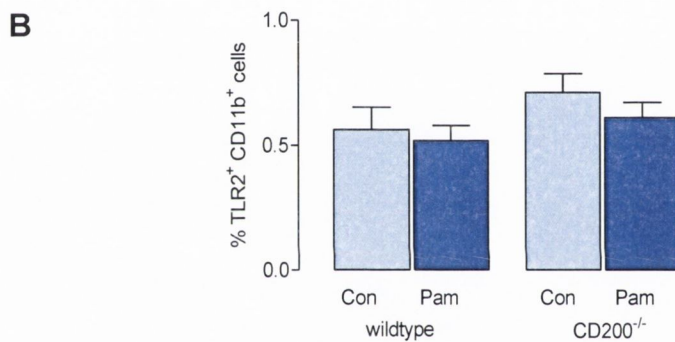
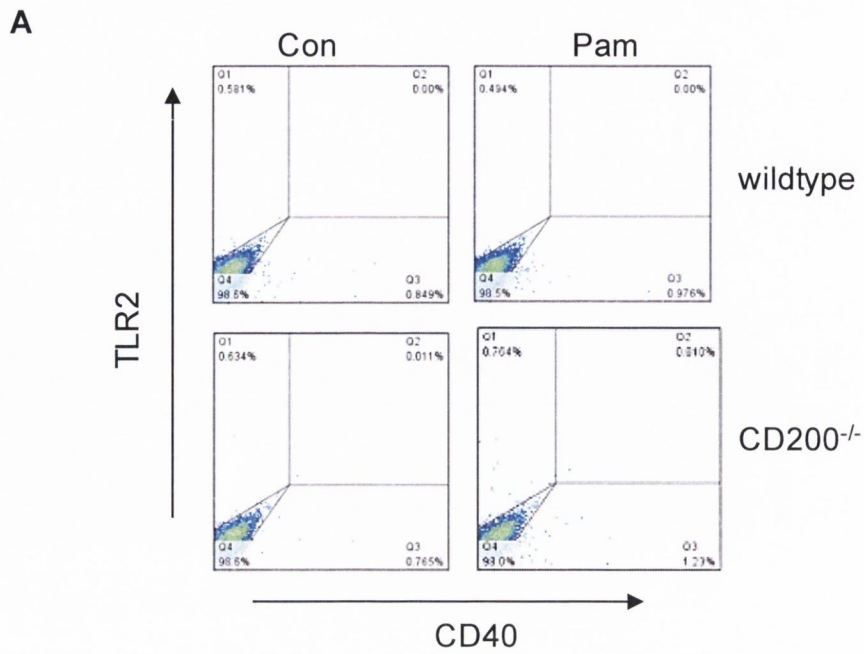


Figure 4.8. Pam₃Csk₄ treatment had no effect on the number of TLR2 expressing CD11b⁺ cells in wildtype and CD200^{-/-} mice.

Wildtype and CD200^{-/-} mice received an i.p. injection of sterile saline (100 μ l) or Pam₃Csk₄ (100 μ g/ml). After 5 hours mice were perfused intracardially and sacrificed. Over half the brain was harvested for percoll separation and microglial isolation for FACS analysis. TLR2 expression was assessed on CD11b⁺ cells. (A) Representative FACS plots. Pam₃Csk₄ treatment had no significant effect on TLR2 expression on CD11b⁺ cells prepared from wildtype and CD200^{-/-} mice (B). Values are expressed as means \pm SEM (n=7).

(B) 2-way ANOVA: Pam₃Csk₄ effect $F(1,23) = 1.010$; $p=0.3253$, Genotype effect $F(1,23) = 2.839$; $p=0.1055$, Interaction effect $F(1,23) = 0.1569$; $p=0.6957$

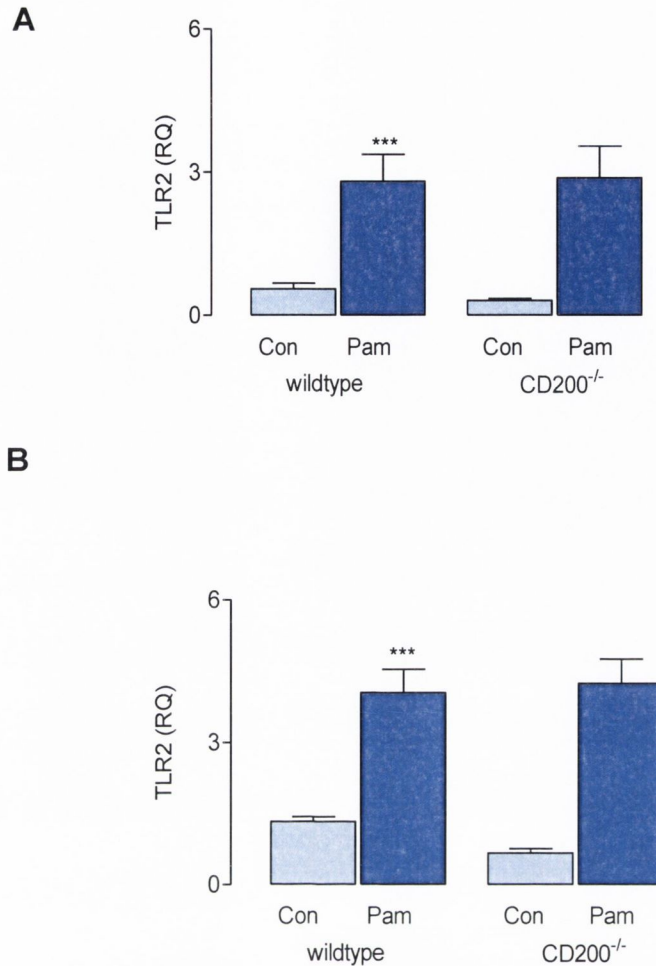


Figure 4.9. Pam₃Csk₄ increased TLR2 mRNA expression in hippocampal and cortical tissue prepared from wildtype and CD200^{-/-} mice.

Hippocampal and cortical tissue was prepared from wildtype and CD200^{-/-} mice for QPCR analysis as described in Figure 4.1. Pam₃Csk₄ treatment significantly increased TLR2 mRNA expression in hippocampal (A) and cortical (B) tissue prepared from wildtype and CD200^{-/-} mice (*** p<0.001, ANOVA). Values are expressed as means ± SEM (n=7-8).

(A) 2-way ANOVA: Pam₃Csk₄ effect F (1,24) = 27.51; p<0.0001, Genotype effect F (1,24) = 0.1575; p=0.6949, Interaction effect F (1,24) = 0.3265; p=0.5731

(B) 2-way ANOVA: Pam₃Csk₄ effect F (1,26) = 66.26; p<0.0001, Genotype effect F (1,26) = 0.3617; p=0.5528, Interaction effect F (1,26) = 1.260; p=0.2718

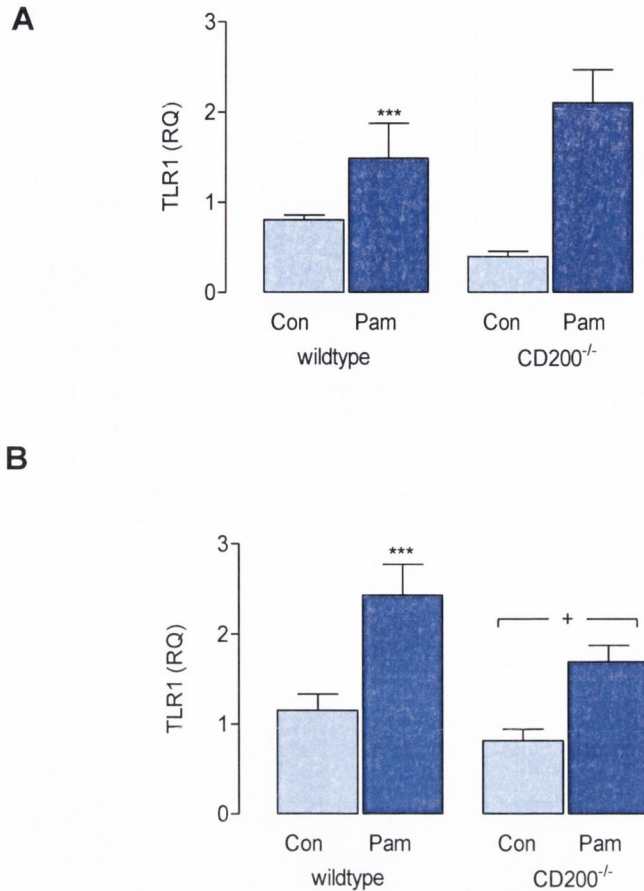


Figure 4.10. Pam₃Csk₄ increased TLR1 mRNA expression in hippocampal and cortical tissue prepared from wildtype and CD200^{-/-} mice.

Hippocampal and cortical tissue was prepared from wildtype and CD200^{-/-} mice for QPCR analysis as described in Figure 4.1. Pam₃Csk₄ treatment significantly increased TLR1 mRNA expression in both hippocampal (A) and cortical (B) tissue prepared from wildtype and CD200^{-/-} mice (**p<0.001, ANOVA). TLR1 mRNA expression was significantly decreased in cortical (B) tissue prepared from CD200^{-/-}, compared with wildtype, mice (+p<0.05, ANOVA). Values are expressed as means ± SEM (n=7-8).

(A) 2-way ANOVA: Pam₃Csk₄ effect F (1,23) = 19.70; p=0.0002, Genotype effect F (1,23) = 0.1513; p= 0.7009, Interaction effect F (1,23) = 3.635; p=0.0692

(B) 2-way ANOVA: Pam₃Csk₄ effect F (1,25) = 24.56; p<0.0001, Genotype effect F (1,25) = 6.118; p= 0.0205, Interaction effect F (1,25) = 0.8640; p=0.3615

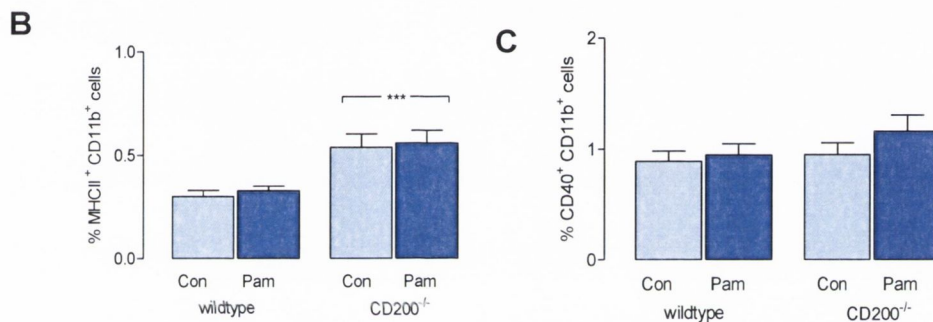
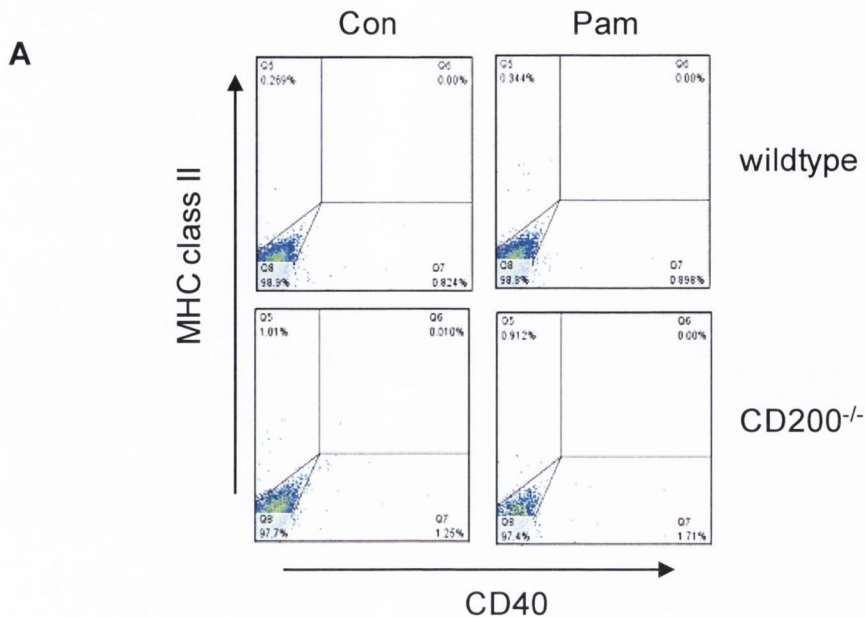


Figure 4.11. Pam₃Csk₄ treatment had no effect on the number of MHC class II and CD40 expressing CD11b⁺ cells in wildtype and CD200^{-/-} mice.

Brain tissue was prepared for FACS analysis from wildtype and CD200^{-/-} mice as described in Figure 4.8. (A) Representative FACS plots. Pam₃Csk₄ treatment had no significant effect on either MHC class II (B) or CD40 (C) expression on CD11b⁺ cells prepared from wildtype and CD200^{-/-} mice. There was a significant increase in MHC class II expression on CD11b⁺ cells prepared from CD200^{-/-} mice compared with wildtype mice (B) (***) p < 0.0001, ANOVA). Values are expressed as means ± SEM (n=7).

(A) 2-way ANOVA: Pam₃Csk₄ effect F (1,20) = 0.2674; p=0.6107, Genotype effect F (1,20) = 23.05; p= 0.0001, Interaction effect F (1,20) = 0.004691; p=0.9461

(B) 2-way ANOVA: Pam₃Csk₄ effect F (1,20) = 1.4447; p=0.2430, Genotype effect F (1,20) = 1.483; p= 0.2374, Interaction effect F (1,20) = 0.4682; p=0.5017

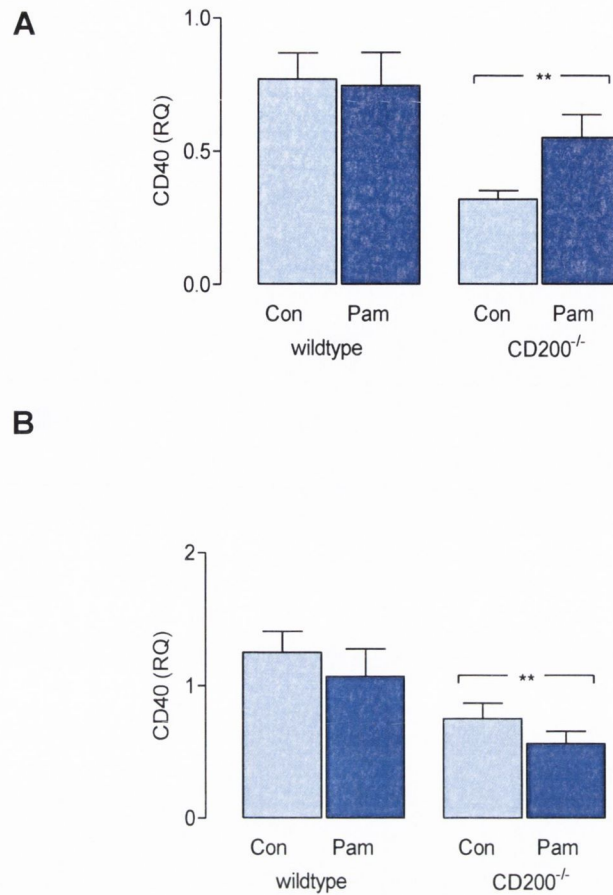


Figure 4.12. CD40 mRNA expression was decreased in hippocampal and cortical tissue prepared from CD200^{-/-} mice.

Hippocampal and cortical tissue was prepared from wildtype and CD200^{-/-} mice for QPCR analysis as described in Figure 4.1. Pam₃Csk₄ treatment had no significant effect on CD40 mRNA expression in either hippocampal (A) or cortical (B) tissue prepared from wildtype and CD200^{-/-} mice. CD40 mRNA expression was significantly decreased in both hippocampal (A) and cortical (B) tissue prepared from CD200^{-/-}, compared with wildtype, mice (**p<0.01, ANOVA). Values are expressed as means ± SEM (n=7-8).

(A) 2-way ANOVA: Pam₃Csk₄ effect F (1,28) = 1.299; p=0.2640, Genotype effect F (1,28) = 12.50; p= 0.0014, Interaction effect F (1,28) = 1.956; p=0.1729

(B) 2-way ANOVA: Pam₃Csk₄ effect F (1,24) = 1.497; p=0.2330, Genotype effect F (1,24) = 11.21; p= 0.0027, Interaction effect F (1,24) = 0.0003998; p=0.9842

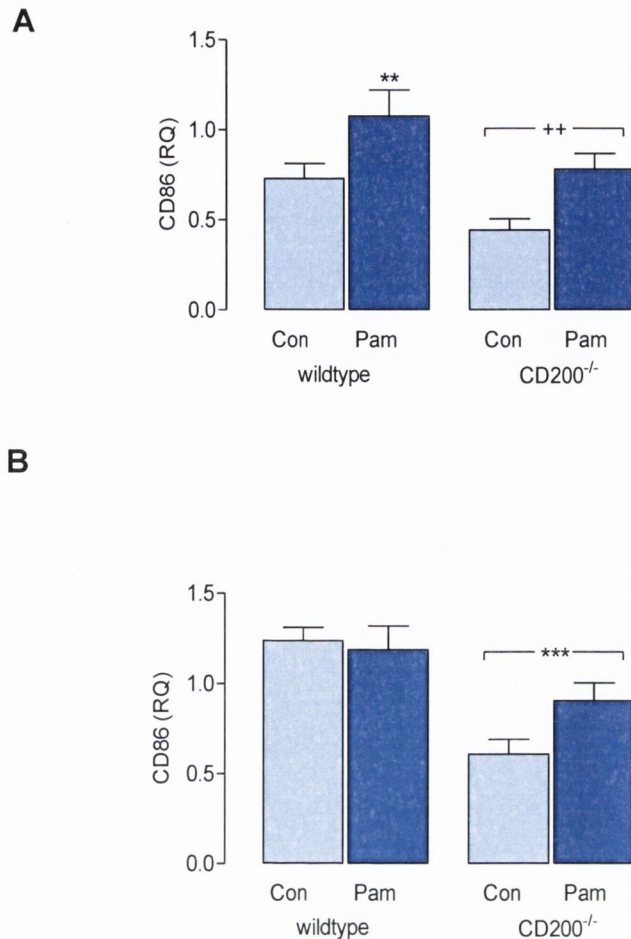


Figure 4.13. CD86 mRNA expression was decreased in hippocampal and cortical tissue prepared from CD200^{-/-} mice.

Hippocampal and cortical tissue was prepared from wildtype and CD200^{-/-} mice for QPCR analysis as described in Figure 4.1. Pam₃Csk₄ treatment significantly increased CD86 mRNA expression in hippocampal (A) tissue prepared from wildtype and CD200^{-/-} mice (** p<0.01, ANOVA). CD86 mRNA expression was significantly decreased in hippocampal (A) and cortical (B) tissue prepared from CD200^{-/-}, compared with wildtype, mice (++ p<0.01, *** p<0.001, ANOVA). Values are expressed as means ± SEM (n=7-8).

(A) 2-way ANOVA: Pam₃Csk₄ effect F (1,28) = 11.83; p=0.0018, Genotype effect F (1,28) = 8.411; p= 0.0072, Interaction effect F (1,28) = 0.0008686; p=0.9767

(B) 2-way ANOVA: Pam₃Csk₄ effect F (1,27) = 1.510; p=0.2297, Genotype effect F (1,27) = 20.55; p= 0.0001, Interaction effect F (1,27) = 2.987; p=0.0954

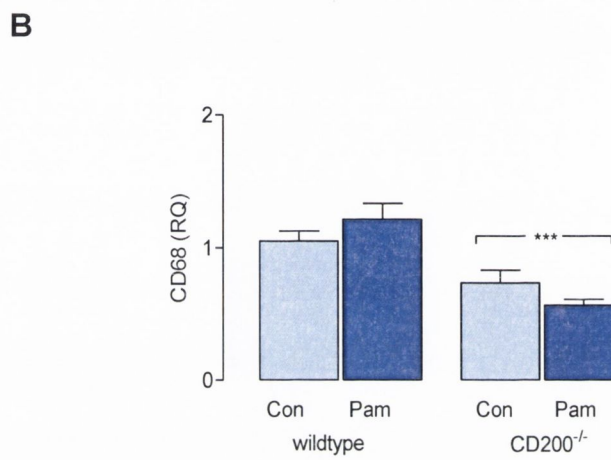
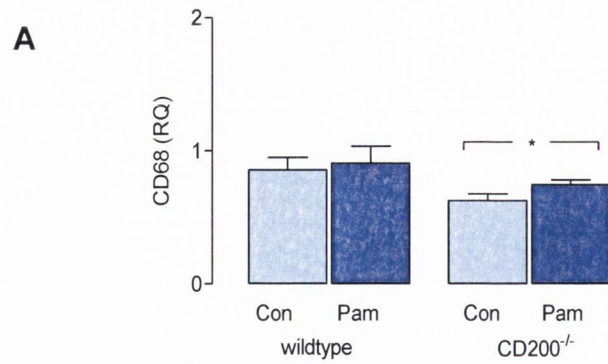


Figure 4.14. CD68 mRNA expression was decreased in hippocampal and cortical tissue prepared from CD200^{-/-} mice.

Hippocampal and cortical tissue was prepared from wildtype and CD200^{-/-} mice for QPCR analysis as described in Figure 4.1. Pam₃Csk₄ treatment had no significant effect on CD68 mRNA expression in either hippocampal (A) or cortical (B) tissue prepared from wildtype and CD200^{-/-} mice. CD68 mRNA expression was significantly decreased in both hippocampal (A) and cortical (B) tissue prepared from CD200^{-/-}, compared with wildtype, mice (* $p < 0.05$, *** $p < 0.001$, ANOVA). Values are expressed as means \pm SEM (n=7-8).

(A) 2-way ANOVA: Pam₃Csk₄ effect $F(1,25) = 0.9145$; $p = 0.3481$, Genotype effect $F(1,25) = 4.962$; $p = 0.0352$, Interaction effect $F(1,25) = 0.1402$; $p = 0.7112$

(B) 2-way ANOVA: Pam₃Csk₄ effect $F(1,24) = 0.0002139$; $p = 0.9885$, Genotype effect $F(1,24) = 29.95$; $p < 0.0001$, Interaction effect $F(1,24) = 3.583$; $p = 0.0705$

4.4. Discussion

One of the fundamental aims of this study was to determine the role of CD200 in the maintenance of microglial responses in an *in vivo* environment in response to a TLR stimulus Pam₃Csk₄. It is well documented that the activation of TLRs may have a major role to play in immune and inflammatory diseases (O'Neill *et al.*, 2009). TLR activation results in a robust inflammatory response characterised by increased production of cytokines, chemokines and the upregulation of cell surface receptors (Kielian *et al.*, 2001; O'Neill *et al.*, 2009). Disruption of the CD200-CD200R partnership has already been widely investigated in several models of disease (Hoek *et al.*, 2000; Broderick *et al.*, 2002; Meuth *et al.*, 2008; Snelgrove *et al.*, 2008) however, the effect of Pam₃Csk₄-induced neurotoxicity in CD200^{-/-} mice has not yet been evaluated. The hypothesis proposed here is that loss of CD200, coupled with Pam₃Csk₄ challenge, will lead to an exaggerated neuroinflammatory response in CD200^{-/-}, compared with wildtype, mice.

Previous studies, using both CD200 knockdown and an increase in the availability of CD200, have documented the role of the CD200-CD200R interaction in regulating cytokine production. The use of CD200Fc in studies has been correlated with a switching of cytokine production away from the production of type-1 cytokines, namely IFN- γ , IL-2 and TNF α , towards the production of type-2 cytokines (Chen *et al.*, 2005). The data here indicate that TNF α and IL-1 β mRNA expression was significantly increased in response to TLR2 activation by Pam₃Csk₄ and was significantly more exaggerated in hippocampal tissue prepared from CD200^{-/-}, compared with wildtype, mice. This is consistent with published data demonstrating that loss of CD200 results in increased TNF α production in a mouse model of *Toxoplasma* encephalitis (TE) (Deckert *et al.*, 2006) and a mouse model of arthritis (Gorczynski *et al.*, 2001). Additionally Gorczynski and colleagues (2002) demonstrated that replacement of CD200 through infusion of CD200Fc or of anti-CD200R could not merely suppress the development of CIA, which occurred in association with decreased serum levels of TNF α , but also ameliorates pre-existing disease in a mouse model of arthritis. Interestingly studies investigating stress which is known to induce a pro-inflammatory response in the CNS, with IL-1 β acting as the main cytokine (Nguyen *et al.*, 1998;

O'Connor *et al.*, 2003), have demonstrated that stress downregulates hippocampal CD200 expression and that this is accompanied by an inflammatory microenvironment in the CNS (Frank *et al.*, 2007).

IL-6 expression was investigated and the results demonstrated an increase in IL-6 mRNA expression following Pam₃Csk₄ treatment in both hippocampal and cortical tissue prepared from wildtype and CD200^{-/-} mice. However, IL-6 mRNA expression was not exacerbated in tissue prepared from CD200^{-/-}, compared with wildtype, mice conversely IL-6 mRNA expression was significantly decreased in cortical tissue prepared from CD200^{-/-}, compared with wildtype, mice. This result was unexpected as previous studies have found that loss of CD200 leads to increased IL-6 production while elevated levels of CD200 reduce IL-6 production. Chitnis and colleagues (2007) demonstrated that elevated expression of CD200 results in reduced IL-6 expression accompanied by diminished accumulation of microglia and macrophages in the CNS in an EAE model (Chitnis *et al.*, 2007). Indeed bone-marrow derived macrophages treated with DX109, a CD200R agonist, decrease the production of IL-6 following IFN- γ stimulation (Copland *et al.*, 2007), while macrophages extracted from anti-CD200R Ab-treated rats exhibited a profound increase in IL-6 secretion (Meuth *et al.*, 2008). *Ex-vivo* studies have shown that alveolar macrophages from CD200^{-/-} mice have enhanced TNF α and IL-6 production in response to another TLR agonist, LPS (Snelgrove *et al.*, 2008). Nonetheless it is difficult to interpret this result as IL-6 is a pluripotent cytokine having both beneficial and destructive effects within the CNS (Dong & Benveniste, 2001).

Previous data from this laboratory has reported an increase in BBB permeability in CD200^{-/-} mice compared with wildtype counterparts and a further increase in BBB breakdown as a consequence of LPS treatment (Kelly *et al.*, unpublished data). It has been established that tight junctions, which modulate the BBB, can be disrupted by cytokines such as TNF α and IL-1 β (Kebir *et al.*, 2007) both of which were found to be exaggerated, in this study, in tissue prepared from CD200^{-/-} mice. Thus with this in mind the expression of chemo attractant mediator's chemokines, which allow for the migration of peripheral immune cells into the CNS, was investigated. These experiments found a significant increase in IP-10, MIP-1 α , MCP-1 and RANTES mRNA expression in response to Pam₃Csk₄ treatment in wildtype and CD200^{-/-} mice. Furthermore IP-10 and MIP-1 α mRNA

expression was exacerbated in tissue prepared from CD200^{-/-}, compared with wildtype, mice. To date, there is not much published data examining chemokines in the CD200-deficient mouse model but some evidence points to a correlation between the loss of CD200 and increased peripheral cell infiltration. Accelerated and increased leukocyte infiltration has been observed in CD200^{-/-} mice undergoing EAU (Broderick *et al.*, 2002). Furthermore the presence of CD200 on endothelium, and the increase in retinal macrophage infiltrate after depletion of CD200, infers a possible control of macrophage trafficking via CD200-CD200R interactions (Broderick *et al.*, 2002). It might be hypothesised that part of the inflammation seen in these CD200^{-/-} mice might be attributed to increased chemokine circulation and a leaky BBB allowing for increased peripheral cell infiltration into the CNS.

It is widely acknowledged that TLRs act to mobilise a robust immune reaction in response to pathogens and a number of studies have reported an association between TLRs and neurodegenerative diseases, that have a large inflammatory component, such as AD (Fassbender *et al.*, 2004; Liu *et al.*, 2005; Jana *et al.*, 2008). Furthermore it has been found that CD200R expression is decreased in AD (Walker *et al.*, 2009). Recent evidence from this lab *in vitro* has suggested that loss of CD200 and the resulting exacerbated microglial response may be attributed to an increase in basal TLR2 and TLR4 expression on microglia in CD200^{-/-} mice (Costello *et al.*, 2011). Considering this evidence, the next aim was to investigate if the exaggerated cytokine and chemokine production in the CD200^{-/-} mice was as a result of altered TLR expression in these animals. Here it was found that there was an apparent but not significant increase in basal TLR2 expression on CD11b⁺ cells prepared from CD200^{-/-}, compared with wildtype, mice. Interestingly Pam₃Csk₄ significantly increased TLR2 mRNA expression in hippocampal and cortical tissue prepared from both wildtype and CD200^{-/-} mice but this effect was not seen at the protein level. It is well established that TLR2 recognises Pam₃Csk₄ through interaction with TLR1 to elicit an inflammatory response (Takeda *et al.*, 2002). The present data show that Pam₃Csk₄ significantly increased TLR1 mRNA expression in hippocampal and cortical tissue prepared from both wildtype, and CD200^{-/-}, mice. In contrast, a significant decrease in TLR1 mRNA expression was seen in cortical tissue prepared from CD200^{-/-}, compared with wildtype, mice.

Having established that there was a profound increase in pro-inflammatory cytokine and chemokine production in CD200^{-/-}, compared with wildtype, mice the extent and phenotype of microglial activation was assessed. There is extensive literature describing the various cell surface markers on microglia and their upregulation in response to pathogenic inflammatory stimuli such as LPS, IL-1 β and A β (Roy *et al.*, 2008). Previous authors have correlated a decrease in CD200 with chronic microglial activation and suggested that disease or endotoxin-induced disruption of the CD200-CD200R axis may contribute to and maintain chronic microglial activation in the brain (Koning *et al.*, 2007; Walker *et al.*, 2009). Increased microglia/macrophage activation in CD200^{-/-} mice has been described in several models of inflammation including; facial nerve transfection, EAE, CIA (Hoek *et al.*, 2000) and EAU (Broderick *et al.*, 2002). Hoek and colleagues (2000) demonstrated that microglia from CD200^{-/-} mice exhibit many features of activation including decreased ramification and increased CD11b and CD45 expression. Furthermore this group showed that microglia from CD200^{-/-} mice were found aggregated together in the spinal cord of EAE animals, a feature that is associated with inflammation and neurodegeneration (Hoek *et al.*, 2000). In this study, it was found that MHC class II expression was significantly increased on CD11b⁺ cells prepared from CD200^{-/-} mice compared with wildtype mice. Unusually it was found that Pam₃Csk₄ treatment had no effect on MHC class II expression on CD11b⁺ cells prepared from wildtype and CD200^{-/-} mice.

Both CD40 and CD86, two co-stimulatory molecules, were found to be significantly decreased in tissue prepared from CD200^{-/-} mice compared with wildtype mice and CD86 expression was only significantly increased following Pam₃Csk₄ treatment in hippocampal tissue prepared from wildtype mice. This result is in agreement with studies from Broderick and colleagues (2002) using CD200^{-/-} mice to investigate EAU. These authors found that despite increased numbers of retinal microglia/macrophages in CD200^{-/-} mice compared with wildtype mice, there was no significant difference in the expression of MHC class II, CD86 and CD40 but found that expression of NOS2 was significantly greater in CD200^{-/-}, compared with wildtype, mice (Broderick *et al.*, 2002). This is important as under normal circumstances microglia in the retina are NOS2-negative, with NOS2 expression associated with peak EAU, and NOS2 inhibitors have been found to protect against photoreceptor destruction (Hoey *et al.*, 1997).

It may be interesting to investigate NOS2 expression in hippocampal and cortical tissue from CD200^{-/-} mice challenged with Pam₃Csk₄ in a future study. Furthermore a study by Deckert and colleagues (2006) examining *Toxoplasma* encephalitis (TE) found no changes in basal levels of the cell surface molecules CD45, CD80, CD86 and MHC class I and II following acute TE in CD200^{-/-}, compared with wildtype, mice. This group demonstrated that these markers of activation only become significantly more enhanced in the CD200^{-/-} mice compared with wildtype mice following chronic TE (Deckert *et al.*, 2006). This evidence raises the question that chronic rather than acute administration of Pam₃Csk₄ is required to see a greater increase in these markers of activation in CD200^{-/-}, compared with wildtype, mice.

CD68 expression was also investigated and the results revealed a significant decrease in tissue prepared from CD200^{-/-}, compared with wildtype, mice and no effect of Pam₃Csk₄ treatment in tissue prepared from wildtype and CD200^{-/-} mice. In contrast, Hoek and colleagues (2000) found increased CD68 staining in CD200^{-/-} mice undergoing EAE. However, it is worth noting that these authors found increased macrophage numbers in spleens from CD200-deficient, compared to wildtype, mice (Hoek *et al.*, 2000). It has been suggested that the increase in CD68 staining seen in the EAE model may not reflect increased phagocytosis but rather an increase in circulating macrophages in the tissue (Nathan & Muller, 2001). Evidence from the literature also suggests that the phagocytic activity of microglia is attenuated by pro-inflammatory cytokines (Hanisch & Kettenmann, 2007). The exaggerated cytokine response seen in tissue prepared from CD200^{-/-} mice, in this study, may account for the decrease in CD68 expression. The discrepancy between the results in the present study and those from Hoek and colleagues needs further investigation.

In conclusion, the data presented here and the data from the previous chapter indicate that loss of CD200, in the presence of Pam₃Csk₄ challenge, results in an exaggerated immune response as measured by cytokine and chemokine expression accompanied by increased MHC class II expression on microglia. The possibility that CD200-CD200R interaction is involved in both cytokine and chemokine regulation in the CNS provides an area for future investigation. Especially targeting modulation of TNF α which, alongside IL-1 β and IL-6 has been found to be elevated during both neurodegenerative and

autoimmune diseases all of which have an inflammatory component as a driving force behind disease progression. TNF α has already been addressed as a therapeutic approach in the treatment of inflammatory disorders. Both decoy TNF α receptor molecules and antibodies to TNF α have been used successfully as treatment (Maini *et al.*, 1999; Moreland *et al.*, 1999) however these treatment are not without significant side effects (Finch & Ruvkun, 2001). Consequently the potential to use CD200 to manipulate pro-inflammatory cytokine production may be of therapeutic benefit. The finding that loss of CD200-CD200R axis can alter chemokine production is a more novel finding and further research will need to be addressed to fully investigate the impact of their regulation by CD200. It is worth noting that a profoundly exaggerated inflammatory response was observed in hippocampal tissue, rather than cortical tissue, prepared from CD200^{-/-} mice. This difference may be accounted for by a regional difference in microglial activation states as already seen in studies using macrophages from different organs. Previous studies have found that the CD200-CD200R axis plays a role in controlling inflammatory reactions in lung macrophages during influenza (Snelgrove *et al.*, 2008) whereas intestinal macrophages are unaffected by the loss of CD200-CD200R axis during dextran sodium sulphate-induced colitis (Bain & Mowat, 2012). These findings may indicate a differential role for the CD200-CD200R interaction in diverse forms of immunopathologies based on the stimulus and the resident myeloid cells present in the affected tissue.

Table 4.1. Results summary of mRNA expression of inflammatory markers assessed in hippocampal and cortical tissue prepared from wildtype and CD200^{-/-} mice.

	Hippocampus			Cortex		
	Pam ₃ Csk ₄ effect	Genotype effect	Interaction effect	Pam ₃ Csk ₄ effect	Genotype effect	Interaction effect
TNF α	↑↑↑	↑↑	↑↑	↑↑↑		
IL-1 β	↑↑↑	↑	↑	↑↑↑		
IL-6	↑↑↑			↑	↓	
IP-10	↑↑↑	↑	↑	↑↑↑	↑	
MIP-1 α	↑↑↑	↑	↑	↑↑↑		
MCP-1	↑↑↑			↑↑↑		
RANTES	↑↑↑			↑↑		
TLR2	↑↑↑			↑↑↑		
TLR1	↑↑↑			↑↑↑	↓	
CD40		↓↓			↓↓	
CD86	↑↑↑	↓↓		↑↑↑	↓↓↓	
CD68		↓			↓↓↓	

Table 4.2. Results summary of cell surface receptor expression on microglia prepared from wildtype and CD200^{-/-} mice.

	Pam ₃ Csk ₄ effect	Genotype Effect	Interaction effect
TLR2			
MHC class II		↑↑↑	
CD40			

Chapter 5

Chapter 5

5.1. Introduction

Microglia are the resident brain mononuclear phagocytes and have functions similar to macrophages such as antigen presentation, phagocytosis, production of complement components, oxidative radicals, nitric oxide, cytokines and chemokines (Benveniste *et al.*, 2001). Although microglia are involved in maintaining homeostasis and secreting neurotrophic factors required for neuronal survival it is believed that exacerbated activation of microglia causes a robust inflammatory response involved in neuronal death and brain injury (Roy *et al.*, 2008). Under normal circumstances it is thought that microglia survey the microenvironment with relevantly low expression of cell surface markers and production of cytokines and chemokines. However during an immune response, resulting in microglial activation, both cytokines and chemokines are rapidly produced and secreted allowing for the activation of other immune cells and importantly the infiltration of peripheral immune cells into the CNS (Lynch, 2009). Activation is identified by the upregulation of several cell surface markers. These markers include MHC class II, CD40 and CD86 all of which are required for effective peripheral T cell activation and proliferation. The role of microglia in neurodegenerative conditions such as AD has received extensive attention in recent years and it is becoming increasingly evident that microglial activation is a fundamental characteristic of AD.

There is compelling evidence from the literature that chronic inflammatory processes participate in the pathophysiology of AD (McGeer & McGeer, 2001; McGeer & McGeer, 2003). These inflammatory changes include microgliosis, astrocytosis, as well as complement activation and increased cytokine and chemokine production. Presently there is extensive literature describing microglial activation both in mouse models of AD and in the AD brain. Activated microglia and astrocytes are found in close proximity to senile plaques (Haga *et al.*, 1989; Itagaki *et al.*, 1989). It has been reported that pro-inflammatory cytokine production is increased in post-mortem brain tissue from AD patients compared with non-demented controls (Griffin *et al.*, 1989) and isolated neuritic plaques and

A β have been shown to induce microglia to release neurotoxins (Giulian *et al.*, 1995; Giulian *et al.*, 1996). It has been suggested that the presence of A β plaques may keep microglia consistently activated resulting in chronic inflammation within the CNS. Indeed it has been proposed that one of the neuropathogenic mechanisms occurring in AD is that A β maintains microglia in an activated state resulting in the production of pro-inflammatory cytokines and neurotoxic mediators resulting in neuronal damage (Benveniste *et al.*, 2001). The release of these neurotoxic factors and cytokines can in turn activate surrounding astrocytes which in turn are capable of damaging neurons through the release of NO (Minagar *et al.*, 2002). It has been suggested that A β activates microglia through an ensemble of cell surface receptors, (Bamberger *et al.*, 2003), resulting in the activation of signalling cascades that results in the activation of microglia into different phenotypes (Combs *et al.*, 2001). Indeed the results presented in Chapter 3 and those of other authors emphasise the production of a range of cytokines and chemokines including IL-1 β , TNF α , IL-6, MCP-1 and MIP-1 α (Meda *et al.*, 1995; Walker *et al.*, 1995) by microglia in response to A β challenge. Furthermore, the upregulation of the co-stimulatory molecule CD40 has been reported to be increased on microglia following A β stimulation *in vitro* while *in vivo* studies have demonstrated enhanced CD40 expression on microglia in a mouse model of AD (Tan *et al.*, 1999). Interaction of CD40 with its ligand CD154 (found predominately on T cells) is critical for an effective immune response and the activation of T cells and APC (Benveniste *et al.*, 2001). Despite the fact that microglia are competent phagocytes there is conflicting evidence over the ability of microglia to phagocytose A β . Indeed it appears that microglia in close proximity to plaques seem unable to internalise A β (Stalder *et al.*, 2001). On the other hand it has been demonstrated that microglia are capable of phagocytosing fibrillar A β through an integrin receptor-dependent manner (Koenigsknecht & Landreth, 2004). Nonetheless it is still not clear if microglial activation and associated inflammatory changes trigger the pathogenesis of AD or whether microglial activation occurs in response to the early changes associated with the disease (Lynch, 2009).

Several studies suggest that inflammation within the CNS arises principally from glia, however with evidence that microglia can act as APCs for peripheral cells it is now thought that peripheral T cells can contribute and

maintain this inflammatory environment (Town *et al.*, 2005). The role of T cells in CNS tissue damage has been widely studied in recent years. The role of T cells, particularly Th1 and Th17 in neurodegenerative pathologies such as MS is clearly demonstrated in studies using an animal model of MS, EAE. Adoptive transfer of MOG-specific Th1 cells can induce EAE (Kroenke *et al.*, 2008). Furthermore previous studies from this laboratory using the EAE model have demonstrated IL-17⁺ and IL-17⁺IFN- γ ⁺ T cells infiltrate the brains of these mice before onset of clinical symptoms and this is associated with enhanced IL-1 β and IL-6 expression. It was also reported that upon onset of clinical symptoms there was a significant increase in IFN- γ producing T cells and upregulation of the expression of CD40, CD86 and CD80 on activated microglia and macrophages (Murphy *et al.*, 2010). There is clear evidence of the detrimental role of T cells in MS through their interaction with glia, however their role in AD is not as clear and there is still much debate if T cells play a beneficial or detrimental role in disease pathology.

It has been proposed that under normal circumstances T cells visit the healthy brain but during AD these visits become more frequent and T cells are thought to begin to accumulate in the brain (Town *et al.*, 2005). Rogers and colleagues (1988) demonstrated that the human leukocyte antigen-DR⁺ could be seen in AD brain tissue. Togo and co-workers (2002), using immunohistochemical analysis, found T cells present in brain tissue taken from individuals with non-AD degenerative dementias, AD and controls but T cell numbers were far greater in brain sections taken from the AD group compared with controls. Several investigators have also addressed whether or not a peripheral T cell response might exist in AD and how this response may or may not contribute to the pathology of the disease. It has been shown that peripheral T cells in AD patients have a switched CD45 isotype from a naive phenotype (as measured by the expression of CD45RA⁺) to a memory phenotype (as measured by the expression of CD45RO⁺) compared with normal aged-matched controls or patients with other forms of dementias (Tan *et al.*, 2002). This finding was corroborated with a finding by Togo and colleagues (2002) that CD45RO⁺-T cells were present in brains of AD patients. Furthermore, it has been shown that T cells isolated from AD patients had increased CD45RO expression compared with controls (Lombardi *et al.*, 2004). This group also reported an increase in CD4⁺ T cells and T-regulatory subsets isolated from AD patients compared with age-

matched controls. Probably the most damning evidence suggesting T cells are more reactive in AD comes from studies examining the presence of A β -reactive T cells in AD patients. Monsonego and colleagues (2003) report the presence of A β -reactive T cells in AD patients and showed that these T cells increase with age. There is clear evidence that T cells can exacerbate inflammation however several studies have implicated T cells in decreasing plaque burden. A clinical trial in which a synthetic A β ₁₋₄₂ peptide (AN-1792) was peripherally administered to AD patients resulted in aseptic T cell meningoencephalitis. It has been suggested that this occurred as a result of an immune response to A β mediated by infiltrating T cells (Pfeifer *et al.*, 2002). Interestingly some of the patients in this study were found to have increased clearance of A β plaque load (Nicoll *et al.*, 2003) and a recent study by Monsonego and co-workers (2006) found increased A β clearance in mice overexpressing IFN- γ immunised with A β . Thus it is clear that T cells are present in the AD brain however the role of T cells in AD pathology is still debatable.

With both activated microglia and T cells present in the AD brain it has become imperative to investigate how these cells may interact with each other and contribute to inflammation. Currently the interaction of T cells and glia and the potential modulatory effects of different T cell subsets on glial activation is not well characterised in relation to AD (McQuillan *et al.*, 2010). However microglia in active MS lesions exhibit an activated phenotype with enhanced expression of MHC class II and co-stimulatory molecules CD40, CD86 and CD80 (Cannella *et al.*, 1995; Cannella & Raine, 1995). Moreover it has been shown that microglia produce pro-inflammatory cytokines in response to T cells (Dasgupta *et al.*, 2005). Microglia isolated from the CNS are able to present antigens to T cells resulting in the production of the pro-inflammatory cytokines IFN- γ and IL-2 (Aloisi *et al.*, 2000b), while IFN- γ can upregulate co-stimulatory molecule expression on microglia (Meda *et al.*, 1995; Nguyen & Benveniste, 2000). On the other hand it has been reported that Th2 cells may have beneficial effects through inhibition of CNS inflammation by the secretion of anti-inflammatory cytokines. Indeed the Th2 cytokine profile is typified by the production of cytokines such as IL-4 and IL-10 which decrease microglial activation, and increase phagocytosis (Koenigsknecht-Talboo & Landreth, 2005). Th2-type cytokines can attenuate A β -induced pro-inflammatory cytokine production by microglia (Szczepanik *et al.*,

2001). While Th17 cells have a pathogenic potential similar to that of Th1 cells, and have been implicated in tissue specific autoimmunity, their role in host defence is not as well defined (Harrington *et al.*, 2005). However adoptive transfer of IL-17-secreting cells induces EAE (Langrish *et al.*, 2005) and IL-17 expressing T cells have been observed in active MS lesions (Kebir *et al.*, 2007). Furthermore, studies have demonstrated that Th1/Th17 cells significantly enhance MHC class II and co-stimulatory molecule expression on microglia (Murphy *et al.*, 2010). It is still uncertain if microglia contribute towards directing infiltrating T cells to a neuroprotective or a neurotoxic function (Melchior *et al.*, 2006).

The aims of this study were to:

- Investigate the consequence of interaction of non antigen-specific and A β -specific Th1, Th2 and Th17 cells with microglia and astrocytes with a focus on investigating their modulation of co-stimulatory molecule expression and cytokine production by glia.
- To establish if the interaction of glia and T cell lines generated from wildtype mice, differed to those generated from APP/PS1 mice.

5.2. Methods

Spleens were harvested from 12 month old APP/PS1 mice and littermate controls and CD4⁺ T cells were isolated using a MACS and a CD4⁺ T cell isolation kit (see section 2.7.1.1 for details). CD4⁺ T cells were plated in 24-well plates and polarized into Th1, Th2 and Th17 cells by incubation of the cells in the presence of specific polarising cytokines for 5 days (see section 2.7.1.2 for details). In addition A β -specific T cell lines were plated in 24-well plates and polarised into A β -specific Th1, Th2 and Th17 cells by incubation of cells in the presence of polarising cytokines and A β ₁₋₄₂ for 5 days (see section 2.7.1.3 for details). On the 5th day of the culture, supernatants were taken for cytokine analysis of IFN- γ , IL-10 and IL-17 by ELISA and cells were harvested for co-culture with microglia and astrocytes.

Mixed glia were prepared from 1-day old C57BL/6 mice and cultured for 12 days before shaking and separation into microglia and astrocytes. Microglia were plated in 24-well plates (1×10^5 cells/well) and astrocytes were plated in 6-well plates (3×10^5 cells/well) and both cell types were incubated for 24 hours prior to T cell co-culture (see section 2.1.2 for details). One group of microglia and astrocytes were co-cultured with non-specific T cell lines and incubated for 24 hours. A second group of microglia and astrocytes were co-cultured with A β -specific T cell lines and treated with A β ₁₋₄₂ (15 μ g/ml) and incubated for 24 hours (see section 2.7.2.2 for details). T cells were co-cultured with microglia and astrocytes at a ratio of 1:2 which has previously been determined to be the optimal ratio for co-culture of these cell types. Following co-culture, supernatants were removed for cytokine analysis of IL-6 and TNF α by ELISA (see section 2.12 for details) and cells were harvested for analysis of cell surface expression of CD40 and CD86 by flow cytometry (see section 2.9.1 for details). Data are expressed as means \pm SEM. ANOVA and Newman's Keuls post-hoc test was applied where appropriate.

5.3. Results

One of the primary aims of this study was to investigate consequences of the interaction between T cell lines and A β -specific T cell lines with microglia and astrocytes by assessing markers of microglial and astrocytic activation and cytokine production. A second aim was to establish if T cells generated from APP/PS1 mice exerted different effects on microglia and astrocytes than T cells generated from littermate controls.

5.3.1. Generation of Th1, Th2 and Th17 T cell lines.

The cytokine environment at the time of T cell activation is crucial for determining the subsequent polarisation into different T cell subsets (Kaiko *et al.*, 2008). Once CD4⁺ T cells are differentiated, specific T cell subtypes secrete an array of cytokines. IFN- γ is primarily released from Th1 cells and NK cells and is strongly associated with a Th1 immune response. IL-10 is an anti-inflammatory cytokine produced by a wide range of cells including Th2, whereas Th17 cells are characterised by their production of IL-17 (Park *et al.*, 2005). In an effort to ensure that the CD4⁺ T cells were correctly polarised into specific Th1, Th2 and Th17 cell lines, supernatants from the specific T cell lines were assessed for the expression of IFN- γ , IL-10 and IL-17. Figure 5.1 demonstrates that cells polarised under Th1-inducing conditions were found to secrete high levels of IFN- γ and IL-10 and low levels of IL-17. Cells polarised under Th2-inducing conditions produced high levels of IL-10 and low levels of IFN- γ and IL-17. Cells polarised under Th17-inducing conditions produced low levels of IFN- γ and high levels IL-10 and IL-17.

5.3.2. Th1 cells increase the expression of co-stimulatory molecules and production of cytokines by microglia and astrocytes.

To examine the effect of Th1 cells on microglial and astrocytic activation, the expression of the co-stimulatory molecules CD40 and CD86 were assessed by FACS and the production of the pro-inflammatory cytokines IL-6 and TNF α were assessed by ELISA. The data show that co-culture of microglia and astrocytes

with Th1 cells generated from wildtype and APP/PS1 mice had no significant effect on CD86 expression (Figure 5.2A and B). Co-culture of microglia with Th1 cells, generated from APP/PS1 mice, significantly increased the expression of CD40 on microglia (** $p < 0.01$, ANOVA; Figure 5.2C). There was a significant increase in the expression of CD40 on microglia co-cultured with Th1 cells generated from APP/PS1 mice compared with Th1 cells generated from wildtype mice ($^+p < 0.05$, ANOVA; Figure 5.2C). Co-culture of astrocytes with Th1 cells, generated from wildtype and APP/PS1 mice, significantly increased the expression of CD40 on astrocytes compared ($^*p < 0.05$, ANOVA; Figure 5.2D).

Co-culture of microglia with Th1 cells, generated from APP/PS1 mice, but not wildtype mice significantly increased supernatant concentrations of TNF α ($^*p < 0.05$, ANOVA; Figure 5.3A). Conversely, co-culture of astrocytes with Th1 cells, generated from wildtype mice but not APP/PS1 mice, significantly increased TNF α supernatant concentrations compared with controls ($^*p < 0.05$, ANOVA; Figure 5.3B). Co-culture of microglia with Th1 cells from wildtype and APP/PS1 mice had no significant effect on IL-6 concentrations (Figure 5.3C) whereas co-culture of astrocytes with Th1 cells generated from both wildtype and APP/PS1 mice significantly increased supernatant concentrations of IL-6 ($^*p < 0.05$, ANOVA; Figure 5.3D).

5.3.3. Th2 cells had no effect on the expression of co-stimulatory molecules and production of cytokines by microglia and astrocytes.

Co-culture of microglia and astrocytes with Th2 cells generated from wildtype and APP/PS1 mice had no significant effect on the expression of CD86 (Figure 5.4A and B) and CD40 on microglia and astrocytes (Figure 5.4C and D). Co-culture of microglia and astrocytes with Th2 cells generated from wildtype and APP/PS1 mice had no significant effect on supernatant concentrations of TNF α (Figure 5.5A and B) or IL-6 (Figure 5.5C and D).

5.3.4. Th17 cells increase the expression of co-stimulatory molecules and production of cytokines by astrocytes but not by microglia.

Co-culture of microglia and astrocytes with Th17 cells from wildtype and APP/PS1 mice had no significant effect on CD86 (Figure 5.6A and B) expression. Co-culture of Th17 cells, generated from wildtype and APP/PS1 mice had no effect on the expression of CD40 on microglia (Figure 5.6C) but co-culture of astrocytes with Th17 cells generated from APP/PS1 mice, but not wildtype mice, significantly increased expression of CD40 on astrocytes (^{***} $p < 0.001$, ANOVA; Figure 5.6D).

Co-culture of microglia with Th17 cells from wildtype and APP/PS1 mice had no significant effect on supernatant concentrations of TNF α and IL-6 (Figure 5.7A and B). Co-culture of astrocytes with Th17 cells from wildtype and APP/PS1 mice significantly increased supernatant concentrations of IL-6 (^{*} $p < 0.05$, ^{**} $p < 0.01$, ANOVA; Figure 5.7C). Supernatant concentrations of TNF α were undetectable following co-culture of Th17 cells with astrocytes. Table 5.1 summarises the expression of co-stimulatory molecules and production of pro-inflammatory cytokines following co-culture of T cell lines with microglia and astrocytes.

5.3.5. Generation of A β -specific Th1, Th2 and Th17 T cell lines.

Having established that co-culture of T cell subsets with glia increased the expression of co-stimulatory molecules and production of pro-inflammatory cytokines, irrespective of whether they were generated from wildtype or APP/PS1 mice, the effect of A β -specific T cells on glial function was assessed. A β -specific T cell lines were generated and assessed for the production of IFN- γ , IL-10 and IL-17 to ensure that they were correctly polarised into A β -specific T cell subtypes. Figure 5.8 demonstrates that cells polarised under A β -specific Th1-inducing conditions produced high levels of IFN- γ and IL-10 and low levels of IL-17. Cells polarised under A β -specific Th2-inducing conditions produced high levels of IL-10 and low levels of IFN- γ and IL-17. Cells polarised under A β -specific Th17-inducing conditions produced low levels of IFN- γ and IL-10 and high levels of IL-17.

5.3.6. A β -specific Th1 cells did not effect the expression of co-stimulatory molecules on microglia and astrocytes but increased production of TNF α .

Co-culture of microglia and astrocytes with A β -specific Th1 cells generated from wildtype and APP/PS1 mice had no significant effect on the expression of CD86 or CD40 on microglia and astrocytes (Figure 5.9A-D). Co-culture of microglia with A β -specific Th1 cells, generated from wildtype and APP/PS1 mice, significantly increased supernatant concentrations of TNF α (* p <0.05, *** p <0.01, ANOVA; Figure 5.10A). Co-culture of astrocytes with A β -specific Th1 cells, from wildtype mice significantly increased supernatant concentrations of TNF α but co-culture of astrocytes with A β -specific Th1 cells generated from APP/PS1 mice significantly decreased supernatant concentration of TNF α (** p <0.001, +++ p <0.001, ANOVA; Figure 5.10B). Co-culture of astrocytes (Figure 5.10D) but not microglia (Figure 5.10C) with A β -specific Th1 cells from wildtype but not APP/PS1 mice significantly increased supernatant concentrations of IL-6 (* p <0.05, ANOVA; Figure 5.10D).

5.3.7. A β -specific Th2 and Th17 cells had no effect on the expression of co-stimulatory molecules and production of cytokines by microglia and astrocytes.

Co-culture of microglia and astrocytes with A β -specific Th2 (Figure 5.11 and 5.12) and Th17 (Figure 5.13 and 5.14) cells generated from wildtype and APP/PS1 mice had no significant effect on the expression of CD86 and CD40 on microglia and astrocytes (Figure 5.11A-D and 5.13A-D). Co-culture of microglia and astrocytes with A β -specific Th2 cells generated from wildtype and APP/PS1 mice had no significant effect on supernatant concentrations of TNF α and IL-6 (Figure 5.12A-C and 5.14A-C). TNF α was undetectable following co-culture of A β -specific Th2 and Th17 cells with astrocytes.

Table 5.2 summarises the expression of co-stimulatory molecules and the production of pro-inflammatory cytokines, following co-culture of A β -specific T cell lines with microglia and astrocytes.

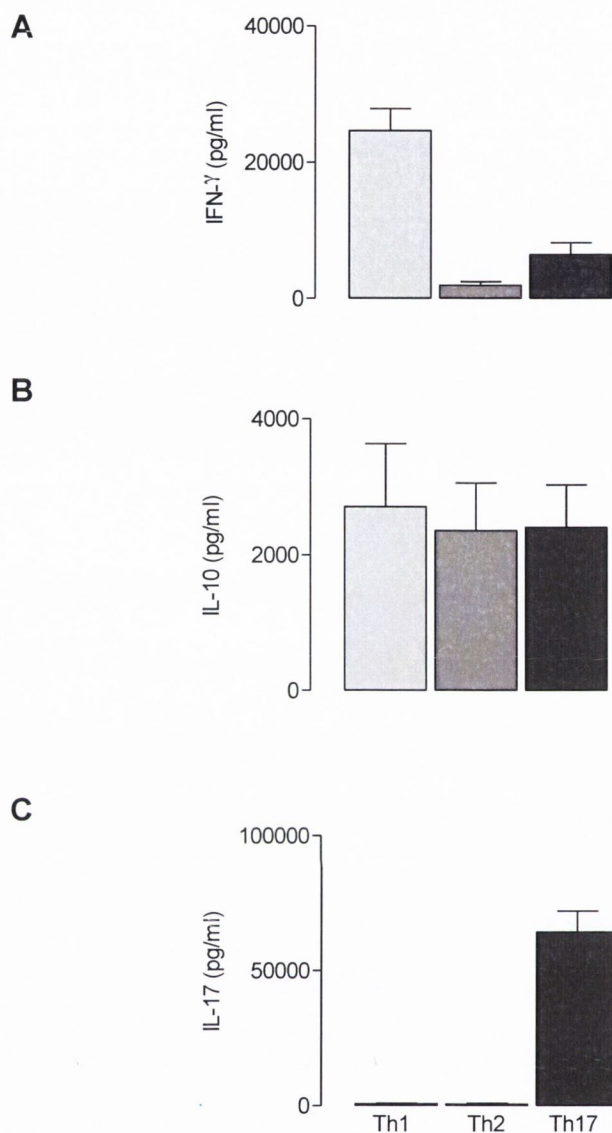


Figure 5.1. Generation of non-specific Th1, Th2 and Th17 T cell lines.

Spleens were harvested from APP/PS1 and wildtype littermate control mice (12 months old), and cells were stimulated into T cell lines under polarising conditions. Th1 polarising conditions with IL-12 (50 ng/ml), Th2 polarising conditions with IL-4 (10 ng/ml) and anti-IFN- γ (5 μ g/ml) and Th17 polarising conditions with TGF- β (5 ng/ml), IL-1 β (25 ng/ml), IL-23 (50 ng/ml) and anti-IFN- γ . On the 4th day of the culture supernatants were removed for analysis of IFN- γ (A), IL-10 (B) and IL-17 (C) concentrations by ELISA. Th1 cells have high IFN- γ and IL-10 and low IL-17 production (A-C). Th2 cells have high IL-10 and low IFN- γ and IL-17 production (A-C). Th17 cells have low IFN- γ and high IL-10 and IL-17 production (A-C). Values are expressed as means \pm SEM (n=10).

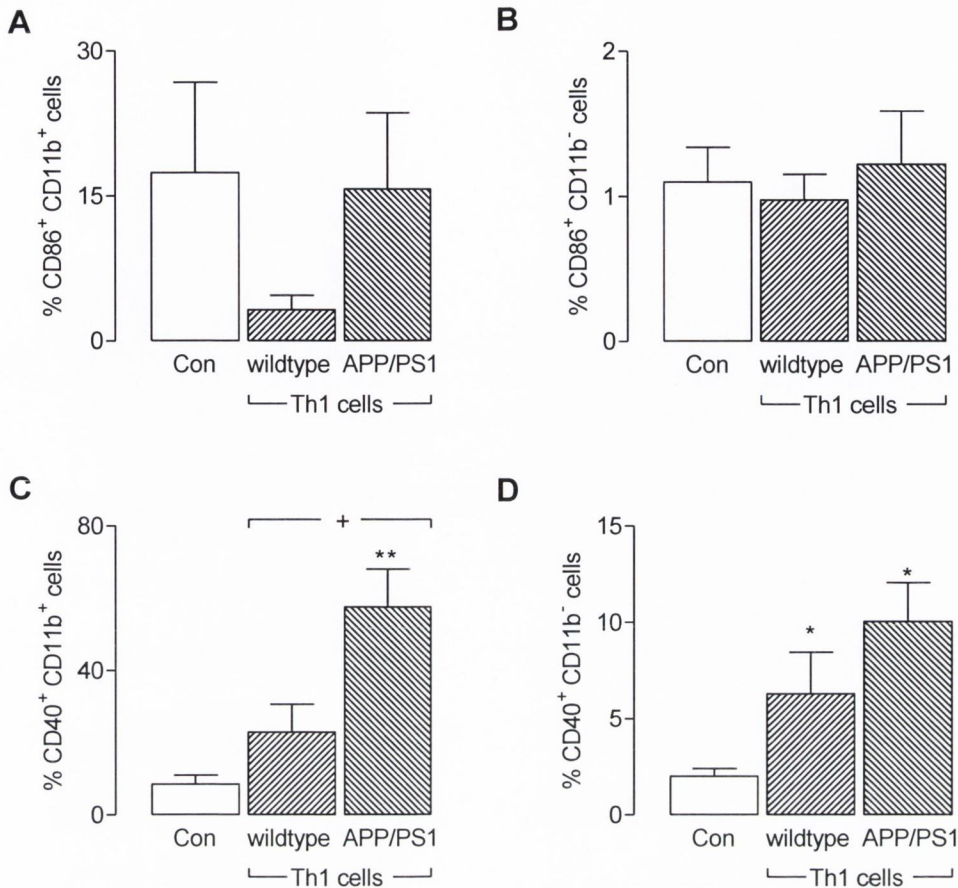


Figure 5.2. Increased CD40 expression on microglia and astrocytes co-cultured with Th1 cells.

Th1 cells were generated from wildtype and APP/PS1 mice as described in Figure 5.1. After 4 days of polarisation Th1 cell lines were co-cultured with microglia (CD11b⁺) and astrocytes (CD11b⁻) prepared from neonatal C57BL/6 mice, for 24 hours. Expression of CD86 and CD40 on CD11b⁺ and CD11b⁻ cells was quantified by FACS. Co-culture of microglia with Th1 cells from wildtype and APP/PS1 mice had no significant effect on the expression of CD86 on microglia or astrocytes (A and B). Co-culture of microglia with Th1 cells, generated from APP/PS1 mice, significantly increased the expression of CD40 on microglia (C) (***p*<0.01, ANOVA). There was a significant increase in the expression of CD40 on microglia co-cultured with Th1 cells generated from APP/PS1 mice compared with Th1 cells generated from wildtype mice (C) ([†]*p*<0.05, ANOVA). Co-culture of astrocytes with Th1 cells, generated from wildtype and APP/PS1 mice, significantly increased expression of CD40 on astrocytes (D) (**p*<0.05, ANOVA). Values are expressed as means ± SEM (n=3-10).

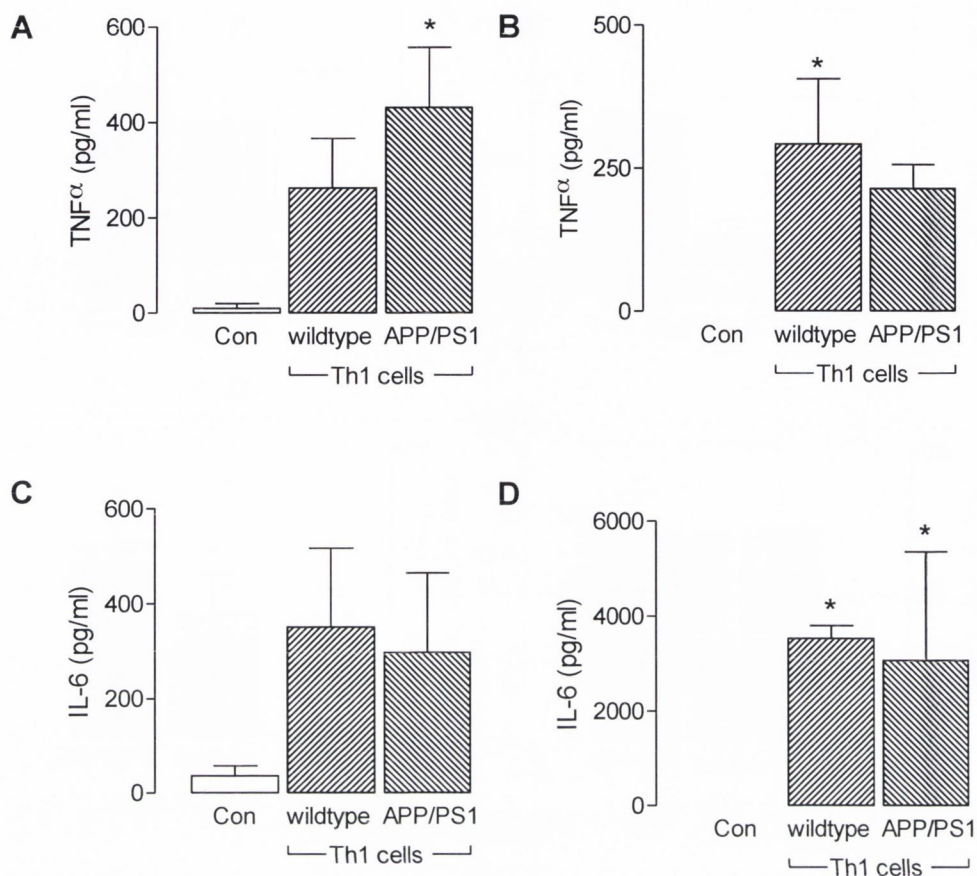


Figure 5.3. Increased cytokine production by microglia and astrocytes following co-culture with Th1 cells.

Th1 cells were generated from wildtype and APP/PS1 mice and co-cultured with microglia and astrocytes as described in Figure 5.1 and 5.2. Supernatants were harvested for analysis of TNF α and IL-6 concentrations by ELISA. Co-culture of microglia with Th1 cells, generated from APP/PS1 mice but not wildtype mice, significantly increased supernatant concentrations of TNF α (A) (* p <0.05, ANOVA). Co-culture of astrocytes with specific Th1 cells, generated from wildtype mice but not APP/PS1 mice, significantly increased supernatant concentrations of TNF α (B) (* p <0.05, ANOVA). Co-culture of microglia with Th1 cells generated from wildtype and APP/PS1 mice had no significant effect on IL-6 concentrations (C) whereas co-culture of astrocytes with Th1 cells generated from wildtype and APP/PS1 mice significantly increased supernatant concentrations of IL-6 (D) (* p <0.05, ANOVA). Values are expressed as means \pm SEM (n=4).

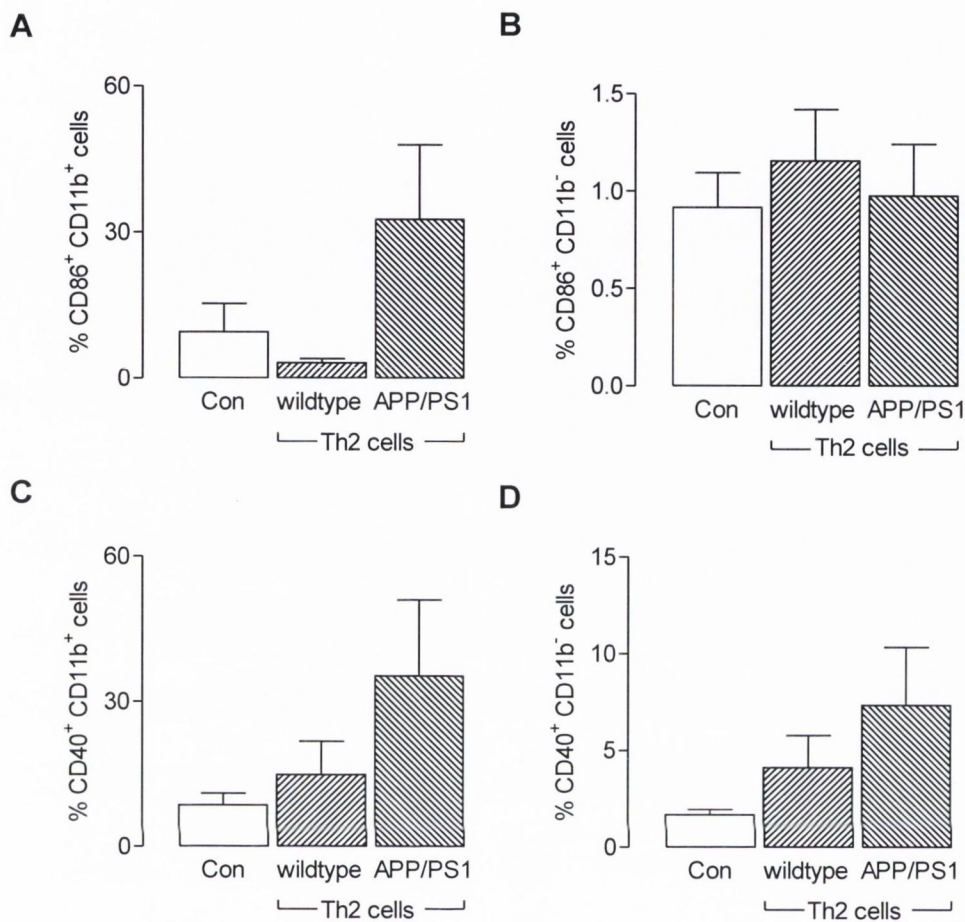


Figure 5.4. CD40 and CD86 expression is unaltered on microglia and astrocytes following co-culture with Th2 cells.

Th2 cells were generated from wildtype and APP/PS1 mice and co-cultured with microglia (CD11b⁺) and astrocytes (CD11b⁻) as described in Figure 5.1 and 5.2. Expression of CD86 and CD40 on CD11b⁺ and CD11b⁻ cells was quantified by FACS. Co-culture of microglia and astrocytes with Th2 cells from wildtype and APP/PS1 mice had no significant effect on the expression of CD86 and CD40 on microglia and astrocytes (A- D). Values are expressed as means \pm SEM (n=4-10).

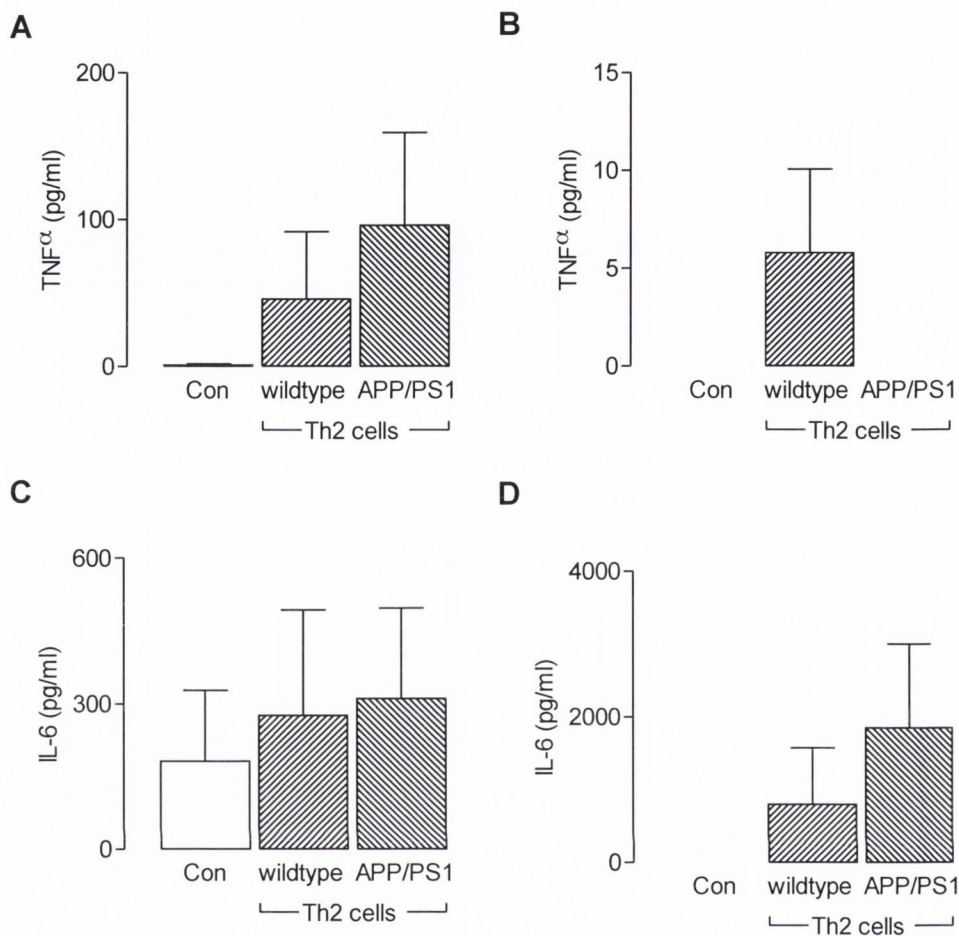


Figure 5.5. Cytokine production by microglia and astrocytes is unaltered following co-culture with Th2 cells.

Th2 cells were generated from wildtype and APP/PS1 mice and co-cultured with microglia and astrocytes as described in Figure 5.1 and 5.2. Supernatants were harvested for analysis of TNF α and IL-6 concentrations by ELISA. Co-culture of microglia and astrocytes with Th2 cells from wildtype and APP/PS1 mice had no significant effect on supernatant concentrations of TNF α or IL-6 (A-D). Values are expressed as means \pm SEM (n=4-5).

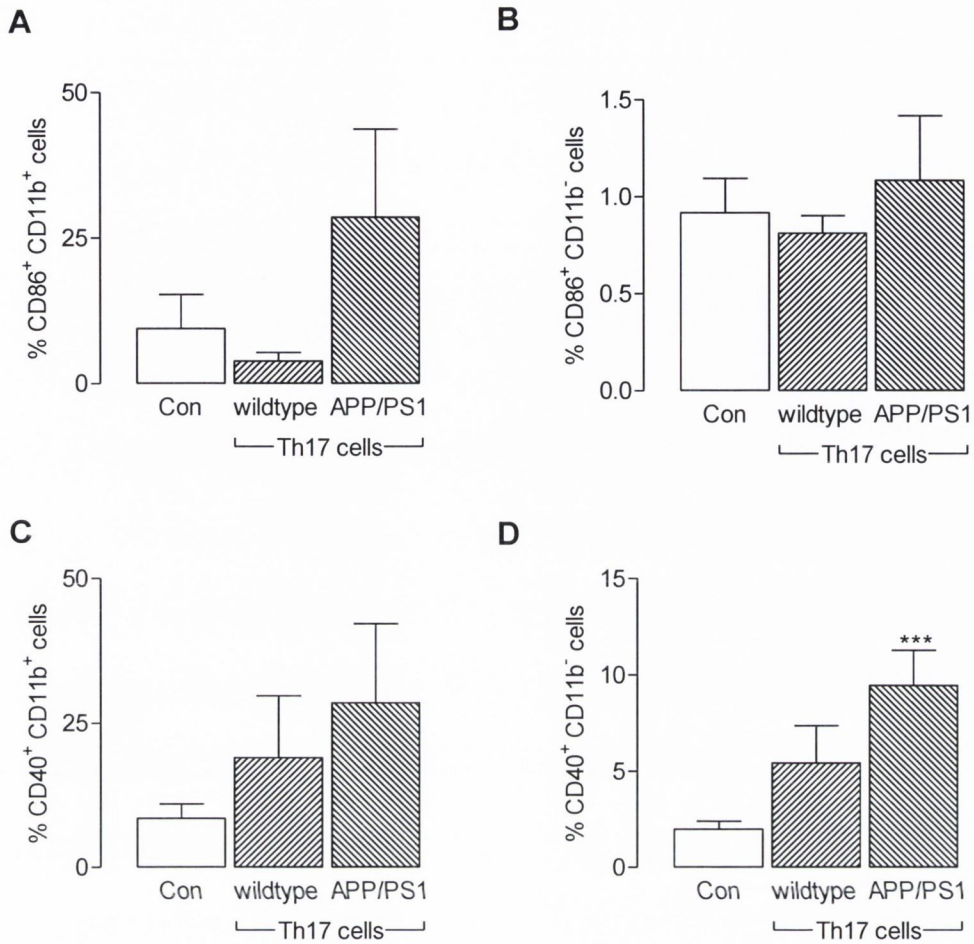


Figure 5.6. Increased CD40 expression on astrocytes following co-culture with Th17 cells.

Th17 cells were generated from wildtype and APP/PS1 mice and co-cultured with microglia (CD11b⁺) and astrocytes (CD11b⁻) as described in Figure 5.1 and 5.2. Expression of CD86 and CD40 on CD11b⁺ and CD11b⁻ cells was quantified by FACS. Co-culture of microglia and astrocytes with Th17 cells generated from wildtype and APP/PS1 mice had no significant effect on expression of CD86 (A and B). Co-culture of microglia with Th17 cells, generated from wildtype and APP/PS1 mice had no effect on CD40 expression (C). Co-culture of astrocytes with Th17 cells, generated from APP/PS1 mice but not wildtype mice, significantly increased the expression of CD40 on astrocytes (D) (***) ($p < 0.001$, ANOVA). Values are expressed as means \pm SEM (n=4-10).

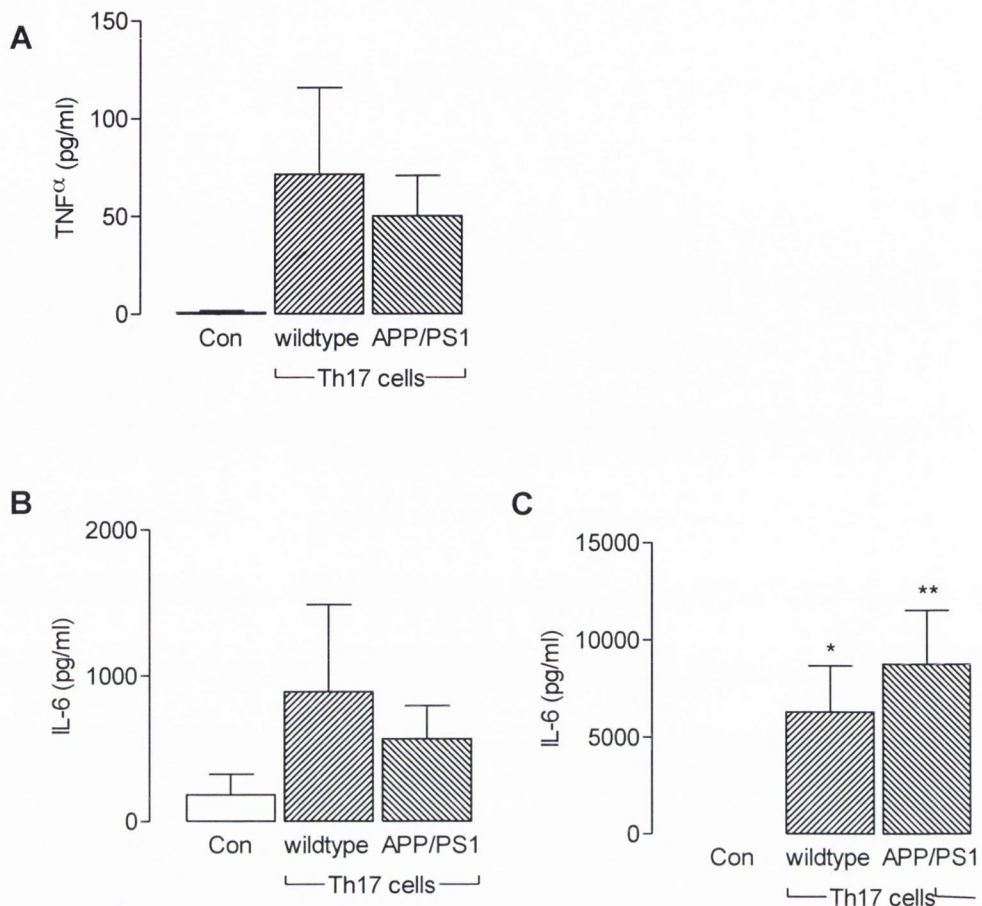


Figure 5.7. IL-6 production is increased by astrocytes following co-culture with Th17 cells

Th17 cells were generated from wildtype and APP/PS1 mice and co-cultured with microglia and astrocytes as described in Figure 5.1 and 5.2. Supernatants were harvested for analysis of TNF α and IL-6 concentrations by ELISA. Co-culture of microglia with Th17 cells generated from wildtype and APP/PS1 mice had no significant effect on supernatant concentration of either TNF α or IL-6 (A and B). Co-culture of astrocytes with Th17 cells generated from wildtype and APP/PS1 mice significantly increased supernatant concentrations of IL-6 (C) (* $p < 0.05$, ** $p < 0.01$, ANOVA). Supernatant concentrations of TNF α were undetectable following co-culture of Th17 cells with astrocytes. Values are expressed as means \pm SEM (n=4).

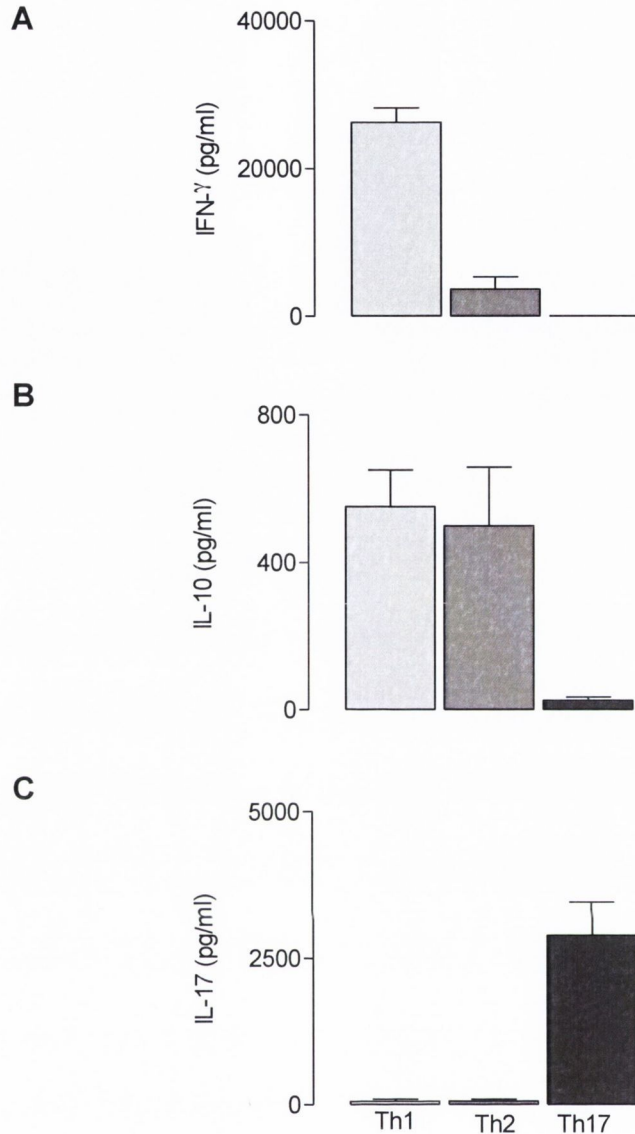


Figure 5.8. Generation of A β -specific Th1, Th2 and Th17 T cell lines.

Spleens were harvested from APP/PS1 and wildtype littermate control mice and cells were stimulated into A β -specific T cell lines under polarising conditions and in the presence of A β_{1-42} (15 μ g/ml). Th1 polarising conditions were IL-12 (50 ng/ml), Th2 polarising conditions were IL-4 (10 ng/ml) and anti-IFN- γ (5 μ g/ml) and Th17 polarising conditions were TGF- β (5 ng/ml), IL-1 β (25 ng/ml), IL-23 (50 ng/ml) and anti-IFN- γ . On the 4th day of the culture supernatants were removed for analysis of IFN- γ (A), IL-10 (B) and IL-17 (C) concentrations by ELISA. Th1 cells have high IFN- γ and IL-10 and low IL-17 production (A-C). Th2 cells have high IL-10 and low IFN- γ and IL-17 production (A-C). Th17 cells have high IL-17 production and low IFN- γ and IL-10 (A-C). Values are expressed as means \pm SEM (n=10).

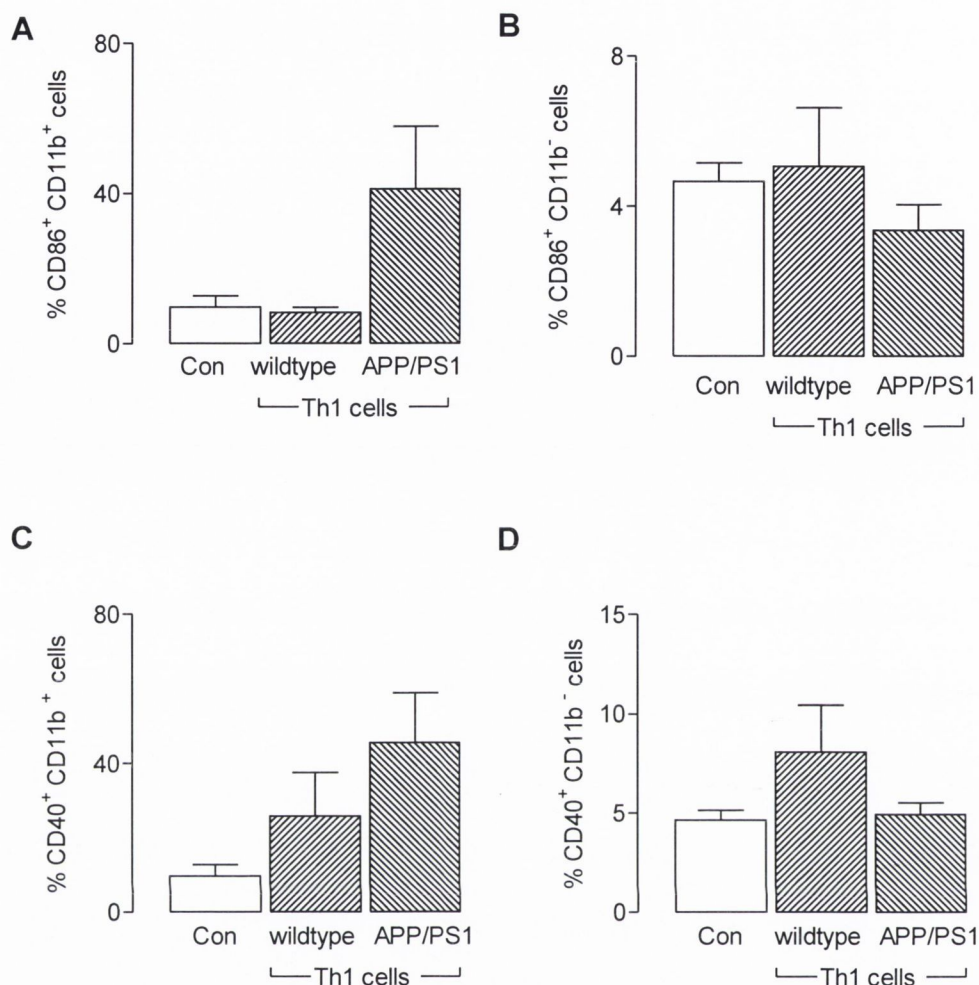


Figure 5.9. CD40 and CD86 expression is unaltered on microglia and astrocytes following co-culture with A β -specific Th1 cells.

A β -specific Th1 cells were generated from wildtype and APP/PS1 mice as described in Figure 5.8. After 4 days of polarisation A β -specific Th1 cell lines were co-cultured with microglia (CD11b⁺) and astrocytes (CD11b⁻) prepared from neonatal C57BL/6 mice, treated with A β ₁₋₄₂ (15 μ g/ml), for 24 hours. Expression of CD86 and CD40 on CD11b⁺ (A and C) and CD11b⁻ (B and D) cells was quantified by FACS. Co-culture of microglia and astrocytes with A β -specific Th1 cells generated from wildtype and APP/PS1 mice had no significant effect on the expression of CD86 or CD40 on microglia and astrocytes (A-D). Values are expressed as means \pm SEM (n=5-10).

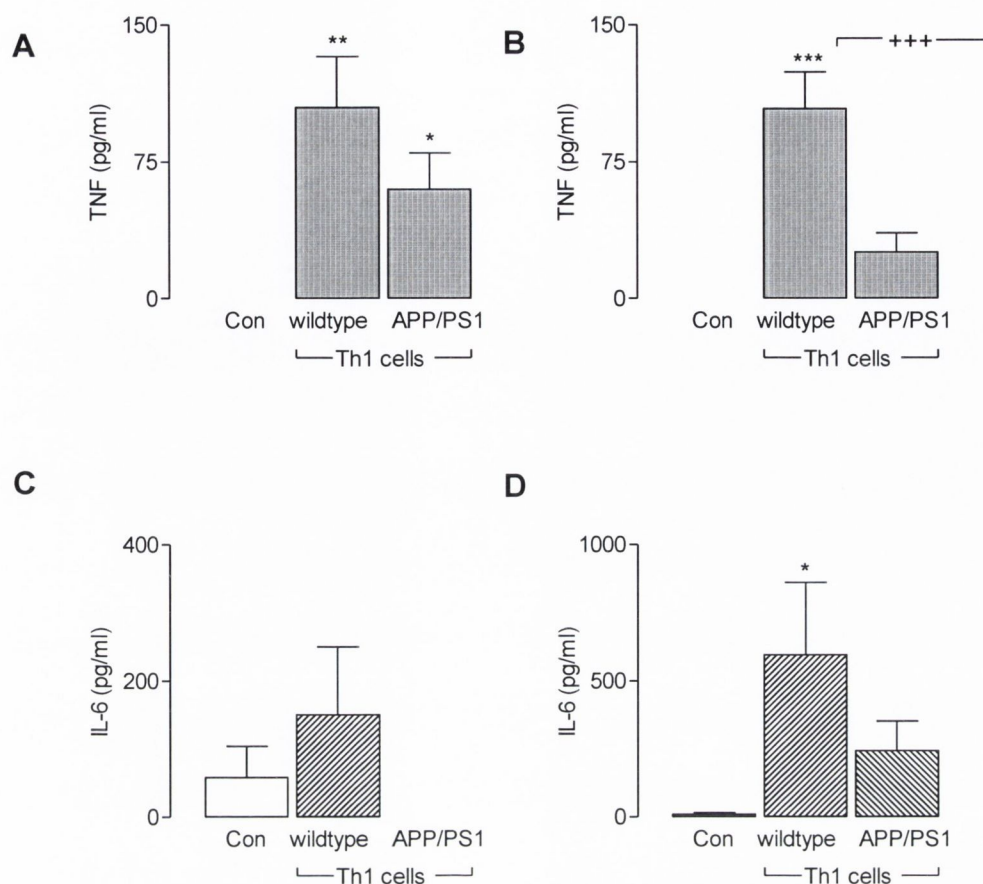


Figure 5.10. TNF α production was increased by microglia and astrocytes following co-culture with A β -specific Th1 cells.

A β -specific Th1 cells were generated from wildtype and APP/PS1 mice and co-cultured with microglia and astrocytes treated with A β_{1-42} as described in Figure 5.8 and 5.9. Supernatants were harvested for analysis of TNF α and IL-6 concentrations by ELISA. Co-culture of microglia with A β -specific Th1 cells, generated from wildtype and APP/PS1 mice, significantly increased supernatant concentrations of TNF α (A) (* $p < 0.05$, *** $p < 0.01$, ANOVA). Co-culture of astrocytes with A β -specific Th1 cells generated from wildtype mice significantly increased supernatant concentrations of TNF α (B) (** $p < 0.001$, ANOVA), and this increase was significantly attenuated by co-culture of astrocytes with A β -specific Th1 cells generated from APP/PS1 mice (B) (*** $p < 0.001$, ANOVA). Co-culture of astrocytes (D), but not microglia (C), with A β -specific Th1 cells generated from wildtype mice significantly increased IL-6 supernatant concentrations (D) (* $p < 0.05$, ANOVA). Values are expressed as means \pm SEM (n=4-8).

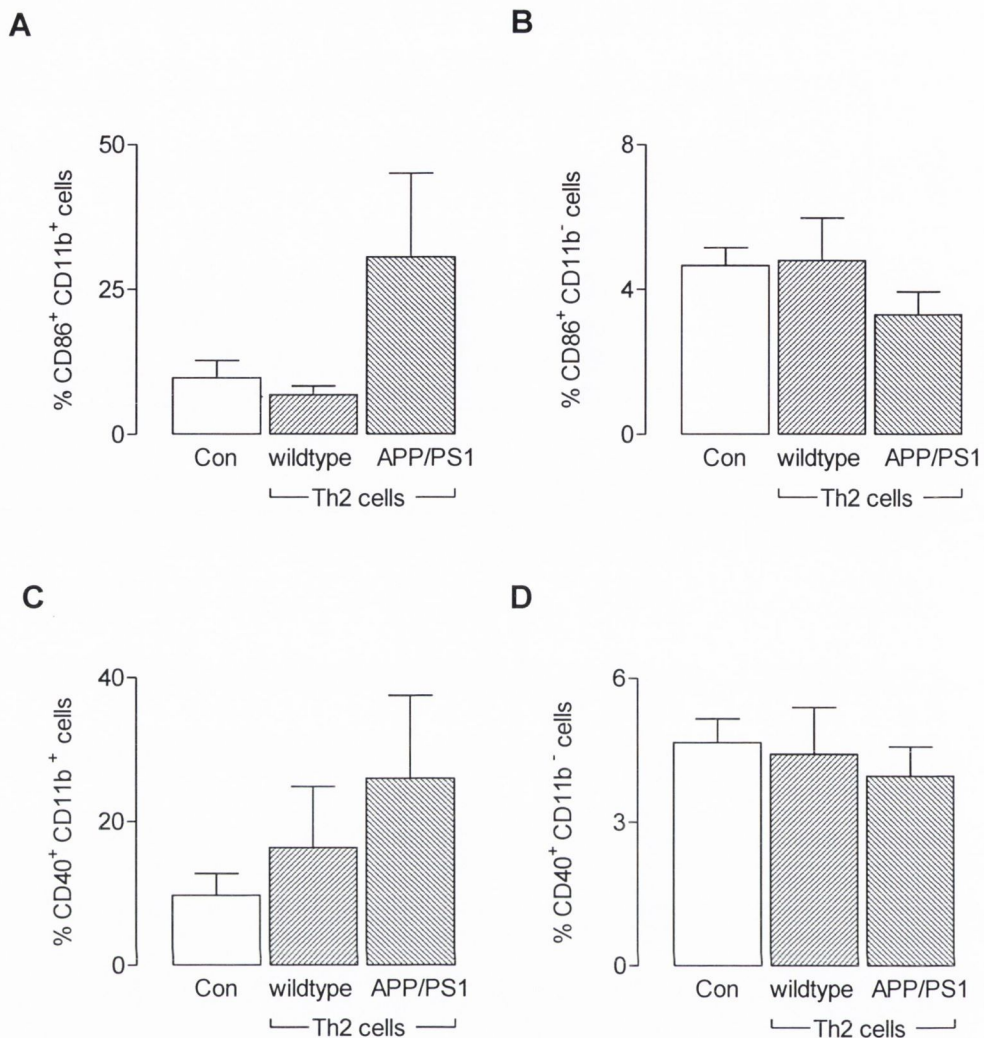


Figure 5.11. CD40 and CD86 expression is unaltered on microglia and astrocytes following co-culture with A β -specific Th2 cells.

A β -specific Th2 cells were generated from wildtype and APP/PS1 mice and co-cultured with microglia (CD11b⁺) and astrocytes (CD11b⁻) treated with A β ₁₋₄₂ as described in Figure 5.8 and 5.9. Expression of CD86 and CD40 on CD11b⁺ (A and C) and CD11b⁻ (B and D) cells was quantified by FACS. Co-culture of microglia and astrocytes with A β -specific Th2 cells generated from wildtype and APP/PS1 mice had no significant effect on the expression of CD86 and CD40 on microglia and astrocytes (A-D). Values are expressed as means \pm SEM (n=5-10).

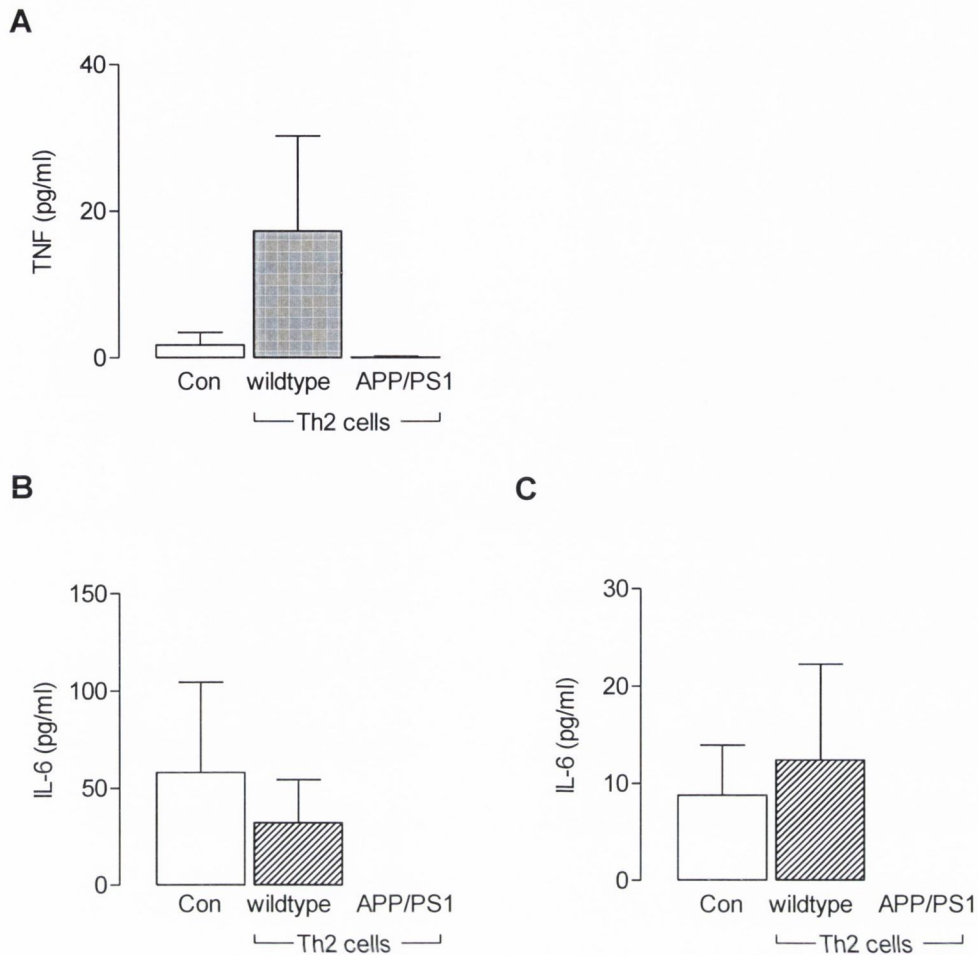


Figure 5.12. Cytokine production by microglia and astrocytes is unaltered following co-culture with A β -specific Th2 cells.

A β -specific Th2 cells were generated from wildtype and APP/PS1 mice and co-cultured with microglia and astrocytes treated with A β ₁₋₄₂ as described in Figure 5.8 and 5.9. Supernatants were harvested for analysis of TNF α and IL-6 concentrations by ELISA. Co-culture of microglia (A and B) and astrocytes (C) with A β -specific Th2 cells generated from wildtype and APP/PS1 mice had no significant effect on supernatant concentrations of TNF α and IL-6 (A-C). Supernatant concentrations of TNF α were undetectable following co-culture of A β -specific Th2 cells with astrocytes. Values are expressed as means \pm SEM (n=4-7).

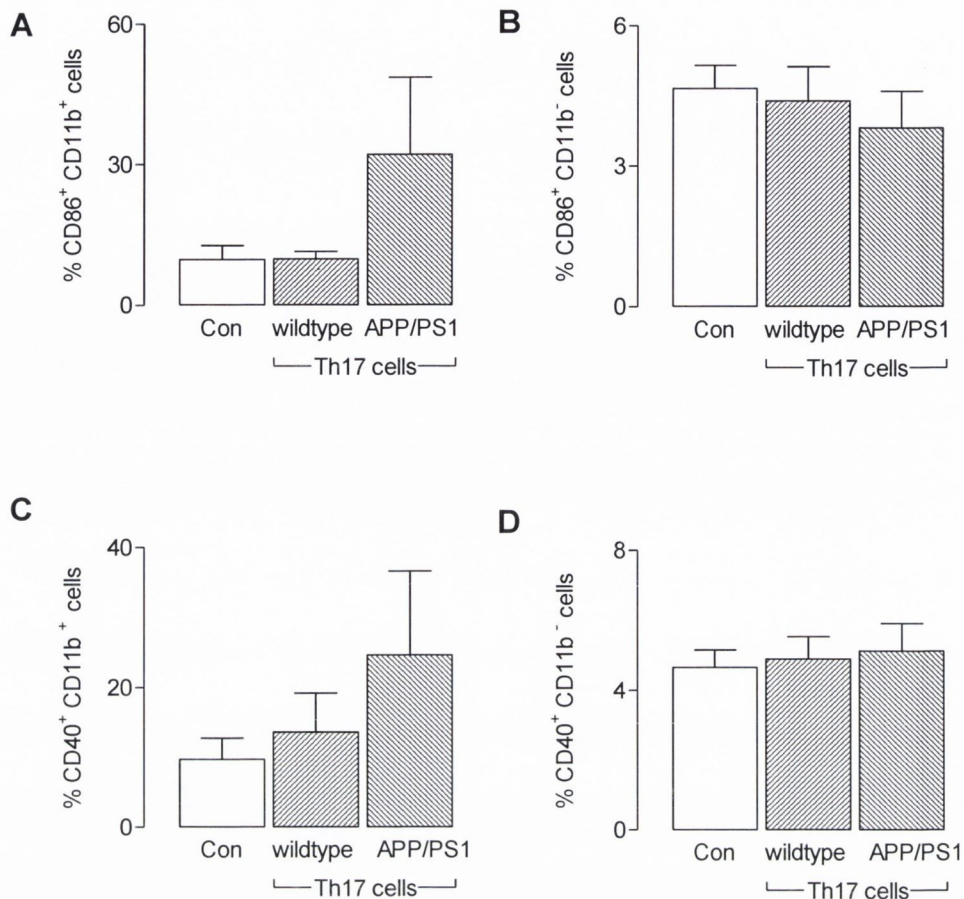


Figure 5.13. CD40 and CD86 expression is unaltered on microglia and astrocytes following co-culture with A β -specific Th17 cells.

A β -specific Th17 cells were generated from wildtype and APP/PS1 mice and co-cultured with microglia (CD11b⁺) and astrocytes (CD11b⁻) treated with A β ₁₋₄₂ as described in Figure 5.8 and 5.9. Expression of CD86 and CD40 on CD11b⁺ (A and C) and CD11b⁻ (B and D) cells was quantified by FACS. Co-culture of microglia and astrocytes with A β -specific Th17 cells generated from wildtype and APP/PS1 mice had no significant effect on the expression of CD86 and CD40 on microglia and astrocytes (A-D). Values are expressed as means \pm SEM (n=5-10).

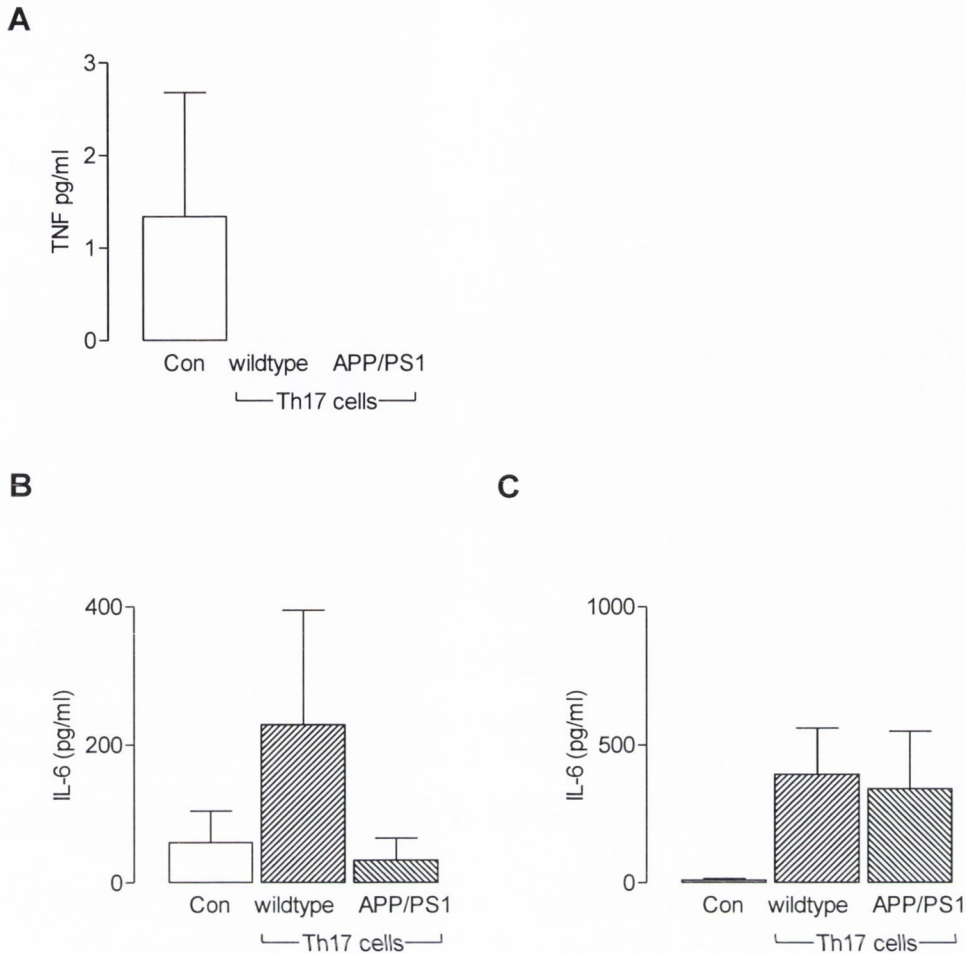


Figure 5.14. Cytokine production by microglia and astrocytes is unaltered following co-culture with A β -specific Th17 cells.

A β -specific Th17 cells were generated from wildtype and APP/PS1 mice and co-cultured with microglia and astrocytes treated with A β_{1-42} as described in Figure 5.8 and 5.9. Supernatants were harvested for analysis of TNF α and IL-6 concentrations by ELISA. Co-culture of microglia (A and B) and astrocytes (C) with A β -specific Th17 cells generated from wildtype and APP/PS1 mice had no significant effect on supernatant concentrations of TNF α and IL-6 (A-C). Supernatant concentrations of TNF α were undetectable following co-culture of A β -specific Th17 cells with astrocytes. Values are expressed as means \pm SEM (n=4-8).

5.4. Discussion

In this chapter the interaction of glia and distinct T cell subsets, including those that were A β -specific was investigated. Specifically the effect of Th1, Th2 and Th17 cells in modulating the expression of CD40 and CD86 and the production of the pro-inflammatory cytokines TNF α and IL-6 by glia was investigated. The effect of T cell subtypes generated from the spleens of wildtype mice were compared with cells generated from APP/PS1 mice. The data revealed that co-culturing of Th1 and Th17 cells with glia markedly enhanced microglial and astrocytic activation and, in some cases, this was enhanced if glia were co-cultured with T cells generated from APP/PS1 mice. In contrast it was found that co-culturing Th2 cells with glia exerted no effect. A β -specific Th1 cells induced glial activation but neither A β -specific Th2 or Th17 cells exerted any significant effect.

The process by which naïve CD4⁺ T cells differentiate into specific effector Th cells is well understood. It has been established that once naïve T cells migrate from the thymus they can become differentiated into appropriate effector cells following activation by two signals. The first signal is delivered through interaction of MHC class II on cells of the innate immune system with their specific TCRs (Huang *et al.*, 1999; Sharpe & Freeman, 2002). This process is accompanied by a secondary signal from co-stimulatory molecules CD80 and CD86 on innate immune cells, to CD28 on T cells. Once both signals are present, naïve CD4⁺ T cells will rapidly divide into a subpopulation of T cells with effector functions (Sharpe & Freeman, 2002). The phenotype of the activated CD4⁺ T cells generated depends, not only on the antigen presented, but on the cytokine environment present at the time of clonal expansion (Mosmann *et al.*, 1986). Naïve T cells differentiate into Th1 cells in the presence of IL-12, Th2 cells in the presence of IL-4 and Th17 cells in the presence of TGF- β , IL-1 β and IL-23 (Schluns & Lefrancois, 2003; Korn *et al.*, 2009; McQuillan *et al.*, 2010). In this study CD4⁺ T cells were polarised into non-specific and A β -specific Th1 cells by incubating cells in the presence of IL-12, Th2 cells by incubating cells in the presence of IL-4 and anti-IFN- γ and Th17 cells by incubating cells in the presence of TGF- β , IL-1 β , IL-23 and anti-IFN- γ . Predictably non-specific and A β -specific

Th1 cells secreted predominantly IFN- γ , Th2 cells secreted predominantly IL-10 and Th17 cells secreted predominantly IL-17. The secretion of a pattern of cytokines by T cells has already been described in both CD4⁺ clones, human and mouse T cells and the function of specific T cell subgroups correlates well with their distinctive cytokine profiles. For example Th1 cytokines are involved in cell mediated-inflammatory reactions and play a role in autoimmune diseases while Th2 promote antibody production and are involved in strong antibody and allergic responses (Mosmann & Sad, 1996). Th17 cells are implicated in pathogen clearance and also play a role in autoimmune disease (Korn *et al.*, 2009).

Previous studies have found that IFN- γ increases the expression of co-stimulatory molecules on human microglia and the secretion of cytokines by microglia (Becher & Antel, 1996). Priming of microglia *in vitro* with IFN- γ upregulates MHC class II expression and co-stimulatory molecules on microglia allowing for antigen processing and T cell restimulation (Aloisi *et al.*, 2000b). The role of astrocytes as APCs is unclear. It has been noted that the type of T cell present renders astrocytes as either efficient or unefficient APCs (Aloisi *et al.*, 2000b). Aloisi and colleagues (1999) demonstrated that astrocytes are more efficient in restimulating Th2 cells compared with Th1 cells and fail to prime naïve T cells. However astrocytes have been found to upregulate MHC class II expression following IFN- γ exposure (Shrikant & Benveniste, 1996). The data presented here indicate that co-culture of glia with non-specific Th1 cells significantly increased the expression of CD40 on both microglia and astrocytes, and the effect on microglia was greater following co-culture with Th1 cells generated from APP/PS1. Co-culture of Th17 cells with glia significantly enhanced expression of CD40 on astrocytes. These results are consistent with previous studies from this lab which have found that co-culture of MOG-specific Th1 and Th17 cells with glia increases the expression of CD40 on microglia (Murphy *et al.*, 2010). It has been proposed that increased expression of CD40 and CD80 is a consequence of cell-cell contact (Wolf *et al.*, 2001). Although Seguin and colleagues (2003) demonstrated that supernatants taken from Th1 cells could induce both CD86 and CD40 expression on microglia. It has been suggested that Th2 cells are inefficient at stimulating microglia due to their secretion of microglia-deactivating factors, IL-4 and IL-10 (Mosmann & Sad, 1996). Consistently no significant change in the expression of CD40 by glia was

observed following co-culture with Th2 cells which supports previous findings that Th2 cells cultured with adult murine microglia failed to increase expression of APC related molecules and in turn microglia failed to restimulate Th2 cells (Aloisi *et al.*, 2000a). Although a study by Gimsa and colleagues (2001) using entorhinal-hippocampal slices demonstrated that prestimulated Th2 cells were able to invade slices to the same degree as Th1 cells and that both Th1 and Th2 cells increased the expression of CD40 on microglia compared to control cultures however total CD40 staining was somewhat higher in Th1 co-cultures. These authors also found that Th2 cells were unable to increase the expression of ICAM-1, an important adhesion and co-stimulatory molecule, on microglial but were able to diminish the Th1-induced increase in microglial expression of ICAM-1 (Gimsa *et al.*, 2001).

It has been suggested that CD40 is fundamental marker of certain disease pathologies and inflammation. A role for CD40-CD40L pathway in MS has been suggested; it has been shown that CD40⁺ microglia and macrophages are present in MS lesions (Gerritse *et al.*, 1996). Indeed studies have shown that myelin basic protein (MBP)-specific TCR mice lacking CD40L have T cell priming deficiencies and EAE could not be provoked in these animals following immunisation with encephalitogenic peptide (Grewal & Flavell, 1996). Whereas blockade of the CD40-CD40L interaction reduces disease severity in experimental autoimmune diseases such as EAE (Gerritse *et al.*, 1996; Grewal & Flavell, 1996). Furthermore it has been shown that CD40-CD40L interaction in the presence of IFN- γ is required for IL-12 production by microglia which in turn promotes polarisation of T cells into Th1 cells and that blockade of this pathway could have the additional advantage of inhibiting IL-12 production without affecting the ability of CNS APCs to produce PGE₂, which has an inhibitory influence on Th1 responses. (Aloisi *et al.*, 1999).

Previously it has been suggested that interaction of CD28 on T cells and CD80/CD86 on APCs is crucial for the onset and course of EAE (Wolf *et al.*, 2001). Both CD80 and CD86 are upregulated on microglia following co-culture with MOG-specific Th1 and Th17 cells (Murphy *et al.*, 2010). However no significant change in CD86 expression on microglia and astrocytes following co-culture with Th1, Th2 and Th17 cells was observed in the present study. However, it has previously been suggested that initial CD86 stimulation can induce the

expression of IL-4, and favour a Th2 response, while CD80 stimulation has been reported to favour a Th1 response (Freeman *et al.*, 1995). Furthermore, Wolf and colleagues (2001) demonstrated that Th1 cells independent of antigen specificity, can switch the expression of the co-stimulatory molecules on microglia from CD86 to CD80. Taking this evidence into account further experiments should assess expression of CD80 as well as CD86.

Activation of microglia during CNS disease leads to the production of the pro-inflammatory cytokines such as TNF α and IL-6, which have been found to contribute to myelin damage and CNS inflammation (Benveniste, 1997). There is extensive literature implicating the production of TNF α specifically as a critical mediator of autoimmune inflammatory pathologies such as MS and EAE. TNF α is detectable in lesions of MS and in EAE and is increased in the serum and CSF of patients with MS. TNF α can induce cytotoxicity in rodent and human primary oligodendrocytes. (Probert *et al.*, 2000) and can influence lymphocyte trafficking across the endothelium and upregulate many of the adhesion molecules involved in this process (Chabot *et al.*, 1997). It has been demonstrated that T cell-microglia interactions *in vitro* significantly increase the production of TNF α by microglia (Chabot *et al.*, 1997). Dasgupta and colleagues (2005) demonstrated that neuroantigen-specific T cells interacting with microglia increase the expression of IL-1 β and IL-6 as well as TNF α . Furthermore supernatants from Th1 cells can induce the secretion of pro-inflammatory cytokines, TNF α and IL-6, and the chemokine IP-10 from microglia (Seguin *et al.*, 2003). While studies have found that in addition to the effect of Th1 cells, Th17 cells co-cultured with glia enhance the production of TNF α and IL-6 (Murphy *et al.*, 2010). The results of the present studies show that Th1 cells increased secretion of TNF α and IL-6 in microglial and astrocytic cultures and Th17 cells increased IL-6 production by astrocytes; no significant change was observed following co-culture of glia with Th2 cells. The increased production of cytokines by glia co-cultured with Th1 and Th17 cells is concomitant with the increase in CD40 expression on microglia and astrocytes which concurs with the finding that ligation of CD40 with CD40L activates NF- κ B and enhances cytokine production. This may also account for the lack of cytokine production observed in Th2 co-cultures as no significant increase in CD40 expression was observed in these cultures. Th17 cells, surprisingly, had no affect on cytokine production from microglia but the difference in cytokine

production by glial cells in response to Th1 and Th17 cells could be explained by a recent study from Kroenke and colleagues (2008). These authors suggest that although Th1 and Th17 cells are involved in the pathology of MS, the form of inflammation generated by the T cells differs between the two subsets. This group reported that Th1-driven EAE favoured the upregulation of monocyte- and lymphocyte-attracting chemokines while Th17-driven EAE favoured the upregulation of neutrophil chemokines (Kroenke *et al.*, 2008). Together the data suggest that co-culture of glia with Th1 and Th17 cells but not Th2 cells significantly exaggerates pro-inflammatory cytokine production as measured by TNF α and IL-6, suggesting that interaction of these cells facilitates a detrimental inflammatory environment. However there is some debate over the role of TNF α in EAE with some evidence suggesting that disease progression is exacerbated in TNF $^{-/-}$ mice immunised with MOG (Liu *et al.*, 1998) and other evidence indicating that TNF α stimulates development and progression of the disease (Probert *et al.*, 2000). The present results might suggest that the production of TNF α by glia has a detrimental role as it was only produced in response to Th1 cells. The production of anti-inflammatory cytokines by glia in response to Th2 cells was not assessed in this study and should be addressed in the future.

Infiltrating T cells are not as common in AD as in conditions such as meningitis and MS (Bitsch *et al.*, 2000) none the less their presence, although low, has been described in several studies (Rogers *et al.*, 1988; Togo *et al.*, 2002). A study from Monsonogo and colleagues (2003) described the presence of A β -reactive T cells in the brains of healthy young and elderly subjects and in AD patients, with the crucial finding that these T cells, although present in all subjects, were significantly increased in elderly patients and patients with AD. These authors postulated that capture of A β by APCs results in the migration of APCs to lymph nodes in turn inducing T cell activation (Monsonogo *et al.*, 2003). However it still remains unclear if the role of T cells is beneficial or detrimental. Evidence suggests that glia act as effective APCs for A β -specific Th1 and Th17 cells and enhance A β -induced pro-inflammatory cytokine production and co-stimulatory molecule expression on glia (McQuillan *et al.*, 2010) and one evidence shows that MHC class II and T cells are co-localised with plaques (McGeer *et al.*, 1987). Furthermore it has been reported that IFN- γ which is derived from Th1 cells is required for A β -induced neuronal toxicity (Li *et al.*,

2004). In contrast Th2-type cytokines can attenuate A β -induced cytokine production by microglia (Szczepanik *et al.*, 2001).

In contrast to the effects of non-specific T cells there was no significant change in either the expression of CD40 or CD86 on microglia and astrocytes following co-culture with A β -specific Th1, Th2 and Th17 cells. This was surprising given the effect of non-specific Th1 and Th17 cells and in view of the findings from another study that both A β -specific Th1 and A β -specific Th17 cells enhanced A β -induced expression of CD40 and CD86 as well as MHC class II and CD80 on microglia (McQuillan *et al.*, 2010). It is worth noting that some of the experimental conditions were different between these two studies and may account for the discrepancies seen. Firstly the concentration of A β used here to stimulate microglia and astrocytes was 15 μ g/ml versus 40 μ g/ml in the published report. Furthermore the A β -specific T cells were generated *ex-vivo* by the addition of A β ₁₋₄₂ to the T cell cultures whereas McQuillan and colleagues (2010) generated their A β -specific T cells through the immunisation of C57BL/6 mice with A β and CpG and then restimulated T cells *ex-vivo* with A β . The lack of effect of Th2 cells concurs with my earlier findings and previous published data from this lab (McQuillan *et al.*, 2010). Interestingly McQuillan and colleagues (2010) reported that Th2 cells were found to decrease Th1-induced CD40 expression.

Both TNF α and IL-6 are secreted by microglia and astrocytes in the AD brain (Lue *et al.*, 2001a). It has been well documented that A β induces the production of pro-inflammatory cytokines in cultured microglia (Davis *et al.*, 1992; Meda *et al.*, 1995). In the present study the role of A β -specific Th1, Th2 and Th17 cells on TNF α and IL-6 production by microglia and astrocytes treated with A β was investigated. Here it was found that both TNF α and IL-6 were produced by glia following co-culture with A β -specific Th1 cells however neither A β -specific Th17 nor A β -specific Th2 cells had any effect on cytokine production by glia. These results are consistent with others suggesting that augmenting factors such as IFN- γ act synergistically with A β to enhance this inflammatory response; previously it has been demonstrated that IFN- γ enhances A β -induced production of TNF α and NO by glia (Goodwin *et al.*, 1995; Meda *et al.*, 1995). A more recent study from Gasic-Milenkovic and colleagues (2003) found that A β synergised with IFN- γ , LPS and advanced glycation endproducts to enhance

TNF α and IL-6 production from microglia. Similarly a study from McQuillan and colleagues (2010) also observed that A β -specific Th1 cells induced the production of TNF α and IL-6 by glia and that A β -specific Th2 cells had no influence on the production of either cytokine by glia. These results implicate the interaction between glia and A β -specific Th1 cells as detrimental in response to A β , while the absence of a Th2 cell response further supports their potential anti-inflammatory role in AD. Furthermore it has been found that both IFN- γ and IL-12 (Th1 cytokines) are enhanced in the cerebral cortex of APP transgenic mice whereas, IL-4 (Th2 cytokine) is decreased (Abbas *et al.*, 2002). Previously it has been suggested that A β -specific Th2 cells could be beneficial by secreting anti-inflammatory cytokines and downregulating an inflammatory environment (Monsonogo *et al.*, 2003). A β -specific Th2 cells can reduce plaque associated microglia in APP/PS1 mice and this is associated with an improvement in cognition in these mice (Cao *et al.*, 2009). The Th2 cytokine IL-4 has been shown to reduce microglia activation in response to IFN- γ (Nguyen & Benveniste, 2000) and modulate co-stimulatory molecule expression on glia in response to Th1 and Th17 cells (McQuillan *et al.*, 2010).

Interestingly in these studies TNF α production was significantly decreased in astrocytes following co-culture with A β -specific Th1 cells generated from APP/PS1 mice compared with A β -specific Th1 cells generated from wildtype mice. This result may be explained by a previous observation that increased T cell reactivity to A β is not observed in APP transgenic mice possibly as a consequence of T cell tolerance (Monsonogo *et al.*, 2001). These authors suggested that the chronic expression of A β increased T cell hyporesponsiveness and tolerance. Thus it might be hypothesised that the decreased responsiveness in glia cytokine production to A β -specific Th1 cells generated from APP/PS1 mice is due to the tolerance of these T cells.

The results from these studies implicate a role for T cells specifically, Th1 and Th17, in inducing and/or exacerbating inflammation as a result of their interaction with microglia and astrocytes. Here it was observed that Th1 cells induced the expression of CD40 on microglia and astrocytes and the production of TNF α and IL-6 by microglia and astrocytes. Th2 cells were found to have no effect on either the expression of co-stimulatory molecules on glia or the production of cytokines by glia. Th17 cells induced the expression of CD40 and

the production of IL-6 in astrocytes. Furthermore it was observed that A β -specific Th1 cells induced the production of TNF α and IL-6 by glia yet A β -specific Th2 and Th17 cells had no effect. Together the data suggest that Th1 cells have the greatest effect on glial activation and this topic needs further investigation in an *in vivo* model which will be addressed in the next chapter.

Table 5.1. Results summary of the expression of co-stimulatory molecules and production of cytokines following co-culture of non-specific T cells with microglia and astrocytes.

		Generated from Wildtype mice			Generated from APP/PS1 mice		
		Th1	Th2	Th17	Th1	Th2	Th17
Microglia	CD86						
	CD40				↑↑		
	TNF α				↑		
	IL-6						
Astrocytes	CD86						
	CD40	↑			↑		↑↑↑
	TNF α	↑					
	IL-6	↑		↑	↑		↑↑

Table 5.2. Results summary of the expression of co-stimulatory molecules and production of cytokines following co-culture of A β -specific T cells with microglia and astrocytes.

		Generated from Wildtype mice			Generated from APP/PS1 mice		
		A β Specific -Th1	A β Specific -Th2	A β Specific -Th17	A β Specific -Th1	A β Specific -Th2	A β Specific -Th17
Microglia	CD86						
	CD40						
	TNF α	↑↑			↑		
	IL-6						
Astrocytes	CD86						
	CD40						
	TNF α	↑↑↑			↓↓↓		
	IL-6	↑					

Chapter 6

Chapter 6

6.1. Introduction

AD is a progressive neurodegenerative disease that is characterized by profound neuronal loss and development of neurofibrillary tau tangles and neuritic plaques. The A β cascade hypothesis is one of the main theories which has been suggested to explain the development of neurodegeneration in AD. This theory suggests that an imbalance between the production and clearance of A β in the brain gives rise to the accumulation and the formation of A β -plaques, exacerbated glial cell activation and neuronal loss which ultimately causes cognitive decline (Karran *et al.*, 2011). There is strong evidence in the literature which supports the A β hypothesis. Of note is the fact that neuritic plaques, which are composed of the A β -protein, are associated with activated microglia whilst diffuse plaques, which have been termed clinically benign A β deposits, are not associated with activated microglia (Benveniste *et al.*, 2001). It has been suggested that interaction of A β with microglia gives rise to chronic inflammation which in turn contributes to both neuronal death and plaque formation (Benveniste *et al.*, 2001; McGeer & McGeer, 2003). One proposal is that the chronic inflammatory environment is not causative but plays a large role in the pathogenesis of AD (McGeer & McGeer, 2003). As a result, research has focused on the development of therapies that could allow A β clearance from the brain, and therapies that could have an anti-inflammatory effect.

The removal of A β from the brain has received substantial attention as a therapeutic strategy and A β clearance after anti-A β immunotherapy was first reported in the PDAPP transgenic mouse model of AD following A β ₁₋₄₂ vaccination by Schenk and colleagues (1999). Since then other investigators, using the same vaccination protocol and other transgenic models of AD, have shown similarly-reduced A β levels which is associated with a decrease in cognitive deficits in the brains of these mice (Janus *et al.*, 2000; Morgan *et al.*, 2000). It is not clear by what mechanism immunotherapy acts although Wilcock and colleagues (2003) have reported that diffuse A β is removed independent of microglial activation whereas removal of compact A β required microglial

activation. In a later study these authors found that vaccination of transgenic mice, over a 3 month period, similarly decreased A β load and this was accompanied by microglial activation and a dramatic increase in circulating A β levels in the plasma (Wilcock *et al.*, 2004). Thus it has been hypothesized that anti-A β immunotherapy and the resultant plaque clearance may be due to the activation of microglia to a phagocytic phenotype, via opsonization of A β (Schenk *et al.*, 1999). It is possible that A β may move down the concentration gradient from the brain into the plasma; this has been termed the peripheral sink mechanism (DeMattos *et al.*, 2001). Following animal trials in which no significant unwanted side effects were observed, an anti-A β immunotherapy clinical trial was initiated. In this clinical trial, a synthetic A β ₁₋₄₂ peptide (AN-1792), with adjuvant QS21, was peripherally administered to AD patients. The trial passed Phase I but was rapidly halted in Phase II when patients developed meningoencephalitis, which was thought to be as a result of an immune response to A β mediated by infiltrating Th1 cells (Pfeifer *et al.*, 2002). However active immunisation promoted plaque clearance in the brains of these AD patients (Nicoll *et al.*, 2003). Despite the negative side effects of the current A β -based immunotherapeutic approaches, it was established that both mouse models of AD and AD patients were capable of developing A β -specific adaptive immune responses suggesting that successful therapeutic intervention may lie in limiting or altering the A β -specific immune response (Ethell *et al.*, 2006).

Previously the CNS was described as an immunologically privileged site but more recently it is more correctly viewed as an immunologically-specialized site (Ransohoff *et al.*, 2003). Extensive literature describes the potential mechanisms of T cell entry into the CNS during AD. It is acknowledged that the BBB may become more permeable during ageing and AD allowing for the invasion of peripheral immune cells into the CNS (Farrall & Wardlaw, 2009). Furthermore, the results presented in chapter 3 suggest that, A β can stimulate the production of a range of cytokines and chemokines *in vitro*, while others have found similar cytokine and chemokine production from human post-mortem microglia stimulated with A β (Lue *et al.*, 2001b). The significance of this is that it has been suggested that the production of different cytokines and chemokines may direct selective peripheral immune cell recruitment into the CNS (Tran *et al.*, 2000b; Stalder *et al.*, 2005). It is also known that A β ₁₋₄₂ can freely cross the BBB

and stimulate naïve T cells outside of the CNS (DeMattos *et al.*, 2002). Indeed there is evidence documenting the presence of T cells in the AD brain (Rogers *et al.*, 1988; Togo *et al.*, 2002; Monsonego *et al.*, 2003), although not to the same degree as seen in autoimmune diseases like MS. None the less, their presence has prompted investigators to assess the role they may have in the pathogenesis of AD and it remains uncertain if the presence of T cells in the brain is beneficial or destructive. A destructive role for T cells specifically A β -specific Th1 cells was implicated in the AN-1792 clinical trial and therefore a newer vaccine, CAD106, designed to avoid the activation of A β -specific T cells has shown reduced A β -accumulation in APP transgenic mice and is now in Phase II trials in AD patients (Wiessner *et al.*, 2011).

It has been shown *in vitro* that both Th1 cells (McQuillan *et al.*, 2010) and Th1 cell-secreted cytokines (Seguin *et al.*, 2003; Li *et al.*, 2004) exacerbate microglial activation and inhibit A β degradation (Yamamoto *et al.*, 2008). A beneficial role for T cells has been implicated in studies from the laboratory of Ethell and colleagues (2006) who found that adoptive transfer of a mixed population of A β -specific T cells into APP/PS1 mice reversed synaptic loss and cognitive decline. These authors observed that the cognitive improvement was attributed to Th2 cells and not Th1 cells (Ethell *et al.*, 2006). A more recent study using APP transgenic mice expressing low levels of IFN- γ showed decreased plaque burden which the authors attributed to the infiltration of A β -specific T cells (Fisher *et al.*, 2010). Correspondingly *in vitro* studies suggest that both Th2 cells (McQuillan *et al.*, 2010) and Th2 cell-secreted cytokines (Szczepanik *et al.*, 2001) decrease microglial activation and thus could have a beneficial effect by downregulating the pro-inflammatory environment. It has been shown that Th2 cell cytokines enhance A β degradation (Yamamoto *et al.*, 2008). Not much is known about the role of Th17 cells in the pathogenesis of AD although their role in the pathogenesis of EAE is well established, (Langrish *et al.*, 2005), and the evidence indicates that they upregulate expression of co-stimulatory molecules and pro-inflammatory cytokine production *in vitro* (McQuillan *et al.*, 2010; Murphy *et al.*, 2010).

The mechanism by which T cells have beneficial or detrimental roles may involve their modulatory effect on microglial activation both through cell-cell contacts and as a consequence of their ability to secrete an array of pro- and anti-

inflammatory cytokines. The results discussed in the previous chapter and evidence from others have established that T cells, specifically Th1 and Th17 cells can induce expression of co-stimulatory molecules on glia and alter the production of pro-inflammatory cytokines, while it was found that Th2 cells exerted no effect on glial activation. It has been established that T cell-induced or A β -induced activation of microglia can be enhanced when these two factors are present together. Specifically, the Th1 cell-secreted cytokine IFN- γ has a profound effect on microglial activation *in vitro*, and it synergises with A β to induce microglia-mediated neurotoxicity (Goodwin *et al.*, 1995; Meda *et al.*, 1995; Li *et al.*, 2004). While it inhibits microglial phagocytosis of A β (Koenigsknecht-Talboo & Landreth, 2005; Yamamoto *et al.*, 2008). Furthermore, microglia stimulated with IFN- γ can present A β to T cells and trigger proliferation of A β -specific T cells (Town *et al.*, 2005), while IFN- γ upregulates β -secretase resulting in increased A β production (Yamamoto *et al.*, 2007).

Interestingly it has been found that IFN- γ is significantly enhanced in the cerebral cortex of APP transgenic mice (Abbas *et al.*, 2002) and higher levels of IFN- γ have been found in the post-mortem brain tissue of AD patients compared with age-matched controls (Huberman *et al.*, 1994). Together these studies suggest that the interaction of Th1 cells with microglia and A β may have a profound effect on the progression of AD, suggesting that perhaps targeting Th1 cells and the secretion of their signature cytokine, IFN- γ , may have beneficial effects.

The aims of this study were to:

- Establish if Th1 and Th17 cells were present in the brains of aged APP/PS1 mice.
- Investigate the effects of Th1 and Th17 cells, and their signature cytokines IFN- γ and IL-17, respectively on microglial activation in mixed glia in the presence or absence of A β ₁₋₄₂.
- Investigate the effect of adoptive A β -specific T cell transfer on microglial activation in APP/PS1 mice.
- Investigate the effect of A β -specific Th1 cell transfer on plaque load and microglial activation and to examine what effect blocking IFN- γ might have on microglial activation and plaque burden in APP/PS1 mice.

6.2. Methods

Male and female APP/PS1, and wildtype littermate control, mice (18 months old) were anaesthetised with sodium pentobarbital (40 μ l) and perfused intracardially with sterile ice-cold PBS (20 ml). Brains were harvested for mononuclear cell isolation by the 5 layer percoll method (see section 2.8 for details). Following separation of the cells into layers based on relative densities using percoll gradients, the mononuclear cell layer was transferred into FACS tubes. Cells were washed and prepared for intracellular staining using a cell permeabilisation kit and stimulated with PMA, ionomycin and BFA for 4 hours. Following stimulation, cells were incubated in the presence of anti-CD16/CD32 to block non-specific binding, incubated with appropriate FACS antibodies and fixed to allow analysis using FlowJo software (see section 2.9.2 for details).

In a separate set of experiments, spleens were harvested from C57BL/6 mice (2 months old) and CD4⁺ T cells were isolated using a MACS and a CD4⁺ T cell isolation kit. CD4⁺ T cells were plated in 24-well plates and polarized into Th1 and Th17 cells in the presence of specific polarising cytokines for 4 days (see section 2.7.3.1 for details). On the 4th day of the culture, supernatants were taken for cytokine analysis of IFN- γ and IL-17 concentrations by ELISA (see section 2.12 for details), and cells were harvested for co-culture with mixed glia. Mixed glia were prepared from 1-day old C57BL/6 mice and cultured for 14 days prior to T cell co-culture (see section 2.1.2 for details). Th1/Th17 cell lines were co-cultured with mixed glia at a ratio of 1:2 and, after 1 hour of incubation, cells were stimulated with A β ₁₋₄₂ (10 μ M) and incubated for 24 hours. Mixed glia were also treated in the presence or absence of IFN- γ (20 ng/ml) or IL-17 (20 ng/ml) (see section 2.7.3.2 for details). Cells were harvested for cell surface marker expression of MHC class II, CD86 and CD40 by flow cytometry (see section 2.9.1 for details).

In a separate series of experiments, A β -specific T cells were generated from wildtype mice which received a footpad immunisation of A β (75 μ g/mouse) and CpG (25 μ g/mouse) and, after 21 days, the mice were boosted with A β and CpG. Mice were sacrificed 7 days after the booster injection and the spleens were harvested. The cell preparation was restimulated *ex vivo* with A β (25 μ g/ml) and appropriate cytokines and/or antibodies depending on the type of T cell line being

developed (see section 2.7.4.1 for details). Following generation of A β -specific T cell lines, A β -specific Th1 and Th17 cells were injected i.v. into APP/PS1 mice (6-7 months old; 15×10^6 cells/mouse; see section 2.7.4.1 for details). After 2 weeks APP/PS1 mice were anaesthetised with sodium pentobarbital (40 μ l) and perfused intracardially with ice-cold PBS (20 ml). The brains were rapidly removed, bisected and snap-frozen for later immunohistochemical analysis (see section 2.14 for details).

In another series of experiments, APP/PS1 and wildtype littermates received an i.p. injection of either anti-IFN- γ or β -galactosidase (600 μ g/mouse). Twenty four hours later, Th1 cells (15×10^6 cells/mouse) were injected (300 μ l) into the lateral tail vein of the mice. Anti-IFN- γ or β -galactosidase antibody injections were repeated several days after adoptive A β -specific T cell transfer (see section 2.7.4.2 for details). Mice were killed 34 days after adoptive A β -specific T cell transfer by cervical dislocation and tissue was taken for later analysis of A β concentration by multi-spot ELISA (see section 2.13 for details) and microglial activation and A β -plaque load by immunohistochemistry (see section 2.14 for details).

6.3. Results

6.3.1. Th1 and Th17 cell are present in the periphery and infiltrate the brains of APP/PS1 mice.

Flow cytometry was used to investigate the presence of T cells in the brains of wildtype and APP/PS1 mice. The data revealed that there were very few CD3⁺CD4⁺ cells in the brain of wildtype mice but a significantly greater number in brain tissue prepared from APP/PS1 mice (***p*<0.001; student's *t*-test; Figure 6.1A and C). Intracellular staining revealed that a proportion of these CD4⁺ cells stained positively for IFN- γ and for IL-17, but there was no significant difference between the numbers of CD4⁺ IFN- γ ⁺ cells and CD4⁺ IL-17⁺ cells, suggesting that equal numbers of Th1 and Th17 cells were present in the brains of APP/PS1 mice (Figure 6.1B and D). The presence of CD3⁺CD8⁺ cells was also assessed and it was found that there was no genotype-related difference in the number of these cells in brain tissue (Figure 6.2A and B), although intracellular staining indicated that a greater proportion of these CD8⁺ cells stained positively for IFN- γ compared with IL-17 (***p*<0.01; student's *t*-test; Figure 6.2C).

6.3.2. Generation of Th1 and Th17 T cell lines.

To assess that CD4⁺ T cells were correctly polarised into Th1 and Th17 cell lines, supernatants from the T cell lines were assessed for the production of IFN- γ and IL-17. Figure 6.3A and B demonstrates that cells polarised under Th1-inducing conditions were found to produce high levels of IFN- γ and low concentrations of IL-17. Cells polarised under Th17-inducing conditions produced low concentrations of IFN- γ and high concentrations of IL-17.

6.3.3. Th1 and Th17 cells and their signature cytokines, IFN- γ and IL-17, alter the expression of MHC class II and co-stimulatory molecules on microglia.

T cells were co-cultured with mixed glia in the presence or absence of A β ₁₋₄₂. Mixed glia were also incubated with IFN- γ or IL-17 in the presence or

absence of A β ₁₋₄₂. To examine the effect of Th1 and Th17 cells and their signature cytokines IFN- γ and IL-17 on microglial activation, the expression of MHC class II and co-stimulatory molecules CD40 and CD86 were assessed by FACS. The data revealed that the percentage of CD11b⁺CD40⁺ cells was not affected by incubating microglia in the presence of Th1 cells or IFN- γ . However A β ₁₋₄₂ markedly increased the percentage of CD11b⁺CD40⁺ cells and this was not affected by the presence of Th1 cells or IFN- γ (**p<0.01, ***p<0.001, ANOVA; Figure 6.4A and B).

The percentage of CD11b⁺CD86⁺ cells was significantly increased by incubating microglia in the presence of Th1 cells or IFN- γ (*p<0.05, ***p<0.001, ANOVA; Figure 6.4A and C). The percentage of CD11b⁺CD86⁺ cells was significantly enhanced by incubating microglia in the presence of IFN- γ compared with Th1 cells (⁺p<0.05, ANOVA; Figure 6.4A and C). However the percentage of CD11b⁺CD86⁺ cells was not altered by incubating microglia in the presence of A β ₁₋₄₂.

The percentage of CD11b⁺MHC class II⁺ cells was significantly increased by incubating microglia in the presence of IFN- γ (**p<0.01, ANOVA; Figure 6.5A and B). The percentage of CD11b⁺MHC class II⁺ cells was significantly enhanced by incubating microglia in the presence of IFN- γ compared with Th1 cells (⁺p<0.05, ANOVA; Figure 6.5A and C). However the percentage of CD11b⁺MHC class II⁺ cells was not altered by incubating microglia in the presence of Th1 cells or A β ₁₋₄₂.

The same parameters were investigated following co-culture of mixed glia with Th17 cells and incubation with IL-17 in the presence or absence of A β ₁₋₄₂. The data revealed that the percentage of CD11b⁺CD40⁺ cells was not affected by incubating microglia in the presence of Th17 cells or IL-17. However A β ₁₋₄₂ markedly increased the percentage of CD11b⁺CD40⁺ cells and this was not affected by the presence of Th17 cells or IL-17 (*p<0.05, **p<0.01, ***p<0.001, ANOVA; Figure 6.6A and B).

The percentage of CD11b⁺CD86⁺ cells and CD11b⁺MHC class II⁺ cells was not affected by incubating microglia in the presence of Th17 cells, IL-17 or A β ₁₋₄₂ (Figure 6.6A and C and 6.7A and B).

6.3.4. A β -specific Th1 and Th17 cells increase microglial activation in the brains of APP/PS1 mice.

Having established, both in this chapter and the previous chapter, that Th1 and Th17 cells increase microglial activation *in vitro* as measured by the expression of co-stimulatory molecules, the effect of adoptive transfer of A β -specific Th1 and Th17 cells was investigated in APP/PS1 mice. The micrographs revealed that CD11b-positive immunoreactivity was low in cortical and hippocampal sections taken from wildtype mice (Figure 6.8A and 6.9A) and there was an apparent increase in CD11b-positive immunoreactivity in cortical and hippocampal sections taken from control APP/PS1 mice (Figure 6.8B and 6.9B). A further increase in CD11b-positive immunoreactivity in cortical and hippocampal sections taken from APP/PS1 mice which received A β -specific Th1 and Th17 cells was observed (Figure 6.8C-D and 6.9C-D). Quantitative analysis of the micrographs by Image J revealed that CD11b expression was significantly increased in cortical sections prepared from APP/PS1 mice which received A β -specific Th1 cells (* $p < 0.05$, ANOVA; Figure 6.8E); an increase in CD11b expression in cortical sections prepared from APP/PS1 mice which received A β -specific Th17 cells was also observed but this did not reach statistical significance (Figure 6.8E). The increase in CD11b expression in hippocampal sections prepared from APP/PS1 mice which received A β -specific Th1 cells did not reach statistical significance (Figure 6.9E).

6.3.5. A β -specific Th1 cells enhance A β load and plaque burden in APP/PS1 mice.

The effect of A β -specific Th1 cells on A β load and plaque burden in APP/PS1 mice was investigated. The concentration of insoluble A β_{1-38} , A β_{1-40} and A β_{1-42} were significantly increased in cortical tissue prepared from APP/PS1 mice compared to wildtype littermates (** $p < 0.01$, *** $p < 0.001$, ANOVA; Figure 6.10A-C). A β_{1-38} , A β_{1-40} and A β_{1-42} concentrations were significantly enhanced in APP/PS1 mice which received A β -specific Th1 cells compared with control APP/PS1 mice (⁺ $p < 0.01$, ⁺⁺⁺ $p < 0.001$, ANOVA; Figure 6.10A-C). The effect that neutralizing IFN- γ might have on A β -specific Th1-induced A β load was

investigated and the data revealed that the A β -specific Th1-induced increase in A β ₁₋₃₈, A β ₁₋₄₀ and A β ₁₋₄₂ concentrations in APP/PS1 mice was attenuated in APP/PS1 mice that received A β -specific Th1 cells and anti-IFN- γ antibody (§ p<0.05, §§§ p<0.001, ANOVA; Figure 6.10A-C). The effect of A β -specific Th1 cells and neutralizing IFN- γ on plaque burden in APP/PS1 mice was also investigated. There was a significant increase in positively-stained A β -plaques in control APP/PS1 sections compared with wildtype sections (** p<0.01, ANOVA; Figure 6.11A) but there was no significant increase in the number of A β -plaques in APP/PS1 mice which received A β -specific Th1 cells compared with control APP/PS1 mice (Figure 6.11A). However further analysis revealed a significant increase in the number of positively-stained A β -plaques in APP/PS1 mice which received A β -specific Th1 cells compared with control APP/PS1 mice (** p<0.01, student's *t* test; Figure 6.11B). The data revealed that this A β -specific Th1-induced increase in A β -plaque load was significantly attenuated in APP/PS1 mice which received A β -specific Th1 cells together with anti-IFN- γ treatment († p<0.05, ANOVA; Figure 6.11A).

6.3.6. A β -specific Th1 cells enhance microglial activation in APP/PS1 mice.

Microglial activation in cortical and hippocampal sections was assessed following adoptive A β -specific Th1 cell transfer and IFN- γ neutralization in APP/PS1 mice. The micrographs revealed that CD11b-positive immunoreactivity was low in cortical and hippocampal sections prepared from wildtype mice and there was an apparent increase in sections prepared from all APP/PS1 groups (Figure 6.12A-E and 6.13A-E). There was an apparent increase in CD11b immunoreactivity in cortical and hippocampal sections prepared from APP/PS1 mice which received A β -specific Th1 cells compared with sections prepared from control APP/PS1 mice (Figure 6.12C and 6.13C) and an attenuation of the A β -specific Th1-induced CD11b-positive immunoreactivity in sections prepared from APP/PS1 mice that received A β -specific Th1 cells and anti-IFN- γ treatment (Figure 6.12D-E and 6.13D-E). Quantitative analysis of the micrographs by Image J revealed that CD11b expression was not significantly increased in cortical sections prepared from any of the APP/PS1 groups (Figure 6.12F).

Quantitative analysis of hippocampal sections revealed that CD11b expression was significantly increased in APP/PS1 mice which received A β -specific Th1 cells ($^*p < 0.05$, ANOVA; Figure 6.13F). The Th1-induced increase in CD11b expression was significantly attenuated in APP/PS1 mice that received A β -specific Th1 cells and anti-IFN- γ treatment ($^{\dagger}p < 0.05$, ANOVA; Figure 6.13F).

6.3.7. Co-localisation of A β and CD11b expression in cortical and hippocampal tissue prepared from APP/PS1 mice.

Having established that adoptive transfer of A β -specific Th1 cells into APP/PS1 mice increased plaque burden and microglial activation in these animals it was investigated if microglia were co-localised to A β -plaques in cortical and hippocampal sections taken from these animals. The micrographs revealed that pan A β -positive immunoreactivity was increased in cortical and hippocampal sections prepared from all APP/PS1 groups (Figure 6.14B-E and 6.15B-E). There was an apparent increase in pan A β -positive immunoreactivity in sections prepared from APP/PS1 mice which received A β -specific Th1 cells and an apparent attenuation in sections prepared from APP/PS1 mice that received A β -specific Th1 cells and anti-IFN- γ treatment and anti-IFN- γ treatment (Figure 6.14C-E and 6.15C-E). CD11b-positive immunoreactivity was found to be co-localised with A β -positive immunoreactivity in all APP/PS1 groups (Figure 6.14B-E and 6.15B-E).

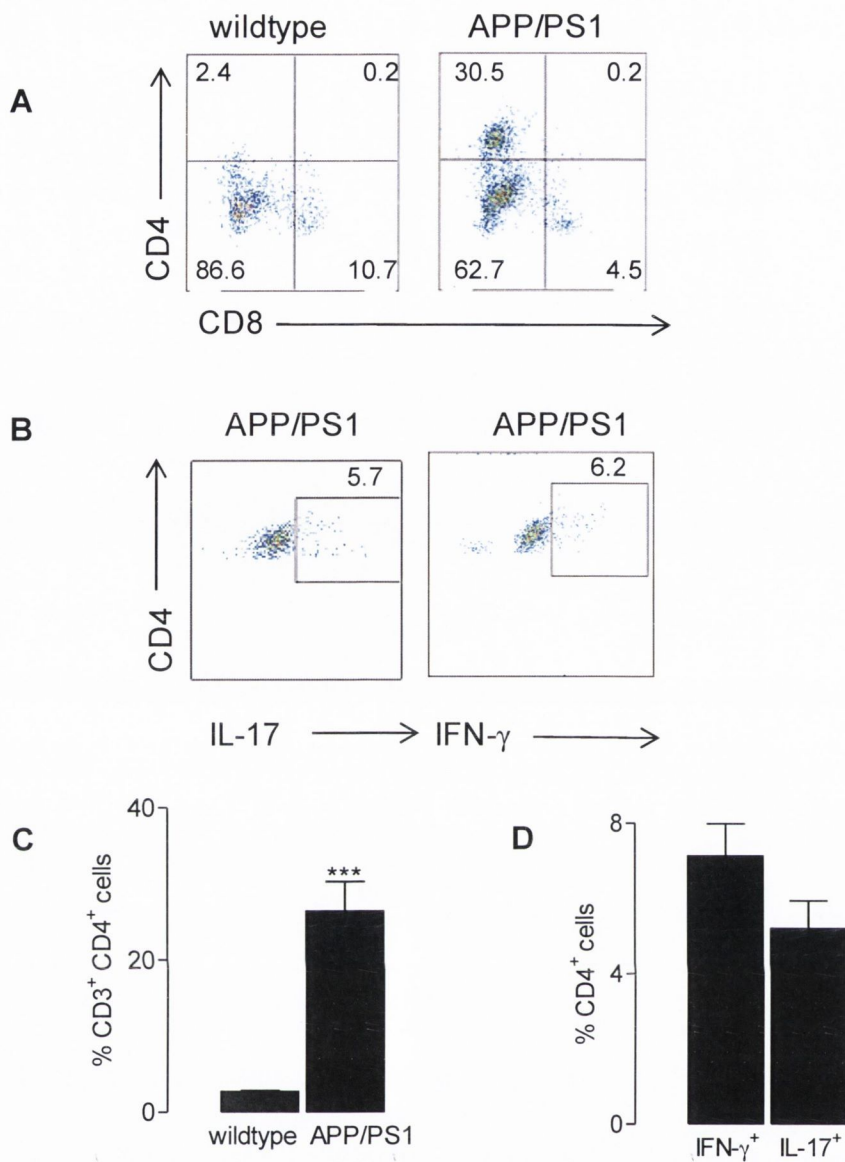


Figure 6.1. CD3⁺CD4⁺ cells infiltrate the brains of wildtype and APP/PS1 mice.

Mononuclear cells were isolated from the brains of APP/PS1 and wildtype littermate control mice and cells were surface stained with antibodies specific for CD3, CD4 and intracellularly for IFN- γ and IL-17 and FACS was performed. (A) Representative FACS plots of CD4⁺ cells in brains of wildtype and APP/PS1 mice. There was a significant increase in the percentage of CD3⁺CD4⁺ cells in brains of APP/PS1 mice compared to wildtype mice (C) (***p*<0.001, student's *t*-test). (B) Representative FACS plots of CD4⁺IFN- γ ⁺ and CD4⁺IL-17⁺ cells in brains of APP/PS1 mice. CD4⁺ cells stained equally for both IFN- γ and IL-17 with no significant difference between the presence of the two cytokines (D). Values are expressed as means \pm SEM (n=4).

(C) ***p*=0.0008; 2.723 \pm 0.09733; n=4 versus 26.48 \pm 3.857; n=4

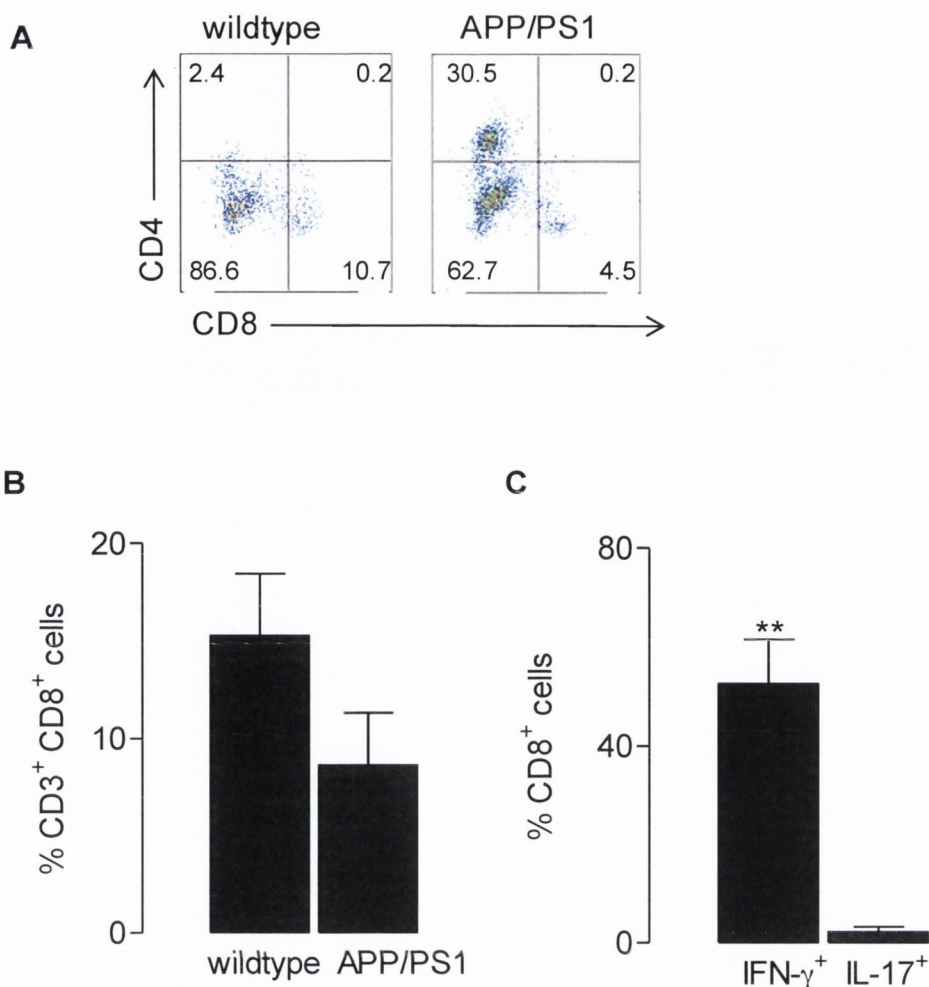


Figure 6.2. CD3⁺CD8⁺ cells infiltrate the brains of wildtype and APP/PS1 mice.

Mononuclear cells were isolated from the brains of APP/PS1 and wildtype littermate control mice and cells were surface stained with antibodies specific for CD8 and intracellularly for IFN- γ and IL-17 and FACS was performed. (A) Representative FACS plots of CD8⁺ cells in brains of wildtype and APP/PS1 mice. There was no significant difference in the percentage of CD8⁺ cells infiltrating the brains of wildtype and APP/PS1 mice (B). There was a significant increase in the percentage of CD8⁺ cells stained positively for IFN- γ compared with the number stained positively for IL-17 in brain tissue prepared from APP/PS1 mice (C) (** $p < 0.01$, student's t -test). Values are expressed as means \pm SEM (n=4).

(C) ** $p=0.0014$; 52.65 ± 8.9111 ; n=4 versus 2.257 ± 1.053 ; n=4

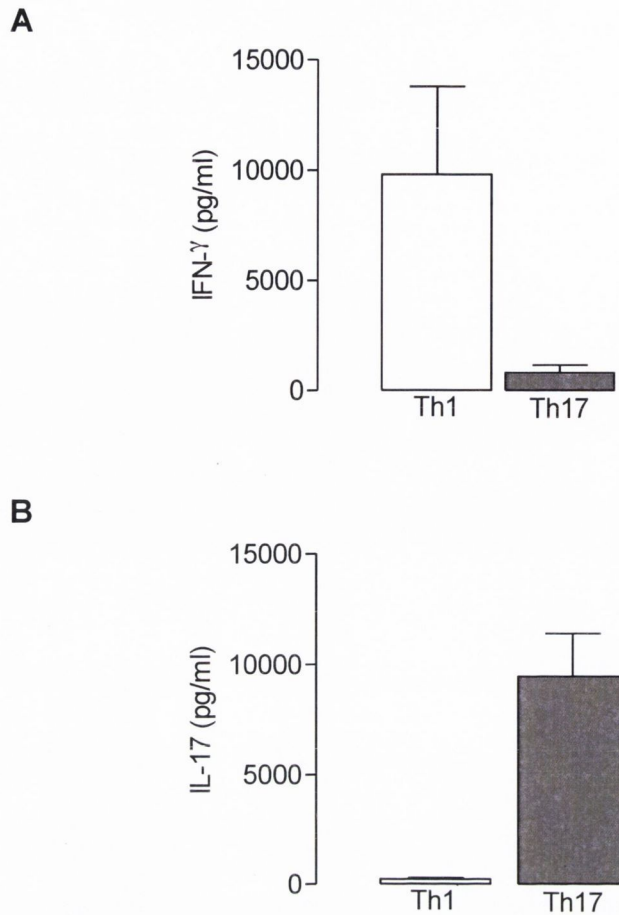


Figure 6.3. Generation of Th1 and Th17 cell lines.

Spleens were harvested from C57BL/6 mice and cells were stimulated under Th1 polarising conditions with IL-12 (50 ng/ml) and Th17 polarising conditions with TGF- β (5 ng/ml), IL-1 β (25 ng/ml), IL-23 (50 ng/ml) and anti-IFN- γ (5 μ g/ml). On the 4th day of the culture supernatants were removed for analysis of IFN- γ and IL-17 concentrations by ELISA. Th1 cells have high IFN- γ , and low IL-17, concentrations (A and B). Th17 cells have low IFN- γ , and high IL-17, concentrations (A and B). Values are expressed as means \pm SEM (n=4).

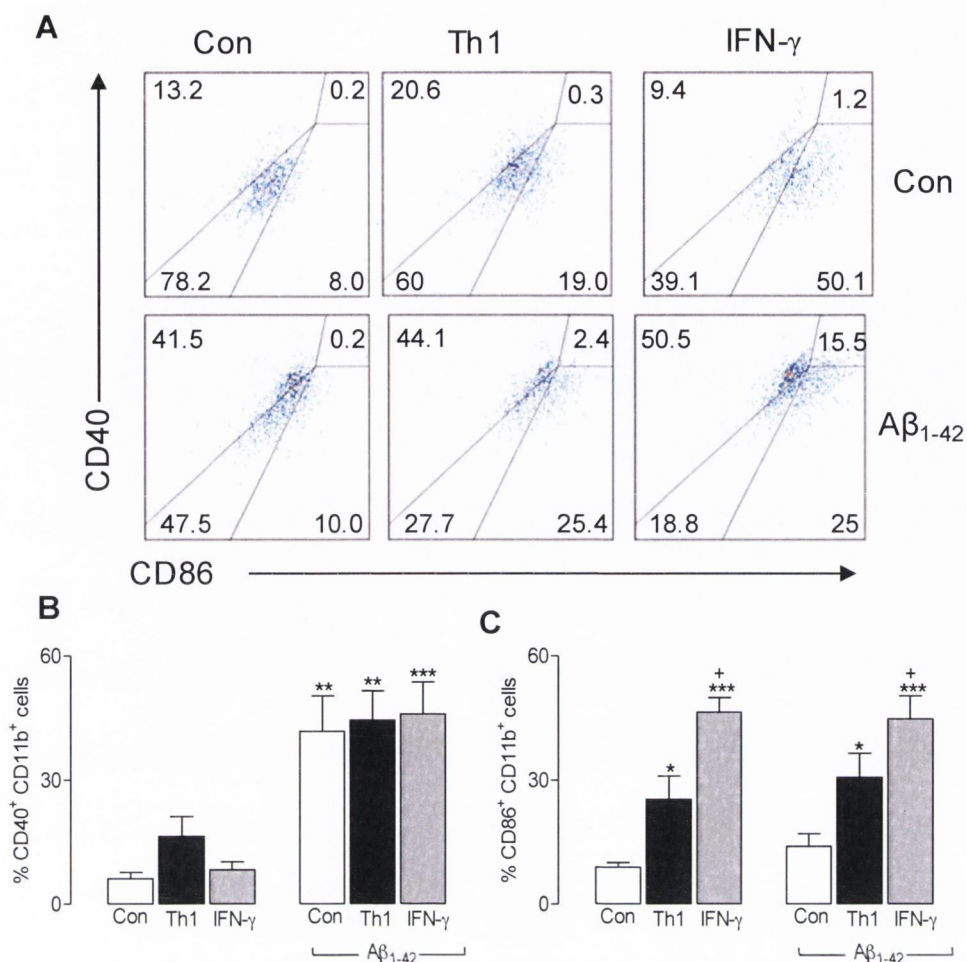


Figure 6.4. Expression of CD40 and CD86 on microglia was assessed following co-culture with Th1 cells and incubation with IFN- γ and A β_{1-42} .

Th1 cell were generated from C57BL/6 mice as described in Figure 6.3. Th1 cell lines were co-cultured with mixed glia, prepared from neonatal C57BL/6 mice, for 24 hours. Mixed glia were also treated with IFN- γ (20 ng) and A β_{1-42} (10 μ M) for 24 hours. Expression of CD86 and CD40 on microglia (CD11b⁺) was quantified by FACS. (A) Representative FACS plots of CD40 and CD86 expression on CD11b⁺ cells. A β_{1-42} significantly increased the expression of CD40 on microglia (B) (**p<0.01, ***p<0.001, ANOVA). Co-culture of mixed glia with Th1 cells and IFN- γ treatment significantly increased the expression of CD86 on microglia (C) (*p<0.05, ***p<0.001, ANOVA). There was a significant increase in the expression of CD86 on microglia treated with IFN- γ compared with Th1 co-culture (C) ([†]p<0.05, ANOVA). Values are expressed as means \pm SEM (n=6).

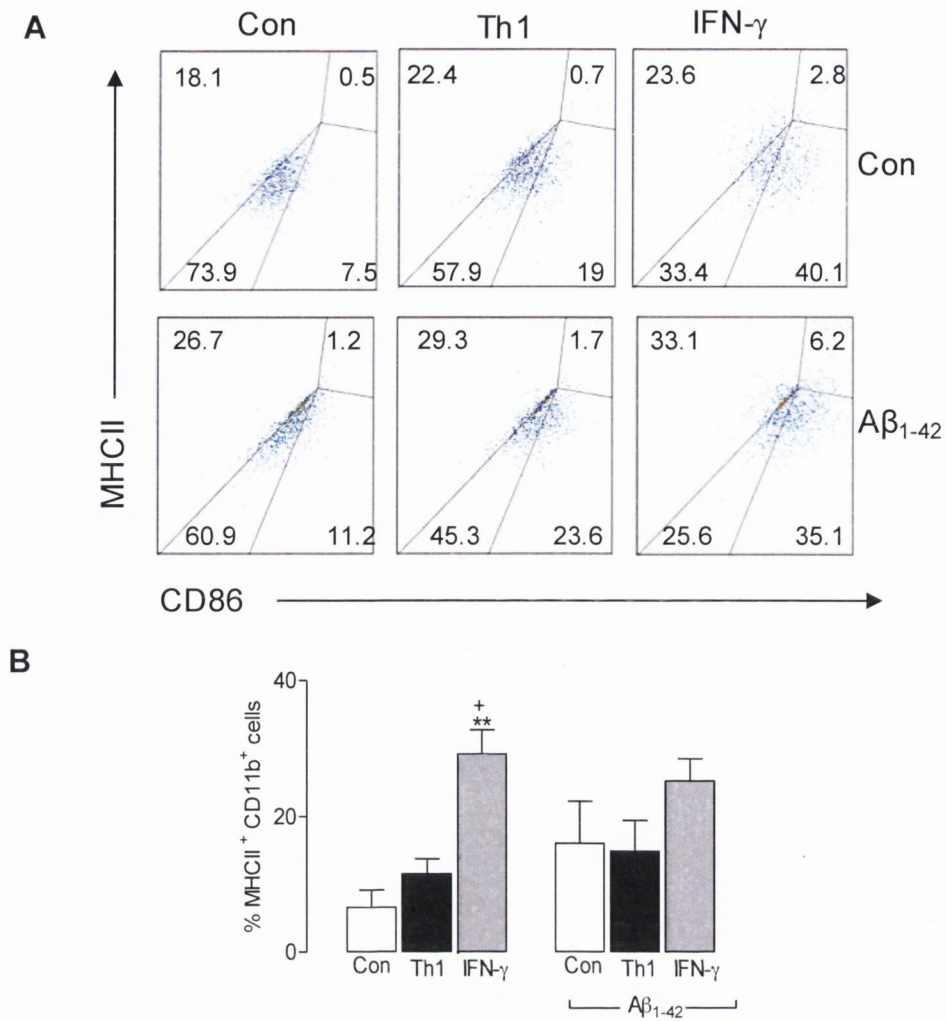


Figure 6.5. Expression of MHC class II on microglia was assessed following co-culture with Th1 cells and incubation with IFN- γ and A β_{1-42} .

Th1 cells were generated from C57BL/6 mice and co-cultured with mixed glia treated with IFN- γ (20 ng) and A β_{1-42} (10 μ M) as described in Figure 6.3 and 6.4. Expression of MHC class II on microglia (CD11b⁺) was quantified by FACS. (A) Representative FACS plots of MHC class II expression on CD11b⁺ cells. Incubation of mixed glia with IFN- γ significantly increased the expression of MHC class II on microglia (B) (** $p < 0.01$, ANOVA). There was a significant increase in the expression of MHC class II on microglia incubated with IFN- γ compared with Th1 co-culture (B) (⁺ $p < 0.05$, ANOVA). Values are expressed as means \pm SEM (n=6).

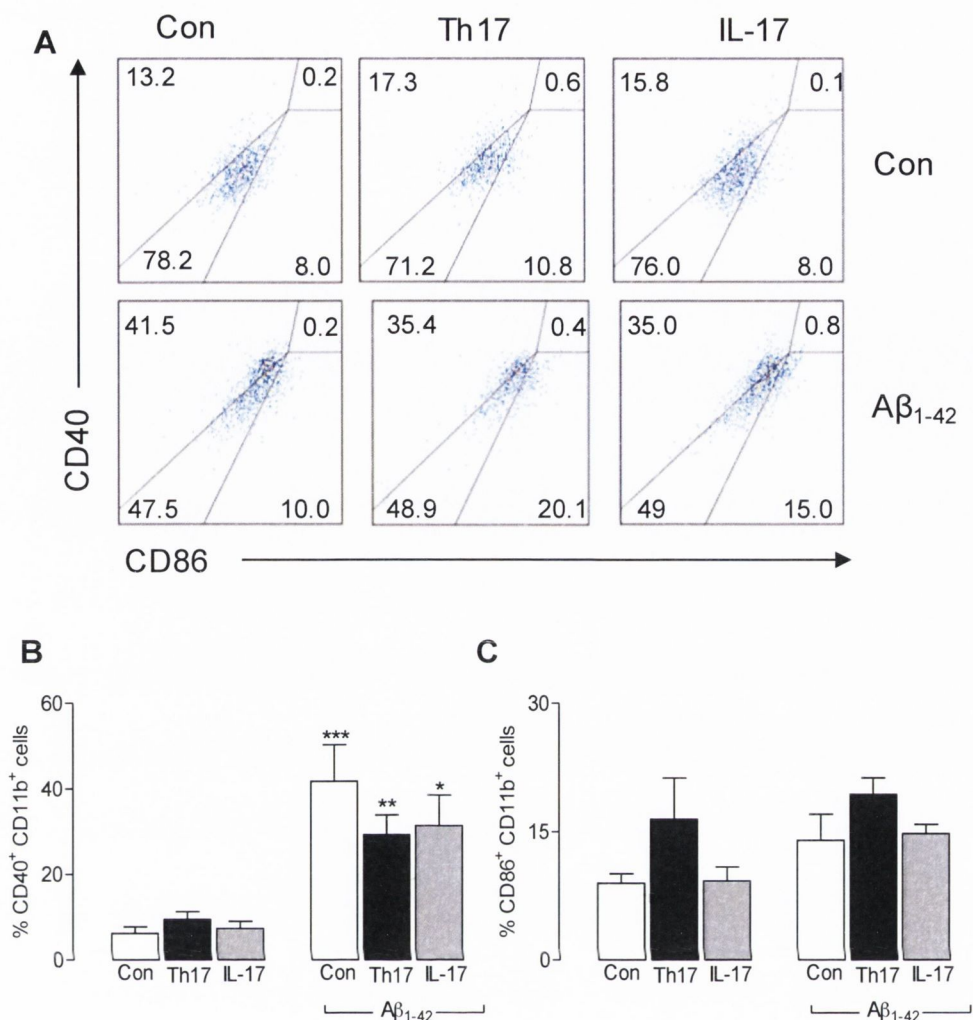


Figure 6.6. Expression of CD40 and CD86 on microglia was assessed following co-culture with Th17 cells and incubation with IL-17 and Aβ₁₋₄₂.

Th17 cells were generated from C57BL/6 mice as described in Figure 6.3. After 4 days of polarisation Th1 cell lines were co-cultured with mixed glia, prepared from neonatal C57BL/6 mice, for 24 hours. Mixed glia were also treated with IL-17 (20 ng) and Aβ₁₋₄₂ (10 μM) for 24 hours. Expression of CD86 and CD40 on microglia (CD11b⁺) was quantified by FACS. (A) Representative FACS plots of CD40 and CD86 expression on CD11b⁺ cells. Aβ₁₋₄₂ significantly increased the expression of CD40 on microglia (B) (*p<0.05, **p<0.01, ***p<0.001, ANOVA). Expression of CD86 on microglia was not significantly altered following co-culture with Th17 cells or incubation with IL-17 or Aβ₁₋₄₂ (C). Values are expressed as means ± SEM (n=6).

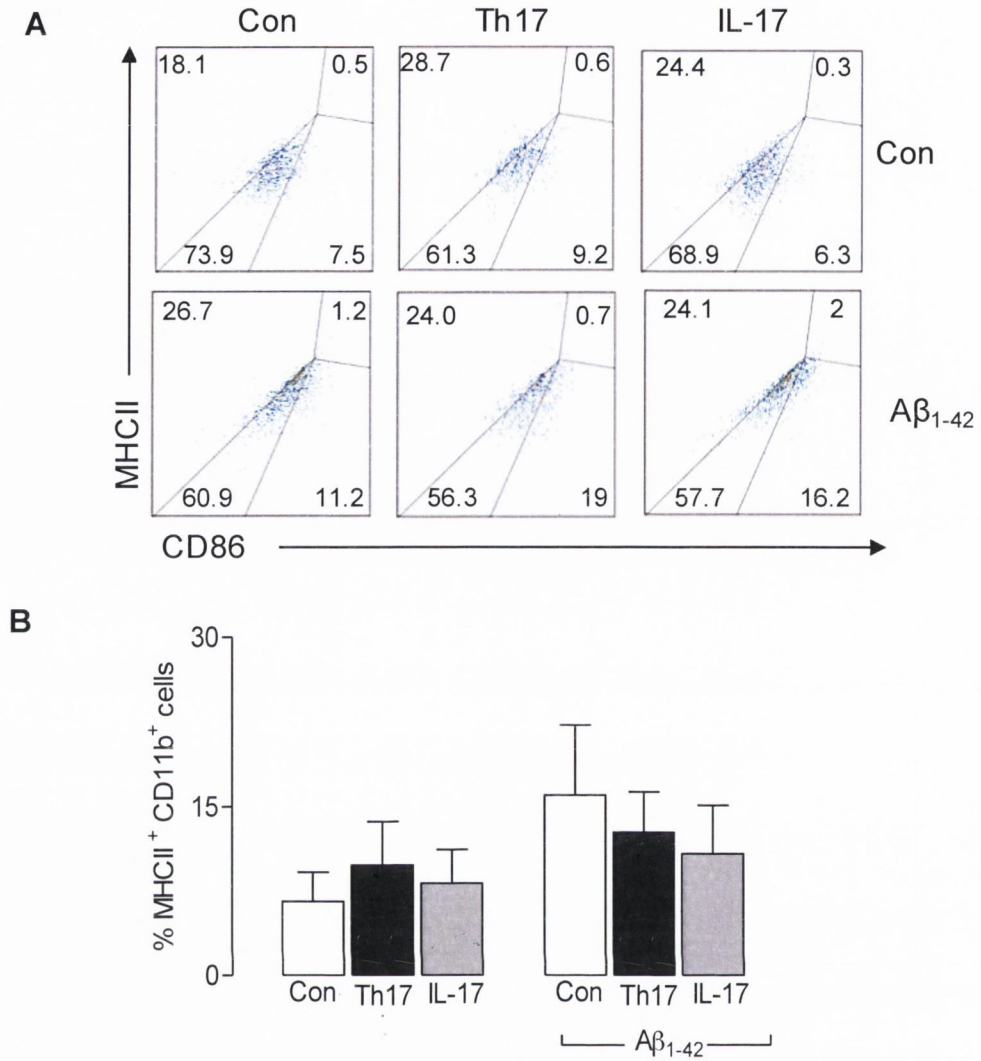


Figure 6.7. Expression of MHC class II on microglia was assessed following co-culture with Th17 cells and incubation with IL-17 and Aβ₁₋₄₂.

Th17 cell were generated from C57BL/6 mice and co-cultured with mixed glia which were also treated with IL-17 (20 ng) and Aβ₁₋₄₂ (10 μM) as described in Figure 6.3 and 6.6. Expression of MHC class II on microglia (CD11b⁺) was quantified by FACS. (A) Representative FACS plots of MHC class II expression on CD11b⁺ cells. MHC class II expression on microglia was not significantly altered following co-culture with Th17 cells and incubation with IL-17 or Aβ₁₋₄₂. Values are expressed as means ± SEM (n=6).

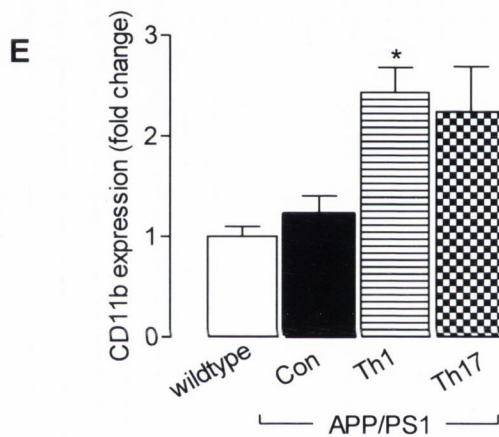
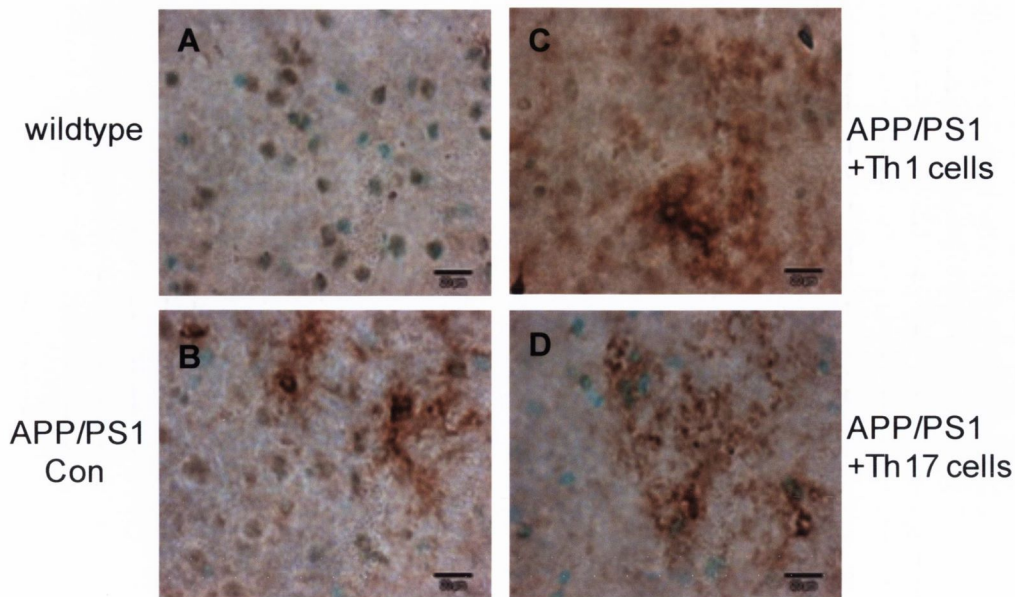


Figure 6.8. CD11b expression is increased in cortical sections prepared from APP/PS1, compared to wildtype, mice.

A β -specific Th1 and Th17 cells were generated in C57BL/6 mice and cells were injected i.v. (15×10^6 cells/mouse) into APP/PS1 mice. Control animals received serum-free medium alone (300 μ l). Animals were sacrificed 2 weeks after adoptive A β -specific Th1 and Th17 cell transfer and tissue was taken for CD11b immunohistochemical analysis of microglial activation. CD11b-positive immunoreactivity was low in cortical sections prepared from wildtype mice (A). There was an apparent increase in CD11b-positive immunoreactivity in sections prepared from all APP/PS1 groups (B-D). CD11b expression was analysed using Image J software and the results were expressed as a fold change. CD11b expression was significantly increased in APP/PS1 mice which received A β -specific Th1 cells (E) (* $p < 0.05$, ANOVA). Values are expressed as means \pm SEM (n=3-5).

(40X magnification)

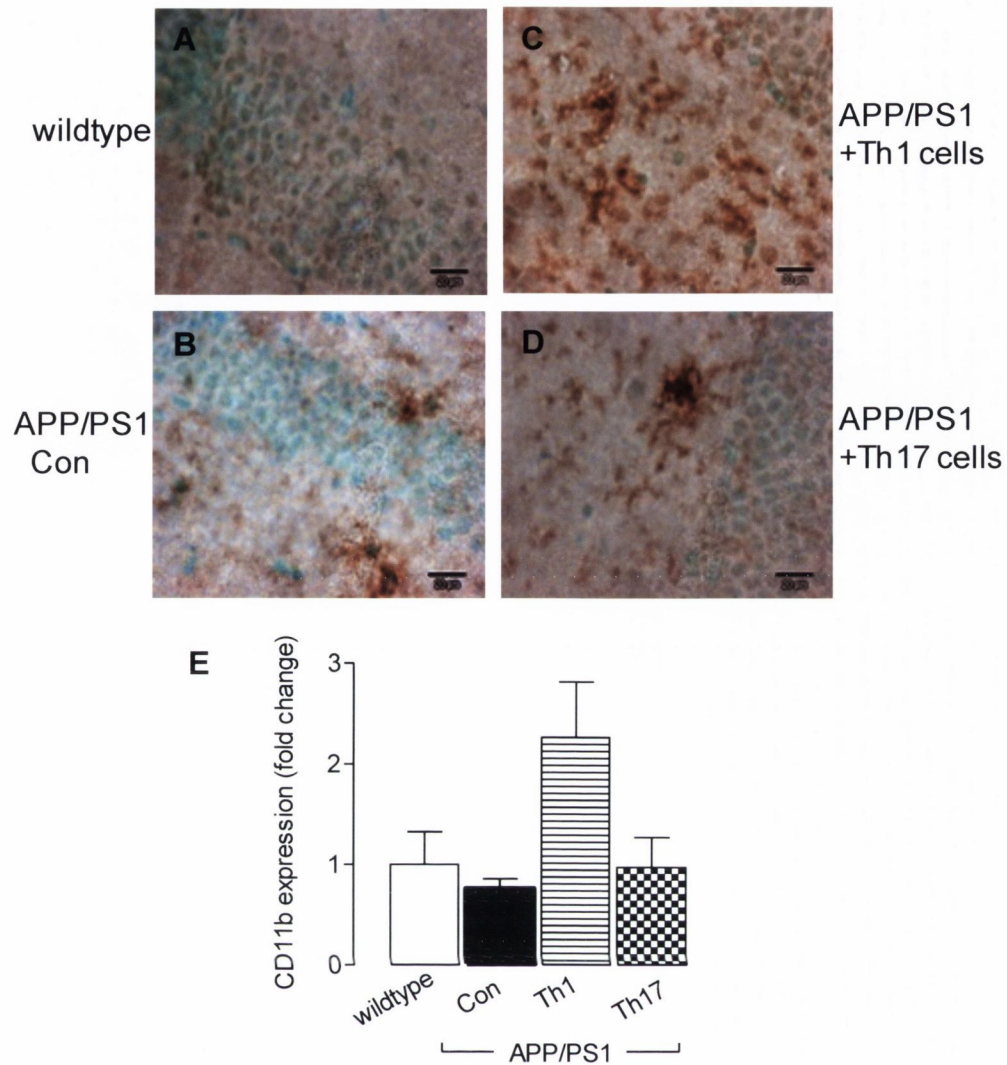


Figure 6.9. CD11b expression is increased in hippocampal sections prepared from APP/PS1, compared with wildtype, mice.

A β -specific Th1 and Th17 cells were generated and adoptively transferred into APP/PS1 mice and sections were stained for CD11b-positive immunoreactivity as described in figure 6.8. CD11b-positive immunoreactivity was low in hippocampal sections prepared from wildtype mice (A). There was an apparent increase in CD11b-positive immunoreactivity in sections prepared from all APP/PS1 groups (B-D). CD11b expression was quantified using Image J software and the results were expressed as a fold change. CD11b expression was not significantly changed between groups (E). Values are expressed as means \pm SEM (n=3-5).

(40X magnification)

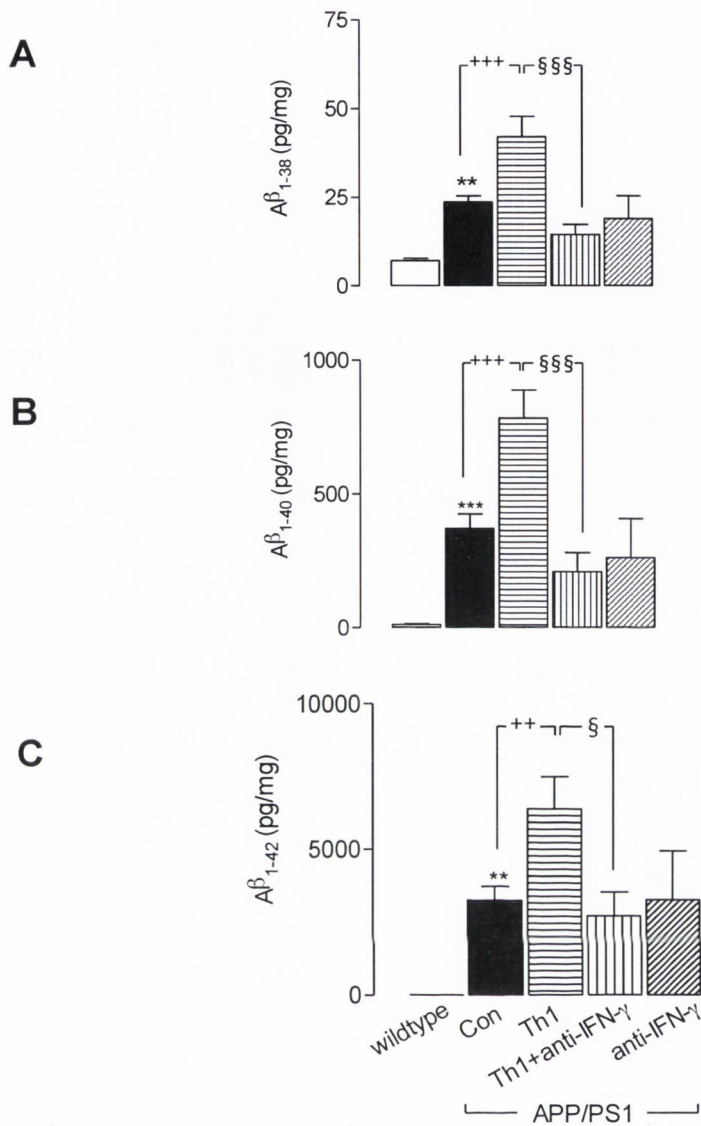


Figure 6.10. Anti-IFN- γ antibody attenuates the A β -specific Th1-induced increase in A β ₁₋₃₈, A β ₁₋₄₀ and A β ₁₋₄₂ concentrations in APP/PS1 mice.

Wildtype and APP/PS1 mice were injected i.p. with anti-IFN- γ antibody or β -galactosidase (600 μ g) and after 24 hours mice were injected i.v. with A β -specific Th1 cells (15×10^6 cells/mouse) as described in Figure 6.8. Anti-IFN- γ or β -galactosidase antibody injections were repeated several days after adoptive Th1 cell transfer. Animals were sacrificed 34 days after adoptive T cell transfer and cortical tissue was taken for analysis of A β load by multi-spot ELISA. A β ₁₋₃₈, A β ₁₋₄₀ and A β ₁₋₄₂ concentrations were significantly increased in control APP/PS1 mice (A-C) (** $p < 0.01$, *** $p < 0.001$, ANOVA). A β ₁₋₃₈, A β ₁₋₄₀ and A β ₁₋₄₂ concentrations were significantly enhanced in APP/PS1 mice which received A β -specific Th1 cells (++ $p < 0.01$, +++ $p < 0.001$, ANOVA). The A β -specific Th1-induced increase in A β ₁₋₃₈, A β ₁₋₄₀ and A β ₁₋₄₂ concentrations was attenuated in APP/PS1 mice that received A β -specific Th1 cells and anti-IFN- γ antibody (A-C) (§ $p < 0.05$, §§§ $p < 0.001$, ANOVA). Values are expressed as means \pm SEM (n=4-13).

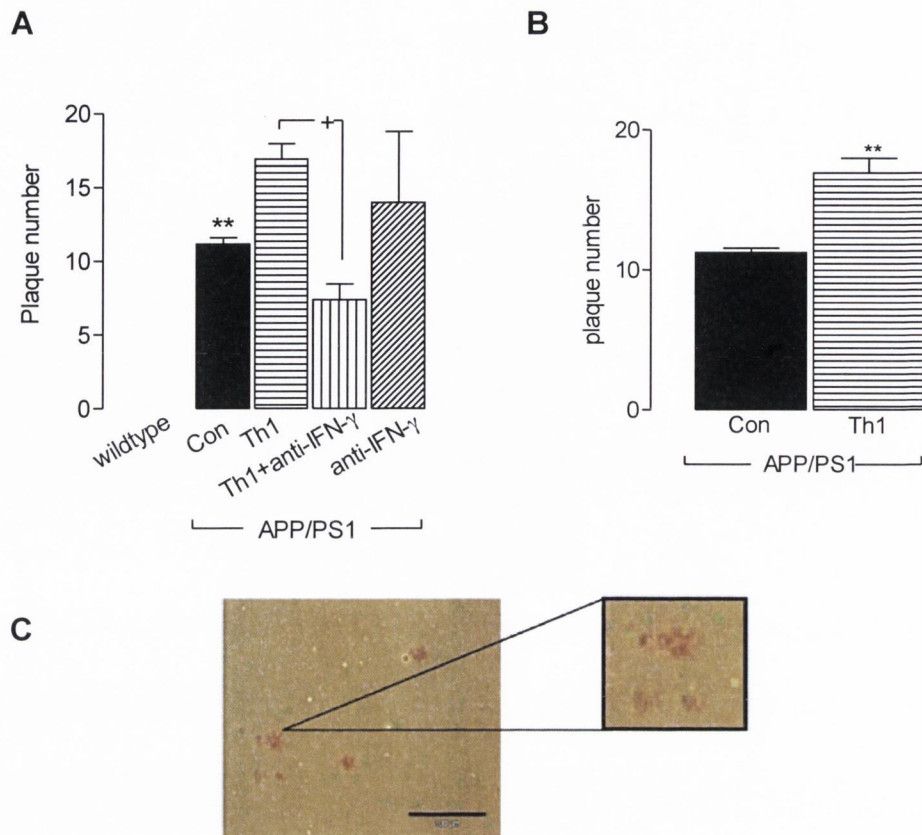


Figure 6.11. A β -specific Th1 cells increase the number of A β -plaques in APP/PS1 mice and this effect is attenuated by anti-IFN- γ treatment.

Wildtype and APP/PS1 mice received A β -specific Th1 cells and an anti-IFN- γ antibody as described in figure 6.10 and tissue was taken for immunohistochemical analysis of A β -plaque load. Sections were stained with congo red to detect compact A β -plaques and plaque numbers were counted across the whole section. There was a significant increase in positively stained A β -plaques in sections prepared from control APP/PS1 mice (A) (** $p < 0.01$, ANOVA). There was a significant increase in the number of positively stained A β -plaques in APP/PS1 mice which received A β -specific Th1 cells compared to control APP/PS1 mice (B) (** $p < 0.01$, student's t test). The A β -specific Th1-induced increase in plaque load was significantly attenuated in APP/PS1 mice which received A β -specific Th1 and anti-IFN- γ treatment (A) ($\dagger p < 0.05$, ANOVA). The micrograph represents congo red positive staining in a section taken from an APP/PS1 (C). Values are expressed as means \pm SEM ($n = 3-5$).

(B) ** $p = 0.0021$; 11.25 ± 0.3227 ; $n = 4$ versus 16.94 ± 1.053 ; $n = 4$

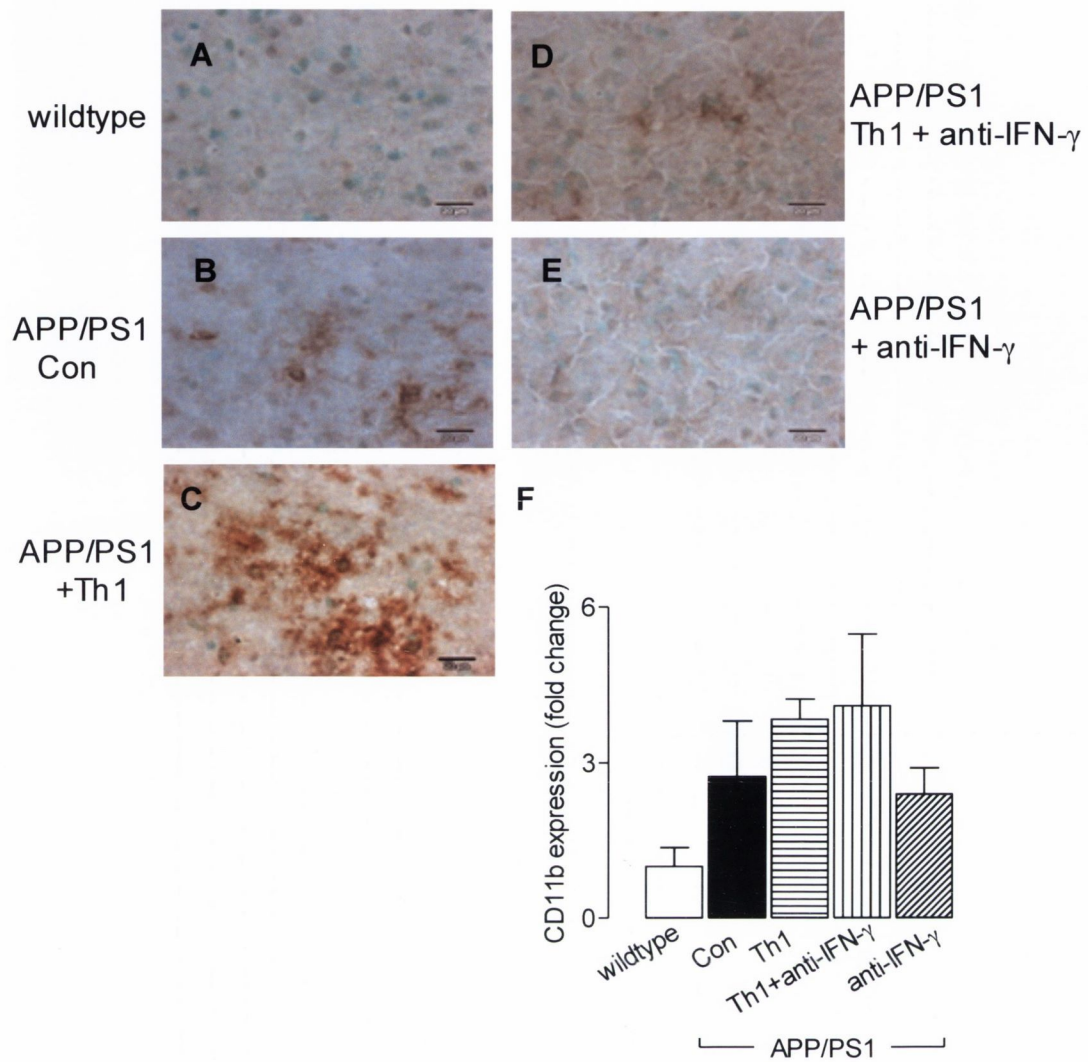


Figure 6.12. CD11b expression was assessed in cortical sections prepared from wildtype and APP/PS1 mice.

Wildtype and APP/PS1 mice received A β -specific Th1 cells and an anti-IFN- γ antibody as described in figure 6.10 and cortical sections were stained for CD11b-positive immunoreactivity as a measure of microglial activation. CD11b-positive immunoreactivity was low in cortical sections prepared from wildtype mice (A). There was an apparent increase in CD11b-positive immunoreactivity in cortical sections prepared from all APP/PS1 groups (B-E). CD11b expression was quantified using Image J software and the results were expressed as a fold change. CD11b expression was not significantly changed between groups (F). Values are expressed as means \pm SEM (n=3-7).

(40X magnification)

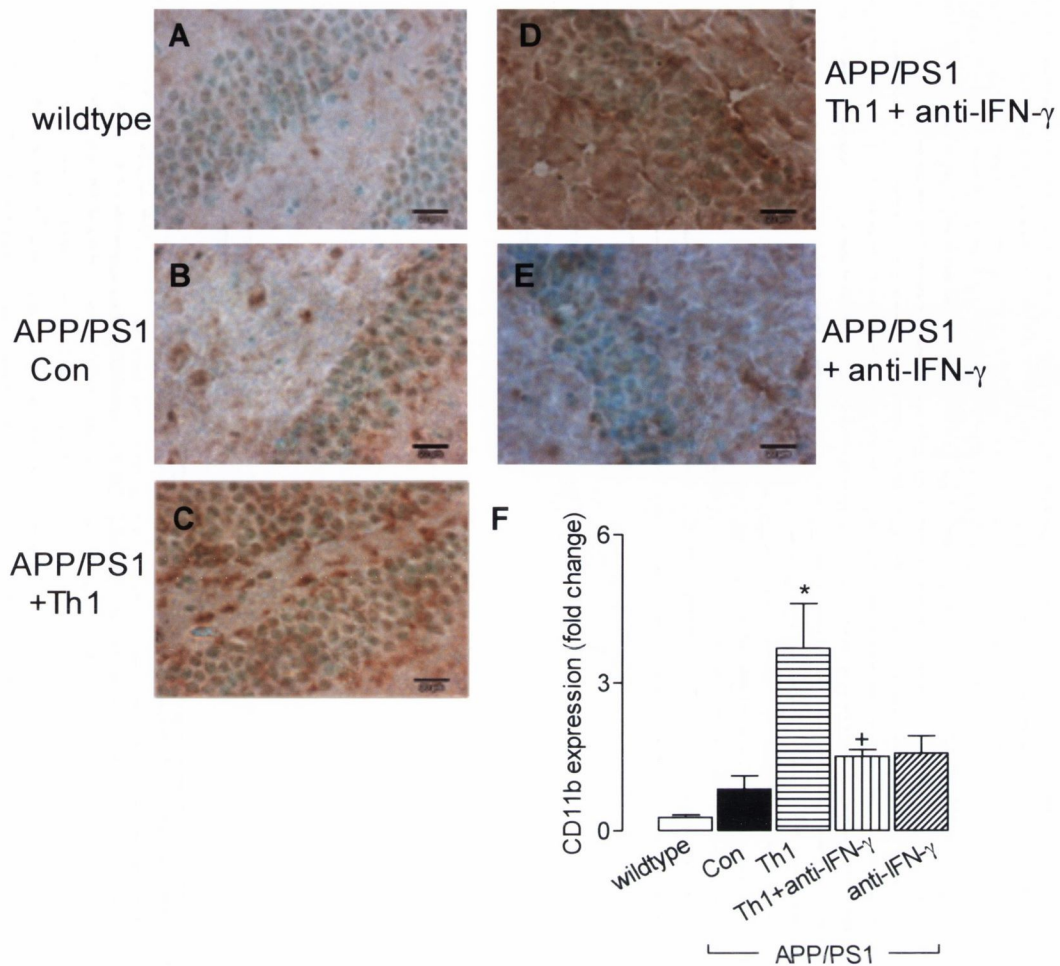


Figure 6.13. CD11b expression was assessed in hippocampal sections prepared from wildtype and APP/PS1 mice.

Wildtype and APP/PS1 mice received A β -specific Th1 cells and an anti-IFN- γ antibody as described in figure 6.10 and hippocampal sections were stained for CD11b-positive immunoreactivity as a measure of microglial activation. CD11b-positive immunoreactivity was low in hippocampal sections prepared from wildtype mice (A). There was an apparent increase in CD11b-positive immunoreactivity in hippocampal sections prepared from all APP/PS1 groups (B-E). CD11b expression was quantified using Image J software and the results were expressed as a fold change. CD11b expression was significantly increased in APP/PS1 mice which received A β -specific Th1 cells (F) (* p <0.05, ANOVA). The Th1-induced increase in CD11b expression was significantly attenuated in APP/PS1 mice that received A β -specific Th1 and anti-IFN- γ treatment (F) (⁺ p <0.05, ANOVA). Values are expressed as means \pm SEM (n=3-7).

(40X magnification)

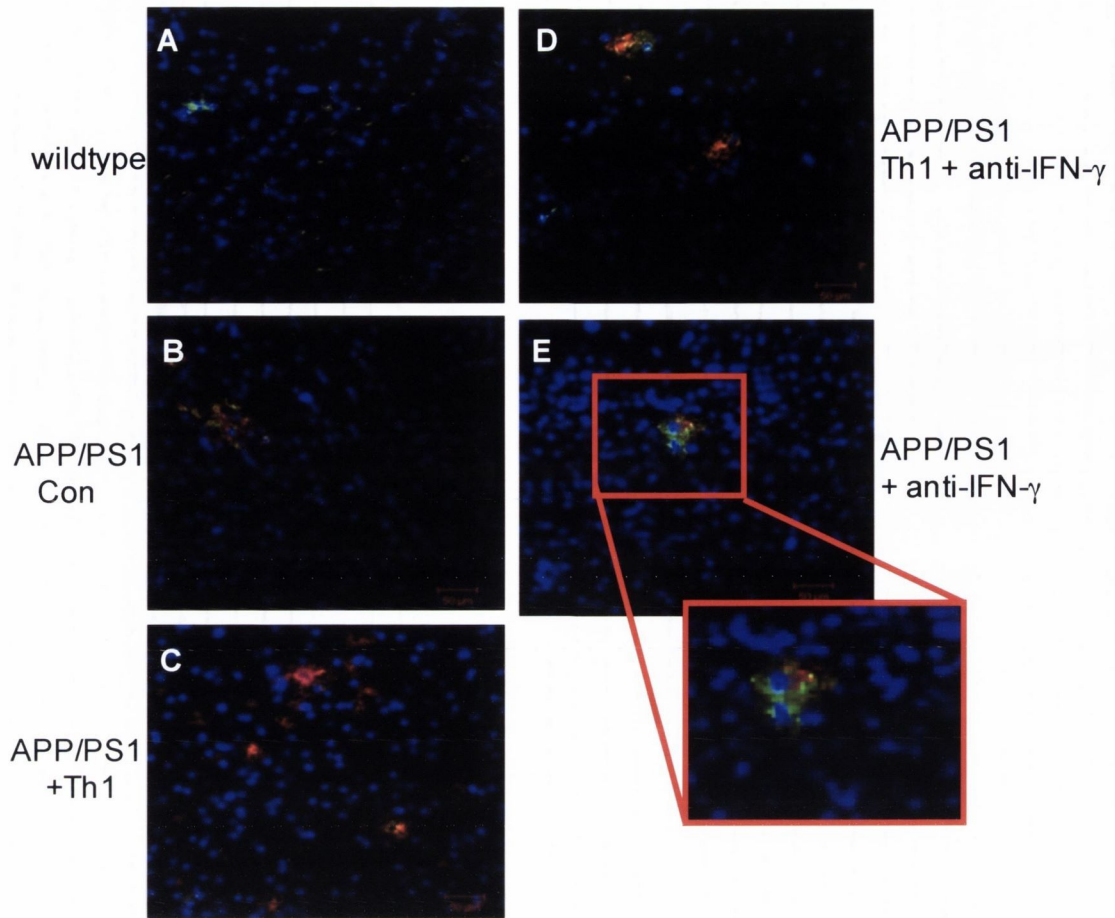


Figure 6.14. Pan A β and CD11b expression was co-localised in cortical sections prepared APP/PS1 mice.

Wildtype and APP/PS1 mice received A β -specific Th1 and an anti-IFN- γ antibody as described in figure 6.10 and sections were stained for CD11b- and A β -positive immunoreactivity. Pan A β -positive immunoreactivity was increased in cortical sections prepared from all APP/PS1 groups compared with sections prepared from wildtype mice (A-E). There was an apparent increase in pan A β -positive immunoreactivity in sections prepared from APP/PS1 mice which received A β -specific Th1 cells and there was an apparent attenuation in sections prepared from APP/PS1 mice that received A β -specific Th1 and anti-IFN- γ treatment and anti-IFN- γ treatment (B-E). CD11b-positive immunoreactivity was found co-localised with pan A β -positive immunoreactivity in all APP/PS1 groups (B-E).

(Pan A β immunoreactivity (red), CD11b immunoreactivity (green), 40X magnification)

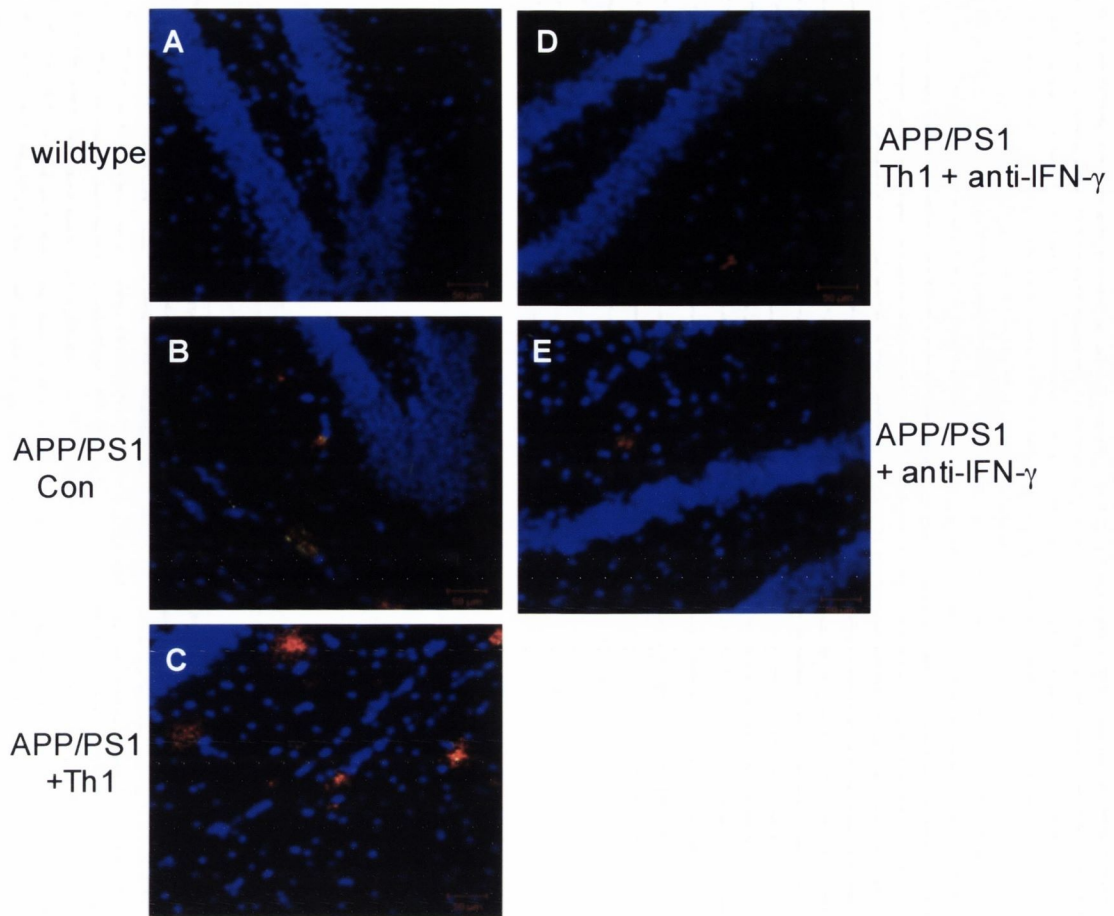


Figure 6.15. Pan A β and CD11b expression was co-localised in hippocampal sections prepared APP/PS1 mice.

Wildtype and APP/PS1 mice received A β -specific Th1 cells and an anti-IFN- γ antibody as described in figure 6.10 and sections were stained for CD11b- and A β -positive immunoreactivity. Pan A β -positive immunoreactivity was increased in hippocampal sections prepared from all APP/PS1 groups compared with sections prepared from wildtype mice (A-E). There was an apparent increase in pan A β -positive immunoreactivity in sections prepared from APP/PS1 mice which received A β -specific Th1 cells and there was an apparent attenuation in sections prepared from APP/PS1 mice that received A β -specific Th1 and anti-IFN- γ treatment and anti-IFN- γ treatment (C-E). CD11b-positive immunoreactivity was found co-localised with pan A β -positive immunoreactivity in all APP/PS1 groups (B-E).

(Pan A β immunoreactivity (red), CD11b immunoreactivity (green), 40X magnification)

6.4. Discussion

In the previous chapter it was established that Th1 and Th17 cells induced a greater effect on glial activation than Th2 cells *in vitro*. Specifically, A β -specific Th1 cells induced an exacerbated inflammatory response in glia compared with A β -specific Th2 and Th17 cells. The focus of this chapter was to investigate if Th1 and Th17 cells were present in the CNS in a mouse model of AD and to establish if A β -specific Th1 and Th17 cells could influence inflammation. A specific aim was to examine if A β -specific Th1-induced inflammation was mediated through the secretion of IFN- γ . The data revealed that T cells which stained intracellularly for IFN- γ and IL-17 were present in greater numbers in the brains of APP/PS1 mice compared with wildtype mice. Furthermore it was found that adoptive transfer of A β -specific Th1 cells enhanced microglial activation and plaque burden in brains of APP/PS1 mice and this effect was attenuated in animals which received an anti-IFN- γ treatment.

The CNS can only deploy a limited range of immune-defence components and, for this reason, peripheral immune cells can gain entry to the CNS as part of normal immune surveillance (Ransohoff *et al.*, 2003). Indeed it has been shown that activated CNS-irrelevant T cells can invade the CNS and promote alterations in the permeability of the BBB without causing any glial pathology while, encephalitogenic T cells similarly enter the CNS and disrupt the BBB; crucially these cells trigger microglial activation, astrogliosis and demyelination (Smorodchenko *et al.*, 2007). It has already been established that disruption of the BBB and trafficking of autoreactive T cells are early events in MS; both MOG-specific Th1 and Th17 cells have been found to expand in the periphery and cross the BBB in mouse models of MS (Kebir *et al.*, 2007). Evidence suggests that, with ageing and during AD, the BBB becomes leakier which could allow for the infiltration of peripheral immune cells which could in turn contribute to the chronic uncontrolled inflammatory environment observed in AD (Farrall & Wardlaw, 2009). Consistent with previous reports that T cells can infiltrate the brains of mice older than 12 months (Stichel & Luebbert, 2007), here CD3⁺CD4⁺ cells were observed in the brains of 18 month-old wildtype and APP/PS1 mice. The data presented here indicate that there is a significant increase in the number of CD3⁺CD4⁺ cells infiltrating the brains of APP/PS1, compared with wildtype,

mice and that these cells stained positively for IFN- γ and IL-17, suggesting the presence of both Th1 and Th17 cells. These results are consistent with previous studies from this laboratory where increased BBB permeability was observed in APP/PS1 mice compared with aged matched controls (Kelly *et al.*, personal communications). Further, a previous study from Stalder and colleagues (2005) using APP23 transgenic mice injected with green fluorescent protein-positive donor cells, found significant invasion of T cells into the brains of transgenic mice, although they found no indication of T cell-mediated inflammation (Stalder *et al.*, 2005). CD3⁺CD8⁺ cells were also observed in the brains of wildtype and APP/PS1 mice, and these cells produced a greater amount of IFN- γ compared with IL-17 in the brains of APP/PS1 mice. Previously it has been observed that CD8⁺ cells, along with CD4⁺ cells, invade the CNS of transgenic mouse models of AD with the greater portion of these cells being CD4⁺ T cells (Fisher *et al.*, 2010). Similarly here it was found that there was a greater portion of CD4⁺ T cells versus CD8⁺ T cells in the brains of APP/PS1 mice. Consistent with this, it has been reported that there is an increase in CD4⁺ T cells while CD8⁺ T cells are decreased in AD and interestingly the CD4/CD8-ratio correlated with cognitive deterioration as measured by MMSE (Schindowski *et al.*, 2007).

It has been suggested that the extent of microglial activation and the degree of co-stimulatory molecule expression in experimental and pathological conditions may affect the outcome of microglia-T cell interactions (Aloisi, 2001). In the previous chapter it was established that Th1 and Th17 cells enhanced the expression of co-stimulatory molecules on microglia. The previous study was extended here with an investigation of the role of Th1 and Th17 cell signature cytokines IFN- γ and IL-17. The data revealed that Th1 cells increased expression of CD86 whilst IFN- γ caused a greater increase in the expression of both CD86 and MHC class II compared with Th1 cells, while Th17 cells and IL-17 had no significant effect on the expression of either CD86 or MHC class II. Interestingly, a previous study from this laboratory observed that Th17 cells enhanced the expression of MHC class II and CD86 whereas the cytokine IL-17 had no effect on their expression suggesting that perhaps the Th17 cell cytokine IL-17 may mediate effects on glia via other receptors (McQuillan *et al.*, 2010). No exaggerated Th1- or Th17-induction of the expression of CD86 and MHC class II in the presence of A β ₁₋₄₂ was observed. This result was a little surprising as

McQuillan and colleagues (2010) observed an increase in the expression of CD86 and MHC class II following co-culture of microglia with Th1 and Th17 cells and A β -stimulation. These results are consistent with the previous chapter and highlight that Th1 cells rather than Th17 cells induce the greatest expression of markers microglial activation although here it was also established that IFN- γ had a more profound effect than Th1 cells. These results suggest IFN- γ may be a major mediator of Th1 cell-induced microglial activation. Incubation of glia with A β ₁₋₄₂ significantly increased the expression of CD40 on microglia however neither Th1 nor Th17 or their signature cytokines IFN- γ or IL-17 had any additional effect on expression of CD40; previously it has been shown that CD40 leads to the synergistic activation of microglia by A β (Townsend *et al.*, 2005). Together the *in vitro* results demonstrated an increase in the expression of CD40 in response to A β ₁₋₄₂ which was accompanied by an increase in the expression of CD86 and MHC class II in response to Th1 cells and IFN- γ . This is consistent with previous suggestions that CD40 ligation in the presence of A β directs microglia away from a phagocytic phenotype towards an MHC class II presentation phenotype (Townsend *et al.*, 2005). These authors suggest that therapeutic intervention in AD might favour selective promotion of a phagocytic-phenotype while downregulating APC function.

Invasion of T cells into the CNS results in microglial and astrocytic activation (Probert *et al.*, 2000). Here the objective was to evaluate the effect of A β -specific Th1 and Th17 cells on microglial activation in APP/PS1 mice and therefore these cells were adoptively transferred into APP/PS1 mice, and CD11b was used as a marker of microglial activation. Previously it has been reported that CD11b expression is increased during neuroinflammation and its expression corresponds with the severity of microglial activation (Roy *et al.*, 2008). The data revealed that microglial activation was low in control APP/PS1 mice and markedly increased in cortical and hippocampal regions in the brains of APP/PS1 mice which received A β -specific Th1 cells. In contrast, microglial activation in the brains of APP/PS1 mice which received A β -specific Th17 cells was similar to control APP/PS1 mice. These data are consistent with the results *in vitro* in both this chapter and the previous chapter which established that Th1 cells, rather than Th17 cells, have a greater impact on microglial activation. Furthermore, previous unpublished data from this laboratory have shown that adoptively transferring A β -

specific Th17 into APP/PS1 mice induces a modest reduction in soluble A β ₁₋₄₀ concentration (Quillan, 2009). Although both Th1 cells (Kroenke *et al.*, 2008) and Th17 cells (Langrish *et al.*, 2005) are pathogenic in EAE, the *in vitro* and *in vivo* data presented here imply that Th1, and not Th17, cells may have a potential pathogenic role in AD.

Activated Th1 cells produce and secrete IFN- γ however the presence of IFN- γ and its role in AD is still not clear (Li *et al.*, 2004). Earlier it was established that IFN- γ has a profound effect on microglial activation *in vitro* thus one of the primary aims of this study was to investigate if neutralizing IFN- γ could attenuate A β -specific Th1 cell-induced inflammation in APP/PS1 mice. Thus A β -specific Th1 cells were adoptively transferred into APP/PS1 mice which were also treated with an anti-IFN- γ antibody at the same time and A β -load and plaque burden was investigated. It was observed that A β ₁₋₃₈, A β ₁₋₄₀ and A β ₁₋₄₂ cortical concentrations were significantly increased in APP/PS1 mice and this was further enhanced in APP/PS1 mice which received A β -specific Th1 cells compared with control APP/PS1 mice. The A β -specific Th1-induced increase in A β ₁₋₃₈, A β ₁₋₄₀ and A β ₁₋₄₂ concentrations was attenuated in APP/PS1 mice that received A β -specific Th1 cells and anti-IFN- γ antibody. These changes were paralleled by changes in plaque burden. Previously it has been suggested that IFN- γ inhibits microglial phagocytosis of A β (Koenigsknecht-Talboo & Landreth, 2005; Yamamoto *et al.*, 2008) and that IFN- γ upregulates β -secretase resulting in increased A β -production (Yamamoto *et al.*, 2007). These results are consistent with a previous study from Yamamoto and colleagues (2007) which demonstrated that IFN- γ receptor-deficient Tg2576 transgenic mice had reduced plaque burden which was accompanied by reduced gliosis. These authors postulated that glial activation mediated A β deposition and reduced A β clearance through IFN- γ , TNF α and increased BACE1 activity (Yamamoto *et al.*, 2007). Interestingly reduced glial-induced inflammation has been demonstrated in IFN- γ -deficient mice undergoing EAE (Tran *et al.*, 2000b). Thus it might be hypothesised that Th1 cells contribute to plaque burden through the production of IFN- γ which increases microglial activation and inhibits phagocytosis. In contrast, a study from Fisher and colleagues (2010) observed a reduction in A β -load and plaque number in the brains of transgenic mice injected with A β ₁₋₄₂, in CFA, which they concluded was due to the occurrence of activated T cells displaying a Th1

phenotype at sites of plaque burden. Monsengo and colleagues (2006) similarly reported reduced plaque burden in APP mice over expressing IFN- γ , and enhanced microglia uptake of A β when stimulated with IFN- γ . It has been suggested that the discrepancies relating to the effect of IFN- γ on plaque burden might be due to the differential mechanisms by which IFN- γ regulates A β uptake and degradation by microglia (Yamamoto *et al.*, 2007).

There is a wealth of literature documenting microglial activation following a range of insults and it has been shown that A β maintains microglia in an activated state both *in vitro* and *in vivo* (Clarke *et al.*, 2007; Lyons *et al.*, 2007). It is well established that microglia can interact with T cells resulting in the production of cytokines, which in turn, cause further activation of both microglia and T cells (Aloisi *et al.*, 2000b; Dasgupta *et al.*, 2005). In parallel with the observed increase in A β -load and plaque burden described here it was found that A β -specific Th1 cells induced a significant increase in microglial activation in hippocampal brain sections, and to a lesser extent cortical sections, of APP/PS1 mice compared with control APP/PS1. This Th1-induced increase in microglial activation was accompanied by a significant attenuation of CD11b-positive microglia in APP/PS1 mice that were simultaneously treated with anti-IFN- γ antibody. Studies from Seguin and colleagues (2003) using human microglia have demonstrated that addition of supernatants from Th1 cells to microglial cultures significantly enhances APC function. This group also showed that incubation of microglia with anti-IFN- γ antibody could attenuate the Th1-induced effects, suggesting that the secretion of IFN- γ by these cells may contribute to the inflammatory response (Seguin *et al.*, 2003). The differences between the cortex and the hippocampus may be as a result of differences between site specific microglia and/or the numbers of microglia present in different brain regions. It has been shown that microglia more densely populate the hippocampus than the cortex in the adult mouse brain (Lawson *et al.*, 1990). It is worth noting that A β enhances microglial activation *in vivo* without the presence of IFN- γ (Muehlhauser *et al.*, 2001), thus suggesting that in the case of microglial activation, as seen in the cortex, cell-cell contacts alone may be enough to mediate an exacerbated inflammatory response and hence the anti-IFN- γ treatment did not have a significant effect.

Inflammatory processes associated with A β -plaques consist of local CNS immune cells including activated microglia and reactive astrocytes. There is extensive literature documenting the presence of microglia immediately adjacent to A β -deposits in both the AD brain (McGeer *et al.*, 1993) and transgenic models of AD (Bornemann *et al.*, 2001). Here the data supported the previous findings that microglia were found co-localised to A β -positive immunoreactivity in both cortical and hippocampal regions of APP/PS1 mice and there was an apparent increase in A β -positive reactivity in APP/PS1 mice which received A β -specific Th1 cells and an apparent attenuation in APP/PS1 mice which received anti-IFN- γ antibody. These results are consistent with previous publications in which plaque-associated microglia have been widely observed in a range of transgenic mouse models of AD (Morgan *et al.*, 2005). A previous study from Bornemann and colleagues (2001) using CD11b, as a microglia marker and a different mouse model of AD, observed the presence of activated microglia in association with A β -plaques. It has also been demonstrated that CD4⁺T cells and CD11b⁺ microglia can be found co-localised with A β -plaques especially in the hippocampus (Fisher *et al.*, 2010).

Immunogenic responses to A β have received ample attention in past few years as a potential therapeutic avenue for the treatment of AD. The role of T cells in the pathogenesis of AD remains speculative. The data here suggests that A β -specific Th1 cells increase microglial activation and potentially influence the development of an APC-phenotype rather than a phagocytic phenotype which would result in a greater inflammatory environment as seen by increased A β -load and microglial activation. The data further imply that A β -specific Th1-induced microglial activation may, to some extent, be due to the production of IFN- γ and perhaps inhibiting this cytokine may have therapeutic advantages although caution must be exercised as low levels of IFN- γ has been noted to have beneficial effects through mediating neurogenesis. Butovsky and colleagues (2006) showed *in vitro* that microglia activated by IFN- γ induced neuronal differentiation, while it has been shown in both wildtype, and APP-transgenic, mice that IFN- γ can induce neurogenesis (Baron *et al.*, 2008). The data presented here suggests that A β -specific Th1 cells are detrimental and that targeting their ability to induce inflammation may be beneficial in therapeutic approaches to AD.

Chapter 7
General Discussion

Chapter 7

7.1. General Discussion

Given the acknowledged importance of inflammation and microglial activation in the pathogenesis of neurodegenerative disorders such as AD the overall objective of this study was to investigate microglial activation in two models of inflammation, the CD200^{-/-} mouse model and the APP/PS1 mouse model, when challenged with immune stimuli. Both of these models have previously been shown to exhibit signs of neuroinflammation. Several investigators have established that CD200^{-/-} mice display an inflammatory phenotype under resting and stress-induced conditions. Hoek and colleagues (2000) established that microglia from CD200^{-/-} mice were localized in clumps and constitutively expressed markers of microglial activation. Specifically, microglia from CD200^{-/-} animals have been found to be strongly CD11b and CD45 positive where normally microglia have low expression of both these molecules (Minas & Liversidge, 2006). Others have suggested that CD200^{-/-} mice are more likely to develop an autoimmune disease and display dysregulated macrophage function (Feuer, 2007). The second model used in this study investigated neuroinflammatory changes in a mouse model of AD, the APP/PS1 mouse model. There is extensive literature describing the activation of immune and inflammatory pathways in this mouse model (Morgan *et al.*, 2005; Wyss-Coray, 2006). Previous studies from this laboratory and my own studies have observed increased expression of markers of microglial activation (CD11b, CD40, CD68 and TLR2) and production of pro-inflammatory cytokines (TNF α and IL-1 β) in the brains of APP/PS1 mice (data not shown).

CD200 is expressed on neurons and oligodendrocytes (Koning *et al.*, 2009), while microglia express the CD200R (Minas & Liversidge, 2006). More recent research has established that CD200 is expressed on astrocytes in post-mortem tissue from MS patients (Koning *et al.*, 2009) and recent work from this laboratory has observed CD200 expression on astrocytes *in vitro* (Costello *et al.*, 2011). Considering that the ligand is knocked out in CD200^{-/-} mice (Minas & Liversidge, 2006), mixed glial cultures which consist of approximately 85%

astrocytes and 15% microglia were used in the *in vitro* study rather than isolated microglia. The data revealed that mixed glia cultured from CD200^{-/-} mice had increased basal expression of CD40 but, surprisingly, none of the other markers of glial activation assessed were increased at basal levels. Interestingly, while the expression of CD11b and CD40 was increased following Pam₃Csk₄ stimulation in CD200^{-/-}, compared with wildtype, mice, expression of CD68 was decreased following Pam₃Csk₄ treatment. These results are consistent with studies from Kielian and colleagues (2002) who using *S. aureus*, another TLR2 agonist, observed enhanced MHC class II, CD40, CD80 and CD86 on microglia.

The CD200 signalling cascade results in the inhibition of signalling cascades involved in cytokine production such as ERK, JNK and p38 MAPK activation (Mihirshahi *et al.*, 2009). The data found that the expression and concentration of pro-inflammatory cytokines TNF α and IL-6 and chemokines MCP-1 and IP-10 were enhanced in glia cultured from CD200^{-/-} mice following Pam₃Csk₄ stimulation, but there was no difference in cytokine and chemokine expression and release when glia were unstimulated. The increase in cytokines and chemokines may be as a result of TLR stimulation. It has been suggested that TLR stimulation results in a positive feedback loop allowing for the increased expression of TLRs in response to stimuli. It has been shown that TLR2 and TLR1/TLR6 levels are enhanced on microglia following bacterial stimulation; this may act as a mechanism to potentate the antibacterial immune response (Kielian *et al.*, 2002). Consistent with this idea both the expression of TLR2 and TLR1 were increased in response to TLR2 stimulation in glia prepared from wildtype and CD200^{-/-} mice.

The data revealed that there was increased expression of TLR2 on microglia cultured from CD200^{-/-} mice. This may provide the mechanism by which Pam₃Csk₄ stimulation had a greater effect in glia cultured from CD200^{-/-}, compared with wildtype, mice. Extensive work from Mukhopadhyay and colleagues (2010) has proposed a mechanism by which CD200 acts as an inhibitory receptor on myeloid cells in response to TLR activation. These authors demonstrated that TLR activation induces CD200 to initiate a negative feedback loop to regulate TLR responses and prevent uncontrolled inflammatory responses without compromising pathogen killing. It has been suggested that this negative feedback loop works by limiting NF- κ B nuclear translocation (Mukhopadhyay *et*

al., 2010). Thus it is possible that in the present study that the Pam₃Csk₄-induced increase in TLR2 expression induces an inflammatory environment which is exaggerated in the CD200^{-/-} mice due to the lack of the negative feedback loop that in wildtype animals downregulates the production of pro-inflammatory cytokines and chemokines.

The same parameters were investigated *in vivo*. Here the data revealed that loss of CD200 resulted in an increase in MHC class II expression. Previous studies from this laboratory have observed that interaction of neuronal CD200 and CD200R on microglia can significantly decrease MHC class II expression (Lyons *et al.*, 2007). Unexpectedly loss of CD200 resulted in a decrease in co-stimulatory molecule expression. However as MHC class II expression is upregulated in virtually all inflammatory conditions, as a marker of activation, it would suggest that these cells are activated. The increase in expression of MHC class II accompanied by a decrease in co-stimulatory molecules could be an indication of how these APCs interact with T cells and suggests that this situation would induce T cell anergy rather than T cell stimulation and proliferation due to the lack of co-stimulatory molecules (Becher *et al.*, 2000b).

The data revealed that the expression of pro-inflammatory cytokines TNF α , IL-1 β and IL-6 and chemokines IP-10, MCP-1, RANTES and MIP-1 α were exacerbated in cortical and hippocampal tissue prepared from wildtype and CD200^{-/-} mice following Pam₃Csk₄ stimulation. Interestingly, it was found that the expression of TNF α , IL-1 β and MIP-1 α were enhanced in hippocampal, but not cortical, tissue following Pam₃Csk₄ stimulation in CD200^{-/-}, compared with wildtype, mice. These results are of particular interest as they suggest that the hippocampus is more susceptible to microglia-induced inflammatory changes following the loss of CD200. Moreover this laboratory has reported that loss of CD200 affects synaptic function; LTP is reduced in CA1 synapses of hippocampal slices prepared from CD200^{-/-}, compared with wildtype, mice (Costello *et al.*, 2011). Furthermore studies have shown decreased CD200 expression is coupled with increased microglial activation in the hippocampus of aged and A β -treated rats (Lyons *et al.*, 2007; Downer *et al.*, 2010).

Activation of TLR2 *in vitro* and *in vivo* consistently increased expression of pro-inflammatory cytokines and chemokines but these changes were not accompanied by upregulation of markers of microglial activation which is

generally reported. This could be because astrocytes, as well as microglia, contribute to the release of these inflammatory mediators which implies that there is a separation between the secretory and APC function of microglia which is uncovered by loss of CD200. It is possible that microglia from CD200^{-/-} animals are in a state of tonic activation at basal levels and that the manner in which they respond to an insult/stimuli is governed by the CD200-CD200R interaction. It is possible that no enhanced increase in the expression of glial markers was observed in CD200^{-/-} animals as Pam₃Csk₄ primarily induces a cytokine and chemokine response rather than the upregulation of the markers that were examined. A future study should investigate a broader range of cell surface markers.

It has been suggested that chronic TLR2 expression leads to an exaggerated inflammatory response and is part of the mechanisms underlying neurodegeneration (Laflamme *et al.*, 2001). Increased expression of TLR2, TLR4 and the co-receptor CD14 in the brains of mouse models of AD and AD patients (Fassbender *et al.*, 2004; Walter *et al.*, 2007; Letiembre *et al.*, 2009) has initiated extensive research into their role in inflammation. The ability of TLR2 to modulate A β -induced microglial activation has been demonstrated *in vitro* and *in vivo* (Jana *et al.*, 2008; Liu *et al.*, 2012). The data from the present study corresponds with those of others and showed that expression of TLR2 is upregulated in response to A β _{1-40/1-42} and that TLR2 activation was having a profound effect on A β -induced glial activation. Pre-treatment of glia with anti-TLR2 attenuated A β -induced expression of co-stimulatory molecules CD40 and CD86 and attenuated the production of pro-inflammatory cytokines, TNF α and IL-6, and chemokines IP-10, MCP-1 and RANTES. These pro-inflammatory molecules have been shown to play a role in neurodegeneration and their upregulation has been correlated with neurodegenerative changes (Lynch, 2009). Microglia from the brains of Parkinson's diseased individuals have been shown to be TNF α and IL-6-positive in areas of the brain associated with dramatic neuronal loss (Sawada *et al.*, 2006) while, IP-10-positive astrocytes are found co-localised to A β -plaques (Xia *et al.*, 2000). In the EAE model it has been suggested that RANTES and MCP-1 are the predominant chemokines which recruit peripheral immune cells to produce a nonlethal remitting EAE while other chemokines like MIP-2 produce acute lethal EAE (Tran *et al.*, 2000b).

Interestingly anti-TLR2 treatment had no effect on CD68 expression. This was somewhat surprising since CD68 expression is considered to be a marker of phagocytosis and since it has been reported that TLR2-deficiency enhances A β -phagocytosis (Liu *et al.*, 2012). It has been observed that TLR2 forms a heterodimer with TLR1 to recognise A β (Liu *et al.*, 2012); in a future study it would be interesting to assess the effect of anti-TLR1 and anti-TLR2 combined on glial activation.

Although the evidence presented here suggests that blocking or removing TLR2 may have beneficial effects by reducing A β -induced inflammation on the other hand, a role for stimulating TLR2 activation has been suggested in several studies. For example a role for TLRs, including TLR2, in phagocytosis of A β has been described. The stimulation of TLR2, TLR4, and TLR9 in BV-2 cell lines causes significant uptake of A β ₁₋₄₂ whereas TLR4-deficient mice exhibit increased A β -load (Tahara *et al.*, 2006). Similarly A β uptake was observed in primary murine microglia following activation of TLR2 by PGN (Chen *et al.*, 2006). It has been proposed that the efficacy of TLRs in the phagocytosis of A β occurs in an age-dependent manner. Studies from Tahara and colleagues (2006), demonstrate an increase in A β -load in 14-16 month old APP/PS1 mice lacking TLR4. Whereas Richard and colleagues (2008), found that TLR2-deficient APP/PS1 mice had delayed plaque burden at 6 months of age but not at 9 months of age. These studies suggest that TLR-independent mechanisms are more effective in the early stages of AD due to the absence of TLR-mediated inflammation but as the disease progresses the potential lack of TLRs enhances A β deposition (Reed-Geaghan *et al.*, 2009). The mechanism through which A β mediates microglial activation/phagocytosis is complex. It has been shown that fibrillar A β binds to a receptor complex consisting of $\alpha_6\beta_1$ integrin, CD47, CD36 and the scavenger receptor A (Bamberger *et al.*, 2003); importantly, CD36 and CD47 associate with TLRs (Reed-Geaghan *et al.*, 2009). Immune cells employ a wide range of receptors to recognize an array of pathogens and tailor immune responses; it is known that A β binds to different receptors and receptor complexes and that, in the absence of one, it will bind to another to initiate a response. Therefore it may be the combination of receptors that A β binds to or the types of A β present (i.e. oligomeric or fibrillar) that will govern the exact immune response elicited.

There is still much dispute in the literature regarding the role of TLRs as potential targets for modulating the pathogenesis of AD. The data presented here suggest a significant role for TLR2 in mediating A β -induced inflammation by activating microglia into an APC phenotype and/or upregulating the production of cytokines and chemokines. The data suggests that blocking TLR2 may have therapeutic advantages, especially give recent evidence that an anti-TLR2 antibody (OPN-301) inhibits detrimental NF- κ B-mediated inflammation, cytokine production and leukocyte infiltration in a mouse model of myocardial ischemia reperfusion injury (Arslan *et al.*, 2010), and a humanized version has now entered phase II clinical trials for reperfusion injury post kidney transplantation. However this topic needs further investigation particularly in an *in vivo* model as the limitations of an *in vitro* model are widely recognised; it has been suggested that microglia in culture have a more reactive phenotype as they have been released from their normal microenvironment where neuronal factors contribute to their quiescence (Ransohoff & Perry, 2009).

The second model of inflammation in which microglial activation was investigated was the APP/PS1 mouse model of AD. The fact that inflammation plays an important role in AD was suggested over 20 year ago, and since then our understanding of the role of microglia in the diseased brain has grown (Cameron & Landreth, 2010). However despite the extensive research, it still remains unclear why these cells which are supposed to provide protection to the CNS become detrimental during disease progression. The literature is replete with evidence that the production of A β and its interaction with microglia results in the production of the characteristic chronic inflammatory environment. As a result research in recent times has focused on A β -immunotherapies to aid the removal of A β (Schenk *et al.*, 1999; Morgan *et al.*, 2000). However following the abrupt termination of an anti-A β vaccination clinical trial due to a small percentage of AD patients developing an unexpected T cell mediated meningoencephalitis (Orgogozo *et al.*, 2003), attention has moved towards the investigation of adaptive immune cell interactions with microglia in the pathogenesis of AD.

In this study the initial findings indicated that Th1 and Th17 cells induced glial cells to adopt an APC phenotype and to secrete cytokines, while Th2 cells were having no effect on glial activation. Of note are the findings that Th1 cells induced expression of CD40 and MHC class II and production of TNF α . These

are consistent with observations that Th1 and Th17 cells propagate inflammation whilst Th2 cells have anti-inflammatory effects (Benveniste *et al.*, 2001; McQuillan *et al.*, 2010). A role for CD40 in AD pathology has been demonstrated in previous studies. Tan and colleagues (2002) reported decreased microgliosis and astrogliosis in an APP mouse model lacking CD40 and this was associated with decreased plaque burden. Neurons express CD40 and treatment with CD40L has been shown to increase the amyloidogenic processing of APP suggesting that interaction of CD40 with CD40L on T cells may contribute to the inflammatory environment (Wyss-Coray, 2006). It has been suggested that ligation of CD40 and CD40L directs microglia away from a phagocytic phenotype towards an APC phenotype (Townsend *et al.*, 2005) and ligation enhances the expression of cytokines and chemokines (Grewal & Flavell, 1996).

The present data also shows that Th1 cells increased MHC class II expression on microglia and this was further increased by IFN- γ . IFN- γ is known to be the most potent inducer of MHC class II expression and MHC class II engagement leads to the production of TNF α and IL-1 β (Benveniste *et al.*, 2001). Thus it is possible that interaction of Th1 cells with microglia alters their phenotype towards a pro-inflammatory APC form which may contribute to the progression of AD. However it has been noted in a facial axotomy model of motorneuron degeneration that T cell mediated neuroprotection is actually dependent on antigen presentation by microglia (Byram *et al.*, 2004).

The finding that the production of TNF α in microglia was increased following the addition of Th1 cells is a significant observation as studies have suggested that TNF α and IFN- γ work together to increase iNOS expression in microglia and enhance NF- κ B nuclear translocation thus enhancing the upregulation of genes involved in inflammation (Mir *et al.*, 2008). Further TNF α has been shown to increase the infiltration of T cells into the brain in an age-dependent manner and this was associated with increased ICAM-1 upregulation (Xu *et al.*, 2010). The observation that both TNF α and CD40 expression were upregulated in glial cultures in response to Th1 cells is interesting since it has been shown that neither TNF α or IFN- γ can induce IL-12 secretion, which allows for further T cells stimulation, without CD40 signalling (Becher *et al.*, 2000a).

A possible mechanism by which T cells induce microglial activation has been proposed by Aloisi and colleagues (1999). These authors suggested that

peripherally-activated T cells may cross the BBB and stimulate microglia to adopt an APC phenotype; the mechanism proposed was that IFN- γ induced the upregulation of MHC class II and CD40 which triggered the interaction of MHC class II and CD40 with TCR and CD40L on T cells, resulting in the secretion of cytokines. Since these cytokines enhance T cell activation, a positive feedback loop is created. These authors also postulated that this loop was downregulated by the secretion of PGE₂ (Aloisi *et al.*, 1999). However more recently knocking out the PGE₂ receptor EP2, has been shown to decrease plaque burden in transgenic animals, leading to the proposal that EP2 signalling promotes BACE cleavage in an age-dependent manner (Liang *et al.*, 2005). Additional experiments investigating the modulatory role of PGE₂ in this situation would be interesting.

T cells were found to infiltrate the brains of aged wildtype and APP/PS1 mice with a significantly greater number infiltrating the brains of APP/PS1 mice. On closer analysis these cells were found to secrete IFN- γ and IL-17, suggesting the presence of both Th1 and Th17 cells. The consequences of the infiltration of T cells into the brain, and the outcome, depends on the manner of interactions of T cells with glia and neurons (Carson *et al.*, 2006). It is interesting that both Th1 and Th17 cells have been implicated in the progression of MS in mouse models (Kebir *et al.*, 2007; Murphy *et al.*, 2010), but their role in AD is not as well examined.

The data described here that Th1 cells significantly impacted on both microglial activation and A β -load and burden in the brains of APP/PS1 mice, which is consistent with other authors. Studies from Stalder and colleagues (2005) have suggested a role for peripheral immune cells in cerebral amyloidogenesis and they found that some of these invading peripheral immune cells were targeted to plaques. In this study, it was found that anti-IFN- γ treatment significantly attenuated Th1-induced A β -load and burden. Furthermore it was found that anti-IFN- γ treatment significantly attenuated Th1-induced microglial activation in the hippocampus of APP/PS1 mice. The decrease in plaque burden and A β -load in APP/PS1 mice treated with anti-IFN- γ may be due several possible mechanisms. Firstly it could lead to increased phagocytosis, as *in vitro* studies have established that IFN- γ inhibits effective phagocytosis of A β by microglia, (Koenigsnecht-Talboo & Landreth, 2005). Secondly anti-IFN- γ treatment could reduce microglial activation as IFN- γ has been shown to synergise with pro-inflammatory cytokines, such as TNF α as described earlier, and with A β , to increase microglia activation

and neurotoxicity (Goodwin *et al.*, 1995; Meda *et al.*, 1995). Finally the treatment could alter A β accumulation since IFN- γ has been observed to increase A β production in the presence of TNF α through increasing β -secretase activity (Yamamoto *et al.*, 2007). The present results suggest that A β accumulation in this model is a consequence of infiltrating Th1 cells which release IFN- γ , activating microglia, and inducing an inflammatory phenotype which triggers APP proteolysis. A future study should include more extensive analysis of microglial activation and focus on evaluating changes in phagocytic ability to make a more conclusive determination of the mechanism by which A β load and burden was reduced.

In conclusion, the results of these studies have provided important insights into the potential roles that CD200, TLR2 and T cells have in modulating glial activation. How these factors interact with one and another to enhance inflammation in neurodegeneration such as AD is not yet clear. AD is associated with altered basal microglial and astrocytic activation, these changes are thought to be in part inherent to the glia although changes may also be due to changes in neuronal health such as the expression of CD200 (Carson *et al.*, 2006). Changes in the expression of both CD200 and TLR have been reported in AD. Indeed CD200 and CD200R has been found to be downregulated in AD (Walker *et al.*, 2009), and CD200R is decreased in brains of APP/PS1 mice (unpublished observation). Previous evidence from this laboratory has identified an inverse relationship between neuronal expression of CD200 and microglial activation, and has established that the anti-inflammatory cytokine IL-4, which is secreted by Th2 cells, can increase the expression of CD200 (Lyons *et al.*, 2007). TLR expression has been found to be upregulated in AD and in mouse models of AD (Fassbender *et al.*, 2004; Walter *et al.*, 2007; Letiembre *et al.*, 2009).

Interestingly the chemokine, RANTES, that was induced by A $\beta_{1-40/1-42}$ and attenuated by anti-TLR2 treatment in the *in vitro* studies has been shown to preferentially recruit Th1 cells to sites of inflammation (Siveke & Hamann, 1998). The definitive roles of chemokines in AD have not been as well established as those in EAE (Tran *et al.*, 2000b), none the less their presence must raise the question of the possibility that they attract peripheral immune cells to sites of inflammation in the CNS during AD. The data highlight the fact that T cells can enter the brains of APP/PS1 mice and that the interaction of Th1 cells with

microglia may contribute to the progression of the disease through glial activation via cell-cell contacts or the secretion of IFN- γ . As described earlier IFN- γ has a potent effect not only on glial activation and the production of inflammatory mediators but also through its potential to increase A β -load and more importantly it has been found that both IFN- γ and IL-12 are increased in the AD brain (Huberman *et al.*, 1994).

Together the data suggest that during AD the loss of CD200 and increased TLR expression, which is a receptor for A β , may result in a pro-inflammatory environment that favours the recruitment of peripheral Th1 cells, rather than Th2 cells, into the CNS. In turn these Th1 cells exacerbate inflammation and plaque development through their interaction with glia and the production of IFN- γ . The data suggest that microglia in an APC phenotype have a detrimental impact and that potential therapeutic targets lie in the switching of microglia to a phagocytic phenotype. Additional experiments are required to unveil the precise mechanisms by which T cells and TLRs, possibly in a joint manner, induce a phenotypic state resulting in a disadvantageous inflammatory environment, and question the role played by different glial phenotypic states in neurodegeneration.

Chapter 8
Bibliography

- Abbas N, Bednar I, Mix E, Marie S, Paterson D, Ljungberg A, Morris C, Winblad B, Nordberg A & Zhu J. (2002). Up-regulation of the inflammatory cytokines IFN-gamma and IL-12 and down-regulation of IL-4 in cerebral cortex regions of APP(SWE) transgenic mice. *Journal of neuroimmunology* **126**, 50-57.
- Aloisi F. (2001). Immune function of microglia. *Glia* **36**, 165-179.
- Aloisi F, De Simone R, Columba-Cabezas S, Penna G & Adorini L. (2000a). Functional maturation of adult mouse resting microglia into an APC is promoted by granulocyte-macrophage colony-stimulating factor and interaction with Th1 cells. *J Immunol* **164**, 1705-1712.
- Aloisi F, Penna G, Polazzi E, Minghetti L & Adorini L. (1999). CD40-CD154 interaction and IFN-gamma are required for IL-12 but not prostaglandin E2 secretion by microglia during antigen presentation to Th1 cells. *J Immunol* **162**, 1384-1391.
- Aloisi F, Ria F & Adorini L. (2000b). Regulation of T-cell responses by CNS antigen-presenting cells: different roles for microglia and astrocytes. *Immunology today* **21**, 141-147.
- Applequist SE, Wallin RP & Ljunggren HG. (2002). Variable expression of Toll-like receptor in murine innate and adaptive immune cell lines. *International immunology* **14**, 1065-1074.
- Arslan F, Smeets MB, O'Neill LA, Keogh B, McGuirk P, Timmers L, Tersteeg C, Hoefler IE, Doevendans PA, Pasterkamp G & de Kleijn DP. (2010). Myocardial ischemia/reperfusion injury is mediated by leukocytic toll-like receptor-2 and reduced by systemic administration of a novel anti-toll-like receptor-2 antibody. *Circulation* **121**, 80-90.
- Ashe KH. (2001). Learning and memory in transgenic mice modeling Alzheimer's disease. *Learn Mem* **8**, 301-308.
- Babcock AA, Kuziel WA, Rivest S & Owens T. (2003). Chemokine expression by glial cells directs leukocytes to sites of axonal injury in the CNS. *The Journal of neuroscience : the official journal of the Society for Neuroscience* **23**, 7922-7930.
- Bain CC & Mowat AM. (2012). CD200 receptor and macrophage function in the intestine. *Immunobiology* **217**, 643-651.
- Bamberger ME, Harris ME, McDonald DR, Husemann J & Landreth GE. (2003). A cell surface receptor complex for fibrillar beta-amyloid mediates microglial activation. *The Journal of neuroscience : the official journal of the Society for Neuroscience* **23**, 2665-2674.
- Bamberger ME & Landreth GE. (2001). Microglial interaction with beta-amyloid: implications for the pathogenesis of Alzheimer's disease. *Microscopy research and technique* **54**, 59-70.
- Barclay AN, Wright GJ, Brooke G & Brown MH. (2002). CD200 and membrane protein interactions in the control of myeloid cells. *Trends in immunology* **23**, 285-290.
- Baron R, Nemirovsky A, Harpaz I, Cohen H, Owens T & Monsonego A. (2008). IFN-gamma enhances neurogenesis in wild-type mice and in a mouse model of

Alzheimer's disease. *FASEB journal : official publication of the Federation of American Societies for Experimental Biology* **22**, 2843-2852.

- Becher B & Antel JP. (1996). Comparison of phenotypic and functional properties of immediately ex vivo and cultured human adult microglia. *Glia* **18**, 1-10.
- Becher B, Bechmann I & Greter M. (2006). Antigen presentation in autoimmunity and CNS inflammation: how T lymphocytes recognize the brain. *J Mol Med (Berl)* **84**, 532-543.
- Becher B, Blain M & Antel JP. (2000a). CD40 engagement stimulates IL-12 p70 production by human microglial cells: basis for Th1 polarization in the CNS. *Journal of neuroimmunology* **102**, 44-50.
- Becher B, Prat A & Antel JP. (2000b). Brain-immune connection: immuno-regulatory properties of CNS-resident cells. *Glia* **29**, 293-304.
- Benveniste EN. (1997). Role of macrophages/microglia in multiple sclerosis and experimental allergic encephalomyelitis. *J Mol Med (Berl)* **75**, 165-173.
- Benveniste EN, Nguyen VT & O'Keefe GM. (2001). Immunological aspects of microglia: relevance to Alzheimer's disease. *Neurochemistry international* **39**, 381-391.
- Biber K, Neumann H, Inoue K & Boddeke HW. (2007). Neuronal 'On' and 'Off' signals control microglia. *Trends in neurosciences* **30**, 596-602.
- Bitsch A, Schuchardt J, Bunkowski S, Kuhlmann T & Bruck W. (2000). Acute axonal injury in multiple sclerosis. Correlation with demyelination and inflammation. *Brain : a journal of neurology* **123 (Pt 6)**, 1174-1183.
- Blum-Degen D, Muller T, Kuhn W, Gerlach M, Przuntek H & Riederer P. (1995). Interleukin-1 beta and interleukin-6 are elevated in the cerebrospinal fluid of Alzheimer's and de novo Parkinson's disease patients. *Neuroscience letters* **202**, 17-20.
- Bornemann KD, Wiederhold KH, Pauli C, Ermini F, Stalder M, Schnell L, Sommer B, Jucker M & Staufenbiel M. (2001). Abeta-induced inflammatory processes in microglia cells of APP23 transgenic mice. *The American journal of pathology* **158**, 63-73.
- Bowman CC, Rasley A, Tranguch SL & Marriott I. (2003). Cultured astrocytes express toll-like receptors for bacterial products. *Glia* **43**, 281-291.
- Broderick C, Hoek RM, Forrester JV, Liversidge J, Sedgwick JD & Dick AD. (2002). Constitutive retinal CD200 expression regulates resident microglia and activation state of inflammatory cells during experimental autoimmune uveoretinitis. *The American journal of pathology* **161**, 1669-1677.
- Bsibsi M, Ravid R, Gveric D & van Noort JM. (2002). Broad expression of Toll-like receptors in the human central nervous system. *Journal of neuropathology and experimental neurology* **61**, 1013-1021.
- Byram SC, Carson MJ, DeBoy CA, Serpe CJ, Sanders VM & Jones KJ. (2004). CD4-positive T cell-mediated neuroprotection requires dual compartment antigen

- presentation. *The Journal of neuroscience : the official journal of the Society for Neuroscience* **24**, 4333-4339.
- Cameron B & Landreth GE. (2010). Inflammation, microglia, and Alzheimer's disease. *Neurobiology of disease* **37**, 503-509.
- Campbell M, Ozaki E & Humphries P. (2010). Systemic delivery of therapeutics to neuronal tissues: a barrier modulation approach. *Expert opinion on drug delivery* **7**, 859-869.
- Cannella B, Aquino DA & Raine CS. (1995). MHC II expression in the CNS after long-term demyelination. *Journal of neuropathology and experimental neurology* **54**, 521-530.
- Cannella B & Raine CS. (1995). The adhesion molecule and cytokine profile of multiple sclerosis lesions. *Annals of neurology* **37**, 424-435.
- Cao C, Arendash GW, Dickson A, Mamcarz MB, Lin X & Ethell DW. (2009). Abeta-specific Th2 cells provide cognitive and pathological benefits to Alzheimer's mice without infiltrating the CNS. *Neurobiology of disease* **34**, 63-70.
- Cao D, Lu H, Lewis TL & Li L. (2007). Intake of sucrose-sweetened water induces insulin resistance and exacerbates memory deficits and amyloidosis in a transgenic mouse model of Alzheimer disease. *The Journal of biological chemistry* **282**, 36275-36282.
- Carpentier PA, Begolka WS, Olson JK, Elhofy A, Karpus WJ & Miller SD. (2005). Differential activation of astrocytes by innate and adaptive immune stimuli. *Glia* **49**, 360-374.
- Carson MJ, Thrash JC & Walter B. (2006). The cellular response in neuroinflammation: The role of leukocytes, microglia and astrocytes in neuronal death and survival. *Clinical neuroscience research* **6**, 237-245.
- Cartier L, Hartley O, Dubois-Dauphin M & Krause KH. (2005). Chemokine receptors in the central nervous system: role in brain inflammation and neurodegenerative diseases. *Brain research Brain research reviews* **48**, 16-42.
- Chabot S, Williams G & Yong VW. (1997). Microglial production of TNF-alpha is induced by activated T lymphocytes. Involvement of VLA-4 and inhibition by interferonbeta-1b. *The Journal of clinical investigation* **100**, 604-612.
- Chen DX, He H & Gorczynski RM. (2005). Synthetic peptides from the N-terminal regions of CD200 and CD200R1 modulate immunosuppressive and anti-inflammatory effects of CD200-CD200R1 interaction. *International immunology* **17**, 289-296.
- Chen K, Huang J, Gong W, Iribarren P, Dunlop NM & Wang JM. (2007). Toll-like receptors in inflammation, infection and cancer. *International immunopharmacology* **7**, 1271-1285.
- Chen K, Iribarren P, Hu J, Chen J, Gong W, Cho EH, Lockett S, Dunlop NM & Wang JM. (2006). Activation of Toll-like receptor 2 on microglia promotes cell uptake of Alzheimer disease-associated amyloid beta peptide. *The Journal of biological chemistry* **281**, 3651-3659.

- Chitnis T, Imitola J, Wang Y, Elyaman W, Chawla P, Sharuk M, Raddassi K, Bronson RT & Khoury SJ. (2007). Elevated neuronal expression of CD200 protects Wlds mice from inflammation-mediated neurodegeneration. *The American journal of pathology* **170**, 1695-1712.
- Chu CQ, Wittmer S & Dalton DK. (2000). Failure to suppress the expansion of the activated CD4 T cell population in interferon gamma-deficient mice leads to exacerbation of experimental autoimmune encephalomyelitis. *The Journal of experimental medicine* **192**, 123-128.
- Clark MJ, Gagnon J, Williams AF & Barclay AN. (1985). MRC OX-2 antigen: a lymphoid/neuronal membrane glycoprotein with a structure like a single immunoglobulin light chain. *The EMBO journal* **4**, 113-118.
- Clarke RM, O'Connell F, Lyons A & Lynch MA. (2007). The HMG-CoA reductase inhibitor, atorvastatin, attenuates the effects of acute administration of amyloid-beta1-42 in the rat hippocampus in vivo. *Neuropharmacology* **52**, 136-145.
- Colton CA. (2009). Heterogeneity of microglial activation in the innate immune response in the brain. *Journal of neuroimmune pharmacology : the official journal of the Society on NeuroImmune Pharmacology* **4**, 399-418.
- Combs CK, Karlo JC, Kao SC & Landreth GE. (2001). beta-Amyloid stimulation of microglia and monocytes results in TNFalpha-dependent expression of inducible nitric oxide synthase and neuronal apoptosis. *The Journal of neuroscience : the official journal of the Society for Neuroscience* **21**, 1179-1188.
- Conant K, Garzino-Demo A, Nath A, McArthur JC, Halliday W, Power C, Gallo RC & Major EO. (1998). Induction of monocyte chemoattractant protein-1 in HIV-1 Tat-stimulated astrocytes and elevation in AIDS dementia. *Proceedings of the National Academy of Sciences of the United States of America* **95**, 3117-3121.
- Constant SL & Bottomly K. (1997). Induction of Th1 and Th2 CD4+ T cell responses: the alternative approaches. *Annual review of immunology* **15**, 297-322.
- Copland DA, Calder CJ, Raveney BJ, Nicholson LB, Phillips J, Cherwinski H, Jenmalm M, Sedgwick JD & Dick AD. (2007). Monoclonal antibody-mediated CD200 receptor signaling suppresses macrophage activation and tissue damage in experimental autoimmune uveoretinitis. *The American journal of pathology* **171**, 580-588.
- Costello DA, Lyons A, Denieffe S, Browne TC, Cox FF & Lynch MA. (2011). Long term potentiation is impaired in membrane glycoprotein CD200-deficient mice: a role for Toll-like receptor activation. *The Journal of biological chemistry* **286**, 34722-34732.
- D'Aversa TG, Weidenheim KM & Berman JW. (2002). CD40-CD40L interactions induce chemokine expression by human microglia: implications for human immunodeficiency virus encephalitis and multiple sclerosis. *The American journal of pathology* **160**, 559-567.
- Dasgupta S, Jana M, Liu X & Pahan K. (2005). Myelin basic protein-primed T cells of female but not male mice induce nitric-oxide synthase and proinflammatory

- cytokines in microglia: implications for gender bias in multiple sclerosis. *The Journal of biological chemistry* **280**, 32609-32617.
- Dasu MR, Riosvelasco AC & Jialal I. (2009). Candesartan inhibits Toll-like receptor expression and activity both in vitro and in vivo. *Atherosclerosis* **202**, 76-83.
- Davis JB, McMurray HF & Schubert D. (1992). The amyloid beta-protein of Alzheimer's disease is chemotactic for mononuclear phagocytes. *Biochemical and biophysical research communications* **189**, 1096-1100.
- Deckert M, Sedgwick JD, Fischer E & Schluter D. (2006). Regulation of microglial cell responses in murine *Toxoplasma* encephalitis by CD200/CD200 receptor interaction. *Acta neuropathologica* **111**, 548-558.
- DeMattos RB, Bales KR, Cummins DJ, Dodart JC, Paul SM & Holtzman DM. (2001). Peripheral anti-A beta antibody alters CNS and plasma A beta clearance and decreases brain A beta burden in a mouse model of Alzheimer's disease. *Proceedings of the National Academy of Sciences of the United States of America* **98**, 8850-8855.
- DeMattos RB, Bales KR, Cummins DJ, Paul SM & Holtzman DM. (2002). Brain to plasma amyloid-beta efflux: a measure of brain amyloid burden in a mouse model of Alzheimer's disease. *Science* **295**, 2264-2267.
- Deng XH, Bertini G, Xu YZ, Yan Z & Bentivoglio M. (2006). Cytokine-induced activation of glial cells in the mouse brain is enhanced at an advanced age. *Neuroscience* **141**, 645-661.
- Dimitrijevic OB, Stamatovic SM, Keep RF & Andjelkovic AV. (2006). Effects of the chemokine CCL2 on blood-brain barrier permeability during ischemia-reperfusion injury. *Journal of cerebral blood flow and metabolism : official journal of the International Society of Cerebral Blood Flow and Metabolism* **26**, 797-810.
- Dong Y & Benveniste EN. (2001). Immune function of astrocytes. *Glia* **36**, 180-190.
- Downer EJ, Cowley TR, Lyons A, Mills KH, Berezin V, Bock E & Lynch MA. (2010). A novel anti-inflammatory role of NCAM-derived mimetic peptide, FGL. *Neurobiology of aging* **31**, 118-128.
- Du X, Fleiss B, Li H, D'Angelo B, Sun Y, Zhu C, Hagberg H, Levy O, Mallard C & Wang X. (2011). Systemic stimulation of TLR2 impairs neonatal mouse brain development. *PloS one* **6**, e19583.
- Duan RS, Yang X, Chen ZG, Lu MO, Morris C, Winblad B & Zhu J. (2008). Decreased fractalkine and increased IP-10 expression in aged brain of APP(swe) transgenic mice. *Neurochemical research* **33**, 1085-1089.
- Dufour JH, Dziejman M, Liu MT, Leung JH, Lane TE & Luster AD. (2002). IFN-gamma-inducible protein 10 (IP-10; CXCL10)-deficient mice reveal a role for IP-10 in effector T cell generation and trafficking. *J Immunol* **168**, 3195-3204.
- Ebert S, Gerber J, Bader S, Muhlhauser F, Brechtel K, Mitchell TJ & Nau R. (2005). Dose-dependent activation of microglial cells by Toll-like receptor agonists alone and in combination. *Journal of neuroimmunology* **159**, 87-96.

- Esen N, Tanga FY, DeLeo JA & Kielian T. (2004). Toll-like receptor 2 (TLR2) mediates astrocyte activation in response to the Gram-positive bacterium *Staphylococcus aureus*. *Journal of neurochemistry* **88**, 746-758.
- Ethell DW, Shippy D, Cao C, Cracchiolo JR, Runfeldt M, Blake B & Arendash GW. (2006). Aβ-specific T-cells reverse cognitive decline and synaptic loss in Alzheimer's mice. *Neurobiology of disease* **23**, 351-361.
- Eugster HP, Frei K, Kopf M, Lassmann H & Fontana A. (1998). IL-6-deficient mice resist myelin oligodendrocyte glycoprotein-induced autoimmune encephalomyelitis. *European journal of immunology* **28**, 2178-2187.
- Falsig J, Latta M & Leist M. (2004). Defined inflammatory states in astrocyte cultures: correlation with susceptibility towards CD95-driven apoptosis. *Journal of neurochemistry* **88**, 181-193.
- Farfara D, Lifshitz V & Frenkel D. (2008). Neuroprotective and neurotoxic properties of glial cells in the pathogenesis of Alzheimer's disease. *Journal of cellular and molecular medicine* **12**, 762-780.
- Farrall AJ & Wardlaw JM. (2009). Blood-brain barrier: ageing and microvascular disease--systematic review and meta-analysis. *Neurobiology of aging* **30**, 337-352.
- Fassbender K, Walter S, Kuhl S, Landmann R, Ishii K, Bertsch T, Stalder AK, Muehlhauser F, Liu Y, Ulmer AJ, Rivest S, Lentsch A, Gulbins E, Jucker M, Staufenbiel M, Brechtel K, Walter J, Multhaup G, Penke B, Adachi Y, Hartmann T & Beyreuther K. (2004). The LPS receptor (CD14) links innate immunity with Alzheimer's disease. *FASEB journal : official publication of the Federation of American Societies for Experimental Biology* **18**, 203-205.
- Feuer R. (2007). Tickling the CD200 receptor: A remedy for those irritating macrophages. *The American journal of pathology* **171**, 396-398.
- Finch CE & Ruvkun G. (2001). The genetics of aging. *Annual review of genomics and human genetics* **2**, 435-462.
- Finsen B & Owens T. (2011). Innate immune responses in central nervous system inflammation. *FEBS letters* **585**, 3806-3812.
- Fisher Y, Nemirovsky A, Baron R & Monsonego A. (2010). T cells specifically targeted to amyloid plaques enhance plaque clearance in a mouse model of Alzheimer's disease. *PloS one* **5**, e10830.
- Frank MG, Baratta MV, Sprunger DB, Watkins LR & Maier SF. (2007). Microglia serve as a neuroimmune substrate for stress-induced potentiation of CNS pro-inflammatory cytokine responses. *Brain, behavior, and immunity* **21**, 47-59.
- Frank MG, Barrientos RM, Biedenkapp JC, Rudy JW, Watkins LR & Maier SF. (2006). mRNA up-regulation of MHC II and pivotal pro-inflammatory genes in normal brain aging. *Neurobiology of aging* **27**, 717-722.

- Frank S, Copanaki E, Burbach GJ, Muller UC & Deller T. (2009). Differential regulation of toll-like receptor mRNAs in amyloid plaque-associated brain tissue of aged APP23 transgenic mice. *Neuroscience letters* **453**, 41-44.
- Freeman GJ, Boussiotis VA, Anumanthan A, Bernstein GM, Ke XY, Rennert PD, Gray GS, Gribben JG & Nadler LM. (1995). B7-1 and B7-2 do not deliver identical costimulatory signals, since B7-2 but not B7-1 preferentially costimulates the initial production of IL-4. *Immunity* **2**, 523-532.
- Fukumoto H, Rosene DL, Moss MB, Raju S, Hyman BT & Irizarry MC. (2004). Beta-secretase activity increases with aging in human, monkey, and mouse brain. *The American journal of pathology* **164**, 719-725.
- Gadient RA & Otten UH. (1997). Interleukin-6 (IL-6)--a molecule with both beneficial and destructive potentials. *Progress in neurobiology* **52**, 379-390.
- Galimberti D, Schoonenboom N, Scarpini E & Scheltens P. (2003). Chemokines in serum and cerebrospinal fluid of Alzheimer's disease patients. *Annals of neurology* **53**, 547-548.
- Games D, Adams D, Alessandrini R, Barbour R, Berthelette P, Blackwell C, Carr T, Clemens J, Donaldson T, Gillespie F & et al. (1995). Alzheimer-type neuropathology in transgenic mice overexpressing V717F beta-amyloid precursor protein. *Nature* **373**, 523-527.
- Garcia-Alloza M, Robbins EM, Zhang-Nunes SX, Purcell SM, Betensky RA, Raju S, Prada C, Greenberg SM, Bacskai BJ & Frosch MP. (2006). Characterization of amyloid deposition in the APP^{swE}/PS1^{dE9} mouse model of Alzheimer disease. *Neurobiology of disease* **24**, 516-524.
- Gasic-Milenkovic J, Dukic-Stefanovic S, Deuther-Conrad W, Gartner U & Munch G. (2003). Beta-amyloid peptide potentiates inflammatory responses induced by lipopolysaccharide, interferon -gamma and 'advanced glycation endproducts' in a murine microglia cell line. *The European journal of neuroscience* **17**, 813-821.
- Gehrmann J, Matsumoto Y & Kreutzberg GW. (1995). Microglia: intrinsic immune effector cell of the brain. *Brain research Brain research reviews* **20**, 269-287.
- Geisberger R, Lamers M & Achatz G. (2006). The riddle of the dual expression of IgM and IgD. *Immunology* **118**, 429-437.
- Gelinas DS, DaSilva K, Fenili D, St George-Hyslop P & McLaurin J. (2004). Immunotherapy for Alzheimer's disease. *Proceedings of the National Academy of Sciences of the United States of America* **101 Suppl 2**, 14657-14662.
- Gemma C, Bachstetter AD & Bickford PC. (2010). Neuron-Microglia Dialogue and Hippocampal Neurogenesis in the Aged Brain. *Aging and disease* **1**, 232-244.
- Gerritse K, Laman JD, Noelle RJ, Aruffo A, Ledbetter JA, Boersma WJ & Claassen E. (1996). CD40-CD40 ligand interactions in experimental allergic encephalomyelitis and multiple sclerosis. *Proceedings of the National Academy of Sciences of the United States of America* **93**, 2499-2504.

- Ghirnikar RS, Lee YL & Eng LF. (1998). Inflammation in traumatic brain injury: role of cytokines and chemokines. *Neurochemical research* **23**, 329-340.
- Gimsa U, Wolf SA, Haas D, Bechmann I & Nitsch R. (2001). Th2 cells support intrinsic anti-inflammatory properties of the brain. *Journal of neuroimmunology* **119**, 73-80.
- Giulian D, Haverkamp LJ, Li J, Karshin WL, Yu J, Tom D, Li X & Kirkpatrick JB. (1995). Senile plaques stimulate microglia to release a neurotoxin found in Alzheimer brain. *Neurochemistry international* **27**, 119-137.
- Giulian D, Haverkamp LJ, Yu JH, Karshin W, Tom D, Li J, Kirkpatrick J, Kuo LM & Roher AE. (1996). Specific domains of beta-amyloid from Alzheimer plaque elicit neuron killing in human microglia. *The Journal of neuroscience : the official journal of the Society for Neuroscience* **16**, 6021-6037.
- Giuliani F, Goodyer CG, Antel JP & Yong VW. (2003). Vulnerability of human neurons to T cell-mediated cytotoxicity. *J Immunol* **171**, 368-379.
- Glezer I, Simard AR & Rivest S. (2007). Neuroprotective role of the innate immune system by microglia. *Neuroscience* **147**, 867-883.
- Goodwin JL, Uemura E & Cunnick JE. (1995). Microglial release of nitric oxide by the synergistic action of beta-amyloid and IFN-gamma. *Brain research* **692**, 207-214.
- Gorczynski R, Chen Z, Kai Y, Lee L, Wong S & Marsden PA. (2004). CD200 is a ligand for all members of the CD200R family of immunoregulatory molecules. *J Immunol* **172**, 7744-7749.
- Gorczynski RM, Chen Z, Lee L, Yu K & Hu J. (2002a). Anti-CD200R ameliorates collagen-induced arthritis in mice. *Clin Immunol* **104**, 256-264.
- Gorczynski RM, Chen Z, Yu K & Hu J. (2001). CD200 immunoadhesin suppresses collagen-induced arthritis in mice. *Clin Immunol* **101**, 328-334.
- Gorczynski RM, Hu J, Chen Z, Kai Y & Lei J. (2002b). A CD200FC immunoadhesin prolongs rat islet xenograft survival in mice. *Transplantation* **73**, 1948-1953.
- Grewal IS & Flavell RA. (1996). A central role of CD40 ligand in the regulation of CD4+ T-cell responses. *Immunology today* **17**, 410-414.
- Griffin WS, Stanley LC, Ling C, White L, MacLeod V, Perrot LJ, White CL, 3rd & Araoz C. (1989). Brain interleukin 1 and S-100 immunoreactivity are elevated in Down syndrome and Alzheimer disease. *Proceedings of the National Academy of Sciences of the United States of America* **86**, 7611-7615.
- Gurley C, Nichols J, Liu S, Phulwani NK, Esen N & Kielian T. (2008). Microglia and Astrocyte Activation by Toll-Like Receptor Ligands: Modulation by PPAR-gamma Agonists. *PPAR research* **2008**, 453120.
- Haga S, Akai K & Ishii T. (1989). Demonstration of microglial cells in and around senile (neuritic) plaques in the Alzheimer brain. An immunohistochemical study using a novel monoclonal antibody. *Acta neuropathologica* **77**, 569-575.

- Hanisch UK & Kettenmann H. (2007). Microglia: active sensor and versatile effector cells in the normal and pathologic brain. *Nature neuroscience* **10**, 1387-1394.
- Harrington LE, Hatton RD, Mangan PR, Turner H, Murphy TL, Murphy KM & Weaver CT. (2005). Interleukin 17-producing CD4+ effector T cells develop via a lineage distinct from the T helper type 1 and 2 lineages. *Nature immunology* **6**, 1123-1132.
- Heinrich PC, Behrmann I, Haan S, Hermanns HM, Muller-Newen G & Schaper F. (2003). Principles of interleukin (IL)-6-type cytokine signalling and its regulation. *The Biochemical journal* **374**, 1-20.
- Henry CJ, Huang Y, Wynne AM & Godbout JP. (2009). Peripheral lipopolysaccharide (LPS) challenge promotes microglial hyperactivity in aged mice that is associated with exaggerated induction of both pro-inflammatory IL-1beta and anti-inflammatory IL-10 cytokines. *Brain, behavior, and immunity* **23**, 309-317.
- Herber DL, Mercer M, Roth LM, Symmonds K, Maloney J, Wilson N, Freeman MJ, Morgan D & Gordon MN. (2007). Microglial activation is required for Abeta clearance after intracranial injection of lipopolysaccharide in APP transgenic mice. *Journal of neuroimmune pharmacology : the official journal of the Society on NeuroImmune Pharmacology* **2**, 222-231.
- Hickey WF. (2001). Basic principles of immunological surveillance of the normal central nervous system. *Glia* **36**, 118-124.
- Higgins GA & Jacobsen H. (2003). Transgenic mouse models of Alzheimer's disease: phenotype and application. *Behavioural pharmacology* **14**, 419-438.
- Hoek RM, Ruuls SR, Murphy CA, Wright GJ, Goddard R, Zurawski SM, Blom B, Homola ME, Streit WJ, Brown MH, Barclay AN & Sedgwick JD. (2000). Down-regulation of the macrophage lineage through interaction with OX2 (CD200). *Science* **290**, 1768-1771.
- Hoey S, Grabowski PS, Ralston SH, Forrester JV & Liversidge J. (1997). Nitric oxide accelerates the onset and increases the severity of experimental autoimmune uveoretinitis through an IFN-gamma-dependent mechanism. *J Immunol* **159**, 5132-5142.
- Holcomb L, Gordon MN, McGowan E, Yu X, Benkovic S, Jantzen P, Wright K, Saad I, Mueller R, Morgan D, Sanders S, Zehr C, O'Campo K, Hardy J, Prada CM, Eckman C, Younkin S, Hsiao K & Duff K. (1998). Accelerated Alzheimer-type phenotype in transgenic mice carrying both mutant amyloid precursor protein and presenilin 1 transgenes. *Nature medicine* **4**, 97-100.
- Hoyer BF, Manz RA, Radbruch A & Hiepe F. (2005). Long-lived plasma cells and their contribution to autoimmunity. *Annals of the New York Academy of Sciences* **1050**, 124-133.
- Hsiao HY, Mak OT, Yang CS, Liu YP, Fang KM & Tzeng SF. (2007). TNF-alpha/IFN-gamma-induced iNOS expression increased by prostaglandin E2 in rat primary astrocytes via EP2-evoked cAMP/PKA and intracellular calcium signaling. *Glia* **55**, 214-223.

- Hsiao K, Chapman P, Nilsen S, Eckman C, Harigaya Y, Younkin S, Yang F & Cole G. (1996). Correlative memory deficits, Abeta elevation, and amyloid plaques in transgenic mice. *Science* **274**, 99-102.
- Hua F, Ma J, Ha T, Kelley J, Williams DL, Kao RL, Kalbfleisch JH, Browder IW & Li C. (2008). Preconditioning with a TLR2 specific ligand increases resistance to cerebral ischemia/reperfusion injury. *Journal of neuroimmunology* **199**, 75-82.
- Huang JF, Yang Y, Sepulveda H, Shi W, Hwang I, Peterson PA, Jackson MR, Sprent J & Cai Z. (1999). TCR-Mediated internalization of peptide-MHC complexes acquired by T cells. *Science* **286**, 952-954.
- Huberman M, Shalit F, Roth-Deri I, Gutman B, Brodie C, Kott E & Sredni B. (1994). Correlation of cytokine secretion by mononuclear cells of Alzheimer patients and their disease stage. *Journal of neuroimmunology* **52**, 147-152.
- Ishizuka K, Kimura T, Igata-yi R, Katsuragi S, Takamatsu J & Miyakawa T. (1997). Identification of monocyte chemoattractant protein-1 in senile plaques and reactive microglia of Alzheimer's disease. *Psychiatry and clinical neurosciences* **51**, 135-138.
- Itagaki S, McGeer PL, Akiyama H, Zhu S & Selkoe D. (1989). Relationship of microglia and astrocytes to amyloid deposits of Alzheimer disease. *Journal of neuroimmunology* **24**, 173-182.
- Jack CS, Arbour N, Manusow J, Montgrain V, Blain M, McCrea E, Shapiro A & Antel JP. (2005). TLR signaling tailors innate immune responses in human microglia and astrocytes. *J Immunol* **175**, 4320-4330.
- Jana M, Palencia CA & Pahan K. (2008). Fibrillar amyloid-beta peptides activate microglia via TLR2: implications for Alzheimer's disease. *J Immunol* **181**, 7254-7262.
- Jankowsky JL, Slunt HH, Ratovitski T, Jenkins NA, Copeland NG & Borchelt DR. (2001). Co-expression of multiple transgenes in mouse CNS: a comparison of strategies. *Biomolecular engineering* **17**, 157-165.
- Janus C, Pearson J, McLaurin J, Mathews PM, Jiang Y, Schmidt SD, Chishti MA, Horne P, Heslin D, French J, Mount HT, Nixon RA, Mercken M, Bergeron C, Fraser PE, St George-Hyslop P & Westaway D. (2000). A beta peptide immunization reduces behavioural impairment and plaques in a model of Alzheimer's disease. *Nature* **408**, 979-982.
- Jenmalm MC, Cherwinski H, Bowman EP, Phillips JH & Sedgwick JD. (2006). Regulation of myeloid cell function through the CD200 receptor. *J Immunol* **176**, 191-199.
- Kaiko GE, Horvat JC, Beagley KW & Hansbro PM. (2008). Immunological decision-making: how does the immune system decide to mount a helper T-cell response? *Immunology* **123**, 326-338.
- Karpus WJ & Kennedy KJ. (1997). MIP-1alpha and MCP-1 differentially regulate acute and relapsing autoimmune encephalomyelitis as well as Th1/Th2 lymphocyte differentiation. *Journal of leukocyte biology* **62**, 681-687.

- Karran E, Mercken M & De Strooper B. (2011). The amyloid cascade hypothesis for Alzheimer's disease: an appraisal for the development of therapeutics. *Nature reviews Drug discovery* **10**, 698-712.
- Kebir H, Kreymborg K, Ifergan I, Dodelet-Devillers A, Cayrol R, Bernard M, Giuliani F, Arbour N, Becher B & Prat A. (2007). Human TH17 lymphocytes promote blood-brain barrier disruption and central nervous system inflammation. *Nature medicine* **13**, 1173-1175.
- Kielian T. (2006). Toll-like receptors in central nervous system glial inflammation and homeostasis. *Journal of neuroscience research* **83**, 711-730.
- Kielian T, Barry B & Hickey WF. (2001). CXC chemokine receptor-2 ligands are required for neutrophil-mediated host defense in experimental brain abscesses. *J Immunol* **166**, 4634-4643.
- Kielian T, Mayes P & Kielian M. (2002). Characterization of microglial responses to *Staphylococcus aureus*: effects on cytokine, costimulatory molecule, and Toll-like receptor expression. *Journal of neuroimmunology* **130**, 86-99.
- Kim TS, Lim HK, Lee JY, Kim DJ, Park S, Lee C & Lee CU. (2008). Changes in the levels of plasma soluble fractalkine in patients with mild cognitive impairment and Alzheimer's disease. *Neuroscience letters* **436**, 196-200.
- Koenigsknecht-Talboo J & Landreth GE. (2005). Microglial phagocytosis induced by fibrillar beta-amyloid and IgGs are differentially regulated by proinflammatory cytokines. *The Journal of neuroscience : the official journal of the Society for Neuroscience* **25**, 8240-8249.
- Koenigsknecht J & Landreth G. (2004). Microglial phagocytosis of fibrillar beta-amyloid through a beta1 integrin-dependent mechanism. *The Journal of neuroscience : the official journal of the Society for Neuroscience* **24**, 9838-9846.
- Koning N, Bo L, Hoek RM & Huitinga I. (2007). Downregulation of macrophage inhibitory molecules in multiple sclerosis lesions. *Annals of neurology* **62**, 504-514.
- Koning N, Swaab DF, Hoek RM & Huitinga I. (2009). Distribution of the immune inhibitory molecules CD200 and CD200R in the normal central nervous system and multiple sclerosis lesions suggests neuron-glia and glia-glia interactions. *Journal of neuropathology and experimental neurology* **68**, 159-167.
- Korn T, Bettelli E, Oukka M & Kuchroo VK. (2009). IL-17 and Th17 Cells. *Annual review of immunology* **27**, 485-517.
- Kreutzberg GW. (1996). Microglia: a sensor for pathological events in the CNS. *Trends in neurosciences* **19**, 312-318.
- Kroenke MA, Carlson TJ, Andjelkovic AV & Segal BM. (2008). IL-12- and IL-23-modulated T cells induce distinct types of EAE based on histology, CNS chemokine profile, and response to cytokine inhibition. *The Journal of experimental medicine* **205**, 1535-1541.
- Laflamme N, Soucy G & Rivest S. (2001). Circulating cell wall components derived from gram-negative, not gram-positive, bacteria cause a profound induction of the

- gene-encoding Toll-like receptor 2 in the CNS. *Journal of neurochemistry* **79**, 648-657.
- Landreth GE & Reed-Geaghan EG. (2009). Toll-like receptors in Alzheimer's disease. *Current topics in microbiology and immunology* **336**, 137-153.
- Langrish CL, Chen Y, Blumenschein WM, Mattson J, Basham B, Sedgwick JD, McClanahan T, Kastelein RA & Cua DJ. (2005). IL-23 drives a pathogenic T cell population that induces autoimmune inflammation. *The Journal of experimental medicine* **201**, 233-240.
- Lawrence DM, Seth P, Durham L, Diaz F, Boursiquot R, Ransohoff RM & Major EO. (2006). Astrocyte differentiation selectively upregulates CCL2/monocyte chemoattractant protein-1 in cultured human brain-derived progenitor cells. *Glia* **53**, 81-91.
- Lawson LJ, Perry VH, Dri P & Gordon S. (1990). Heterogeneity in the distribution and morphology of microglia in the normal adult mouse brain. *Neuroscience* **39**, 151-170.
- Letiembre M, Liu Y, Walter S, Hao W, Pfander T, Wrede A, Schulz-Schaeffer W & Fassbender K. (2009). Screening of innate immune receptors in neurodegenerative diseases: a similar pattern. *Neurobiology of aging* **30**, 759-768.
- Li M, Pisalyaput K, Galvan M & Tenner AJ. (2004). Macrophage colony stimulatory factor and interferon-gamma trigger distinct mechanisms for augmentation of beta-amyloid-induced microglia-mediated neurotoxicity. *Journal of neurochemistry* **91**, 623-633.
- Li M, Shang DS, Zhao WD, Tian L, Li B, Fang WG, Zhu L, Man SM & Chen YH. (2009). Amyloid beta interaction with receptor for advanced glycation end products up-regulates brain endothelial CCR5 expression and promotes T cells crossing the blood-brain barrier. *J Immunol* **182**, 5778-5788.
- Liang X, Wang Q, Hand T, Wu L, Breyer RM, Montine TJ & Andreasson K. (2005). Deletion of the prostaglandin E2 EP2 receptor reduces oxidative damage and amyloid burden in a model of Alzheimer's disease. *The Journal of neuroscience : the official journal of the Society for Neuroscience* **25**, 10180-10187.
- Liu J, Marino MW, Wong G, Grail D, Dunn A, Bettadapura J, Slavin AJ, Old L & Bernard CC. (1998). TNF is a potent anti-inflammatory cytokine in autoimmune-mediated demyelination. *Nature medicine* **4**, 78-83.
- Liu S, Liu Y, Hao W, Wolf L, Kiliaan AJ, Penke B, Rube CE, Walter J, Heneka MT, Hartmann T, Menger MD & Fassbender K. (2012). TLR2 is a primary receptor for Alzheimer's amyloid beta peptide to trigger neuroinflammatory activation. *J Immunol* **188**, 1098-1107.
- Liu Y, Walter S, Stagi M, Cherny D, Letiembre M, Schulz-Schaeffer W, Heine H, Penke B, Neumann H & Fassbender K. (2005). LPS receptor (CD14): a receptor for phagocytosis of Alzheimer's amyloid peptide. *Brain : a journal of neurology* **128**, 1778-1789.

- Lombardi VR, Fernandez-Novoa L, Etcheverria I, Seoane S & Cacabelos R. (2004). Association between APOE epsilon4 allele and increased expression of CD95 on T cells from patients with Alzheimer's disease. *Methods and findings in experimental and clinical pharmacology* **26**, 523-529.
- Lue LF, Rydel R, Brigham EF, Yang LB, Hampel H, Murphy GM, Jr., Brachova L, Yan SD, Walker DG, Shen Y & Rogers J. (2001a). Inflammatory repertoire of Alzheimer's disease and nondemented elderly microglia in vitro. *Glia* **35**, 72-79.
- Lue LF, Walker DG & Rogers J. (2001b). Modeling microglial activation in Alzheimer's disease with human post-mortem microglial cultures. *Neurobiology of aging* **22**, 945-956.
- Lynch AM, Loane DJ, Minogue AM, Clarke RM, Kilroy D, Nally RE, Roche OJ, O'Connell F & Lynch MA. (2007). Eicosapentaenoic acid confers neuroprotection in the amyloid-beta challenged aged hippocampus. *Neurobiology of aging* **28**, 845-855.
- Lynch MA. (2009). The multifaceted profile of activated microglia. *Molecular neurobiology* **40**, 139-156.
- Lyons A, Downer EJ, Crotty S, Nolan YM, Mills KH & Lynch MA. (2007). CD200 ligand receptor interaction modulates microglial activation in vivo and in vitro: a role for IL-4. *The Journal of neuroscience : the official journal of the Society for Neuroscience* **27**, 8309-8313.
- Lyons A, Lynch AM, Downer EJ, Hanley R, O'Sullivan JB, Smith A & Lynch MA. (2009a). Fractalkine-induced activation of the phosphatidylinositol-3 kinase pathway attenuates microglial activation in vivo and in vitro. *Journal of neurochemistry* **110**, 1547-1556.
- Lyons A, McQuillan K, Deighan BF, O'Reilly JA, Downer EJ, Murphy AC, Watson M, Piazza A, O'Connell F, Griffin R, Mills KH & Lynch MA. (2009b). Decreased neuronal CD200 expression in IL-4-deficient mice results in increased neuroinflammation in response to lipopolysaccharide. *Brain, behavior, and immunity* **23**, 1020-1027.
- Ma X, Reynolds SL, Baker BJ, Li X, Benveniste EN & Qin H. (2010). IL-17 enhancement of the IL-6 signaling cascade in astrocytes. *J Immunol* **184**, 4898-4906.
- Mahad D, Callahan MK, Williams KA, Ubogu EE, Kivisakk P, Tucky B, Kidd G, Kingsbury GA, Chang A, Fox RJ, Mack M, Sniderman MB, Ravid R, Staugaitis SM, Stins MF & Ransohoff RM. (2006). Modulating CCR2 and CCL2 at the blood-brain barrier: relevance for multiple sclerosis pathogenesis. *Brain : a journal of neurology* **129**, 212-223.
- Maini R, St Clair EW, Breedveld F, Furst D, Kalden J, Weisman M, Smolen J, Emery P, Harriman G, Feldmann M & Lipsky P. (1999). Infliximab (chimeric anti-tumour necrosis factor alpha monoclonal antibody) versus placebo in rheumatoid arthritis patients receiving concomitant methotrexate: a randomised phase III trial. ATTRACT Study Group. *Lancet* **354**, 1932-1939.

- Masocha W. (2009). Systemic lipopolysaccharide (LPS)-induced microglial activation results in different temporal reduction of CD200 and CD200 receptor gene expression in the brain. *Journal of neuroimmunology* **214**, 78-82.
- McGeer EG & McGeer PL. (2003). Inflammatory processes in Alzheimer's disease. *Progress in neuro-psychopharmacology & biological psychiatry* **27**, 741-749.
- McGeer PL, Itagaki S, Tago H & McGeer EG. (1987). Reactive microglia in patients with senile dementia of the Alzheimer type are positive for the histocompatibility glycoprotein HLA-DR. *Neuroscience letters* **79**, 195-200.
- McGeer PL, Kawamata T, Walker DG, Akiyama H, Tooyama I & McGeer EG. (1993). Microglia in degenerative neurological disease. *Glia* **7**, 84-92.
- McGeer PL & McGeer EG. (2001). Inflammation, autotoxicity and Alzheimer disease. *Neurobiology of aging* **22**, 799-809.
- McManus C, Berman JW, Brett FM, Staunton H, Farrell M & Brosnan CF. (1998). MCP-1, MCP-2 and MCP-3 expression in multiple sclerosis lesions: an immunohistochemical and in situ hybridization study. *Journal of neuroimmunology* **86**, 20-29.
- McManus CM, Weidenheim K, Woodman SE, Nunez J, Hesselgesser J, Nath A & Berman JW. (2000). Chemokine and chemokine-receptor expression in human glial elements: induction by the HIV protein, Tat, and chemokine autoregulation. *The American journal of pathology* **156**, 1441-1453.
- McQuillan K, Lynch MA & Mills KH. (2010). Activation of mixed glia by Abeta-specific Th1 and Th17 cells and its regulation by Th2 cells. *Brain, behavior, and immunity* **24**, 598-607.
- Meda L, Cassatella MA, Szendrei GI, Otvos L, Jr., Baron P, Villalba M, Ferrari D & Rossi F. (1995). Activation of microglial cells by beta-amyloid protein and interferon-gamma. *Nature* **374**, 647-650.
- Medawar PB. (1948). Immunity to homologous grafted skin; the fate of skin homografts transplanted to the brain, to subcutaneous tissue, and to the anterior chamber of the eye. *British journal of experimental pathology* **29**, 58-69.
- Medzhitov R & Janeway CA, Jr. (1997). Innate immunity: the virtues of a nonclonal system of recognition. *Cell* **91**, 295-298.
- Melchior B, Puntambekar SS & Carson MJ. (2006). Microglia and the control of autoreactive T cell responses. *Neurochemistry international* **49**, 145-153.
- Mennicken F, Maki R, de Souza EB & Quirion R. (1999). Chemokines and chemokine receptors in the CNS: a possible role in neuroinflammation and patterning. *Trends in pharmacological sciences* **20**, 73-78.
- Meuth SG, Simon OJ, Grimm A, Melzer N, Herrmann AM, Spitzer P, Landgraf P & Wiendl H. (2008). CNS inflammation and neuronal degeneration is aggravated by impaired CD200-CD200R-mediated macrophage silencing. *Journal of neuroimmunology* **194**, 62-69.

- Mihrshahi R, Barclay AN & Brown MH. (2009). Essential roles for Dok2 and RasGAP in CD200 receptor-mediated regulation of human myeloid cells. *J Immunol* **183**, 4879-4886.
- Mihrshahi R & Brown MH. (2010). Downstream of tyrosine kinase 1 and 2 play opposing roles in CD200 receptor signaling. *J Immunol* **185**, 7216-7222.
- Mills KH. (2008). Induction, function and regulation of IL-17-producing T cells. *European journal of immunology* **38**, 2636-2649.
- Mills KH & Dunne A. (2009). Immune modulation: IL-1, master mediator or initiator of inflammation. *Nature medicine* **15**, 1363-1364.
- Milner R & Campbell IL. (2003). The extracellular matrix and cytokines regulate microglial integrin expression and activation. *J Immunol* **170**, 3850-3858.
- Minagar A, Shapshak P, Fujimura R, Ownby R, Heyes M & Eisdorfer C. (2002). The role of macrophage/microglia and astrocytes in the pathogenesis of three neurologic disorders: HIV-associated dementia, Alzheimer disease, and multiple sclerosis. *Journal of the neurological sciences* **202**, 13-23.
- Minas K & Liversidge J. (2006). Is the CD200/CD200 receptor interaction more than just a myeloid cell inhibitory signal? *Critical reviews in immunology* **26**, 213-230.
- Mir M, Tolosa L, Asensio VJ, Llado J & Olmos G. (2008). Complementary roles of tumor necrosis factor alpha and interferon gamma in inducible microglial nitric oxide generation. *Journal of neuroimmunology* **204**, 101-109.
- Monsonogo A, Maron R, Zota V, Selkoe DJ & Weiner HL. (2001). Immune hyporesponsiveness to amyloid beta-peptide in amyloid precursor protein transgenic mice: implications for the pathogenesis and treatment of Alzheimer's disease. *Proceedings of the National Academy of Sciences of the United States of America* **98**, 10273-10278.
- Monsonogo A, Zota V, Karni A, Krieger JI, Bar-Or A, Bitan G, Budson AE, Sperling R, Selkoe DJ & Weiner HL. (2003). Increased T cell reactivity to amyloid beta protein in older humans and patients with Alzheimer disease. *The Journal of clinical investigation* **112**, 415-422.
- Moore S & Thanos S. (1996). The concept of microglia in relation to central nervous system disease and regeneration. *Progress in neurobiology* **48**, 441-460.
- Moreland LW, Schiff MH, Baumgartner SW, Tindall EA, Fleischmann RM, Bulpitt KJ, Weaver AL, Keystone EC, Furst DE, Mease PJ, Ruderman EM, Horwitz DA, Arkfeld DG, Garrison L, Burge DJ, Blosch CM, Lange ML, McDonnell ND & Weinblatt ME. (1999). Etanercept therapy in rheumatoid arthritis. A randomized, controlled trial. *Annals of internal medicine* **130**, 478-486.
- Morgan D, Diamond DM, Gottschall PE, Ugen KE, Dickey C, Hardy J, Duff K, Jantzen P, DiCarlo G, Wilcock D, Connor K, Hatcher J, Hope C, Gordon M & Arendash GW. (2000). A beta peptide vaccination prevents memory loss in an animal model of Alzheimer's disease. *Nature* **408**, 982-985.
- Morgan D, Gordon MN, Tan J, Wilcock D & Rojiani AM. (2005). Dynamic complexity of the microglial activation response in transgenic models of amyloid deposition:

- implications for Alzheimer therapeutics. *Journal of neuropathology and experimental neurology* **64**, 743-753.
- Mosmann TR, Cherwinski H, Bond MW, Giedlin MA & Coffman RL. (1986). Two types of murine helper T cell clone. I. Definition according to profiles of lymphokine activities and secreted proteins. *J Immunol* **136**, 2348-2357.
- Mosmann TR & Sad S. (1996). The expanding universe of T-cell subsets: Th1, Th2 and more. *Immunology today* **17**, 138-146.
- Mrak RE. (2012). Microglia in Alzheimer brain: a neuropathological perspective. *International journal of Alzheimer's disease* **2012**, 165021.
- Muehlhauser F, Liebl U, Kuehl S, Walter S, Bertsch T & Fassbender K. (2001). Aggregation-Dependent interaction of the Alzheimer's beta-amyloid and microglia. *Clinical chemistry and laboratory medicine : CCLM/ FESCC* **39**, 313-316.
- Mukhopadhyay S, Pluddemann A, Hoe JC, Williams KJ, Varin A, Makepeace K, Akin ML, Bowdish DM, Smale ST, Barclay AN & Gordon S. (2010). Immune inhibitory ligand CD200 induction by TLRs and NLRs limits macrophage activation to protect the host from meningococcal septicemia. *Cell host & microbe* **8**, 236-247.
- Murphy AC, Lalor SJ, Lynch MA & Mills KH. (2010). Infiltration of Th1 and Th17 cells and activation of microglia in the CNS during the course of experimental autoimmune encephalomyelitis. *Brain, behavior, and immunity* **24**, 641-651.
- Murray CA & Lynch MA. (1998). Evidence that increased hippocampal expression of the cytokine interleukin-1 beta is a common trigger for age- and stress-induced impairments in long-term potentiation. *The Journal of neuroscience : the official journal of the Society for Neuroscience* **18**, 2974-2981.
- Nagele RG, Wegiel J, Venkataraman V, Imaki H & Wang KC. (2004). Contribution of glial cells to the development of amyloid plaques in Alzheimer's disease. *Neurobiology of aging* **25**, 663-674.
- Nathan C, Calingasan N, Nezezon J, Ding A, Lucia MS, La Perle K, Fuortes M, Lin M, Ehrt S, Kwon NS, Chen J, Vodovotz Y, Kipiani K & Beal MF. (2005). Protection from Alzheimer's-like disease in the mouse by genetic ablation of inducible nitric oxide synthase. *The Journal of experimental medicine* **202**, 1163-1169.
- Nathan C & Muller WA. (2001). Putting the brakes on innate immunity: a regulatory role for CD200? *Nature immunology* **2**, 17-19.
- Nguyen KT, Deak T, Owens SM, Kohno T, Fleshner M, Watkins LR & Maier SF. (1998). Exposure to acute stress induces brain interleukin-1beta protein in the rat. *The Journal of neuroscience : the official journal of the Society for Neuroscience* **18**, 2239-2246.
- Nguyen VT & Benveniste EN. (2000). IL-4-activated STAT-6 inhibits IFN-gamma-induced CD40 gene expression in macrophages/microglia. *J Immunol* **165**, 6235-6243.

- Nicoll JA, Wilkinson D, Holmes C, Steart P, Markham H & Weller RO. (2003). Neuropathology of human Alzheimer disease after immunization with amyloid-beta peptide: a case report. *Nature medicine* **9**, 448-452.
- O'Connor KA, Johnson JD, Hansen MK, Wieseler Frank JL, Maksimova E, Watkins LR & Maier SF. (2003). Peripheral and central proinflammatory cytokine response to a severe acute stressor. *Brain research* **991**, 123-132.
- O'Garra A. (1998). Cytokines induce the development of functionally heterogeneous T helper cell subsets. *Immunity* **8**, 275-283.
- O'Neill LA. (2008). The interleukin-1 receptor/Toll-like receptor superfamily: 10 years of progress. *Immunological reviews* **226**, 10-18.
- O'Neill LA, Bryant CE & Doyle SL. (2009). Therapeutic targeting of Toll-like receptors for infectious and inflammatory diseases and cancer. *Pharmacological reviews* **61**, 177-197.
- Ohno M, Sametsky EA, Younkin LH, Oakley H, Younkin SG, Citron M, Vassar R & Disterhoft JF. (2004). BACE1 deficiency rescues memory deficits and cholinergic dysfunction in a mouse model of Alzheimer's disease. *Neuron* **41**, 27-33.
- Okun E, Griffioen KJ, Lathia JD, Tang SC, Mattson MP & Arumugam TV. (2009). Toll-like receptors in neurodegeneration. *Brain research reviews* **59**, 278-292.
- Olson JK & Miller SD. (2004). Microglia initiate central nervous system innate and adaptive immune responses through multiple TLRs. *J Immunol* **173**, 3916-3924.
- Orgogozo JM, Gilman S, Dartigues JF, Laurent B, Puel M, Kirby LC, Jouanny P, Dubois B, Eisner L, Flitman S, Michel BF, Boada M, Frank A & Hock C. (2003). Subacute meningoencephalitis in a subset of patients with AD after Abeta42 immunization. *Neurology* **61**, 46-54.
- Owens T, Babcock AA, Millward JM & Toft-Hansen H. (2005). Cytokine and chemokine inter-regulation in the inflamed or injured CNS. *Brain research Brain research reviews* **48**, 178-184.
- Ozinsky A, Underhill DM, Fontenot JD, Hajjar AM, Smith KD, Wilson CB, Schroeder L & Aderem A. (2000). The repertoire for pattern recognition of pathogens by the innate immune system is defined by cooperation between toll-like receptors. *Proceedings of the National Academy of Sciences of the United States of America* **97**, 13766-13771.
- Palm NW & Medzhitov R. (2009). Pattern recognition receptors and control of adaptive immunity. *Immunological reviews* **227**, 221-233.
- Pandey S & Agrawal DK. (2006). Immunobiology of Toll-like receptors: emerging trends. *Immunology and cell biology* **84**, 333-341.
- Park H, Li Z, Yang XO, Chang SH, Nurieva R, Wang YH, Wang Y, Hood L, Zhu Z, Tian Q & Dong C. (2005). A distinct lineage of CD4 T cells regulates tissue inflammation by producing interleukin 17. *Nature immunology* **6**, 1133-1141.

- Parvathy S, Rajadas J, Ryan H, Vaziri S, Anderson L & Murphy GM, Jr. (2009). Abeta peptide conformation determines uptake and interleukin-1alpha expression by primary microglial cells. *Neurobiology of aging* **30**, 1792-1804.
- Pfeifer M, Boncristiano S, Bondolfi L, Stalder A, Deller T, Staufenbiel M, Mathews PM & Jucker M. (2002). Cerebral hemorrhage after passive anti-Abeta immunotherapy. *Science* **298**, 1379.
- Prat A, Biernacki K, Wosik K & Antel JP. (2001). Glial cell influence on the human blood-brain barrier. *Glia* **36**, 145-155.
- Prinz M, Garbe F, Schmidt H, Mildner A, Gutcher I, Wolter K, Piesche M, Schroers R, Weiss E, Kirschning CJ, Rochford CD, Bruck W & Becher B. (2006). Innate immunity mediated by TLR9 modulates pathogenicity in an animal model of multiple sclerosis. *The Journal of clinical investigation* **116**, 456-464.
- Probert L, Eugster HP, Akassoglou K, Bauer J, Frei K, Lassmann H & Fontana A. (2000). TNFR1 signalling is critical for the development of demyelination and the limitation of T-cell responses during immune-mediated CNS disease. *Brain : a journal of neurology* **123 (Pt 10)**, 2005-2019.
- Proudfoot AE. (2002). Chemokine receptors: multifaceted therapeutic targets. *Nature reviews Immunology* **2**, 106-115.
- Qin S, Rottman JB, Myers P, Kassam N, Weinblatt M, Loetscher M, Koch AE, Moser B & Mackay CR. (1998). The chemokine receptors CXCR3 and CCR5 mark subsets of T cells associated with certain inflammatory reactions. *The Journal of clinical investigation* **101**, 746-754.
- Querfurth HW & LaFerla FM. (2010). Alzheimer's disease. *The New England journal of medicine* **362**, 329-344.
- Quillan KM. (2009). The role of T cells in the pathogenesis and prevention of the inflammatory and neurodegenerative changes associated with Alzheimer's disease. *PhD thesis*.
- Ransohoff RM, Kivisakk P & Kidd G. (2003). Three or more routes for leukocyte migration into the central nervous system. *Nature reviews Immunology* **3**, 569-581.
- Ransohoff RM & Perry VH. (2009). Microglial physiology: unique stimuli, specialized responses. *Annual review of immunology* **27**, 119-145.
- Reed-Geaghan EG, Savage JC, Hise AG & Landreth GE. (2009). CD14 and toll-like receptors 2 and 4 are required for fibrillar A{beta}-stimulated microglial activation. *The Journal of neuroscience : the official journal of the Society for Neuroscience* **29**, 11982-11992.
- Ribes S, Ebert S, Regen T, Czesnik D, Scheffel J, Zeug A, Bunkowski S, Eiffert H, Hanisch UK, Hammerschmidt S & Nau R. (2010). Fibronectin stimulates Escherichia coli phagocytosis by microglial cells. *Glia* **58**, 367-376.
- Richard KL, Filali M, Prefontaine P & Rivest S. (2008). Toll-like receptor 2 acts as a natural innate immune receptor to clear amyloid beta 1-42 and delay the

- cognitive decline in a mouse model of Alzheimer's disease. *The Journal of neuroscience : the official journal of the Society for Neuroscience* **28**, 5784-5793.
- Rogers J, Lubner-Narod J, Styren SD & Civin WH. (1988). Expression of immune system-associated antigens by cells of the human central nervous system: relationship to the pathology of Alzheimer's disease. *Neurobiology of aging* **9**, 339-349.
- Roy A, Jana A, Yatish K, Freidt MB, Fung YK, Martinson JA & Pahan K. (2008). Reactive oxygen species up-regulate CD11b in microglia via nitric oxide: Implications for neurodegenerative diseases. *Free radical biology & medicine* **45**, 686-699.
- Sastre M, Walter J & Gentleman SM. (2008). Interactions between APP secretases and inflammatory mediators. *Journal of neuroinflammation* **5**, 25.
- Sawada M, Imamura K & Nagatsu T. (2006). Role of cytokines in inflammatory process in Parkinson's disease. *Journal of neural transmission Supplementum*, 373-381.
- Schenk D, Barbour R, Dunn W, Gordon G, Grajeda H, Guido T, Hu K, Huang J, Johnson-Wood K, Khan K, Kholodenko D, Lee M, Liao Z, Lieberburg I, Motter R, Mutter L, Soriano F, Shopp G, Vasquez N, Vandeventer C, Walker S, Wogulis M, Yednock T, Games D & Seubert P. (1999). Immunization with amyloid-beta attenuates Alzheimer-disease-like pathology in the PDAPP mouse. *Nature* **400**, 173-177.
- Schindowski K, Eckert A, Peters J, Gorriz C, Schramm U, Weinandi T, Maurer K, Frolich L & Muller WE. (2007). Increased T-cell reactivity and elevated levels of CD8+ memory T-cells in Alzheimer's disease-patients and T-cell hyporeactivity in an Alzheimer's disease-mouse model: implications for immunotherapy. *Neuromolecular medicine* **9**, 340-354.
- Schluns KS & Lefrancois L. (2003). Cytokine control of memory T-cell development and survival. *Nature reviews Immunology* **3**, 269-279.
- Seguin R, Biernacki K, Prat A, Wosik K, Kim HJ, Blain M, McCrea E, Bar-Or A & Antel JP. (2003). Differential effects of Th1 and Th2 lymphocyte supernatants on human microglia. *Glia* **42**, 36-45.
- Shah VB, Williams DL & Keshvara L. (2009). beta-Glucan attenuates TLR2- and TLR4-mediated cytokine production by microglia. *Neuroscience letters* **458**, 111-115.
- Sharief MK & Hentges R. (1991). Association between tumor necrosis factor-alpha and disease progression in patients with multiple sclerosis. *The New England journal of medicine* **325**, 467-472.
- Sharpe AH & Freeman GJ. (2002). The B7-CD28 superfamily. *Nature reviews Immunology* **2**, 116-126.
- Shrikant P & Benveniste EN. (1996). The central nervous system as an immunocompetent organ: role of glial cells in antigen presentation. *J Immunol* **157**, 1819-1822.
- Simpson JE, Newcombe J, Cuzner ML & Woodroffe MN. (1998). Expression of monocyte chemoattractant protein-1 and other beta-chemokines by resident glia

- and inflammatory cells in multiple sclerosis lesions. *Journal of neuroimmunology* **84**, 238-249.
- Siveke JT & Hamann A. (1998). T helper 1 and T helper 2 cells respond differentially to chemokines. *J Immunol* **160**, 550-554.
- Smorodchenko A, Wuerfel J, Pohl EE, Vogt J, Tysiak E, Glumm R, Hendrix S, Nitsch R, Zipp F & Infante-Duarte C. (2007). CNS-irrelevant T-cells enter the brain, cause blood-brain barrier disruption but no glial pathology. *The European journal of neuroscience* **26**, 1387-1398.
- Snelgrove RJ, Goulding J, Didierlaurent AM, Lyonga D, Vekaria S, Edwards L, Gwyer E, Sedgwick JD, Barclay AN & Hussels T. (2008). A critical function for CD200 in lung immune homeostasis and the severity of influenza infection. *Nature immunology* **9**, 1074-1083.
- Sorensen TL, Tani M, Jensen J, Pierce V, Lucchinetti C, Folcik VA, Qin S, Rottman J, Sellebjerg F, Strieter RM, Frederiksen JL & Ransohoff RM. (1999). Expression of specific chemokines and chemokine receptors in the central nervous system of multiple sclerosis patients. *The Journal of clinical investigation* **103**, 807-815.
- Stalder AK, Ermini F, Bondolfi L, Krenger W, Burbach GJ, Deller T, Coomaraswamy J, Staufenbiel M, Landmann R & Jucker M. (2005). Invasion of hematopoietic cells into the brain of amyloid precursor protein transgenic mice. *The Journal of neuroscience : the official journal of the Society for Neuroscience* **25**, 11125-11132.
- Stalder M, Deller T, Staufenbiel M & Jucker M. (2001). 3D-Reconstruction of microglia and amyloid in APP23 transgenic mice: no evidence of intracellular amyloid. *Neurobiology of aging* **22**, 427-434.
- Stichel CC & Luebbert H. (2007). Inflammatory processes in the aging mouse brain: participation of dendritic cells and T-cells. *Neurobiology of aging* **28**, 1507-1521.
- Streit WJ. (2005). Microglia and neuroprotection: implications for Alzheimer's disease. *Brain research Brain research reviews* **48**, 234-239.
- Sutton C, Brereton C, Keogh B, Mills KH & Lavelle EC. (2006). A crucial role for interleukin (IL)-1 in the induction of IL-17-producing T cells that mediate autoimmune encephalomyelitis. *The Journal of experimental medicine* **203**, 1685-1691.
- Szczepanik AM, Funes S, Petko W & Ringheim GE. (2001). IL-4, IL-10 and IL-13 modulate A beta(1-42)-induced cytokine and chemokine production in primary murine microglia and a human monocyte cell line. *Journal of neuroimmunology* **113**, 49-62.
- Szelenyi J. (2001). Cytokines and the central nervous system. *Brain research bulletin* **54**, 329-338.
- Tahara K, Kim HD, Jin JJ, Maxwell JA, Li L & Fukuchi K. (2006). Role of toll-like receptor signalling in Aβ uptake and clearance. *Brain : a journal of neurology* **129**, 3006-3019.
- Takeda K & Akira S. (2004). TLR signaling pathways. *Seminars in immunology* **16**, 3-9.

- Takeda K, Takeuchi O & Akira S. (2002). Recognition of lipopeptides by Toll-like receptors. *Journal of endotoxin research* **8**, 459-463.
- Takeuchi O, Hoshino K, Kawai T, Sanjo H, Takada H, Ogawa T, Takeda K & Akira S. (1999). Differential roles of TLR2 and TLR4 in recognition of gram-negative and gram-positive bacterial cell wall components. *Immunity* **11**, 443-451.
- Tamagno E, Guglielmotto M, Aragno M, Borghi R, Autelli R, Giliberto L, Muraca G, Danni O, Zhu X, Smith MA, Perry G, Jo DG, Mattson MP & Tabaton M. (2008). Oxidative stress activates a positive feedback between the gamma- and beta-secretase cleavages of the beta-amyloid precursor protein. *Journal of neurochemistry* **104**, 683-695.
- Tan J, Town T, Abdullah L, Wu Y, Placzek A, Small B, Kroeger J, Crawford F, Richards D & Mullan M. (2002). CD45 isoform alteration in CD4+ T cells as a potential diagnostic marker of Alzheimer's disease. *Journal of neuroimmunology* **132**, 164-172.
- Tan J, Town T, Paris D, Mori T, Suo Z, Crawford F, Mattson MP, Flavell RA & Mullan M. (1999). Microglial activation resulting from CD40-CD40L interaction after beta-amyloid stimulation. *Science* **286**, 2352-2355.
- Thornton P, Pinteaux E, Gibson RM, Allan SM & Rothwell NJ. (2006). Interleukin-1-induced neurotoxicity is mediated by glia and requires caspase activation and free radical release. *Journal of neurochemistry* **98**, 258-266.
- Togo T, Akiyama H, Iseki E, Kondo H, Ikeda K, Kato M, Oda T, Tsuchiya K & Kosaka K. (2002). Occurrence of T cells in the brain of Alzheimer's disease and other neurological diseases. *Journal of neuroimmunology* **124**, 83-92.
- Town T, Tan J, Flavell RA & Mullan M. (2005). T-cells in Alzheimer's disease. *Neuromolecular medicine* **7**, 255-264.
- Townsend KP, Town T, Mori T, Lue LF, Shytle D, Sanberg PR, Morgan D, Fernandez F, Flavell RA & Tan J. (2005). CD40 signaling regulates innate and adaptive activation of microglia in response to amyloid beta-peptide. *European journal of immunology* **35**, 901-910.
- Tran EH, Kuziel WA & Owens T. (2000a). Induction of experimental autoimmune encephalomyelitis in C57BL/6 mice deficient in either the chemokine macrophage inflammatory protein-1alpha or its CCR5 receptor. *European journal of immunology* **30**, 1410-1415.
- Tran EH, Prince EN & Owens T. (2000b). IFN-gamma shapes immune invasion of the central nervous system via regulation of chemokines. *J Immunol* **164**, 2759-2768.
- Udan ML, Ajit D, Crouse NR & Nichols MR. (2008). Toll-like receptors 2 and 4 mediate Aβ(1-42) activation of the innate immune response in a human monocytic cell line. *Journal of neurochemistry* **104**, 524-533.
- Van Wagoner NJ & Benveniste EN. (1999). Interleukin-6 expression and regulation in astrocytes. *Journal of neuroimmunology* **100**, 124-139.

- Walker DG, Dalsing-Hernandez JE, Campbell NA & Lue LF. (2009). Decreased expression of CD200 and CD200 receptor in Alzheimer's disease: a potential mechanism leading to chronic inflammation. *Experimental neurology* **215**, 5-19.
- Walker DG, Kim SU & McGeer PL. (1995). Complement and cytokine gene expression in cultured microglial derived from post-mortem human brains. *Journal of neuroscience research* **40**, 478-493.
- Walsh DM & Selkoe DJ. (2007). A beta oligomers - a decade of discovery. *Journal of neurochemistry* **101**, 1172-1184.
- Walter S, Letiembre M, Liu Y, Heine H, Penke B, Hao W, Bode B, Manietta N, Walter J, Schulz-Schuffer W & Fassbender K. (2007). Role of the toll-like receptor 4 in neuroinflammation in Alzheimer's disease. *Cellular physiology and biochemistry : international journal of experimental cellular physiology, biochemistry, and pharmacology* **20**, 947-956.
- Wiessner C, Wiederhold KH, Tissot AC, Frey P, Danner S, Jacobson LH, Jennings GT, Luond R, Ortmann R, Reichwald J, Zurini M, Mir A, Bachmann MF & Staufenbiel M. (2011). The second-generation active Abeta immunotherapy CAD106 reduces amyloid accumulation in APP transgenic mice while minimizing potential side effects. *The Journal of neuroscience : the official journal of the Society for Neuroscience* **31**, 9323-9331.
- Wilcock DM, Rojiani A, Rosenthal A, Levkowitz G, Subbarao S, Alamed J, Wilson D, Wilson N, Freeman MJ, Gordon MN & Morgan D. (2004). Passive amyloid immunotherapy clears amyloid and transiently activates microglia in a transgenic mouse model of amyloid deposition. *The Journal of neuroscience : the official journal of the Society for Neuroscience* **24**, 6144-6151.
- Wilson EH, Weninger W & Hunter CA. (2010). Trafficking of immune cells in the central nervous system. *The Journal of clinical investigation* **120**, 1368-1379.
- Wolf SA, Gimsa U, Bechmann I & Nitsch R. (2001). Differential expression of costimulatory molecules B7-1 and B7-2 on microglial cells induced by Th1 and Th2 cells in organotypic brain tissue. *Glia* **36**, 414-420.
- Wright GJ, Puklavec MJ, Willis AC, Hoek RM, Sedgwick JD, Brown MH & Barclay AN. (2000). Lymphoid/neuronal cell surface OX2 glycoprotein recognizes a novel receptor on macrophages implicated in the control of their function. *Immunity* **13**, 233-242.
- Wyss-Coray T. (2006). Inflammation in Alzheimer disease: driving force, bystander or beneficial response? *Nature medicine* **12**, 1005-1015.
- Xia MQ, Bacskai BJ, Knowles RB, Qin SX & Hyman BT. (2000). Expression of the chemokine receptor CXCR3 on neurons and the elevated expression of its ligand IP-10 in reactive astrocytes: in vitro ERK1/2 activation and role in Alzheimer's disease. *Journal of neuroimmunology* **108**, 227-235.
- Xu J & Ling EA. (1995). Induction of major histocompatibility complex class II antigen on amoeboid microglial cells in early postnatal rats following intraperitoneal injections of lipopolysaccharide or interferon-gamma. *Neuroscience letters* **189**, 97-100.

- Xu YZ, Nygard M, Kristensson K & Bentivoglio M. (2010). Regulation of cytokine signaling and T-cell recruitment in the aging mouse brain in response to central inflammatory challenge. *Brain, behavior, and immunity* **24**, 138-152.
- Yamamoto M, Kiyota T, Horiba M, Buescher JL, Walsh SM, Gendelman HE & Ikezu T. (2007). Interferon-gamma and tumor necrosis factor-alpha regulate amyloid-beta plaque deposition and beta-secretase expression in Swedish mutant APP transgenic mice. *The American journal of pathology* **170**, 680-692.
- Yamamoto M, Kiyota T, Walsh SM, Liu J, Kipnis J & Ikezu T. (2008). Cytokine-mediated inhibition of fibrillar amyloid-beta peptide degradation by human mononuclear phagocytes. *J Immunol* **181**, 3877-3886.
- Zaheer A, Zaheer S, Thangavel R, Wu Y, Sahu SK & Yang B. (2008). Glia maturation factor modulates beta-amyloid-induced glial activation, inflammatory cytokine/chemokine production and neuronal damage. *Brain research* **1208**, 192-203.
- Zhang S, Cherwinski H, Sedgwick JD & Phillips JH. (2004). Molecular mechanisms of CD200 inhibition of mast cell activation. *J Immunol* **173**, 6786-6793.
- Zhou S, Halle A, Kurt-Jones EA, Cerny AM, Porpiglia E, Rogers M, Golenbock DT & Finberg RW. (2008). Lymphocytic choriomeningitis virus (LCMV) infection of CNS glial cells results in TLR2-MyD88/Mal-dependent inflammatory responses. *Journal of neuroimmunology* **194**, 70-82.

Appendix I

List of Publications

Costello D, Lyons A, Denieffe S, **Browne TC**, Cox F, Lynch MA. (2011)
Long-term potentiation is impaired in membrane glycoprotein CD200-deficient mice: a role for Toll-like receptor activation. *Journal of Biological Chemistry*, 286, 34722-32.

Blau CW, Cowley TR, O'Sullivan J, Grehan B, **Browne TC**, Kelly L, Birch A, Murphy N, Kelly AM, Kerskens CM, Lynch MA. (2011)
The age-related deficit in LTP is associated with changes in perfusion and blood-brain barrier permeability. *Neurobiology of ageing*, 33, 1005.e23–1005.e35.

Browne TC, McQuillan K, McManus RM, O'Reilly JA, Mills KHG, Lynch MA.
IFN- γ production by amyloid β -specific Th1 cells promotes microglial activation and increases plaque burden in a mouse model of Alzheimer's disease. *The Journal of Immunology*.

Appendix II

List of Materials

Acetone	Sigma-Aldrich
Acrodisc syringe filters	Pall Corporation
Ammonium chloride	Sigma-Aldrich
Anti- CD3/CD28	BD Biosciences
Anti-CD11b	AbD Serotec
Anti-CD16/CD32	BD Biosciences
Anti-IFN- γ /IL-17	BD Biosciences
Anti-TLR2	Hycult Biotech
A β	Invitrogen
BFA	Sigma-Aldrich
BSA	Sigma-Aldrich
β -galactosidase	R&D Systems
β -mercaptoethanol	Sigma-Aldrich
cDNA kit	Applied Biosystems
Chromium potassium sulphate	Sigma-Aldrich
Collagenase D	Roche
Confocal secondary antibodies	Invitrogen
Congo red	Sigma-Aldrich
CpG	Sigma-Aldrich
Cryostat	Leica
Cytokines (recombinant)	R&D Systems
Cytomation pen	Dako
DAB	Sigma-Aldrich
Dapi mounting medium	Vector
Dexamethasone	Sigma-Aldrich
Dulbecco's modified eagles medium	Gibco
DNeasy [®] blood and tissue kit	Qiagen
DNA ladder	Promega
DNase-RNase free water	Sigma-Aldrich

DPX	VWR
EDTA	Invitrogen
EGTA	Sigma-Aldrich
ELISA kits	R&D Systems
ELISA plates	NUNC
ELISA plates (black)	Labsystems
Ethanol	Sigma-Aldrich
Euthatal	Merial Animal Health
FACS antibodies	BD Biosciences
FACS tubes	BD Biosciences
Falcon tubes	Fisher Scientific
Filters	BD Bioscience
Filter paper	Whatman
Fixable viability dye	Ebiosciences
Flasks (T25)	Fisher Scientific
Flow-check fluorospheres	Beckman Coulter
Foetal bovine serum	Sigma-Aldrich
Gel red	Biotium
Gelatine	Fluka
Glycine	Sigma-Aldrich
Green GoTaq	Biolegend
Guanidine HCl	Sigma-Aldrich
Haematocytometer	Hycor Biomedical
HBSS	Sigma-Aldrich
HEPES	Sigma-Aldrich
Homogenizer	Kinematica
Hydrochloric acid	Lennox
Ionomycin	Sigma-Aldrich
Intracellular permeabilisation kit	Dako
L-Glutamine	Gibco
MACS isolation kit	Miltenyi Biotec
MACS columns	Miltenyi Biotec
Methyl green	Sigma-Aldrich

MSD 96-well multi-spot 4G8 A β	Meso Scale Discovery
Triple ultra-sensitive assay kit	
NanoDrop spectrophotometer	NanoDrop Technologies Inc
Nuaire Flow CO ₂ incubator	Jencons
NucleoSpin® RNA extraction kit	Macherey-Nagel
NRS/NGS	Vector
OCT compound	Sakura
Pam ₃ Csk ₄	Invivogen
Pan A β	Calbiochem
Penicillin/streptomycin	Gibco
Petri-dish	Fisher Scientific
Percoll	Sigma-Aldrich
Phosphate buffered saline	Sigma-Aldrich
PIPES	Sigma-Aldrich
Plates (6/24 well)	Fisher Scientific
PMA	Sigma-Aldrich
Polytron homogeniser	Kinematica
Primers for genotyping	MWG Biotech
RA1 buffer	Macherey-Nagel
Reaction buffer (10X)	Promega
Scalpel	Swann-Morton
Sodium Hydroxide	Sigma-Aldrich
Sodium chloride	Sigma-Aldrich
Sulphuric acid	Lennox
Taq polymerase	Sigma-Aldrich
Taqman® gene expression assays	Applied Biosystems
Thioflavin T	Sigma-Aldrich
Tris-HCl	Sigma-Aldrich
Trypan Blue	Sigma-Aldrich
Trypsin-EDTA	Invitrogen
Tubes (1.5 ml)	Sarstedt
Tween-20	Sigma-Aldrich
Vectorstain Elite ABC reagent	Vector

Xylene

VWR

X-vivo media

Lonza

Appendix III

List of Solutions

Calcium Solution

2.94g CaCl₂ in 20 ml dH₂O

Cell culture media

Dulbecco's Modified Eagles Medium (DMEM) (GIBCO, UK) was supplemented with 10% heat activated (56⁰C for 60 minutes) foetal bovine serum (FBS), 100 µg/ml penicillin/streptomycin.

Congo red staining solution

2.5 g Congo red

500 ml Saturated sodium chloride solution

Stir overnight before use

ELISA wash buffer

500 ml 20X PBS

9.5 L dH₂O

5 ml Tween 20

ELISA stopping solution (1 M)

26.6 ml 18.8M (H₂SO₄)

473.4 ml dH₂O

ELISA substrate solution

3,3',5,5'-Tetramethylbenzidine (TMB)

FACS buffer

500 ml PBS

10 ml FBS

Glycine stock solution (100 mM)

7.51 g Glycine

1 L dH₂O

pH 8.5

Krebs Solution

3.975 g NaCl

0.095 g KCl

0.08 g KH₂PO₄

0.135 g MgSO₄

0.67 g NaHCO₃

0.9 g Glucose

Make up to 500 ml with dH₂O and pH 7.3

Krebs Calcium solution

For short term use or storage CaCl₂ is added to Krebs buffer (1:500 dilution).

For long term storage 10% DMSO is added to the above Krebs/ CaCl₂ buffer.

PHEM Buffer

18.14 g PIPES

6.5 g HEPES

3.8 g EGTA

0.99 g MgSO₄

Saturated sodium chloride solution

50 g Sodium chloride (NaCl)

500 ml 80% ethanol

Stir overnight before use.

Thioflavin T stock solution (2 mM)

500 ml dH₂O

0.32 g ThT

Filter before use.

Appendix IV

List of Company Addresses

Alexis	Axxora (UK) Ltd. P.O. Box 6757 Bingham Nottingham NG13 8LS UK
AbD Serotec	Medical Supply Ltd., Damastown Mulhuddart Dublin 15 Ireland
Applied Biosystems	Applied Biosystems Frankfurter Str. 129b 64293 Darmstadt Germany
BD Biosciences	BD Pharmingen 10975 Torreyana Road San Diego CA 92121 US
Beckman Coulter	Beckman Coulter Inc. 4300 N Harbor Boulevard PO Box 3100 Fullerton CA 92834 US

Biolegend

Medical Supply Ltd.,
Damastown
Mulhuddart
Dublin 15
Ireland

Bioimaging Systems

UVP
2066 W 11th Street
Upland
CA 91786
US

Biosciences

Biosciences Ltd.
3 Charlemont Terrace
Crofton Road
Dun Laoghaire
Co Dublin
Ireland

Calbiochem

Merck Biosciences
Boulevard Industrial Park
Padge Road
Beeston
Nottingham
UK

Dako

Alere Ltd
Pepper Road Hazel Grove
Stockport SK7 SBW
UK

eBiosciences

eBiosciences

2nd Floor

Titan Court

3 Bishop Square

Hatfield AL 10 9NA

UK

Fisher Scientific

Fisher Scientific

Suit 3, Plaza Q12

Blanchardstown Corporate Pk

Ballycoolin

Dublin 15

Ireland

Gibco

Gibco Ltd.,

3 Fountain drive

Linchinnan Drive

Paisley PA4 9RF

Scotland

UK

Hycor Biomedical

Hycor

Pentlands Science Park

Bush Loan

Penicuik

Edinburgh EH26 0PL

UK

Hycult Biotech

Frontstraat 2A

5405 PB UDEN

Netherlands

Invitrogen	Invitrogen Ltd 3 Fountain drive Linchinnan Drive Paisley PA4 9RF Scotland UK
Invivogen	5, Rue Jean Rodier F-31400 Toulouse France
Jencons	Jencons Unit 15 The Birches Willard Way Imberhome Industrial Estate East Grinstead West Sussex RH19 1XZ UK
Kinematica	Kinematica AG Luzernerstrasse 147a Littau-Lucerne 6014 Switzerland
Labsystems	Labsystems OY Sorvaajankatu 15 SF-FIN-00811 Helsinki Finland

Lennox

Lennox Laboratory Supplies
Ltd
John F. Kennedy Drive
Naas Road
Dublin 12
Ireland

Macherey-Nagel

Labquip Ireland
12 The Business Centre
Fonthill Industrial Park
Clondalkin
Dublin 22
Ireland

Merial Animal Health Limited

Merial Animal Health Ltd.,
PO Box 327
Sandringham House
Sandringham Avenue
Harlow Business Park
Harlow
Essex CM19 5TG
UK

Meso Scale Discovery

Meso Scale Discovery
9238 Gaither Road
Gaithersburg
Maryland 20877
US

Miltenyi Biotech

Miltenyi Biotech
Almac House
Church Lane
Surrey GU24 9DR
UK

Molecular Devices

1311 Orleans Drive

Sunnyvale

CA 94089-1136

US

MWG Biotech

MWG Biotech

Anzinger Strasse 7A

Ebersberg D-85560

US

NanoDrop Technologies

NanoDrop Technologies Inc.

NanoDrop products

3411 Silverside Road

Bancroft Building

Wilmington

DE 19810

US

NUNC

Thermo Fisher Scientific

Kamstrupvej 90

Postbox 280

Roskilde

Denmark

Pall Corporation

Pall Corporation

2200 Northern Boulevard

East Hills

NY 11548

Pierce

Pierce Biotechnology Inc.
3747 N Meridian Road
PO Box 117
Rockford
IL 61105
US

Promega

Promega US
2800 Woods Hollow Road
Madison
WI 53711
US

Qiagen

Qiagen House
Fleming Way
Crawley
West Sussex RH10 9NQ
UK

R & D Systems

R & D Systems
19 Barton Lane
Abingdon Science Park
Abingdon OX143N3
UK

Roche

Roche Ireland Ltd.
Clarecastle
Co.Clare
Ireland

Sarstedt

Sarstedt Ltd.
Sinnottstown Lane
Drinagh
Wexford
Ireland

Sigma-Aldrich

Sigma-Aldrich Company Ltd,
Vale Road
Arklow
Wicklow
Ireland

Whatman

Whatman Plc
Whatman House
St Leonards Road
Maidstone
Kent ME160LS
UK

Vector Laboratories

Balydoyle Industrial Estate
Balydoyle
Dublin 13
Ireland

VWR

VWR International
Orion Business Campus
Northwest Business Park
Ballycoolin
Dublin 15
Ireland

The age-related deficit in LTP is associated with changes in perfusion and blood-brain barrier permeability

Christoph W. Blau, Thelma R. Cowley*, Joan O'Sullivan, Belinda Grehan, Tara C. Browne, Laura Kelly, Amy Birch, Niamh Murphy, Aine M. Kelly, Christian M. Kerskens, Marina A. Lynch

Trinity College, Institute of Neuroscience, Trinity College, Dublin, Ireland

Received 18 April 2011; received in revised form 22 September 2011; accepted 30 September 2011

Abstract

In view of the increase in the aging population and the unavoidable parallel increase in the incidence of age-related neurodegenerative diseases, a key challenge in neuroscience is the identification of clinical signatures which change with age and impact on neuronal and cognitive function. Early diagnosis offers the possibility of early therapeutic intervention, thus magnetic resonance imaging (MRI) is potentially a powerful diagnostic tool. We evaluated age-related changes in relaxometry, blood flow, and blood-brain barrier (BBB) permeability in the rat by magnetic resonance imaging and assessed these changes in the context of the age-related decrease in synaptic plasticity. We report that T2 relaxation time was decreased with age; this was coupled with a decrease in gray matter perfusion, suggesting that the observed microglial activation, as identified by increased expression of CD11b, MHCII, and CD68 by immunohistochemistry, flow cytometry, or polymerase chain reaction (PCR), might be a downstream consequence of these changes. Increased permeability of the blood-brain barrier was observed in the perivascular area and the hippocampus of aged, compared with young, rats. Similarly there was an age-related increase in CD45-positive cells by flow cytometry, which are most likely infiltrating macrophages, with a parallel increase in the messenger mRNA expression of chemokines IP-10 and MCP-1. These combined changes may contribute to the deficit in long-term potentiation (LTP) in perforant path-granule cell synapses of aged animals.

© 2012 Elsevier Inc. All rights reserved.

Keywords: Microglial activation; Long-term potentiation (LTP); Age; magnetic resonance imaging (MRI); blood-brain barrier (BBB); Hippocampus; T2 relaxation time; Perfusion imaging

1. Introduction

The age-related deterioration in synaptic function is associated with neuroinflammatory changes which are typified by activation of both microglia and astrocytes (Lynch, 2010). Emerging evidence suggests that these changes may be evaluated noninvasively by magnetic resonance imaging (MRI). Thus local increases in brain T1 relaxation time have been linked with acute astrocyte activation (Anderson et al.,

2006; Sibson et al., 2008), while the age-related increase in glial fibrillary acidic protein (GFAP) expression and immunoreactivity was also accompanied by increased T1 relaxation time (Cowley et al., 2010). Decreased T2 relaxation time has been correlated with microglial activation in a rat model of ischemic stroke (Justicia et al., 2008). T2 also decreases with age in humans (Siemonsen et al., 2008) although the evidence indicates that its effect is more profound in advanced age. However, T1 and T2 relaxation times are also affected by several factors including localized edema, altered vascular dynamics, and axonal loss (Fabene et al., 2003; Grohn et al., 2000; van Walderveen et al., 1998).

An age-related decrease in cerebral blood flow has been reported using arterial spin labeling (ASL) whereby the

C. Blau and T. Cowley contributed equally to this work.

* Corresponding author at: Trinity College-University of Dublin, Trinity College Institute of Neuroscience, Dublin, Ireland. Tel.: +353 1 896 8477; fax: +353 1 896 3545.

E-mail address: tcowley@tcd.ie (T.R. Cowley).

mean transit time (MTT) and capillary transit time (CTT) of magnetically labeled blood water can be measured by MRI (Kelly et al., 2010; Mitschelen et al., 2009). Consistent with this, Small and colleagues reported an age-related decrease in brain oxygenation, particularly in the hippocampus (Small et al., 2004). These changes are likely to have a significant effect on synaptic function (Reitz et al., 2009).

The factors which trigger the age-related activation of glia are not known, although a change in the balance between pro- and anti-inflammatory cytokines, as well as dysregulation of antioxidative processes, which are likely to promote activation, have been reported (Nolan et al., 2005; Roy et al., 2008). In addition, glial cell activation by infiltrating peripheral cells has been reported recently (McQuillan et al., 2010; Murphy et al., 2010). The evidence suggests that there is minimal infiltration of peripheral cells in the healthy brain; this is probably primarily due to the fact that expression of chemotactic agents is low, because migration of cells appears to be controlled mainly by expression of chemokines and adhesion molecules and their receptors. However, there is a marked increase in cell infiltration following trauma (Shichita et al., 2009) and in neurodegenerative conditions (Stone et al., 2009; Togo et al., 2002) when the blood-brain barrier (BBB) is breached and when expression of chemotactic agents is increased.

Here we set out to assess whether the age-related increase in microglial activation, as indicated by cell surface markers CD11b, MHCII (OX6), and CD68, was accompanied by changes in T2 relaxation time. Furthermore, we aimed to evaluate whether these changes were associated with evidence of altered perfusion (assessed by ASL) and BBB permeability (using the MRI contrast agent meglumine gadopentate). These measures may provide a further understanding of the factors which contribute to the age-related decrease in hippocampal synaptic plasticity, assessed by the ability to sustain long-term potentiation (LTP). The evidence suggests that perfusion and BBB permeability are altered in aged rats compared with young rats, particularly in the hippocampus, and that these modifications are linked with a decrease in T2 relaxation time. It is proposed that one consequence of these combined age-related changes is a decrease in the ability of aged rats to sustain LTP.

2. Methods

2.1. Animals

Groups of young (3–5 months old) and aged (20–26 months old) male Wistar rats (B&K Universal, Hull, UK) were housed in the BioResources Unit, Trinity College Dublin under standard conditions (2–3 per cage; 12-hour light-dark cycle; 22 °C–23 °C; food and water ad libitum). For some experiments, male Wistar rats of intermediate ages (14–26 months old and 18–20 months old) were also

used. Experiments were performed under license and in accordance with ethical guidelines.

2.2. Magnetic resonance imaging

MRI was carried out on a dedicated rodent Bruker Biospec system (Bruker Biospin, Germany) with a 7 Tesla magnet and a 30 cm diameter core, equipped with a 20 cm actively-shielded gradient system. A pair of actively decoupled 12 cm Helmholtz transmitters, and 3 cm surface quadrature receive coils (Bruker Biospin), were used for signal transmission and reception respectively. The machine was connected to a workstation running ParaVision 4.0 software (Bruker Biospin) for data reconstruction and analysis.

Animals were anesthetized with 4% isoflurane (Isoflo; Abbott Animal Health, Maidenhead, UK) in 100% oxygen and maintained with 1.5%–2% isoflurane administered by facemask in either 100% oxygen, or, in the case of the perfusion imaging, a 30%:70% oxygen:nitrogen mix; the depth of anesthesia was monitored using respiratory rate and heart rate and controlled by altering isoflurane concentration. To carry out MRI, animals were placed in a custom-built magnetic resonance (MR)-compatible Perspex rat cradle, positioned using a bite bar and ear supports with the receive coil placed over the skull. Accurate positioning was ensured by acquiring an initial pilot image using a fast gradient echo scan and a single-slice high contrast scan taken at the isocenter of the B0 magnetic field to ensure that the imaging region was centered at bregma –3.60 mm and allow consistent imaging of the cortical and hippocampal regions of interest (ROIs).

2.2. Arterial spin labeling

The ASL sequence consisted of a 5-second preparation interval containing the inversion pulse, followed by a snapshot fast low-angle shot (FLASH) image acquisition (echo time [TE] = 3.5 ms, repetition time [TR] = 11 ms, flip angle [FA] = 30°, bandwidth [BW] = 25 kHz, number of repetitions [NR] = 6, slice thickness = 1.6 mm, number of slices = 1, field of view [FOV] = 3.0 × 3.0 cm, matrix = 128 × 64, acquisition time = 2 minutes, 34 seconds per repetition [Kerskens et al., 1996]). Flow-induced fast adiabatic passage of inflowing inverted arterial spins was performed using a rectangular pulse, inverting arterial spins that then travel to the imaging plane (Dixon et al., 1986; Kelly et al., 2009). The inversion pulse radio frequency power (–22 dB) and offset frequency (–12 kHz) were determined to give optimal perfusion contrast by achieving inversion 20 mm proximal to the imaging plane. Control images with the offset frequency reversed (12 kHz), in which inflowing spins were left undisturbed, were also acquired, in an interleaved fashion. Six repetitions of each image type were acquired for signal averaging, and corresponding pairs of labeled and control images were subtracted to provide perfusion-weighted maps. A theoretical

model to facilitate the quantification of cerebral perfusion with ASL (Kelly et al., 2010) was applied to the data. The model uses a bolus-tracking ASL sequence to provide 11 data points on a signal-time curve of the passage of a 3-second bolus through the imaging slice, and yields values for the MTT, CTT, and relative cerebral blood volume of labeled water (rCBV) in a user-defined region of interest.

2.3. T1 and T2 relaxometry

A rapid acquisition with relaxation enhancement (RARE) and with variable repetition time (RARE-VTR) scan was used to calculate T1 relaxation times (TE = 12.637 ms, TR = 300, 589.116, 942.255, 1396.084, 2031.981, 3103.081, and 8000 ms, FA = 180°, BW = 100 kHz, RARE factor = 4, slice thickness = 1.5 mm, number of slices = 1, FOV = 3.0 × 3.0 cm, matrix = 128 × 128; giving a resolution of 234 × 234 × 1500 μm; and an acquisition time of 8 minutes, 43 seconds). A multislice multiecho (MSME) scan was used to calculate T2 relaxation times (echo spacing = 8.06 ms, number of echoes = 12, TR = 2000 ms, FA = 180°, BW = 100 kHz, slice thickness = 1.5 mm, number of slices = 5, FOV = 3.0 × 3.0 cm, matrix = 128 × 128, acquisition time = 4 minutes, 16 seconds). A fast imaging with steady-state precession (FISP) scan (TE = 1.5 ms, TR = 3.0 ms, FA = 60°, BW = 150 kHz, NR = 60, inversion time = 6 ms, slice thickness = 1.5 mm, number of slices = 5, FOV = 3.0 × 3.0 cm, matrix = 128 × 128, acquisition time = 5 minutes, 20 seconds) was performed from which T1 and T2 relaxation times were derived using an in-built macro in the scan acquisition software (Schmitt et al., 2004). To allow colocalization of relaxation times, the 3 scans shared the same geometry. Additionally, a “slice scout” anatomical RARE scan (TE = 12 ms, TR = 6250 ms, RARE partitions = 8, acquisition time 55 seconds) using the same matrix, field of view, and slice thickness as in the relaxometry experiments. This was used as the template for selection of the ROI from which local mean T1 and T2 relaxation times were calculated.

2.4. Contrast agent MRI

For analysis of BBB permeability, using the contrast agent meglumine gadopentate (Magnevist, HE Clissmann, Dublin, Ireland), tail veins were bilaterally cannulated to allow intravenous administration of the contrast agent and the propofol anesthetic. Animals were allowed to recover from isoflurane anesthesia until spontaneous movement occurred, and then reanesthetized with a single bolus of intravenous propofol (7.5 mg; Rapinovel, MSD Animal Health, Tallaght, Ireland) and, after 6 minutes, continuously infused with propofol, 45 mg kg⁻¹ hour⁻¹ while breathing room air (Griffin et al., 2010). Propofol was used to maintain anesthesia in these experiments because it has been reported that isoflurane opens the BBB (Tétrault et al., 2008).

A fast T1-weighted fast low-angle shot sequence (TE = 2.5 ms, TR = 4.5 ms, FA = 30°, BW = 100 kHz, NR = 60,

slice thickness = 1.5 mm, number of slices = 11, FOV = 3.0 × 3.0 cm, matrix = 128 × 128, acquisition time = 15 minutes [Kerskens et al., 1996]) with T2*-crusher gradients was developed to assess blood brain barrier permeability to the contrast agent meglumine gadopentate. The tail vein catheter was flushed with saline, and the cannula and tubing were loaded with the contrast agent. Five repetitions of the scan were acquired prior to delivery of a bolus of contrast agent (0.2 mmol/kg) and scanning continued for 15 minutes. Following scanning, animals were allowed to recover on a heat pad, breathing room air, until they were sufficiently awake to be reintroduced to their home cage.

2.5. MRI analysis

MRI data were analyzed using the data acquisition and analysis software, ParaVision (Bruker Biospin), and scripts written in Interactive Data Language (IDL; Exelis Visual Information Solutions UK, Bracknell, UK) software. For T2 relaxation time analysis, a voxel-wise linear fitting to the logarithm of the echo train decay was performed using a region of interest mask superimposed on a high resolution scan. For T1 relaxation time analysis, a voxelwise least squares curve fit of the signal recovery curve was performed and the same region of interest mask was used. ASL data were analyzed in IDL: the MTT and CTT were quantified using the previously described bolus tracking ASL method (Kelly et al., 2010). Briefly, a noncompartmental model of cerebral perfusion was fitted to the bolus tracking ASL data. The MTT and CTT were calculated from the first and second statistical moments of the signal-time curves, respectively. The rCBV was also calculated from the amplitude of the fitted curve, which is directly proportional to the area under the curve (Kelly et al., 2010). This parameter was therefore used to estimate the rCBV in the ROI. Contrast MRI data were analyzed in IDL: the average signal intensity change in the whole dataset was plotted against time, to determine the iteration at which the bolus first became detectable on the dataset. ROI were drawn on the first image of the dataset, and the progression of the logarithm of the contrast change, compared with baseline levels, was extracted and normalized to the average of the precontrast agent signal intensity in that region. Because the animals received the bolus of contrast agent in situ, the positioning of the pre- and postcontrast scans was identical enabling anatomically identical ROIs to be evaluated over time. A standard stereotaxic atlas (Paxinos and Watson, 2004) was used to ensure that the same ROIs were assessed in young and aged rats and all ROIs were drawn on high resolution scans and transferred to the contrast-enhanced datasets of the same animals.

2.6. Analysis of LTP

Rats were allowed to recover for at least 48 hours after MRI scanning before LTP was assessed in vivo. Animals were anesthetized by intraperitoneal injection of urethane

(1.5 g/kg) and, if necessary, a top-up dose of urethane (maximum dose 2.5 g/kg) was given to achieve deep anesthesia as indicated by the absence of a pedal reflex. LTP was assessed in perforant path-granule cell synapses as previously described (Loane et al., 2009). Briefly, a bipolar stimulating electrode and a unipolar recording electrode were positioned in the perforant path (4.4 mm lateral to lambda) and in the dorsal cell body region of the dentate gyrus (2.5 mm lateral and 3.9 mm posterior to bregma). Test shocks were delivered at 30-second intervals, and after a stabilization period, responses were recorded for 10 minutes before and 45 minutes after tetanic stimulation (3 trains of stimuli; 250 Hz for 200 ms; 30 seconds intertrain interval). Rats were killed by decapitation at the end of the period of electrophysiological recording and the brains were rapidly removed. One portion of the brain was stored in Tissue Tek OCT (Sakura Finetek Europe B.V., Alphen aan den Rijn, The Netherlands) at -80°C and used for preparation of cryostat sections and subsequent immunohistochemical analysis of CD11b and CD68. The hippocampus and cortex were dissected from the remaining brain tissue and placed in RNAlater (Applied Biosystems, Warrington, UK) to ensure that the integrity of the ribonucleic acid (RNA) was maintained for later gene expression analysis.

2.7. Analysis of CD11b, CD68, IP-10, and MCP-1 mRNA

We also assessed age-related changes in microglial activation by evaluating messenger (m) mRNA expression of markers of activation, CD11b and CD68, and the chemokines IP-10 and MCP-1. RNA was extracted from hippocampal tissue using a NucleoSpin RNAII isolation kit (Macherey-Nagel Inc., Düren, Germany) and concentrations were equalized to 1 μg prior to cDNA synthesis using a high capacity cDNA RT Kit (Applied Biosystems), according to the manufacturer's instructions. Equal concentrations of cDNA were used for RT-polymerase chain reaction (PCR) amplification. Real-time polymerase chain reaction primers were delivered as "Taqman Gene Expression Assays" containing forward and reverse primers, and a FAM-labeled MGB TaqMan probe for each gene (Applied Biosystems, UK) as described previously (Downer et al., 2010). The assay IDs were as follows: CD11b (Rn00709342_m1), CD68 (Rn01495631_m1), IP-10 (Rn00594648_m1), and MCP-1 (Rn00580555_m1). Gene expression was calculated relative to the endogenous control samples (β -actin) to give a relative quantification (RQ) value ($2^{-\text{DDCT}}$, where CT is threshold cycle).

2.8. CD11b and CD68 immunohistochemical staining

To assess CD11b immunohistochemistry by light microscopy brain sections were thawed, kept at room temperature for 30 minutes, fixed using ice-cold alcohol and washed in Tris-buffered saline (TBS, pH 7.5). The sections were incubated in blocking solution (10% normal horse serum (Vector Laboratories Ltd., Peterborough, UK) and 4% bo-

vine serum albumin, (BSA; Sigma-Aldrich Ireland Ltd., Arklow, Ireland), in TBS) for 30 minutes at room temperature and overnight in anti-CD11b primary antibody solution (1/100 antibody in 2% BSA/TBS; AbD Serotec, Kidlington, UK). Negative controls were incubated in 2% BSA in TBS. The sections were washed, incubated in the secondary antibody solution (1/200 in 2% BSA/TBS; IgG anti-mouse biotinylated; Vector Laboratories Ltd., Peterborough, UK; 1 hour; room temperature). The sections were washed, endogenous peroxidases were blocked by incubating in 0.3% hydrogen peroxide in TBS for 15 minutes and sections were washed again and incubated in ABC reagent (2 drops of A/B in 5 mL TBS; Vector Laboratories Ltd) for 1 hour at room temperature. Sections were washed, incubated in DAB stain (Dako, USA) for 10 minutes and this reaction was stopped by washing the slides with double deionized water. The sections were counterstained by incubating in the presence of methyl green (Sigma-Aldrich Ireland Ltd.) for 10 minutes, dehydrated by submerging the slides in a series of alcohols, cleared in xylene, mounted in DPX (p-xylene-bis-pyridinium bromide) and stored for later examination.

To assess CD68 immunohistochemistry, sections were permeabilized for 5 minutes with Triton X-100 surfactant, (Sigma-Aldrich Ireland Ltd.) and nonspecific interactions were blocked (10% normal goat serum (Vector Laboratories Ltd.), in PHEM buffer (60 mM PIPES, 25 mM HEPES, 10 mM EGTA, 2 mM MgCl_2 , pH 6.9; Sigma-Aldrich Ireland Ltd., Arklow, Ireland) containing 1% BSA for 4 hours at room temperature. Sections were incubated overnight in primary antibody solution (1/200 anti-CD68 antibody raised in mouse in 1% normal goat serum in PHEM). Negative controls were incubated in 1% normal goat serum in PHEM alone in the presence of a concentration-matched control anti-IgG antibody. Sections were rinsed 3 times in PHEM, incubated in fluorescein isothiocyanate (FITC)-conjugated secondary antibody for 2 hours at room temperature in the dark and washed. Slides were mounted with DAPI nucleic counterstain enhanced mountant (Vector Laboratories Ltd.) and coverslipped. A thin line of nail polish was applied around the coverslip to further stabilize it, and slides were stored at 4°C .

2.9. Preparation of cells from young and aged rats and flow cytometric analysis

In one series of experiments, we used flow cytometry to assess age-related changes in expression of MHCII on CD11b⁺ cells as an indicator of microglial activation and expression of CD45 on CD11b⁺ cells as an indicator of macrophage infiltration. To do so, young rats (4–6 months; $n = 8$) and aged rats (24–26 months; $n = 6$) were transcardially perfused with 200–300 mL saline before tissue was harvested. In this case, brain tissue was cross-chopped and enzymatically digested in 5 mL Krebs buffer containing 10% collagenase D and 1% DNase, in a humidified incu-

bator at 37 °C, 95% air and 5% CO₂ for 30 minutes. Tissue was flushed through a 70- μ m cell strainer using Dulbecco's modified Eagles medium (DMEM; Gibco, Invitrogen, Ireland) supplemented with 10% fetal calf serum (FCS) and 1% penicillin/streptomycin (Invitrogen). The resultant single cell suspension was centrifuged (300g, 5 minutes, room temperature) and the pellet was resuspended and incubated for 30 minutes in 5 mL complete DMEM containing 0.5 M sucrose and 10% wt/vol PEG-1000 (Fluka, UK). Samples were centrifuged at 300g for 5 minutes at 4 °C and resuspended in flow cytometry buffer (phosphate-buffered saline, 137 mM NaCl, 8.1 mM Na₂HPO₄, 1.5 mM KH₂PO₄, 2.7 mM KCl; pH 7.4) containing 2% FCS and 0.1% sodium azide; hereafter referred to as FCM buffer) and washed 3 times to remove DMEM. Cell suspensions were blocked in FCM buffer containing 50% FCS for 15 minutes at 4 °C, washed as before to remove FCM buffer, and stained with mouse anti-rat CD11b-Alexa Fluor 647 (AbD Serotec), mouse anti-rat CD45-Alexa Fluor 488 (AbD Serotec) and mouse anti-rat OX6-PerCP (BD Pharmingen, BD Bioscience, Oxford, UK) for 30 minutes at 4 °C in the dark. Cell suspensions were washed and the number of CD11b-positive cells expressing CD45 or OX6 (MHCII) was analyzed using a DakoCytomation (Dublin, Ireland) CyAn ADP flow cytometer and Summit software V4.3.

2.10. Statistical analysis

The data were assessed using Student *t* tests for independent means, 1-way analysis of variance (ANOVA) for more than 2 groups or where time and age were factors a 2-way ANOVA was used. Post hoc Newmann-Keuls tests were used to compare means. Correlations were performed and Pearson's *r* is reported.

3. Results

Analysis of MTT in propofol-anesthetized rats revealed that it was significantly increased in the hippocampus and cortex of aged, compared with young, rats (* *p* < 0.05; ** *p* < 0.01; Student *t* test for independent means; Fig. 1a and c). Similarly, analysis of CTT revealed an age-related increase in both brain areas (** *p* < 0.01; *** *p* < 0.001; Student *t* test for independent means; Fig. 1b and d). These data concur with previous findings indicating a generalized decrease in cerebral perfusion with age (Mitschelen et al., 2009), which has been associated with cognitive decline (Murphy et al., 2008) and with impairment in synaptic plasticity (Lin et al., 2010). To evaluate whether the changes in MTT and CTT described here were associated with any deficits in synaptic plasticity, we assessed LTP in perforant path-granule cell synapses and show that the mean amplitude of the population spike was significantly decreased following the tetanic stimulation in aged, compared with young, rats (*p* < 0.001; ANOVA; Fig. 2a). Analysis of the amplitude in the last 10 minutes of the experiment con-

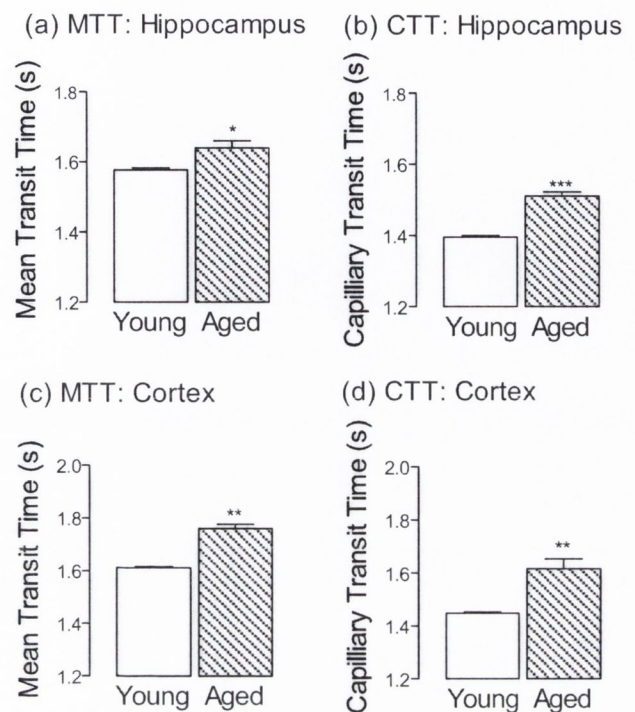


Fig. 1. Mean transit time (MTT) (a, c) and capillary transit time (CTT) (b, d) were significantly increased in the hippocampus (a, b) and cortex (c, d) of aged, compared with young, rats (* *p* < 0.05; ** *p* < 0.01; *** *p* < 0.001; Student *t* test for independent means; *n* = 8).

firmed that there was a significant age-related deficit in synaptic plasticity (*** *p* < 0.001; ANOVA; Fig. 2b).

Several factors have been associated with decreased LTP, 1 of which is glial activation which is considered to significantly contribute to the age-related inflammatory changes which have been consistently reported (Lynch, 2010). Here we assessed expression of CD11b mRNA, CD11b immunoreactivity, and the number of CD11b⁺ OX6⁺ cells prepared from whole brain of young and aged rats using FCM. CD11b mRNA was significantly higher, and immunoreactivity for CD11b was markedly greater in hippocampal (Fig. 3a and b) and cortical (Fig. 3c and d) tissue prepared from aged, compared with young, rats (* *p* < 0.05; *** *p* < 0.001; Student *t* test for independent means). The number of CD11b⁺ OX6⁺ cells, which is indicative of microglial activation, was also significantly greater in dissociated cells prepared from the whole brain of aged, compared with young, rats (*** *p* < 0.001; Student *t* test for independent means; Fig. 1e). The changes in CD11b mRNA and CD11b immunoreactivity were mirrored by changes in CD68; CD68 mRNA was significantly greater in tissue prepared from hippocampus (Fig. 1f) and cortex (Fig. 1h) of aged, compared with young rats (* *p* < 0.05; ** *p* < 0.01; Student *t* test for independent means) and an age-related increase in CD68 immunoreactivity was similarly observed in hippocampus (Fig. 1g) and cortex (Fig. 1i).

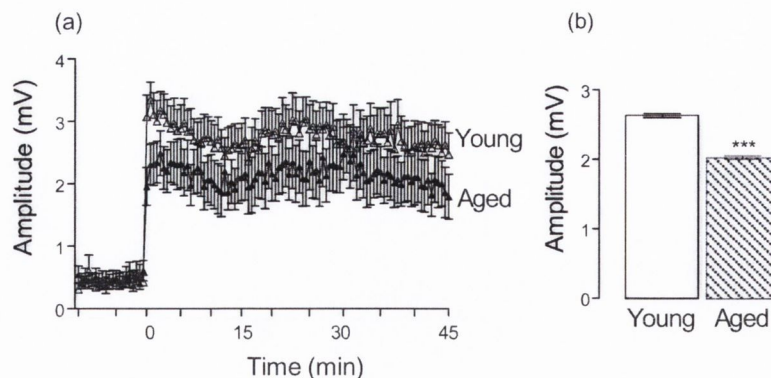


Fig. 2. Long-term potentiation (LTP), as assessed by the mean change in population spike amplitude, was significantly attenuated in dentate gyrus of aged, compared with young, rats ($p < 0.001$; analysis of variance [ANOVA]; a) and the mean change in the last 10 minutes of the experiment also revealed a significant age-related change ($*** p < 0.001$; Student t test for independent means; $n = 14$; b).

There was a significant correlation between LTP and hippocampal expression of CD11b mRNA ($r = -0.77$, $p < 0.01$, $n = 11$; Fig. 3j) and CD68 mRNA ($r = -0.75$, $p < 0.01$, $n = 11$; Fig. 3k).

We used MSME to assess T2 relaxation time, and comparison of the sample maps from a young and aged rat indicated a generalized decrease throughout the brain with age (Fig. 4a). Analysis of the mean data indicated that T2 relaxation time was significantly decreased in cortex and hippocampus of aged, compared with young, rats ($** p < 0.01$; Student t test for independent means; Fig. 4b and c). A similar, though quantitatively different, age-related change was observed when T2 was assessed by the FISP method; in this case the mean values (\pm standard error of the mean [SEM]) in hippocampus were 69.85 ± 1.02 and 63.08 ± 2.14 in young and aged animals respectively ($p < 0.05$) and the mean values in the cortex were 74.37 ± 0.78 and 66.40 ± 1.03 in young and aged animals respectively ($p < 0.001$). There was a significant negative correlation between CTT and T2 relaxation in both hippocampus ($r = -0.51$, $p < 0.01$; Fig. 4d) and cortex ($r = -0.53$, $p < 0.05$; Fig. 4e). Furthermore, T2 relaxation in the hippocampus significantly correlated with LTP ($r = 0.78$, $p < 0.01$, $n = 11$; Fig. 4f) and negatively correlated with hippocampal CD11b ($r = -0.72$, $p < 0.01$, $n = 11$; Fig. 4g) and CD68 ($r = -0.82$, $p < 0.01$, $n = 11$; Fig. 4h) mRNA expression. The data presented were obtained from isoflurane-anesthetized rats and similar data were obtained from propofol-anesthetized rats (data not shown).

In contrast to the change in T2 relaxation time, analysis of T1 relaxation time using RARE revealed no significant age-related changes in either hippocampus (Fig. 5a) or cortex (Fig. 5c). However previous data indicated that T1 relaxation time was higher in 20-month-old rats than in younger animals (Cowley et al., 2010) and it has been reported by others that T1 relaxation time peaks at middle age (Aquino et al., 2009). To further evaluate this, data from several cohorts of rats were pooled and the findings support

the contention that T1 relaxation time is age-dependent in hippocampus (Fig. 5b) and cortex (Fig. 5d).

Contrast-enhanced imaging was performed under propofol anesthesia because it has been reported that isoflurane opens the BBB (Tétrault et al., 2008). The periventricular region, hippocampus, and cortex of young and aged rats were analyzed for pre- versus postcontrast signal intensity. The images presented (Fig. 6a) are exemplary and suggest that signal intensity was significantly higher in the brain of an aged rat compared with a young rat 2 minutes after injection of contrast agent. Analysis of the periventricular region (Fig. 6b) indicated that there was a marked age-related and time-associated difference in diffusion and clearance of the contrast agent ($p < 0.001$; ANOVA; Fig. 6b). The periventricular region sampled comprises the ventricle (and therefore cerebrospinal fluid [CSF]) and also tissue adjacent to the ventricle which did not contain any major blood vessels (established by making reference to the ASL scans). The presence of the CSF explains the greater impact of the contrast agent on the signal in this, compared with hippocampal and cortical, ROIs. The data may be indicative of an age-related increase in permeability in the blood-CSF barrier (time \times age interaction, $p < 0.05$; repeated measures 2-way ANOVA). A significant age-related decrease in clearance of the contrast agent from the hippocampus was observed ($p < 0.001$; ANOVA; Fig. 6c) and the interaction between time and age was significant ($p < 0.05$; repeated measures 2-way ANOVA). It should be noted that an age-related difference in signal enhancement was evident about 2 minutes following intravenous administration of the contrast agent in the periventricular area compared with about 7 minutes after administration in the hippocampus. The delay in contrast enhancement in the hippocampal tissue probably reflects the slower diffusion of contrast agent deeper into the tissue, which is particularly evident in aged animals. A similar gradual increase in signal intensity has also been reported following temporary breakdown of the BBB by claudin 5 knockdown (Campbell et al.,

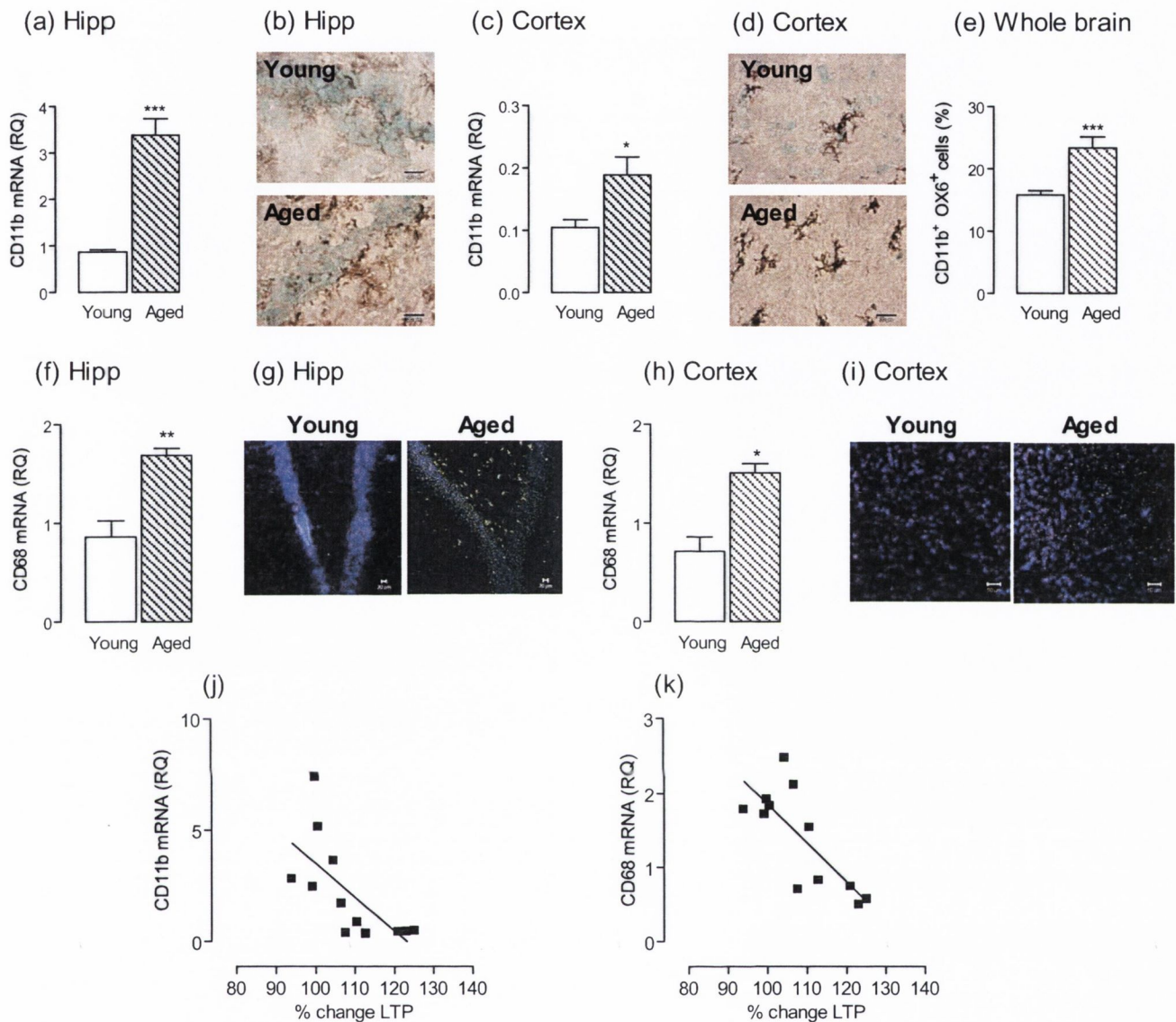


Fig. 3. CD11b messenger Ribonucleic Acid (mRNA) was significantly increased in hippocampal (a) and cortical (c) tissue prepared from aged, compared with young, rats (* $p < 0.05$; *** $p < 0.001$; Student t test for independent means; $n = 6$). CD11b immunoreactivity in hippocampal (b) and cortical (d) tissue was also markedly increased with age. (e) The number of CD11b⁺ cells which also stained positively for OX6 was significantly increased in cells prepared from cortical tissue obtained from aged, compared with young, rats (*** $p < 0.001$; Student t test for independent means; $n = 14$). CD68 mRNA was significantly increased in hippocampal (f) and cortical (h) tissue prepared from aged, compared with young, rats (* $p < 0.05$; ** $p < 0.01$; Student t test for independent means; $n = 6$) and similarly CD68 immunoreactivity in hippocampal (g) and cortical (i) tissue were also markedly increased with age. There was a significant negative correlation between LTP and (j) hippocampal expression of CD11b mRNA ($r = -0.77$; $p < 0.01$; $n = 11$) and (k) CD68 mRNA ($r = -0.75$; $p < 0.01$; $n = 11$).

2008); poor junctional localization of claudin-5 with loss of integrity of the BBB in the hippocampus have previously been reported in female middle-aged rats (Bake et al., 2009). In contrast to the change in hippocampus, there was no significant age-related change in signal intensity in the cortex (Fig. 6d). The possibility exists that changes in hippocampal volume may impact on measurement of BBB permeability. In this study, there was no evidence of a change in hippocampal volume ($4.18 \pm 0.34\%$ and $3.93 \pm$

0.49% of intracranial volume in young and aged rats respectively; $p > 0.1$) although a decrease in cortical thickness at the level of the dorsal hippocampus (bregma -3.6 mm) was observed (1.78 ± 0.13 mm and 1.45 ± 0.24 mm in young and aged rats respectively; $p < 0.01$; Student t test for independent means).

Although the blood-brain barrier is considered primarily to be a barrier to the movement of solutes and molecules, evidence suggests that an increase in its permeability may

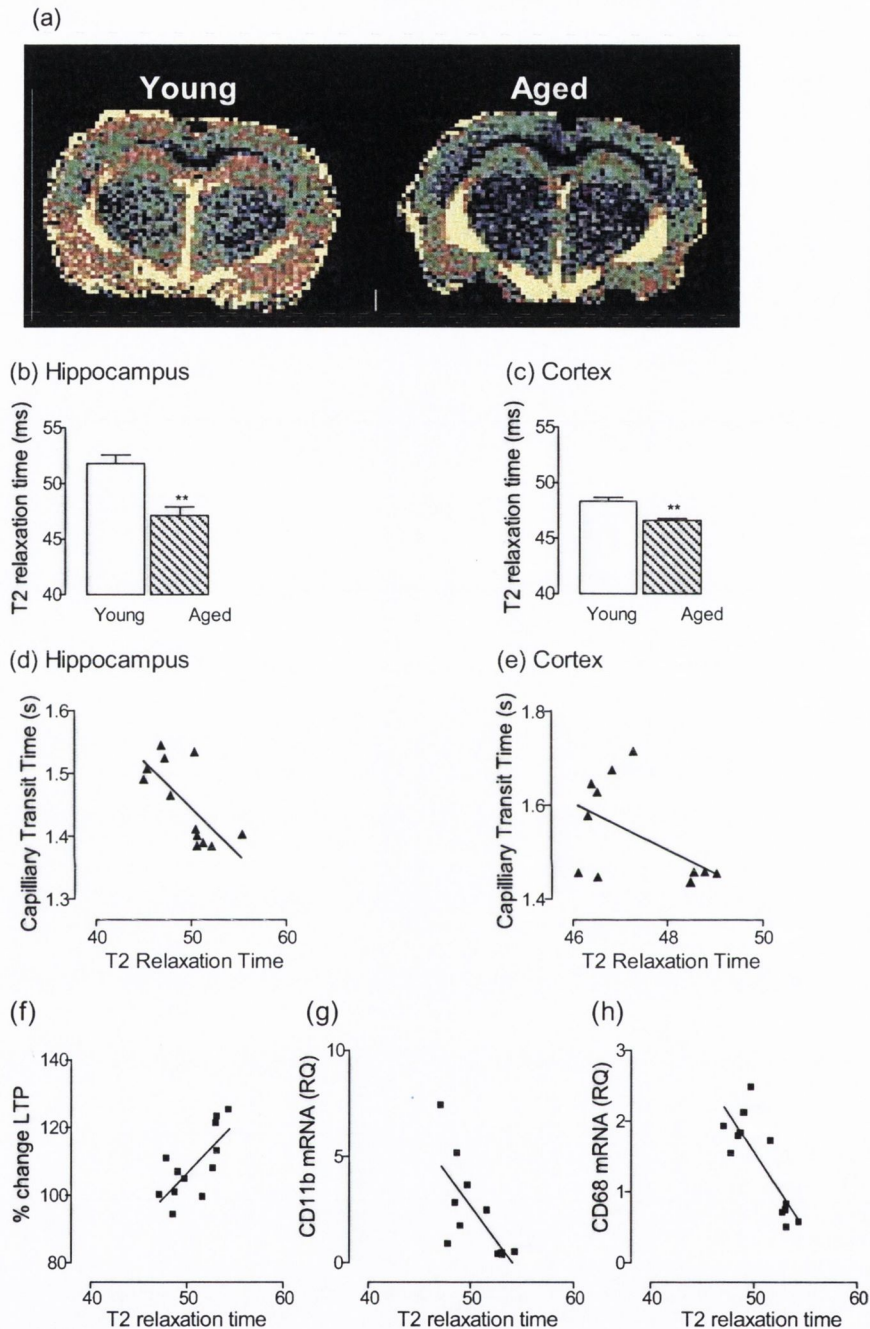


Fig. 4. T2 relaxation time was decreased in the brains of aged, compared with young, rats (a) and analysis of the data in hippocampal (b) and cortical (c) tissue revealed a significant age-related decrease (** $p < 0.01$; Student t test for independent means; $n = 6$). There was a significant correlation between capillary transit time (CTT) and T2 relaxation in hippocampus ($r = 0.51$; $n = 12$; $p < 0.01$; d) and cortex ($r = 0.53$; $n = 12$; $p < 0.05$; e). T2 relaxation in the hippocampus significantly correlated with (f) long-term potentiation (LTP) ($r = 0.78$; $p < 0.01$; $n = 11$) and (g) hippocampal CD11b ($r = -0.72$; $p < 0.01$; $n = 11$) and (h) CD68 ($r = -0.82$; $p < 0.01$; $n = 11$) mRNA expression.

also permit infiltration of cells (Popescu et al., 2009), although this mainly occurs under the influence of chemotactic molecules. Here we show that expression of IP-10 and MCP-1 which play a significant role in chemotaxis of peripheral cells (Babcock et al., 2003) were increased in brain

tissue prepared from aged, compared with young, rats (* $p < 0.05$; *** $p < 0.001$; Student t test for independent means; Fig. 7a and b). These changes were accompanied by an increase in the number of CD11b⁺ CD45⁺ cells (which are probably macrophages [Carson et al., 1998]) in whole

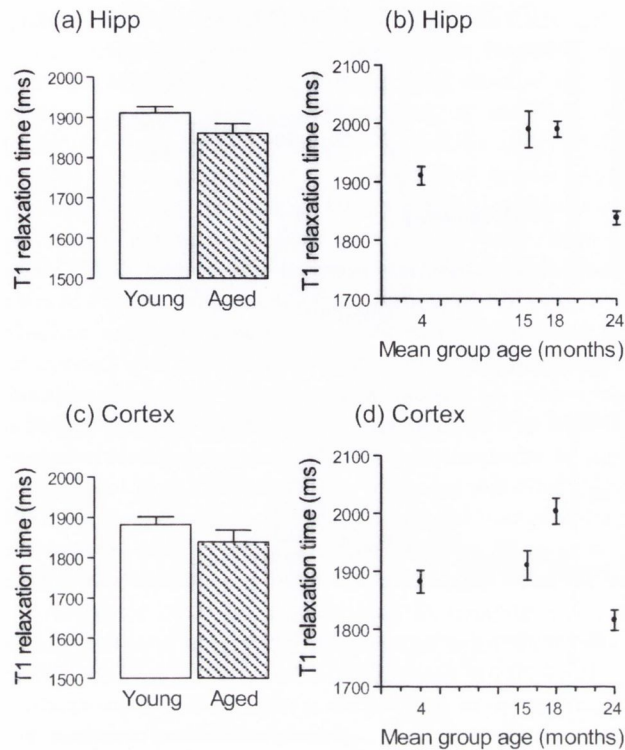


Fig. 5. T1 relaxation time was similar in hippocampus (a) and cortex (c) of aged and young rats. However, when data from other studies in which rats of different ages were assessed, it was evident that T1 relaxation time was increased in 18-month-old compared with 24-month-old rats in hippocampus and cortex ($p < 0.001$; analysis of variance [ANOVA]; $n = 12$; b and d).

brain; ** $p < 0.01$; Student t test for independent means; Fig 7c.

4. Discussion

A key challenge in neuroscience is to understand the mechanisms underlying the age-related neuroinflammatory changes which contribute to the characteristic deficit in neuronal function. The ability to noninvasively detect age-related changes in vivo to which neuroinflammation may be contributing, and to link these changes to well-established ex vivo markers of neuroinflammation has the potential to provide valuable insights into the mechanisms behind age-related cognitive decline. In this study, we set out to evaluate whether the increase in microglial activation and the associated deficit in LTP in aged animals was linked with changes in perfusion or BBB permeability as assessed by MRI. In addition, we also investigated T1 and T2 relaxation times because previous findings suggested that these parameters are altered in several neuroinflammatory conditions and changes in these parameters may reflect changes in glial activation.

The evidence indicates that MTT and CTT were increased in hippocampus and cortex of aged, compared with

young, rats and that these changes were accompanied by increased BBB permeability. An increase in the number of CD11b⁺ CD45⁺ cells were observed in the brain of aged rats and this was associated with upregulation of MCP-1 and IP-10. Interestingly the data show that there was an age-related decrease in T2 relaxation time and this, as previously reported, was accompanied by evidence of microglial activation (Falangola et al., 2005; Justicia et al., 2008; Teipel et al., 2011). Overall the evidence suggests that multiple changes occur in the brain with age which might contribute to the deficit in LTP observed here and elsewhere.

The data demonstrate an age-related increase in both MTT and CTT in hippocampus and cortex, although similar changes were observed in most areas of the brain and also in a whole brain slice (data not shown). This suggests a generalized decrease in cerebral perfusion with age and concurs with the observations that cerebral blood flow is decreased in rat and humans with age (Mitschelen et al., 2009; van Es et al., 2010) and that cerebral blood flow changes in hippocampal subregions are inversely correlated with age in nonhuman primates and rats (Small et al., 2004). The increases in MTT and CTT are probably due to a combination of decreased blood flow and altered perfusion coefficient of the tissue (Kelly et al., 2009). MTT has been shown to correlate with accumulation of lactate following stroke suggesting that it may provide a marker of ischemia (Cvoro et al., 2009) and, in this context, it is interesting that there is evidence of oxidative changes in the brain of aged rats (Kelly et al., 2011; O'Donnell et al., 2000). These changes cannot be attributed to any age-related difference in hippocampal volume because, although a decrease in cortical thickness was observed, we found no evidence of any difference in hippocampal volume in aged, compared with young, rats. However, analysis using a 9.4 Tesla magnet revealed an age-dependent decrease in hippocampal volume of Fisher 344 × Brown Norway hybrid rats (Driscoll et al., 2006), suggesting that there may be strain differences between these rats and the Wistar rats used here, or that the field strength used in this study may not be strong enough to highlight subtle volumetric differences.

Chronic hypoperfusion has been associated with a decrease in cognitive function and neuronal plasticity, specifically LTP (Lin et al., 2010) and similar changes were observed following ischemia which is also associated with decreased perfusion (Li et al., 2010). Here we show that the age-related decrease in MTT and CTT in the hippocampus is associated with a decrease in LTP, which is reported here and elsewhere (Cowley et al., 2010; Kelly et al., 2010), indicating that a relatively modest decrease in cerebral perfusion may impact on synaptic function.

Among the several factors which accompany, and probably contribute to, the age-related decrease in synaptic plasticity is microglial activation (Lynch, 2010), probably because these cells are the main source of inflammatory

Several factors contribute to the deterioration of synaptic plasticity with age and 1 of these factors appears to be a heightened level of activation of microglia, which may reflect impairment in the homeostatic ability of these cells with age, or an increase in responsiveness to modulatory molecules. The evidence presented here indicates that the age-related decrease in tissue perfusion, together with the increase in BBB permeability may alter the microenvironment in the brain; this, combined with the proposed age-related compromised homeostatic capability of microglia, may be a significant factor in maintaining the neuroinflammatory changes which have been described in the aged brain and which exert a negative impact on synaptic function.

Disclosure statement

C.W.B., T.R.C., J.O., and N.M. were funded by GlaxoSmithKline. Otherwise there are no conflicts of interest.

All experiments were performed under a license issued by the Department of Health (Ireland) and in accordance with the guidelines laid down by the Trinity College ethical committee.

Acknowledgements

This work was supported by grants from GlaxoSmithKline and the Industrial Development Agency, Ireland, Health Research Board (Ireland) and Science Foundation, Ireland.

References

- Anderson, V.M., Fox, N.C., Miller, D.H., 2006. Magnetic resonance imaging measures of brain atrophy in multiple sclerosis. *J. Magn. Reson. Imaging* 23, 605–618.
- Aquino, D., Bizzi, A., Grisoli, M., Garavaglia, B., Bruzzone, M.G., Nardocci, N., Savoirdo, M., Chiapparini, L., 2009. Age-related iron deposition in the basal ganglia: quantitative analysis in healthy subjects. *Radiology* 252, 165–172.
- Babcock, A.A., Kuziel, W.A., Rivest, S., Owens, T., 2003. Chemokine expression by glial cells directs leukocytes to sites of axonal injury in the CNS. *J. Neurosci.* 23, 7922–7930.
- Bake, S., Friedman, J.A., Sohrabji, F., 2009. Reproductive age-related changes in the blood brain barrier: expression of IgG and tight junction proteins. *Microvasc. Res.* 78, 413–424.
- Barnes, D., McDonald, W.I., 1988. A magnetic resonance imaging study of experimental cerebral edema and its response to dexamethasone. *Magn. Reson. Med.* 7, 125–131.
- Bartzokis, G., Sultzer, D., Cummings, J., Holt, L.E., Hance, D.B., Henderson, V.W., Mintz, J., 2000. In vivo evaluation of brain iron in Alzheimer disease using magnetic resonance imaging. *Arch. Gen. Psychiatry* 57, 47–53.
- Breger, R.K., Yetkin, F.Z., Fischer, M.E., Papke, R.A., Haughton, V.M., Rimm, A.A., 1991. T1 and T2 in the cerebrum: correlation with age, gender, and demographic factors. *Radiology* 181, 545–547.
- Campbell, M., Kiang, A.S., Kenna, P.F., Kerskens, C., Blau, C., O'Dwyer, L., Tivnan, A., Kelly, J.A., Brankin, B., Farrar, G.J., Humphries, P., 2008. RNAi-mediated reversible opening of the blood-brain barrier. *J. Gene Med.* 10, 930–947.
- Carson, M.J., Reilly, C.R., Sutcliffe, J.G., Lo, D., 1998. Mature microglia resemble immature antigen-presenting cells. *Glia* 22, 72–85.
- Cowley, T.R., O'Sullivan, J., Blau, C., Deighan, B.F., Jones, R., Kerskens, C., Richardson, J.C., Virley, D., Upton, N., Lynch, M.A., 2010. Rosiglitazone attenuates the age-related changes in astrocytosis and the deficit in LTP. *Neurobiol. Aging*. doi: 10.1016/j.neurobiolaging.2010.02.002.
- Cvoro, V., Wardlaw, J.M., Marshall, I., Armitage, P.A., Rivers, C.S., Bastin, M.E., Carpenter, T.K., Wartolowska, K., Farrall, A.J., Dennis, M.S., 2009. Associations between diffusion and perfusion parameters, N-acetyl aspartate, and lactate in acute ischemic stroke. *Stroke* 40, 767–772.
- Dixon, W.T., Du, L.N., Faul, D.D., Gado, M., Rossnick, S., 1986. Projection angiograms of blood labeled by adiabatic fast passage. *Magn. Reson. Med.* 3, 454–462.
- Downer, E.J., Cowley, T.R., Lyons, A., Mills, K.H., Berezin, V., Bock, E., Lynch, M.A., 2010. A novel anti-inflammatory role of NCAM-derived mimetic peptide, FGL. *Neurobiol. Aging* 31, 118–128.
- Driscoll, I., Howard, S.R., Stone, J.C., Monfils, M.H., Tomanek, B., Brooks, W.M., Sutherland, R.J., 2006. The aging hippocampus: a multi-level analysis in the rat. *Neuroscience* 139, 1173–1185.
- Fabene, P.F., Marzola, P., Sbarbati, A., Bentivoglio, M., 2003. Magnetic resonance imaging of changes elicited by status epilepticus in the rat brain: diffusion-weighted and T2-weighted images, regional blood volume maps, and direct correlation with tissue and cell damage. *Neuroimage* 18, 375–389.
- Falangola, M.F., Lee, S.P., Nixon, R.A., Duff, K., Helpem, J.A., 2005. Histological co-localization of iron in Abeta plaques of PS/APP transgenic mice. *Neurochem. Res.* 30, 201–205.
- Griffin, K.M., Blau, C.W., Kelly, M.E., O'Herlihy, C., O'Connell, P.R., Jones, J.F., Kerskens, C.M., 2010. Propofol allows precise quantitative arterial spin labelling functional magnetic resonance imaging in the rat. *Neuroimage* 51, 1395–1404.
- Grohn, O.H., Kettunen, M.I., Penttonen, M., Oja, J.M., van Zijl, P.C., Kauppinen, R.A., 2000. Graded reduction of cerebral blood flow in rat as detected by the nuclear magnetic resonance relaxation time T2: a theoretical and experimental approach. *J. Cereb. Blood Flow Metab.* 20, 316–326.
- Helpem, J.A., Lee, S.P., Falangola, M.F., Dyakin, V.V., Bogart, A., Ardekani, B., Duff, K., Branch, C., Wisniewski, T., de Leon, M.J., Wolf, O., O'Shea, J., Nixon, R.A., 2004. MRI assessment of neuropathology in a transgenic mouse model of Alzheimer's disease. *Magn. Reson. Med.* 51, 794–798.
- Justicia, C., Ramos-Cabrer, P., Hoehn, M., 2008. MRI detection of secondary damage after stroke: chronic iron accumulation in the thalamus of the rat brain. *Stroke* 39, 1541–1547.
- Kelly, L., Grehan, B., Chiesa, A.D., O'Mara, S.M., Downer, E., Sahyoun, G., Massey, K.A., Nicolaou, A., Lynch, M.A., 2011. The polyunsaturated fatty acids, EPA and DPA exert a protective effect in the hippocampus of the aged rat. *Neurobiol. Aging* 32, 2318.e1–2318.e15.
- Kelly, M.E., Blau, C.W., Griffin, K.M., Gobbo, O.L., Jones, J.F., Kerskens, C.M., 2010. Quantitative functional magnetic resonance imaging of brain activity using bolus-tracking arterial spin labeling. *J. Cereb. Blood Flow Metab.* 30, 913–922.
- Kelly, M.E., Blau, C.W., Kerskens, C.M., 2009. Bolus-tracking arterial spin labelling: theoretical and experimental results. *Phys. Med. Biol.* 54, 1235–1251.
- Kerskens, C.M., Hoehn-Berlage, M., Schmitz, B., Busch, E., Bock, C., Gyngell, M.L., Hossmann, K.A., 1996. Ultrafast perfusion-weighted MRI of functional brain activation in rats during forepaw stimulation: comparison with T2-weighted MRI. *NMR Biomed.* 9, 20–23.
- Li, S., He, Z., Guo, L., Huang, L., Wang, J., He, W., 2010. Behavioral alterations associated with a down regulation of HCN1 mRNA in hippocampal cornu ammon 1 region and neocortex after chronic incomplete global cerebral ischemia in rats. *Neuroscience* 165, 654–661.

- Lin, Q., Hai, J., Yao, L.Y., Lu, Y., 2010. Neuroprotective effects of NSTyr on cognitive function and neuronal plasticity in rats of chronic cerebral hypoperfusion. *Brain Res.* 1325, 183–190.
- Loane, D.J., Deighan, B.F., Clarke, R.M., Griffin, R.J., Lynch, A.M., Lynch, M.A., 2009. Interleukin-4 mediates the neuroprotective effects of rosiglitazone in the aged brain. *Neurobiol. Aging* 30, 920–931.
- Lynch, M.A., 2010. Age-related neuroinflammatory changes negatively impact on neuronal function. *Front. Aging Neurosci.* 1, 6.
- McQuillan, K., Lynch, M.A., Mills, K.H., 2010. Activation of mixed glia by Abeta-specific Th1 and Th17 cells and its regulation by Th2 cells. *Brain Behav. Immun.* 24, 598–607.
- Mitschelen, M., Garteiser, P., Carnes, B.A., Farley, J.A., Doblas, S., Demoe, J.H., Warrington, J.P., Yan, H., Nicolle, M.M., Towner, R., Sonntag, W.E., 2009. Basal and hypercapnia-altered cerebrovascular perfusion predict mild cognitive impairment in aging rodents. *Neuroscience* 164, 918–928.
- Murphy, A.C., Lalor, S.J., Lynch, M.A., Mills, K.H., 2010. Infiltration of Th1 and Th17 cells and activation of microglia in the CNS during the course of experimental autoimmune encephalomyelitis. *Brain Behav. Immun.* 24, 641–651.
- Murphy, M.J., Grace, G.M., Tartaglia, M.C., Orange, J.B., Chen, X., Rowe, A., Findlater, K., Kozak, R.I., Freedman, M., Strong, M.J., Lee, T.Y., 2008. Cerebral haemodynamic changes accompanying cognitive impairment in primary lateral sclerosis. *Amyotroph. Lateral Scler.* 9, 359–368.
- Nolan, Y., Maher, F.O., Martin, D.S., Clarke, R.M., Brady, M.T., Bolton, A.E., Mills, K.H., Lynch, M.A., 2005. Role of interleukin-4 in regulation of age-related inflammatory changes in the hippocampus. *J. Biol. Chem.* 280, 9354–9362.
- O'Donnell, E., Vereker, E., Lynch, M.A., 2000. Age-related impairment in LTP is accompanied by enhanced activity of stress-activated protein kinases: analysis of underlying mechanisms. *Eur. J. Neurosci.* 12, 345–352.
- O'Shea, J.M., Williams, S.R., van Bruggen, N., Gardner-Medwin, A.R., 2000. Apparent diffusion coefficient and MR relaxation during osmotic manipulation in isolated turtle cerebellum. *Magn. Reson. Med.* 44, 427–432.
- Pakulski, C., Drobnik, L., Millo, B., 2000. Age and sex as factors modifying the function of the blood-cerebrospinal fluid barrier. *Med. Sci. Monit.* 6, 314–318.
- Parry, A., Clare, S., Jenkinson, M., Smith, S., Palace, J., Matthews, P.M., 2002. White matter and lesion T1 relaxation times increase in parallel and correlate with disability in multiple sclerosis. *J. Neurol.* 249, 1279–1286.
- Paxinos, G., Watson, C., 2004. *The Rat Brain in Stereotaxic Co-Ordinates*. Academic Press, New York.
- Pelegrí, C., Canudas, A.M., del Valle, J., Casadesus, G., Smith, M.A., Camins, A., Pallàs, M., Vilaplana, J., 2007. Increased permeability of blood-brain barrier on the hippocampus of a murine model of senescence. *Mech. Ageing Dev.* 128, 522–528.
- Popescu, B.O., Toescu, E.C., Popescu, L.M., Bajenaru, O., Muresanu, D.F., Schultzberg, M., Bogdanovic, N., 2009. Blood-brain barrier alterations in ageing and dementia. *J. Neurol. Sci.* 283, 99–106.
- Reitz, C., Brickman, A.M., Brown, T.R., Manly, J., DeCarli, C., Small, S.A., Mayeux, R., 2009. Linking hippocampal structure and function to memory performance in an aging population. *Arch. Neurol.* 66, 1385–1392.
- Roy, A., Jana, A., Yatish, K., Freidt, M.B., Fung, Y.K., Martinson, J.A., Pahan, K., 2008. Reactive oxygen species up-regulate CD11b in microglia via nitric oxide: Implications for neurodegenerative diseases. *Free Radic. Biol. Med.* 45, 686–699.
- Schindowski, K., Eckert, A., Peters, J., Gorris, C., Schramm, U., Weinandi, T., Maurer, K., Frolich, L., Muller, W.E., 2007. Increased T-cell reactivity and elevated levels of CD8⁺ memory T-cells in Alzheimer's disease-patients and T-cell hyporeactivity in an Alzheimer's disease-mouse model: implications for immunotherapy. *Neuromol. Med.* 9, 340–354.
- Schmitt, F., Grosu, D., Mohr, C., Purdy, D., Salem, K., Scott, K.T., Stoeckel, B., 2004. 3 Tesla MRI: successful results with higher field strengths [in German]. *Radiologie* 44, 31–47.
- Shichita, T., Sugiyama, Y., Ooboshi, H., Sugimori, H., Nakagawa, R., Takada, I., Iwaki, T., Okada, Y., Iida, M., Cua, D.J., Iwakura, Y., Yoshimura, A., 2009. Pivotal role of cerebral interleukin-17-producing gammadeltaT cells in the delayed phase of ischemic brain injury. *Nat. Med.* 15, 946–950.
- Sibson, N.R., Lowe, J.P., Blamire, A.M., Martin, M.J., Obrenovitch, T.P., Anthony, D.C., 2008. Acute astrocyte activation in brain detected by MRI: new insights into T(1) hypointensity. *J. Cereb. Blood Flow Metab.* 28, 621–632.
- Siemonsen, S., Finsterbusch, J., Matschke, J., Lorenzen, A., Ding, X.Q., Fiehler, J., 2008. Age-dependent normal values of T2* and T2' in brain parenchyma. *AJNR Am. J. Neuroradiol.* 29, 950–955.
- Small, S.A., Chawla, M.K., Buonocore, M., Rapp, P.R., Barnes, C.A., 2004. Imaging correlates of brain function in monkeys and rats isolates a hippocampal subregion differentially vulnerable to aging. *Proc. Natl. Acad. Sci. U. S. A.* 101, 7181–7186.
- Stamatovic, S.M., Keep, R.F., Andjelkovic, A.V., 2008. Brain endothelial cell-cell junctions: how to "open" the blood brain barrier. *Curr. Neuropharmacol.* 6, 179–192.
- Stone, D.K., Reynolds, A.D., Mosley, R.L., Gendelman, H.E., 2009. Innate and adaptive immunity for the pathobiology of Parkinson's disease. *Antioxid. Redox Signal.* 11, 2151–2166.
- Teipel, S.J., Kaza, E., Hadlich, S., Bauer, A., Brüning, T., Plath, A.S., Krohn, M., Scheffler, K., Walker, L.C., Lotze, M., Pahnke, J., 2011. Automated detection of amyloid- β -related cortical and subcortical signal changes in a transgenic model of Alzheimer's disease using high-field MRI. *J. Alzheimers Dis.* 23, 221–237.
- Tétrault, S., Chever, O., Sik, A., Amzica, F., 2008. Opening of the blood-brain barrier during isoflurane anaesthesia. *Eur. J. Neurosci.* 28, 1330–1341.
- Togo, T., Akiyama, H., Iseki, E., Kondo, H., Ikeda, K., Kato, M., Oda, T., Tsuchiya, K., Kosaka, K., 2002. Occurrence of T cells in the brain of Alzheimer's disease and other neurological diseases. *J. Neuroimmunol.* 124, 83–92.
- van Es, A.C., van der Grond, J., ten Dam, V.H., de Craen, A.J., Blauw, G.J., Westendorp, R.G., Admiraal-Behloul, F., van Buchem, M.A., PROSPER Study Group, 2010. Associations between total cerebral blood flow and age related changes of the brain. *PLoS One* 5, e9825.
- van Walderveen, M.A., Kamphorst, W., Scheltens, P., van Waesberghe, J.H., Ravid, R., Valk, J., Polman, C.H., Barkhof, F., 1998. Histopathologic correlate of hypointense lesions on T1-weighted spin-echo MRI in multiple sclerosis. *Neurology* 50, 1282–1288.

Long Term Potentiation Is Impaired in Membrane Glycoprotein CD200-deficient Mice

A ROLE FOR TOLL-LIKE RECEPTOR ACTIVATION*

Received for publication, July 11, 2011. Published, JBC Papers in Press, August 11, 2011, DOI 10.1074/jbc.M111.280826

Derek A. Costello^{1,2}, Anthony Lyons¹, Stephanie Denieffe, Tara C. Browne, F. Fionnuala Cox, and Marina A. Lynch

From the Department of Physiology and the Trinity College Institute of Neuroscience, Trinity College, Dublin 2, Ireland

The membrane glycoprotein CD200 is expressed on several cell types, including neurons, whereas expression of its receptor, CD200R, is restricted principally to cells of the myeloid lineage, including microglia. The interaction between CD200 and CD200R maintains microglia and macrophages in a quiescent state; therefore, CD200-deficient mice express an inflammatory phenotype exhibiting increased macrophage or microglial activation in models of arthritis, encephalitis, and uveoretinitis. Here, we report that lipopolysaccharide (LPS) and Pam₃CysSerLys₄ exerted more profound effects on release of the proinflammatory cytokines, interleukin (IL)-1 β , IL-6, and tumor necrosis factor- α (TNF α), in glia prepared from CD200^{-/-} mice compared with wild type mice. This effect is explained by the loss of CD200 on astrocytes, which modulates microglial activation. Expression of Toll-like receptors 4 and 2 (TLR4 and -2) was increased in glia prepared from CD200^{-/-} mice, and the evidence indicates that microglial activation, assessed by the increased numbers of CD11b⁺ cells that stained positively for both MHCII and CD40, was enhanced in CD200^{-/-} mice compared with wild type mice. These neuroinflammatory changes were associated with impaired long term potentiation (LTP) in CA1 of hippocampal slices prepared from CD200^{-/-} mice. One possible explanation for this is the increase in TNF α in hippocampal tissue prepared from CD200^{-/-} mice because TNF α application inhibited LTP in CA1. Significantly, LPS and Pam₃CysSerLys₄, at concentrations that did not affect LTP in wild type mice, inhibited LTP in slices prepared from CD200^{-/-} mice, probably due to the accompanying increase in TLR2 and TLR4. Thus, the neuroinflammatory changes that result from CD200 deficiency have a negative impact on synaptic plasticity.

CD200 is a type-1 membrane glycoprotein which has been identified as an immunosuppressive molecule, consistent with its expression on cells of the immune system, including dendritic cells, T and B cells, and endothelial and epithelial cells (1). Diverse immunomodulatory roles for CD200 have been reported; these include antigen-specific T cell responses, suppression of regulatory T cells (2), cytotoxic T cell-mediated

tumor suppression (3), graft survival (4), and apoptosis-associated immune tolerance (5).

In the brain, CD200 is expressed on neurons (6) and oligodendrocytes (7) but not on microglia (8). A recent report has indicated that CD200 is expressed on reactive astrocytes in lesions from post-mortem multiple sclerosis brains (7). Expression of CD200R is mainly restricted to cells of the myeloid lineage and therefore, in the brain, has been identified on microglia (6, 7) but not on neurons (8). The complementary expression of ligand and receptor on neurons and microglia, respectively, suggests that their interaction may play a role in modulating microglial activation, and recent evidence has supported this contention. The LPS-induced increases in expression of cell surface markers of microglial activation and inflammatory cytokine production were inhibited by the addition of neurons, and this attenuating effect of neurons was blocked by an anti-CD200 antibody (8). This finding suggests that interaction of CD200 with its receptor has the capacity to modulate microglial activation.

In CD200-deficient mice, increased microglial and/or macrophage activation has been described in several models of inflammation (e.g. facial nerve transection, experimental autoimmune encephalomyelitis, an animal model of arthritis (9), and experimental autoimmune uveoretinitis (10)). Conversely, administration of a CD200 fusion protein ameliorates the inflammatory changes observed in collagen-induced arthritis (11, 12), whereas the decrease in experimental autoimmune encephalomyelitis-like symptoms in *Wld^s* mice has been attributed to increased expression of CD200 on spinal cord neurons (13).

Reduced expression of CD200 is coupled with increased microglial activation in hippocampus of aged and β -amyloid (A β)³-treated rats (8, 14), and synaptic plasticity, specifically long term potentiation (LTP), is impaired when microglial activation is increased (15, 16). Therefore, we predicted that glia prepared from CD200-deficient mice would respond more profoundly to LPS and that this would be coupled with evidence of impaired LTP. The data show that LPS and Pam₃Csk₄ exert a greater effect on glia prepared from CD200^{-/-} mice, presumably due to the observed increase in expression of TLR4 and TLR2 on these cells. In addition, LTP was markedly reduced at

* This work was supported by Science Foundation Ireland and the Health Research Board, Ireland.

¹ Both authors contributed equally to this work.

² To whom correspondence should be addressed: Dept. of Physiology, Trinity College Institute of Neuroscience, Trinity College, Dublin 2, Ireland. E-mail: derek.costello@tcd.ie.

³ The abbreviations used are: A β , β -amyloid; LTP, long term potentiation; Pam₃Csk₄, Pam₃CysSerLys₄; EPSP, excitatory postsynaptic potential; TLR, Toll-like receptor; TBS, θ -burst stimulation; ANOVA, analysis of variance; PE, phycoerythrin; GFAP, glial fibrillary acidic protein; GLAST, L-glutamate/L-aspartate transporter.

CA1 synapses of hippocampal slices prepared from CD200^{-/-}, compared with wild type, mice. LPS and Pam₃Csk₄ further attenuated LTP in slices prepared from CD200^{-/-} mice. The data provide further evidence for an important immunomodulatory role for CD200 and couple the loss of CD200 with a deficit in synaptic function and with increased expression of TLR2 and -4.

EXPERIMENTAL PROCEDURES

Animals—1-day-old and 2–6-month-old C57BL/6 or CD200^{-/-} mice were used for preparation of glial cultures or for preparation of hippocampal slices, respectively. Tissue from 2–6-month-old mice was also used for analysis of expression of TLR2 and -4. All experiments were performed under license (Department of Health and Children, Ireland) and with ethical approval (BioResources, Trinity College, Dublin) in accordance with local guidelines. Animals were housed under controlled conditions (20–22 °C, food and water *ad libitum*) and maintained under veterinary supervision.

Preparation and Treatment of Primary Glial Cultures—Mixed glial cultures were prepared from 1-day-old C57BL/6 mice or CD200^{-/-} mice as described previously (8). These cultures contained ~70% astrocytes and 30% microglia as assessed by expression of CD11b using FACS. We used mixed glia because CD200 is expressed on astrocytes but not microglia. This means that knocking out CD200 will have no impact on microglia unless they are in culture with astrocytes, and, in this case, the effect can be attributed to the loss of signaling through CD200R. In the context of this study, isolated microglia prepared from wild type and CD200^{-/-} are essentially the same.

In one series of experiments, cells were harvested for flow cytometric analysis to evaluate expression of cell surface markers of microglial activation, for GLAST to identify astrocytes, or for PCR to evaluate expression of TLR2 and -4. In a second series of experiments, cells were incubated in the presence or absence of LPS (100 ng/ml; Alexis Biochemical) or Pam₃Csk₄ (100 ng/ml; InvivoGen), and, 24 h later, supernatant was collected and assessed for concentration of IL-1 β , IL-6, and TNF α .

Purified astrocytes were prepared as described previously, using the shaking method to remove microglia (17), and membranes were isolated using a subcellular protein fractionation kit (Thermo Scientific). Cells were incubated in trypsin-EDTA (1 ml, 15 min, 37 °C), centrifuged (500 \times g, 5 min), washed with ice-cold PBS, resuspended in PBS, and centrifuged (500 \times g, 5 min). The pellet was resuspended in ice-cold Cytoplasmic Extraction Buffer containing protease inhibitors (Thermo Scientific), incubated (4 °C, 10 min), and centrifuged (3,000 \times g, 5 min); the supernatant provided the cytosolic fraction, whereas the pellet, which contained the membrane fraction, was resuspended in ice-cold Membrane Extraction Buffer containing protease inhibitors (Thermo Scientific), incubated (4 °C, 10 min), and centrifuged (3,000 \times g, 5 min). The resultant supernatant provided the membrane fraction.

To prepare microglia, cells were initially seeded onto 25-cm² flasks, and, after 24 h, medium was replaced with cDMEM containing GM-CSF (10 ng/ml) and M-CSF (20 ng/ml). After 10–14 days in culture, non-adherent microglia were harvested by shaking (110 rpm, 2 h, room temperature), tapping, and cen-

trifuging (2,000 rpm, 5 min). The pellet was resuspended in cDMEM, and the microglia were plated onto 24-well plate at a density of 1 \times 10⁵ cells/ml and maintained at 37 °C in a 5%CO₂ humidified atmosphere for up to 3 days prior to treatment.

Flow Cytometry—Glial cells were trypsinized (0.25% trypsin-EDTA; Sigma) and washed three times in FACS buffer (2%FBS, 0.1% NaN₃ in PBS). Whole brain tissue was harvested and passed through a cell strainer (70 μ m) and centrifuged (170 \times g, 10 min). The pellet was resuspended in PBS containing collagenase D (1 mg/ml) and DNase I (200 μ g/ml), incubated at 37 °C for 30 min, and centrifuged (170 \times g, 5 min). Pellets were resuspended in 1.088 g/ml Percoll (9 ml), overlaid with 1.122 g/ml Percoll (5 ml), and overlaid with 1.072 and 1.030 g/ml 9 ml each) Percoll and PBS (9 ml) and centrifuged (1,250 \times g, 45 min). The mononuclear cells (between 1.088:1.072 g/ml and between 1.072:1.030 g/ml) were centrifuged, and the pellets were washed. All cells were blocked for 15 min at room temperature in FACS block (Mouse BD Fc Block (BD Pharmingen); 1:500 in FACS buffer). Cells were incubated with PE-Cy7- or allophycocyanin-rat anti-mouse CD11b (BD Biosciences), FITC-rat anti-mouse CD40 (BD Biosciences), PE-rat anti-mouse MHCII (BD Biosciences), allophycocyanin-rat anti-mouse CD200 (BD Biosciences), PE-rat anti-mouse CD200R (Serotec), FITC-rat anti-mouse TLR2 (Cambridge Biosciences), FITC-rat anti-mouse TLR4 (Cambridge Biosciences), PE-Cy7-anti-mouse CD45 (BD Biosciences), and allophycocyanin-rat anti-mouse GLAST (BD Biosciences). Antibodies were diluted (1:400) in FACS buffer. Immunofluorescence analysis was performed on a DAKO Cyan ADP 7 color flow cytometer (DAKO Cytomation) with Summit version 4.3 software.

Real-time PCR Analysis of CD11b, CD40, TLR2, and TLR4—Total RNA was extracted from snap-frozen hippocampal tissue and harvested mixed glial cells using a NucleoSpin[®] RNAII isolation kit (Macherey-Nagel Inc.), and cDNA synthesis was performed on 1 μ g of total RNA using a High Capacity cDNA RT kit (Applied Biosystems); the protocols used were according to the manufacturer's instructions. Real-time PCR was performed as described previously (8) using an ABI Prism 7300 instrument (Applied Biosystems). The primer IDs were as follows: CD11b, Mm01271265_m1; CD40, Mm00441895_m1; TLR2, Mm00442346_m1; TLR4, Mm00445273_m1 (Applied Biosystems). Samples were assayed in duplicate, and gene expression was calculated relative to the endogenous control samples (β -actin) to give a relative quantity value ($2^{-\Delta\Delta Ct}$, where Ct is the threshold cycle).

Analysis of IL-1 β , IL-6, and TNF α —The concentrations of IL-1 β , IL-6, and TNF α were analyzed in triplicate by ELISA in samples of supernatant obtained from *in vitro* experiments as described previously (8).

Analysis of CD200, GFAP, pI κ B α , IL-1 α , IL-1 β , and TNF α by Western Immunoblotting—Hippocampal lysate was assessed for expression of IL-1 α , IL-1 β , and TNF α ; glial cell lysate was evaluated for expression of pI κ B α ; and membrane and cytosolic preparations obtained from purified astrocytes were evaluated for expression of CD200 and GFAP using standard Western immunoblotting methods (8, 18). Primary antibodies directed against CD200 (anti-goat; 1:500; Santa Cruz Biotechnology,

Increased TLR Enhances Susceptibility in CD200^{-/-} Mice

Inc., Santa Cruz, CA), GFAP (anti-rabbit; 1:1000; Invitrogen), p1κBα (Ser-32) (anti-rabbit; 1:1000; Cell Signaling), IL-1α (anti-goat; 1:1000; R&D Systems), IL-1β (anti-goat; 1:500; Santa Cruz Biotechnology, Inc.), and TNFα (anti-rabbit; 1:500; Cell Signaling) were incubated overnight at 4 °C. The secondary antibodies were conjugated to horseradish peroxidase (1:5000; Jackson ImmunoResearch), and after a 2-h incubation step, membranes were washed, and protein complexes were visualized (Immobilon Western chemiluminescent substrate, Millipore). Membranes were stripped and probed for β-actin (to confirm equal loading) as described previously (8, 18). Images were captured using the Fujifilm LAS-3000 imager, and densitometric analysis was used to quantify expression of the proteins. Values are presented as mean ± S.E., normalized to β-actin.

Hippocampal Slice Preparation and LTP Recording—Acute hippocampal slices (400 μm) from C57BL/6 and CD200^{-/-} mice were prepared using a McIlwain tissue chopper as described previously (18) and maintained in oxygenated artificial cerebrospinal fluid (125 mM NaCl, 1.25 mM KCl, 2 mM CaCl₂, 1.5 mM MgCl₂, 1.25 mM KH₂PO₄, 25 mM NaHCO₃, and 10 mM D-glucose) at room temperature (21–23 °C) in a holding chamber for a minimum of 1 h before being transferred to a submersion recording chamber. Slices were continuously perfused (2–3 ml/min) with oxygenated artificial cerebrospinal fluid at room temperature (21–23 °C). The Schaffer collateral-commissural pathway was stimulated at 0.033 Hz (0.1-ms duration; 30–50% of maximal excitatory postsynaptic potential (EPSP) amplitude) using a bipolar tungsten stimulation electrode (Advent Materials). Stable field EPSPs were recorded from the CA1 stratum radiatum using a monopolar glass recording electrode filled with artificial cerebrospinal fluid. We assessed input-output response and paired pulse facilitation to evaluate neurotransmission at CA1 synapses and found that there were no differences between slices obtained from wild type and CD200^{-/-} mice. In addition, there was no evidence of epileptiform activity in any slice. Stable base line EPSPs were recorded for 20 min prior to application of θ-burst stimulation (TBS; 10 trains (4 pulses at 100 Hz) repeated at 5 Hz (18)). In some experiments, LPS (Alexis Biochemicals) or Pam₃Csk₄ (InvivoGen) was added to the perfusate (10 μg/ml for 20 min or 20 μg/ml for 60 min) prior to TBS. In an additional set of experiments, slices were perfused with mouse recombinant TNFα (R&D Systems; 3 ng/ml in 0.002% BSA) or vehicle alone (0.002% BSA), for 20 min prior to LTP induction. This concentration of TNFα is less than that previously demonstrated to impair LTP in hippocampal slices prepared from rats (19, 20). Data were acquired using WinWCP version 4.0.7 software (Dr. J. Dempster, Strathclyde, UK). Evoked EPSPs were normalized to the slope recorded in the 5-min period prior to LTP induction. The level of LTP was evaluated as the mean percentage EPSP slope during the last 5 min of recording, and data are presented as mean percentage EPSP slope ± S.E.

Hippocampal slices not used for electrophysiology were prepared for Western immunoblot analysis of IL-1α, IL-1β, and TNFα expression (described above). These slices were incubated as described for a minimum of 1 h following the slicing procedure plus a further incubation period equivalent to the duration of LTP recording.

Statistical Analysis—Data were analyzed using either Student's *t* test for independent means or analysis of variance (ANOVA) followed by *post hoc* Student Newman-Keuls test to determine which conditions were significantly different from each other. Data are expressed as means ± S.E.

RESULTS

Loss of CD200 has been associated with evidence of increased inflammatory changes in hippocampal tissue prepared from aged animals as well as LPS- and Aβ-treated animals (8, 21). In this study, the effects of the TLR4 and TLR2 agonists, LPS and Pam₃Csk₄, were assessed on cytokine production in mixed glia prepared from wild type and CD200^{-/-} mice. The data indicate that incubation of cells prepared from wild type mice in the presence of LPS (100 ng/ml) increased release of the proinflammatory cytokines, IL-1β, IL-6, and TNFα, and the effect was significant in the case of IL-6 and TNFα (***, *p* < 0.001; ANOVA; Fig. 1, *a–c*). The effect of LPS was significantly greater in cells prepared from CD200^{-/-} mice (+++, *p* < 0.001; ANOVA; Fig. 1). Incubation of mixed glia prepared from wild type mice in the presence of Pam₃Csk₄ (100 ng/ml) also significantly increased release of inflammatory cytokines (**, *p* < 0.01; ***, *p* < 0.001; ANOVA; Fig. 1, *d–f*). The effect of Pam₃Csk₄ was greater in mixed glia prepared from CD200^{-/-} mice, and this was statistically significant in the case of IL-6 and TNFα (+++, *p* < 0.001; wild type versus CD200^{-/-}; ANOVA). Both LPS and Pam₃Csk₄ also increased mRNA expression of these inflammatory cytokines, and the effect was greater in cells prepared from CD200^{-/-} mice (data not shown). These data indicate that tonic activation by CD200 modulates cytokine release from glia. Analysis of the effect of LPS on cytokine release prepared from purified microglia obtained from wild type and CD200^{-/-} mice revealed no genotype-related change for IL-1β (99.64 ± 26.52 pg/ml versus 67.80 ± 8.03 pg/ml for wild type and CD200^{-/-} cells, respectively), IL-6 (3,837 ± 171.8 versus 3,875 ± 144.8), and TNFα (1,559 ± 88.31 versus 1,533 ± 204.5). This is consistent with the view that isolated microglia prepared from CD200^{-/-} mice are unaffected, whereas when cultured with astrocytes that are deficient in CD200, an activated phenotype is evident.

Using CD11b as a marker of microglia, we show that the number of CD11b⁺ MHCII⁺ cells and CD11b⁺ CD40⁺ cells was increased in a mixed glial population prepared from CD200^{-/-} compared with wild type mice (Fig. 2). These data suggest that CD200 contributes to maintenance of microglia (in a mixed glial preparation) in a quiescent state and therefore suggest that CD200 is expressed on astrocytes. To date, its expression on astrocytes has been reported only on reactive astrocytes in lesions from post-mortem brains of individuals with multiple sclerosis (7). Here, flow cytometry was used to evaluate CD200 expression on GLAST⁺ cells in a purified culture of astrocytes prepared from wild type and CD200^{-/-} mice (Fig. 3, *a* and *b*). Although CD200 expression was evident on GLAST⁺ cells prepared from wild type mice, expression was absent on GLAST⁺ cells prepared from CD200^{-/-} mice. To confirm astrocytic expression of CD200, purified astrocytes were used to prepare membrane and cytosolic fractions for analysis by Western immunoblotting. CD200 was evident in

Increased TLR Enhances Susceptibility in CD200^{-/-} Mice

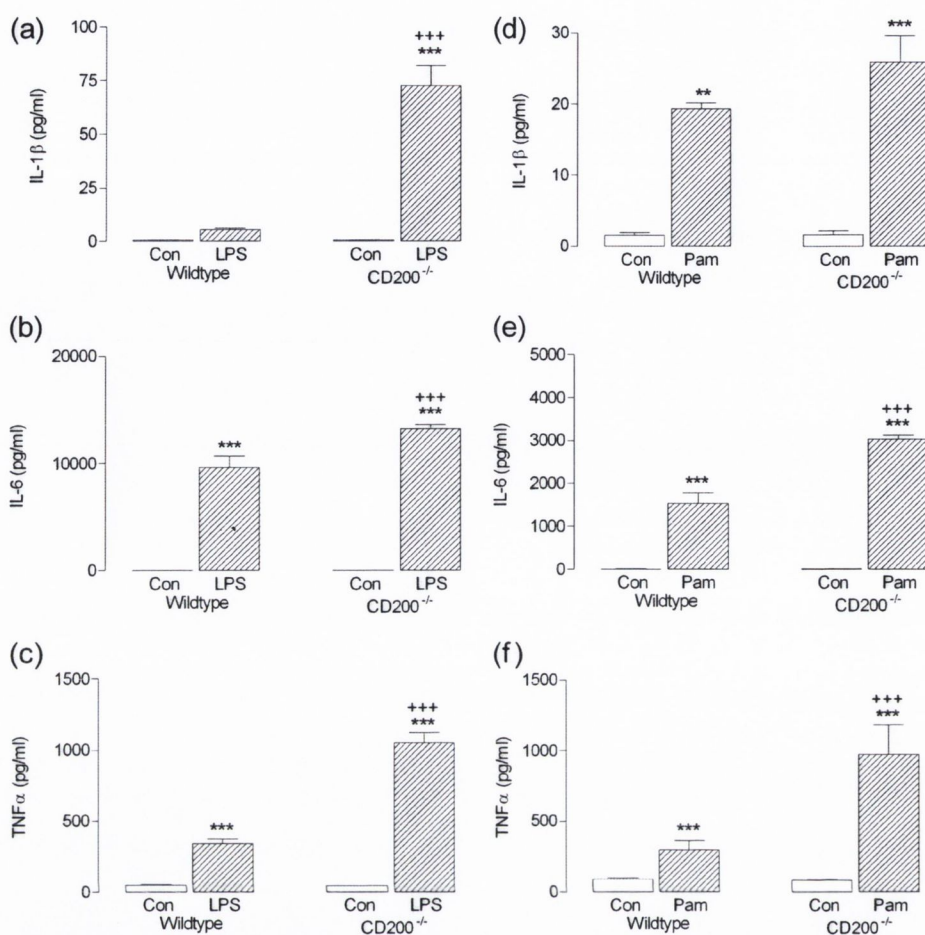


FIGURE 1. TLR2- and TLR4-induced increases in inflammatory cytokines are enhanced in glia prepared from CD200^{-/-} mice. Incubation of mixed glia prepared from wild type mice in the presence of LPS (100 ng/ml; a–c) or Pam₃Csk₄ (Pam; 100 ng/ml; d–f) increased supernatant concentrations of IL-1β, IL-6, and TNFα (**, $p < 0.01$; ***, $p < 0.001$; ANOVA; $n = 4–8$), and the effect of LPS and Pam₃Csk₄ was significantly greater in cells prepared from CD200^{-/-} mice (+ + +, $p < 0.001$; ANOVA; $n = 4–8$). Error bars, S.E.

membrane, but not cytosolic, fractions (Fig. 3c), whereas GFAP expression was, predictably, largely confined to the cytosolic fractions.

A possible explanation for the increase in responsiveness of cells from CD200^{-/-} mice to LPS and Pam₃Csk₄ is the significant increase in expression of both TLR2 and TLR4 mRNA in mixed glia prepared from CD200^{-/-} compared with wild type mice (*, $p < 0.05$; Student's *t* test for independent means; Fig. 4, a and d). Flow cytometric analysis demonstrated that cell surface expression of both receptors was increased on CD11b⁺ cells obtained from CD200^{-/-} compared with wild type mice, but the increase was significant only in the case of TLR2 (**, $p < 0.01$; Student's *t* test for independent means; Fig. 4, b, c, e, and f). The significant increase in phosphorylated IκBα in cells prepared from CD200^{-/-} compared with wild type mice (*, $p < 0.05$; Student's *t* test for independent means; Fig. 4g) indicates that signaling through TLR is up-regulated in cells prepared from CD200^{-/-} mice.

CD200 deficiency is accompanied by inflammatory changes (9, 10), and, in the brain, microglial activation is coupled with decreased CD200 in brains of aged animals and also in LPS-treated and Aβ-treated animals (8, 21). To investigate this correlation further, we evaluated expression of surface markers of

microglial activation on cells prepared from CD200^{-/-} and wild type mice using PCR and flow cytometry and show that CD40 mRNA, but not CD11b mRNA, was significantly increased in tissue prepared from CD200^{-/-} compared with wild type mice (*, $p < 0.05$; Student's *t* test for independent means; Fig. 5, a and b). Analysis by flow cytometry indicated that there was no genotype-related change in CD11b⁺ cells (Fig. 5c), but the percentage of CD11b⁺ cells that were positive for MHCII and CD40 was significantly increased (*, $p < 0.05$; ***, $p < 0.001$; Student's *t* test for independent means; Fig. 5, d–g).

CD45 has been used as a means of discriminating between macrophages (which express high levels of CD45) and microglial (which express low levels of CD45 (22)). Flow cytometric analysis revealed that the numbers of CD11b⁺ CD45^{low} cells were significantly increased in hippocampus of CD200^{-/-} compared with wild type mice (***, $p < 0.001$; Student's *t* test for independent means; Fig. 6a) and that CD200R expression (b), CD40 (c), TLR2 (d), and TLR4 (f) on these cells was greater in tissue prepared from CD200^{-/-} compared with wild type mice. The numbers of macrophages in the brain (*i.e.* CD11b⁺ CD45^{high} cells) were negligible in CD200^{-/-} and wild type mice. Analysis of expression of TLR in hippocampus revealed

Increased TLR Enhances Susceptibility in $CD200^{-/-}$ Mice

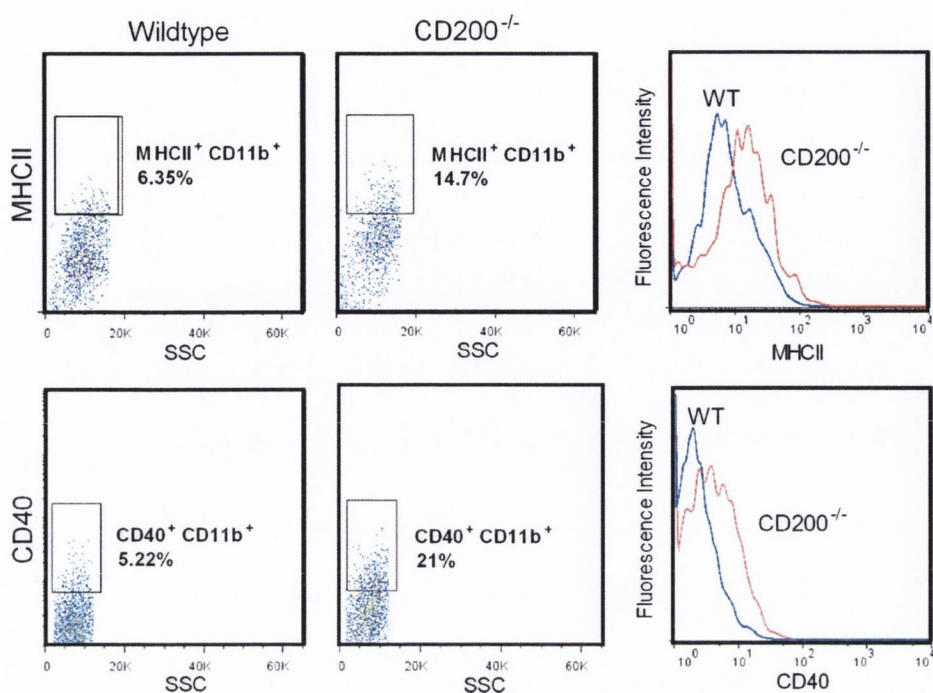


FIGURE 2. $MHCII^+ CD11b^+$ and $CD40^+ CD11b^+$ cells are increased in glia prepared from $CD200^{-/-}$ mice. Shown is the mean percentage of $CD11b^+$ cells that also stained positively for $MHCII^+$ (top panels) and $CD40$ (bottom panels). Data are presented as target proteins versus side scatter (SSC). The right-hand panels illustrate representative overlays.

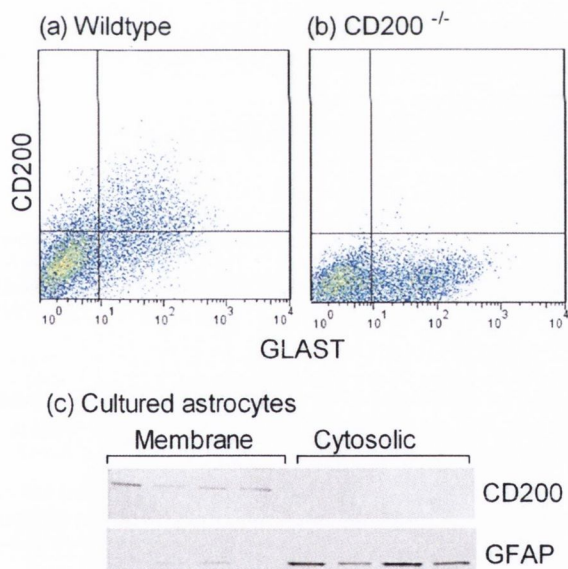


FIGURE 3. **CD200 is expressed on astrocytes.** CD200 expression was observed on $GLAST^+$ cells from purified astrocytic cultures obtained from wild type (a) but not $CD200^{-/-}$ (b) mice. CD200 was observed in membrane, but not cytosolic, fractions prepared from purified astrocytes obtained from wild type mice. GFAP expression was observed in the cytosolic fraction (c).

that both TLR2 and -4 were increased in $CD200^{-/-}$ compared with wild type mice (*, $p < 0.05$; **, $p < 0.01$; Student's t test for independent means; Fig. 6, e and g). These changes indicate that microglial activation occurs in brain tissue of $CD200^{-/-}$ mice, and therefore the changes *in vitro* are reflected *in vivo*, although the increase in expression of TLR2 mRNA in hippocampus is markedly greater than the change observed in cultured cells. Significantly, this was accompanied by a deficit in LTP in CA1

synapses where the response, 60 min following application of TBS, was markedly reduced in slices prepared from $CD200^{-/-}$ mice (12 slices from seven mice) compared with wild type mice (15 slices from 11 mice; $p < 0.001$; unpaired Student's t test; Fig. 6h). Although a number of inflammatory cytokines released from activated microglia might exert this effect (17–21), here we show that whereas expression of IL-1 α and IL-1 β were similar in hippocampal tissue prepared from wild type and $CD200^{-/-}$ mice (Fig. 7, a and b), TNF α was increased ($p < 0.05$; Student's t test for independent means; Fig. 7c). As previously demonstrated in hippocampal slices prepared from rats (19, 20, 23), application of TNF α (3 ng/ml) to mouse hippocampal slices significantly impaired LTP relative to vehicle controls ($p < 0.05$; unpaired Student's t test; three slices from two mice; Fig. 7d).

Because cells prepared from $CD200^{-/-}$ mice showed increased susceptibility to LPS, we predicted that concentrations of LPS that exerted no effect on LTP in wild type mice may attenuate it in $CD200^{-/-}$ mice. Application of LPS (20 μ g/ml) to hippocampal slices from wild type mice for 60 min prior to TBS inhibited LTP (five slices from five mice) compared with controls (15 slices from 11 mice; $p < 0.001$; Fig. 8a). In contrast, a lower concentration of LPS (10 μ g/ml; 20-min pretreatment), which exerted no effect on LTP in slices prepared from wild type mice (seven slices from six mice; Fig. 8b), significantly decreased LTP in slices from $CD200^{-/-}$ mice (13 slices from nine mice) relative to control (12 slices from seven mice; $p < 0.05$; Fig. 8c).

Like LPS, Pam₃Csk₄ exerted a greater effect on inflammatory markers in cells prepared from $CD200^{-/-}$ mice, and therefore we predicted that its effect on LTP would be genotype-specific. Application of Pam₃Csk₄ (20 μ g/ml) to hippocampal slices pre-

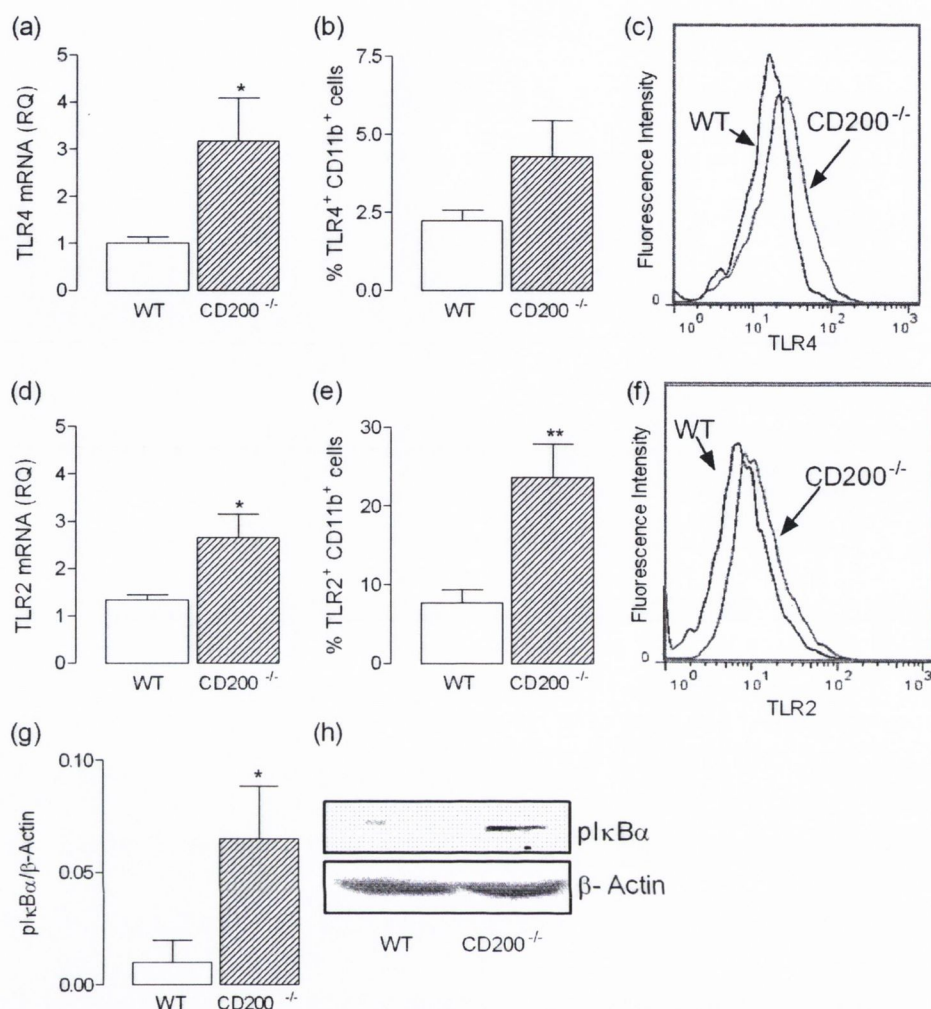


FIGURE 4. Expression of TLR2 and TLR4 is increased in glia prepared from CD200^{-/-} mice. TLR4 mRNA (a) and TLR2 mRNA (d) and the number of CD11b⁺ cells that stained positively for TLR4 (b and c) and TLR2 (e and f) were increased in glia prepared from CD200^{-/-} compared with wild type mice (*, $p < 0.05$; Student's t test for independent means; $n = 5$). Mean data from densitometric analysis (g) and a sample immunoblot (h) reveal that phosphorylated IκBα is increased in cells prepared from CD200^{-/-} compared with wild type mice (*, $p < 0.05$; Student's t test for independent means; $n = 4-6$). Error bars, S.E.

pared from wild type mice for 60 min prior to TBS inhibited LTP (three slices from three mice) compared with untreated controls (15 slices from 11 mice; $p < 0.001$; Fig. 9a). A lower concentration of Pam₃Csk₄ (10 μg/ml), applied for 20 min prior to TBS, did not affect LTP in slices prepared from wild type mice (four slices from three mice; Fig. 9b) but significantly reduced LTP in slices prepared from CD200^{-/-} mice (six slices from five mice) compared with control (12 slices from seven mice; $p < 0.05$; Fig. 9c).

DISCUSSION

The loss of CD200 has a significant impact on activation of microglia in response to inflammatory stimuli, probably because of increased expression of TLR4 and TLR2 *in vitro* and *in vivo*. Whereas LTP in Schaffer collateral-CA1 synapses was markedly impaired in slices prepared from CD200-deficient mice under control conditions, activation of TLR4 and TLR2, by LPS and Pam₃Csk₄, respectively, exerted a more profound effect on LTP in slices prepared from CD200^{-/-} mice. We pro-

pose that the increased expression of TLR4 and TLR2 provides a plausible explanation for the increased responsiveness of CD200^{-/-} mice to inflammatory stimuli.

LPS and Pam₃Csk₄ increased the release of proinflammatory cytokines, IL-1β, IL-6, and TNFα, from mixed glial cultures, confirming previously described effects of TLR4 and TLR2 (21, 24, 25). Both agonists exerted a greater effect on release of proinflammatory cytokines in mixed glia prepared from CD200^{-/-} mice, compared with wild type mice. Thus tonic activation of CD200 receptor by CD200 is required to modulate inflammatory cytokine production. This concurs with data indicating that the interaction of neurons and microglia by means of CD200 receptor engagement by CD200 decreased microglial activation and production of IL-1β (8). In the current study, in which a mixed glial preparation was used, we propose that the modulating effect is a consequence of the interaction between microglia and astrocytes, which we demonstrate express CD200. It is known that CD200 is widely expressed on numerous cell types, although, in the case of astrocytes, expres-

Increased TLR Enhances Susceptibility in CD200^{-/-} Mice

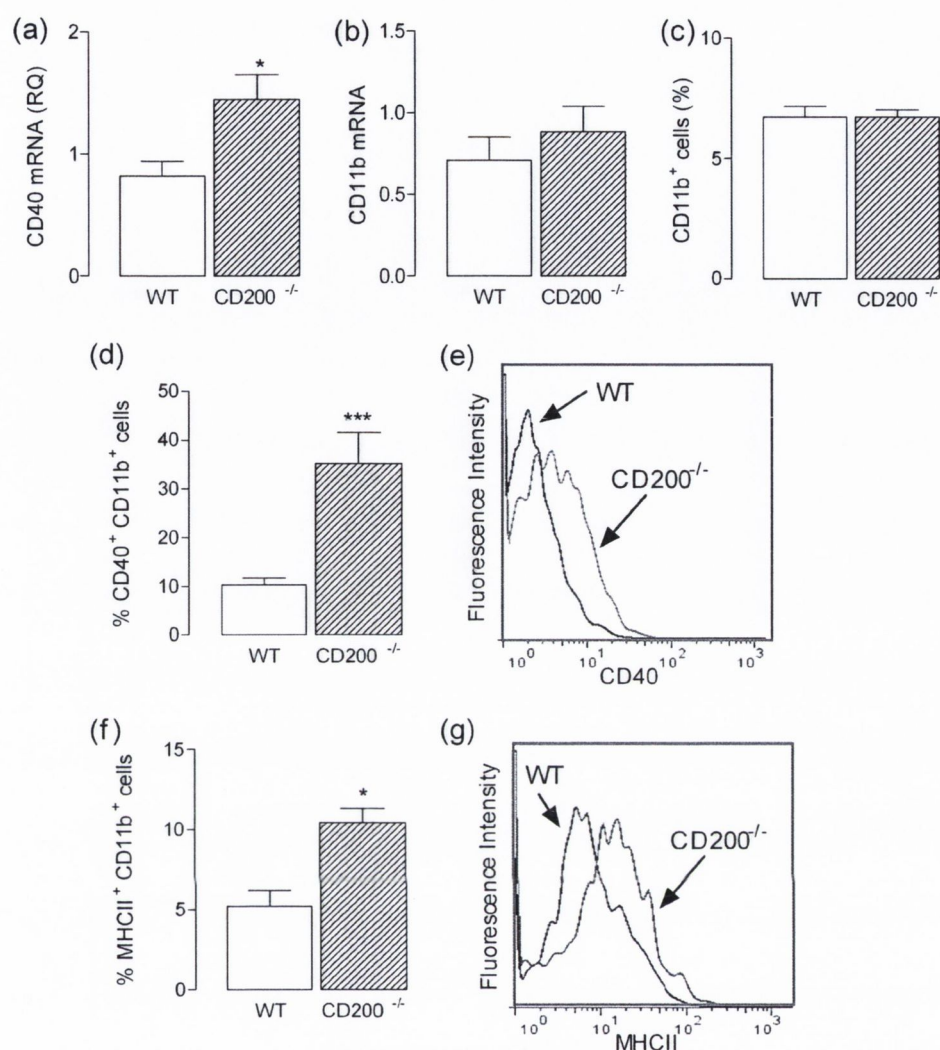


FIGURE 5. Markers of microglial activation are increased in cells prepared from CD200^{-/-} mice. *a* and *b*, expression of CD40 mRNA, but not CD11b mRNA, was significantly greater in mixed glia prepared from CD200^{-/-} compared with wild type mice (*, $p < 0.05$; Student's *t* test for independent means; $n = 4-5$). *c-f*, flow cytometric analysis revealed that the percentage of CD11b⁺ cells was similar in wild type and CD200^{-/-} (*c*), but the percentage of CD11b⁺ cells that also stained positively for CD40 (*d* and *e*) and MHCII (*f* and *g*) was significantly greater in mixed glia obtained from CD200^{-/-} compared with wild type mice (*, $p < 0.05$; ***, $p < 0.001$; Student's *t* test for independent means; $n = 4-8$). Error bars, S.E.

sion to date has been reported only on reactive astrocytes in lesions from post-mortem brains of individuals with multiple sclerosis (7). An interesting possibility is that the relatively activated state of microglia in a purified microglial culture may be a consequence of the loss of the CD200-controlled modulating effect of astrocytes.

The present findings in glia mirror those observed in peritoneal macrophages; thus, stimulation with LPS and peptidoglycan and also poly(I:C) increased release of TNF α and IL-6 to a greater extent in macrophages prepared from CD200^{-/-} mice compared with wild type mice (26). Similarly, alveolar macrophages prepared from CD200^{-/-} mice, when stimulated *ex vivo* with LPS or IFN γ , expressed more MHCII and released more inflammatory cytokines than macrophages from wild type mice (27). It has been known for many years that astrocytes are capable of modulating microglial/macrophage function. They have been shown to modulate LPS-induced changes in inducible nitric oxide synthase and NO production (28, 29) and

expression of MHCII (30), effects that have been attributed to astrocytic release of soluble factors like transforming growth factor TGF β . The present findings uncover another mechanism by which astrocytes can modulate microglial activation.

Several studies have established that responses to insults that induce inflammatory changes are exacerbated in CD200^{-/-} mice. Thus, the symptoms and inflammation associated with experimental autoimmune encephalomyelitis, *Toxoplasma* encephalitis, experimental autoimmune uveoretinitis, collagen-induced arthritis, and facial nerve transection are more profound in CD200-deficient mice (9, 10, 31). In addition, the response to an influenza dose of hemagglutination was much more severe (inducing some fatalities) in CD200-deficient compared with wild type mice (27). Although it has been shown that CD200R activation by a CD200Fc ameliorates the symptoms associated with these conditions and although CD200R-mediated regulation of macrophages relies on the binding of Dok2 to the PTB binding motif in the cytoplasmic region of CD200R and

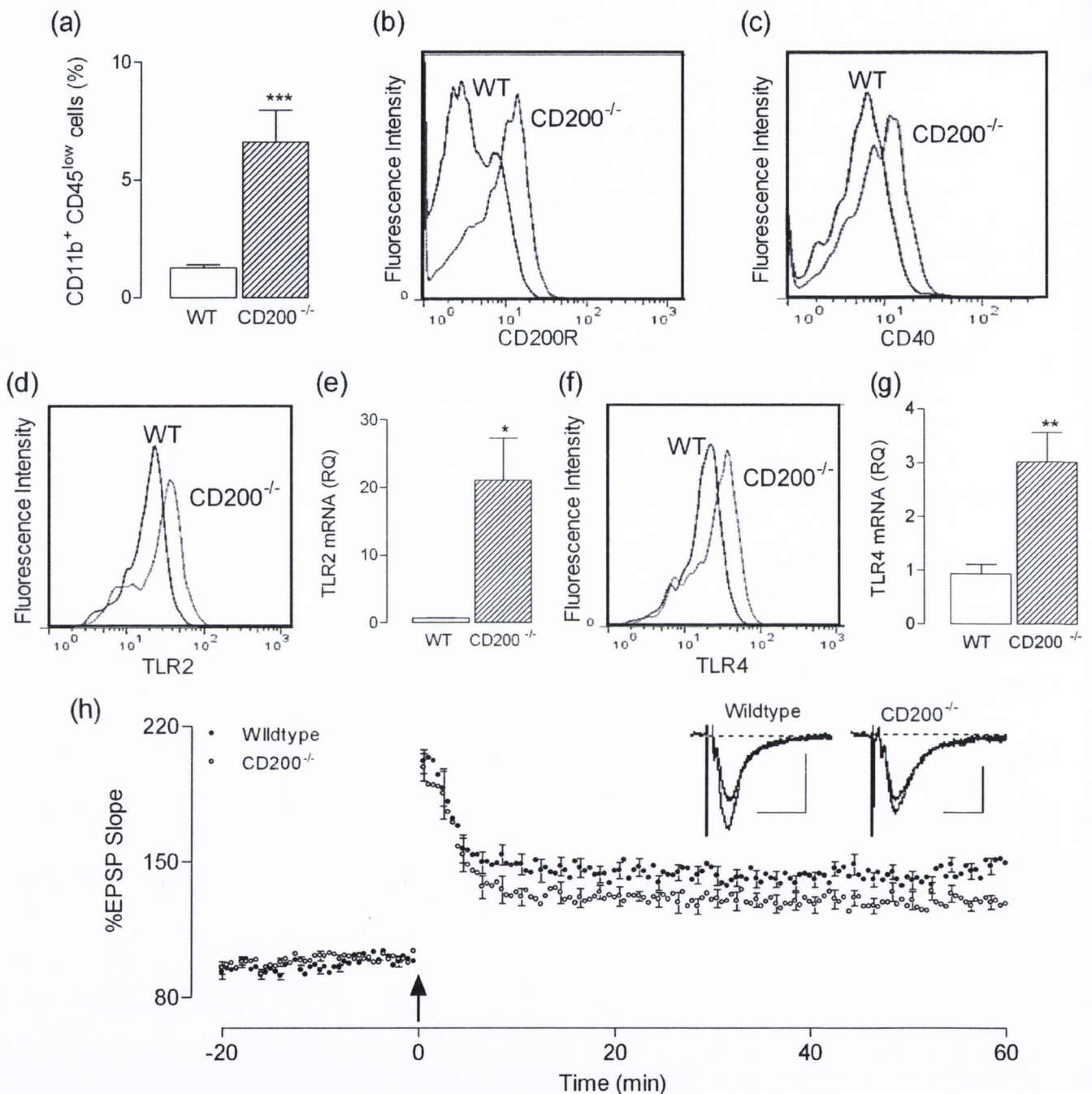


FIGURE 6. The increase in hippocampal expression of TLR2 and TLR4 in CD200^{-/-} mice is coupled with a deficit in LTP. *a*, greater numbers of CD11b⁺CD45^{low} cells were found in the hippocampus of CD200^{-/-} compared with wild type mice (***, $p < 0.001$; Student's *t* test for independent means), and expression of CD200R expression (*b*) and CD40 (*c*) was greater in tissue prepared from CD200^{-/-} compared with wild type mice. TLR2 (*d*) and TLR4 (*f*) expression on CD11b⁺CD45^{low} cells was greater in tissue prepared from CD200^{-/-} compared with wild type mice, whereas TLR2 mRNA (*e*) and TLR4 mRNA (*g*) expression were significantly increased in hippocampal tissue prepared from CD200^{-/-} compared with wild type mice (*, $p < 0.05$; **, $p < 0.01$; Student's *t* test for independent means; $n = 5$). *h*, TBS (arrow) induced LTP in CA1 synapses of hippocampal slices prepared from wild type mice (15 slices from 11 mice). LTP, measured as mean percentage EPSP slope in the last 5 min of the experiment, was significantly reduced in slices prepared from CD200^{-/-} mice relative to wild type mice ($p < 0.001$; 12 slices from seven mice). Sample recordings immediately before and 60 min following TBS are shown for wild type and CD200^{-/-} mice (scale bars, 1 mV/20 ms). Error bars, S.E.

the subsequent recruitment and activation of RasGAP (32), the mechanism by which these changes lead to dampening the activation of macrophage/microglia remains to be fully explained. In this study, we show that increased expression of both TLR4 and TLR2 was observed in glia prepared from CD200^{-/-} mice, and this may,

at least in part, provide an explanation for the susceptibility of CD200^{-/-} mice to inflammatory stimuli. Both TLR2 and TLR4 ultimately lead to activation of NFκB, and, in this study, the increased receptor expression in glia prepared from CD200^{-/-} mice is coupled with increased expression of phosphorylated IκB,

Increased TLR Enhances Susceptibility in CD200^{-/-} Mice

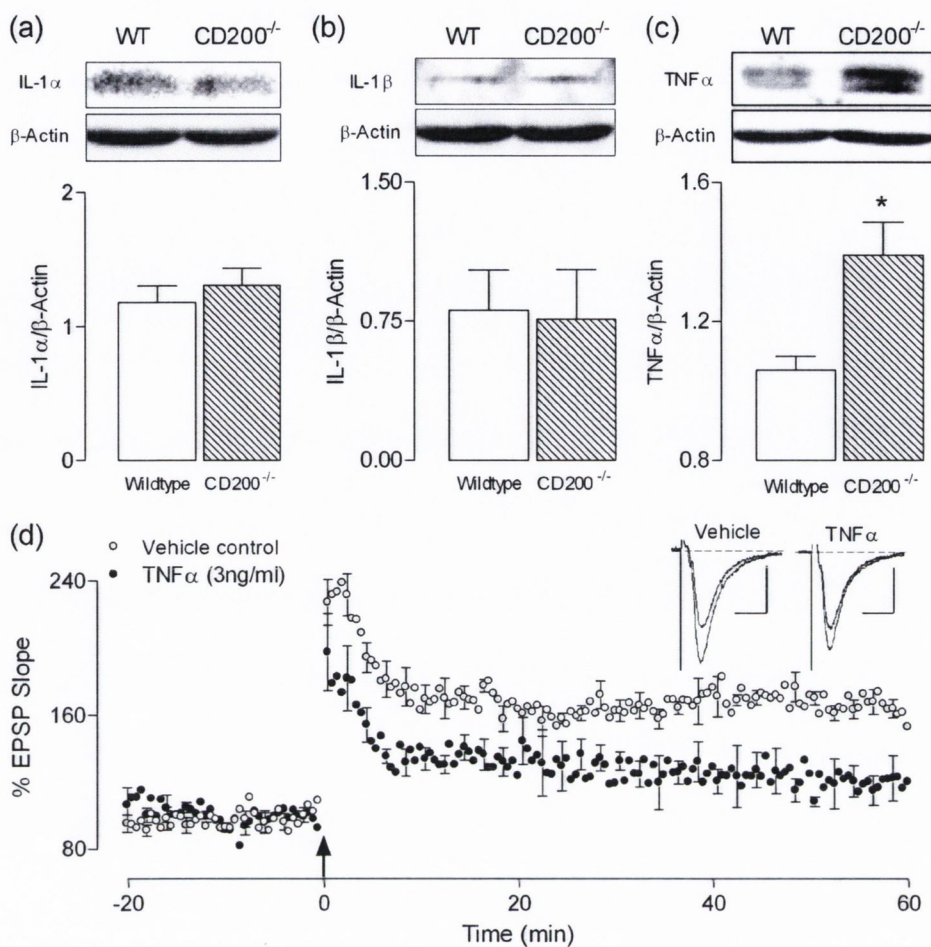


FIGURE 7. Increased hippocampal expression of TNF α in CD200^{-/-} mice may underlie the associated deficit in LTP. IL-1 α and IL-1 β were similar in tissue prepared from wild type and CD200^{-/-} mice (a and b), but TNF α was significantly increased ($p < 0.05$; Student's t test for independent means; c), as revealed by sample immunoblots and analysis of densitometric data. Application of TNF α (3 ng/ml) to hippocampal slices significantly impaired LTP relative to vehicle controls ($p < 0.05$; unpaired Student's t test; three slices from two mice; d). Sample EPSP traces immediately prior to and 60 min following TBS are presented (scale bars, 1 mV/20 ms). Error bars, S.E.

which is indicative of NF κ B activation. These changes clearly provide one possible explanation for the increased responsiveness of these cells to LPS and Pam₃Csk₄ in the present study and perhaps also in other models.

Loss of CD200 increases expression of markers of microglial activation in mixed glial cultures; CD200 deficiency was associated with enhanced expression of CD40 mRNA but not CD11b mRNA. In parallel, flow cytometry revealed that these markers and also MHCII were increased on CD11b-positive cells prepared from CD200^{-/-} mice. Previous studies have highlighted the importance of the interaction between CD200 and CD200R in maintaining the quiescent state of microglia and have revealed that the age-related and A β -induced increases in microglial activation are coupled with decreased CD200 expression on neurons (8, 14, 21). The present observations also concur with the findings that under resting conditions, spinal cord microglia adopt an inflammatory morphology expressing more CD11b (9), and the number of CD45⁺CD11b⁺ cells prepared from retina of CD200^{-/-} mice was increased (10).

In the past decade, it has become clear that neuroinflammatory changes, coupled with increased microglial activation,

negatively affect synaptic plasticity in aged, LPS-treated, and A β -treated rats (15, 33–35). These observations are corroborated in this study, where we directly associate the loss of CD200 with microglial activation and a deficit in LTP. The evidence indicates that slices prepared from CD200^{-/-} mice do not display LTP to the same degree as slices prepared from wild type mice. One possible explanation for this is that TNF α , which is increased in hippocampal tissue prepared from these mice, is released from activated microglia and inhibits LTP. We demonstrate that TNF α inhibits TBS-induced LTP in mouse Schaffer collateral-CA1 synapses, which concurs with previous evidence indicating that it exerts a similar effect on tetanus-induced LTP in rats *in vitro* and *in vivo* (17, 19, 23).

In addition to the decrease in LTP observed in untreated slices prepared from CD200^{-/-} mice, the data indicate that a subthreshold concentration of LPS or Pam₃Csk₄, which exerts minimal effects on LTP in wild type mice, markedly impairs LTP in slices prepared from CD200^{-/-} mice. These findings show for the first time that activation of TLR2 leads to inhibition of LTP and further emphasize the protective effect of CD200-CD200R interaction, such that a deficit in CD200 leads to increased susceptibility to inflammatory stimuli. At this

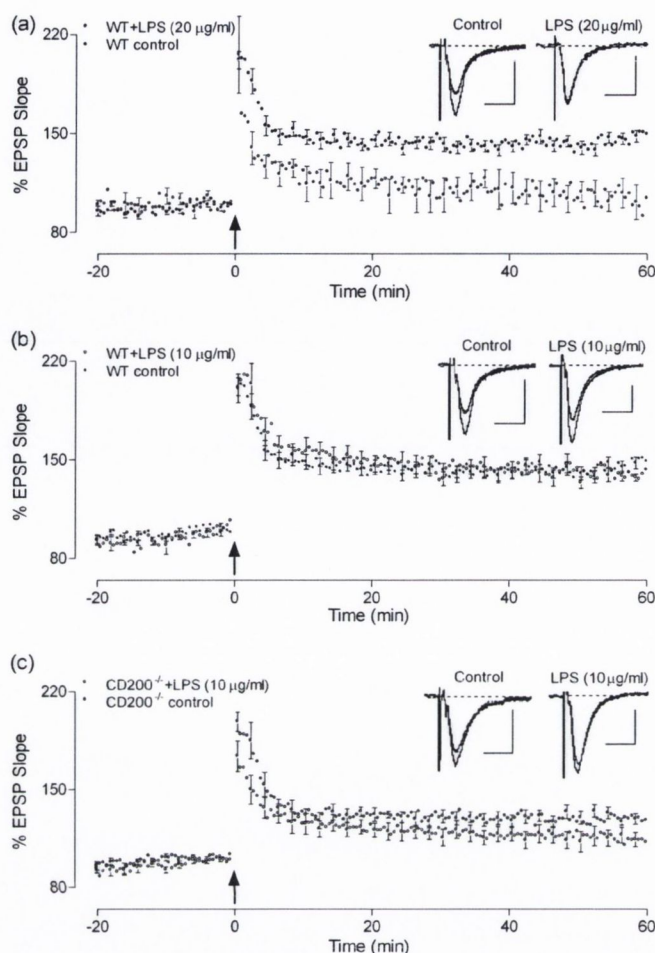


FIGURE 8. LTP is attenuated by LPS in $CD200^{-/-}$ mice. *a*, perfusion of LPS ($20 \mu\text{g/ml}$) for 60 min prior to TBS (arrow) decreased LTP in slices prepared from wild type mice (five slices from five mice), and the mean percentage EPSP slope in the last 5 min of the experiment was significantly decreased compared with control slices ($p < 0.0001$; 15 slices from 11 mice). *b* and *c*, LTP in slices prepared from wild type mice was unaffected by perfusion of $10 \mu\text{g/ml}$ LPS for 20 min prior to TBS (*b*; seven slices from six mice relative to control 15 slices from 11 mice), but LTP was attenuated in slices from $CD200^{-/-}$ mice (*c*; $p < 0.05$; 13 slices from nine mice relative to control 12 slices from seven mice). Sample EPSP traces immediately prior to and 60 min following TBS are presented (scale bars, $1 \text{ mV}/20 \text{ ms}$). Error bars, S.E.

point, it is unclear whether the effects of LPS or Pam₃Csk₄ on LTP are secondary to changes in glia or are a consequence of a direct effect on neuronal TLR4 and TLR2. In this regard, it is important to note that although some groups have reported neuronal expression of most TLRs both *in vitro* and *in vivo* (36, 37), others have been unable to demonstrate expression of TLR2 on neurons (38). The implication of this finding for the present study is that the mechanism underlying the Pam₃Csk₄-induced depression in LTP may result from its ability to release IL-1 β , IL-6, and TNF α from glia; each of these inflammatory cytokines has been shown to inhibit LTP (17, 39, 40).

Although there is an accumulating body of evidence indicating that CD200 deficiency is associated with increased inflammatory changes in several tissues, including the brain, the effect on neuronal function is relatively unexplored. Here we report that activation of TLR4 and -2 exacerbates neuroinflammatory changes in the absence of CD200 and, importantly, demon-

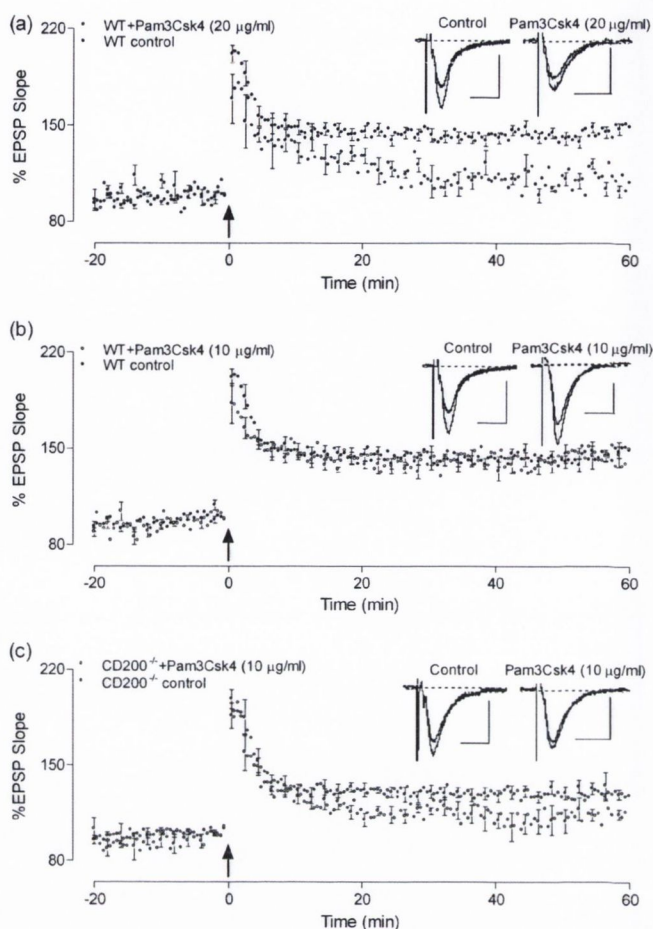


FIGURE 9. LTP is attenuated by Pam₃Csk₄ in $CD200^{-/-}$ mice. *a*, perfusion of Pam₃Csk₄ ($20 \mu\text{g/ml}$) for 60 min prior to TBS (arrow) decreased LTP in slices prepared from wild type mice (three slices from three mice), and the mean percentage EPSP slope in the last 5 min of the experiment was significantly decreased compared with control slices (15 slices from 11 mice; $p < 0.001$). *b* and *c*, LTP in slices prepared from wild type mice was unaffected by perfusion of $10 \mu\text{g/ml}$ Pam₃Csk₄ for 20 min prior to TBS (*b*; four slices from three mice relative to control 15 slices from 11 mice). However, LTP was attenuated in slices from $CD200^{-/-}$ mice following treatment with $10 \mu\text{g/ml}$ Pam₃Csk₄ (*c*; six slices from five mice relative to control 12 slices from seven mice; $p < 0.05$). Sample EPSP traces immediately prior to and 60 min following TBS are presented (scale bars, $1 \text{ mV}/20 \text{ ms}$). Error bars, S.E.

strate that CD200 deficiency also exerts a negative effect on LTP. A key factor underlying these changes is increased expression of these receptors. The findings highlight the importance of CD200 as a potential therapeutic target in disorders that are characterized by neuroinflammatory changes, coupled with loss of synaptic function.

Acknowledgment—We thank Dr. Jonathon D. Sedgwick for the gift of $CD200^{-/-}$ mice.

REFERENCES

- Barclay, A. N. (1981) *Immunology* **44**, 727–736
- Pallasch, C. P., Ulbrich, S., Brinker, R., Hallek, M., Uger, R. A., and Wendtner, C. M. (2009) *Leuk. Res.* **33**, 460–464
- Siva, A., Xin, H., Qin, F., Oltean, D., Bowdish, K. S., and Kretz-Rommel, A. (2008) *Cancer Immunol. Immunother.* **57**, 987–996
- Gorczynski, R. M., Yu, K., and Clark, D. (2000) *J. Immunol.* **165**,

Increased TLR Enhances Susceptibility in CD200^{-/-} Mice

4854–4860

5. Rosenblum, M. D., Olasz, E., Woodliff, J. E., Johnson, B. D., Konkol, M. C., Gerber, K. A., Orentas, R. J., Sandford, G., and Truitt, R. L. (2004) *Blood* **103**, 2691–2698
6. Barclay, A. N., Wright, G. J., Brooke, G., and Brown, M. H. (2002) *Trends Immunol.* **23**, 285–290
7. Koning, N., Swaab, D. F., Hoek, R. M., and Huitinga, I. (2009) *J. Neuro-pathol. Exp. Neurol.* **68**, 159–167
8. Lyons, A., Downer, E. J., Crotty, S., Nolan, Y. M., Mills, K. H., and Lynch, M. A. (2007) *J. Neurosci.* **27**, 8309–8313
9. Hoek, R. M., Ruuls, S. R., Murphy, C. A., Wright, G. J., Goddard, R., Zurawski, S. M., Blom, B., Homola, M. E., Streit, W. J., Brown, M. H., Barclay, A. N., and Sedgwick, J. D. (2000) *Science* **290**, 1768–1771
10. Broderick, C., Hoek, R. M., Forrester, J. V., Liversidge, J., Sedgwick, J. D., and Dick, A. D. (2002) *Am. J. Pathol.* **161**, 1669–1677
11. Gorczynski, R. M., Chen, Z., Yu, K., and Hu, J. (2001) *Clin. Immunol.* **101**, 328–334
12. Gorczynski, R. M., Chen, Z., Lee, L., Yu, K., and Hu, J. (2002) *Clin. Immunol.* **104**, 256–264
13. Chitnis, T., Imitola, J., Wang, Y., Elyaman, W., Chawla, P., Sharuk, M., Raddassi, K., Bronson, R. T., and Khoury, S. J. (2007) *Am. J. Pathol.* **170**, 1695–1712
14. Downer, E. J., Cowley, T. R., Lyons, A., Mills, K. H., Berezin, V., Bock, E., and Lynch, M. A. (2010) *Neurobiol. Aging* **31**, 118–128
15. Lynch, M. A., Loane, D. J., Minogue, A. M., Clarke, R. M., Kilroy, D., Nally, R. E., Roche, O. J., O'Connell, F., and Lynch, M. A. (2007) *Neurobiol. Aging* **28**, 845–855
16. Nolan, Y., Maher, F. O., Martin, D. S., Clarke, R. M., Brady, M. T., Bolton, A. E., Mills, K. H., and Lynch, M. A. (2005) *J. Biol. Chem.* **280**, 9354–9362
17. Cowley, T. R., O'Sullivan, J., Blau, C., Deighan, B. F., Jones, R., Kerskens, C., Richardson, J. C., Virley, D., Upton, N., and Lynch, M. A. (2010) *Neurobiol. Aging*, in press
18. Costello, D. A., Watson, M. B., Cowley, T. R., Murphy, N., Murphy Royal, C., Garlanda, C., and Lynch, M. A. (2011) *J. Neurosci.* **31**, 3871–3879
19. Butler, M. P., O'Connor, J. J., and Moynagh, P. N. (2004) *Neuroscience* **124**, 319–326
20. Cunningham, A. J., Murray, C. A., O'Neill, L. A., Lynch, M. A., and O'Connor, J. J. (1996) *Neurosci. Lett.* **203**, 17–20
21. Lyons, A., McQuillan, K., Deighan, B. F., O'Reilly, J. A., Downer, E. J., Murphy, A. C., Watson, M., Piazza, A., O'Connell, F., Griffin, R., Mills, K. H., and Lynch, M. A. (2009) *Brain Behav. Immun.* **23**, 1020–1027
22. Carson, M. J., Reilly, C. R., Sutcliffe, J. G., and Lo, D. (1998) *Glia* **22**, 72–85
23. Tancredi, V., D'Arcangelo, G., Grassi, F., Tarroni, P., Palmieri, G., Santoni, A., and Eusebi, F. (1992) *Neurosci. Lett.* **146**, 176–178
24. Lin, H. Y., Tang, C. H., Chen, J. H., Chuang, J. Y., Huang, S. M., Tan, T. W., Lai, C. H., and Lu, D. Y. (2010) *J. Cell Physiol.* **226**, 1573–1582
25. Lotz, M., Ebert, S., Esselmann, H., Iliev, A. I., Prinz, M., Wiazewicz, N., Wiltfang, J., Gerber, J., and Nau, R. (2005) *J. Neurochem.* **94**, 289–298
26. Mukhopadhyay, S., Plüddemann, A., Hoe, J. C., Williams, K. J., Varin, A., Makepeace, K., Akin, M. L., Bowdish, D. M., Smale, S. T., Barclay, A. N., and Gordon, S. (2010) *Cell Host Microbe* **8**, 236–247
27. Snelgrove, R. J., Goulding, J., Didierlaurent, A. M., Lyonga, D., Vekaria, S., Edwards, L., Gwyer, E., Sedgwick, J. D., Barclay, A. N., and Hussell, T. (2008) *Nat. Immunol.* **9**, 1074–1083
28. Vincent, V. A., Tilders, F. J., and Van Dam, A. M. (1997) *Glia* **19**, 190–198
29. Vincent, V. A., Van Dam, A. M., Persoons, J. H., Schotanus, K., Steinbusch, H. W., Schoffemeer, A. N., and Berkenbosch, F. (1996) *Glia* **17**, 94–102
30. Hailer, N. P., Heppner, F. L., Haas, D., and Nitsch, R. (1998) *Brain Pathol.* **8**, 459–474
31. Deckert, M., Sedgwick, J. D., Fischer, E., and Schlüter, D. (2006) *Acta Neuropathol.* **111**, 548–558
32. Mirshahi, R., Barclay, A. N., and Brown, M. H. (2009) *J. Immunol.* **183**, 4879–4886
33. Hauss-Wegrzyniak, B., Lynch, M. A., Vraniak, P. D., and Wenk, G. L. (2002) *Exp. Neurol.* **176**, 336–341
34. Rosi, S., Vazdarjanova, A., Ramirez-Amaya, V., Worley, P. F., Barnes, C. A., and Wenk, G. L. (2006) *Neuroscience* **142**, 1303–1315
35. Griffin, R., Nally, R., Nolan, Y., McCartney, Y., Linden, J., and Lynch, M. A. (2006) *J. Neurochem.* **99**, 1263–1272
36. Tang, S. C., Arumugam, T. V., Xu, X., Cheng, A., Mughal, M. R., Jo, D. G., Lathia, J. D., Siler, D. A., Chigurupati, S., Ouyang, X., Magnus, T., Camandola, S., and Mattson, M. P. (2007) *Proc. Natl. Acad. Sci. U.S.A.* **104**, 13798–13803
37. Mishra, B. B., Mishra, P. K., and Teale, J. M. (2006) *J. Neuroimmunol.* **181**, 46–56
38. Lehnardt, S., Henneke, P., Lien, E., Kasper, D. L., Volpe, J. J., Bechmann, I., Nitsch, R., Weber, J. R., Golenbock, D. T., and Vartanian, T. (2006) *J. Immunol.* **177**, 583–592
39. Tancredi, V., D'Antuono, M., Cafè, C., Giovedi, S., Buè, M. C., D'Arcangelo, G., Onofri, F., and Benfenati, F. (2000) *J. Neurochem.* **75**, 634–643
40. Murray, C. A., and Lynch, M. A. (1998) *J. Neurosci.* **18**, 2974–2981

IFN- γ Production by Amyloid β -Specific Th1 Cells Promotes Microglial Activation and Increases Plaque Burden in a Mouse Model of Alzheimer's Disease

Tara C. Browne,^{*,1} Keith McQuillan,^{*,†,1} Róisín M. McManus,^{*,†} Julie-Ann O'Reilly,^{*} Kingston H. G. Mills,^{†,2} and Marina A. Lynch^{*,2}

Alzheimer's disease (AD) is characterized by the presence of amyloid- β (A β)-containing plaques, neurofibrillary tangles, and neuronal loss in the brain. Inflammatory changes, typified by activated microglia, particularly adjacent to A β plaques, are also a characteristic of the disease, but it is unclear whether these contribute to the pathogenesis of AD or are a consequence of the progressive neurodegenerative processes. Furthermore, the factors that drive the inflammation and neurodegeneration remain poorly understood. CNS-infiltrating T cells play a pivotal role in the pathogenesis of multiple sclerosis, but their role in the progression of AD is still unclear. In this study, we examined the role of A β -specific T cells on A β accumulation in transgenic mice that overexpress amyloid precursor protein and presenilin 1 (APP/PS1). We found significant infiltration of T cells in the brains of APP/PS1 mice, and a proportion of these cells secreted IFN- γ or IL-17. A β -specific CD4⁺ T cells generated by immunization with A β and a TLR agonist and polarized in vitro to Th1-, Th2-, or IL-17-producing CD4⁺ T cells, were adoptively transferred to APP/PS1 mice at 6 to 7 mo of age. Assessment of animals 5 wk later revealed that Th1 cells, but not Th2 or IL-17-producing CD4⁺ T cells, increased microglial activation and A β deposition, and that these changes were associated with impaired cognitive function. The effects of Th1 cells were attenuated by treatment of the APP/PS1 mice with an anti-IFN- γ Ab. Our study suggests that release of IFN- γ from infiltrating Th1 cells significantly accelerates markers of diseases in an animal model of AD. *The Journal of Immunology*, 2013, 190: 2241–2251.

A role for inflammation in the pathogenesis of Alzheimer's disease (AD) is suggested by epidemiological studies that have reported a decreased incidence of AD in patients treated with nonsteroidal anti-inflammatory drugs (1, 2); these findings are supported by evidence of preventative effects of these drugs in animal models of AD (3). Whereas the classical characteristics of AD are the presence of amyloid- β (A β) plaques and neurofibrillary tangles, together with selective neuronal loss, there is also evidence of innate immune activation in AD, with activation of microglia, the primary resident immune cell of the CNS. Activated microglia are found in the brain of AD patients with mild to moderate dementia (4) and in a significant proportion of cases with mild cognitive impairment (5). Microglia secrete

inflammatory cytokines like IL-1 β and TNF- α , which increase activity and expression of secretases (6, 7), contributing to A β deposition and the early pathogenic changes in AD (8). Inflammatory cytokines released from activated microglia are known to be potentially cytotoxic, but there is evidence indicating a positive effect of an inflammatory environment on A β clearance (9–11). Microglia demonstrate significant plasticity and also adopt other phenotypes that are associated with tissue repair (12). Furthermore, immune cells in the AD brain can have an alternative activated state as well as the classical proinflammatory phenotype (13). Cell-surface expression of MHC class II and costimulatory molecules is enhanced on activated microglia (14, 15), enabling them to act as APC. However, circulating cells, including T cells, are infrequently observed in the normal CNS, although there is a population of perivascular macrophages, distinct from microglia (16–18), and these cells may play an important anti-inflammatory function, perhaps mediated by a change in hypothalamic–pituitary–adrenal axis function (19).

The blood–brain barrier plays a key role in protecting the brain, restricting the entry of pathogens and macromolecules. An intact blood–brain barrier is also important in restricting entry of circulating cells, and increased blood–brain barrier permeability, which is a characteristic of several neurodegenerative conditions including multiple sclerosis, AD, and Parkinson's disease (20–22), is associated with infiltration of circulating immune cells. Studies in multiple sclerosis and experimental allergic encephalomyelitis (EAE), a mouse model of multiple sclerosis, have shown that T cells, particularly IL-17-producing CD4⁺ T cells (Th17) cells, infiltrate the brain and spinal cord and are central to the pathogenesis of the disease (23). The role of Th1 cells in CNS inflammation associated with EAE is more controversial, with some studies suggesting that Th1 cells contribute to pathology and

^{*}Trinity College Institute of Neuroscience, Trinity Biomedical Sciences Institute, Trinity College Dublin, Dublin 2, Ireland; and [†]School of Biochemistry and Immunology, Trinity Biomedical Sciences Institute, Trinity College Dublin, Dublin 2, Ireland

¹T.C.B. and K.M. contributed equally to this work.

²K.H.G.M. and M.A.L. contributed equally to this work.

Received for publication April 4, 2012. Accepted for publication December 18, 2012.

This work was supported by grants from Science Foundation Ireland, the Health Research Board of Ireland, and the Irish Research Council for Science, Engineering and Technology.

Address correspondence and reprint requests to Prof. Kingston H.G. Mills, Immune Regulation Research Group, School of Biochemistry and Immunology, Trinity Biomedical Sciences Institute, Trinity College Dublin, 152–160 Pearse Street, Dublin 2, Ireland. E-mail address: kingston.mills@tcd.ie

The online version of this article contains supplemental material.

Abbreviations used in this article: A β , amyloid- β ; AD, Alzheimer's disease; APP, amyloid precursor protein; dH₂O, distilled H₂O; EAE, experimental autoimmune encephalomyelitis; HBSS/FBS, HBSS containing 3% FBS; PS1, presenilin 1; RT, room temperature; Th17 cells, IL-17-producing CD4⁺ T cells; WT, wild-type.

Copyright © 2013 by The American Association of Immunologists, Inc. 0022-1767/13/\$16.00

others suggesting a protective role for IFN- γ through inhibition of Th17 cells. As well as their role in demyelination, the interaction of T cells with microglia contributes to the inflammatory changes observed in EAE (24).

T cells are also present in the brain of patients with AD (25–28), and infiltration may result from increased expression of CXCR2 and MIP-1 α on the T cells (29). Although T cells, in particular Th2 or regulatory T cells, can have a protective role in the brain (30, 31), the entry of activated effector T cells, particularly Th1 or Th17 cells, into the brain in which inflammatory changes are ongoing, is likely to escalate the inflammatory cascade. Consistent

with this is the finding that A β -induced release of inflammatory cytokines from glia was exacerbated by Th1 and Th17 cells (32), and this effect was attenuated by Th2 cells. Immunization with A β peptides, formulated with various adjuvants, is being evaluated both in preclinical models and in the clinic as a potential therapy for AD based on Ab-mediated reduction of A β plaque burden (33). However, a proportion of AD patients who received a vaccine containing A β peptide formulated with the adjuvant QS21 (AN1792) developed meningoencephalitis (34). It is possible that the generation of certain subtypes of A β -specific T cells may contribute to inflammatory pathology in AD.

In this study, we used a transgenic mouse model of AD that overexpresses amyloid precursor protein (APP) with the Swedish mutation and exon-9-deleted presenilin 1 (PS1; APP/PS1 mice) to determine whether A β -specific T cell subsets can modulate A β burden and affect microglial activation. A β -specific effector T cells were generated by immunization with A β and CpG, polarized *in vitro* to Th1, Th2, and Th17 cells, and adoptively transferred to 6- to 7-month-old APP/PS1 mice. We found that A β -specific Th1 cells increased A β deposition and microglial activation in APP/PS1 mice and negatively impacted on spatial

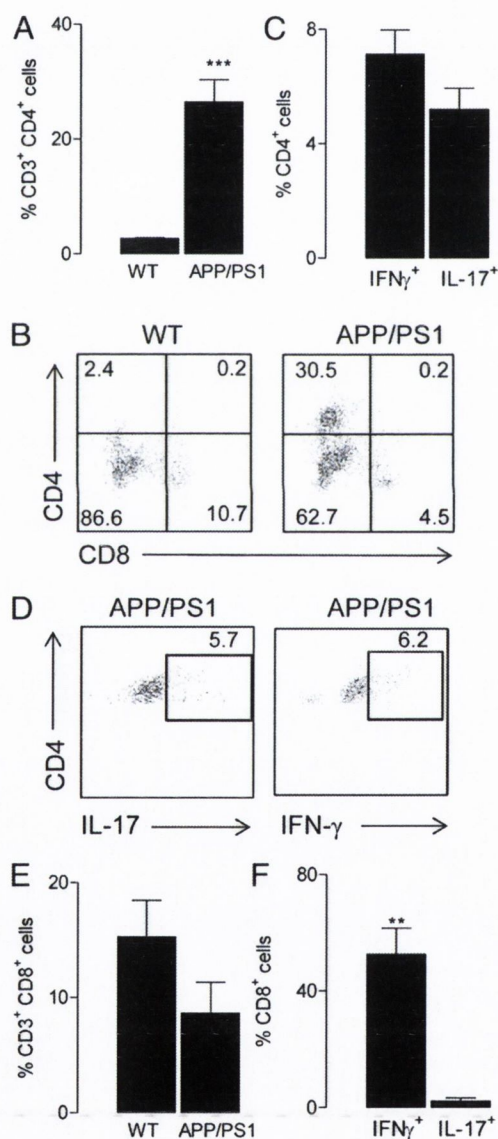


FIGURE 1. Th1 and Th17 infiltrate the brain of APP/PS1 mice. Mononuclear cells were prepared from the brain of APP/PS1 and WT mice, and cells were surface stained with Abs specific for CD3, CD4, CD8, intracellular IL-17, and IFN- γ , and flow cytometric analysis was performed. Mean frequency (A) and representative dot plots (B) of CD4⁺ and CD8⁺ cells in brain of WT and APP/PS1 mice. Mean frequency (C) and representative dot plots (D) of CD4⁺ cells stained positively for IFN- γ and IL-17 in brain of APP/PS1 mice. (E) Mean frequency of CD8⁺ in brain of tissue prepared from WT and APP/PS1 mice. (F) Mean frequency of CD8⁺ cells stained positively for IFN- γ and IL-17 in brain tissue prepared from APP/PS1 mice. ** p < 0.01, Student *t* test for independent means ($n \geq 4$), *** p < 0.001, Student *t* test for independent means. Representative of three experiments.

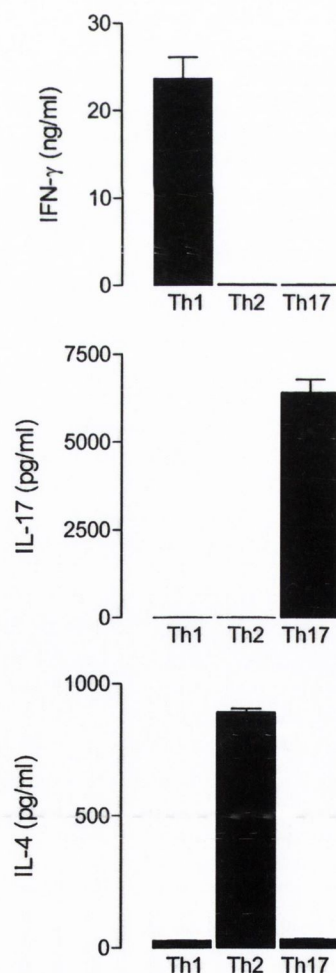


FIGURE 2. Cytokine production by *in vitro* polarized A β -specific T cells. Popliteal lymph nodes harvested from mice immunized with A β and CpG were cultured with A β _{1–42} in the presence of IL-12 to generate Th1 cells, dexamethasone, IL-4, and anti-IFN- γ to generate Th2 cells, or IL-23 and anti-IFN- γ to generate Th17 cells. IFN- γ , IL-4, and IL-17 concentrations were determined by ELISA on supernatants removed 3 d after stimulation with Ag and APC. Values are expressed as means \pm SEM ($n = 4$); representative of four experiments.

learning. Treatment of mice with anti-IFN- γ Ab ameliorated these changes, suggesting that release of IFN- γ from infiltrating Th1 cells accelerates the pathology in these animals.

Materials and Methods

Animals

APP/PS1 mice and wild-type (WT) littermates (6 to 7 mo old) were obtained from The Jackson Laboratory and subsequently bred in a specific pathogen-free unit in the Bioresources Unit in Trinity College Dublin. GFP mice were a gift from Matthew Campbell, School of Genetics and Microbiology, Trinity College Dublin. Mice used were transgenic animals on a C57/Bl6J background expressing eGFP cDNA under the control of a chicken β -actin promoter and CMV enhancer. All mice were maintained in controlled conditions (temperature 22 to 23°C, 12-h light-dark cycle, and food and water ad libitum) under veterinary supervision, and experimentation was carried out under a license granted by the Minister for Health and Children (Ireland) and with the appropriate ethical approval.

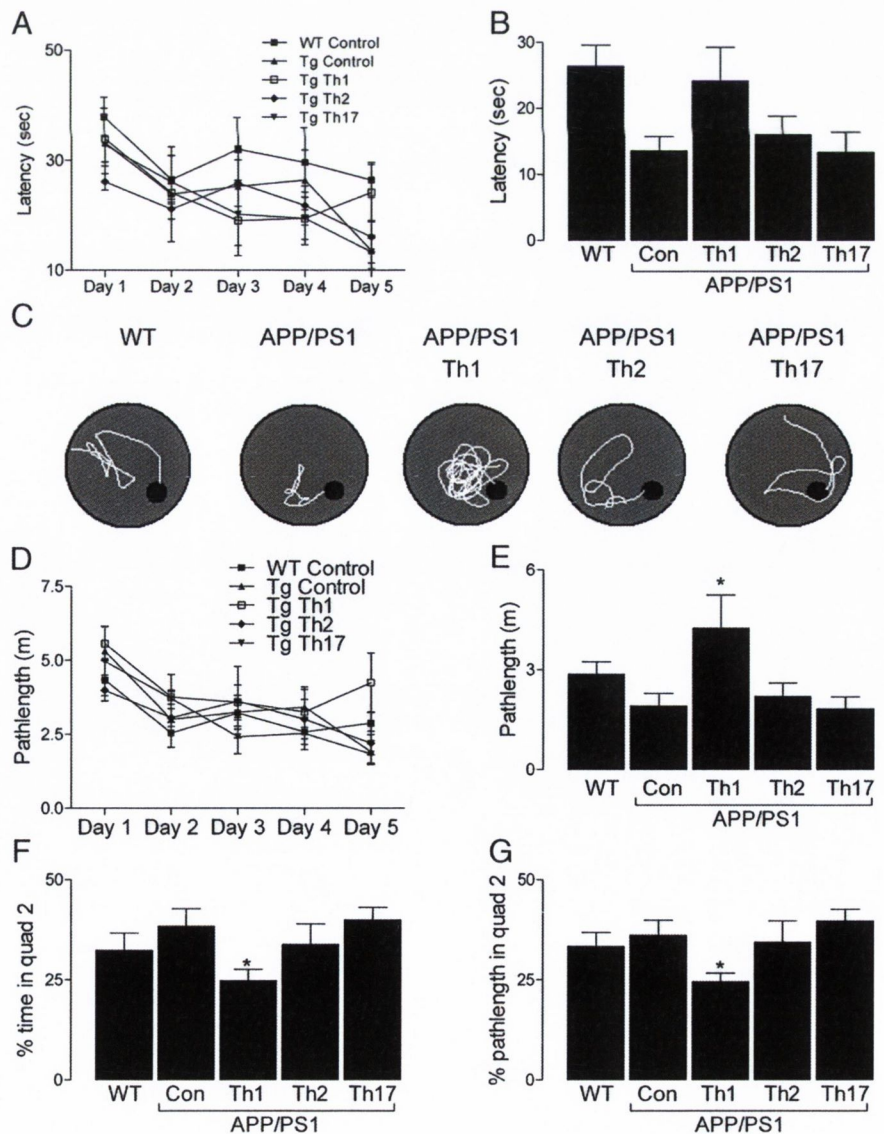
Isolation and FACS analysis on mononuclear cell isolation from CNS tissue

APP/PS1 mice and nontransgenic littermates were anesthetized with sodium pentobarbital (40 μ l) and perfused intracardially with sterile ice-cold PBS (20 ml). The brain was removed and placed in HBSS (2 ml) containing 3% FBS (HBSS/FBS; Sigma-Aldrich). Tissue was dissociated through a sterile 70- μ m nylon mesh filter, washed with HBSS/FBS, and

centrifuged at 170 \times g for 10 min at room temperature (RT). The supernatant was removed and the remaining pellet resuspended in HBSS/FBS (2 ml) containing collagenase D (1 mg/ml; Roche) and DNase I (10 μ g/ml; Sigma-Aldrich) and incubated for 1 h at 37°C. Cells were washed in HBSS/FBS and centrifuged at 1200 rpm for 5 min. Supernatants were removed, and cells were resuspended in 1.088 g/ml Percoll (9 ml; Sigma-Aldrich). This was underlaid with 1.122 g/ml Percoll (5 ml) and overlaid with 1.072 g/ml Percoll (9 ml) followed by 1.030 g/ml Percoll (9 ml) and finally PBS (9 ml). Percoll gradients were centrifuged at 1250 \times g for 45 min at 18°C. Mononuclear cells were removed from between the 1.088/1.072 and 1.072/1.030 g/ml interfaces, washed twice in HBSS/FBS, and counted.

Mononuclear cells prepared from CNS tissue were prepared for intracellular staining using a cell permeabilization kit (DakoCytomation). Cells were centrifuged at 1200 rpm for 5 min before stimulation with X-Vivo media (200 μ l) containing PMA (10 ng/ml; Sigma-Aldrich), ionomycin (1 μ g/ml; Sigma-Aldrich), and brefeldin A (5 μ g/ml; Sigma-Aldrich) for 5 h. Following stimulation, cells were centrifuged at 1200 rpm for 5 min and resuspended. Low-affinity IgG receptors (Fc γ RIII) were blocked by incubating cells in FACS buffer (50 μ l/sample) containing CD16/CD32 Fc γ RIII (1:100) for 10 min at RT. Cells were incubated in 50 μ l/sample FACS buffer containing the appropriate FACS Abs for 15 min at RT and fixed in IntraStain Reagent A (50 μ l/sample; DakoCytomation) for 15 min at RT. Cells were washed twice with FACS buffer and centrifuged at 1200 rpm for 5 min, permeabilized with IntraStain Reagent B (50 μ l/sample; DakoCytomation) plus intracellular Abs for 15 min at RT in the dark, washed twice in FACS buffer, and centrifuged at 1200 rpm for 5 min. Immunofluorescence analysis was performed on a DakoCytomation Cyan,

FIGURE 3. Spatial learning is impaired in APP/PS1 mice that received A β -specific Th1 cells. A β -specific Th1, Th2, and Th17 cells, generated as described in Fig. 2, were injected i.v. into APP/PS1 mice at 6 to 7 mo of age. Two weeks after injection, cognitive function was analyzed in the Morris Water Maze test. Training commenced after 1 d of habitation and continued for 5 consecutive days on which the mice underwent four 1-min trials with an inter-trial interval of 5 min. The day after the final day of training, the platform was removed, and mice were given a single 60-s probe trial. The percentage of time each animal spent swimming in the quadrant previously containing the platform was measured. Path length was also assessed. **(A)** The latency to reach the platform of all groups. **(B)** Mean latency on day 5 of training. **(C)** Sample paths for individual mice in each treatment group. **(D and E)** The path length taken to reach the platform. **(F and G)** In the probe test, the percentage of the total time and distance (i.e., path length) each animal spent swimming in the quadrant was measured. * $p < 0.05$, ANOVA; $n \geq 5$; representative of two experiments. Con, Control; Tg, transgenic.



data acquired using Summit software (DakoCytomation), and the results analyzed using FlowJo software (Tree Star).

Generation of A β -specific T cell lines and in vivo transfer

WT mice were immunized in the footpad with A β_{1-42} (75 μ g/mouse) and CpG (25 μ g/mouse) and boosted after 21 d. Mice were sacrificed 7 d later; the spleens and popliteal lymph nodes were harvested and restimulated with A β_{1-42} (25 μ g/ml) in the presence of IL-12 (10 ng/ml) to generate Th1 cells, dexamethasone (1×10^{-8} M), IL-4 (10 ng/ml), and anti-IFN- γ (5 μ g/ml) to generate Th2 cells, or IL-23 (10 ng/ml) and anti-IFN- γ (5 μ g/ml) to generate Th17 cells. After 4 d, IL-2 (5 ng/ml) was added to the Th1 and Th2 cell preparations, RPMI-1640 culture medium only was added to the Th17 cell cultures, and incubation continued for a further 7 d. Cells were washed and injected i.v. (15×10^6 cells/mouse in 300 μ l serum-free medium) into 6- to 7-mo-old APP/PS1 mice. Control animals received in 300 μ l serum-free medium alone. Behavior analysis was assessed 2 wk after T cell transfer. Samples of supernatant were assessed by ELISA (see below) for IFN- γ , IL-4, IL-10, IL-17, and IL-5 production.

In a separate series of experiments, 6- to 7-mo-old APP/PS1 and WT control mice were injected i.p. with anti-IFN- γ Ab (600 μ g) or a control Ab (anti- β -galactosidase: 600 μ g; R&D Systems) and after 24 h were injected i.v. with Th1 cells (15×10^6 cells/mouse) as described above. Anti-IFN- γ or anti- β -galactosidase Ab injections were repeated 3, 7, 10, 14, 17, 21, 24, 28, and 31 d after T cell transfer. Behavioral analysis was assessed 21 d after T cell transfer.

Tracking of A β -specific Th1 cells into the brain

A β -specific Th1 were generated from GFP mice immunized with A β_{1-42} and CpG, restimulated in vitro with A β_{1-42} and IL-12, and expanded with IL-2 as described above. Cells were washed and injected i.v. (15×10^6 cells/mouse) into 6- to 7-mo-old APP/PS1 mice or WT mice. Mice were sacrificed 14 d later and mononuclear cells prepared from CNS tissue. Cells were stimulated with PMA and ionomycin and stained for surface CD3, CD4, CD8, and intracellular IFN- γ . Immunofluorescence analysis was performed on a DakoCytomation Cyan as described above.

Behavioral analysis

Gait was analyzed in WT and APP/PS1 mice using the footprint test to assess stride length and hind and front limb base widths. Muscular strength and coordination were assessed using the inverted screen and wire-hang tests. Two days later, 2 wk after administration of A β -specific T cells, mice were tested for spatial memory in the Morris water maze. The pool (1.2 m diameter; 0.6 m high; 0.24 m water depth; 0.15 m platform diameter placed in the northwest quadrant of the pool; 0.13 m from the edge of the

pool) was sited in a well-lit room (22 to 23°C), and distinct visual cues were placed on the curtains that encircled the pool. Training commenced after 1 d of habitation and continued for 5 consecutive days on which the mice underwent four 1-min trials with an intertrial interval of 5 min. Each trial ended when mice located the platform or after 60 s when mice that failed to locate the platform were led to it; animals remained on the platform for 20 s. The day after the final day of training, the platform was removed, and mice were given a single 60-s probe trial. The percentage of time each animal spent swimming in the quadrant previously containing the platform was measured. Path length was also assessed.

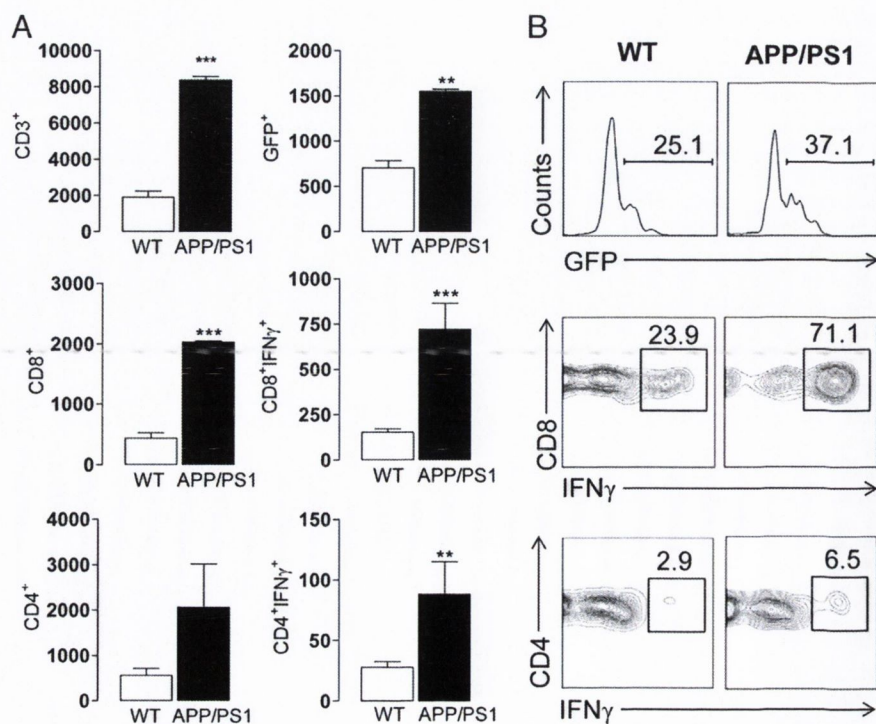
Preparation of tissue

In the first study, in which the effect of transfer of Th1, Th2, and Th17 cells was assessed, mice were killed 24 h after the last behavioral analysis. In the second study, in which the effect of anti-IFN- γ Ab was assessed, mice were killed 34 d after the first injection of Ab. They were anesthetized with sodium pentobarbital (40 μ l; Euthatal; Merial Animal Health) and perfused intracardially with ice-cold PBS (20 ml). The brains were rapidly removed, and one half of the brain was stored for later extraction and analysis of A β . The second half of the brain, which was used for immunohistochemical analysis, was placed onto cork discs, coated with optimum cooling temperature compound (Sakura Tissue-Tek), snap-frozen in prechilled isopropanol, and stored at -80°C . Before sectioning, the tissue was allowed to equilibrate to -20°C for 2 h. Sagittal sections (10- μ m thick) were prepared using a cryostat (Leica, Meyer, U.K.), mounted on gelatin-coated (Flukaerland) glass slides, allowed to dry for 20 min, and stored at -20°C for later immunohistochemical analysis.

Detection of A β

Snap-frozen cortical tissue was homogenized in five volumes (w/v) of homogenizing buffer (SDS/NaCl in distilled H $_2$ O [dH $_2$ O]) with proteases and centrifuged (15,000 rpm, 40 min, 4°C). The supernatant samples were removed to extract SDS-soluble A β , and the pellets were kept for extraction of insoluble A β . Supernatants were equalized (3 mg/ml) with homogenizing buffer using a BCA protein assay, and samples were neutralized by the addition of 10% (w/v) 0.5 M Tris-HCl (pH 6.8). Samples were stored at -20°C for later detection of soluble A β . Pellets were incubated in guanidine buffer (50 μ l; 5 M guanidine-HCl/50 mM Tris-HCl, pH 8; Sigma-Aldrich) for 4 h on ice. Samples were centrifuged (15,000 rpm, 30 min, 4°C), and the supernatant samples were equalized (0.3 mg/ml) with guanidine buffer and stored at -20°C for later detection of insoluble A β using MSD 96-well multi-spot 4G8 A β triple ultra-sensitive assay kits according to the manufacturer's instructions (Meso Scale Discovery). Standards (A β_{1-38} , 0–3,000 pg/ml; A β_{1-40} , 0–10,000 pg/ml; A β_{1-42} , 0–3,000 pg/ml) and samples were added to the 96-well plates, incubated

FIGURE 4. Transferred A β -specific Th1 cells migrate into the brain of APP/PS1 mice. A β -specific Th1 cells, generated from GFP mice were injected i.v. into 6- to 7-mo-old WT or APP/PS1 mice. Two weeks after injection, mice were sacrificed, and mononuclear cells were prepared from the brain. Cells were surface-stained with Abs specific for CD3, CD4, and CD8 and intracellularly stained for IFN- γ , and flow cytometric analysis was performed to quantify GFP-expressing and IFN- γ -secreting T cells in the brain. **(A)** Results are mean absolute number of the indicated cells in the brain. **(B)** Sample FACS plots of GFP $^+$ T cells (gated on CD3), IFN- γ^+ CD8 $^+$, and IFN- γ^+ CD4 $^+$ cells; number represent percentage positive. Data in (A) represent mean \pm SEM from four animals per experimental group from one experiment; data in (B) representative of four mice. ** $p < 0.01$, *** $p < 0.001$, Student t test for independent means.



(2 h, RT), washed, and read in a Sector Imager plate reader (Meso Scale Discovery) immediately after addition of the MSD read buffer. A β concentrations were calculated with reference to the standard curves and expressed as picograms per milliliter.

Immunohistochemistry

Cryostat sections were assessed for A β plaque deposition by staining with Congo red. Sections, equilibrated to RT, were fixed in ice-cold methanol for 5 min, washed in PBS, and incubated at room temperature for 20 min in an alkaline solution prepared by adding NaOH (2 ml; 1 M) to saturated NaCl (200 ml; 80% ethanol in dH₂O). Thereafter, sections were incubated in filtered Congo red solution (0.2% Congo red dye in the same alkaline solution) for 30 min, rinsed in dH₂O, incubated in methyl green solution (1% in dH₂O) for 30 s, washed, and dehydrated by dipping in 80, 95, and then 100% ethanol. Sections were dried, incubated in 100% xylene (3 \times 5 min), mounted onto slides using dibutyl phthalate in xylene (RA Lamb), and allowed to dry overnight.

To assess CD11b, sections were fixed in an acetone/ethanol mixture (1:1) for 5–10 min, and endogenous peroxidase activity was blocked by incubating in 0.3% H₂O₂ in PBS for 5 min. Sections were washed, blocked in 10% rabbit serum (Vector Laboratories), incubated overnight at 25°C in rat anti-CD11b Ab (1:100 in 5% rabbit serum in PBS; clone 5C6; Serotec), washed, and incubated for 2 h at RT in biotinylated rabbit anti-rat IgG (1:200 in 5% rabbit serum in PBS; Vector Laboratories). Sections were washed, incubated in Vectastain Elite ABC reagent (two drops of A/B in 5 ml PBS; Vector Laboratories) for 1 h at RT, washed, and developed using the substrate 3,3 diaminobenzidine–enhanced liquid substrate system tetrahydrochloride (one drop solution B in 1 ml solution A) for ~10 min until the color developed and counterstained with 1% methyl green for 10 min. Samples were dehydrated by dipping in graded ethanol (70, 80, 95, and 100%) and incubating in xylene (VWR International). Sections were

mounted with dibutyl phthalate in xylene, dried overnight, and stored at RT. The sections were examined using an Olympus lx51 light microscope (Olympus, Tokyo, Japan), and micrographs were taken using an Olympus UCMAD3 (Olympus) at \times 40 magnification. Data were quantified using the Immunoratio plugin (<http://imtmicroscope.uta.fi/immunoratio/>) available for the ImageJ software package (National Institutes of Health) (35). Colocalization of A β and CD11b was examined by confocal microscopy. Frozen brain sections brought to RT, fixed in ice-cold methanol, washed, permeabilized in 0.1% Triton (Sigma-Aldrich) in PHEM buffer, and washed. Nonspecific binding was blocked by incubating sections in 10% normal goat serum (2 h, RT), and sections were incubated overnight with pan-A β Ab (1:1000; Calbiochem) and rat anti-CD11b Ab (1:100, clone 5C6, AbD; Serotec) in 5% normal goat serum in PHEM buffer. Sections were washed, incubated in secondary Ab ALEXA 488 (1:4000; Invitrogen) and Alexa 546 (1:1000; Invitrogen; 90 min, RT), washed, mounted, and analyzed using confocal microscopy (Axioplan 2; Zeiss).

Statistical analysis

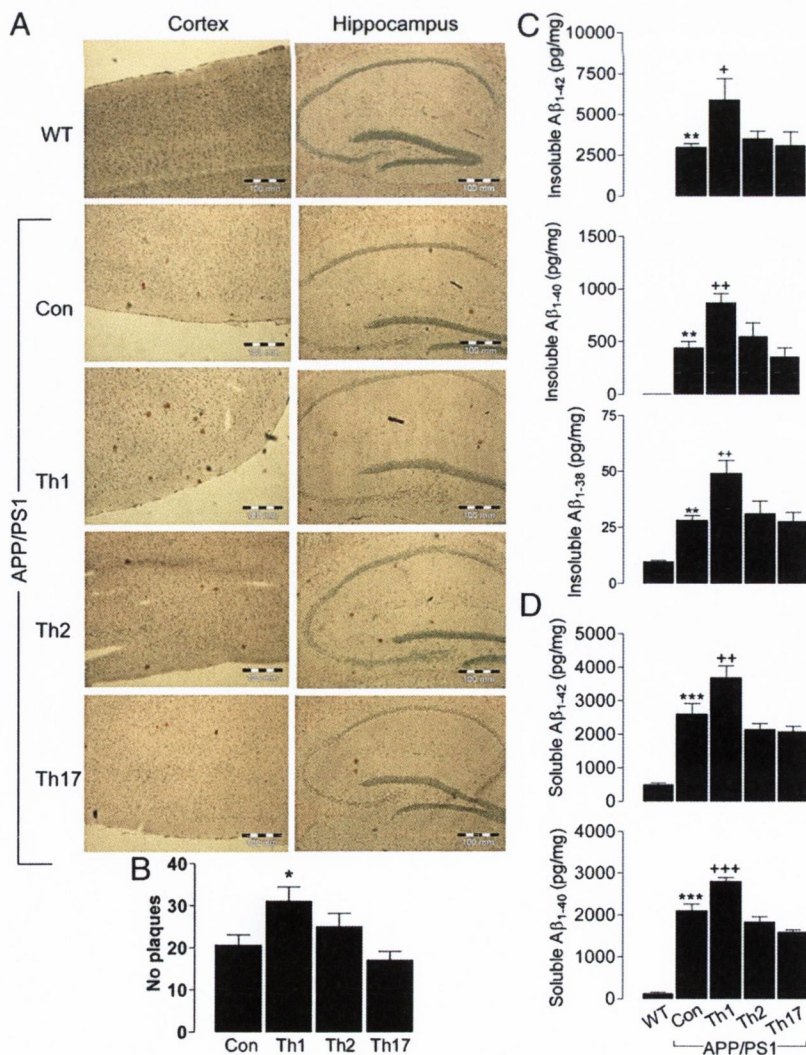
Statistical analysis was performed using GraphPad Prism (GraphPad). Data were analyzed using Student *t* test, two-way ANOVA, or one-way ANOVA followed by Newman–Keuls post hoc test. Data are expressed as means with SEM and deemed statistically significant when *p* < 0.05.

Results

Th1 and Th17 cell are present in the periphery and infiltrate the brains of APP/PS1 mice

We used flow cytometry to assess the presence of T cells in the brain of WT and APP/PS1 mice. We found that there were very few CD3⁺CD4⁺ cells in the brain of WT mice but a significantly

FIGURE 5. Transfer of A β -specific Th1 cells enhanced A β deposition in brains of APP/PS1 mice. APP/PS1 mice were injected with A β -specific Th1, Th2, or Th17 cells as described in Fig. 3. **(A)** Cryostat sections were stained with Congo red to assess A β -containing plaques in hippocampus and cortex; the mean number of plaques was recorded **(B)**. **(C)** The concentrations of insoluble A β _{1–42}, A β _{1–40}, and A β _{1–38} in the cortical tissue were quantified by ELISA. **(D)** The concentrations of soluble A β _{1–42} and A β _{1–40} in cortical tissue were quantified by ELISA. **p* < 0.05, ***p* < 0.01, ****p* < 0.001, ANOVA, APP/PS1 versus WT. †*p* < 0.05, ††*p* < 0.01, †††*p* < 0.001, ANOVA versus control untreated APP/PS1 mice (*n* = 5 to 6); representative of two experiments. Con, Control.



greater number in brain tissue prepared from APP/PS1 mice ($***p < 0.001$; Student *t* test for independent means; Fig. 1A). Intracellular staining revealed that a proportion of CD4⁺ cells stained positively for IFN- γ and also for IL-17 (Fig. 1B–D). There was no genotype-related difference in the number of CD3⁺CD8⁺ cells in the brain (Fig. 1E), although intracellular staining indicated that a greater proportion of these cells stained positively for IFN- γ compared with IL-17 ($**p < 0.01$; Student *t* test for independent means; Fig. 1F).

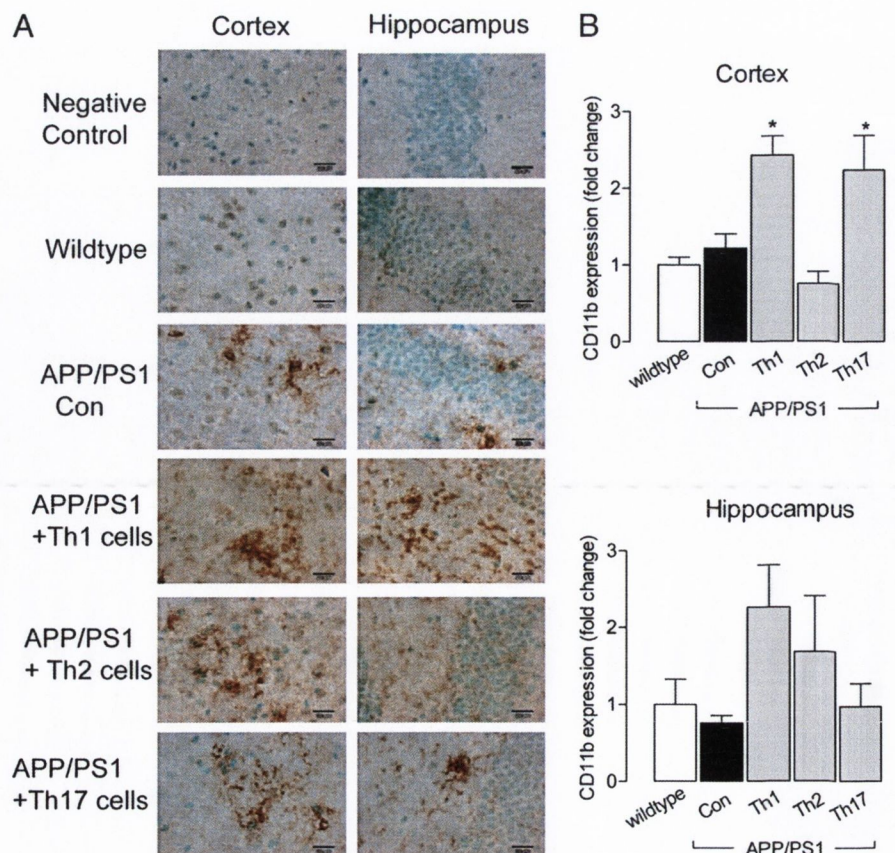
A β -specific Th1 cells impair cognitive function in APP/PS1 mice

Having demonstrated the presence of Th1 and Th17 cells in the brain of APP/PS1 mice, we set out to evaluate the effect of administration of A β -specific T cells on cognitive function, A β accumulation, and microglial activation in 6- to 7-mo-old APP/PS1 mice in which early pathological changes have been reported (36). To amplify A β -specific T cells, WT mice were immunized twice (0, 21 d) with A β and CpG, an adjuvant known to promote Th1 and Th17 responses. Short-term A β -specific Th1, Th2, and Th17 cell lines were generated by restimulation with Ag and APC in the presence of polarizing mixture described in the *Materials and Methods* section. This protocol resulted in the generation of highly polarized populations of Th1, Th2, and Th17 cells; Th1 cells produced high levels of IFN- γ and low IL-4 and IL-17, Th2 cells secreted high levels of IL-4 and low IL-17 and IFN- γ , and Th17 cells produced high levels of IL-17 and no IL-4 or IFN- γ (Fig. 2). After one round of Ag-stimulation, surviving T cells were washed and injected i.v. (15×10^6 cells/mouse) into 6- to 7-mo-old APP/PS1 or WT mice. Mice were tested for spatial memory in the Morris water maze 2 wk after administration of A β -specific T cells. The latency to reach the platform decreased over the 5-d training period but changes were similar in WT mice and control-treated APP/PS1 mice or APP/PS1 mice that received

T cells (Fig. 3A), and no treatment effect was observed on day 5 of training (Fig. 3B). The path length taken to reach the platform decreased with training, except in APP/PS1 mice, which received Th1 cells (Fig. 3D) as shown by the representative traces obtained on day 5 (Fig. 3C). The mean path length on day 5 was significantly increased in these mice compared with untreated APP/PS1 mice ($*p < 0.05$; ANOVA; Fig. 3E). In contrast, transfer of Th1 cells into WT mice had no significant effect on path length taken to reach the platform or mean path length on day 5 (Supplemental Fig. 1). The day after the final day of training, the platform was removed, and mice underwent a single 60-s probe trial. The percentage of the total time and distance (i.e., path length) each animal spent swimming in the quadrant that previously contained the platform was significantly decreased in APP/PS1 mice that received Th1 cells compared with untreated APP/PS1 mice ($*p < 0.05$; ANOVA; $n \geq 5$; Fig. 3F, 3G). Therefore, Th1 cell transfer induces a deficit in spatial learning in APP/PS1 mice at an age at which such deficits are not generally observed. Importantly, no motor deficits were observed in these animals; stride length, hind limb base width, and front limb base width were similar in all groups of mice, and, on the hangwire task, there were no differences in the latency to fall between groups (data not shown). These findings suggest that transfer of Th1, but not Th2 or Th17 cells, around the time of onset of A β plaque formation impairs cognitive function in APP/PS1 mice.

We tracked the migration of transferred T cells into the CNS using A β -specific Th1 cells generated from GFP mice immunized with A β and CpG and polarized with IL-12. We found a higher proportion of CD3⁺ T cells in the brain of APP/PS1, compared with WT, mice after transfer of A β -specific Th1 cells (Fig. 4). Furthermore, we detected GFP⁺ cells in the brain 14 d following transfer of Th1 cells, and this was significantly greater in APP/PS1 mice. Finally, we found that CD8⁺ as well as CD4⁺ cells infiltrated

FIGURE 6. Transfer of A β -specific Th1 cells increase CD11b immunoreactivity in hippocampus and cortex of APP/PS1 mice. APP/PS1 mice were injected with A β -specific Th1, Th2, or Th17 cells as described in Fig. 3. (A) Microglial activation was assessed by CD11b immunoreactivity. (B) Data are means \pm SEM. $*p < 0.05$, ANOVA versus control ($n = 3$ –5) representative of two experiments. Con, Control.



the brain, and a significant number of these secreted IFN- γ (Fig. 4). These findings suggested that at least a proportion of A β -specific Th1 cells migrate into the brain following systemic de-

livery, and this is more pronounced in APP/PS1 when compared with WT mice. In addition, IFN- γ -secreting CD8 T cells are detected in higher numbers in the brains of APP/PS1 compared with WT mice.

A β -specific Th1 cells enhance A β plaque burden and enhance microglial activation in APP/PS1 mice

A β deposition has been reported in the brain of APP/PS1 mice as early as 6 mo of age (37). Cryostat sections prepared from the 6- to 7-mo-old APP/PS1 mice used in this study confirm the presence of A β -containing plaques in cortex and hippocampus. Adoptive transfer of A β -specific Th1 cells markedly increased A β load, particularly in cortex, whereas transfer of Th2 or Th17 cells had little effect (Fig. 5A). Mean plaque number was significantly increased in sections prepared from mice that received Th1 cells ($*p < 0.05$; ANOVA; Fig. 5B). Insoluble A β_{1-38} , A β_{1-40} , and A β_{1-42} were all significantly increased in tissue prepared from APP/PS1, compared with WT, mice ($*p < 0.05$; $**p < 0.01$; ANOVA; Fig. 5C). Injection of Th1 cells induced a further increase in the concentration of the three A β species ($*p < 0.05$; $**p < 0.01$, ANOVA, versus control APP/PS1 mice). Furthermore, soluble A β_{1-40} and A β_{1-42} were also significantly increased in tissue prepared from APP/PS1 following transfer of Th1 cells (Fig. 5D), although soluble A β_{1-38} was unchanged between treatment groups (data not shown). Neither Th2 nor Th17 cells exerted any significant effect on soluble or insoluble A β .

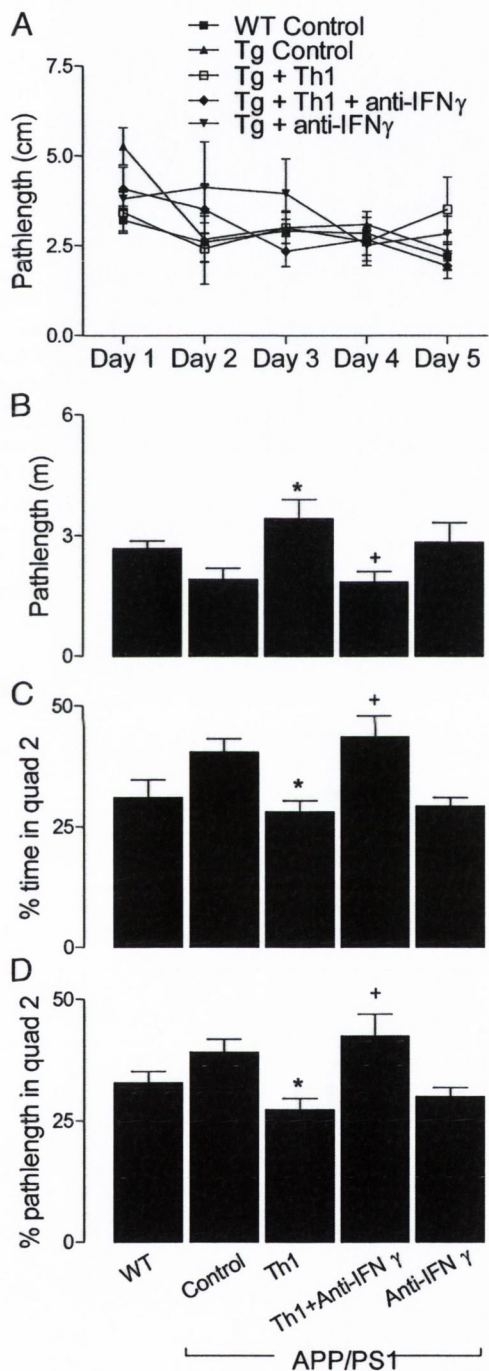


FIGURE 7. Anti-IFN- γ Ab attenuated the effect of Th1 cells on behavioral deficits. APP/PS1 mice were injected with A β -specific Th1 cells as described in Fig. 3, and mice were treated with anti-IFN- γ Ab or anti- β -galactosidase as a control Ab before and after injection of the cells. Three weeks after injection, cognitive function was analyzed in the Morris Water Maze test as described in Fig. 3. (A) The path length taken to reach the platform. (B) Mean path length on day 5 of training. (C and D) In the probe test, the time and path length in the quadrant that previously contained the platform (expressed as a percentage of the total) was measured. Data represent mean \pm SEM from four to five animals per experimental group from two experiments. $*p < 0.05$, ANOVA, APP/PS1+Th1 cells versus control APP/PS1 mice, $^+p < 0.05$, ANOVA, APP/PS1 + Th1 cells versus APP/PS1 plus Th1 cells plus anti-IFN- γ Ab. Tg, Transgenic.

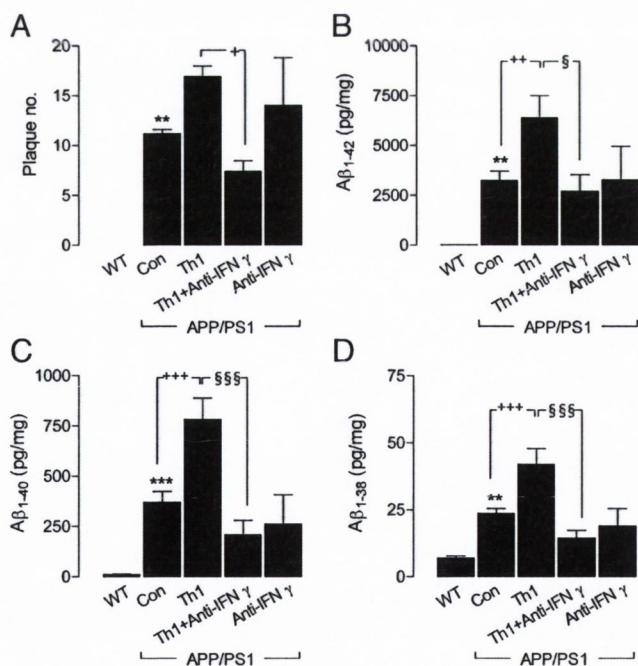


FIGURE 8. Anti-IFN- γ Ab attenuated the effect of Th1 cells on A β accumulation. APP/PS1 mice were injected with A β -specific Th1 cells and treated with anti-IFN- γ Ab or a control Ab as described in Fig. 6. Mice were sacrificed 5 wk after cell transfer. Cryostat sections were stained with Congo red to assess A β -containing plaques in hippocampus and cortex; the mean number of plaques was recorded (A), and the concentrations of insoluble A β_{1-42} (B), A β_{1-40} (C), and A β_{1-38} (D) were quantified by ELISA in brain tissue prepared from APP/PS1 and WT mice. Data represent mean \pm SEM from four to five animals per experimental group from two experiments. $**p < 0.01$, $***p < 0.001$, ANOVA; ($n = 4-6$); $^+p < 0.05$, $^{++}p < 0.01$, $^{+++}p < 0.001$, ANOVA; control APP/PS1 mice versus APP/PS1 mice that received Th1 cells; $^{\S}p < 0.05$; $^{\S\S\S}p < 0.001$, ANOVA, APP/PS1 + Th1 cells versus APP/PS1 + Th1 cells + anti-IFN- γ Ab. Con, Control.

Sections prepared from WT and APP/PS1 mice were assessed for CD11b immunoreactivity as a measure of microglial activation. Immunoreactivity was negligible in sections of hippocampus and cortex prepared from WT mice (Fig. 6), whereas CD11b staining was observed in both areas in some but not all APP/PS1 mice. Quantification of the data indicated that CD11b expression was markedly increased in APP/PS1 mice that received Th1 cells, and the increase was significant in the case of the cortex ($*p < 0.05$; ANOVA), where Th17 cells exerted a similar effect.

Neutralization of IFN- γ attenuates the effect of Th1 cells on behavioral deficits

Having shown a specific effect of Th1 cells on spatial memory and A β accumulation, we assessed the role of the key Th1 cytokine, IFN- γ , by treating APP/PS1 mice with a neutralizing anti-IFN- γ Ab prior to, and following, Th1 cell transfer. There was no significant effect of treatment on latency to reach the platform (data not shown), confirming the data shown in Fig. 3. However, we found that the path length taken to reach the platform decreased with training in all groups except in APP/PS1 mice, which received Th1 cells (Fig. 7A), and analysis of the mean data indicates that path length was significantly increased in this group compared with APP/PS1 mice that did not receive Th1 cells ($*p < 0.05$; ANOVA; Fig. 7B). Administration of anti-IFN- γ Ab significantly attenuated the Th1 cell-induced effect ($^{\dagger}p < 0.05$, ANOVA, versus APP/PS1 mice that received Th1 cells). In the probe test, treatment with Th1 cells decreased the percentage of the total time and distance each animal spent swimming in the quadrant that previously contained the platform ($*p < 0.05$; ANOVA; Fig. 7C, 7D), confirming the findings presented in Fig. 3. Treatment with anti-IFN- γ significantly reversed the effect of Th1 cells ($^{\dagger}p < 0.05$, ANOVA, versus APP/PS1 mice that received Th1 cells).

Neutralization of IFN- γ attenuates the effect of Th1 cells on A β plaque burden

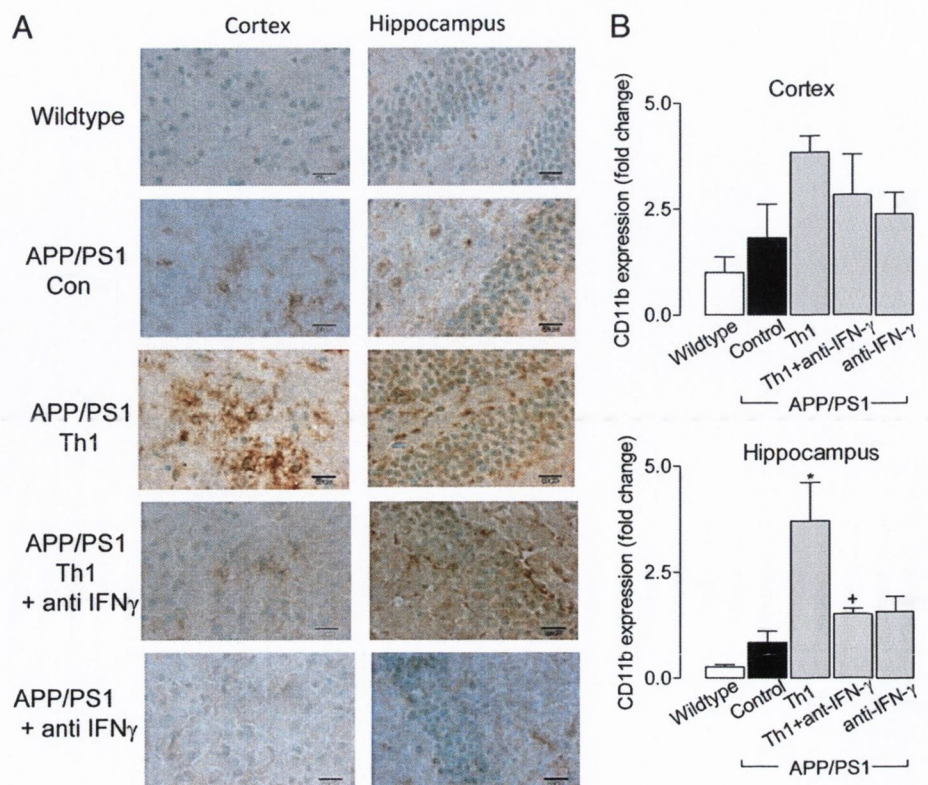
Anti-IFN- γ Ab attenuated the effects of Th1 cells on plaque number and concentration of insoluble A β_{1-38} , A β_{1-40} , and A β_{1-42} in tissue prepared from APP/PS1 mice (Fig. 8). These measures were increased in tissue prepared from APP/PS1 mice compared with WT mice ($**p < 0.01$, $***p < 0.001$, ANOVA; Fig. 8), and these were significantly increased by administration of Th1 cells ($^{\dagger}p < 0.05$, $^{++}p < 0.01$, $^{+++}p < 0.001$, ANOVA, control APP/PS1 mice versus APP/PS1 mice that received Th1 cells). The increase in A β_{1-38} , A β_{1-40} , and A β_{1-42} induced by Th1 cells was attenuated when mice were treated with anti-IFN- γ Ab ($^{\dagger}p < 0.05$, $^{§§}p < 0.001$, ANOVA, APP/PS1 mice that received Th1 cells versus Ab-treated APP/PS1 mice that received Th1 cells).

CD11b immunoreactivity was negligible in sections prepared from hippocampus and cortex of WT mice (Fig. 9), whereas some staining was observed in both areas in APP/PS1 mice. This was greater in APP/PS1 mice that received Th1 cells, but this effect was ameliorated to some degree in sections prepared from APP/PS1 mice that received Th1 cells and anti-IFN- γ Ab. Immunoreactivity was similar in sections prepared from control APP/PS1 mice and APP/PS1 mice, which received anti-IFN- γ Ab. Analysis of staining using confocal microscopy indicated that CD11b immunoreactivity (green staining; Fig. 10) was colocalized with A β deposition (red staining) in hippocampus and cortex. As shown in Figs. 6 and 9, A β accumulation was increased in sections prepared from APP/PS1 mice, which received Th1 cells, and this effect was attenuated by anti-IFN- γ Ab treatment (Fig. 10). These findings demonstrate that the impact of Th1 cells on A β plaque burden and microglial activation was mediated through IFN- γ .

Discussion

The significant finding of this study is that adoptive transfer of Th1 cells increases A β accumulation and microglial activation in

FIGURE 9. Anti-IFN- γ Ab attenuated the effect of Th1 cells on CD11b immunoreactivity. APP/PS1 mice were injected with A β -specific Th1 cells and treated with anti-IFN- γ Ab or a control Ab as described in Fig. 6. Mice were sacrificed 5 wk after T cell transfer. **(A)** Microglial activation was assessed by CD11b immunoreactivity in the cortex and hippocampus. **(B)** Data are means \pm SEM. Data represent mean \pm SEM from four to seven animals per experimental group from two experiments. $*p < 0.05$, ANOVA, versus control, $^{\dagger}p < 0.05$, ANOVA, versus Th1. Con, Control.



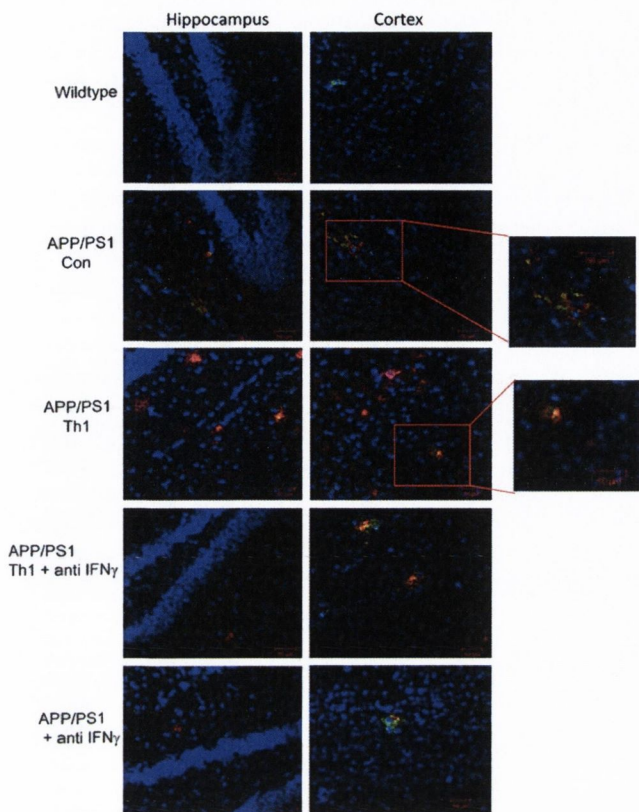


FIGURE 10. Anti-IFN- γ Ab attenuated the effect of Th1 cells on CD11b immunoreactivity. APP/PS1 mice were injected with A β -specific Th1 cells and treated with anti-IFN- γ Ab or a control Ab as described in Fig. 6. Mice were sacrificed 5 wk after T cell transfer. Microglial activation and A β deposition was assessed by confocal microscopy. Cells were stained with DAPI (nuclei; blue), amyloid- β (red), and CD11b (green). Original magnification $\times 40$ and enlarged panels $\times 60$. Data are representative of five mice per experimental group from two experiments. Con, Control.

the brain of 6- to 7-mo-old APP/PS1 mice and impairs performance in a Morris water maze; these effects are attenuated by treatment of mice with anti-IFN- γ Ab.

It has been recognized for some time that T cells can infiltrate the brain (38, 39). T cell infiltration is significantly enhanced under pathological conditions (for example, in multiple sclerosis and EAE), and this is due, at least to some extent, to an increase in blood-brain barrier permeability (23, 40). In this study, we report that there is a significant increase in the number of CD3⁺CD4⁺ cells in the brain of APP/PS1 mice compared with WT mice and that a proportion of these are Th1 and Th17 cells. Consistent with this is the observation that significant numbers of peripheral T cells are present in the postmortem brain of AD patients compared with the relatively low numbers of cells in other degenerative dementia cases and, importantly, that these cells are clustered in areas of the brain in which pathology is more marked, such as the hippocampus and limbic regions (25). However, the role of T cells in the pathogenesis of AD is not clear, with circumstantial evidence of both host protective and damaging roles for A β -specific T cells. Peripheral T cells specific for A β_{1-40} have been detected in healthy individuals, but were absent in patients with AD (41), possibly suggesting that A β_{1-40} -specific T cells may prevent the development of A β plaques. It has also been reported that Th1 cells directed against A β_{1-42} are present in young individuals but decline with age and are lost in patients with AD, in whom IL-10-producing regulatory T cells predominate (42).

Vaccine studies in mouse models have shown that immunization with A β_{42} in CFA prevented the development of A β plaques and reduced the development of AD-like neuropathology (33, 43). The protection was associated with Ab and could be mimicked by passive transfer of A β -specific Abs (44). There is also evidence from a clinical trial that active immunization with A β_{42} , formulated with the adjuvant QS21 (AN 1792), can reduce plaque burden in AD patients (45), though a number of patients developed meningoencephalitis, and the trial was halted. Although the cause of the meningoencephalitis is not clear, it has been suggested that it could result from the induction of inflammatory T cell responses (46). Interestingly, QS-21, the adjuvant used in AD vaccine, has been shown to promote Th1 responses to coadministered foreign Ag in mice (47). Our findings are consistent with a pathogenic role for Th1 cells, at least in a mouse model of AD.

To evaluate the impact of different T cell subtypes on plaque burden in the brain, we adoptively transferred A β -specific Th1, Th2, and Th17 cells into 6- to 7-mo-old APP/PS1 mice. Consistent with previous findings (36), we found that there was some A β accumulation in the brain of the 6-mo-old APP/PS1 mice. This was accompanied by increased concentrations of A β_{1-42} , A β_{1-40} , and A β_{1-38} in cortical tissue. However, transfer of Th1 cells increased deposition of A β (determined by Congo red staining) and markedly increased cortical A β concentration. This suggests that A β -specific Th1 cells may play a role in the development of A β plaques in the brain. This was confirmed by treatment of mice with a neutralizing anti-IFN- γ Ab, which attenuated the effect of Th1 cells on A β accumulation. In contrast with the effect of Th1 cells, transfer of Th17 cells, which have been associated with pathology in EAE and other autoimmune/inflammatory diseases, and Th2 cells, which have a more anti-inflammatory function in other diseases, did not enhance A β accumulation in the brain. These findings are consistent with our earlier report that A β -specific Th1 cells enhance proinflammatory cytokine production and MHC class II and costimulatory molecule expression by A β -stimulated microglia, whereas A β -specific Th2 cells suppress cytokine production by glial cells (32).

Under resting conditions, microglia are maintained in a quiescent state in the brain because of the presence of neuroimmune regulatory molecules that enable the interaction with other cells, low concentrations of stimulatory factors such as IFN- γ and other inflammatory cytokines, and the presence of minimal numbers of immune cells like T cells (13). However, microglial activation occurs following any insult, and an activated state is a characteristic of most, if not all, neurodegenerative diseases in which these cells can assume the role of APC. Modest microglial activation was observed in the hippocampus and cortex of 6- to 7-mo-old APP/PS1 mice but transfer of Th1 cells markedly increased activation. This is consistent with our previous findings that showed that A β -specific Th1 cells increased microglial activation *in vitro* (32). In parallel with its effect on A β accumulation, treatment of mice with anti-IFN- γ Ab attenuated the effect of Th1 cells on microglial activation. It is well established that IFN- γ is among the most potent activators of microglia (15, 48) and synergizes with A β to increase expression of cell-surface markers of activation and production of inflammatory cytokines (15, 49). Chakrabarty et al. (50) reported that viral delivery of IFN- γ gene promotes microglial activation and clearance of A β . We observed that Th1 cells also promoted microglial activation but that this was associated with an increase in A β plaques. We do not have a definitive explanation for the discrepancy in these studies other than the differences in the experimental approaches: virally-delivered IFN- γ , which had effects, such as basal ganglia calcification, in

WT as well as Tg mice, compared with i.v. injected A β -specific Th1 cells, in which the effects were largely confined to Tg mice. One interpretation of the data, as suggested in this study, is that anti-IFN- γ prevents Th1 cell-induced activation of microglia, but it is possible that the Ab treatment affects infiltration of cells, perhaps by altering chemotaxis or exerting an effect on blood-brain barrier permeability.

Our studies with Th1 cells expressing GFP demonstrated that at least a proportion of the transferred Th1 cells did migrate from the periphery into the CNS. Interestingly, IFN- γ -secreting CD8 as well as CD4 T cells were detected in the brain following i.v. injection of A β -specific Th1 cells. This is consistent with studies in the EAE model that have demonstrated that Th1 cells preferentially infiltrate the CNS and facilitate recruitment of other inflammatory T cells (51). Interestingly, the migration of T cells into the brain and subsequent behavioral deficits was significantly more pronounced following transfer of A β -specific Th1 cells into APP/PS1 when compared with WT mice. This may reflect the higher A β burden in the APP/PS1 mice and might suggest local Ag stimulation of IFN- γ -secreting T cells, which were at a significantly higher frequency in the brains of APP/PS1 compared with WT mice.

Previous studies from this laboratory have shown that A β -specific Th1 cells enhanced A β -induced activation of microglia (32). Furthermore, the increase in microglial activation in APP/PS1 mice was accompanied by increased expression of inflammatory cytokines, including TNF- α and IL-1 β (52). Interestingly, TNF- α and IL-1 β have been shown to increase activity and/or expression of γ - and β -secretases (6, 7), which leads to A β deposition. Although activated microglia may phagocytose and remove A β aggregates (50), IL-1 β -expressing microglia are associated with A β plaques and neurofibrillary tangles in the brain of AD patients, where they correlate with progressive neuronal damage (53). Furthermore, IL-1 β can promote synthesis of APP in endothelial cells (54). It has also been reported that IFN- γ -induced activation of microglia enhanced processing of APP and suppressed A β clearance (55). We found that Th1 cells, which increase IL-1 β expression by microglia (32), enhanced soluble and insoluble A β concentrations in the brains of APP/PS1 mice. However, it must be acknowledged that A β potently activates microglia in vitro and in vivo (56, 57), and therefore it is possible that there may be a feedback loop, leading to persistent microglial activation and A β accumulation with the subsequent pathogenic consequences.

Although there was significant A β accumulation in the brain of 6- to 7-mo-old APP/PS1 mice, we found no evidence of genotype-related changes during the training phase in the Morris water maze or during the probe test, contrasting with previous reports that indicated a deficit in slightly older (8-mo-old) APP/PS1 mice (58, 59). It has been suggested that cognitive deficits correlate with insoluble A β in Tg2576 mice (60) and APP/PS1 mice (61), but this view is not supported by the present findings. However, we report that transfer of Th1 cells doubled the concentration of insoluble A β in brain tissue, and this was associated with deterioration in cognitive function in the probe test; this raises the possibility that a threshold concentration of A β must be reached before an impact on spatial learning is exerted. In contrast to the effect of Th1 cells on APP/PS1 mice, transfer of Th2 cells or Th17 cells exerted no effect in the spatial learning task or on either plaque number or A β accumulation. The present findings are at variance with an earlier report that indicated that adoptive transfer of a mixed T cell preparation improved performance of 10-mo-old APP/PS1 mice in a radial arm maze task (62). Although no effect on insoluble A β or A β plaque numbers was observed, the authors

suggested that microglia or monocytes were stimulated to clear A β because the distribution of A β -immunoreactive cells in hippocampus of mice that received T cells was similar to the distribution of MHC class II-positive cells. More recent data from this group suggested that the beneficial effects on behavior may be Th2 cell-mediated because the effect was evident when T cells had been incubated in vitro in the presence of IL-2 and IL-4 (31). We have recently reported that the A β -induced microglia activation in vitro is attenuated by Th2 cells (32), and the current study found that Th2 cells, unlike Th1 cells, did not enhance plaque burden in vivo.

Although beneficial effects of T cells in the brain have also been observed (63), the evidence presented in this study indicates that Th1 cells, but not Th2 or Th17 cells, contribute to A β accumulation and development of a functional deficit in APP/PS1 mice during the early stages of development of pathology. In this model, the effects appear to be mediated by IFN- γ and are associated with enhanced microglial activation, which may trigger inflammatory changes that propagate a damaging cascade of events and further development of pathology.

Acknowledgments

We thank Barry Moran (School of Biochemistry and Immunology, Trinity College Dublin) for assistance with cell sorting and Mathew Campbell (School of Genetics and Microbiology, Trinity College Dublin) for supplying GFP mice.

Disclosures

K.H.G.M. is a cofounder and shareholder in Opona Therapeutics and TriMod Therapeutics Ltd., startup companies involved in the development of immunotherapeutics. The other authors have no financial conflict of interest.

References

- Breitner, J. C. 1996. The role of anti-inflammatory drugs in the prevention and treatment of Alzheimer's disease. *Annu. Rev. Med.* 47: 401-411.
- Heneka, M. T., M. P. Kummer, S. Weggen, B. Bulic, G. Multhaup, L. M. Hünter, M. Hüll, T. Pflanzner, and C. U. Pietrzik. 2011. Molecular mechanisms and therapeutic application of NSAIDs and derived compounds in Alzheimer's disease. *Curr. Alzheimer Res.* 8: 115-131.
- Varvel, N. H., K. Bhaskar, M. Z. Kounnas, S. L. Wagner, Y. Yang, B. J. Lamb, and K. Herrup. 2009. NSAIDs prevent, but do not reverse, neuronal cell cycle reentry in a mouse model of Alzheimer disease. *J. Clin. Invest.* 119: 3692-3702.
- Cagnin, A., D. J. Brooks, A. M. Kennedy, R. N. Gunn, R. Myers, F. E. Turkheimer, T. Jones, and R. B. Banati. 2001. In-vivo measurement of activated microglia in dementia. *Lancet* 358: 461-467.
- Okello, A., P. Edison, H. A. Archer, F. E. Turkheimer, J. Kennedy, R. Bullock, Z. Walker, A. Kennedy, N. Fox, M. Rossor, and D. J. Brooks. 2009. Microglial activation and amyloid deposition in mild cognitive impairment: a PET study. *Neurology* 72: 56-62.
- Liao, Y. F., B. J. Wang, H. T. Cheng, L. H. Kuo, and M. S. Wolfe. 2004. Tumor necrosis factor- α , interleukin-1 β , and interferon- γ stimulate gamma-secretase-mediated cleavage of amyloid precursor protein through a JNK-dependent MAPK pathway. *J. Biol. Chem.* 279: 49523-49532.
- Sastre, M., J. Walter, and S. M. Gentleman. 2008. Interactions between APP secretases and inflammatory mediators. *J. Neuroinflammation* 5: 25.
- Glass, C. K., K. Saijo, B. Winner, M. C. Marchetto, and F. H. Gage. 2010. Mechanisms underlying inflammation in neurodegeneration. *Cell* 140: 918-934.
- Tan, J., T. Town, F. Crawford, T. Mori, A. DelleDonne, R. Crescentini, D. Obregon, R. A. Flavell, and M. J. Mullan. 2002. Role of CD40 ligand in amyloidosis in transgenic Alzheimer's mice. *Nat. Neurosci.* 5: 1288-1293.
- Tan, J., T. Town, D. Paris, T. Mori, Z. Suo, F. Crawford, M. P. Mattson, R. A. Flavell, and M. J. Mullan. 1999. Microglial activation resulting from CD40-CD40L interaction after beta-amyloid stimulation. *Science* 286: 2352-2355.
- Town, T., Y. Laour, C. Pittenger, T. Mori, C. A. Szekely, J. Tan, R. S. Duman, and R. A. Flavell. 2008. Blocking TGF- β -Smad2/3 innate immune signaling mitigates Alzheimer-like pathology. *Nat. Med.* 14: 681-687.
- Colton, C. A., and D. M. Wilcock. 2010. Assessing activation states in microglia. *CNS Neurol. Disord. Drug Targets* 9: 174-191.
- Colton, C. A., R. T. Mott, H. Sharpe, Q. Xu, W. E. Van Nostrand, and M. P. Vitek. 2006. Expression profiles for macrophage alternative activation genes in AD and in mouse models of AD. *J. Neuroinflammation* 3: 27.
- Aloisi, F. 2001. Immune function of microglia. *Glia* 36: 165-179.

15. Benveniste, E. N., V. T. Nguyen, and G. M. O'Keefe. 2001. Immunological aspects of microglia: relevance to Alzheimer's disease. *Neurochem. Int.* 39: 381–391.
16. Kim, W. K., X. Alvarez, J. Fisher, B. Bronfin, S. Westmoreland, J. McLaurin, and K. Williams. 2006. CD163 identifies perivascular macrophages in normal and viral encephalitic brains and potential precursors to perivascular macrophages in blood. *Am. J. Pathol.* 168: 822–834.
17. Guillemin, G. J., and B. J. Brew. 2004. Microglia, macrophages, perivascular macrophages, and pericytes: a review of function and identification. *J. Leukoc. Biol.* 75: 388–397.
18. Audoy-Rémus, J., J. F. Richard, D. Soulet, H. Zhou, P. Kubes, and L. Vallières. 2008. Rod-shaped monocytes patrol the brain vasculature and give rise to perivascular macrophages under the influence of proinflammatory cytokines and angiopoietin-2. *J. Neurosci.* 28: 10187–10199.
19. Serrats, J., J. C. Schiltz, B. García-Bueno, N. van Rooijen, T. M. Reyes, and P. E. Sawchenko. 2010. Dual roles for perivascular macrophages in immune-to-brain signaling. *Neuron* 65: 94–106.
20. Desai, B. S., A. J. Monahan, P. M. Carvey, and B. Hendey. 2007. Blood-brain barrier pathology in Alzheimer's and Parkinson's disease: implications for drug therapy. *Cell Transplant.* 16: 285–299.
21. Garbuzova-Davis, S., S. Saporta, E. Haller, I. Kolomey, S. P. Bennett, H. Potter, and P. R. Sanberg. 2007. Evidence of compromised blood-spinal cord barrier in early and late symptomatic SOD1 mice modeling ALS. *PLoS ONE* 2: e1205.
22. Rosenberg, G. A. 2012. Neurological diseases in relation to the blood-brain barrier. *J. Cereb. Blood Flow Metab.* 32: 1139–1151.
23. Fletcher, J. M., S. J. Lalor, C. M. Sweeney, N. Tubridy, and K. H. Mills. 2010. T cells in multiple sclerosis and experimental autoimmune encephalomyelitis. *Clin. Exp. Immunol.* 162: 1–11.
24. Murphy, A. C., S. J. Lalor, M. A. Lynch, and K. H. Mills. 2010. Infiltration of Th1 and Th17 cells and activation of microglia in the CNS during the course of experimental autoimmune encephalomyelitis. *Brain Behav. Immun.* 24: 641–651.
25. Togo, T., H. Akiyama, E. Iseki, H. Kondo, K. Ikeda, M. Kato, T. Oda, K. Tsuchiya, and K. Kosaka. 2002. Occurrence of T cells in the brain of Alzheimer's disease and other neurological diseases. *J. Neuroimmunol.* 124: 83–92.
26. Town, T., J. Tan, R. A. Flavell, and M. Mullan. 2005. T-cells in Alzheimer's disease. *Neuromolecular Med.* 7: 255–264.
27. Itagaki, S., P. L. McGeer, and H. Akiyama. 1988. Presence of T-cytotoxic suppressor and leucocyte common antigen positive cells in Alzheimer's disease brain tissue. *Neurosci. Lett.* 91: 259–264.
28. Rogers, J., J. Luber-Narod, S. D. Styren, and W. H. Civin. 1988. Expression of immune system-associated antigens by cells of the human central nervous system: relationship to the pathology of Alzheimer's disease. *Neurobiol. Aging* 9: 339–349.
29. Town, T., V. Nikolic, and J. Tan. 2005. The microglial "activation" continuum: from innate to adaptive responses. *J. Neuroinflammation* 2: 24.
30. Carson, M. J., J. C. Thrash, and B. Walter. 2006. The cellular response in neuroinflammation: The role of leukocytes, microglia and astrocytes in neuronal death and survival. *Clin. Neurosci. Res.* 6: 237–245.
31. Cao, C., G. W. Arendash, A. Dickson, M. B. Mamczarz, X. Lin, and D. W. Ethell. 2009. Abeta-specific Th2 cells provide cognitive and pathological benefits to Alzheimer's mice without infiltrating the CNS. *Neurobiol. Dis.* 34: 63–70.
32. McQuillan, K., M. A. Lynch, and K. H. Mills. 2010. Activation of mixed glia by Abeta-specific Th1 and Th17 cells and its regulation by Th2 cells. *Brain Behav. Immun.* 24: 598–607.
33. Schenk, D., R. Barbour, W. Dunn, G. Gordon, H. Grajeda, T. Guido, K. Hu, J. Huang, K. Johnson-Wood, K. Khan, et al. 1999. Immunization with amyloid-beta attenuates Alzheimer-disease-like pathology in the PDAPP mouse. *Nature* 400: 173–177.
34. Orgogozo, J. M., S. Gilman, J. F. Dartigues, B. Laurent, M. Puel, L. C. Kirby, P. Jouanny, B. Dubois, L. Eisner, S. Flitman, et al. 2003. Subacute meningo-encephalitis in a subset of patients with AD after Abeta42 immunization. *Neurology* 61: 46–54.
35. Tuominen, V. J., S. Ruotoistenmäki, A. Viitanen, M. Jumppanen, and J. Isola. 2010. ImmunoRatio: a publicly available web application for quantitative image analysis of estrogen receptor (ER), progesterone receptor (PR), and Ki-67. *Breast Cancer Res.* 12: R56.
36. Jankowsky, J. L., D. J. Fadale, J. Anderson, G. M. Xu, V. Gonzales, N. A. Jenkins, N. G. Copeland, M. K. Lee, L. H. Younkin, S. L. Wagner, et al. 2004. Mutant presenilins specifically elevate the levels of the 42 residue beta-amyloid peptide in vivo: evidence for augmentation of a 42-specific gamma secretase. *Hum. Mol. Genet.* 13: 159–170.
37. Janus, C., and D. Westaway. 2001. Transgenic mouse models of Alzheimer's disease. *Physiol. Behav.* 73: 873–886.
38. Hickey, W. F. 1991. Migration of hematogenous cells through the blood-brain barrier and the initiation of CNS inflammation. *Brain Pathol.* 1: 97–105.
39. Hickey, W. F. 2001. Basic principles of immunological surveillance of the normal central nervous system. *Glia* 36: 118–124.
40. Minagar, A., and J. S. Alexander. 2003. Blood-brain barrier disruption in multiple sclerosis. *Mult. Scler.* 9: 540–549.
41. Trieb, K., G. Ransmayr, R. Sgonc, H. Lassmann, and B. Grubeck-Loebenstein. 1996. APP peptides stimulate lymphocyte proliferation in normals, but not in patients with Alzheimer's disease. *Neurobiol. Aging* 17: 541–547.
42. Loewenbrueck, K. F., J. T. Tigno-Aranjuez, B. O. Boehm, P. V. Lehmann, and M. Tary-Lehmann. 2010. Th1 responses to beta-amyloid in young humans convert to regulatory IL-10 responses in Down syndrome and Alzheimer's disease. *Neurobiol. Aging* 31: 1732–1742.
43. Janus, C., J. Pearson, J. McLaurin, P. M. Mathews, Y. Jiang, S. D. Schmidt, M. A. Chishti, P. Horne, D. Heslin, J. French, et al. 2000. A beta peptide immunization reduces behavioural impairment and plaques in a model of Alzheimer's disease. *Nature* 408: 979–982.
44. Bard, F., C. Cannon, R. Barbour, R. L. Burke, D. Games, H. Grajeda, T. Guido, K. Hu, J. Huang, K. Johnson-Wood, et al. 2000. Peripherally administered antibodies against amyloid beta-peptide enter the central nervous system and reduce pathology in a mouse model of Alzheimer disease. *Nat. Med.* 6: 916–919.
45. Schenk, D. 2002. Amyloid-beta immunotherapy for Alzheimer's disease: the end of the beginning. *Nat. Rev. Neurosci.* 3: 824–828.
46. Ferrer, I., M. Boada Rovira, M. L. Sánchez Guerra, M. J. Rey, and F. Costa-Jussà. 2004. Neuropathology and pathogenesis of encephalitis following amyloid-beta immunization in Alzheimer's disease. *Brain Pathol.* 14: 11–20.
47. Moore, A., L. McCarthy, and K. H. Mills. 1999. The adjuvant combination monophosphoryl lipid A and QS21 switches T cell responses induced with a soluble recombinant HIV protein from Th2 to Th1. *Vaccine* 17: 2517–2527.
48. Lyons, A., K. J. Murphy, R. Clarke, and M. A. Lynch. 2011. Atorvastatin prevents age-related and amyloid- β -induced microglial activation by blocking interferon- γ release from natural killer cells in the brain. *J. Neuroinflammation* 8: 27.
49. Meda, L., M. A. Cassatella, G. I. Szendrei, L. Otvos, Jr., P. Baron, M. Villalba, D. Ferrari, and F. Rossi. 1995. Activation of microglial cells by beta-amyloid protein and interferon-gamma. *Nature* 374: 647–650.
50. Chakrabarty, P., C. Ceballos-Diaz, A. Beccard, C. Janus, D. Dickson, T. E. Golde, and P. Das. 2010. IFN-gamma promotes complement expression and attenuates amyloid plaque deposition in amyloid beta precursor protein transgenic mice. *J. Immunol.* 184: 5333–5343.
51. O'Connor, R. A., C. T. Prendergast, C. A. Sabatos, C. W. Lau, M. D. Leech, D. C. Wraith, and S. M. Anderton. 2008. Cutting edge: Th1 cells facilitate the entry of Th17 cells to the central nervous system during experimental autoimmune encephalomyelitis. *J. Immunol.* 181: 3750–3754.
52. Gallagher, J. J., M. E. Finnegan, B. Grehan, J. Dobson, J. F. Collingwood, and M. A. Lynch. 2012. Modest amyloid deposition is associated with iron dysregulation, microglial activation, and oxidative stress. *J. Alzheimers Dis.* 28: 147–161.
53. Mrak, R. E. 2012. Microglia in Alzheimer brain: a neuropathological perspective. *Int. J. Alzheimers Dis.* 2012: 165021.
54. Goldgaber, D., H. W. Harris, T. Hla, T. Maciag, R. J. Donnelly, J. S. Jacobsen, M. P. Vitek, and D. C. Gajdusek. 1989. Interleukin 1 regulates synthesis of amyloid beta-protein precursor mRNA in human endothelial cells. *Proc. Natl. Acad. Sci. USA* 86: 7606–7610.
55. Yamamoto, M., T. Kiyota, M. Horiba, J. L. Buescher, S. M. Walsh, H. E. Gendelman, and T. Ikezu. 2007. Interferon-gamma and tumor necrosis factor-alpha regulate amyloid-beta plaque deposition and beta-secretase expression in Swedish mutant APP transgenic mice. *Am. J. Pathol.* 170: 680–692.
56. Clarke, R. M., F. O'Connell, A. Lyons, and M. A. Lynch. 2007. The HMG-CoA reductase inhibitor, atorvastatin, attenuates the effects of acute administration of amyloid-beta1-42 in the rat hippocampus in vivo. *Neuropharmacology* 52: 136–145.
57. Lyons, A., E. J. Downer, S. Crotty, Y. M. Nolan, K. H. Mills, and M. A. Lynch. 2007. CD200 ligand receptor interaction modulates microglial activation in vivo and in vitro: a role for IL-4. *J. Neurosci.* 27: 8309–8313.
58. Cao, D., H. Lu, T. L. Lewis, and L. Li. 2007. Intake of sucrose-sweetened water induces insulin resistance and exacerbates memory deficits and amyloidosis in a transgenic mouse model of Alzheimer disease. *J. Biol. Chem.* 282: 36275–36282.
59. Jankowsky, J. L., T. Melnikova, D. J. Fadale, G. M. Xu, H. H. Slunt, V. Gonzales, L. H. Younkin, S. G. Younkin, D. R. Borchelt, and A. V. Savonenko. 2005. Environmental enrichment mitigates cognitive deficits in a mouse model of Alzheimer's disease. *J. Neurosci.* 25: 5217–5224.
60. Westerman, M. A., D. Cooper-Blacketer, A. Mariash, L. Kotilinek, T. Kawarabayashi, L. H. Younkin, G. A. Carlson, S. G. Younkin, and K. H. Ashe. 2002. The relationship between Abeta and memory in the Tg2576 mouse model of Alzheimer's disease. *J. Neurosci.* 22: 1858–1867.
61. Liu, L., T. Tapiola, S. K. Herukka, M. Heikkilä, and H. Tanila. 2003. Abeta levels in serum, CSF and brain, and cognitive deficits in APP + PS1 transgenic mice. *Neuroreport* 14: 163–166.
62. Ethell, D. W., D. Shippy, C. Cao, J. R. Cracchiolo, M. Runfeldt, B. Blake, and G. W. Arendash. 2006. Abeta-specific T-cells reverse cognitive decline and synaptic loss in Alzheimer's mice. *Neurobiol. Dis.* 23: 351–361.
63. Hauben, E., O. Butovsky, U. Nevo, E. Yoles, G. Moalem, E. Agranov, F. Mor, R. Leibowitz-Amit, E. Pevsner, S. Akselrod, et al. 2000. Passive or active immunization with myelin basic protein promotes recovery from spinal cord contusion. *J. Neurosci.* 20: 6421–6430.